august 1962

the institute of radio engineers

Proceedings of the IRE

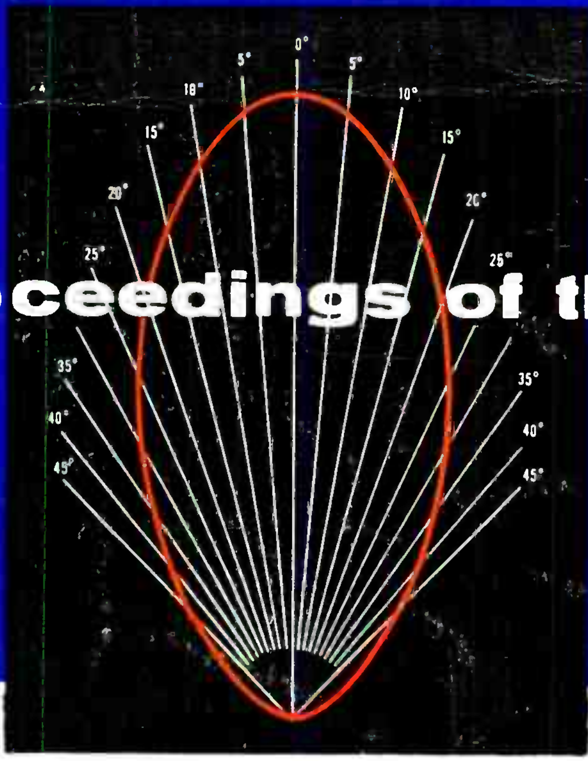

in this issue

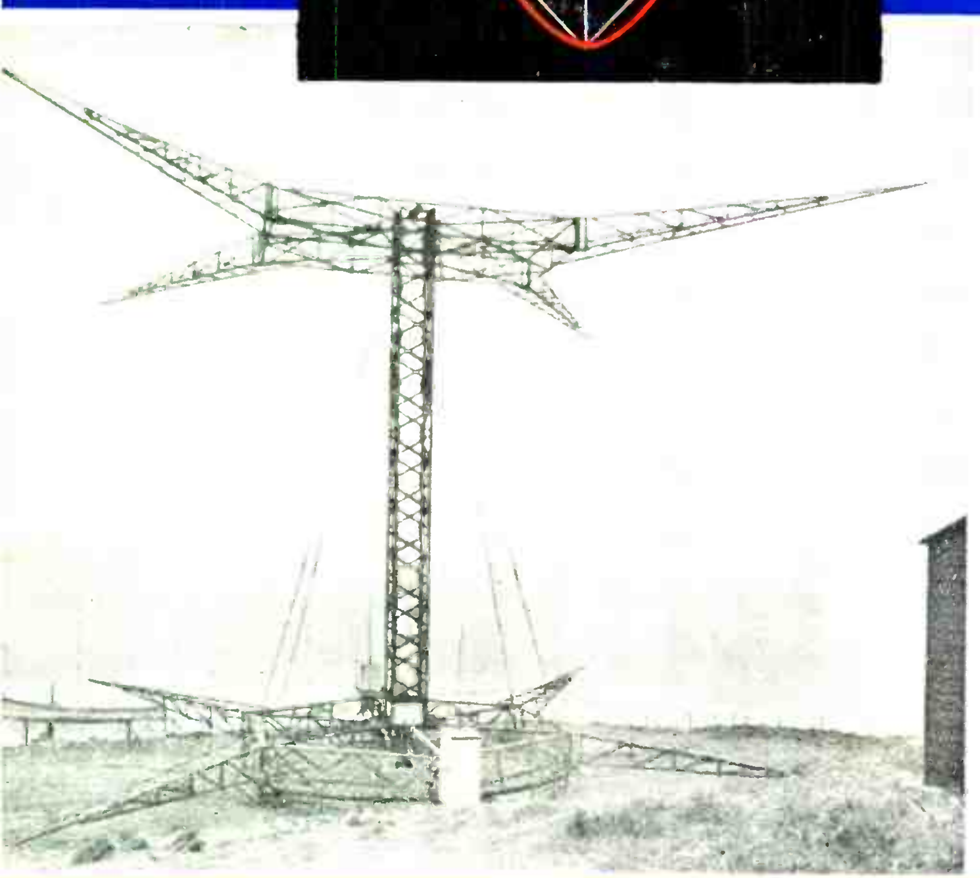

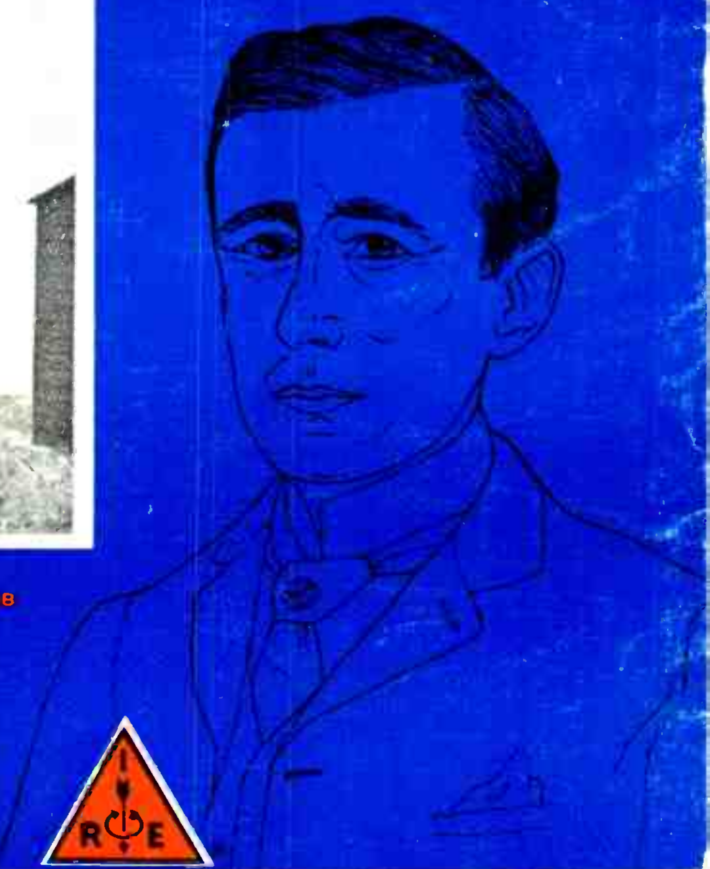

MARCONI'S DIRECTIONAL RADIO EXPERIMENTS: Page 1748

SPECIAL FILTERS

TO YOUR REQUIREMENTS

Almost thirty years of experience in the design and production of special filters have resulted in UTC being a first source for difficult units. Present designs incorporate a wide variety of core structures, winding methods, and capacitors to provide maximum performance, stability, and reliability. The units illustrated show a few of the thousands of specials produced by UTC to customers' requirements, and only slightly indicate the possibilities in present special filter design. Range of frequencies on special units is from .1 cycles to 400 MC.

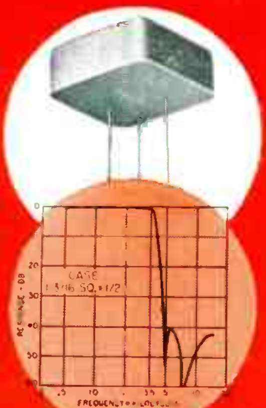

Miniaturized 3.5 KC low pass filter, 10K ohms to 10K ohms. Within 1 db up to 3500 cycles. Greater than 40 db beyond 4800 cycles.

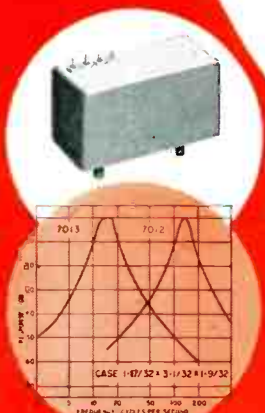

Fifteen cycle and 135 cycle filters for Tacan, 600 ohms to high impedance. Extreme stability —55°C. to + 100°C.

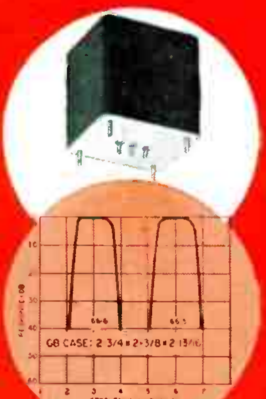

Three KC and 6 KC flat top band pass filters, 400 ohms to 20K ohms, MIL-T-27A, each filter 1.7 lbs.

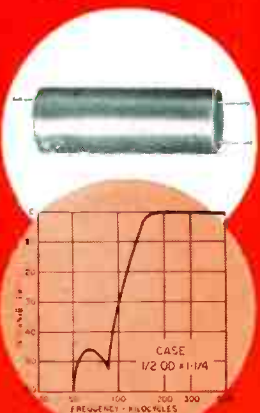

High frequency Mini-filters, .33 oz. MIL-T-27A Grade 5. 150 KC High Pass 3 db to 150 KC, down 45 db below 85 KC, 7500 ohms.

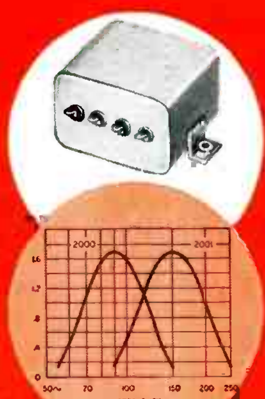

Curves of our miniturized 90 and 150 cycle filters for glide path systems. 1¼" x 1¾" x 1¾".

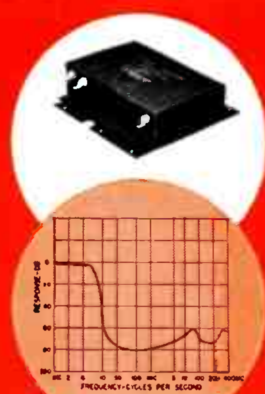

Power line filter from sources of 50 to 400 cycles ... attenuation from 14 KC to 400 MC ... 25 cubic inches.

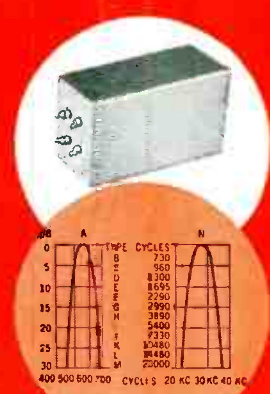

Multi-channel telemetering band pass filters for 400 cycle to 40 KC. Miniaturized units for many applications.

Plus over 1,000 STOCK ITEMS with UTC High Reliability from your local distributor

write for catalog

UNITED TRANSFORMER CORP.

150 VARICK STREET, NEW YORK 13, N. Y.

PACIFIC MFG. DIVISION: 3630 EASTHAM DRIVE, CULVER CITY, CALIF.
EXPORT DIVISION: 13 EAST 40th STREET, NEW YORK 16, N. Y. CABLES: "ARLAB"

VOLUME 50, NUMBER 8

August, 1962

published monthly by The Institute of Radio Engineers, Inc.

Proceedings of the IRE®

contents

COVER

One of Marconi's early experiments with directional short waves took the form of this rotating radio beacon for ship navigation as described in his 1922 IRE Medal of Honor speech reprinted on page 1748.

AUGUST

published monthly by The Institute of Radio Engineers, Inc.

Proceedings of the IRE

continued

AUGUST

PROCEEDINGS OF THE IRE, published monthly by The Institute of Radio Engineers, Inc., at 1 East 79 Street, New York 21, N. Y. Cable Address: IRADENGS Manuscripts should be submitted in triplicate to the Editorial Department. Correspondence column items should not exceed four double-spaced pages (illustrations count as one half page each). Responsibility for contents of papers published rests upon the authors, and not the IRE or its members. All republication rights, including translations, are reserved by the IRE and granted only on request. Abstracting is permitted with mention of source.

Thirty days notice is required for change of address. Price per copy: members of The Institute of Radio Engineers, one additional copy, $1.25; non-members, $2.25. Yearly subscription price: members $9.00, one additional subscription $13.50; public libraries and colleges $13.50; non-members in United States, Canada, and U. S. Possessions $18.00; abroad $19.00. Second-class postage paid at Menasha, Wisconsin, under the act of March 3, 1879. Acceptance for mailing at a special rate of postage is provided for in the act of February 28, 1925, embodied in Paragraph 4, Section 412, P. L. and R., authorized October 26, 1927. Printed in U.S.A.

New from Sprague!

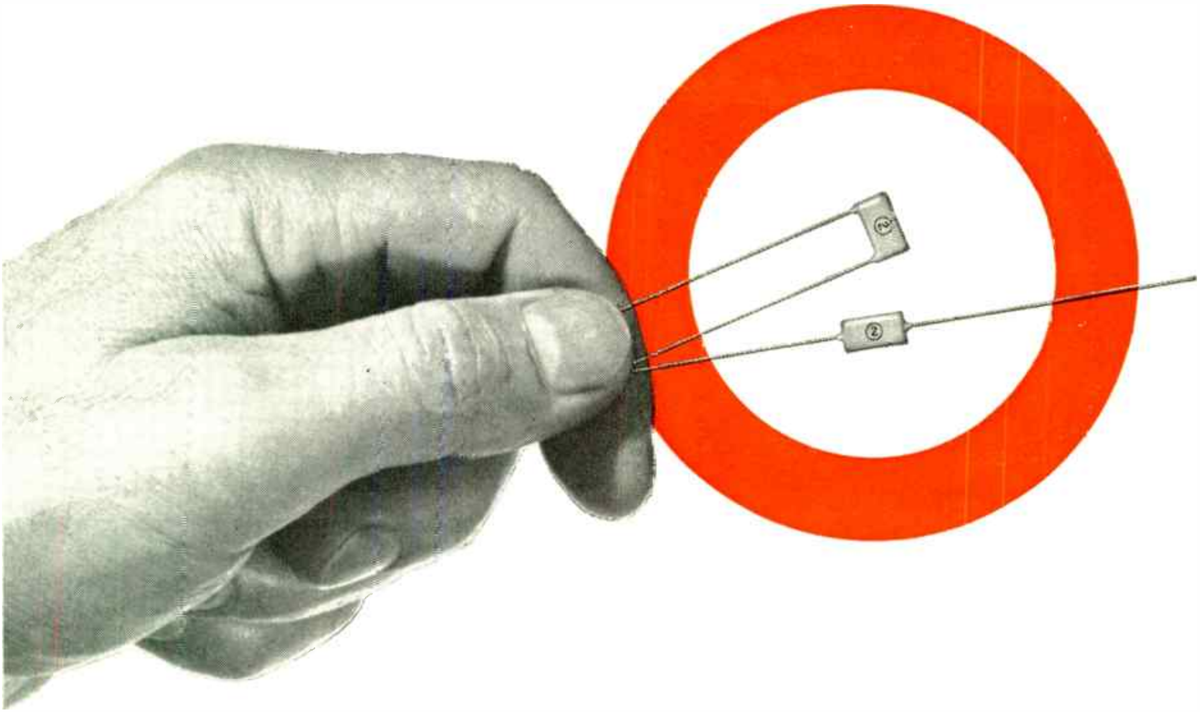

N030 MONOLYTHIC® Ceramic Capacitors offer unparalleled size and circuit stability

Here is a new kind of capacitor . . . with a combination of stability, weight, and size advantages never before achieved in a "compact" capacitor!

Layer-built by a unique automated process, MONOLYTHIC Ceramic Capacitors exhibit extremely low capacitance change with temperature (about one-fourth that of comparable capacitors using other dielectrics). Their special construction also permits a new order of compactness—MONOLYTHICS pack more capacitance per unit volume, resulting in substantial reductions in size and weight.

In addition to single-section capacitors, MONOLYTHICS can also be obtained as multiple-section units, allowing circuit designers to replace several conventional capacitors with a single compact device. The availability of these tiny yet highly stable units with either axial or radial leads offers further flexibility to the circuit design engineer.

Cumulative test data prove the low failure rate of these epoxy or phenolic coated capacitors in service—established by thousands of life, moisture resistance, shock, and vibration tests.

For application engineering assistance without obligation, write to Commercial Engineering Section. For complete technical data, write for Engineering Bulletins to Technical Literature Section. **Sprague Electric Company, 235 Marshall Street, North Adams, Mass.**

SPRAGUE COMPONENTS

CAPACITORS	INTERFERENCE FILTERS	HIGH TEMPERATURE MAGNET WIRE
TRANSISTORS	PULSE TRANSFORMERS	CERAMIC-BASE PRINTED NETWORKS
MAGNETIC COMPONENTS	PIEZOELECTRIC CERAMICS	PACKAGED COMPONENT ASSEMBLIES
RESISTORS	PULSE-FORMING NETWORKS	FUNCTIONAL DIGITAL CIRCUITS
MICROCIRCUITS	TOROIDAL INDUCTORS	ELECTRIC WAVE FILTERS

4S-314R

SPRAGUE®
THE MARK OF RELIABILITY

GET THE FULL STORY AT WESCON BOOTH 640

As the state-of-the-art generally grows more complex, the complexity of antenna problems appears to be keeping pace. It used to be that a radar antenna was required to produce only a single beam which could be moved about to scan the coverage volume. Now, many applications require that the antenna form several beams simultaneously. This month and next month Warren White discusses a problem unique to the multiple beam antenna.

Orthogonality in Multiple Beam Antennas

PART I

Despite several attacks on the validity of Einstein's relativity theories, no one has ever come up with a method of transmitting energy at velocities faster than the speed of light. Consequently, as the requirements on radar systems in terms of data rate and range performance grow ever more demanding, a point is reached in which the old sequential probing of space beamwidth-by-beamwidth must be abandoned and systems devised in which several beams are investigated in parallel.

A variety of techniques have been developed for providing multiple simultaneous beams from a common aperture. One of the earliest of these involved simply placing multiple feed horns in the focal plane of a paraboloid reflector. In other cases, more complex systems have been used, such as cassegrain two-reflector optics and various types of lens antennas, including the Luneberg lens. More recently, techniques have been developed in which a matrix network is used to feed an array antenna.

Regardless of the method used, designers have been plagued with problems of obtaining suitable crossovers and at the same time achieving satisfactory side lobe levels. In the case of the multiple feeds feeding a simple paraboloid, if the individual feeds are large enough to provide proper illumination control, there is physical interference before they can be placed close enough to provide satisfactory crossover levels. On the other hand, if the feeds are positioned to provide the desired crossover levels, the largest structure that will fit is inadequate to provide suitable illumination control, and considerable spillover results.

At one time, it was thought that the problem could be solved by increasing the effective focal length, thereby increasing the distance between feed centers. It was soon found, however, that the size of the required feed also increased in proportion, and the crossover problem was not alleviated. The realization gradually spread that some fundamental principle was at work.

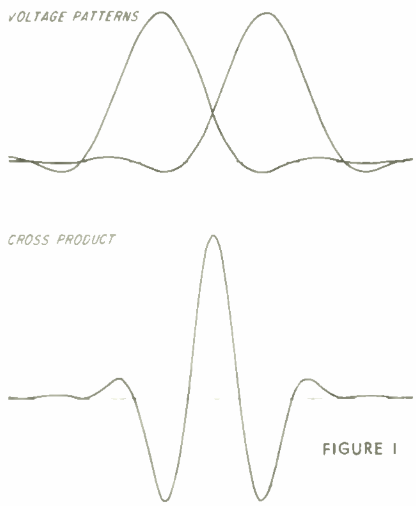

FIGURE 1

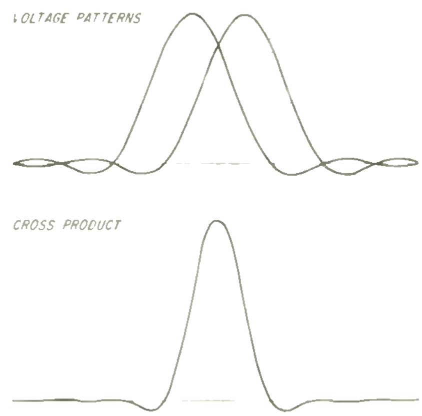

FIGURE 2

However, not until a recent paper by Allen* had any definitive writing on the problem appeared in the generally available literature.

Allen showed, by using certain theorems concerning lossless networks, that in an array antenna fed by a lossless reciprocal matrix, the beams can be decoupled only if the array factor is orthogonal in space. This means that if we multiply one pattern by the other and integrate the product over all space, the result should be zero. Actually, this principle of orthogonality is of much greater application, and can be established for any lossless passive antenna regardless of the beam-forming mechanism and regardless of any possible use of nonreciprocal elements. Simple conservation of energy relations show that for any two antenna beams to be decoupled in a lossless passive system, the radiation patterns must be orthogonal in space.

With uniformly illuminated rectangular apertures, the pattern is, of course, of the sin x/x shape. Patterns of this type, spaced so as to be orthogonal, cross over at about 4 db down and have about 13.2 db side lobes. If we taper the illumination to provide better side lobe control, the crossover level deteriorates. For example, with a cosine taper, if the beams are orthogonal, the crossover level becomes about 9.5 db. Figure 1 shows the individual radiation patterns and the cross product of two cosine tapered beams spaced for orthogonality, and Figure 2 shows similar plots when the beams are spaced for good crossover (about 2 db). As can readily be seen, the latter case is far from orthogonal.

At first glance, it would appear that the problem of obtaining satisfactory operation of a multiple beam antenna is unsolvable, since the conservation of energy principle on which our conclusions are based is rather basic. Actually, the picture is not quite so dark. There are several methods by which acceptable solutions can be achieved in a majority of cases. We will discuss these more fully next month.

* J. L. Allen, "A Theoretical Limitation on the Formation of Lossless Multiple Beams in Linear Arrays," IRE Trans. on Antennas and Propagation, Vol. AP-9, No. 4, p. 350-352, July 1961.

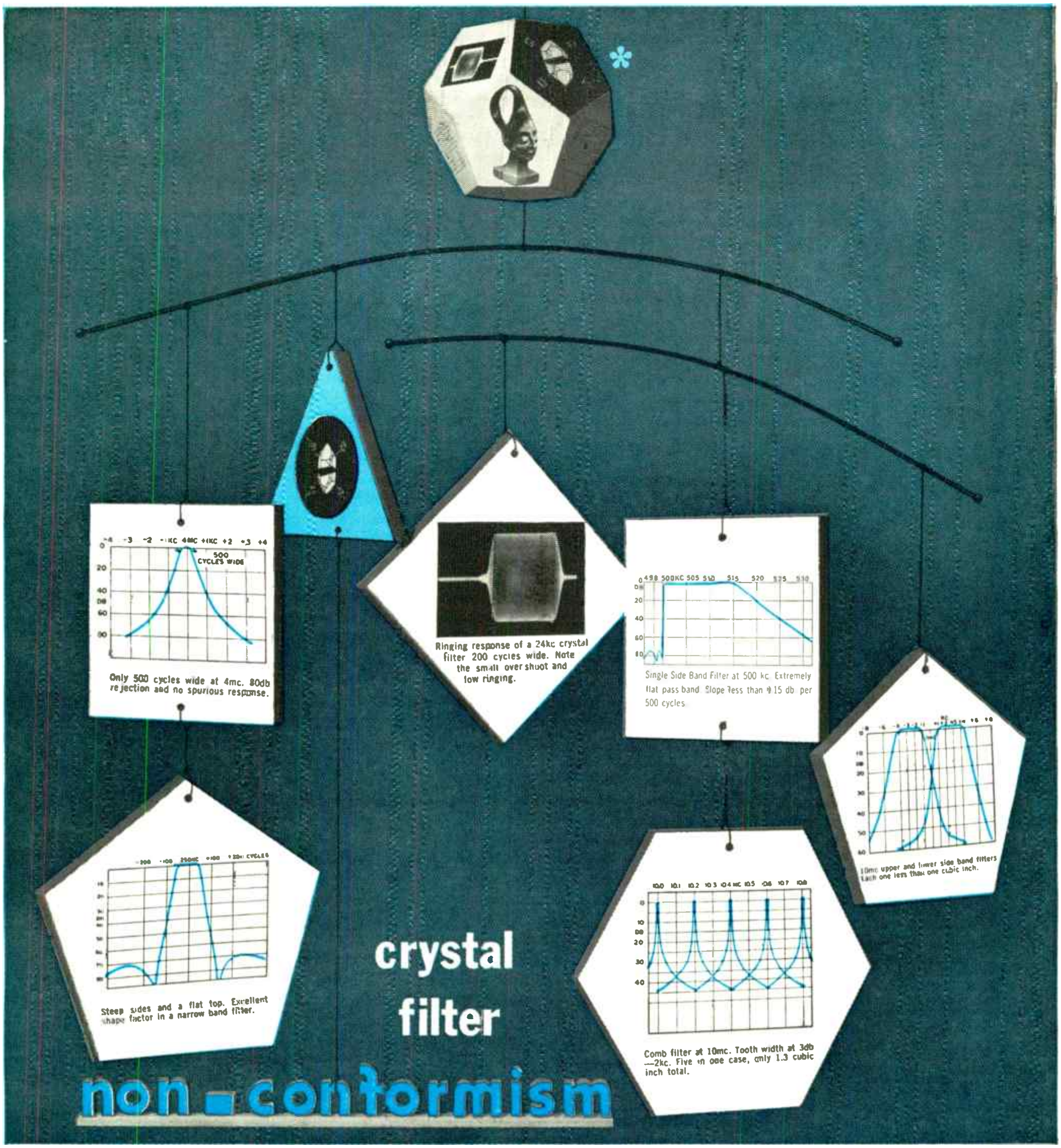

Those *non-conformists* at Burnell's engineering laboratory aren't satisfied with just producing the broadest range of crystal filters, toroids and communication networks: through their constant efforts to satisfy tomorrow's space age electronics problems, they have developed a whole new family of sophisticated crystal filters, with exceptional and unusual characteristics, contributing to increased circuit flexibility as graphically demonstrated above.

Those same *non-conformists* have also made considerable progress solving other electronics/space age problems. A typical example of this has been their work with the application of Time Domain Synthesis; producing an unlimited inventory of wave forms for new applications, and resulting in substantial reductions of size and weight, eliminating the need for complex active circuitry for its support.

*Join the *non-conformists*—write today for your free ***Non-Conformist*** paper weight and Crystal Filter Catalog XT-455. Yes! Your circuits *can* profit today from tomorrow's research.

Burnell & Co., Inc.

PIONEERS IN microminiaturization OF TOROIDS, FILTERS AND RELATED NETWORKS

EXECUTIVE OFFICE AND PLANT
DEPT. PI-8
PELHAM, NEW YORK
PELHAM 8-5000
TELETYPE PELHAM 3633

PACIFIC DIVISION
SOUTH PASADENA, CAL.
MFD. IN CANADA
BY EDO (CANADA) LTD.
CORNWALL, ONT.
WELLINGTON 2-6774

DIVISIONS: Gray & Kuhn, Inc., Pelham, New York • GLP Electronics, Inc., Bristol, Conn. • Guillemin Research Laboratory, Cambridge, Mass.

Telephone craftsman uses special pneumatic tool to flatten connector onto insulated wires. Metal tangs pierce insulation and produce a splice that is equivalent to a soldered joint.

Along the cable routes of the Bell System, wires are spliced at a rate of 250,000,000 a year. Conventionally, connections are made by "skinning" the insulation, twisting the bare wires together, and slipping on an insulating sleeve. Now, with a new connector initiated at Bell Telephone Laboratories, (diagram at lower right) splices can be made faster, yet are even more reliable.

The craftsman slips the two wire ends—with insulation intact—into the connector, then flattens the connector with a pneumatic tool. Springy phosphor bronze tangs inside the connector bite through the insulation to contact the copper wire. The stable, low-resistance splice established is maintained for many years, even under conditions of high humidity, corrosive atmospheres and vibration.

Ultrasensitive measuring techniques devised by our engineers demonstrate that the new connector provides the equivalent of a soldered connection, even with voltages as low as 25 millionths of a volt.

Working with our manufacturing partners at Western Electric, our engineers developed this connector into a design capable of being mass-produced at low cost. It is being introduced in the Bell System.

NEW WIRE CONNECTOR HAS THREE PARTS:

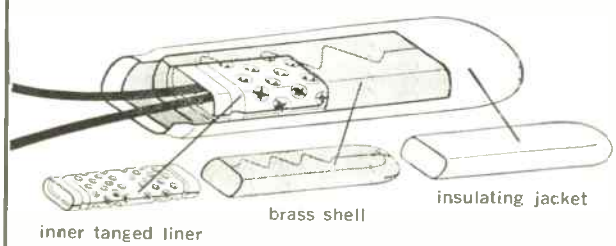

BELL TELEPHONE LABORATORIES

World center of communications research and development

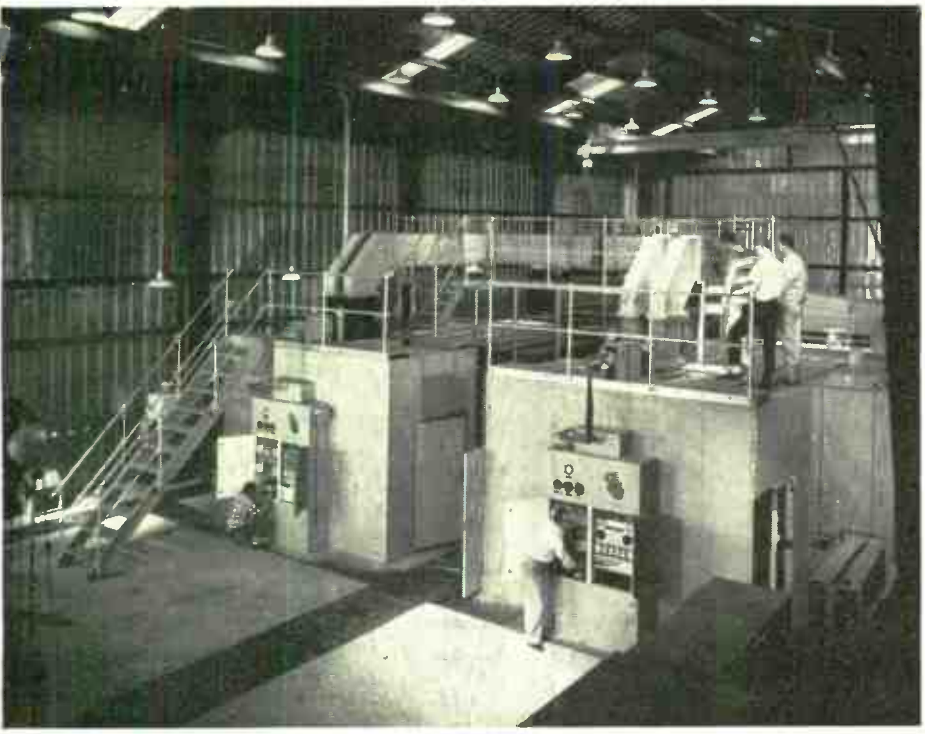

BMEWS . . . the Ballistic Missile Early Warning System is the free world's first warning of enemy ICBM attack.

Powerful radars with an accurate range of thousands of miles can detect incoming ICBMs minutes after launching. The transmitters for this defense system are being built by Continental Electronics . . . specialists in super power transmitting equipment.

Provided under sub-contract to General Electric and R.C.A., these transmitters from Continental Electronics are another contribution to our country's defense.

Continental Electronics

MANUFACTURING COMPANY • MAILING ADDRESS: BOX 17040 • DALLAS 17, TEXAS
4212 S. BUCKNER BLVD. • EV 1-7161 • LTV SUBSIDIARY OF LING-TEMCO-VOUGHT, INC.
Designers and Builders of the World's Most Powerful Radio Transmitters

ENGINEERS . . . FOR STIMULATING WORK ON THE ELECTRONICS FRONTIERS OF TOMORROW WITH A DYNAMIC, CREATIVE ORGANIZATION, SEND RESUME TO DIR. OF PERSONNEL.

Meetings with Exhibits

● As a service both to Members and the industry, we will endeavor to record in this column each month those meetings of IRE, its sections and professional groups, which include exhibits.

Δ

August 21-24, 1962

Western Electronics Show and Conference (WESCON), Statler-Hilton Hotel & Memorial Sports Arena, Los Angeles, Calif.

Exhibits: Mr. Don Larson, WESCON, 1435 S. La Cienega Blvd., Los Angeles, Calif.

August 29-September 1, 1962

Second International Conference on Information Processing, Munich, Germany

Exhibits: Dr. Heinz Billing, Max Planck Institute, Munich, Germany

September 3-7, 1962

National Advanced Technology Management Conference, Opera House, Seattle World's Fair Grounds, Seattle, Wash.

Exhibits: Mr. Hugh Fairclough, 1624 22nd Avenue East, Seattle 2, Wash.

September 21-22, 1962

Conference on Communications, Roosevelt Hotel, Cedar Rapids, Iowa

Exhibits: Mr. Richard L. Jaycox, P.O. Box 918, Cedar Rapids, Iowa

October 1-3, 1962

Eighth National Communications Symposium, Hotel Utica & Utica Municipal Auditorium, Utica, N.Y.

Exhibits: Mr. Charles Glaviano, 45 Meadow Dr., Rome, N.Y.

October 2-4, 1962

Seventh National Symposium on Space Electronics & Telemetry, Fontainebleau Hotel, Miami Beach, Fla.

Exhibits: Mr. Charles H. Doersam, Jr., Instruments for Industry, 101 New South Road, Hicksville, L.I., N.Y.

October 8-10, 1962

National Electronics Conference, McCormick Place, Chicago, Ill.

Exhibits: Mr. Rudy Napolitan, National Electronics Conference, 228 N. LaSalle St., Chicago, Ill.

October 15-18, 1962

Symposium on Space Phenomena & Measurement, Statler-Hilton Hotel, Detroit, Mich.

Exhibits: Mr. J. B. Bullock, University of Michigan, Ann Arbor, Mich.

(Continued on page 10A)

A NEW SUBMINIATURE VARACTOR DIODE

Bomac Laboratories' new ThermoBond* silicon varactor diode provides the microwave designer with a subminiature silicon component offering great reliability, uniformity, packaging simplicity, and size advantages.

Reliability is achieved through matching metal-to-ceramic seals and welded construction. There is no C-spring to work loose from environmental shock, and extreme temperature; an important noise source is eliminated. Uniformity is assured through heat bonding and batch process manufacturing techniques. Packaging simplicity is evident in the extremely small size of the ThermoBond diode. It easily withstands normal soldering temperatures. In addition, hermetically-sealed case construction provides long-life stability, independent of environmental conditions. Retrofit packaging is available. A single case dimension covers 252 electrical values.

Bomac ThermoBond silicon varactor diodes are designed for use in microwave limiters, sideband modulators, harmonic generators, low-noise parametric amplifiers, as tuning elements in voltage control oscillators, and in solid state duplexers.

Write for technical data on the ways in which ThermoBond diodes by Bomac can aid your microwave system design problems.

*Trademark

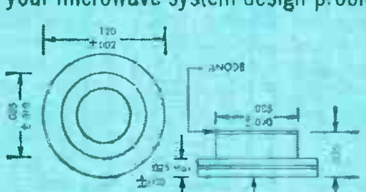

BOMAC laboratories, inc.
BEVERLY 2, MASSACHUSETTS
A Varian Subsidiary

Other Subsidiaries of Varian Associates: S-F-D LABORATORIES, INC. • VARIAN ASSOCIATES OF CANADA, LTD. SEMICON ASSOCIATES, INC. • SEMICON OF CALIFORNIA, INC. • VARIAN A. G. (SWITZERLAND)

Meetings with Exhibits

(Continued from page 8A)

November 1-2, 1962

Sixth National Conference on Product Engineering and Production, Jack Tar Hotel, San Francisco, Calif.

Exhibits: Mr. W. Dale Fuller, Lockheed Missiles & Space Div., P.O. Box 504, Sunnyvale, Calif.

November 4-7, 1962

Fifteenth Annual Conference on Electronic Techniques in Medicine & Biology, Conrad Hilton Hotel, Chicago, Ill.

Exhibits: Professional Associates, Inc., 6520 Clayton Rd., Saint Louis 17, Mo.

November 5-7, 1962

NEREM (Northeast Research & Engineering Meeting), Commonwealth Armory & Somerset Hotel, Boston, Mass.

Exhibits: Mr. S. K. Gibson, Instruments of New England, 108 Greenwood Lane, Waltham 5, Mass.

November 12-15, 1962

Eighth Annual Conference on Magnetism & Magnetic Materials, Penn-Sheraton Hotel, Pittsburgh, Pa.

Exhibits: Mr. J. L. Whitlock, John Leslie Whitlock Associates, 253 Waples Mill Rd., Oakton, Va.

November 16-17, 1962

Communications Symposium, Queen Elizabeth Hotel, Montreal, P.Q., Canada

Exhibits: Mr. Arthur H. Gregory, Northern Electric Co., Ltd., 1600 Dorchester Blvd. W., Montreal, P.Q., Canada

November 19-20, 1962

MAECON (Mid-America Electronics Conference), Continental Hotel, Kansas City, Mo.

Exhibits: Dr. Arthur Goldsmith, Wilcox Electric Co., 1400 Chestnut, Kansas City 27, Mo.

December 4-6, 1962

Fall Joint Computer Conference, Sheraton Hotel, Philadelphia, Pa.

Exhibits: Mr. R. A. C. Lane, RCA Building 204-1, Camden 8, N.J.

December 6-7, 1962

13th National Conference on Vehicular Communications, Mayfair Hotel, Los Angeles, Calif.

Exhibits: Mr. Leslie M. Walker, Los Angeles County Dept. of Communications, 500 West Temple St., Los Angeles 12, Calif.

Note on Professional Group Meetings: Some of the Professional Groups conduct meetings at which there are exhibits. Working committeemen on these groups are asked to send advance data to this column for publicity information. You may address these notices to the Advertising Department and of course listings are free to IRE Professional Groups.

AMPLIFICATION/DISPLAY of TRANSDUCER SIGNALS

Compact portable unit includes oscillator for transducer ac excitation, high-gain carrier-type amplifier, phase-sensitive demodulator, power supply and large, multi-scale meter. Model 311, $375. Battery-operated 2-pound version, Model 312, $300. Wide range of Sanborn transducers also available for linear displacement, velocity, low force, pressure; prices on request.

100th Sec. X-Y RECORDING

Optical recording speeds to 2500 in/sec., frequency response to 130 cps within 3 db. Direct readout 8" x 8" daylight-loading charts; 1% linearity; interchangeable "850" preamps for each axis. Model 670A X-Y Recorder including case, $2,335 (without preamps).

7-CHANNEL FM or DIRECT RECORD DATA RECORDING

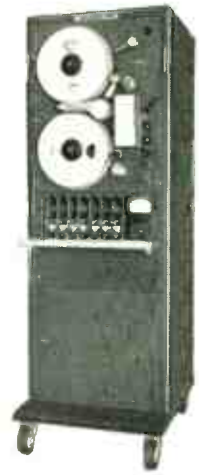

Economical 4-speed (3¾" to 30"/sec) magnetic data recording system, with interchangeable FM and direct record/reproduce electronics in 7" panel space. Compatible with Sanborn preamplifiers and systems, meets IRIG telemetry standards. Series 2000 with FM electronics, $7200. Compatible Model 769 17" Multi-Trace scope, for visual readout or input monitoring, $1145 (not including Gating Amplifiers).

EVENT RECORDING

Up to 120 channels of on/off events as short as 1.3 ms, on 16" wide, dry-process electrically-sensitive chart; complete system with blowers in 19¼" panel space. 9 standard speeds, 9 more optional. Model 360 Event Recorder, $3900; Model 360-2100 Writing Control, $975. Rack mounted 30-channel Model 361 also available, price on request.

Sanborn

RECORDING, READOUT AND DATA HANDLING INSTRUMENTATION

Ask your nearby Sanborn Industrial Sales Engineering Representative for a complete Industrial Catalog and experienced application help. Representatives in principal cities throughout the U.S., Canada and foreign countries.

INDUSTRIAL DIVISION

SANBORN COMPANY

WALTHAM 54, MASSACHUSETTS

A Subsidiary of Hewlett Packard Company

DC-5 KC DIRECT-READOUT RECORDING

Up to 24 channels of direct-readout optical oscillographic recording; response to 3 KC over full scale, DC to 5 KC over 4" amplitudes with single set of galvanometers; 7" high medium-gain amplifier in 8-channel modules. Model 650 system with 8-channel galvanometer block but without inserts or amplifier, $3200.

DATA AMPLIFIERS

Miniaturized (2" x 7" panel), versatile amplifiers. DC-10 KC "FIFO" (Floating Input, Floating Output), completely transistorized; gain 1000, particularly useful for extracting low level signals in the presence of high common mode. 1 ms recovery from 20 V overload, high common mode rejection. Other models with DC-50 KC and DC-100 cps bandwidths. Model 860-4000 FIFO, $825. Prices of others on request.

DIRECT WRITING OSCILLOGRAPHIC RECORDING — 1 to 16 Channels

Clear, rectangular coordinate recording by heated stylus. Wide choice of basic systems for 1, 2, 4, 6, 8, 12, 14 and 16 channels; most have plug-in interchangeable preamplifiers or 8-channel amplifier modules. Basic assembly prices (without amplifiers) range from $3300 for 8-channel "950" style to $6270 for 8-channel "350" style. Typical 2-channel mobile basic assembly, $1575. Single channel portables from $700-$750. Prices of wide variety of amplifiers on request.

ALL PRICES F.O.B. WALTHAM, MASS., U.S.A., AND SUBJECT TO CHANGE WITHOUT NOTICE. STATE AND LOCAL TAXES ADDED WHERE APPLICABLE.

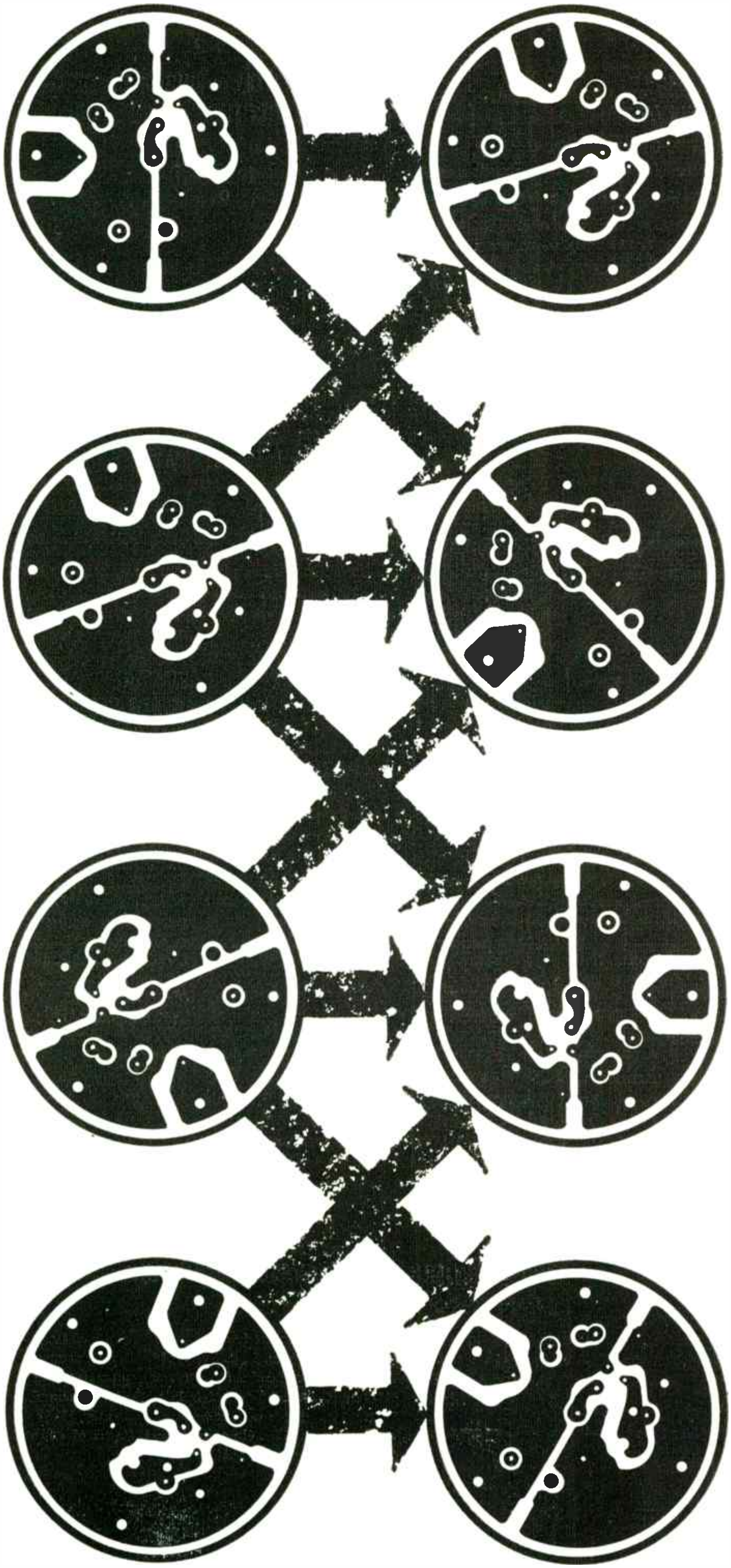

500 MEGACYCLE LOGIC SYSTEM, the first to take full advantage of the ultra high speed capabilities of the tunnel-diode, operates 50 times faster than present circuitry.

NEWS OF DEFENSE TECHNOLOGIES

DATA

To perform effectively, modern defense systems must continuously evaluate every dynamic influence within their environments. Data must be speedily collected, rapidly compared with voluminous memories, and be presented in an organized, accurate and lucid display — *in real time.* All this to assist human judgment, that unassailable prime factor of military strategy.

General Electric has played a major role in advancing the technologies of data utilization and display far beyond their early forms where manual computations of range and track data were accomplished at the plot board. In 1955, for example, General Electric introduced the AN/GPA-37 Radar Course Directing Group, the first mass produced equipment to perform semi-automatic tracking and automatic computation of the intercept problem. Later developments included the AN/FSA-12 Detector Tracking Group—the first equipment to demonstrate automatic detection and tracking of radar targets in all three dimensions—and the new Air Weapons Control System 412L, which provides the U. S. Air Force with the most modern aerospace management system available.

Today's accelerating progress in data technologies is evolving from leap-frog advances in logic and memory circuits and display techniques, and from an expanding scope of responsibility for the data processing and display functions. General Electric continues to make significant contributions to these technologies.

CRYOGENIC ASSOCIATIVE MEMORY enables computers to function like a human brain by instantaneously comparing and associating a new fact with all data in its memory.

THREE-DIMENSIONAL DISPLAY provides a realistic presentation of all spatial activity within its radar's range, in true perspective with scale references in all three dimensions.

CONTACT ANALOG DISPLAY for blind flying or flight simulation uses a digital computer to "paint" a moving TV picture of the ground analogous to the obscured real ground.

TDS-90 DATA SYSTEM transmits up to 62,500 characters a second via coaxial cable or microwave radio to link central processing equipment with remotely located computers.

Progress Is Our Most Important Product

GENERAL ELECTRIC

DEFENSE ELECTRONICS DIVISION

IRE News and Radio Notes

Three Appointments Made to IRE-AIEE Merger Committee

The final three appointments to a 14-man committee that will arrange details of the forthcoming merger of the Institute of Radio Engineers and the American Institute of Electrical Engineers were announced on July 10, 1962 by IRE President Patrick E. Haggerty. The committee, composed of seven representatives of each society, is to begin work immediately. It will go out of existence on January 1, 1963, the date on which the two societies are scheduled to merge to form the Institute of Electrical and Electronic Engineers.

The three IRE appointments to the committee, announced after IRE members had approved the proposed merger by seven to one at a special meeting are: *John T. Henderson*, Principal Research Officer of the National Research Council, Ottawa, Ontario, Canada, and former IRE President; *Walter E. Peterson*, President of Automation Development Corporation, Culver City, Calif., and former Chairman of the IRE Los Angeles Section; and *John D. Ryder*, Dean of Engineering of Michigan State University, East Lansing, Mich., and former IRE President and Editor.

Four others previously selected as IRE representatives on the committee are: Patrick E. Haggerty, President of Texas Instruments Inc., Dallas, Tex.; Secretary Haraden Pratt, Pompano Beach, Fla.; Past President Lloyd V. Berkner, President of the Graduate Research Center, Dallas, Tex.; and Past President Ronald L. McFarlan, Consultant, Chestnut Hill, Mass.

Among the duties of the merger committee are the nomination of candidates for the 1963 Board of Directors, including a President and Vice President, the selection of a General Manager, and the preparation of Bylaws, all of which action must be submitted to the Boards of Directors of the present two societies for approval. The proposed slate of officers and directors must then be ratified by the voting members of both societies.

AIEE representatives previously appointed to the merger committee are: President Warren H. Chase, Vice President of Ohio Bell Telephone Co., Cleveland, Ohio; President-Elect B. R. Teare, Dean of Science and Engineering, Carnegie Institute of Technology, Pittsburgh, Pa.; Past President C. H. Linder, Vice President, General Electric Co., Scarsdale, N. Y.; Past President Elgin B. Robertson, President of Elgin B. Robertson, Inc., Dallas, Tex.

Also appointed are: Treasurer W. R. Clark, Assistant Chief Engineer, Leeds and Northrup Co., Philadelphia, Pa.; Hendley Blackmon, Engineering Manager, Westinghouse Electric Corp., Pittsburgh, Pa.; and L. M. Robertson, Manager of Engineering, Public Service Company of Colorado, Denver, Colo.

IRE President Patrick E. Haggerty (*right*) presents a specially bound copy of the Anniversary Issue of the PROCEEDINGS OF THE IRE to AIEE President Warren H. Chase.

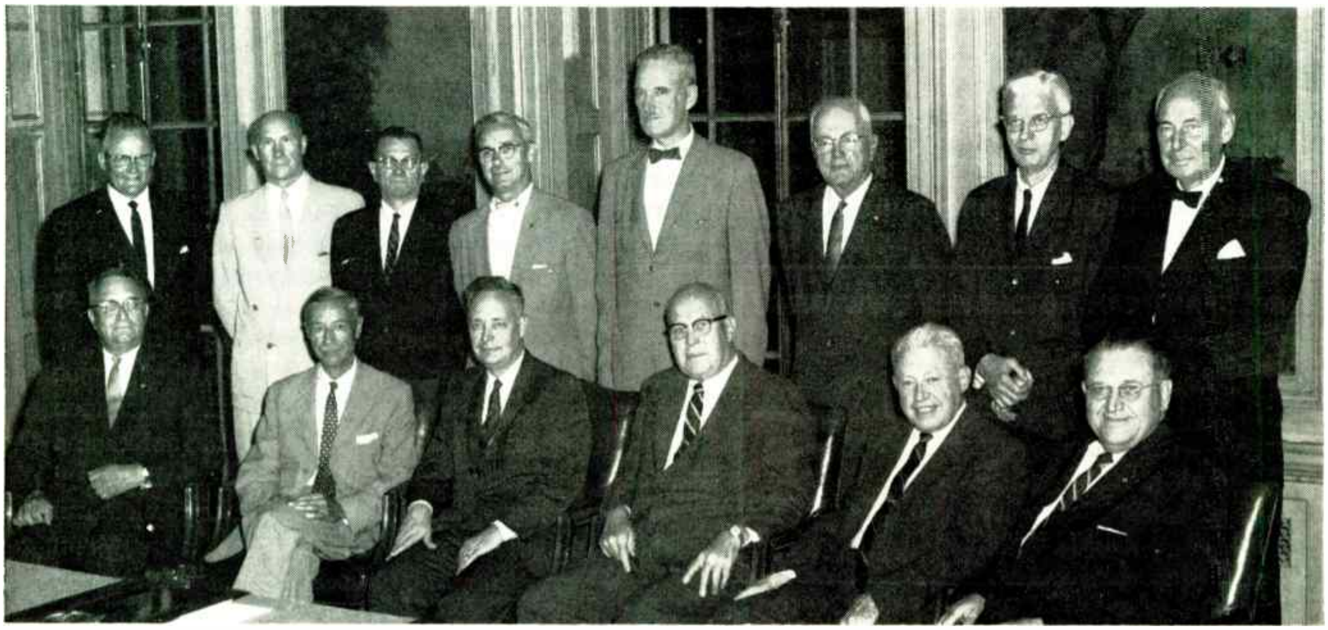

Members of the IRE-AIEE Merger Committee (*left to right*): Front Row: John D. Ryder, Haraden Pratt, Patrick E. Haggerty, Warren H. Chase, L. M. Robertson, and B. R. Teare; Back Row: Walter E. Peterson, John T. Henderson, Hendley Blackmon, W. R. Clark, Ronald L. McFarlan, Elgin B. Robertson, C. H. Linder, and Lloyd V. Berkner.

Current IRE Statistics

(As of April 30, 1962)

Membership—100,075
Sections*—111
Subsections*—33
Professional Groups*—29
Professional Group Chapters—299
Student Branches† —229

* See July, 1962 issue for a list.
† See June, 1962 for a list.

Calendar of Coming Events and Author's Deadlines*

1962

Aug. 13–16: 7th Symposium on Ballistic Missile and Space Technology, United States Air Force Academy, Colorado Springs, Colo.

Aug. 14–17: Internat'l. Conf. on Precision Electromagnetic Measurements (former title: Conf. on Standards and Electronic Measurements), Nat'l. Bur. Standards, Boulder, Colo.

Aug. 21–24: WESCON (Western Electronics Show and Conf.) Statler Hilton and Sports Arena, Los Angeles, Calif.

Aug. 29–Sept. 1: 2nd Internat'l. Conf. on Information Processing, Munich, Germany.

Sept. 3–7: Internat'l. Symp. on Information Theory, Brussels, Belgium.

Sept. 3–7: Nat'l. Advanced Technology, Management Conf., World Fair Grounds, Opera House, Seattle, Wash.

Sept. 3–7: 45th Internat'l. Congress on Microwave Tubes, Kurhaus Hotel, Scheveningen, Netherlands.

Sept. 4–7: ACM Natl. Conf., Hotel Syracuse, Syracuse, N. Y.

Sept. 13–14: 10th Annual Engineering Management Conf., Hotel Roosevelt, New Orleans, La.

Sept. 13–14: Nat'l. Symp. on Engineering Writing and Speech, Mayflower Hotel, Washington, D. C.

Sept. 19–20: 11th Annual Industrial Electronics Symp., Hotel Sheraton, Chicago, Ill.

Sept. 28–29: 12th Annual Broadcast Symp., Willard Hotel, Washington, D. C.

Oct. 1–3: 8th Nat'l. Communications Symp., Hotel Utica, Utica, N. Y.

Oct. 2–4: Nat'l. Symp. on Space Elec. and Telemetry, Fontainebleau Hotel, Miami Beach, Fla.

Oct. 7–12: AIEE 1962 Fall General Meeting—3rd Ann. Symp. on Switching, Circuit Theory and Logical Design, Chicago, Ill.

Oct. 8–10: Nat'l. Elec. Conf., McCormick Pl., Chicago, Ill.

Oct. 12–13: 7th Annual North Carolina Section Symp., Greensboro Coliseum, Greensboro, S. C.

Oct. 15–17: URSI-IRE Fall Meeting, Ottawa, Canada.

Oct. 15–18: Symp. on Space Phenomena and Measurement, Statler-Hilton, Detroit, Mich.

Oct. 22–24: ECCANE (East Coast Conf. on Aerospace and Navigational Elec.), Emerson Hotel, Baltimore, Md.

* DL = Deadline for submitting abstracts.

(*Continued on page 16A*)

H. Rinia, (*left*) Chairman of the Benelux Section, presenting the Makkum plate to Dr. Bruce B. Barrow (*right*). Behind them stand (*from left to right*): W. Metzelaar, G. J. Siezen, Prof. B. D. H. Tellegen, C. B. Broersma, and Dr. H. P. Williams.

Benelux Section Honors Bruce B. Barrow

In recognition of his services for the IRE in Europe, the Benelux Section recently honored its former Secretary-Treasurer, Bruce B. Barrow, at a dinner given by the Executive Committee. The Section Chairman, H. Rinia, presented him with a large plate designed for the occasion and made in Makkum, in the Dutch province of Friesland.

The plate shows along its border an intricate, traditional design in many colors. In the center is the IRE emblem, fired in gold to commemorate the IRE's Golden Anniversary. Above are seen the coats of arms of the three countries of the Benelux Section—Belgium, the Netherlands, and Luxembourg—while below is the inscription "To Dr. B. B. Barrow, from his friends in the Benelux Section of the IRE, 1959–1962." In making the presentation, Mr. Rinia praised the recipient for his contributions to the development of the IRE in Europe, in particular, his efforts as one of the founders of the Benelux Section, as its first Secretary-Treasurer, as one of the organizers of international IRE symposia, and as one of those who worked for the establishment of IRE Region 9.

Conference on Magnetism and Magnetic Materials Solicits Papers

The Eighth Annual Conference on Magnetism and Magnetic Materials will be held on November 12–15, 1962, at the Penn Sheraton Hotel, Pittsburgh, Pa. The Conference is being sponsored by the American Institute of Electrical Engineers and the American Institute of Physics, in cooperation with the IRE, the Office of Naval Research, the Metallurgical Society of AIME, and the American Society for Testing and Materials. It will continue to emphasize the value of bringing together those interested in both basic and applied work from the many disciplines of magnetism.

Contributed papers are solicited on basic theoretical and experimental investigations, potential engineering applications and apparatus and techniques which utilize recent advances in magnetism. Invited papers will be presented by eminent scientists and engineers, both from America and abroad. In addition to the usual topics, the committee is encouraging papers in High Fields, Superconductivity and Magnetism, and Biological Magnetism. Programs containing abstracts of all papers will be distributed before the Conference.

Prospective authors should submit two copies of a 200–500-word abstract in the format of the American Institute of Physics, indicating title, author and affiliation. Abstracts must be sent no later than August 18, 1962, to: G. W. Wiener, Westinghouse Electric Corp., Research Labs., Churchill Borough, Pittsburgh 35, Pa. The AIP style manual may be obtained without charge from H. C. Wolfe, AIP, 335 E. 45 St., New York 17, N. Y. Time allotted for presentation will be ten–fifteen minutes. Final selection of papers and time schedules will be made by the Program Committee. The selection will be based on new technical information contained in the abstract. Consequently, the principal results to be presented should be clearly stated.

The Proceedings of the Conference will be published in the March or April, 1963 supplement to the *Journal of Applied Physics*. Manuscript instructions, including submission deadlines, will be sent to authors whose papers are accepted for presentation. The selection of papers for publication will be determined by their significant scientific or engineering contribution to the present fields of magnetism.

IRE Facsimile Test Charts Now Available

The Technical Committee on Facsimile of the IRE has released a new printing of the Facsimile Test Charts to the Electronic Industries Association. The first printing has been out of stock for some time, and there have been many inquiries for these test charts. Information about prices may be obtained from EIA, 11 West 42 Street, New York, N. Y.

Call for Papers

1963 IRE International Convention

March 25–28, 1963

Waldorf-Astoria Hotel and the New York Coliseum, New York, N. Y.

Prospective authors are requested to submit all of the following information by the

Deadline Date of October 19, 1962

1. 100-word abstract *in triplicate*, title of paper, name and address
2. 500-word summary *in triplicate*, title of paper, name and address
3. Indicate the technical field in which your paper should be classified:

Aerospace & Navigational Electronics
Antennas & Propagation
Audio
Automatic Control
Bio-Medical Electronics
Broadcast & Television Receivers
Broadcasting
Circuit Theory
Communications Systems
Component Parts
Education
Electron Devices
Electronic Computers
Engineering Management
Engineering Writing & Speech
Geoscience Electronics
Human Factors in Electronics
Industrial Electronics
Information Theory
Instrumentation
Microwave Theory & Techniques
Military Electronics
Nuclear Science
Product Engineering & Production
Radio Frequency Interference
Reliability & Quality Control
Space Electronics & Telemetry
Ultrasonics Engineering
Vehicular Communications

Note: Only original papers, not published or presented prior to the 1962 IRE International Convention, will be considered. *Any necessary military or company clearance of papers must be granted prior to submission.*

Address all material to: Dr. Donald B. Sinclair, Chairman
1963 Technical Program Committee
The Institute of Radio Engineers, Inc.
1 East 79 Street, New York 21, N. Y.

Paris Symposium Scheduled

The Third International Symposium on Quantum Electronics will be held at the UNESCO Palace in Paris on February 11–15, 1963. It is being sponsored by the Office of Naval Research, IRE and Société Française des Electroniciens et des Radio-électriciens. It is also receiving support from the Féderation Nationale des Industries Electroniques, which will hold an exposition of apparatus pertaining to quantum electronics during the same week. Professor Louis de Broglie, Nobel Laureate and Secretary of the French Academy, is the Honorary President of the Symposium. Professor P. Grivet, of the University of Paris, is Chairman of the Organizing Committee, and Professor N. Bloembergen, of Harvard University, is Chairman of the Program Committee.

The first two Symposia on Quantum Electronics were sponsored by the Office of Naval Research and were held at High View, N. Y. in 1959 and at Berkeley, Calif. in 1961. As in the previous case, this Symposium will deal with such topics in Quantum Electronics as masers, lasers, coherence, optical pumping, atomic clocks, and applications to spectroscopy, magnetism and relativity. Emphasis will be on basic physical principles rather than on engineering. Scientists desiring to present papers should submit abstracts in triplicate before October 1, 1962 to: The Third International Symposium on Quantum Electronics, 7 Rue de Madrid, Paris 8, France.

Papers may be presented in either French or English. There will be simultaneous translation of each paper into the other language for the benefit of the audience. A registration fee of $12.00 will be required of all participants. Further information can be obtained from the address above.

PGMTT Call for Papers

The 1963 PGMTT National Symposium, sponsored by the IRE Professional Group on Microwave Theory and Techniques, will be held on May 20–22, 1963, at the Miramar Hotel, Santa Monica, Calif.

Original papers in the field of microwave theory and techniques are being sought. Any approval necessary from cognizant authority must be granted prior to submission. Prospective authors are requested to submit a 100-word abstract and a 1000-word summary, in duplicate, with title, name, and address, in English, by January 5, 1963. Address all material to: Dr. I. Kaufman, Chairman, Technical Program Committee, Space Technology Labs., Inc., 1 Space Park, Redondo Beach, Calif.

Authors accepted will be requested to provide 1000-word summaries accompanied by up to six figures suitable for reproduction in a Symposium digest. Publication will not prejudice later consideration of the complete paper for publication in the IRE Transactions on Microwave Theory and Techniques.

Calendar of Coming Events and Author's Deadlines*

(Continued from page 15A)

Oct. 25–27: Electron Devices Meeting, Sheraton Park Hotel, Wash., D. C.
Oct. 30–31: Conf. on Spaceborne Computer Engineering, Disneyland Hotel, Anaheim, Calif.
Nov. 1–2: 6th Nat'l. Conf. on Product Engr. and Production, Jack Tar Hotel, San Francisco, Calif.
Nov. 4–7: 15th Annual Conf. on Engineering in Medicine and Biology, Conrad Hilton Hotel, Chicago, Ill.
Nov. 5–7: NEREM (Northeast Res. and Engr. Meeting, Commonwealth Armory, Somerset Hotel, Boston, Mass.
Nov. 12–14: Radio Fall Meeting, King Edward Hotel, Toronto, Ont., Canada.
Nov. 12–15: 8th Annual Conf. on Magnetism and Magnetic Mat., Penn-Sheraton, Pittsburgh, Pa.
Nov. 16–17: 2nd Canadian IRE Communications Symposium, Queen Eliz. Hotel, Montreal, P.Q., Canada.
Nov. 19–20: MAECON (Mid-America Electronic Conf.), Continental Hotel, Kansas City, Mo.
Nov. 28–30: 1962 Ultrasonics Symp., Columbia Univ., New York, N. Y. (DL*: August 13, 1962, for 200-word abstracts.)
Dec. 4–6: FJCC (Fall Joint Computer Conf.), Sheraton Hotel, Philadelphia, Pa.
Dec. 6–7: 13th Nat'l. Conf. on Vehicular Communications, Disneyland Hotel, Anaheim, Calif. (DL*: Aug. 15, 1962, W. J. Weisz, Motorola, Inc., 4545 W. Augusta Blvd., Chicago 51, Ill.)

1963

Jan. 8–10: Millimeter and Submillimeter Conf., Cherry Plaza Hotel, Orlando, Fla. (DL*: Sept. 15, 1962, J. J. Gallagher, MP-172-Box 5837, The Martin Co., Orlando, Fla.)
Jan. 21–24: 9th Nat'l. Symp. on Reliability and Quality Control, Sheraton Palace Hotel, San Francisco, Calif.
Jan. 30–Feb. 1: 4th Winter Convention on Military Electronics, Ambassador Hotel, Los Angeles, Calif.
Feb. 11–15: 3rd Internat'l. Symp. on Quantum Electronics, UNESCO Bldg., Paris, France. (DL*: Oct. 1, 1962, Madame Cauchy, Secretaire 3ème Congrès d'Electronique Quantique, 7 Rue de Madrid, Paris 8ème, France.)
Feb. 20–22: Internat'l. Solid State Circuits Conf., Sheraton Hotel and Univ. of Pa., Phila., Pa. (DL*: Nov. 1, 1962, S. K. Ghandi, Philco Scientific Lab., Blue Bell, Pa.)
Mar. 25–28: IRE International Convention, Coliseum and Waldorf-Astoria Hotel, New York, N. Y. (DL*: Oct. 19, 1962, Dr. Donald B. Sinclair, IRE, 1 E. 79 St., New York 21, N. Y.)
Apr. 17–19: Southwestern IRE Conf. and Elec. Show, Dallas Memorial Auditorium, Dallas, Tex.
Apr. 17–19: Internat'l. Special Tech. Conf. on Non-Linear Magnetics, Shoreham Hotel, Washington, D. C. (DL*: Nov. 5, 1962, J. J. Suozzi, BTL Labs., Whippany, N. J.)
Apr. 24–26: 7th Region Tech. Conf., San Diego, Calif.

* DL = Deadline for submitting abstracts.

SENSITIVE RESEARCH

10 PPM ACCURACY

5-YEAR RELIABILITY WARRANTY

The Dauphinee Potentiometer is a 6 figure instrument with a 6 year history of stability to a few parts per million. Ranges of −10 μv to +2.101010 v (X1) and −1 μv to +0.2101010 v (X0.1) read out directly on only 4 dials in calibrated steps of 1 μv and 0.1 μv (no slidewire). Thermal emfs are less than 0.1 μv. Contains 2 saturated standard cells in an internally thermostatted enclosure. Separate galvanometer circuits permit continuous monitoring of both the measuring and standardizing functions. Instrument is completely "Self Checking".

The Type 9144 is the only precision DC potentiometer that can be employed equally well as a 2 ppm resistance comparator, a standard cell comparator and a precision 4 terminal 21 Ω standard resistor (variable in steps of 10 μΩ). In the near future an accessory instrument will be made available that will enable this potentiometer to be used in conjunction with a platinum resistance thermometer for the measurement of temperature.

Design is by Dr. T. M. Dauphinee of Canada's National Research Council. All rights are protected by a United States patent application.

TYPE 9144

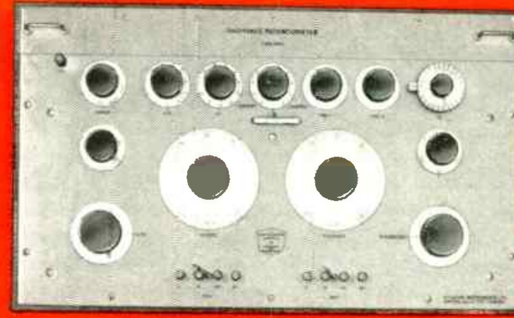

15 PPM ACCURACY

5-YEAR RELIABILITY WARRANTY

The Type 9120 is a new 4 dial, 7 figure precision DC potentiometer with single window readout and a resolution of 1 part in 20 million. Total measuring range of 2.099,999,9 v in steps of 0.1 μv is achieved without the necessity of switching ranges. Instrument is completely "Self Checking". All positions on the measuring dials are individually calibrated steps (no slidewire). Measuring circuit switches are potential contacts and do not carry current. Switch contact resistance is, therefore, of no importance. Thermal emfs are less than 0.1 μv.

The design of the Type 9120 places special emphasis on simplicity of operation and readability. This potentiometer has particular value when voltages requiring usage of the first dial are to be compared to a fraction of a microvolt.

SINGLE WINDOW READOUT

TYPE 9120

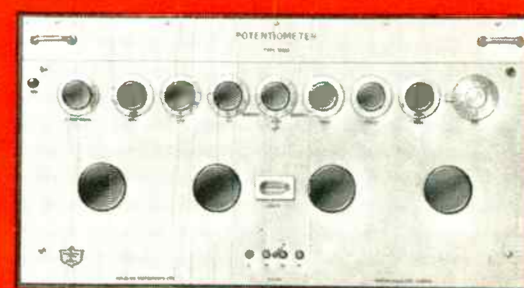

20 PPM ACCURACY

5-YEAR RELIABILITY WARRANTY

The Type 9180 is a 3 dial, 5 figure version of the Dauphinee Potentiometer described above. Particular attention has been paid in construction to the elimination of thermal emfs (less than 0.05 μv). Instrument is completely "Self Checking". Every switch position is an individually calibrated step (no slidewire).

The design of the Type 9180 combines all the advantages of high and low range potentiometers in an economically priced general purpose instrument.

Range Factor	Measuring Range	Resolution
X1.0	−10 μv to +2.10100 v	10 μv
X0.1	−1 μv to +0.210100 v	1 μv
X0.01	−0.1 μv to +0.0210100 v	0.1 μv
*X0.001	−0.01 μv to +0.00210100 v	0.01 μv

*Optional range

TYPE 9180

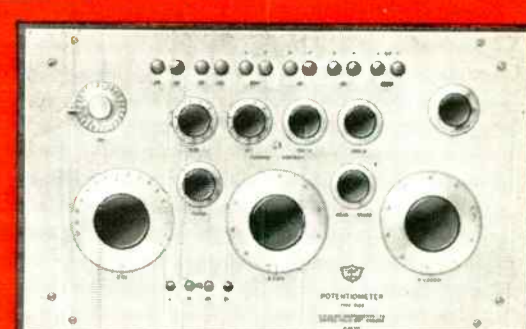

COMMANDER instruments are meticulously manufactured for Sensitive Research by Guildline Instruments Ltd. of Smiths Falls, Canada, whose engineering heritage in the production of fine standards dates back to 1895. The "new" potentiometers described above have many years of "facts and figures" to substantiate their specifications for accuracy and reliability. They are "new" only in the sense that their design concept is so much further advanced than similar instrumentation presently in the field.

COMMANDER potentiometers can be furnished with either NBS or NRC certification. Copies of past performance data are available upon request.

For the most important standard in the world — yours — specify a Sensitive Research COMMANDER Potentiometer. In 1960 and 1961 over 200 other standards people did!

SENSITIVE RESEARCH INSTRUMENT CORPORATION

NEW ROCHELLE, N. Y. ELECTRICAL INSTRUMENTS OF PRECISION SINCE 1927

1962 ACM Conference

The 17th Annual National Conference of the Association for Computing Machinery will be held at the War Memorial Auditorium and the Syracuse Hotel, Syracuse, N. Y. on September 4–7, 1962. Eleven significant fields of interest will be surveyed by over 100 computer authorities from the United States and abroad, covering information retrieval, artificial intelligence, education and training, numerical analysis, and applications in the physical sciences. Engineering applications, automatic programming and compilers, artificial languages, and business and management data processing, as well as real time information processing, and computer design will also be included.

The program will be highlighted by eight invited talks, accenting such vital topics as information processing in military commands, programming languages, and the legal implications of the computer revolution. Also scheduled are panel discussions on ALGOL in use today and the social responsibilities of computer people. The Halls of Discussion periods will be continued at ACM'62, with five topical areas on the agenda: marketing, installation management, business data processing, information retrieval and programmer training. Illustrated condensations of all of the talks will be published in a *Digest of Technical Papers.* Copies will be available on the opening day and distributed free to all conference registrants, except students.

General Chairman of the Syracuse Conference is R. S. Jones, Sylvania Electric Products Inc., Camillus, N. Y.

Florida Conference Call for Papers

The Millimeter and Submillimeter Conference, sponsored by the IRE Orlando Section and PGMTT, will be held in Orlando, Fla., January 8–10, 1963. There will be eleven informative sessions on the following topics:

Millimeter and Submillimeter Transmission Lines

Quasi-Optical Techniques

Millimeter Sources and Stability Considerations

Millimeter and Submillimeter Resonant Structures

Millimeter Components and Power Measurements

Millimeter Receivers, Radiometry, and Propagation

Harmonic Generation and Detection Techniques

Millimeter Spectroscopy—Resonance Phenomenon

Millimeter Masers—Optical Pumping with Millimeter Outputs, and Multiple Quantum Transitions

Millimeter Pulse Work, Plasmas, Measurements and Instrumentation, and Phase Locking and Frequency Control

Survey of Control Millimeter and Submillimeter Work, and Millimeter and Submillimeter Techniques—Future Trends.

Several invited papers will be presented by authorities in the field. Original papers on any of the above topics will be considered for presentation. Speakers should plan on 20 minutes for presentation, and 5 minutes for discussion. The deadline for three copies of a 500-word abstract is September 15, 1962. Abstracts, should be mailed to: J. J. Gallagher, The Martin Co., MP-172, Box 5837, Orlando, Fla.

Authors whose papers cannot be included in the regular sessions will be encouraged to give a brief resume of their papers in the open sessions. Suitable conference papers will be published in the IRE Transactions on Microwave Theory and Techniques.

1962 Ultrasonics Symposium

The 1962 Ultrasonics Symposium, sponsored by the IRE Professional Group on Ultrasonics Engineering, will be held at Columbia University, New York, N. Y. on November 28–30, 1962. In planning the program, the Symposium Committee has invited a number of papers intended to cover both current developments and future trends in the field. The list of authors and papers includes: E. A. Hiedemann, "Optical Effects of Ultrasonic Waves"; A. Kiis, F. G. Hahneman, D. Hornbostel, and B. Small, "A High-Frequency Ultrasonic Spectrum Analyzer"; S. W. Tehon, "Development and Application of Dispersive Ultrasonic Delay Lines"; H. E. Bommel, "Microwave Ultrasonic Absorption in Solids I (Metals and Vitreous Silica)"; K. Dransfeld, "Microwave Ultrasonic Absorption in Solids II (Dielectric Crystals and Ferromagnetic Materials)" R. C. LeCraw, "High-Frequency Acoustic Losses in Ferromagnetic Insulators"; H. Matthews and R. C. LeCraw, "Acoustic Wave Rotation and Magnetoelastic Coupling"; R. T. Denton and E. G. Spencer, "Microwave Acoustic Measurements in Garnets"; M. H. Seavey, Jr., "Microwave Phonon Generation by Thin Magnetic Films"; N. S. Shiren, "Detection of Microwave Ultrasonics by Phonon-Photon Double Quantum Transitions"; E. H. Jacobsen, "Anomalous Dispersion of Ultrasonic Waves by Electron Spins"; E. B. Tucker, "Interactions Between Microwave Phonons and Electron Spins in Solids"; A. R. Hutson, "Prospects for Active Ultrasonic Devices"; and D. L. White, "Ultrasonic Traveling-Wave Amplifier."

In addition to contributed papers related to topics covered by the invited papers, papers are sought on any topic in the general field of ultrasonics. Three copies of a 200-word abstract should be sumbitted before August 13, 1962 to: R. N. Thurston, Technical Program Chairman, Bell Telephone Laboratories, Murray Hill, N. J.

The Symposium Committee includes: General Chairman: J. E. May, Jr.; Vice Chairman: A. H. Meitzler; Arrangements: W. F. Konig; Program: R. N. Thurston, S. E. Jacke, W. F. Konig, J. E. May, Jr., A. H. Meitzler; Publicity and Finance: A. Rothbart.

Obituaries

Martin V. Kiebert Jr. (A'31–M'38–SM'43–F'59). Notification of his death was received. He was former Head of the Electronics Unit of the Advanced Development Division of The Martin Co., Denver, Colo.

Born on November 27, 1908, in Wallace, Idaho, he attended the University of Idaho from 1928 to 1931, and Reed College, Portland, Ore., in 1933 and 1934, majoring in electrical engineering and physics. In 1929 he received the Idaho Edison Scholarship

Award. From 1934 to 1937, he was chief engineer at KIRO, Seattle, Wash. In 1937, he became radio inspector for the Federal Communications Commission at Seattle, and in 1938, he was transferred to Washington, D. C., where he was associate engineer in the broadcast division. During 1939, he became affiliated with Jansky and Bailey, Washington, D. C., as a consulting radio engineer, and in 1941, as a consultant with McNary and Chambers, Washington, D. C.

Before joining The Martin Co., Mr. Kiebert was also proposals coordinator for Datalab, a division of Consolidated Electrodynamics Corp.; director of electronics for the Miami Shipbuilding Corp.; director of research and development for Tele-Dynamics, Inc.; director, Special Products Research Lab., Bendix Aviation Corp.; chief engineer, Tuner Division of P. R. Mallory Co.; assistant to the chief engineer, Convair Guided Missiles Division, General Dynamics Corp.; and director of research and electronics, Applied Research, Inc. A former Navy Commander, he was head of the Special Weapons Branch of the government's Bureau of Aeronautics during World War II. In this capacity, he was responsible for all of the bureau's electronic activities in guided missiles.

Mr. Kiebert was Chairman of the IRE Orange Belt Subsection and of the Radio Telemetry and Remote Control Administrative Committee. He received awards from the American Chemical Society (1928), and from the Royal Aeronautical Society (1947).

John I. Bohnert (M'46–SM'49–F'60) Superintendent of the Electronics Division of the U. S. Naval Research Laboratory, Washington, D. C., died on May 11, 1962. As Laboratory Division Superintendent, he was in charge of a complex of programs devoted to research in solid-state electronics, energy conversion, electron tubes, antennas, identification systems and wave propagation.

He was born in Pittsburgh, Pa., in August, 1910. He received the B.S. degree in mathematics from the Carnegie Institute of Technology in 1932, and the M.A. degrees from the University of Pittsburgh in 1935. He was awarded the Ph.D. degree from the latter institution in 1940.

During World War II, he was engaged in antenna and propagation studies for the Radiation Laboratory of the Massachusetts Institute of Technology. Upon dissolution of the Radiation Laboratory in 1945, he joined the Naval Research Laboratory's Boston field station as a radio engineer, but transferred to the Naval Research Laboratory in Washington in 1946, as a

now see this

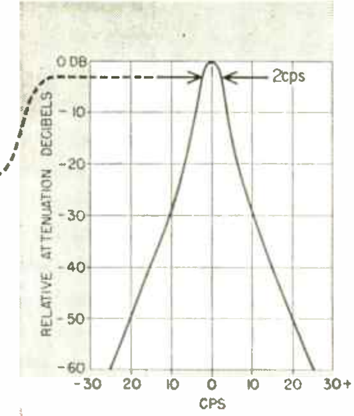

Bandpass response for 2 cps I-F bandwidth

2 cps resolution from 5 cps through 20 kc

with Panoramic's SY-1 SONIC ANALYSIS SYSTEM

a combination of the

LP-1a SONIC SPECTRUM ANALYZER

C-2 AUXILIARY FUNCTION UNIT

RC-3b CHART RECORDER

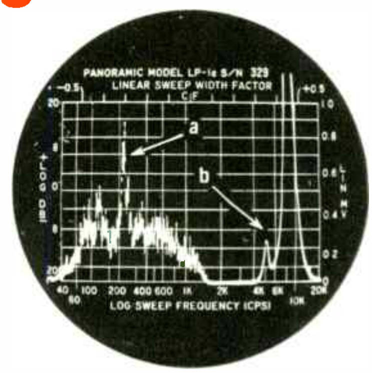

Narrow I-F bandwidths with steep skirts enable:

a) analysis of CW signal deep in noise

b) amplitude measurement of weak signal close to very strong signal.

Panoramic's new low cost system, consisting of the famed Model LP-1a Sonic Analyzer, new C-2 Auxiliary Function Unit and RC-3b Recorder, is designed to solve an extremely wide range of noise, vibration and other waveform analysis problems.

The system is designed for simplicity in use. Its operating parameters are readily adjustable to fit widely varying analysis requirements. *For quick spectrum appraisal* . . . 1 sec. log scan from 40 cps to 20 kc. *For precise detailed analysis* . . . 30 preset linear scan widths of 20 to 5000 cps, centerable between 0 and 20 kc; 1 sec. to 16 hrs. scan intervals; 2 cps to 200 cps steep skirted selectivity range.

Direct frequency and amplitude readouts of discrete and random waveform contents are fast and accurate . . . simplifying use at production test stations or in the laboratory.

Indeed, whether your need is to analyze random or line spectra either with components deep in noise or widely apart in level but close in frequency, this new Panoramic system is your assurance of faster, easier solutions.

AMONG THE SYSTEM'S OUTSTANDING CAPABILITIES:

Overall frequency range: 5 cps to 22,500 cps.

Scan provisions: Precalibrated "quick look" log scan 40 cps to 20 kc in only one second. For precise detailed analysis 30 selectable pre-set linear scans 20 to 5000 cps wide, centerable anywhere between 0 and 20 kc. Scan times: 1 and 10 sec. with C-2 and 30 sec. to 16 hrs. with RC-3b Recorder. Latter permits unattended analysis, provides longer sampling times required for best selectivity and quantitative random signal analysis.

Selectivity characteristics: Automatic optimum resolution (1 second scan) plus adjustable I-F bandwidths from 2 cps to 200 cps with extremely steep skirts—**see graph above**—closely approaches idealized filter desired in random signal analysis.

Readout: 5" CRT and 12" x 4½" inked chart (with RC-3b Recorder).

Calibrated amplitude scales: Linear and 40 db log.

Residual distortion: Dynamic range better than 60 db.

Analyzer stability: Less than 5 cps/HOUR drift (after warm-up) insures meaningful analysis with 2 cps resolution

Sensitivity compensation, random and discrete: Sensitivity remains constant for all I-F bandwidth settings for either random or discrete input signals.

Adjustable smoothing time constant: Smooths random fluctuations, clearly displays average noise level at each frequency for faster more easily appreciated analysis.

Manual scan control: CRT beam and analyzer tuning positioned anywhere within sweep width range for extended time vs. amplitude studies. Amplitude vs. time analysis also provided with RC-3b Recorder.

eem

Sec. 2900

Be sure to see us at WESCON: Booth #3354-5.

Panoramic electronics, inc.

For detailed information on the SY-1 and other sonic systems, CALL, WRITE OR WIRE:

dependable CERTIFIED SPECIFICATIONS for accurate data

522 South Fulton Avenue, Mount Vernon, N.Y. • Phone: (Area Code 914) OWens 9-4600 • TWX: MT-V-N.Y.—5229 • Cables: Panoramic, Mount Vernon, New York State

member of the staff of the newly constituted Microwave Antennas and Components Branch. Assuming positions of increasing importance at the Laboratory, he became Division Superintendent in 1955.

Dr. Bohnert was the author of several papers and reports, and held patents in the antenna field. He was a member of the International Scientific Radio Union, and principal founder of the Inter-Service (Army Navy, Air Force) Antenna Group.

John M. Miller (A'17–F'20) (L), former Navy electronics expert, died on May 18, 1962 in Pompano Beach, Fla. He was widely known for the Miller effect in electronics—the change in the input admittance of a triode value caused by variation of the impedance in the anode circuit.

Born on June 22, 1882 in Hanover, Pa.,

he attended Yale University, where he received the B.A. degree in 1904, the M.A. degree in 1907, and the Ph.D. degree in physics in 1915. From 1907 to 1919, he was a physicist with the National Bureau of Standards. During the period from 1925 to 1936, he was in charge of radio receiver research at the Atwater Kent Manufacturing Co., Philadelphia, Pa., and from 1936 to 1940, he was assistant head of the research laboratory for the RCA Radiotron Co.

From 1923 to 1925, Dr. Miller was associated with the original group at the U. S. Naval Research Laboratory, Washington, D. C. He returned in 1940 as associate superintendent of the Radio Division, and was promoted to the position of Superintendent of Radio Division I in 1945, where he served until his retirement in 1952. During this service, he received several awards for his scientific contributions, among which was the Navy Distinguished Civilian Service Award (1945) for the development of a new flexible frequency cable needed in radio and radar equipment.

Dr. Miller was presented the IRE Medal of Honor in 1953, in recognition of his pioneering contributions to our basic knowledge of electron tube theory, of radio instruments and measurements, and of crystal controlled oscillators. He was a member of several professional groups and was the author of many articles on electronics for scientific journals and Navy publications.

Sixth National Symposium on Engineering Writing and Speech

MAYFLOWER HOTEL, WASHINGTON, D. C., SEPTEMBER 13–14, 1962

The Sixth National Symposium on Engineering Writing and Speech, sponsored by the IRE Professional Group on Engineering Writing and Speech will be held on September 13–14, 1962 at the Mayflower Hotel, Washington, D. C.

The theme of the Symposium is: "EWS—an Art or a Science?" Sixteen papers have been selected and are scheduled for presentation in four consecutive sessions during the two-day meeting. Texts of the technical papers will be published in a Symposium *Proceedings* which will be distributed free to all registrants.

Members of the Symposium Committee include: Chairman: P. J. Martin, Office of the Chief of Naval Operations; Program: J. E. Durkovic, Aeronautical Radio, Inc.; Registration: R. H. Schaaf, Dept. of Defense; Arrangements: T. R. Davis, Technical Scriveners Co.; Publications: J. Carter, RCA; Public Relations: C. De Vore, CREI Atomics; and Finance: J. E. Voyles, Ramo Wooldridge Co.

Advance registration fees (to September 1, 1962) for the Symposium are: $7.00 for IRE and PGEWS members and PGEWS affiliates; $8.00 for advance registration of non-IRE members. Registration at the Symposium will add one dollar to each of the above fees. Further information on registration may be obtained from: R. H. Schaaf, Washington IRE Section, 2029 K St., N.W., Washington 6, D. C.

The program is as follows:

Thursday Morning, September 13
Session I—EWS is an Art

Moderator: *D. C. Ports.*

"The Sound of Good Writing," *G. M. Arnold, Sperry Rand Corp., St. Paul, Minn.*

"Case Against Writer vs Engineer," *E. H. Galinsky, IBM Corp., Owego, N. Y.*

"The New Art," *S. G. Smith, Applied Physics Labs., Johns Hopkins University, Silver Spring, Md.*

"A Moving Finger in the Sand," *G. L. Seielstad, Applied Physics Labs., Johns Hopkins University, Silver Spring, Md.*

Thursday Afternoon
Session II—EWS is a Science

Moderator: *Gladys Montgomery.*

"The Clinical Approach to Creative Speech," *J. C. Connelly, IBM Corp., Owego, N. Y.*

"Technical Writer, the Myth vs the Man," *R. M. D'Aprix, General Electric Co., Utica, N. Y.*

"Economics of EWS Service," *H. N. Hubbs, Glenn L. Martin Co., Denver, Colo.*

"Cost Effectiveness of Several Page Formats," *P. E. T. Jensen, Sylvania Electric Products, Inc., Mountain View, Calif.*

Thursday Evening
Reception and Banquet

Speaker: *Henry Loomis, Director, Voice of America, U. S. Information Agency.*

Friday Morning, September 14
Session III—EWS is Both Art and Science

Moderator: *Phil Klass.*

"Effective Presentation," *R. S. Blicq, Canadian Aviation Electronics Ltd., Winnipeg, Manitoba, Can.*

"EWS—Techniques or Fundamentals?" *A. E. Javitz, Electro-Technology, New York, N. Y.*

"Guide to Winning Proposals," *A. T. Koch, General Electric Co., Syracuse, N. Y.*

"Write It and Read It Right," *W. A. Ternent, General Electric Co., Syracuse, N. Y.*

Friday Afternoon
Session IV—EWS for the Engineer, Writer, Speaker

Moderator: *Paul Martin.*

"How to Not Write a Science Film," *B. E. Strasser, Bell Telephone Labs., New York, N. Y.*

"PERT—A Tool for Subcontract Administration," *A. McHugh, General Electric Co., Syracuse, N. Y.*

"Put the Cart Before the Horse," *H. Gettings, Dynatronics, Inc., Orlando, Fla.*

"A New Recipe for Old Chestnuts," *Dr. Elise Gilmore, Sylvania Electric Products, Inc., Buffalo, N. Y.*

Summary and Adjournment: *Symposium Chairman.*

Tenth Annual Engineering Management Conference

Roosevelt Hotel, New Orleans, La., September 13–14, 1962

The program for the 1962 Engineering Management Conference to be held September 13–14, 1962 at the Roosevelt Hotel, New Orleans, La., has been announced. Sponsoring organizations include the IRE Professional Group on Engineering Management, AIEE, and ASME. The program is as follows:

Thursday, September 13

Session I—The Challenge of the Future

Chairman: *Lloyd Smiley*

"Engineering as a Growing Source of Permanent Wealth," *D. W. Oakley, Vice President, Metal and Thermit Corp., New York, N. Y.*

"The Engineer and the Challenge of Economic Development," *Samuel Lurie, Director, Division of Industrial Development, Department of Economic and Social Affairs, United Nations Headquarters, New York, N. Y.*

"Partners in Progress," *G. C. Rawls, President, Louisiana Power and Light Co., New Orleans, La.*

"The Engineer's Changing Role in Industry," *Morley H. Mathewson, President Elect, AIEE, and Director of Corporate Industrial Engineering and Operations Research, International Minerals and Chemical Corp., Skokie, Ill.*

Thursday Afternoon

Luncheon Speaker: "A Philosophy for Management," *C. H. Shumaker, Southern Methodist University, Dallas, Tex.; President Elect, ASME.*

Session II—Engineering Education

Chairman: *O. J. Sizelove*

"Education for the Complex of Professional Objectives in Engineering," *Newman Hall, Chairman, Dept. of Mechanical Engineering, Yale University, New Haven, Conn.*

"A Forward Look at the Education of Engineers," *W. W. Gagerty, Dean, College of Engineering, University of Texas, Austin, Tex.*

"Objectives and Design of Company Programs For Graduate Education," *D. L. Polenz, Manager, Advanced Systems Development Division Education, IBM, Yorktown Heights, N. Y.*

Friday, September 14

Session III—Managerial Contribution to Engineering Work

Chairman: *Hugh Estes*

"The Motives of Men at Work," *Olaf Sorensen, Manager, Personnel Register and Placement, Engineering Personnel Service, General Electric Co., New York, N. Y.*

"Salary Evaluation of Engineering Positions," *Herbert Hubben, McKinsey and Co., Washington, D. C.*

"Engineering Organization in Transition," *E. J. Tangerman, McGraw-Hill Publishing Co., New York, N. Y.*

Friday Afternoon

Luncheon Speaker: "Latin America – Key to the Future," *Ambassador de Lesseps S. Morrison, U. S. Representative on the Council, Organization of American States.*

Session IV—Contributions by Engineers to Managerial Work

Chairman—*Gardner Reynolds*

"Examples of Computer Usage in Technical Work," *R. R. Johnson, Manager of Engineering, Computer Dept., General Electric Co., Phoenix, Ariz.*

"The Management of a Product Assurance Program," *Landis S. Gephart, Director, Product Assurance, Space Systems Div., Lockheed Missiles and Space Corp., Sunnyvale, Calif.*

Eleventh Annual Joint Industrial Electronics Symposium

Sheraton-Chicago Hotel, Chicago, Ill., September 19–20, 1962

The Eleventh Annual Joint Industrial Electronics Symposium, sponsored by the IRE, AIEE, and Instrument Society of America, will be held at the Sheraton-Chicago Hotel, Chicago, Ill. on September 19–20, 1962. The program of the Symposium is as follows:

Wednesday September 19

Session I—Electro-Mechanical Techniques

Chairman: *Edward A. Roberts, Victor Electronic Systems Co., Chicago, Ill.*

"Low Voltage Percussion Welding," *John Gellatly, Western Electric Co., Chicago, Ill.*

"Versatile Automation," *Harold Johnson, American Machine and Foundry Co., Elk Grove Village, Ill.*

"Future of Numerical Control in Industry," *Dr. Shizuo Hori, Armour Research Foundation, Chicago, Ill.*

"Recent Advances in TWX Mechanization," *Robert E. Stoeffels, Automatic Electric Labs., Inc., Northlake, Ill.*

Wednesday Afternoon

Luncheon Speaker: "Investment Aspects of the Electronics Industry," *Dudley Herr, Vice President, Television Shares Management Corp., Chicago, Ill.*

Session II—Electro-Optical Techniques

Chairman: *Benjamin Griffith, Chairman, Chicago Section IRE; Teletype Corp., Skokie, Ill.*

"Magneto-Optic Positioning," *Dr. Robert Meltzer, Bausch and Lomb, Inc., Rochester, N. Y.*

"Fully Integrated Digital Graphic Processor," *Norman Taylor, Itek Labs., Lexington, Mass.*

"Fiber Optics—A New Tool for Industry," *T. J. Gallagher, Chicago Aerial Industries, Barrington, Ill.*

"Industrial Applications of Lasers," *D. Monteith, Trion Instruments, Inc., Ann Arbor, Mich.*

"Digital Applications of Thermoplastic Recording," *R. G. Reeves, General Electric Co., Schenectady, N. Y.*

Thursday September 20

Session III—Electro-Magnetic Techniques

Chairman: *Joseph Enenbach, Chairman, Chicago Section, AIEE; Illinois Bell Telephone Co., Chicago, Ill.*

"Industrial Applications of Hall Effect Devices," *David Silverman and Kermit Heid, Helipot Division, Beckman Instruments, Fullerton, Calif.*

"Metal Forming with Pulsed-Magnetic Field," *David Brower, General Atomics Division, General Dynamics Corp., San Diego, Calif.*

"Doppler Radar for Cellophane Mill Rolls," *F. Alexander, American Viscose Corp., Marcus-Hook, Pa.*

"Potential Industrial Applications of Magnetohydrodynamics," *Don Marquis, General Electric Co., Schenectady, N. Y.*

Thursday Afternoon

Luncheon Speaker: "Management Decisions in Selecting New Products and Entering New Technical Areas," *Dr. Albert H. Rubenstein, Assoc. Professor, Dept. of Industrial Engineering, Northwestern University.*

Session IV—Electro-Chemical Techniques

Chairman: *John Anagnost, Chairman, Chicago Section, ISA; DeVry Technical Institute, Chicago Ill.*

"Solions, Their Characteristics and Commercial Applications," *Nelson Estes, Tracor, Inc., Austin, Tex.*

"Improved Analytical Technique for Moisture Determination in Non-Newtonian Materials," *John Shaeffer, Consolidated Electrodynamics Corp., Pasadena, Calif.*

"Preliminary Observations on the Effect of Super-Atmospheric Electrolyte Pressures in Electrolytic Metalworking," *Lynn Williams, Anocut Engineering Co., Chicago, Ill.*

"An Energy System for the Future," *H. Jack Allison, Dr. William Hughes, and C. M. Summers, Oklahoma State University, Stillwater, Okla.*

"H_2-O_2 Capillary Fuel Cell System," *H. J. Welch, Allis Chalmers Manufacturing Co., Milwaukee, Wis.*

Industrial Engineering Notes*

Electronic Sales Hit $13.85 Billion

Factory sales of the electronics industry in 1962 are expected to reach a new peak of $13.85 billion, of which almost 60 per cent will go to the U. S. Government, retiring President L. Berkley Davis told EIA members at the annual membership luncheon at the Pick Congress Hotel. He foresaw a substantial rise in Government business this year, due largely to rising sales for space exploration and airport safety controls, and modest gains in consumer and industrial markets. Concluding his second term as EIA President, Mr. Davis said that the electronics industry's "technological advances have continued unabated" with "many promising discoveries in both basic and applied research." Discussing the outlook for the industry, Mr. Davis reported "all signs point to a continuing growth in dollar volume and further penetration into the economy of our country and perhaps the world. Yet the industry of the seventies may well be greatly different from the electronics industry of today," he added. "The electronics manufacturer who keeps abreast of technological progress and adapts to changing markets will not only survive but prosper. Those who stick stubbornly to outworn patterns may well disappear like the buggy whip manufacturer of our grandfather's day." The electronics industry today ranks fifth, or possibly fourth, among manufacturing groups in the United States, the EIA President said.

The Wave of the Future

"The wave of the future" in commercial broadcasting is FM stereo radio and ultra high frequency television, Edward R. Taylor, Chairman of the EIA Consumer Products Division, reported to the annual Convention. "FM stereo radio will provide the entertainment electronics industry with its best business opportunity since television," Mr. Taylor declared. "The future course for UHF-TV is up also," he added, "and the rise over the next 10 years could be significant for the receiver industry. EIA Consumer Products Division members anticipate what can be described as an orderly boom in FM for the next few years. Influencing the course of developments are a number of factors. A very important one, of course, is the high quality of FM stereo sound. Another is the recent move of the FCC partially to freeze AM broadcasting at its present level. The FCC has made it clear that it intends to slow down AM and promote FM. But prior to the Commission freeze announcement, FM had been showing healthy signs of growth. The number of FM stations, for instance, had increased from several hundred a few years ago to about 1100 today. That many Division members anticipate greater demand for UHF equipment than the industry has experienced in many years is indicated in EIA Marketing Services Department figures showing a rise of more than 100 per cent in UHF receiver production in the first quarter of 1962 compared with the same period of last year. While the controversy over all-channel legislation considerably awakened public interest in UHF, other factors influenced UHF receiver output. Not the least of these was educational TV which this month was given its biggest boost in years by enactment of legislation authorizing $22 million in Federal grants. It seems to us that UHF television today is in very much the same position as FM radio was some years ago—at the bottom of its develpment. We believe the future course for UHF is up. The rise over the next 10 years could be very significant for the television receiver industry."

Gain in Electronic Imports and Exports

U. S. exports of electronic equipment and parts during 1961 were valued at more than $635.4 million or nearly 32 per cent above the $483.4 the industry shipped overseas in 1960, Thomas P. Collier, Director of EIA International Department, reported at the annual Convention. "This is a very enviable record for an industry which is faced with substantial competition abroad as well as high tariff and freight rates and a number of other formidable obstacles to its export business," Mr. Collier said. Noting a rise of $50 million in electronic imports into the United States, Mr. Collier commented: "Although exports still are more than three times as large as imports, we are well aware of problems which have been created for some segments of the domestic electronics industry by gains in imports of their products. For instance, 12.4 million radios were imported last year compared with 7.6 million in 1960. Imports of radio tubes went up from 27.6 million in 1960 to 36.6 million in 1961. There also was a substantial gain in the importation of radar equipment, television apparatus and parts, sound equipment, and business dictating machines using a magnetic medium." He pointed out, however, that while imports are a growing problem for certain U. S. electronics manufacturers, many producers are experiencing new exports gains this year. During the first quarter of 1962, he said, exports were $161.9 million, or $15.2

(*Continued on page 24A*)

* The data on which these Notes are based were selected by permission from *Weekly Reports*, issues of May 21, 28 and June 18, 1962, published by the Electronic Industries Association, whose helpfulness is gratefully acknowledged.

ANDREW

HUBLOC ANTENNAS

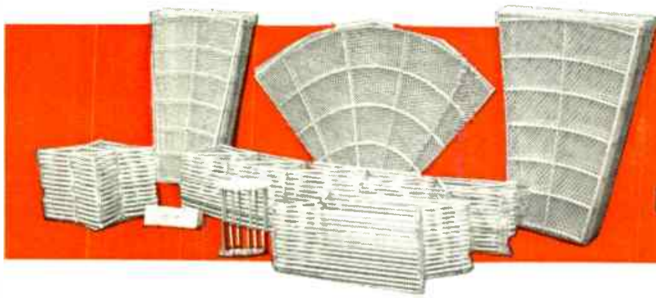

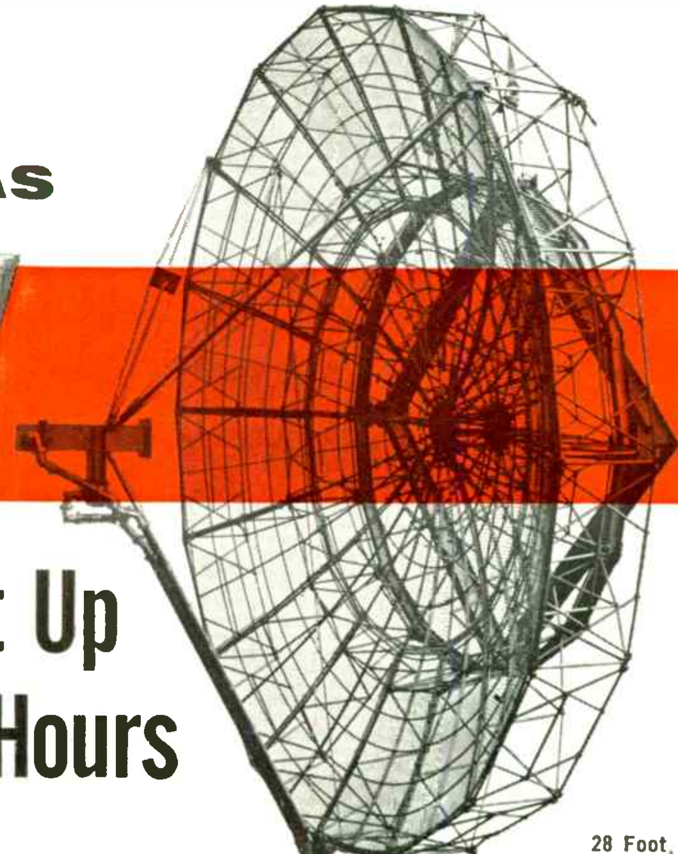

28 Foot Dish Set Up in 12 Man Hours

28 Foot, 1 Gc Antenna

Andrew HUBLOC antennas are setting new standards in performance, cost and ease of assembly. Based on a unique patented structural connection, savings up to 30% are achieved. The model shown is a 28 foot, 1 Gc version. 30, 40 and 60 foot models are currently in production for advanced new communication systems.

Rely on Andrew for all your antenna equipment needs. In addition to the antennas shown and described, Andrew is also the leading producer of Coaxial Cables, Waveguides and accessory items, as well as Microwave, Telemetry and other antennas. Write for catalogs, or call your nearest Andrew office.

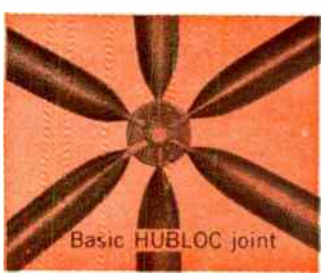
Basic HUBLOC joint


Lightweight subassemblies


Key rib assembly


Backup framework

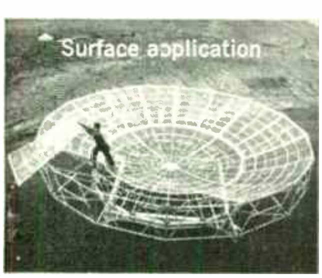
Surface application

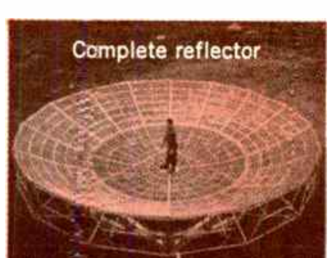
Complete reflector

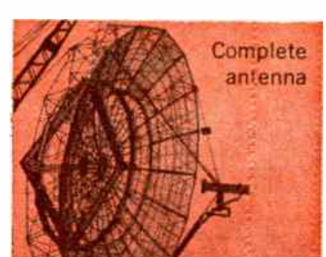
Complete antenna

SPECIFICATIONS

Type Number	26045
Diameter, feet	28
Focal length, feet	10.5
Surface tolerance	±¾″
Windload rating, psf	100
Thrust due to rated windload	44,350
Net weight, pounds	1,250

CHICAGO:	LOS ANGELES:	TORONTO:	NEW YORK:	WASH., D. C.:	BOSTON:
P. O. Box 807	941 E. Marylind	606 Beech Street	P. O. Box 416	P. O. Box 5897	P. O. Box 296
Chicago 42, Illinois	Claremont, Calif.	Whitby, Ontario	Ridgewood, N. J.	Wash. 14, D. C.	Westwood, Mass.
Fieldbrook 9-3300	NAtional 6-3505	MOhawk 8-3348	GIlbert 5-2500	OLiver 4-2540	DAvis 6-6500

Andrew

ANTENNAS • ANTENNA EQUIPMENT • TRANSMISSION LINES

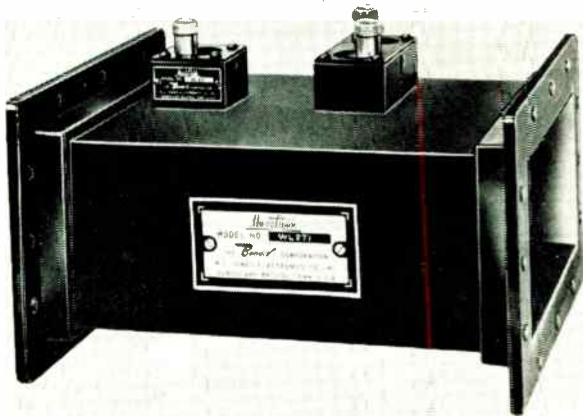

Industrial Engineering Notes

(Continued from page 22A)

million ahead of the like 1961 period. "The American electronics company which gives the overseas customer what he wants, when he wants it, how he wants it and with realistic pricing and credit terms will find the export market to be highly rewarding," Mr. Collier said. "The export record of the industry for 1961 attests to the fact that we are not a too-little and too-late industry."

Governmental and Legislative

President Kennedy last week ordered administrative measures aimed at improving the prestige and environment of scientific and engineering professionals working in federal research and development laboratories in order to meet the competition from industry for their services. The directive to heads of all departments and agencies is part of a White House drive to retain the scientists and engineers the government now has and hire others into federal service through salary increases and pay-raise benefits and improved working conditions. Guidelines for implementing the administrative measures are contained in a special report called "The Competition for Quality" prepared by the Federal Council for Science and Technology, a group of heads of the government's science-oriented agencies. The report recommends that scientists and engineers be given greater participation in decision-making and that government laboratory directors be granted more technical responsibility and administrative authority. Actions are also suggested for improving public information on the "opportunities and challenges" offered by science and technology in government and for developing short and long-term opportunities for scientists and engineers. Other recommendations deal with increasing the flexibility of work schedules, the need for more relocation assistance for transferred employees, and the requirement for government-wide guidelines for official travel and attendance at scientific meetings. The report also recommends sharp increases in government salaries and pay benefits to meet industry levels. The President's legislation to establish the boosts is already before Congress. . . . **The rule prohibiting use of portable FM radios on all United States commercial airplanes and restricting their use on other U. S. civil aircraft has been extended by the Federal Aviation Agency for an additional year to May 25, 1963.** The rule originally was put into effect for a one-year period on May 25, 1961, after tests conducted by the FAA revealed that FM radios adversely affected the operation of very high frequency radio navigation equipment in aircraft. The restriction was issued as a temporary rule pending completion of extended FAA tests. The termination data of the rule has been advanced because final evaluation of the tests has not been completed.

IRE People

Dr. Morton A. Astrahan (S'45–A'50–M'51–SM'57) of International Business Machines Corp., San Jose, has joined the IBM World Trade Corp. in Paris. His new assignment is as senior technical adviser to the manager of WTC Laboratories. He has been with IBM since 1949, and at San Jose since 1956. From 1956 to 1958 he was manager of systems research in the San Jose Research Laboratory.

He received the B.S.E.E. degree from Northwestern University, the M.S.E.E. degree from the California Institute of Technology, and the Ph.D. degree from Northwestern.

He was the first chairman of the IRE Professional Group on Electronic Computers in 1952–1953, chairman of the National Joint Computer Committee from 1956 to 1958, and chairman of the NJCC delegation to Russia in 1959 to observe computer development. He is now chairman of the finance committee of the American Federation of Information Processing Societies.

❖

John W. Ballard (M'60) of Granger Associates, Palo Alto, Calif., has been advanced to the position of director of marketing. He was previously manager of applications engineering. He joined Granger Associates after four years service in the U. S. Navy, as a pilot and as an electronics officer specializing in electronic countermeasures. In the latter specialty he was responsible for ECM system development, modification, testing and operations. During 1959 he developed a complete special-purpose airborne ECM system.

Mr. Ballard received the A.B. and M.S. degrees in electrical engineering from Dartmouth College. He is a member of the Dartmouth Society of Engineers.

❖

The appointment of **Max Krawitz** (A'48–SM'50) as manager of color tube manufacturing for the Electronic Tube Division of Sylvania Electric Products Inc. has been announced. He joined Sylvania in 1947 as a senior engineer assigned to cathode ray and microwave tube development at the company's research laboratories in Bayside, N. Y. In 1950, he was appointed section head in charge of the color tube program. He was transferred to Seneca Falls in 1953 as an engineering manager in the Picture Tube Operations and was in charge of color and monochrome tube design. He was promoted to assistant chief engineer in 1957. In this position, his responsibilities included the engineering, merchandising and manufacturing of electroluminescent devices. Prior to joining Sylvania, he was associated with the Amperex Electronic Corporation, Brooklyn, N. Y., and the Ajax X-Ray Tube Corporation, Staten Island, N. Y.

Mr. Krawitz graduated from the City College of New York with a Bachelor of Science Degree in physics. He also attended Brooklyn Polytechnic Institute. He has published articles on electron optics, cathode ray tubes and electroluminescent devices. He holds several patents on cathode ray tube and electroluminescent device developments.

❖

E. Eugene Ecklund (A'51–SM'53), a marketing executive with wide experience in the development of new products and new product lines, has been named President of Thomas Electronics, Inc., Passaic, N. J. He brings to Thomas more than 20 years' experience in business administration with electronic firms, with special emphasis on the initiation and direction of new product development. His background also includes engineering, sales and manufacturing management.

Most recently associated with ITT Federal Labs. in Clifton, N. J., as a business planning executive, he served as Program Manager of several communications projects, including one of the world's longest tropospheric scatter links. Earlier, in his capacity as sales manager for Allen B. DuMont Labs., Clifton, N. J., he initiated and directed that firm's Automotive Test Equipment program, in which he pioneered the successful acceptance of the oscilloscope as a prime tool in testing internal-combustion engines. While he was managing the Special Instrument Design section for DuMont, the company was awarded a letter of commendation by the Navy for his group's work on an airborne countermeasure analyzer utilizing a specially developed multi-gun cathode ray tube display.

Mr. Ecklund holds a B.E.E. degree

(Continued on page 28A)

IRE People

(Continued from page 26A)

from the University of Minnesota and an M.E.E. from Polytechnic Institute of Brooklyn. He is a senior member of the American Rocket Society, and the author of a number of technical papers as well as three books dealing with electronic servicing.

❖

The appointment of **Dr. Constantine D. J. Generales** (SM'59) as a consultant for RCA, David Sarnoff Research Laboratories, Princeton, N. J., was recently announced. He was formerly an assistant professor of space medicine and coordinator of the Space Medicine Program at New York Medical College, Metropolitan New York Medical Center.

He graduated from Harvard College, and received his medical education at the Universities of Athens, Heidelberg, Paris, Zurich, and Berlin. He holds the degrees of Doctor of Medicine and Doctor of Philosophy, the latter received at the University of Berlin. He has served as a flight surgeon in the Air Force, and has been affiliated with numerous hospitals. In 1960, he traveled with the Space Science group on its visits to Leningrad and Moscow after the International Aeronautical Congress held in Stockholm.

Recently, Dr. Generales was the recipient of an honorary certificate from the Greek government for original research in space science and space medicine. He is a fellow of the New York Academy of Sciences, and a member of many medical and scientific societies, including the American Astronautical Society, American Rocket Society, British Interplanetary Society, and American Medical Association.

❖

Dr. Lawrence J. Giacoletto (S'37–A'42–M'44–SM'48–F'58) was recently elected to the Board of Directors of Thomas and Skinner, Inc., Indianapolis, Ind.

An internationally known expert in the area of semiconductors, he is Professor in the Departments of Electrical Engineering and Engineering Research at Michigan State University, East Lansing, Mich.; he is also President of CoRes Institute. He has formerly been associated with Ford Motor Scientific Lab., R.C.A. Princeton Labs., and the U. S. Army Signal Corps Engineering Labs. In addition to a B.S. in electrical engineering from

(Continued on page 30A)

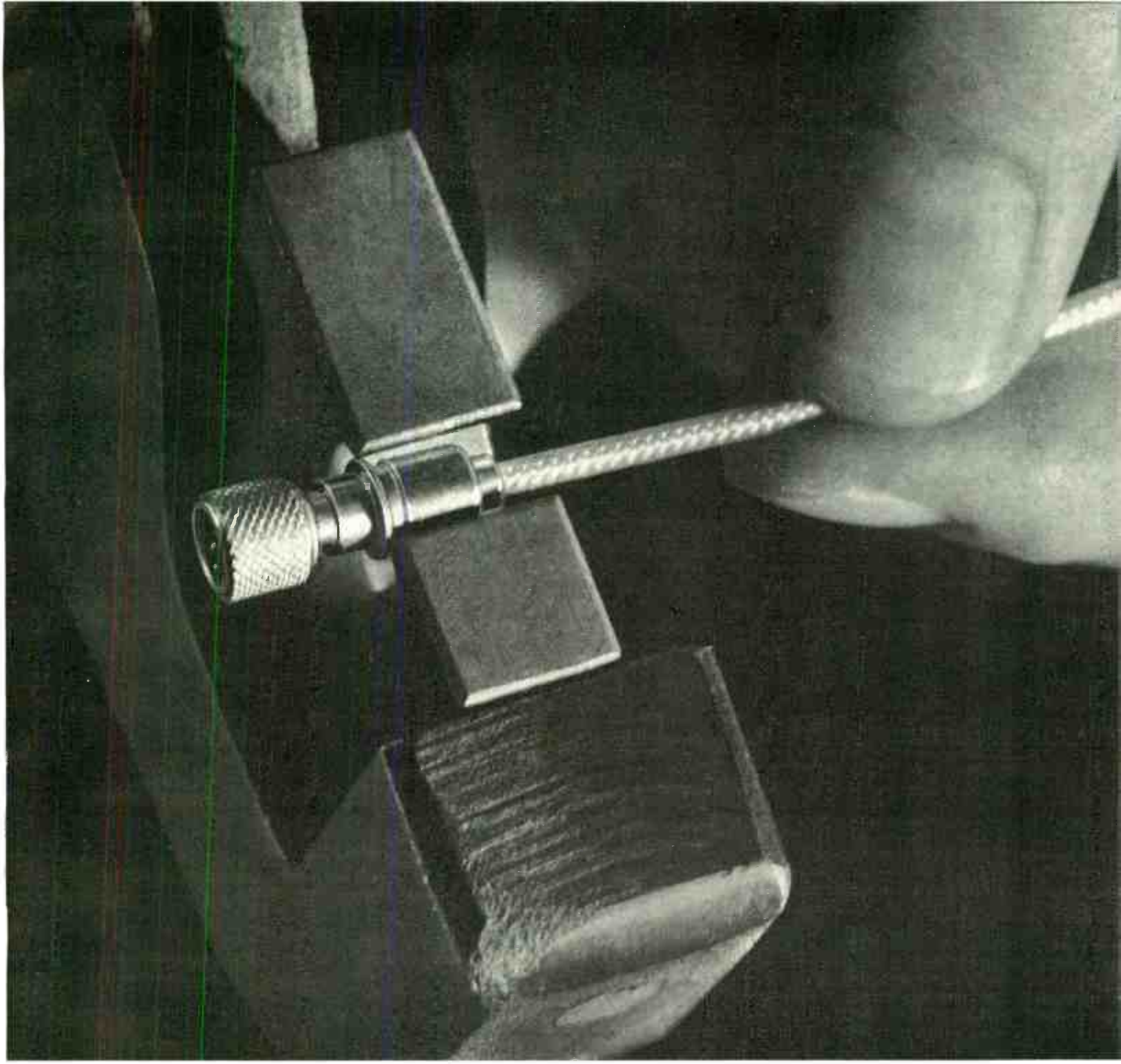

IRE People

(Continued from page 28A)

Rose Polytechnic Institute, he holds graduate degrees in physics and electrical engineering from State University of Iowa and the University of Michigan, respectively. He is a member of several learned societies and a Fellow of the American Association for the Advancement of Science.

❖

Edward S. Hensperger (S'52–A'53–M'56–SM'61) has joined Airtron, a division of Litton Industries, as engineering manager of the company's subsystems section. He joined Airtron after ten years of microwave engineering and sales experience, most recently holding the position of sales manager for the Narda Microwave Corp. His engineering background includes: principal engineer in the Microwave and Missile Guidance Lab. of the W. L. Maxson Corp.; chief engineer for Waveline, Inc., and engineering section head in charge of waveguide and antenna projects with Airtron, Inc., prior to its acquisition by Litton Industries.

Mr. Hensperger was graduated from Rutgers University in 1952 with a B.S. degree in electrical engineering. He has written several technical papers on the design of such microwave components as band-pass filters in waveguide, and multi-hole coupling arrays. He has been secretary of the Northern New Jersey Chapter of the IRE, and is a charter member of Electronic Sales Managers Associates.

❖

Professor C. H. Hoffman (A'54–M'57–SM'59) has accepted an appointment as Associate Professor of Electrical Engineering at the Illinois Institute of Technology, Chicago, where he will continue educational and research activities in computing and control systems. In addition to his duties at I.I.T., he will serve as a consultant to the Armour Research Foundation of the Institute on problems arising in control systems employed in missile and space systems and on problems in industrial control systems.

He was formerly with the Electrical Engineering Department of the University of Notre Dame where he introduced, developed, and taught courses in computers and controls, promoted the acquisition of computing equipment, and recently received a $10,000 National Science Foundation grant for control laboratory equipment. While at Notre Dame, he carried on research work in connection with submarine, missile, and industrial control systems.

Dr. Hoffman has been active in area and national professional societies, being

(Continued on page [illegible])

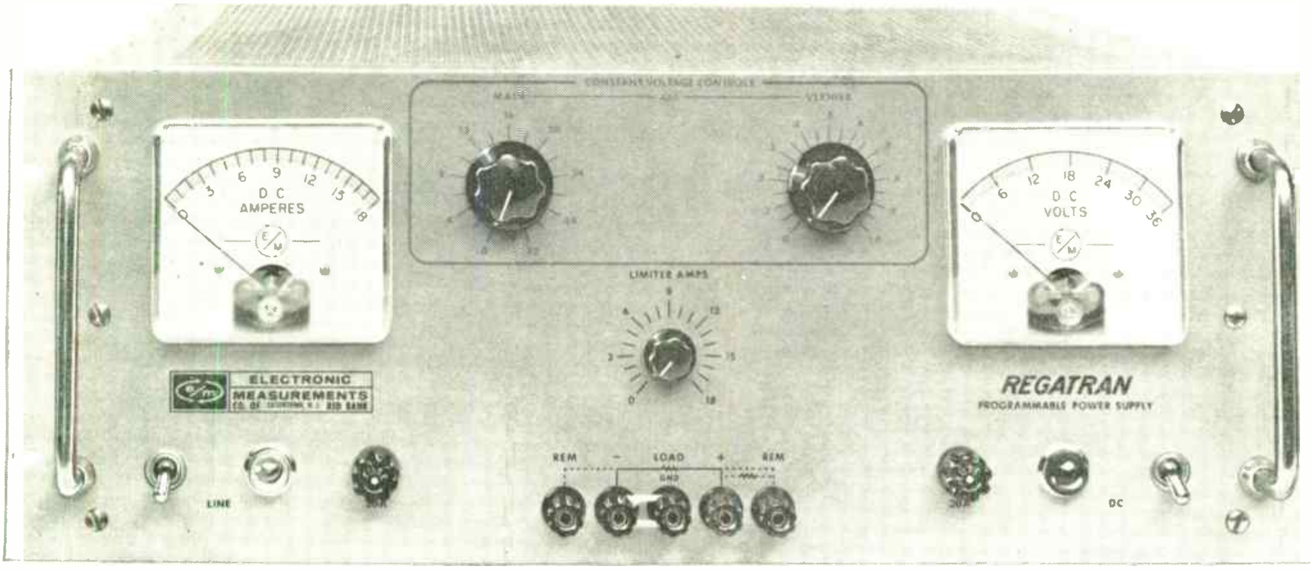

another first from Electronic Measurements

NEW "PV" Series Power Supplies

BRIEF SPECIFICATIONS

BASIC MODEL NO.	DC OUTPUT VOLTS	DC OUTPUT AMPERES	DIMENSIONS IN INCHES PANEL HEIGHT	PANEL WIDTH	DEPTH BEHIND PANEL
PV32-5	0-32	0-5	3½	19	17¼
PV32-10	0-32	0-10	5¼	19	16½
PV32-15	0-32	0-15	7	19	15 7/16
PV32-30	0-32	0-30	8¾	19	16¼
PV36-5	0-36	0-5	3½	19	17½
PV36-10	0-36	0-10	5¼	19	16½
PV36-15	0-36	0-15	7	19	15 7/16
PV36-30	0-36	0-30	8¾	19	16¼
PV60-2.5	0-60	0-2.5	3½	19	17¼
PV60-5	0-60	0-5	5¼	19	16½
PV60-7.5	0-60	0-7.5	7	19	15 7/16
PV60-15	0-60	0-15	8¾	19	16¼

- 0.01% or 2 millivolts regulation
- All solid-state with SCR input
- Programmable over the entire voltage and current range
- Long-line remote sensing
- Continuously variable current limiting
- Slaved series or parallel operation
- Up to 44% reduction in panel height

SEE THEM AT WESCON BOOTHS 3419-3420

request specification sheet 2020

ELECTRONIC MEASUREMENTS
COMPANY OF RED BANK
EATONTOWN • NEW JERSEY

IRE People

(Continued from page 30A)

past Chairman of the IRE South Bend-Mishawaka Section, faculty advisor to the student branch of the society at Notre Dame, a member of the national Education Committee and chairman of the Region V Education Committee in 1960 and 1961. In addition to other society memberships, he has been active in the management of the National Electronics Conference, the leading national symposium on the latest advancements in the electronic art and science, held each year in Chicago. He served as editor of the *Proceedings* in 1958 and 1959 and presently is a member of several committees of the Board of Directors. He will retain his seat on the Board of Directors of the conference through the board action voting him as representative of I.I.T. at the June 9, 1962 meeting of the Board held at McCormick Place, the site of the 1962 Conference in October.

❖

David G. DeHaas (M'57) was promoted to the position of Field Engineer by Neely Enterprises. In this position he will represent the products of Neely's principals. He joined the company in December, 1961.

In 1959, he formed the David G. DeHaas Company, an electronic manufacturers' representatives firm covering San Diego and Imperial Counties. The company was maintained until he became associated with Neely.

Mr. DeHaas received the B.S. degree in applied physics from the University of California, Los Angeles, in 1948. He has served on the Executive Committee of the Aerospace Electrical Society of San Diego, and has been Chairman (1961) and Vice Chairman (1960) of the San Diego Section of the IRE, and Business Manager of the *San Diego IRE Bulletin* since 1957.

❖

Abraham I. Dranetz (S'43–A'48–M'54), former vice president of Gulton Industries, Inc., has established an independent consulting service in the fields of electromechanical instrumentation, underwater sound and electroacoustic technology. Based in Scotch Plains, N. J., the organization will provide technical, marketing and management services for industrial, financial and government groups.

He had been associated with Gulton Industries, Inc., since 1948 and has re-

(Continued on page 34A)

CLARE Stepping Switches

give designers—

- *more levels per switch*
- *more levels in less space*
- *more simplified circuitry*
- *NO synchronization problem*

TYPE 26

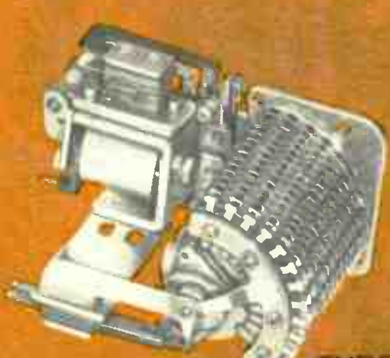

TYPE 211

Type for type, CLARE Stepping Switches provide more levels per switch . . . more levels per inch of height. The 12-level, 52-point, switch shown (CLARE Type 26), for instance, is 4$\frac{11}{16}$ in. high. It has four more 52-point levels than comparable 52-point switches, yet it is but $\frac{13}{16}$ in. higher than a comparable 8-level, 52-point switch. The smaller (Type 211), five-level, 33-point switch provides twice the levels of any comparable 33-point switch.

This greater working capacity per switch . . . and per inch . . . of CLARE Stepping Switches permits more simplified circuitry and avoids synchronization problems which arise when multiple stepping switches are necessary to do what is often a one-switch job with these high-capacity CLARE units.

CLARE Stepping Switches include a full line of spring-driven cam-operated or direct-drive switches with capacities from 10 to 52 points. CLARE engineering will cooperate with designers to develop special switches to meet unique requirements.

For precise stepping switches famous for long life, high capacity and freedom from maintenance

IT HAS TO BE CLARE

Send for DESIGN MANUAL 202A

C. P. Clare & Co., 3101 W. Pratt Blvd., Chicago 45, Illinois. Cable Address: CLARELAY. In Canada: C. P. Clare Canada Ltd., 840 Caledonia Road, Toronto 19, Ontario. In Europe: Europelec, les Clayes-sous-Bois (S. et O.), France

C. P. CLARE & CO.

Relays and related control components

IRE People

(Continued from page 32A)

ceived a number of patents in these fields. From 1944 to 1946 he served with the U. S. Army Signal Corps as a fixed-radio station officer in the Philippine Islands and Japan.

Mr. Dranetz received the B.S. degree in electrical engineering in 1944 from Tufts College and the M.S. degree in electrical engineering in 1948 from the Massachusetts Institute of Technology. He is a member of the Acoustical Society of America, Instrument Society of America, Tau Beta Pi, and American Association for the Advancement of Science.

❖

The appointment of **Marwin R. Johnson** (SM'46) as general manager of the newly formed Military Communications Department within General Electric Company's Defense Electronics Division, was announced recently. He previously was general manager of the Light Military Electronics Department's Arma-

(Continued on page 38A)

Now from LAMBDA new LE SERIES Transistorized Regulated

DESIGNED

TO PERFORM

TO MILITARY

ENVIRONMENT

SPECIFICATIONS

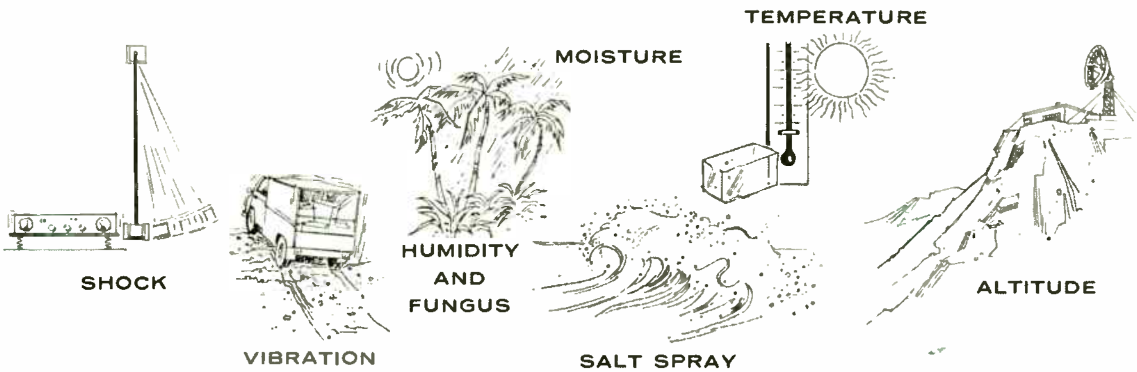

nvironment-engineered...

...at mass-production prices

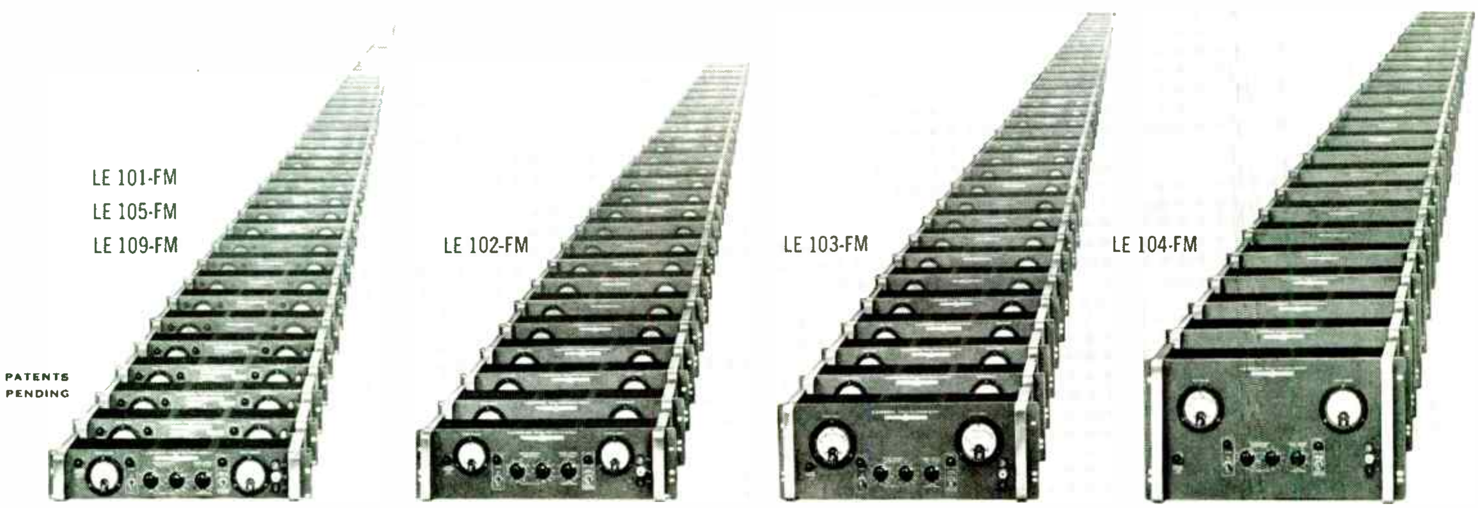

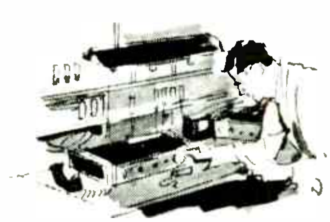

LABORATORY

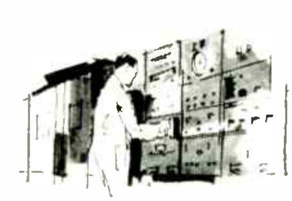

INDUSTRIAL

MILITARY APPLICATIONS

LAMBDA ELECTRONICS CORP.

515 BROAD HOLLOW ROAD • HUNTINGTON, L. I., NEW YORK • 516 MYRTLE 4-4200

Western Regional Office: 230 North Lake Avenue, Pasadena, California • Phone: Code 213, MUrray 1-2544
New England Regional Office: 275 Boston Post Road, Marlboro, Massachusetts • Phone: Code 617, HUntley 5-7122
Middle Atlantic District Office: 515 Broad Hollow Road, Huntington, L. I., New York • Phone: Code 516, MYrtle 4-4200
Southeastern Region: W. A. Brown & Associates, Inc., Engineering Representatives
Orlando, Fla. • Fort Lauderdale, Fla. • Huntsville, Ala. • Alexandria, Va. • Winston-Salem, N. C.

Power Supplies

CONVECTION COOLED

No blowers or filters; maintenance free.

CONSTANT VOLTAGE CONSTANT CURRENT

by automatic switchover.

6 MODELS AVAILABLE

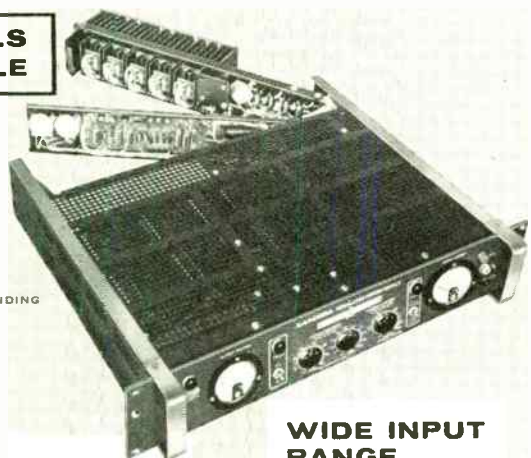

PATENTS PENDING

COMPLETELY PROTECTED

against—short circuit and electrical overload; input line voltage transients; excessive ambient temperatures. No voltage spikes due to "turn-on, turn-off" or power failure.

WIDE INPUT RANGE

Wide input voltage and frequency range —105-135 VAC, 45-66 CPS and 320-480 CPS in two bands selected by switch.

REMOTELY PROGRAMMABLE AND CONTINUOUSLY VARIABLE

Voltage continuously variable over entire range. Programmable over voltage and current range.

OTHER FEATURES

- Adjustable automatic current limiting.
- 0°C to +50°C ambient.
- Grey ripple finish.
- Ruggedized voltmeters and ammeters per MIL-M-10304B on metered models.

5-YEAR GUARANTEE

covers all Lambda Power Supplies including LE Series models

Every Lambda power supply sold since 1953 has been backed by Lambda's 5-year guarantee, which covers workmanship and materials (except for tubes and fuses).

Visit

LAMBDA

at the Wescon Show

Booths 3421-3422.

LE SERIES
CONDENSED TENTATIVE DATA

DC OUTPUT (VOLTAGE REGULATED FOR LINE AND LOAD)[1]

Model	Voltage Range	Current Range	Price[2]
LE101	0-36 VDC	0- 5 Amp	$420
LE102	0-36 VDC	0-10 Amp	525
LE103	0-36 VDC	0-15 Amp	595
LE104	0-36 VDC	0-25 Amp	775
LE105	0-18 VDC	0- 8 Amp	425
LE109	0- 9 VDC	0-10 Amp	430

(1) Current rating applies over entire voltage range.
(2) Prices are for nonmetered models. For models with ruggedized MIL meters add suffix "M" to model number and add $40 to the nonmetered price. For metered models and front panel control add suffix "FM" and add $50 to the nonmetered price.

REGULATED VOLTAGE:

Regulation (line) ...... Less than .05 per cent or 8 millivolts (whichever is greater). For input variations from 105-135 VAC.

Regulation (load) ...... Less than .05 per cent or 8 millivolts (whichever is greater). For load variations from 0 to full load.

Transient Response
(line) .... Output voltage is constant within regulation specifications for any 15 volt line voltage change within 105-135 VAC.
(load) .... Output voltage is constant within 25 MV for load change from 0 to full load or full load to 0 within 50 microseconds of application.

Remote Programming ... 50 ohms/volt constant over entire voltage range.

Ripple and Noise ...... Less than 0:5 millivolt rms either positive or negative terminal grounded.

Temperature Coefficient.. Less than 0.015%/°C.

DC OUTPUT (CURRENT REGULATED FOR LINE AND LOAD)[3]
Current range 10% to 100% rated load for entire voltage range. Full specifications upon request.

AC INPUT .... 105-135 VAC; 45-66 CPS and 320-480 CPS in two bands selected by switch.

OPERATING AMBIENT TEMPERATURE AND DUTY CYCLE.............. Continuous duty at full load 0°C to +50°C (122°F) ambient.

OVERLOAD PROTECTION:
Thermal .... Thermostat, reset by power switch, thermal overload indicator light front panel.

Electrical:
External Overload Protection .... Adjustable, automatic electronic current limiting circuit limits the output current to the preset value upon external overloads, including direct short, thereby providing protection for load as well as power supply. Current limiting settable from 10% to 110% of load.

METERS:.................. Ruggedized voltmeter and ammeter to Mil-M-10304B specifications on metered models.

CONTROLS:
DC Output Controls .. Coarse and fine voltage adjust and current adjust on front panel for models with suffix "FM", all other models same controls are mounted in rear.

PHYSICAL DATA:
Mounting.................... Standard 19" rack mounting.

Size.......		
	LE101, LE105, LE109	3½" H x 19" W x 16" D
	LE102,	5¼" H x 19" W x 16" D
	LE103,	7" H x 19" W x 16½" D
	LE104,	10½" H x 19" W x 16½" D

WRITE FOR COMPLETE CATALOG

IRE People

(Continued from page 14A)

ment and Control Product Section, Johnson City, N. Y.

He joined General Electric's former Radio Transmitter Department, Schenectady, N. Y. in 1932. During his stay there until 1944, he made important contributions in the transmitter field and received several patents. He joined what then was known as the Electronics Division in 1944, specializing in electronics engineering, particularly in airborne equipment. He became manager of engineering in the Light Military Electronics Department, Utica, N. Y. in 1952. During his five years in that position, he fostered a number of new engineering concepts and techniques. He was named manager of the Armament and Control Section of the Light Military Electronics Department, Johnson City, N. Y. in 1957.

Mr. Johnson received the B.S.E.E. degree from the University of Utah. He is a licensed professional engineer of New York State, a member of the American Society of Naval Engineers, Scientific Research Society of America, Society of Advancement of Management, and the Armed Forces Communications and Electronics Association. In 1939 he received the Charles A. Coffin Award, General Electric's highest honor, for work on the first directly calibrated airborne transmitter.

❖

Robert Kent (M'59) has recently been appointed to the Technical Staff of Damon Engineering, Inc. He was previously Manager of the Electronic Systems Engineering Department of Itek Electro-Products where he developed miniature FM communication devices and multiple-channel spectrographic systems.

From June 1952 to December 1960, he was a member of the Research Staff of the M.I.T. Research Laboratory of Electronics. His work there included circuit development in missile guidance and electronically scanned radar systems. He participated in ARPA sponsored study programs concerned with communication satellites and ballistic missile defense. From 1959 to 1960 he led a group investigating satellite techniques for measuring the gravitational red shift postulated by the General Theory of Relativity.

Mr. Kent received the B.S. degree in electrical engineering from the University of Pennsylvania in 1950 and the M.S. degree from M.I.T. in 1952. He is a member of Eta Kappa Nu, Tau Beta Pi, and an Associate of Sigma Xi. He is a co-author of papers on satellite techniques for measurement of the gravitational red shift and closed-loop phase control for electronic scanning.

❖

(Continued on page 124A)

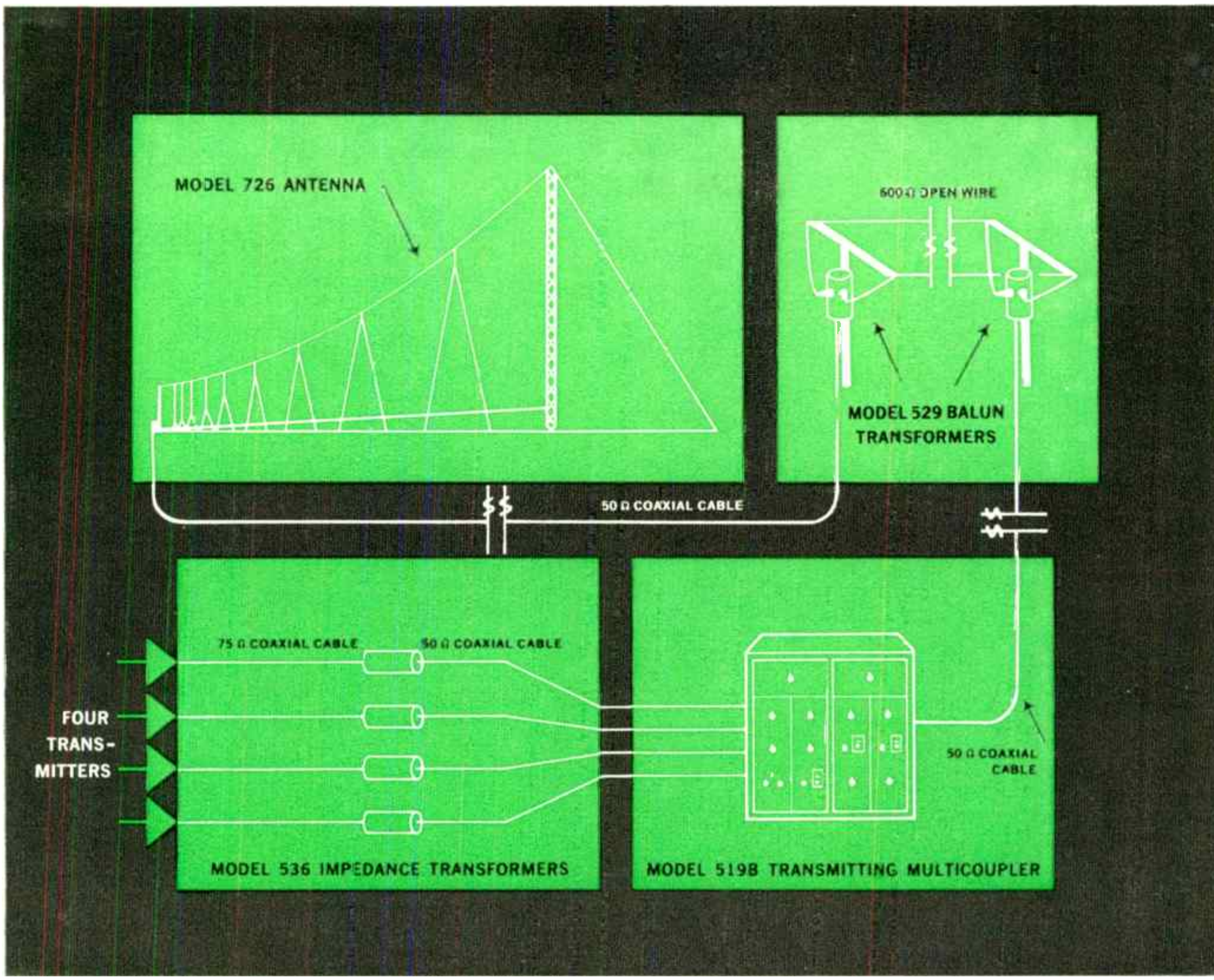

For h-f communications: sensible solutions to practical problems

If you are involved in practical problems of h-f communications, you may want to save this ad. It's a reminder of sensible, proven hardware to increase the *efficiency, flexibility* and *economy* of your operations. For example, in the typical installation shown above, our *Model 726 vertically-polarized log-periodic antenna* provides 10.5 db gain from 2.5 to 32 Mc for long-haul transmission—on a minimum of real estate; the *Model 529 balun transformer* lets you take maximum advantage of both open wire and coaxial transmission lines—with efficiency greater than 97%; the *Model 519B transmitting multicoupler* couples up to four transmitters to one broad-band antenna—saving real estate, installation, and antennas; and the *Model 536 impedance transformer* mates 50-ohm and 75-ohm components or lines at power levels up to 50 kw peak rating—with greater than 99% efficiency. Come to think of it, don't save the ad. Write your name and address at the top and mail it to us. We'll respond with details.

VISIT US AT WESCON BOOTH 2106-2107


Model 536 impedance transformer

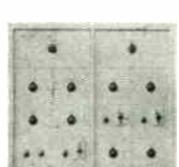
Model 519B multicoupler


Model 529 balun transformer


Model 726 antenna

Granger Associates

an equal opportunity employer

Granger Associates / 974 Commercial Street, Palo Alto, California *DAvenport 1-4175 (area code 415)*

NOW! RECTANGULAR CERAMIC CRT ▸ ILLUMINATED INTERNAL GRATICULE ▸ NEW DUAL-TRACE AND NEW DELAYED SWEEP PLUG-INS

with the Tektronix Type 561A Oscilloscope

The Type 561A employs a unique 5-inch rectangular "ceramic envelope" cathode-ray tube with the following features:

1. Illuminated "no parallax" internal graticule on a high-quality parallel-ground plate-glass face.
2. Controllable graticule lighting, permitting trace photography with the same convenience as provided by external graticules.

Other features of this compact new oscilloscope include: Improved regulated power supplies • Regulated dc heater supply • Z-axis input • 3.5-KV accelerating potential • Amplitude calibrator with 18 steps from 0.2 mv to 100 v • Operation from 105 v to 125 v or 210 v to 250 v, 50 to 400 cps.

A wide range of performance characteristics is provided by available plug-in units—from the simple single-channel 2A60 to the dual-channel 0.4 nsec-risetime 3S76. For example, the two latest additions to this ever-growing family of plug-ins, the 3A1 and 3B3, provide high-sensitivity wide-band dual-trace operation combined with calibrated sweep delay.

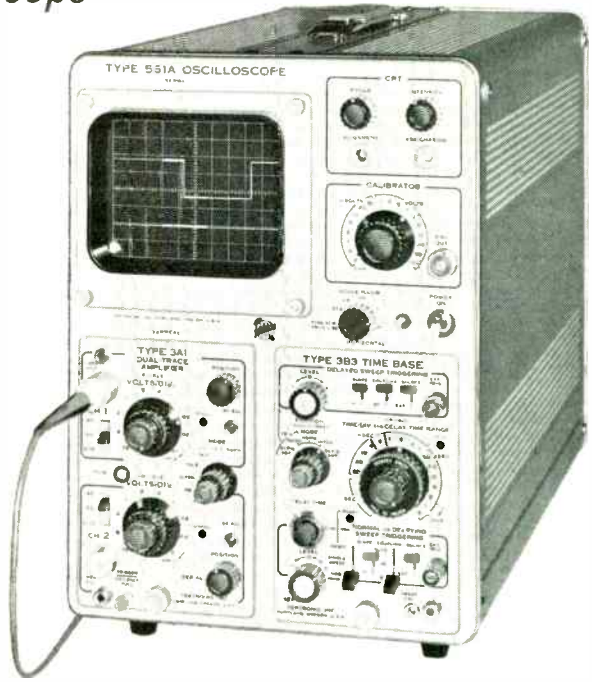

Type 3A1 Dual-Trace Amplifier Unit

Passband—dc to 10 Mc at 3-db down.

Displays—single trace, dual trace, or algebraic addition. 6-cm linear scan.

Sensitivity—10 mv/cm to 10 v/cm in 10 calibrated steps, 1-2-5 sequence. Variable sensitivity between steps.

No Signal delay.

Type 3B3 Time-Base Unit

Normal and Delayed Sweeps—0.5 μsec/cm to 1 sec/cm in 20 calibrated steps, 1-2-5 sequence. Variable adjustment between steps. 5X Magnifier extends calibrated range to 0.1 μsec/cm.

Precision Delay Interval—0.5 microseconds to 10 seconds.

Triggering—Flexible Tektronix triggering, plus single-sweep operation for normal sweep. Triggered operation to above 10 Mc.

Type 3B1 Same as 3B3 except has uncalibrated delay and does not have single sweep feature.

TYPE 561A OSCILLOSCOPE (without plug-ins)	$470
TYPE 3A1 DUAL-TRACE AMPLIFIER UNIT	$410
TYPE 3B1 TIME-BASE UNIT	$475
TYPE 3B3 TIME-BASE UNIT	$525

U. S. Sales Prices, f.o.b. Beaverton, Oregon

For more information on a Type 561A Oscilloscope and plug-in combinations, please call your Tektronix Field Engineer.

OTHER 2-SERIES AND 3-SERIES PLUG-INS AVAILABLE

AMPLIFIER UNITS TYPE	PASSBAND (3-db down)	SENSITIVITY	PRICE
2A60	dc—1 Mc.	50 mv/cm—50 v/cm 4 decade steps with variable control.	$105
2A63—Differential (50:1 rejection ratio)	dc—300 kc.	1 mv/cm—20 v/cm 1-2-5 sequence with variable control.	$130
3A72—Dual Trace (Identical Channels)	dc—650 kc. (each channel).	10 mv/cm—20 v/cm, 1-2-5 sequence, with variable control.	$250
3A74—Four Trace	dc—2 Mc (each channel).	20 mv/cm—10 v/cm, 1-2-5 sequence, with variable control.	$550
3A75—Wide Band	dc—4 Mc.	50 mv/cm—20 v/cm, 1-2-5 sequence, with variable control.	$175
3S76—Dual Trace Sampling (for use with 3T77)	equivalent dc-to-875 Mc. (0.4-nsec risetime)	2 mv/cm—200 mv/cm, 1-2-5 sequence, with variable control.	$1100

TIME-BASE UNITS TYPE	SWEEP FEATURES	TRIGGERING	PRICE
2B67	1 μsec/cm to 5 sec/cm 1-2-5 sequence, variable between rates. 5X Magnifier. Single Sweep.	Internal, External, Line; Amplitude-Level Selection; AC or DC-Coupling; Automatic or Free-Run; ± Slope.	$175
3T77 Sampling Sweep (for use with 3S76)	Equivalent to 0.2 nsec/cm to 10 μsec/cm, 1-2-5 sequence, variable between rates. 10X Magnifier.	Internal or External, ± Slope.	$650

Tektronix, Inc. *P. O. BOX 500 · BEAVERTON, OREGON / Mitchell 4-0161 · TWX—BEAV 311 · Cable: TEKTRONIX*

TEKTRONIX FIELD OFFICES are located in principal cities throughout the United States. Please consult your Telephone Directory.

TEKTRONIX CANADA LTD: Montreal, Quebec • Toronto (Willowdale) Ontario

ENGINEERING REPRESENTATIVES: Kentron Hawaii Ltd., Honolulu, Hawaii. Tektronix is represented in twenty-five overseas countries by qualified engineering organizations.

European and African countries, the countries of Lebanon and Turkey, please contact TEKTRONIX INTERNATIONAL A.G., Terrassenweg 1A, Zug, Switzerland, for the name of your local engineering representative.

Other Overseas areas, please write or cable directly to Tektronix, Inc., International Marketing Department, P. O. Box 500, Beaverton, Oregon, U.S.A. Cable: TEKTRONIX.

SEE THIS TEKTRONIX OSCILLOSCOPE AT WESCON—BOOTHS 751-752-753-754.

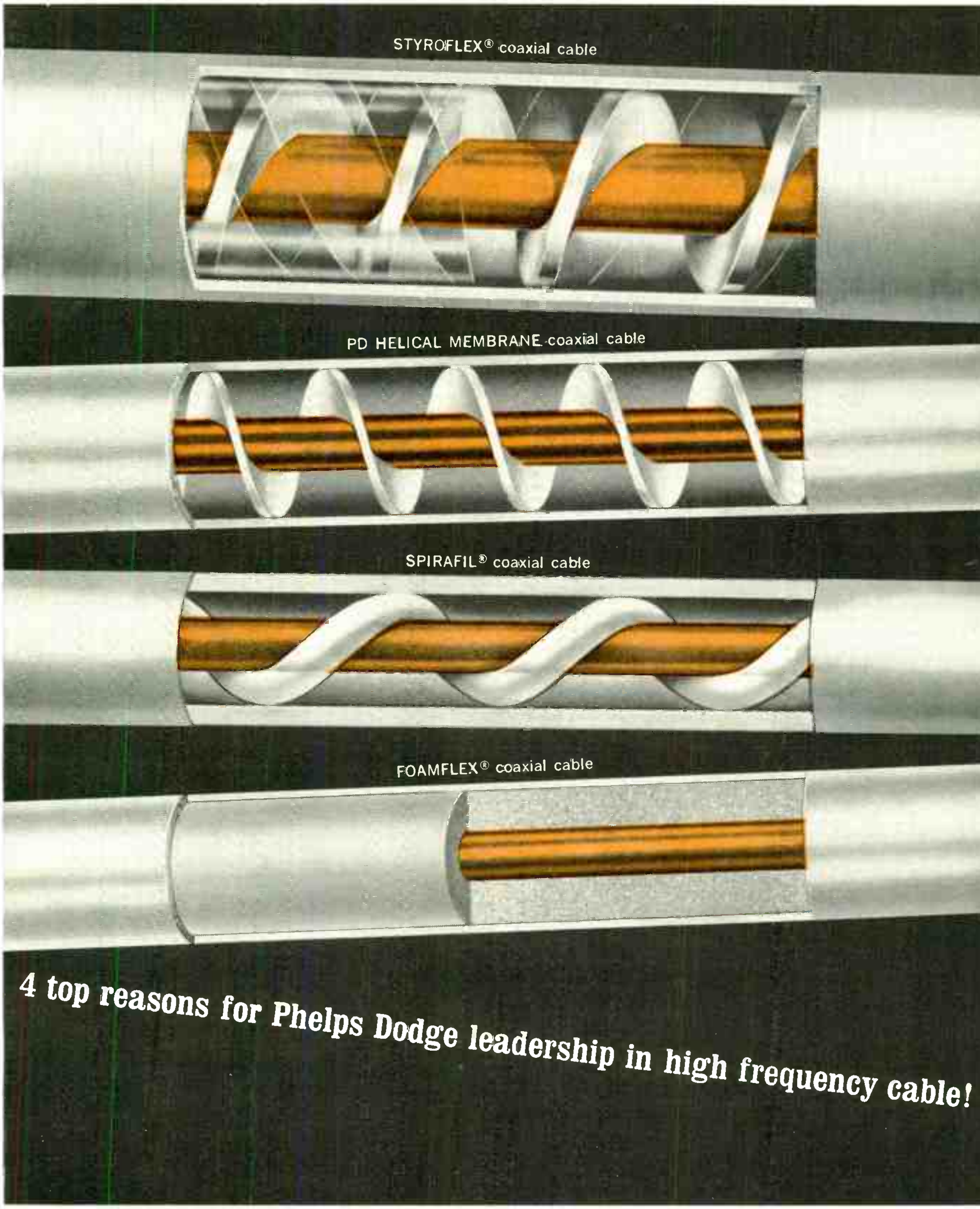

These semi-flexible, air dielectric coaxial cables have demonstrated their superiority as electronic transmission links in a number of advanced communications projects in space research, national defense and industry.

☐ No radiation ☐ Low attenuation ☐ Excellent frequency response ☐ Uniform electrical properties over wide temperature variations ☐ Unlimited operating life ☐ Continuous 1000-foot lengths

Complete cable systems including attachments and connectors are available. These cables are fabricated by Phelps Dodge Copper Products Corporation at Yonkers, N. Y.

PHELPS DODGE ELECTRONIC PRODUCTS
CORPORATION • 300 PARK AVENUE, NEW YORK 22, N.Y.

IRE People

(Continued from page 38A)

Dr. Peter D. Kennedy (S'48–A'51–M'56–SM'59) has been appointed project engineer on research activity in the Antenna Department of Granger Associates.

He came from Lockheed Missiles and Space Co., where, as a section head, he worked on propagation theory, communication and tracking systems and antenna feasibility studies. Earlier he was a supervisor in the Antenna Lab. of Ohio State University Research Foundation and an electrical engineer with the U. S. Army Frankfort Arsenal at Philadelphia and with Westinghouse Electric Co. at Baltimore.

Dr. Kennedy received the B.S. degree from Newark College of Engineering, the M.S. degree from Purdue University and the Ph.D. degree from Ohio State University. He is a member of Tau Beta Pi, Eta Kappa Nu and Sigma Xi.

(Continued on page 46A)

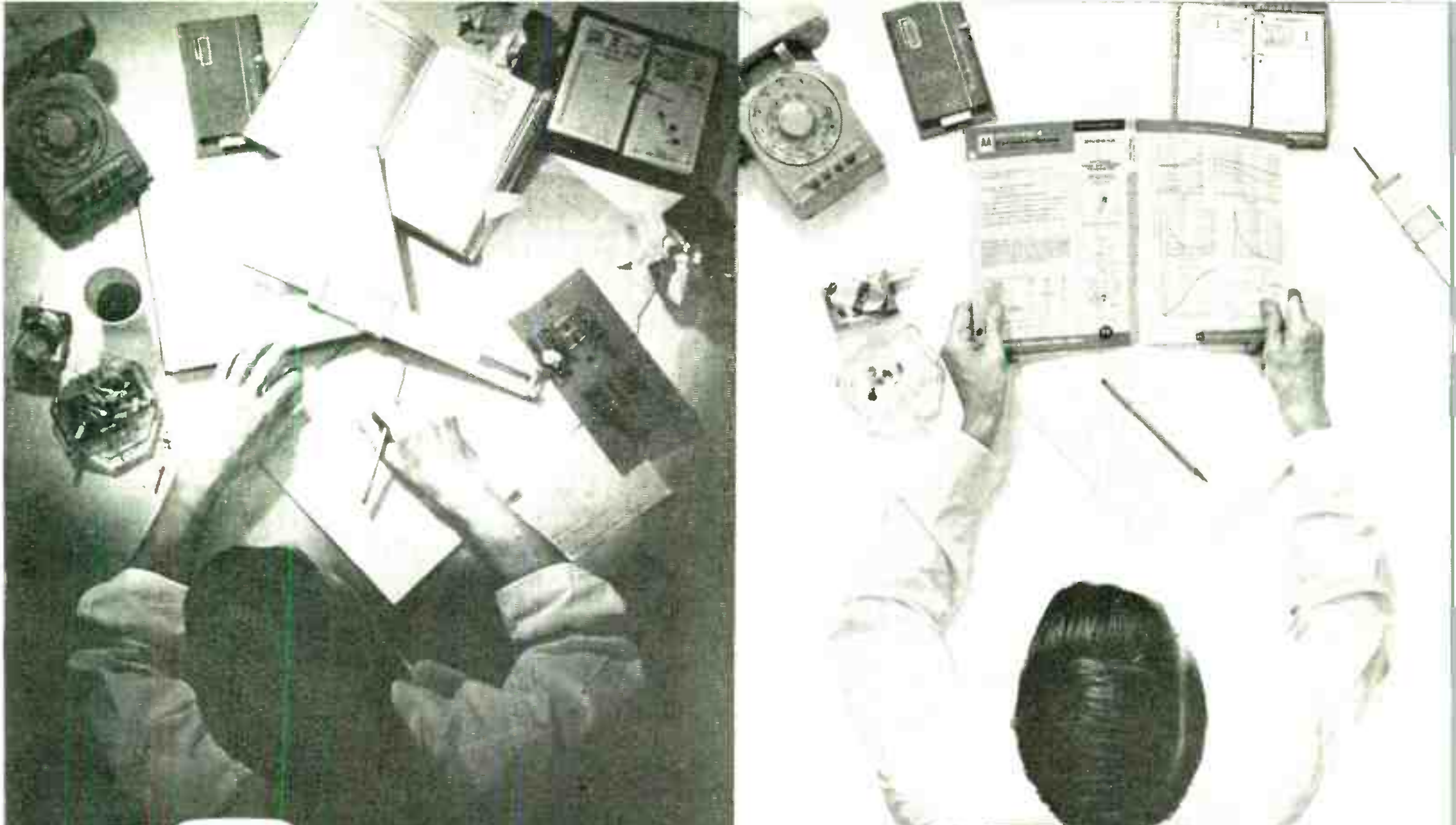

8 hrs.... or 15 min

Some engineers now design high-frequency switching circuits by:

1. Estimating transistor electrical characteristics at the design operating points rather than at points specified on the manufacturer's data sheet.
2. Allowing for variation in specification limits of devices due to changes in current and voltage.
3. Allowing for parameter variations resulting from changes in temperature.
4. Throwing in a safety factor based upon educated estimates.
5. Breadboarding circuits with limit transistors and checking operation at temperature extremes. Then, when necessary, due to unsatisfactory performance of breadboarded circuits by:
   - Trimming safety margins
   - Refining circuit design
   - Writing specs for special devices
   - Selecting specials at Incoming Inspection

Making these estimates and calculations and doing expensive breadboard testing and analysis wastes valuable time and frequently results in marginal or over-designed circuits...

But not YOU if you use Motorola's new 2N964A Designer's Data Sheet

1. It contains limit curves that fully define "on" conditions from 2 to 100 mAdc (h_{FE}, $V_{CE(SAT)}$, $V_{BE(SAT)}$); "off" conditions (leakage, latchup); and "transient" conditions (total charge, rise and fall time constants).
2. Sufficient curves are given on important design parameters to permit easy construction of any other curve desired.
3. Curves define necessary min-max limits.
4. Curves are given for various junction temperatures.
5. Safety factors are included in the curves.
6. Breadboard is used merely to check circuit analysis.
7. The 8-page Motorola "Designer's Data Sheet" contains typical calculations showing step-by-step how you use this complete design information for switching circuits.

In fifteen minutes you'll learn more about this transistor from the Designer's Data Sheet than you could in days of testing. Tightly specified in characteristics, but designed for a broad range of application, the Motorola 2N964A transistor is the ideal high frequency switch for most of your requirements.

For a copy of the Motorola 2N964A Designer's Data Sheet, or for more information, write or call your local Motorola Semiconductor Engineering Representative.

MOTOROLA Semiconductor Products Inc.

A SUBSIDIARY OF MOTOROLA INC

5005 EAST McDOWELL ROAD • PHOENIX 8, ARIZONA

1986

For further information visit **WESCON Booth 302-303.**

IRE People

(Continued from page 12A)

Commander Paul H. Lee, USNR (A'42–M'48–SM'52) has been appointed by the Director of Naval Communications as Officer-in-Charge of the National Naval Reserve Network. This position involves supervision of on-the-air training of naval communications personnel for service in time of mobilization.

In June of this year he resigned from the position of Manager of Research and Development for Communications in the Bureau of Ships, to join the consulting engineering staff of Booz-Allen Applied Research, Bethesda, Md. He had previously served as Deputy Chief, Technical Division, at the "Voice of America," and has been a member of that agency's Science Advisory Board since 1959, concerned with the planning and installation of high-power transmitter plants and receiving facilities. From 1954 to 1956 he was Assistant Chief Engineer of INTELEC, Caracas, Venezuela, where he supervised the planning and construction of communications facilities for the Venezuelan government. His civilian work also included positions as Chief Engineer of WNDR, Syracuse; WHOM, New York; and WWNY, Watertown, N. Y.

In active naval service during World War II, he was Radio Design Officer in the Bureau of Ships; Electronics Inspection Officer at Inspector of Naval Materiel, New York; and had special duty involving test and evaluation of communications equipment aboard the USS *New York*. From 1948 to 1954 he held communications and electronics engineering billets at U. S. Naval Operating Base, Trinidad, BWI; Charleston Naval Shipyard; and the Office of Director of Naval Communications. For three years he was Instructor in Naval Electronics and Advanced Guided Missiles at Naval Reserve Officers' School 5-6, Washington, D. C. With over 24 years' Naval Reserve service, his service career began as a Radioman 3rd Class, and he has been an active radio amateur since 1931, having written over 20 technical articles for amateur radio journals. His present call letters are W3JHR, known the world over.

Commander Lee received the B.S.E.E. degree (*cum laude*) from Syracuse University. He is a member of the American Society of Naval Engineers, the National Society of Professional Engineers, the Veteran Wireless Operators' Association, and the Armed Forces Communications and Electronics Association. He has been a Registered Professional Engineer in the District of Columbia since 1954, and as such has served as consultant for several radio and television stations and in presentations to the Federal Communications Commission.

(Continued on page 121A)

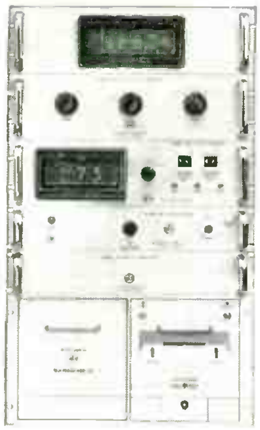

For Instrumentation

In these digital voltmeters, designed to satisfy critical standards for missile work, Non-Linear Systems, Inc., uses about 1,000 A-B hot molded resistors in each instrument.

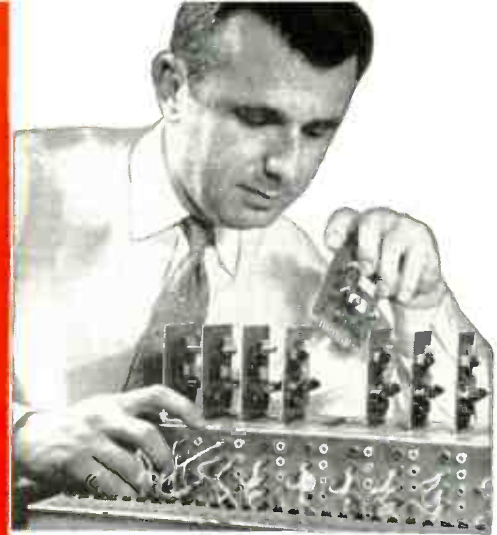

For Research

In experiments at Bell Telephone Laboratories, A-B hot molded resistors are used in artificial electronic nerve cells, designed to study information processing in nervous systems.

No Question—

Allen-Bradley are a "Must" for

Shown Actual Size

For Ground Exploration

At Schlumberger's Research Center, hundreds of thousands of A-B hot molded resistors are assembled into interchangeable grids. These grids are used in a variety of networks to simulate ground formation characteristics.

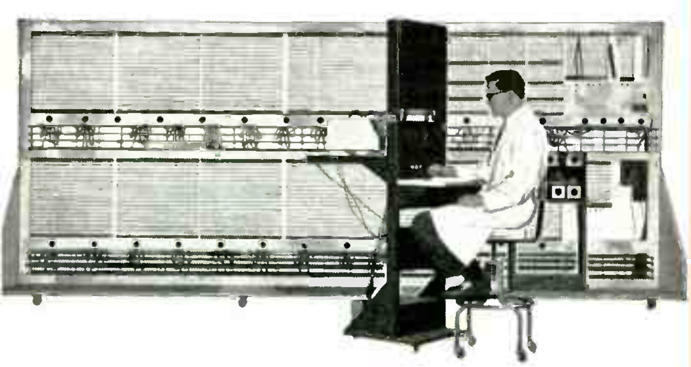

For Product Improvement

To miniaturize the circuitry in their new electronic timepiece, without sacrificing reliability, Accutron designers chose the smallest of A-B standard hot molded resistors—which are exactly as reliable as the higher rated resistors.

DRAWING OF ACCUTRON SHOWS BASIC MECHANISM

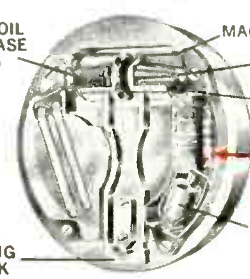

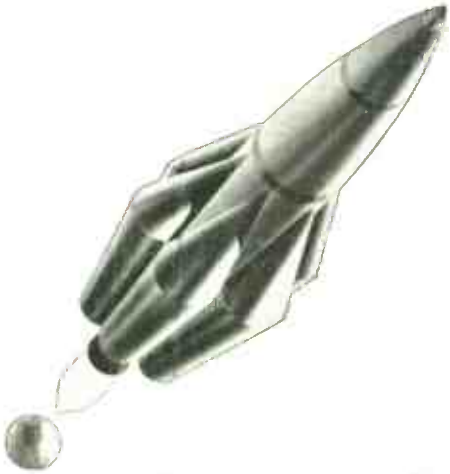

For Space Exploration

Allen-Bradley hot molded resistors have proved their complete reliability in the environmental extremes of shock and vibration so common in missile work.

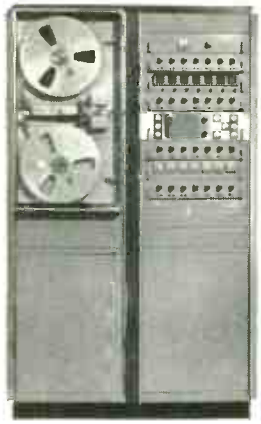

For Data Recording

For meeting the critical requirements of the highly sophisticated circuits in their advanced recorder/reproducer. Ampex engineers could take no chances—they used Allen-Bradley hot molded resistors.

SEE US AT THE WESCON SHOW — BOOTHS 405-6-7-8

Hot Molded Resistors
Critical Applications

Allen-Bradley hot molded resistors—for more than 30 years—have proved their complete reliability and superior performance in all types of circuits

All over the world you'll find Allen-Bradley fixed resistors bringing reliability and superior performance to all types of critical circuits. The exclusive hot molding process—developed and perfected by A-B—assures such consistent uniformity from resistor to resistor that performance can be accurately predicted over long periods of time. Where Allen-Bradley hot molded resistors are used, "catastrophic resistor failure" is unknown. With their conservative ratings and stable characteristics, Allen-Bradley hot molded resistors will assure resistor dependability in *your* equipment—and they cost no more than ordinary resistors.

For complete details please write for Publication 6024—it also includes information about other A-B *quality* electronic components.

Allen-Bradley Co., 114 W. Greenfield Ave., Milwaukee 4, Wis.
In Canada: Allen-Bradley Canada Ltd., Galt, Ontario

ALLEN-BRADLEY

Quality Electronic Components

NEWS New Products

These manufacturers have invited PROCEEDINGS readers to write for literature and further technical information. Please mention your IRE affiliation.

Microwave Diplexer

A new line of microwave diplexers has been announced by **the Special Products Div., I-T-E Circuit Breaker Co.,** 1900 Hamilton St., Philadelphia 30, Pa.

Available over the standard waveguide range WR 430 through WR 2300, the diplexers are fixed tuned at the factory.

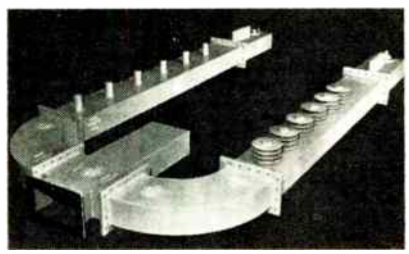

Shown here is a WR 975 diplexer which is operable in the 0.750 to 1.120 gc frequency band. Minimum separation between receive and transmit frequencies is eight percent of the higher frequency and each pass band is 8 mc wide. A minimum of 120 db isolation is guaranteed and the VSWR is less than 1.1:1. Diplexers to these specifications can be delivered immediately.

Very prompt delivery is also available on similar units, to varying specifications to meet customers' requirements.

Additional information is available on request to the firm.

Frequency Meter X Band

Budd-Stanley Co., Inc., 175 Eileen Way, Syosset, N. Y., announces the availability of its Model X1301A Precision Direct Reading Frequency Meter covering the range from 8.2 to 12.4 gc.

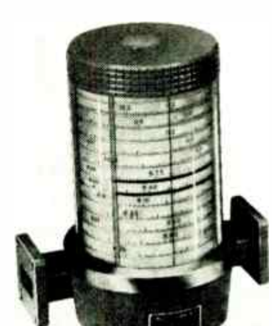

This meter uses a TE_{111} resonant cavity coupled to WR-90 waveguide with a dip of approximately 1 db in the transmitted power at resonance. The frequency can be read directly from the scale with an overall accuracy of .08%.

The high Q cavity is tuned by means of a choke plunger and no sliding contacts are used. A precision lead screw spring loaded to prevent backlash provides a resetability of 0.01%. The instrument is finished in fine wrinkle baked grey enamel with standard X Band cover flanges.

The price of this unit is $157.50 and delivery is immediate from stock.

Storage Register

ARA, Inc., 4130 Kensington Ave., Kensington, Md., announces a new low cost 10 line input Decimal Storage Register, Model No. 234, which includes the write and read gating. It is used with electronic counters in applications that require a buffer storage to read out from, while the counter system continues to operate without interruption during the readout period.

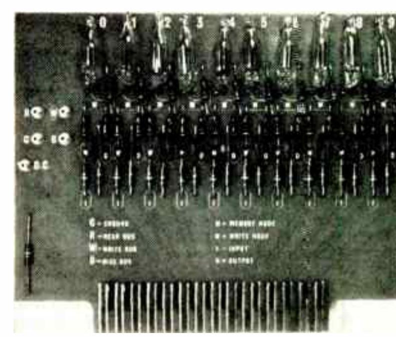

Each storage register contains the memory cells and their associated write and read gating mounted on a 4"×5" printed circuit card. The card layout is such that it may employ Elco pins and connectors.

It employs a specially processed gas diode in each of the ten memory cells and in operation only one cell can be "On" to the exclusion of the other nine. The use of gas diodes also provides a visual indication of the number stored.

The input is typically from a ten position device such as a glow transfer gas counter tube, beam switching vacuum counter tube or Nixie display tube. In the writing operation *no* "memory clear" function is required.

The readout operation is high speed, non-destructive and can be furnished in a number of codes to meet the user's requirements. It reads out to IBM or other typical types of sequential entry equipment.

The Storage Register cards can be simply interconnected by back board wiring to form storage banks for several hundred decimal digits. A Sequential Magnetic Core Switch with Driver for scanning a bank of Model 234 Storage Registers is available as optional equipment.

Available from stock. Price approximately $30.00 each, FOB Kensington, Md.

2N996

SILICON PLANAR EPITAXIAL PNP for HIGH SPEED, HIGH CURRENT LOGIC

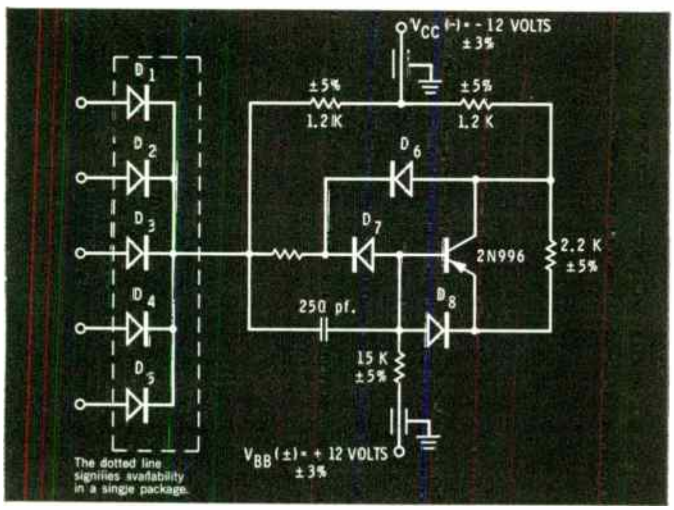

FAN OUT MAXIMUM = 5; TYPICAL PROPAGATION DELAY = 15 nSec.
D_1 through D_8 : All FD6002.

- 60 mA High Current Operation
- 15 nSec Typical Propagation Delay
- 200° C Maximum Junction Temperature
- Direct Replacement for Many Germanium Transistors

The advantages of the Silicon Planar construction are now available in a wide variety of direct replacements for germanium. In addition, the diode gate now is available in a single package TO-5 type can (special product FSP-463) for miniaturized packaging.

FD-6002*

V_F	@ $I_F = 100$ mA	1 V Max.
I_R	@ $V_R = 25$ V	100 mμA Max.
t_{rr}	@ $I_F = I_R$ recover to 10% of I_F for all I_F from 10 mA to 200 mA	4 nSec Max.

2N996*

BV_{CBO}	@ $I_C = 10\ \mu$A	15.0 V Min.
h_{fe}	@ f = 100 mc, $I_C = 10$ mA	2.3 typical
V_{CE}(sat)	@ $I_C = 60$ mA, $I_B = 2$ mA	0.3 V Max.

*OFF-THE-SHELF FROM DISTRIBUTORS

WESCON BOOTHS
2129-2131

FAIRCHILD SEMICONDUCTOR
545 WHISMAN ROAD, MOUNTAIN VIEW, CALIF. • YORKSHIRE 8-8161 • TWX: MN VW CAL 853
A DIVISION OF FAIRCHILD CAMERA AND INSTRUMENT CORPORATION

Membership

The following transfers and admissions have been approved and are now effective:

Transfer to Senior Member

Ackley, E. H., Syracuse, N. Y.
Anderson, C. T., Syracuse, N. Y.
Anthony, I. B., Oradell, N. J.
Bloom, G. M., Plainview, L. I., N. Y.
Brown, D. J., Dover, N. J.
Cassedy, E. S., Jr., Brooklyn, N. Y.
Ceccanti, L. P., St. Albans, N. Y.
Chomet, M., East Northport, L. I., N. Y.
Craddock, G. L., Montgomery, Ala.
Creusere, M. C., China Lake, Calif.
Dickson, F. H., Fair Haven, N. J.
Dutton, F. L., Sr., Greenwich, Conn.
Fortin, R. J., Newport, R. I.
Henry, W. E., Albuquerque, N. M.
Holmes, W. R., Coronado, Calif.
Holub, A. J., Santa Ana, Calif.
Houseman, E. O., Jr., Orlando, Fla.
Jansen, J. J., Topsfield, Mass.
Lanford, W. E., Winston Salem, N. C.
Marshall, F. M., San Rafael, Calif.
McFarland, R. T., Winston Salem, N. C.
Mita, S., Tokyo, Japan
Parrott, J. E., Seattle, Wash.
Pereda, E. F., Albuquerque, N. M.
Pogust, F. B., Oyster Bay, L. I., N. Y.
Roake, W. C., Great Neck, L. I., N. Y.
Robinson, H. L., Kew Gardens, L. I., N. Y.
Rose, W., Los Angeles, Calif.
Ryesky, A., Plymouth Meeting, Pa.
Schreitmueller, R. F., Garden City Park, L. I., N. Y.
Tressa, F. J., Deer Park, L. I., N. Y.
Unger, D. M., Winchester, Mass.
Wade, O., San Diego, Calif.
Weber, D. C., Jacksonville, Fla.
Wilson, W. H., Locust Valley, N. Y.
Yonker, F. H., State College, Pa.

Admission to Senior Member

Akers, S. B., Jr., Syracuse, N. Y.
Bryant, M. O., Harlow, Essex, England
Carlson, M. W., Davenport, Iowa
Evans, R. O., Salt Lake City, Utah
Flint, C. W., Fort Monmouth, N. J.
Gillanders, B. W., Sacramento, Calif.
Hall, B. C., Fort Worth, Tex.
Hanson, O. W., Bountiful, Utah
Hart, S. V., San Francisco, Calif.
Hauri, E. R., Bern, Switzerland
Hecker, K. J., Riverside, Calif.
Hill, W. J., Framingham, Mass.
Inniss, C. F., Camarillo, Calif.
Kaye, R. L., Waltham, Mass.
Kramer, B. A., North Caldwell, N. J.
LeVine, B. A., Orlando, Fla.
Longton, A. C., North Andover, Mass.
Lundholm, J. G., Jr., Lynnfield, Mass.
Ma, J., Algonquin, Ill.
Newby, N. D., Leonia, N. J.
Odle, J. W., Lexington, Mass.
Olivier, R. P., Versailles, France
Russell, J. E., Tulsa, Okla.
Seidl, M. G., Bellevue, Wash.
Sekimoto, T., Kawasaki, Japan
Shuffler, B. B., Fort Worth, Tex.
Smith, F. B., Williamsburg, Va.
Sponsler, G. C., III, Bethesda, Md.
Sucher, M., Levittown, L. I., N. Y.
Swensen, N. E., North Hollywood, Calif.
Tabor, N. E., Sunnyvale, Calif.
Tillwick, F. H., Marlton, N. J.
Touger, M. L., Camden, N. J.
Van Blerkom, R., Arlington, Va.
Walker, N. C., San Diego, Calif.
Weatherspoon, G., Culver City, Calif.
Weber, H. E., Meilen, Switzerland
Welsh, A. Y., Framingham, Mass.
Wheeler, J. W., Greensboro, N. C.
Williams, K. A., Marshfield, Mass.
Young, J. M., Austin, Tex.
Zink, H. D., Jr., Silver Spring, Md.

Transfer to Member

Alexander, L. D., North Palm Beach, Fla.
Barghausen, A. F., Boulder, Colo.
Barrows, J. H., Tacoma, Wash.
Bouse, G. B., Los Angeles, Calif.
Bush, A., Los Angeles, Calif.
Caruana, P. A., Kokomo, Ind.
Case, E. E., Fort Worth, Tex.
Cornett, V., Kansas City, Mo.
England, S. J. M., Columbus, Ohio
Fricke, C. A., Philadelphia, Pa.
Hananel, M. D., Galata, Istanbul Turkey
Honert, G. B., Fort Washington, Pa.
Jones, R. T., El Paso, Tex.
Laughlin, J. L., Downers Grove, Ill.
Lim, R. S., Seattle, Wash.
MacMillan, A. U., Vancouver, B. C., Canada
Pestel, T. L., Ogallala, Neb.
Taylor, S. L., Trenton, Ont., Canada
Tinsler, H. C., Biloxi, Miss.
Todd, H. C., Seattle, Wash.
Trullinger, L., El Paso, Tex.
Weibley, J. E., North Chicago, Ill.
Weiner, E. G., York, Pa.
Wolf, P. L., Minneapolis, Minn.

Admission to Member

Adler, J. J., China Lake, Calif.
Ahmed, M. I., London, England
Akers, A. E., San Diego, Calif.
Archer, J. E., Bel Air, Md.
Arnow, S., Great Neck, L. I., N. Y.
Badr, H. A., Zurich, Switzerland
Baker, J. L., Bethesda, Md.
Barber, M. R., Murray Hill, N. J.
Bartlett, R. E., Raleigh, N. C.
Bartz, A. T., Jr., Oswego, N. Y.
Beck, P. E., Enon, Ohio
Becker, G. M., Santa Barbara, Calif.
Bell, A., Long Island City, L. I., N. Y.
Betz, R. J., Ferndale, Md.
Blais, C. A., Rome, N. Y.
Bloom, L., Pikesville, Md.
Blount, G. A., Jr., Raleigh, N. C.
Borges, L. E., St. Petersburg, Fla.
Bottorff, P. S., Gainesville, Fla.
Brani, R. F., Owego, N. Y.
Browder, L. B., Arcadia, Calif.
Bruner, J. J., Tulsa, Okla.
Bryans, L. G., Fremont, Calif.
Bush, J., Syracuse, N. Y.
Callahan, R. M., Jr., Fredericksburg, Va.
Campbell, E. S., Fairfax, Va.
Carroll, C. L., Fort Huachuca, Ariz.
Carroll, S. H., Sunnyvale, Calif.
Ceglowski, F. E., Madison, N. J.
Cianciola, M., Vista, Calif.

(Continued on page 54A)

Membership

(Continued from page 52A)

Clark, R. W., Centerville, Ohio
Cleary, L. J., Framingham, Mass
Coates, W. J., Fullerton, Calif.
Cohen, D. B., Akron, Ohio
Cohen, M. E., Mantua, N. J.
Comes, R. G., Denver, Colo.
Cone, P. F., Wakefield, Mass.
Conger, C. R., State College, Pa.
Cornish, A. F., Camden, N. J.
Courts, H. R., Austin, Tex.
Cox, E. S., Canonsburg, Pa.
Cowlishaw, J. D., Baltimore, Md.
Cummins, C. C., Melbourne, Fla.
Czecha, S. J., Glen Rock, N. J.
Davis, D. B., Mountain View, Calif.
Davis, J. R., Jr., Lexington, Ky.
DeBoice, W. F., Long Beach, Calif.
DeVera, G. E., Succasunna, N. J.
Dierking, D. L., Orlando, Fla.
DiStefano, R. G. V., Orlando, Fla.
Dodds, B. L., State College, Pa.
Donovan, R. P., Bowie, Md.
Dosick, L., Owings Mills, Md
Dunn, W. T., Mobile, Ala.
Earl, J. L., Santa Clara, Calif.
Edelsohn, H., Hollis, L. I., N. Y.
Ennis, N. F., Cedar Rapids, Iowa
Everett, P. G., Chicago, Ill.
Farotto, R. M., St. Ann, Mo.
Fellows, R. A., Newbury Park, Calif.
Fischer, W. C., Jr., Fairfield, Conn.
Fitzgerald, R. W., Norwalk, Conn.
Francesconi, J. G., Poughkeepsie, N. Y.
Frank, J. H., Rhinebeck, N. Y.
Frazier, M. J., Glen Ellyn, Ill.
Freeland, K. L., Penfield, N. Y.
Freeman, D. G., Rockville, Md.
Freeman, W. S., Winston Salem, N. C.
Frisch, A., Brooklyn, N. Y.
Fry, J. J., Prairie Village, Kan
Furchner, C. J., Anaheim, Calif.
Gabany, V., Jr., Media, Pa.
Gartland, J. P., Washington, D. C.
Gerding, E. Y., Torrance, Calif.
Gilbert, B., Bournemouth, Hants, England
Gaze, W., Mountain View, Calif.
Glaze, H. B., Woodland Hills, Calif
Glover, J. F., Vienna, Va.
Goldstein, R., Highland Park, N. J.
Grant, W. V., Falls Church, Va.
Greer, C. H., Watertown, Mass.
Gupta, K. R. C., Bangalore, India
Haas, P., New York, N. Y.
Hall, J. A., Lynchburg, Va.
Hammon, R. L., Las Vegas, Nev.
Hampton, I. H., Winston Salem, N. C
Hanes, L. F., Dayton, Ohio
Harstad, A. J., Cocoa Beach, Fla
Henness, J. M., Davenport, Iowa
Henoch, B. T., Alvsjo, Sweden
Hinnah, H. D., Davenport, Iowa
Hjelle, D. G., Dayton, Ohio
Holley, O. M., Fullerton, Calif.
Houston, R. W., Torrance, Calif.
Hsieh, P., Poughkeepsie, N. Y.
Hughes, W. F., Windsor, Conn

(Continued on page 58A)

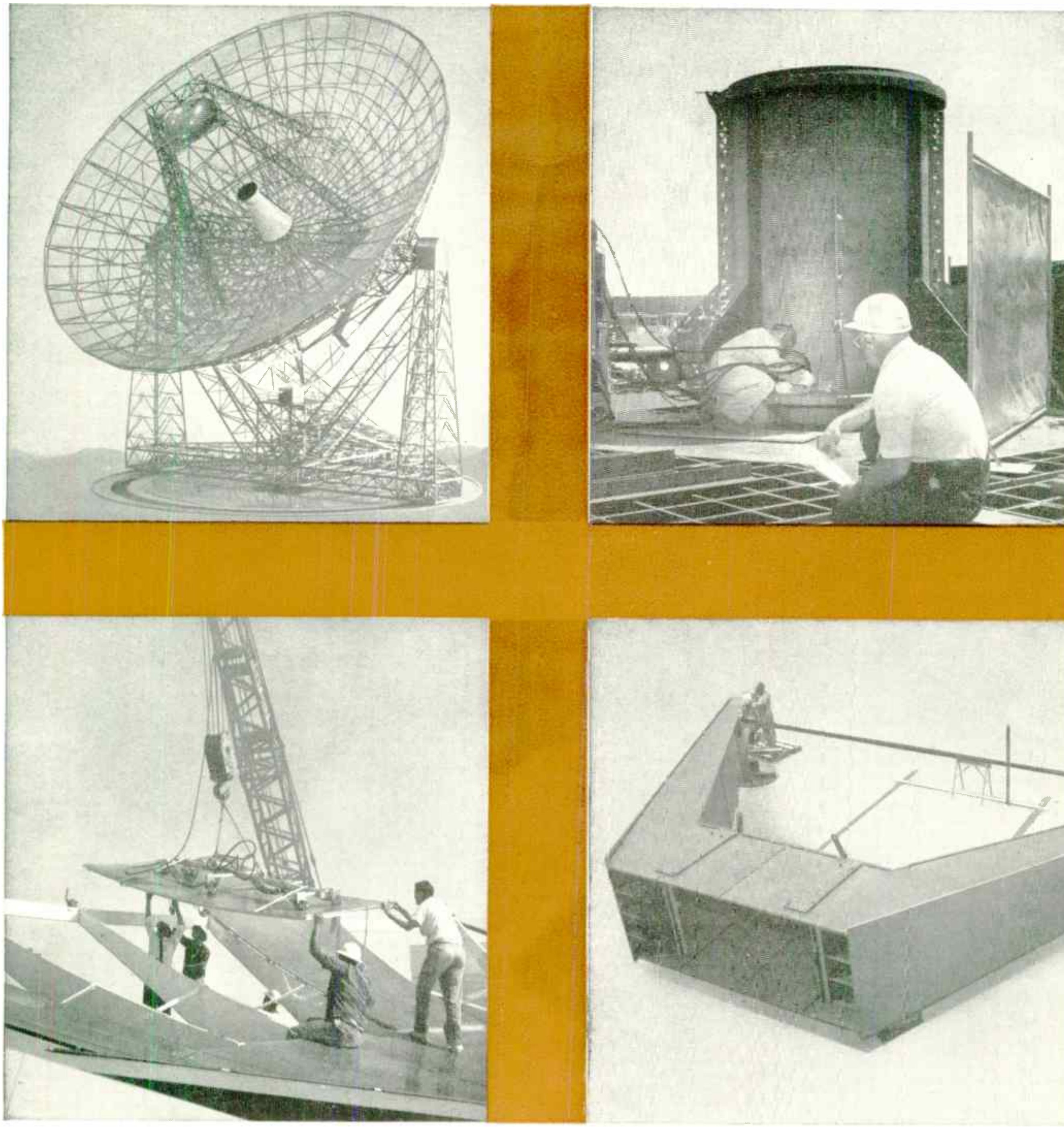

Rohr precision—a natural plus in large antenna hardware

Our successful performance in the manufacture of massive antenna structures results from a unique blending of engineering and manufacturing experience in the field of large and precise metal components. From the beginning, our antenna philosophy called for a new degree of precision to meet new levels of antenna performance. This led to a long and continuing Rohr antenna research program . . . research in design, fabrication and erection problems with consideration of environmental requirements. The result is that today Rohr is producing under contract some of the largest and most advanced antenna structures in the world. For more information, write for our brochure titled, "Large Antenna Structures." Address Marketing Manager, Dept. 130, Rohr Corporation Chula Vista, California.

Main Plant and Headquarters. Chula Vista, Calif. / Plant: Riverside, Calif./ Assembly Plants: Winder, Ga.; Auburn, Wash.

Offices in Washington, D C. and Huntsville Ala.

ROHR
CORPORATION

ELECTRONICS
progress in semiconductors

The Schizoid Switch

Two separate and distinct personalities is pretty unusual, in people that is. Three is almost unheard of. But in electronics, a new G-E device is a real hip schizoid character with *eight* separate and distinct personalities; (1) extremely sensitive NPNP controlled switch (complement of SCR); (2) extremely sensitive PNPN controlled switch (SCR configuration); (3) NPN silicon transistor; (4) PNP silicon transistor; (5) N type negative resistance (trigistor, transwitch); (6) S type negative resistance (binistor); (7) four layer diode; (8) zener diode. (As you can see, the schizoid switch doesn't create problems, it solves 'em.)

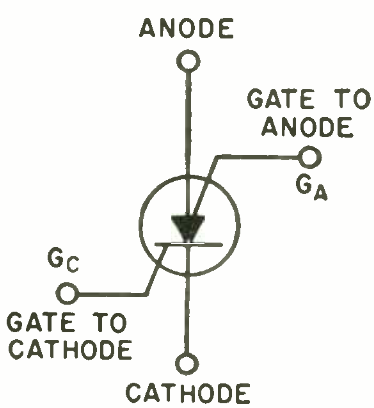

We call this versatile new 8-headed beauty the Silicon Controlled Switch. As the pictured symbol illustrates, it's a four layer (PNPN) device with all four layers accessible, and therein lies the secret of its versatility. We can't divulge the secret of its amazingly low cost and its military-type reliability, but we can sure talk about it. And we can also talk about the wide range of jobs it can perform in industrial and military digital computer and control applications. To name a few: time delay generator, SCR trigger pulse generator, tone generator, telemetry oscillator, sensitive voltage level detector, bistable memory element, binary counter, shift register, indicator lamp driver. And there are more . . . many more.

To complete the schizoid switch story, the SCS is available in three types, 3N58, 3N59 and 3N60 . . . all furnished in a TO-5 case. And they're available *now* in production quantities. Call your District Sales Manager, or write to us at Section 23H133. We have several psychiatrists with engineering degrees who have done extensive analysis of the schizoid switch. They know how to handle 'em, and they'll be glad to answer your questions.

MIL types galore! Newest approved types include JAN 2N696 and 697 silicon planars, and JAN 2N497, 8, 2N656, 7 silicon double-diffused NPN amplifiers — giving you a broad selection from among 34 JEDEC types. (One of our unijunctions is used in the Mercury capsule.) For a complete list see your District Sales Manager, or write to Section 23H133 and ask for the latest Semiconductor Products Full Line Catalog.

Improving the Breed

. . . wins horse races and dog shows. It also makes for better semiconductor devices (although we're not looking for laurel wreaths or blue ribbons). Our "PEP" line of silicon computer diodes now features new high temperature Anode and Cathode contacts so good that we now bake our "PEP" units at 300°C for a solid week (168 hours) before we test 'em. Talk about stability! But please, no complimentary letters. Just buy some!

Any questions? Write us at Section 23H133, General Electric Company, Semiconductor Products Department, Electronics Park, Syracuse, New York. In Canada: Canadian General Electric, 189 Dufferin St., Toronto, Ont. Export: International General Electric, 159 Madison Avenue, New York 16, N. Y.

GENERAL ELECTRIC

with the NEW
AM SIGNAL GENERATOR
Model 144H **$1190**

WIDER FREQUENCY RANGE
10 kc to 72 mc
GREATER STABILITY
0.002%
ELECTRONIC FINE TUNING
0.01%
HIGHER OUTPUT
2 v to 0.1μV, $\pm$ 0.5 db
AND . . . AT LOWER COST

WESCON Booth #2043-44

MARCONI
INSTRUMENTS

DIVISION OF ENGLISH ELECTRIC CORPORATION
111 CEDAR LANE • ENGLEWOOD, NEW JERSEY
Main Plant: St. Albans, England

revolutionary new single point resistance MICROWELDER

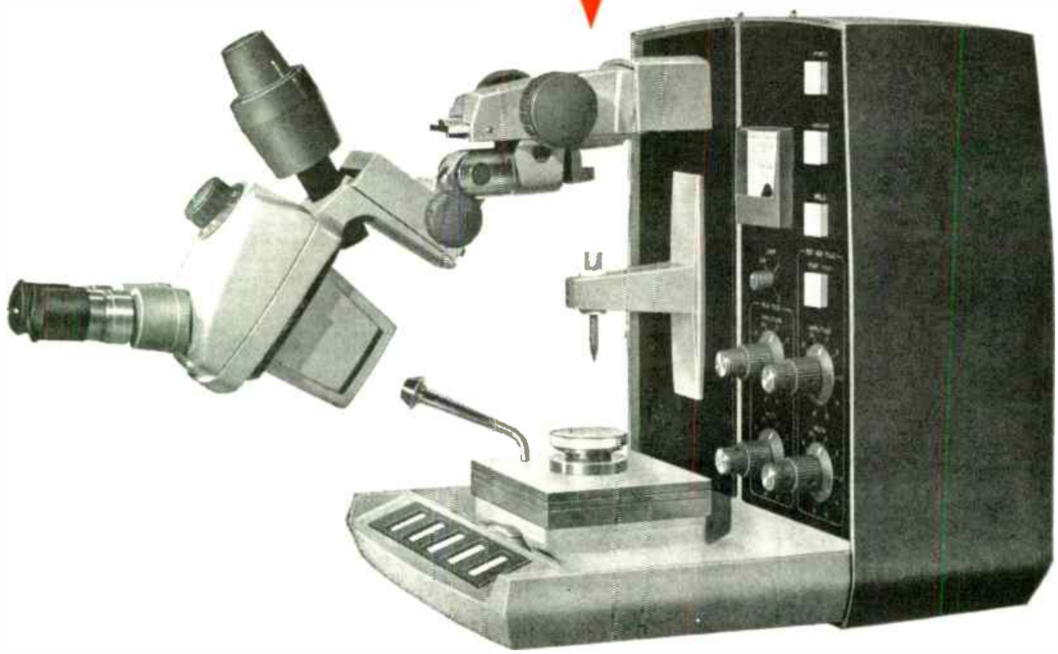

WELDS ½-MIL WIRE ON 3-MIL CENTERS

■ Metal-to-glass bonds ■ Metal-to-ceramic bonds ■ Metal-to-semiconductor substrates ■ Bonds to angstrom-thick thin-films ■ Portable—110-115 V, ac, 60-cycle operation

Provides reliable bonds…from printed circuitry to molecular electronic functional blocks.

For further information write Aerojet-General® Corporation Astrionics Division, Dept. 505, Azusa, California

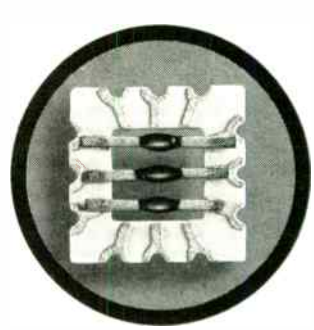

WELDED WINDOW-FRAME MICROELECTRONICS

See the MICROWELDER at Wescon Booth No. 3817, 3818

AEROJET GENERAL TIRE GENERAL ASTRIONICS DIVISION / AZUSA, CALIFORNIA

Membership

(Continued from page 51A)

Hunsicker, F. L., Washington, D. C.
Huppert, W. W., Rock Island, Ill.
Hynd, J. A. S., Hamilton, Ont., Canada
Ignagni, M. B., Detroit, Mich.
Ingham, H. J., Dallas, Tex.
Irvine, J. J., Ottawa, Ont., Canada
Jackson, J. H., Salt Lake City, Utah
Jaffe, J. C., Norwalk, Conn.
Jelen, G. F., Jr., Silver Spring, Md
Johnson, L. O., Inglewood, Calif.
Jonas, J. C., Grand Rapids, Mich.
Juliano, C. V., Los Angeles, Calif.
Kastanas, G. E., Athens, Greece
Kastella, K. G., Albuquerque, N. M.
Keegan, J. P., Nashua, N. H.
Kelly, E. J., Lexington, Mass.
Khan, M. A., Karachi, West Pakistan
Konsowski, S. G., Jr., New Hyde Park, L. I., N. Y.
Kostelec, J., Stamford, Conn.
Krupanszky, S., New York, N. Y.
Kulle, T. J., East Northport, L. I., N. Y
LaBanca, F. A., Bronx, N. Y.
LaGalante, J. K., Elmwood Park, Ill.
Latourette, C. D., Los Angeles, Calif.
Laubscher, P. R., Bath, N. Y.
Lawrence, J. L., Jr., Pasadena, Calif
Leland, R. F., Tempe, Ariz.
Lemley, V. F., San Marcos, Calif.
Lenhart, D. W., Syracuse, N. Y.
Leonard, T. C., Williamsville, N. Y
Liebler, K. A., South Beloit, Ill.
London, E. P., Palos Verdes Estates, Calif.
Lukman, F. J., Palmerton, Pa.
Lundqvist, A. L., Jakobsberg, Sweden
Lynn, V. L., Sudbury, Mass.
Mandra, S. A., New York, N. Y.
Mann, O. S., Emporium, Pa.
Mannion, J. J., Santa Monica, Calif.
Mapother, T. C., Liverpool, N. Y.
Martin, J. L., Summit, N. J.
Maze, L., Bellwood, Ill.
McCally, L. R., Great Falls, Mont
McElroy, R. E., Roswell, N. M.
McKenny, H. T., Winooski, Vt.
McMillan, T. T., Reseda, Calif.
Mears, K. E., Port Hueneme, Calif
Medendorp, L. E., Hamilton, Ohio
Merle, R. T., Malibu, Calif.
Miko, A. S., Chicago, Ill.
Miller, G. K., II, Boston, Mass
Miller, J. G., Dayton, Ohio
Miller, M. W., Dayton, Ohio
Miller, T. A., Woodland Hills, Calif
Misra, S. S., Minneapolis, Minn.
Mitchell, P. A., Paso Robles, Calif.
Molthen, E. H., Chicago, Ill.
Moyers, W. D., Amityville, L. I., N. Y.
Mundl, W. J., Duverday East, Que., Canad
Murphy, J. H., Medford Lakes, N. J.
Murthy, S. V., Bangalore, South India
Nath, P. N., Philadelphia, Pa.
Newman, P. A., Oakhurst, N. J.
Nunnally, C. H., Old Bethpage, L. I., N. Y
O'Meara, W. M., Toronto, Ont., Canada
Paiewonsky, B. H., Princeton, N. J
Paltauf, R. C., Medway, Ohio
Panzieri, A., Bogota, Colombia
Paredes, A. E., Miami, Fla
Parin, F. S., Iselin, N. J.
Paterson, V. Z., Davenport, Iowa
Patterson, E. E., San Francisco, Calif
Pescetelli, P. P., Rome, Italy
Pezaris, S. D., Lexington, Mass
Phillips, W. B., Poughkeepsie, N. Y.

(Continued on page 60A)

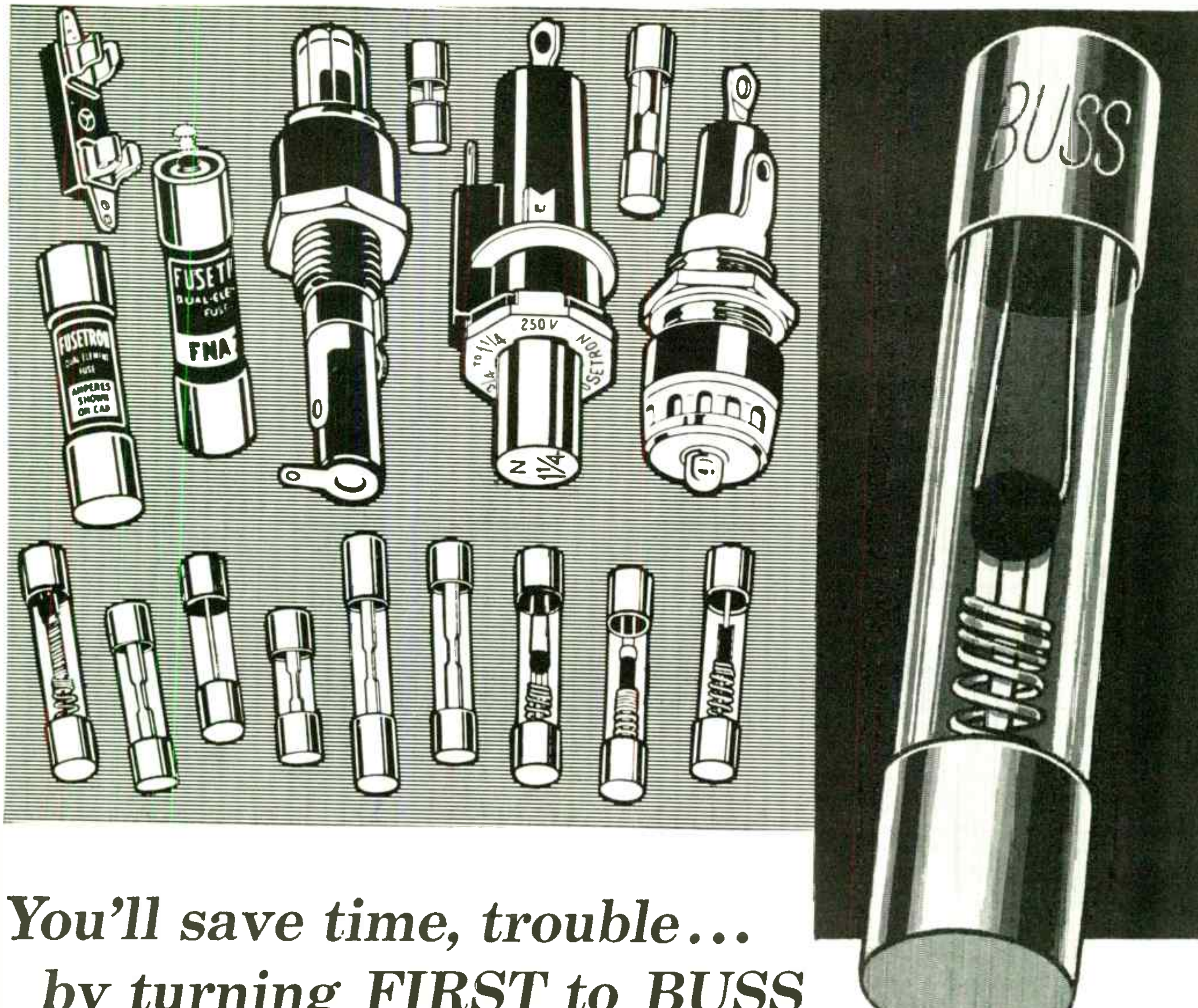
FUSETRON
AMPERES SHOWN ON CAP
FNA
250 V
BUSS

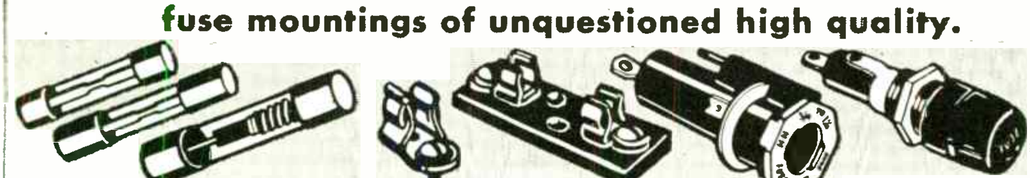

Membership

(Continued from page 58A)

Piston, H. H., Nashua, N. H.
Platt, A. H., Poughkeepsie, N. Y.
Poetzl, H. W., Vienna, Austria
Pool, E. T., Glendale, Calif.
Psutka, M. E., Ottawa, Ont., Canada
Puvogel, R. L., Santiago, Chile
Quintiliani, D. A., Newton, Mass.
Radcliff, R. E., Dover, N. J.
Radosavljevic, S. M., Chicago, Ill.
Rea, L. T., Camillus, N. Y.
Reardon, J. E., Glenside, Pa.
Reegan, J. E., Bedford, Mass.
Rehberg, C. A., Little Falls, N. J.
Richard, C. A., Montreal, Que., Canada
Riedler, W. W., Vienna, Austria
Rimini, A., Milano, Italy
Roberts, S. M., Utica, N. Y.
Rogness, D. F., Davenport, Iowa
Rosenbusch, J. M., Baltimore, Md.
Rowson, R. G., New York, N. Y.
Ruckstuhl, R. E., Norristown, Pa.
Salmon, T. F., West End, N. J.
Salzer, W. E., Somerdale, N. J.
Samuels, S. R., Bellerose, L. I., N. Y.
Sarkar, B., Roorkee, India
Schmager, N. F., APO, San Francisco, Calif.
Schramm, L. P., Princeton, N. J.
Schultz, D. O., North Springfield, Va.
Schwartz, L., Torrance, Calif.
Schwartz, L., Dayton, Ohio
Shaw, C. W., Vestal, N. Y.
Shoemaker, R. L., Harrisburg, Pa.
Shube, E. E., Elmont, N. Y.
Shumsky, J., Binghamton, N. Y.
Sikaitis, P. E., Detroit, Mich.
Silverstein, M., Melbourne, Fla.

(Continued on page 68A)

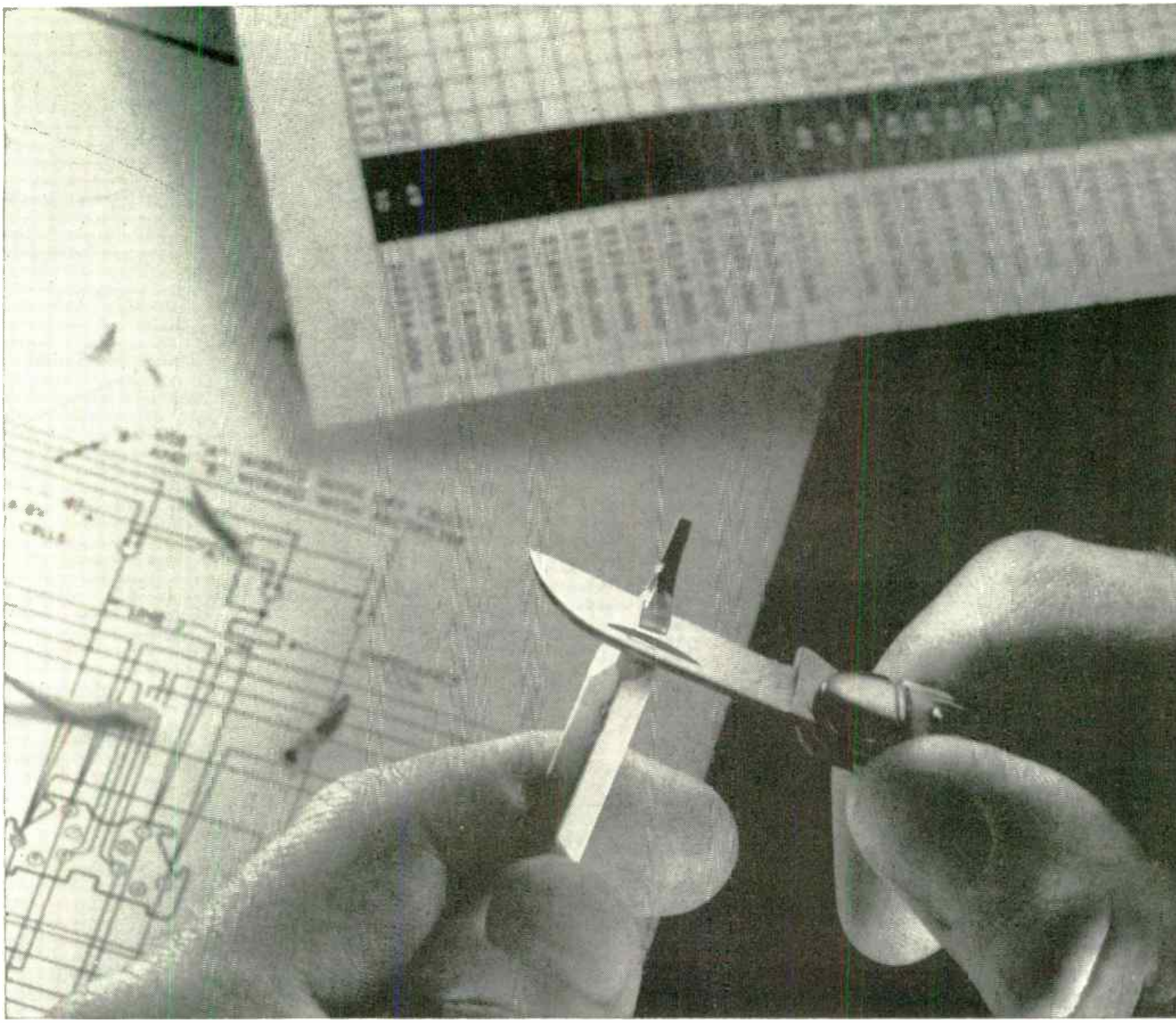

Sorry,
but your resistor specs just went out of date

Now Corning supplies total ΔR less than 3% with no derating

Start a design with known limits of resistance deviation as tight as that and you can specify other components with more certainty and more freedom.

Drop an amplifier stage? Use broader tolerance, cheaper tubes or transistors?

That's what our new *Corning Design Tolerances* are all about. They give you a percent deviation from nominal that includes the purchase tolerance, maximum ΔR due to TC, and maximum load-life drift. They're based on extended performance at full power and 70°C. ambient for over 30,000 hours.

We've assigned them to resistors that cover the 10 ohm—1 meg. range: the fusion-sealed NF, the precision N, and the low-cost, high-performance general purpose C. They're available fast, and at factory prices, from your local Corning distributor.

A new folder, "Design Tolerances for Tin Oxide Resistors," gives you full information. Write for a copy to Corning Glass Works, 3902 Electronics Drive, Raleigh, N.C. . . . and sharpen your pencil.

	Model	Resistance (ohms)	Corning Design Tolerance
NF (Meets Mil-R-10509D)	60 65	100 to 100K 100 to 348K	3%
N (Meets Mil-R-10509D)	60 65 70	10 to 133K 10 to 499K 10 to 1 meg.	3%
C (Meets Mil-R-22684)	20 32 42S	51 to 150K 51 to 470K 10 to 1.3 meg.	5% (plus purchase tolerance of either 2% or 5%)

CORNING
Electronic Components

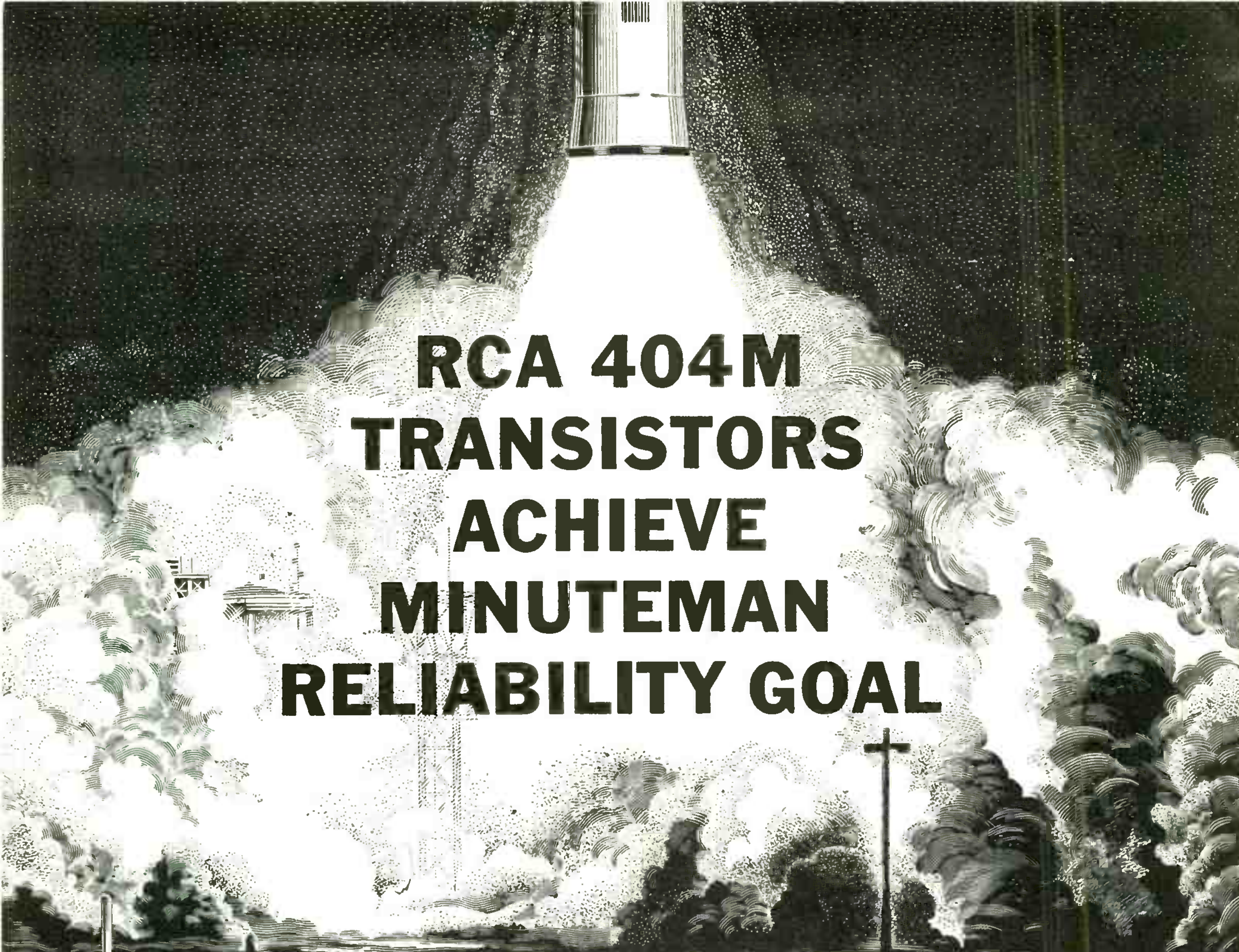

Surpass Failure-Rate Requirement of 0.001% per 1000 Hours

Failure-free performance of RCA 404M Germanium-alloy switching transistors in final-phase tests surpassed the established failure rate goal of 0.001% per 1000 hours at a 60% confidence level.

In achieving these outstanding results, on the MINUTEMAN program, RCA accumulated test data covering over 13,000,000 transistor hours. Each 404M is tested to tight limits in the following tests:

- 250 hours of power stress (150mw at 25° C)
- 750 hours of 100° C storage
- Helium bomb and detergent bomb leak test
- 8 hours of temperature cycling (from −65° to 100° C)
- 100 G tap tests while energized
- High-temperature leakage

Also, the Environmental and Mechanical requirements of MIL-S-19500B are met.

The ultra-high reliability of the RCA 404M again demonstrates RCA capability to design, develop, and manufacture transistors to meet the strictest requirements of industrial and military applications.

The RCA 404M is now available in quantity. For technical data and delivery information on the RCA 404M or any other transistor in RCA's broad line, call your local field office.

Here's your close-up tour showing how RCA builds quality and reliability into all its transistor types.

RCA's 16mm Color Sound Film..."53 Steps to Electronic Progress through Transistor Quality" will show you and your organization how RCA achieves outstanding quality and reliability. Contact your RCA field office for a date to see this outstanding film.

THE MOST TRUSTED NAME IN ELECTRONICS

Visit the RCA Exhibit at WESCON—Booths 1043-1050.

RCA SEMICONDUCTOR & MATERIALS DIVISION FIELD OFFICES . . . EAST: Newark, N. J., 744 Broad St., HU 5-3900 • (Camden-Philadelphia Area) Erlton, N. J., 605 Marlton Pike, HA 8-4802 • Syracuse, N. Y., 731 James St., Rm. 402, GR 4-5591 • Baltimore, Md., EN 9-1850 • **NORTHEAST:** Needham Heights 94, Mass., 64 "A" St., HI 4-7200 • **SOUTHEAST:** Orlando, Fla., 1520 Edgewater Dr., Suite #1, GA 4-4768 • **EAST CENTRAL:** Detroit 2, Mich., 714 New Center Bldg., TR 5-5600 • **CENTRAL:** Chicago, Ill., Suite 1154, Merchandise Mart Plaza, WH 4-2900 • Indianapolis 5, Ind., 2132 East 52nd St., CL 1-1405 • Minneapolis 16, Minn., 5805 Excelsior Blvd., WE 9-0676 • Denver 11, Colorado, Continental Terrace Bldg., Suite 301, 2785 N. Speer Blvd., 477-1688 • **WEST:** Los Angeles 22, Calif., 6801 E. Washington Blvd., RA 3-8361 • (San Francisco Area) Burlingame, Calif., 1838 El Camino Real, OX 7-1620 • Seattle 4, Wash., 2250 First Ave. S., MA 2-8816 • **SOUTHWEST:** Dallas 7, Texas, 7905 Carpenter Freeway, ME 1-9720 • **GOV'T:** Dayton, Ohio, 224 N. Wilkinson St., BA 6-2366 • Washington, D. C., 1725 "K" St., N.W., FE 7-8500 • **RCA INTERNATIONAL DIVISION,** 30 Rockefeller Plaza, New York 20, N. Y. Cable Address: RADIOINTER, N. Y.

August, 1962 *Vol. 50* *No. 8*

Proceedings of the IRE

Poles and Zeros

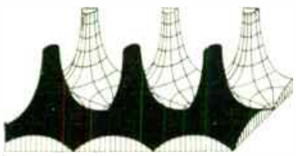

Merger Approved. IRE members approved plans to merge with the AIEE by a $6\frac{1}{2}$-to-1 margin at the special membership meeting on July 10. A full report on this important meeting appears on the following page.

Students, Attention! The IRE Board of Directors has decided that the IRE STUDENT QUARTERLY will be expanded to provide a greater amount of material of direct interest and value to students. The resulting increase in cost will make it impossible to provide both the student publication and the PROCEEDINGS to Student Members for the present annual dues of $5.00.

Student Members joining or renewing their membership after September 15, 1962, will have the option of receiving only the expanded student publication by paying annual dues of $5.00, or of receiving both the student publication and the PROCEEDINGS by paying annual dues of $9.00. The second plan is equivalent to obtaining the PROCEEDINGS for a modest portion of the cost of printing and postage.

Interdisciplinary. As engineers and scientists pursue with enthusiasm their task of gleaning knowledge from this earth (and the universe!), and of exploiting this knowledge for man's benefit, they are continually discovering (or becoming aware of) unifying concepts, principles, and techniques which shatter traditional boundaries between disciplines and demand new alliances and team efforts. Early in the history of our profession we found common interests and fellowship with physicists in such areas as electromagnetic theory, theoretical mechanics, and acoustics. For a time the infatuation of physicists with atomic and nuclear phenomena looked like a parting of the ways. But developments such as nuclear power, nuclear propulsion, and the phenomenal applications of the solid state have brought about new and stronger relationships. The tie with mathematics—and mathematicians—has been similarly close through the years. A few years ago engineers sought applied mathematics, and the colleagueship of applied mathematicians. Today engineers working on the mathematical forefronts of our profession speak of "applicable mathematics" and draw upon esoteric mathematical topics such as measure theory, group theory, and topology.

Interdisciplinary ties have been so effective in the immediate past that significant efforts are being made by local and national groups, including government bureaus, to foster interdisciplinary-team attacks on forefront technical areas.

Biomedical Engineering. Engineering advances of the last two decades in communication, information, and control theory; in artificial intelligence; in computers; and in energy conversion have been found to have broad applicability to the fields of biology and medicine. These mutual interests were strong among the factors which led the IRE in January, 1957 to adopt the Professional Group Affiliate plan whereby members of other professional societies might function as affiliate members of IRE Professional Groups without themselves being IRE members. The Canadian Medical Association is the latest society approved for affiliation of its members with the IRE Professional Group on Bio-Medical Electronics. Over the last several years biomedical research has been greatly stimulated by grants from the National Institute of Health and other sources within and without the Government. On almost every campus electronic researchers are joining with colleagues in biology and medicine to pursue mutual interests. In anticipation of continued and rapid growth of activity in this "interdiscipline," President Haggerty, in consultation with members of the Executive Committee, has appointed the following to the IRE Ad Hoc Committee on Bio-Medical Electronics: F. K. Willenbrock (Chairman), E. Finley Carter, A. N. Goldsmith, R. L. McFarlan, Otto Schmitt, J. H. U. Brown, and A. K. Solomon. They are charged to study and make recommendations to the Executive Committee on: 1) the appropriate scope of IRE activities in the broad field of applications of electronics and electrical engineering to biology and medicine; 2) the service that IRE might be expected to render in these areas; and 3) feasible ways of implementation of these recommendations.

"The Engineer and the Life Sciences." On page 1758 of this issue is a very timely article by Dr. J. H. U. Brown which delineates the field of Biomedical Engineering and which outlines explicit scientific interest of the Government.

Census of Engineers. The Bureau of Census is mailing a questionnaire to a sample group of 20,000 engineers. About one in fifty of our members thereby will be given an opportunity to serve his profession. If you should be so honored, please complete the questionnaire with care and return it promptly as directed. The result of this preliminary survey will be very useful to IRE and to the profession.

Historic Papers. The Editorial Board of IRE recently adopted the suggestion of Managing Editor E. K. Gannett to continue our celebration of IRE's 50th Anniversary Year by republishing a series of historical PROCEEDINGS papers. The first paper, Marconi's "Radio Telegraphy," was published in the August, 1922 issue. Of today's 100,000-plus members, less than one-half of one per cent (503) saw the article when it first arrived in the mail to the 1922 membership of 2896. We beg forebearance of our 503 venerable members while 99,600 of us newcomers enjoy the rich past of IRE!—T.F.J.

IRE Members Approve Merger with AIEE

AT A SPECIAL MEETING of the membership, held at IRE Headquarters at 9 A.M., July 10, 1962, IRE members approved, by a $6\frac{1}{2}$-to-1 margin, plans to merge with the American Institute of Electrical Engineers to form the Institute of Electrical and Electronic Engineers on January 1, 1963.

Voting by proxy and in person, 36,221 members, or 86.8 per cent of those voting, expressed themselves in favor of merger, with 5,489, or 13.2 per cent, opposed. Of the 66,152 members eligible to vote, 63.1 per cent voted, an unusually high percentage.

AIEE members previously approved the proposed merger, by a virtually identical vote, on June 18, at their annual meeting in Denver, Colo., with 87.1 per cent in favor, 12.9 per cent opposed, and 61.4 per cent of the eligible members voting.

IRE members also approved a resolution modifying the nomination and election procedures provided in the Constitution while the proposed merger is pending. The vote was 36,622 for and 5,090 against.

IRE President Patrick E. Haggerty presided over the meeting, and Haraden Pratt, Secretary of the IRE, acted as proxy for those who voted by mail, both for and against. At the conclusion of the meeting, President Haggerty introduced Warren H. Chase, President of the AIEE, B. Richard Teare, AIEE President-Elect, who takes office August 1, 1962, and L. M. Robertson, Hendley Blackmon, and W. R. Clark, AIEE representatives on the AIEE-IRE Merger Committee. On behalf of the IRE Board of Directors and IRE members of the Merger Committee, President Haggerty presented AIEE President Chase a specially bound volume of the May Anniversary Issue of the PROCEEDINGS.

President Haggerty closed the meeting by stating, on behalf of the Committee, that any deficiencies which may exist in their documentation, procedures, or actions are the deficiencies of human beings. For in all cases the Committee has been endeavoring to act in a constructive and positive fashion for the welfare of both societies, ever conscious of the fact that no matter what point is brought up there are always those who, for good reason, feel otherwise. He pointed out that all of these points have been discussed and labored over by the Committee, in many instances as long as a year ago.

No matter how these points have been resolved, President Haggerty noted, they have apparently been resolved in such fashion that the heavy and almost identical majority in each society was in concurrence. He expressed the regret of the Committee members concerning their inability to so express themselves and to so state the measures to be taken as to satisfy all of the membership, especially those who have such a strong and sincere interest in the society. To all of them he expressed, for the members of the Fourteen-Man Committee, and for the IRE Board, their desire, and their full confidence, that the IEEE on its formation will be a far superior society to either of those which now exist. He pointed out that since it is a human institution, the IEEE, too, will bear the marks of human frailty and that hence it will urgently need the advice, support, and action, of all of the members of the new society.

As a result of the favorable vote by members of both societies, a 14-man merger committee, seven from each society, is proceeding with plans to prepare for and implement the merger (see page 14A of this issue).

Scanning the Issue

Radio Telegraphy (Marconi, p. 1748)— Of the 2896 members who saw the IRE celebrate its tenth birthday, a surprisingly large proportion, 503, have seen it reach its fiftieth. These individuals had the privilege to be present during a period when the early giants of radio were doing their most important work—and to read first-hand accounts of it in the PROCEEDINGS. It is a privilege which has not been shared, however, by the other 99,500 "newcomers" who make up the IRE of today. It is planned, therefore, to reprint during this Golden Anniversary year a few early PROCEEDINGS papers which it is believed will be of outstanding historical interest to the 99 per cent of the membership who have never read them before. The first paper in this series takes the reader back to 1922. Marconi had traveled to the United States that year, and on June 20th was presented the IRE Medal of Honor before a joint meeting of the IRE and AIEE. In response, he stepped to the lectern and delivered a discourse that electrified his audience and made radio history. He began with a remarkable, wide-ranging discussion of recent developments in radio communication which, even after 40 years, will strike many a familiar note in the mind of today's engineer. For example, his comments on the possible enhancement of radio waves as they converge on the opposite side of the earth will remind many readers of the phenomenon reported in the March, 1958 PROCEEDINGS where 40 Mc signals from Sputnik I created a virtual radio image of the satellite on the opposite of the earth. But the main force of his remarks was directed toward the important possibilities he foresaw in the future for the then unused VHF and UHF portion of the spectrum, and the novel experiments he was undertaking with short waves and reflectors to develop a point-to-point communication system and a rotating-beam radio beacon as a navigation aid for ships. The climax of his lecture came when he demonstrated on the stage the directional properties of 1-meter waves and then went on to make one of the famous prognostications of radio history—that these waves might be used to detect the presence and directions of distant ships. It was a virtuoso performance which remains as one of the high moments in IRE's 50-year past.

The Engineer and the Life Sciences (Brown, p. 1758)—It has been generally recognized for a number of years that the field of engineering can contribute much to the fields of medicine and biology, and vice versa. During the past decade, research organizations, professional societies and others have made a notable start toward fostering activities which permit and encourage a greater collaboration among professionals in these diverse fields. The IRE, for example, has contributed importantly in this through its Professional Groups of Bio-Medical Electronics. It has become increasingly evident, however, that the fruits of the marriage between engineering and the life sciences will not fully ripen by dealing with this area in piecemeal fashion, that is, as branches within each of several existing disciplines. What is needed, and what indeed is arising, is a new science which is a discipline in its own right, known to many as biomedical engineering. To flourish, it must be populated by a new type of professional who has a new kind of training. This timely article discusses the kind of professionals needed, the work they will do, and the training they require. Equally important, it calls attention to the role of the National Institutes of Health in nurturing a new discipline which is currently doubling in size every $2\frac{1}{2}$ years.

Group Theory and the Energy Band Structure of Semiconductors (Nussbaum, p. 1762)—This paper is the complement of one which appeared in the special issue on solid-state electronics seven years ago. The earlier paper dealt also with the energy band structure of semiconductors, with the emphasis on how to apply the results of energy band calculations to the interpretation of experimental data. In the present paper the author devotes himself to the principles involved in making the calculations, showing how quantum mechanics and the crystal structure lead to the various kinds of bands. The result is an excellent tutorial paper aimed primarily at workers in the solid-state field, who will find it broadly helpful in reading and interpreting the literature as well as directly useful in energy band calculations.

Injection Currents in Insulators (Lampert, p. 1781)—The subject of this paper—conduction phenomena in insulators—is one which is of growing current interest and of major potential importance. Indeed, it is felt that this area will become as important to electronics engineers during the next ten years as conduction processes in semiconductors did during the last decade. Already there are two amplifying devices which utilize conduction in insulators. Moreover, the basic processes involved are also applicable to photoconductive and electroluminescent materials. This paper can be described quite simply. It is a review and tutorial paper which sets forth in a manner intelligible to a wide range of readers, the fundamental principles of a phenomena that is destined to become of widespread importance in the near future.

Theoretical Considerations on Millimeter Wave Generation by Optical Frequency Mixing (Fontana and Pantell, p. 1796)—The development of optical and near-infrared masers has not only opened up the optical portion of the spectrum to the communications engineer but, it appears, has finally provided him the means for closing the microwave-infrared gap. In principle it should now be possible to mix two optical signals to produce an output at a difference frequency which lies in the 1 to 0.01-millimeter band. To achieve this result, an appropriate nonlinear element must be found. The analysis presented here shows that, contrary to the situation in harmonic generation, lossless nonlinear elements have very low conversion efficiencies, but that nonlinear resistive elements can give efficiencies up to 25 per cent.

Electron Guns for Forming Solid Beams of High Perveance and High Convergence (Frost, *et al.*, p. 1800)—A new method of designing solid-beam electron guns has been developed which results in an impressive advance in the art of producing high-density electron beams. Because of the pressing need for higher density beams for high-power klystrons and traveling-wave tubes in the microwave and millimeter wave range, the substantial improvement reported here will be of general interest to systems people.

Thermal Noise in Field-Effect Transistors (van der Ziel, p. 1808)—This paper describes the limiting noise mechanism in a device which is becoming more and more important because of improvements in semiconductor device technology. Hence, the results are likely to interest those who work in fields other than semiconductor devices and who will be using field-effect transistors in the future. It is not unlikely that this paper will become a classic in the field, similar to the author's earlier papers on noise in transistors and diodes.

Higher-Order Temperature Coefficients of the Elastic Stiffness and Compliances of Alpha-Quartz (Bechmann, *et al.*, p. 1812)—The authors present the results of precise work on the elastic data of quartz as a function of temperature, with application to numerous cuts of special interest. These new data have a range and show a degree of completeness markedly exceeding previous determinations. The results will be of considerable importance to all readers interested in frequency control.

Scanning the Transactions appears on page 1862.

Radio Telegraphy*

SENATORE GUGLIELMO MARCONI
G.C.V.O., D.SC., LL.D., Etc.

During the first decade of its existence, the PROCEEDINGS *published a number of important papers by foremost pioneers of the infant radio engineering art which today are of major historical interest. Since less than one per cent of the present generation of IRE members were* PROCEEDINGS *readers at that time, it is planned to republish a few of these early papers during the coming months in commemoration of IRE's Golden Anniversary year.*

The following paper is the first of the series. It was first presented before a joint meeting of the IRE and the American Institute of Electrical Engineers on June 20, 1922, on the occasion when the IRE presented Marconi with the Medal of Honor. His response, which included a live demonstration, added a memorable and historically important chapter to the extension of the radio art into the UHF region of the spectrum.—The Editor

THE FIRST OCCASION on which I had the honor of speaking before the members of the American Institute of Electrical Engineers was of a very festive nature.

It is over twenty years ago, to be exact on January 13, 1902; (there was not then any Radio Institute in existence) and on that date, memorable for me, I was entertained by over 300 members of your Institute at a dinner at the Waldorf-Astoria in this City. I was offered that dinner following my announcement of the fact that I had succeeded in getting the first radio signal across the Atlantic Ocean.

Many men, whose names are household words in electrical science, were present, men such as Dr. Alexander Graham Bell, Professor Elihu Thompson, Dr. Steinmetz, Dr. Pupin, Mr. Frank Sprague, and many others.

The function was one I shall never forget, and displayed to the full American resource and originality, as only forty-eight hours' notice of the dinner had been given, but what has left the greatest impression on my mind during all the long twenty years that have passed is the fact that you believed in me and in what I told you about having got the simple letter "S" for the first time across the ocean from England to Newfoundland without the aid of cables or conductors.

It gives me now the greatest possible satisfaction to say that, in some measure, perhaps, your confidence in my statement was not misplaced, for those first feeble signals which I received at St. John's, Newfoundland, on the 12th of December, 1901, had proved once and for all that electric waves could be transmitted and received across the ocean, and that long-distance radiotelegraphy, about which so many doubts were then entertained, was really going to become an established fact.

You will easily understand my feelings and how very happy I am to have the honor of addressing you again tonight, and when I say that I will always treasure the recollection of the generous encouragement and valid support so heartily extended to me practically at the commencement of my career, when perhaps I most needed it, by such a distinguished and authoritative body as the American Institute of Electrical Engineers.

The subject of my lecture, "Radiotelegraphy," has become so vast and so complex that you will readily understand my difficulty as to where I shall begin and as to when I ought to stop. It would be quite impossible for me to descant at any length on present achievements in a country which in a very short time has made gigantic strides in the scientific development and practical application of the science and art of radiotelegraphy. Moreover, time will not allow me to do more than skim over only a very few of the many problems which have lately been solved, or which there is a good prospect of solving in the near future.

Although we have, or believe we have, all the necessary data for the generation, transmission, and reception of electrical waves, as at present utilized for radiotelegraphy, we are still far from possessing exact knowledge concerning the conditions governing the transmission, or rather the propagation, of these waves through

* Reprinted from PROC. IRE, vol. 10, pp. 215–238: August, 1922.

space, especially across long distances.

I propose now to bring to your notice some of the recent results attained in Europe and elsewhere and to call your attention particularly to what I consider a somewhat neglected branch of the art; and which is the study of the characteristics and properties of very short electrical waves. My belief is always that, only by the careful study and analysis of the greatest possible number of well-authenticated facts and results, will it be possible to overcome the difficulties that still lie in the way of the practical application of radio in the broadest possible sense.

A very great impulse has been given to radiotelegraphy and telephony by the discovery and utilization of the oscillating electron tube or triode valve based on the observations and discoveries of Edision and Fleming, of those of De Forest and of those of Meissner in Germany, Langmuir and Armstrong in America, and H. W. Round in England, who have also brought it to a practical form as a most reliable generator of continuous electric waves.

As the electron tube, or triode valve, or valve, as it is now generally called in England, is able, not only to act as a detector, but also to generate oscillations, it has supplied us with an arrangement which is fundamentally similar for both transmitter and receiver, providing us also by a simple and practical method with the means for obtaining beat reception and an almost unlimited magnification of the strength of signals.

A result of the introduction of the triode valve has been that the basic inventions which made long-distance radiotelegraphy possible have become more and more valuable.

It may perhaps be of interest if I give some information as to the progress made by the Marconi Company in England, with the practical application of the triode valve.

It has been so far our practice to use a plurality of tubes in parallel at our long distance stations. High power has been obtained in practice up to 100 kilowatts in the antenna by means of a number of glass tubes in parallel, and for the present we are standardizing units capable of supplying 4 kilowatts to the antenna, in the numbers required and sufficient for each particular case.

Some difficulty was at first experienced in paralleling large tubes in considerable numbers, but no difficulties now occur with groups of 60 bulbs working on voltages of 12,000 on the plate.

I am told that no insurmountable difficulty would be encountered if it were desired to supply 500 kilowatts to the antenna from a number of these bulbs (Fig. 1). The life of the bulbs has been very materially increased and the 4-kilowatt units are expected to have a life, which, based on a great number of tests carried out both in the laboratory and at our Clifden station, should be well in excess of 5000 hours.

The development of single unit tubes of considerable power is also progressing. We have lately concentrated on the production of high power tubes made of quartz, and two sizes of each bulb are now being made, one for 25 kilowatts to the antenna, and another for 75 kilowatts, but it is not expected that the efficiency of the high power single units will be as good as that of the multiple units, and the work on the large tubes is being considered so far as experimental.

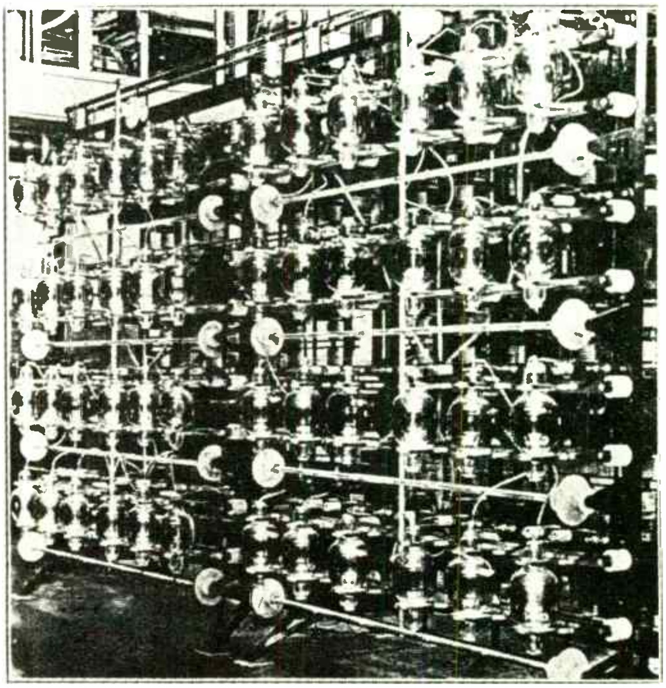

Fig. 1—Tube panel at Carnarvon

In transmission work a large amount of investigation has been carried out during the last two years on the efficiency of the circuits and in regard to the best way of utilizing the available energy.

Considerable increases in efficiency have been obtained in the aerial or antenna circuits and also in minimizing the losses in the attendant loading coils, and the latest results indicate that it is possible to obtain efficiency of radiation into space as high as 50 per cent on wavelengths as long as 20,000 meters, when, in this particular case, towers of a height of 250 meters would, of course, have to be used, owing to the length of the wave.

Very careful investigations have been carried out by Mr. H. W. Round, of all the losses in the loading coils and other parts of the tube circuits, and actual measurements on considerable power have shown that an overall efficiency from the input power on the plates of the tubes to the aerial of 70 per cent is possible with a complete avoidance of harmonics, that is, an efficiency from the power input to the plates of the tubes to actual radiation into space of about 35 per cent.

On shorter wave stations it is quite practicable still further to increase this efficiency, although possibly it is hardly worth the extra expense involved. We have at present one station in England working on a 3000-meter wavelength with a height of mast of 100 meters which has an efficiency from plates to radiation into space of 40 per cent.

Aside from the question of efficiency, great attention has been paid to maintaining an extremely constant frequency, and this can now be guaranteed to an extraordinary degree of constancy. Simple and reliable methods of high speed keying have been developed which on the shorter waves can be used up to over 200 words per minute, and on the longer waves to whatever speed the aerial constants will permit.

In high speed transmission, we are maintaining public services at 100 words per minute to two places in Europe, namely, Paris and Berne, using a single aerial transmitter with 2 wavelengths on the same aerial, and although the operation of utilizing a single aerial for 2 wavelengths is not an advisable one for high power work, it has certain points to recommend it in medium power work, where the consequent loss of efficiency can be made up for by a slight increase of power.

These 2 waves are working duplex to both Paris and Berne and practically all traffic is taken on printing machinery, although there are occasions when, because of static, reception has to be done on undulator tape, and in some rare cases, on the telephones, by sound.

The reception at these shorter distance stations is carried out by means of a cascade arrangement of high- and low-frequency tuned amplifier circuits attached to the directional aerial system of the Bellini type, arranged for unidirectional reception when necessary. Very great care is taken in the receiving circuits to shield them so that the tuned circuits come well into action and to prevent any direct effect or influence of the aerial on circuits other than those intended to be acted upon. The characteristics of all these circuits have been very accurately measured so as to give filter curves suitable to the required speeds of working, and the adjustments are easily performed by the operators. Aside from the protection from interference given by directional reception, a close filtering, and an element of saturation, no particularly sensational methods or ideas in regard to static elimination have been so far introduced into practice.

The careful measurement and study of the constants of all circuits in use and the design of more efficient circuits from the result of those measurements is being systematically carried out, but as a result of these investigations considerable improvements have suggested themselves, which will be applied in the future if certain appropriate means can be devised.

The protection of receivers against the troubles of atmospherics or static can only be, and is likely to continue to be, a relative matter, as it is quite obvious that a static eliminator under certain conditions will cease to be effective, where the static arrives with much greater intensity than had been anticipated, and will also frequently fail when, in consequence of the weakness of the received signals, amplification has to be increased to any considerable extent.

It would be really interesting to know how much the increase in CW transmitters, the development in directional reception, and the improvements in tuning that have taken place during the last few years have really increased our speed of readability and reliability over given distances.

As the development has been gradual, the tendency is towards pessimism, but I think we are now able at the same expense to work at about 8 to 10 times the effective speed that we were able to work at in 1912 under the same atmospheric conditions.

Interference from other stations has, of course, enormously increased and this has perhaps somewhat checked the increase of speed, but fortunately prevention of interference from other radio stations is a very much easier problem than the prevention of the disturbances caused by natural electric waves, or static.

Amongst the different types of tube amplifiers used in modern radio receiving stations, the tuned high-frequency and audio-frequency amplifier is probably the one which excites the greatest technical interest. In fact, its selective qualities, combined with the comparatively better ratio of signal strength to interference which it secures, justifies such interest.

These advantages were fully realized by most radio workers during the war, and I do not think that at the time the Armistice was signed there remained many radio laboratories where some time had not been utilized in experimenting on that type of receiver.

If those researches were generally not quite successful in regard to preparing or fixing the design of practical apparatus, they however indicated that the main difficulty to be overcome was to combine considerable amplification with stability and that the solution of the problem became rapidly more difficult with the increase of the number of tubes used in cascade.

By stability, in this case, I mean the freedom from any sudden generation of oscillations in any part of the circuits of the amplifier.

In 1920, however, an important step was made by Mr. G. Mathieu, as to the path to be followed out in order to obtain a practical solution of the problem. This consisted in the design of a new type of air-core tuned intervalve transformer arranged in such a manner as to possess only an extremely small electrostatic capacity between the windings, and having its effective primary impedance about equal to the effective internal plate to filament resistance of the tube in use when the secondary circuit was brought into resonance with the frequency of the oscillations to be amplified.

The results achieved during the first tests of these new transformers appeared to be quite amazing, the amplification factor for one tube having passed suddenly from 5 to about 15 for the particular tube tested, whilst the stability proved incomparably better than what had been obtained previously, even when the grid of the tube was kept to a negative potential of 1 or 2 volts.

The same principle has proved quite as successful when applied to the design of iron-core low-frequency transformers. In this case, however, it was found necessary to adopt an iron magnetic shunt between the windings so as to provide a sufficiently loose coupling between the primary and secondary circuits of the transformer. Recently, Mr. Mathieu has further improved the design of his high-frequency transformer by making it astatic.

One of these new appliances including high-frequency and low-frequency tuned transformers has been used daily on my yacht during my trip from England to America and the results of the tests carried out on board fully confirm the reliability of the apparatus and its marked superiority over the ordinary type of amplifier.

It has been clearly realized by most radio workers for some years that the science of radiotelegraphy had reached a stage of development where mere guesswork had done nearly all that could be expected from it, and that the improvement and development of commercial telegraphic services over what we once considered exceedingly long distances necessitated some very definite knowledge on the following points:

First: The strength of signals that can be relied upon with given arrangements over these distances, and

Second: The all-important question of the ratio of the strength of signals to that of the natural disturbances and interferences acting on the receiving station in various parts of the world.

First of all, suitable and reliable apparatus for the purpose of obtaining the necessary data on both these points had to be developed. This apparatus is now in systematic daily use in a good many far distant places, with the result that a vast amount of most valuable information is being collected, and is now coming to hand.

At these observation points, the signals from distant stations are measured at all times of the day and night, together with the strength of the interference of static, and also the direction or bearing from which the static appears to be coming.

The measurements are done in such a way that the power that would be required at the transmitting station to give readability is used as a measure of the static, as this is the actual thing a radio engineer requires for the proper calculation of his transmitting station.

It is a method which gives a very satisfactory and reliable result in practice, and which I think could well be used universally.

In short, this method consists in inducing in the aerial CW signals from the measuring apparatus, which signals are made equal to those received from the distant transmitting station. The voltage applied to the aerial can then be directly read off. An aerial of a standard size is used for the purpose, and from this the strength of the signals in microvolts per meter can be calculated. If the signals are then unreadable, due to static, the measuring apparatus is used to send to an operator at a standard rate of 20 words per minute, 5-letter code, and the voltage applied to the aerial from the local sender is increased until complete readability is obtained, thus the ratio of the new voltage applied to the aerial to that of the old voltage equal to that of the signals received gives at once a very correct estimate of how much the power of the transmitting station would have to be increased in order to insure readability. As this variation can be carried out on aerial systems giving direction diagrams the method is obviously of great practical utility.

The question as to whether it would or would not be possible to transmit radio signals right round the world as far as the Antipodes is one which has always fascinated me. In fact the distance to the Antipodes is the greatest possible useful distance that can be covered by radio on this little earth of ours, and from this point of view the question was also important as such a distance included all minor distances between all other places on earth.

Sixteen years ago at a lecture I delivered on the 3rd of March, 1905, before the Royal Institution in London I expressed the belief that if it were proved that transmission to the Antipodes were possible, the waves ought to go over and travel round different parts of the globe from one station to the other, and perhaps all converge and concentrate at the Antipodes, and in this way I thought it might be possible to send messages to such distant places by utilizing only a moderate amount of electrical energy; and at that lecture I also showed a model globe and tried to explain how I thought the waves would help each other if arriving in proper phase, or in other words, concentrate at places at or near the Antipodes of the sending station.

The results recently obtained and which go to show the relative facility with which radio signals can now be sent from England to Austrialia seems to indicate that there is something in the idea of the wireless waves traveling round the earth by various ways and reuniting at places near the Antipodes.

But still more interesting and precise data has been obtained during other more recent tests.

Two expeditions, one to Brazil, and the other to New Zealand, have carried out a number of most interesting and instructive observations, and although complete reports have not yet been received, I think it will nevertheless be of interest if I give you the results of some of their important tests.

The expedition to Brazil of which Mr. H. H. Beverage, of the Radio Corporation of America, Mr. N. W. Rust, of Marconi's Wireless Telegraph Company of England, and Mr. W. Eichkoff and Dr. A. Esau of the Gesellschaft für Drahtlose Telegraphie (Telefunken) of Berlin formed part, has just completed a series of observations at various points on the Atlantic Coast of South America, where the intensity of the signals from European and other stations has been observed and measured at all times of the day and night, and where also the direction and intensity of atmospherics or static has been equally observed and recorded over considerable periods of time.

Another expedition under the direction of Mr. E. Tremellen, of the English Marconi Company, has just completed its work in measuring signals from all European and American high power stations, on a journey between England and New Zealand via the Panama Canal, and from the mass of information obtained on both day and night signals it should be possible, among other things, to reconstruct the attenuation formula. Incidentally, I may say that the signals exceed greatly in strength what should be expected according to the Austin-Cohen formula, otherwise super-long-distance working would not be a practical proposition.

Complete measurements from England to the Antipodes have been made on the Carnarvon, Nauen, Bordeaux, and Hanover signals; and also in Brazil on the American high power stations and on the U. S. Naval station, N.P.O. at Cavite (Philippine Islands).

In both these expeditions to Brazil and New Zealand the fact has been noted definitely and independently, and I think for the first time, that signals from stations at very great distances do not always retain their direction along one great circle, but reach the receiver from either way or various ways round the earth.

These important observations were made by means of loop aerial direction finders arranged so as to give the well-known heart-shape diagram and the very interesting fact has been recorded independently by both expeditions, that on many occasions during what might be called a transition period, when the wave is changing from one way round the earth to another way round, the two or more sets of waves when received on a simple vertical aerial produced fairly slow beats resembling Morse signals, caused by the mutual interference or addition of the two sets of waves, whereas on the direction-finder heart-shape diagram arrangement, the signals were quite steady and normal when it was turned so as to receive only from one way or the other.

Of course it should be noted that when one is very near to the Antipodes there is only such a slight difference between any of the great circles leading from the sending station that the constancy of direction is not maintained, but this direction seemed to keep definitely true at distances of about 2000 miles from the Antipodes.

The observers noted American signals from Radio Central and from Tuckerton coming from a direction which indicated that they preferred to travel a distance of three quarters of the way round the earth, rather than come by the shortest way round. Also, according to the reports received from the observers on other occasions at or near the Antipodes of the English or German stations, the direction finder often indicated the signals as coming from directions all round.

Another interesting and rather extraordinary result was noted on several occasions, according to the report of Mr. Tremellen from Rocky Point, New Zealand, where during last March the signals from Nauen appeared to travel to him via the South Pole, whilst those from Hanover, also situated in Germany, and not very far from Nauen, appeared to prefer to travel via the North Pole.

A much more complete and exhaustive series of observations at fixed stations in Australia is now being made so as to obtain if possible all the variations from one period of the year to the other.

It seems to have been definitely ascertained in a general way that the sources of bad atmospheric disturbances, or static, are situated chiefly over land, but observations in Brazil indicate that a type of static known as "grinder" is a disturbance originating a long way off and coming from a direction which indicates the African Coast and at a time of the day when static there would be at a maximum, whereas a very violent "click" type of static came from a direction indicating its source as being nearby in South America.

During my present journey across the Atlantic, on board the Yacht *Elettra*, we noticed that up to about halfway across (apart from the effects of local storms) static interference appeared to be coming mainly from the European and African continents, while at more than halfway across they were coming from Westerly directions, that is, from the American continent.

The changing over of the direction of origin of these disturbances has also been noted under similar circumstances by Mr. Tremellen in crossing the Pacific.

It is very fortunate for the North Atlantic transatlantic radio service, carried out at stations in North America and Europe, particularly for those in Western Europe, that this strong nearby type of static comes from directions which greatly differ from those from which one has to receive, and that the continents which lie in the direction of the sending stations are so far distant and sufficiently temperate as not to project troublesome static to the receiving stations on the other side of the ocean.

Another fact which can be fairly well deduced from these tests over very great distances is that transmission from West to East is apparently easier than from East to West, and shows the necessity for qualifying or modifying the transmission formula for great distances.

A scientific paper giving the results of measurements and of all the work carried out and observations made in these two expeditions will shortly be published.

I shall now deal with another and most important branch of the science of radiotelegraphy; a branch which I might say has been for a long time most sadly neglected. It concerns the use that can be made of very short waves, especially in regard to their application to directional radiotelegraphy and radiotelephony.

Some years ago, during the war, I could not help feeling that we had perhaps got rather into a rut by confining practically all our researches and tests to what I may term long waves, or waves of some thousands of feet in length, especially as I remembered that during my very early experiments, as far back as 1895 and 1896, I had obtained some promising results with waves not more than a few inches long.

The study of short waves dates from the time of the discovery of electric waves themselves, that is, from the time of the classical experiments of Hertz and his contemporaries, for Hertz used short electric waves in all his experiments, and also made use of reflectors to prove their characteristics and to show among many other things that the waves, which he had discovered, obeyed the ordinary optical laws of reflection.

As I have already stated, short electric waves were also the first with which I experimented in the very early stages of wireless history, and I might perhaps recall the fact that when, over twenty-six years ago, I first went to England, I was able to show to the late Sir William Preece, then Engineer in Chief of the British Post Office, the transmission and reception of intelligible signals over a distance of 1¾ miles by means of short waves and reflectors (Figs. 2 and 3), whilst, curiously enough, by means of the antenna or elevated wire system, I could only get, at that time, signals over a distance of half a mile.

The progress made with the long-wave or antenna system was so rapid, so comparatively easy, and so spectacular, that it distracted practically all attention and research from the short waves, and this I think was regrettable, for there are very many problems that can be solved, and numerous most useful results to be obtained by, and only by, the use of the short-wave system.

Sir William Preece described my early tests at a meeting of the British Association for the Advancement of Science, in September, 1896, and also at a lecture he delivered before the Royal Institution in London on the 4th of June, 1897.

On the 3rd of March, 1899, I went into the matter more fully in a paper I read before the Institution of Electrical Engineers in London, to which paper I would recall your attention as being of some historical interest.

At that lecture I showed how it was possible, by means of short waves and reflectors, to project the rays in a beam in one direction only, instead of allowing them to spread all around, in such a way that they could not affect any receiver which happened to be out of the angle of propagation of the beam.

I also described tests carried out in transmitting a beam of reflected waves across country over Salisbury Plain in England, and pointed out the possible utility of such a system if applied to lighthouses and lightships, so as to enable vessels in foggy weather to locate dangerous points around the coasts.

I also showed results obtained by a reflected beam of waves projected across the lecture room, and how a receiver could be actuated and a bell rung only when the aperture of the sending reflector was directed towards the receiver.

Since these early tests of over twenty years ago practically no research work was carried out or published in regard to short waves, so far as I can ascertain, for a very long period of years.

Research along these lines did not appear easy or promising; the use of reflectors of reasonable dimensions

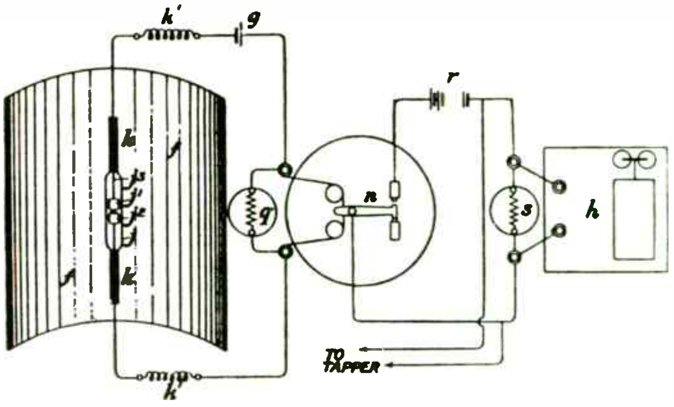

Fig. 2—Early short-wave directional receiver.

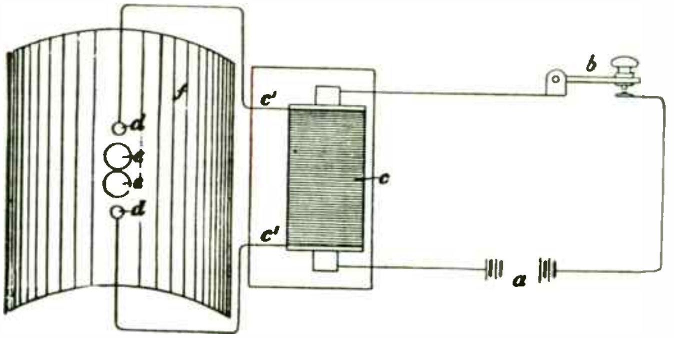

Fig. 3—Early short-wave directional transmitter.

implied the use of waves of only a few meters in length, which were difficult to produce, and, up to a comparatively recent date, the power that could be utilized by them was small. This and the fact of the very high attenuation of such waves, over any distance of land or sea, gave results which appeared to be very disappointing.

The investigation of the subject was again taken up by me in Italy early in 1916 with the idea of utilizing very short waves combined with reflectors for certain war purposes, and at subsequent tests during that year, and afterwards, I was most valuably assisted by Mr. C. S. Franklin, of the British Marconi Company.

Mr. Franklin has since then followed up the subject with great thoroughness and the results obtained have been described by him in a paper read before the Institution of Electrical Engineers in London on the 3rd of April, 1922.

Most of the facts and results which I propose to bring to your notice are taken from Mr. Franklin's paper.

The work carried out in experimenting with these waves in 1916 was most interesting, as it was like going back to the early days of wireless, when one had a perfectly clear field.

The waves used had a length of 2 meters and 3 meters. With these waves, disturbances caused by static can be said to be almost nonexistent, and the only interference experienced came from the ignition apparatus of automobiles and motor boats. These machines apparently emit electric waves from near 0 to about 40 meters in length, and the day may come when they will perhaps have to have their ignition systems screened, or carry a Government license for transmitting.

Incidentally I might mention that one of these short-wave receivers will act as an excellent device for testing, even from a distance, whether or not one's ignition is working all right. Some motorists would have a shock if they realized how often their magnetos and sparking plugs are working in a deplorably irregular manner.

During my tests in 1916, I used a coupled spark transmitter, the primary having an air condenser and spark in compressed air. By these means the amount of energy was increased and the small spark gap in compressed air appeared to have a very low resistance.

The receiver at first used was a crystal receiver, whilst the reflectors employed were made of a number of strips or wires tuned to the wave used, arranged on a cylindrical parabolic curve with the aerial in the local line.

The transmitting reflector was arranged so that it could be revolved and the effects studied at a distance on the receiver.

Mr. Franklin has calculated the polar curve of radiation into space (Fig. 4), in the horizontal plane, which should be obtained from reflectors of various apertures, by assuming that the waves leave the reflector as plane waves of uniform intensity, having a width equal to the aperture of the reflector. The calculated curves agree very well with the observed results. In Fig. 4 are shown the calculated curves for reflectors having apertures equal to 1, 2, 3, and 5 wavelengths.

Reflectors with apertures up to $3\frac{1}{2}$ wavelengths were tested, and the measured polar curves agreed very well indeed with the calculated values.

The Italian experiments showed that good directional working could always be obtained with reflectors properly proportioned in respect to the wavelength employed, and with the apparatus then available the range obtained was 6 miles.

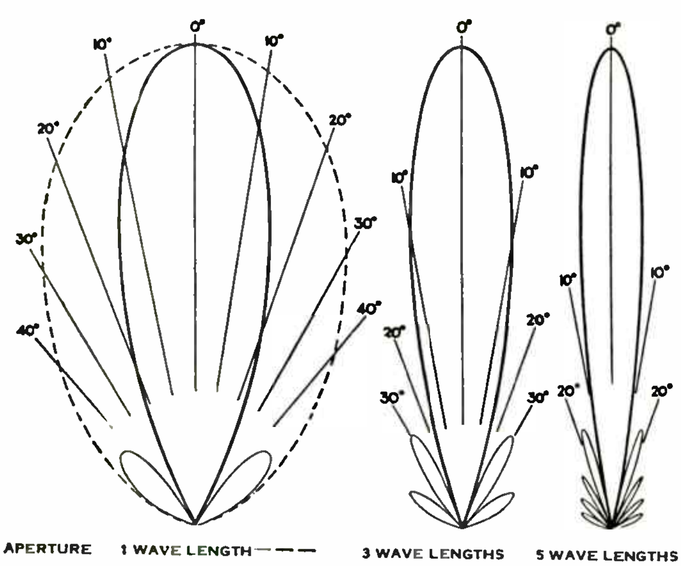

Fig. 4—Calculated polar curves of reflectors.

The tests were continued in England at Carnarvon during 1917. With an improved compressed air spark gap transmitter, a 3-meter wave, and a reflector having an aperture of 2 wavelengths and a height of 1.5 wavelengths, a range of over 20 miles was readily obtained with a receiver used without a reflector.

In 1919 further experiments were commenced by Mr. Franklin at Carnarvon for which electron tubes or valves were used to generate these very short waves, the object being to evolve a directional radiotelephonic system.

A 15-meter wave was chosen, which could quite easily be generated by the type of electron tube employed.

After overcoming a few practical difficulties, very strong and clear speech was received in Holyhead 20 miles away. Longer distance tests were next undertaken and a receiving set of apparatus was installed on one of the mail boats running between England and Ireland.

During these tests clear speech was received all the way over to the Irish coast and into Kingstown Harbour at a distance of 78 miles from Carnarvon. The important fact was also noticed that there was no rapid diminution of the strength of signals after the ship had passed the horizon line from Carnarvon.

As a result of the success of these experiments it was decided to carry out further tests over land across a distance of 97 miles between Hendon (London) and Birmingham.

It was proved at once that, with reflectors at both ends, good and clear speech could be exchanged at all times between the two places.

The following are some particulars of the arrangements employed at Hendon and at Birmingham (Figs. 5 and 6).

The power supplied to the tubes employed is usually 700 watts. The aerial is rather longer than half a wavelength and has a radiation resistance which is exceedingly high. The efficiency input to the tubes to aerial power is between 50 and 60 per cent, and about 300 watts are actually radiated into space.

With the reflectors in use at both ends speech is strong and of very good quality. It is usually strong enough to be just audible with a $\frac{1}{4}$- to $\frac{1}{2}$-ohm shunt across a 60-ohm telephone.

With both reflectors down and out of use, speech is only just audible with no shunt. Average measurements made by Mr. Franklin indicate that the value of the energy received when both reflectors are used is about 200 times that of the energy received without any reflectors.

These figures have been lately confirmed by local measurements taken round the stations.

Fig. 7 shows a measured polar curve of the field of Hendon station taken in the vicinity of the reflector. It is rather unsymmetrical in consequence perhaps of the ground being on a slope, and owing to local reflection from trees and wires.

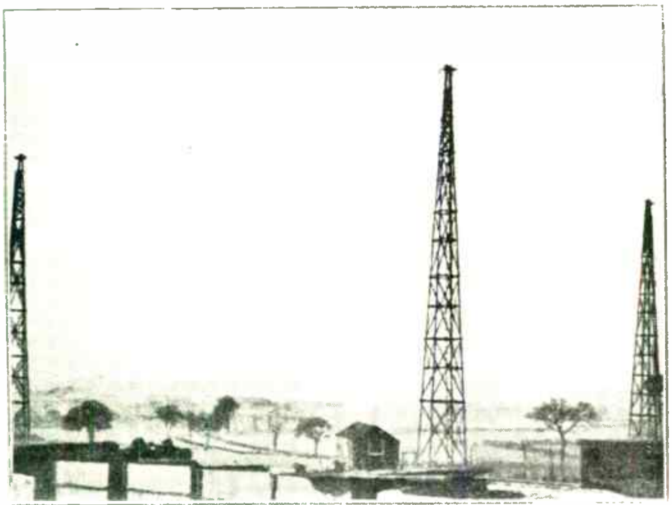

Fig. 5—Directional transmitter (Hendon).

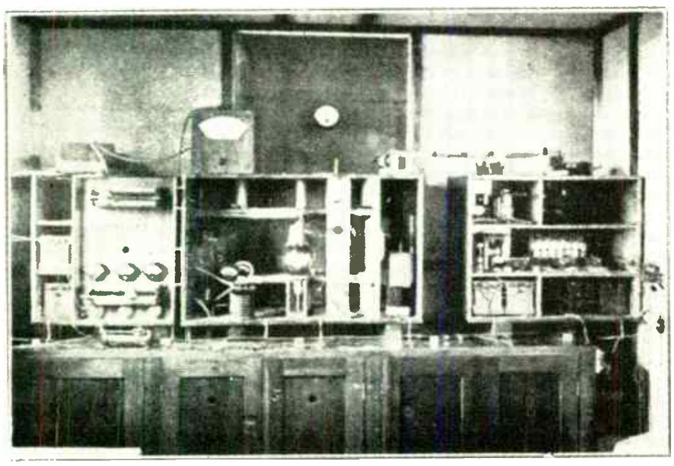

Fig. 6—Experimental short-wave transmitter and receiver at Hendon.

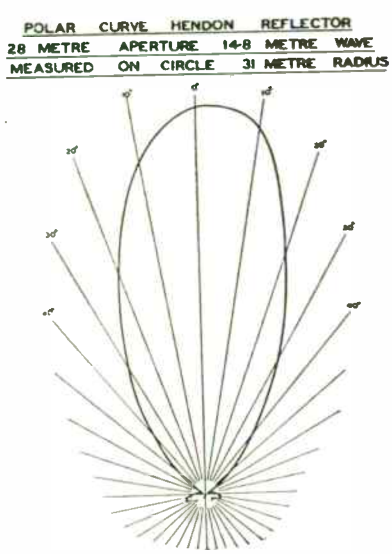

Fig. 7—Polar curve of Hendon reflector.

It has occurred to some of my assistants that a polar curve taken locally round the station may not be the same as a curve taken at a distance, and that at a distance the directional effect may be lost. I am, however, in agreement with Mr. Franklin that such is not the case.

Experiments carried out with revolving reflectors, which make it easy to read measurements at any distance, prove that the polar diagram for a given reflector and wavelength is practically constant at all ranges.

By means of suitable electron tubes or valves, it is now quite practicable to produce waves from about 12 meters and upwards utilizing a power of several kilowatts, and it is also practicable to utilize valves in parallel.

During the CW tests at Carnarvon, it was found that reception was quite possible on the transmitting aerial whilst the transmitter was operating.

This system is being used successfully for duplexing between Hendon and Birmingham, as it avoids all switching.

Reflectors besides giving directional working, and economizing power, are showing another unexpected advantage, which is probably common to all sharply directional systems. It has been noted that practically no distortion of speech takes place, such as is often noticed with nondirectional transmitters and receivers, even when using short waves.

The results between Hendon and Birmingham easily constitute a record for radiotelephony in respect to the ratio of distance to wavelength, as Birmingham, it may be interesting to note, is 10,400 wavelengths from Hendon.

We consider, however, that these results represent only what could be obtained from a first attempt, and not what could now be done after the experience gained.

It has thus been shown for the first time that electric waves of the order of 15 to 20 meters in length are quite capable of providing a good and reliable point-to-point directional service over quite considerable ranges.

In these days of broadcasting, it may still be very useful to have a practically new system which will be to a very large degree secret, when compared to the usual kind of radio.

The results obtained by reflectors appeared to be so good that I was tempted to try out my old idea of twenty-six years ago, and test the system as a position finder for ships near dangerous points. This is now being done in Scotland through the courtesy of Messrs. D. and C. Stevenson and of the Commissioners of Northern Lights. Trials are being carried out under the supervision of Mr. Franklin with a revolving reflector erected at Inchkeith Island in the Firth of Forth near Edinburgh. The transmitter and reflector, revolving, act as a kind of wireless lighthouse or beacon, and, by means of the revolving beam of electrical radiation, it is possible for ships, when within a certain distance, to ascertain in thick weather the bearing and position of the lighthouse.

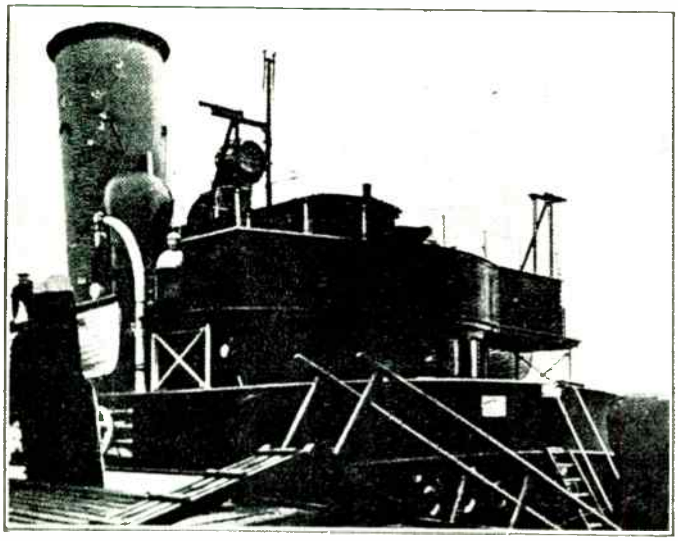

Fig. 8—Short-wave receiver on Steamship *Pharos*.

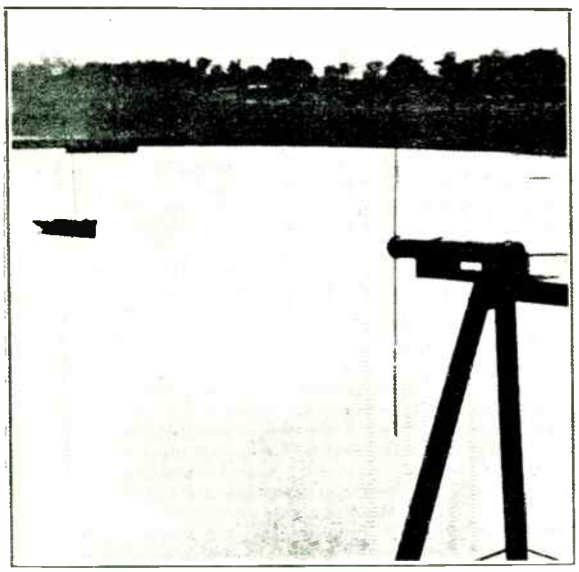

Fig. 9—Short-wave receiver.

The experimental revolving reflector was erected and the first tests were carried out with the S. S. *Pharos* during the autumn of 1920 (Fig. 8).

With a 4-meter wave spark transmitter, a reflector, and a single tube receiver, suitably tuned, on the ship, a working range of 7 miles was obtained.

The reflector was caused to make a complete revolution every two minutes, and a distinctive signal was sent every half-point of the compass. It was ascertained on the steamer that this enabled the bearing of the transmitter to be accurately determined within a quarter-point of the compass, or within 2.8 degrees. At a later date a new reflector was designed and erected and is now being tested (Fig. 12).

Fig. 10 shows measured polar curves taken recently with the new reflector. The curves were measured at a distance of 4 miles.

With the revolving beam the exact times of maximum signals are not easy to judge, by ear, but the times of

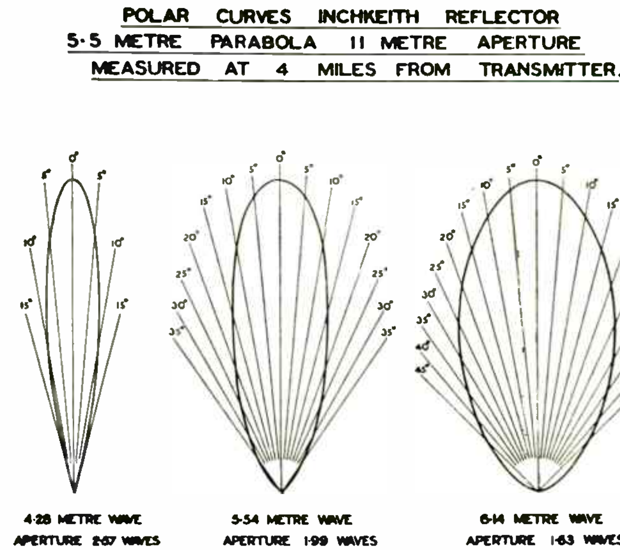

Fig. 10—Polar curves of Inchkeith reflector.

starting and vanishing are easy to determine, as the rate of rise and fall of the signals is extremely rapid. The time halfway between these two times gives, with great exactness, the moment when the beam is pointing to the ship (Fig. 11).

By means of a clockwork arrangement a distinctive letter is sent out every two points, and short signs mark intermediate points and half-points; and this is done in practice by contact segments arranged on the base of the revolving reflector, so that a definite and distinctive signal is transmitted at every half- or quarter-point of the compass (Fig. 12).

I will now try to show you the working of a roughly constructed 1-meter wave transmitter and reflector.[1]

The attenuation of these short waves over sea is so surprisingly regular that a little experience enables distance to be judged by the strength of signals, and this can be measured by means of a potentiometer.

Before I conclude I should like to refer to another possible application of these waves which, if successful, would be of great value to navigators.

As was first shown by Hertz, electric waves can be completely reflected by conducting bodies. In some of my tests I have noticed the effects of reflection and deflection of these waves by metallic objects miles away.

It seems to me that it should be possible to design apparatus by means of which a ship could radiate or project a divergent beam of these rays in any desired direction, which rays, if coming across a metallic object, such as another steamer or ship, would be reflected back to a receiver screened from the local transmitter on the sending ship, and thereby immediately reveal the presence and bearing of the other ship in fog or thick weather.

[1] At this point, Senatore Marconi demonstrated the transmission of 1-meter continuous waves from a parabolic reflector of the type shown in Fig. 3, and composed of parallel wires, over a distance of approximately 15 meters to a tube receiver with reflector similar to that of Fig. 2. Absorption of the waves by a tuned resonator was also shown—EDITOR.

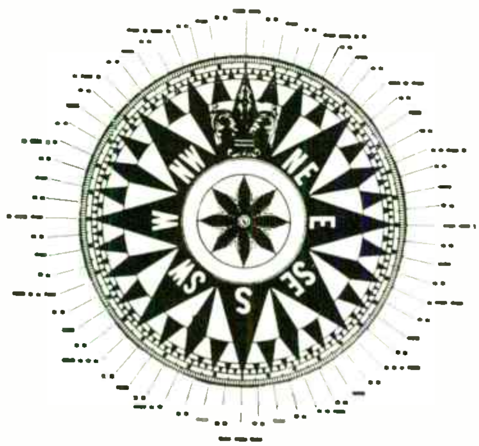

Fig. 11—Compass bearings with letter designations for radio direction finding.

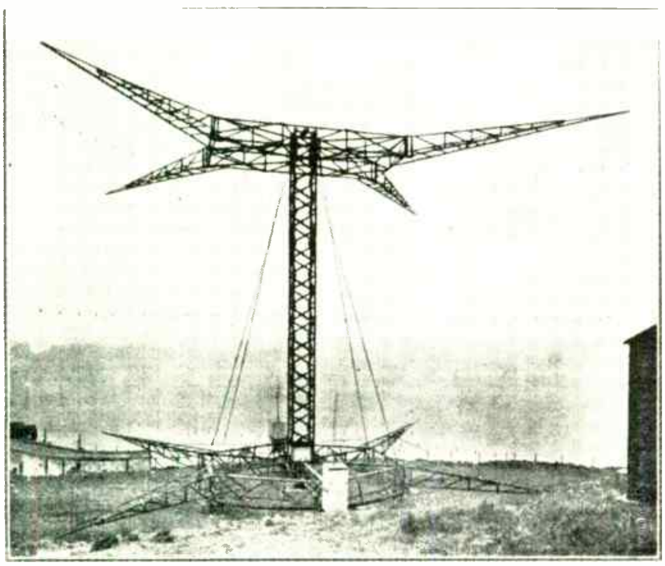

Fig. 12—Rotating short-wave directional transmitter, Inchkeith.

One further great advantage of such an arrangement would be that it would be able to give warning of the presence and bearing of ships, even should these ships be unprovided with any kind of radio.

I have brought these results and ideas to your notice as I feel—and perhaps you will agree with me—that the study of short electric waves, although sadly neglected practically all through the history of wireless, is still likely to develop in many unexpected directions, and open up new fields of profitable research.

Having referred so lengthily to what is essentially a directional system, that is, a system that does not spread its waves all round, you will perhaps expect a few words from me before I bring this rather lengthy discourse to a close, on the subject of "Broadcasting."

No remarks from me or from anyone else are required to tell you what has already been done with radio in America, as a means of broadcasting human speech, and other kinds of sound which may also be entertaining if not always instructive.

In thousands of homes in this country there are radiotelephonic receivers, and intelligent people, young and old, well able to use them—often able to make them and in many instances contributing valuable information to the general body of knowledge concerning the problems great and small of radiotelegraphy and radiotelephony.

But I think I am safe in saying that if radio has already done so much for the safety of life at sea, for commerce, and for commercial and military communications it is also destined to bring new and, until recently, unforeseen opportunities for healthy recreation and instruction into the lives of millions of human beings.

Abstract

The lecture first deals briefly with the early history of long distance radio communication.

The work carried out by the engineers and experts of the Marconi Company in England with electron tubes or triode valves shows that, according to their experience, greater efficiency can be obtained at present by a number of bulbs used in parallel than by the employment of large single unit tubes.

Information is given in a general way in regard to recent practice in the design and construction of receivers with the object especially of improving selectivity, reducing interference, and concerning the possible speed of working.

The lecture also deals briefly with results obtained at receiving observation stations situated in various far distant parts of the world, where it has been ascertained that radio signals arriving from high power stations situated at or near the antipodes of the observation stations, reach the receivers by various ways around the earth, not always following the shortest great circle route, and also that at such places the electric waves coming round by different ways do in certain cases increase this effect on the receivers whilst in others interfere with each other.

It has also been noticed that apparently transmission is easier from west to east than from east to west, and that it may be necessary to modify somewhat the transmission formula for long distances.

It has also been ascertained that the most troublesome atmospheric disturbances or static usually come from the continents and not from the oceans.

The lecture further deals with a study of short electrical waves and the results which have been obtained with such waves of a length from 1 meter to 20 meters, and describes tests which show for the first time that electric waves of under 20 meters in length, used in connection with suitable reflectors, are quite capable of providing a good and reliable point-to-point, unidirectional system of radio over quite considerable distances.

The application of this system as a direction finder in aid of navigation, and as a method for preventing collisions at sea, is also dealt with.

The Engineer and the Life Sciences*

J. H. U. BROWN†, SENIOR MEMBER, IRE

Summary—**Within recent years the life sciences have realized the significance of the contributions which can be made by the engineer, and the engineering sciences are beginning to realize the value of the contributions which can be made by the life sciences in bionics. A new field has developed which may be called bio-medical engineering. The National Institutes of Health is now engaged in a program designed to provide support in research, training, and facilities for this broad area. Support will be largely in the field of the application of engineering theory to the biological sciences, and may not include some of the aspects of applied engineering or instrumentation except as they arise as a result of theoretical development.**

WITHIN THE LAST few years a new science has arisen which is bridging the gap between the engineer and the life sciences. This area has been called life science engineering, bio-medical engineering, biosciences engineering, bioengineering, and a variety of other names. It includes widely divergent areas embracing cybernetics, bionics, and medical electronics. It may be included as portion of the area known as biophysics.

This area is not composed of a homogeneous group of laboratories or individuals. Research interests can and do range through all forms of engineering (mechanical, electrical, chemical), all forms of life science (clinical medicine to pure biology), and many phases of physics and mathematics. By the same token, researchers in the area can represent several different levels of training and capability. It is apparent that the top level should be composed of individuals holding the doctoral degree in engineering or a life science with adequate training in the corollary disciplines and who will be capable of initiating research, developing basic theory and training the upcoming generation of bio-medical engineers. Below this will be a competent group of scientists at the Master's level who can develop sophisticated instrumentation for a particular research project and assist in carrying out the programs of a senior investigator. At a still lower level will be the Bachelor of Science in engineering with perhaps some training in the biological sciences who will serve as a very high grade technical associate. Still lower may be the usual electronics technician.

It should also be emphasized at the outset that the word "engineering" does not here refer to construction, design, or architectural applications of design, but to the abstract engineering theory which is founded in mathematics and in physical concepts.

This new engineering includes a previously unmentioned aspect—that of data collection. As finer techniques are developed for the recognition of variables in biological systems, mountains of data will accumulate requiring reduction, analysis, evaluation, and statistical correlation. This type of problem can be solved *only* by computers—and computer theory and design is another form of engineering. The importance of the field is shown by the establishment of computer centers at many universities about the country. As biological data become more complex, engineering will be needed to produce the right type of computer to handle the information. The computer engineer will need to know a great deal of biology in order to understand the type of information wanted and the correct method to obtain that information.

Over and above theoretical applications of engineering to the biological sciences mentioned above, a more practical joint endeavor has now developed. The instruments used by the medical scientist have become more and more complex. The extension of investigations into the micro, submicro, and atomic realms has led to greater requirements of sensitivity, accuracy, and compactness. The simultaneous measurement of many variables in this region, the study of transient phenomena, the recording of rate processes, and many other experimental problems require transducers which have not yet been designed or built.

Too often the biological scientist has envisioned a method of approach to a specific problem through engineering, has read on the subject, partially designed an apparatus and had it constructed by an electronics technician only to find that the engineering lack has produced a less than satisfactory instrument. The reverse is also true. Engineers called in consultation on a particular problem will produce designs perfectly satisfactory from an engineering viewpoint only to find that the peculiar properties of biological systems make the design inoperable. Examples of both cases are legion.

The engineering and basic life sciences can carry out a mutually advantageous cooperative program in at least three major areas of science:

1) Design of experiments, their instrumentation, and the processing of data.
2) Development of *new* experimental methods combining the best features of both fields.
3) Design of physical models of many complex biological systems which will aid in understanding and analysis.

Ideally, the solution would be to have a single individual competent in both fields, *i.e.*, a man with an advanced degree in engineering and a similar degree in

* Received April 27, 1962.
† Division of General Medical Sciences, National Institutes of Health, Bethesda, Md.

one of the medical sciences. This presupposes an individual with time to take 8 years of graduate study before entering into the field. In practice, a collaborative approach is the present solution. In this arrangement, both men trained in engineering with a good background in medical science and men trained in the basic medical sciences but with a good background in engineering could be brought together for cooperative training and research. As the area of bio-medical engineering develops it is anticipated that undergraduate programs will emerge. This will provide the foundations for graduate programs in the field and a broadly trained individual will finally be produced. The retraining of biologists or engineers in the ancillary field is at best a stop gap measure.

The addition of simple biological knowledge to an engineer or of simple engineering concepts to a biologist is not sufficient even for those engaged in such cooperative effort. The person so trained is still a technician, unable to think in conceptual terms in the field in which he is not primarily trained. This is demonstrated by the fact that many engineers could design an apparatus if given a clear statement of its requirements. However, the biologist cannot formulate his needs in engineering terms, and the engineer cannot understand the design in biological terms. The problem becomes more acute when it is realized that a major task of individuals and groups in this new field will be to develop and organize basic knowledge in the engineering principles for biological systems.

The foregoing exposition has been presented to illustrate the need for bio-medical engineers as distinguished from the instrument engineers, and to distinguish engineering from instrumentation. There is ample evidence that the number of individuals in either of the above groups is small. In order to secure a continuing supply in sufficient number, training programs must be expanded. As training programs can only be conducted on a satisfactory level by the Ph.D. bio-medical engineer, it is apparent that the number of such people must be increased. At the present, the time required for training a Ph.D. in bio-medical engineering after high school is about 9 years. On this time scale, it is obvious that any plans made now will reach fruition in the year 1970 when the present entering group will finally enter active work in the area. All plans must be based on numbers to be expected approximately 10 years in the future rather than on present demand. At the present time and for the last 10–15 years, the size of the bio-medical engineering area has been doubling every $2\frac{1}{2}$ years. On this basis, about three generations of doubling will occur by 1970. At the moment, about \$20,000,000 per year is spent on research in this area which suggests a budget of \$150,000,000 per year by 1970.

In order to provide the best training, special courses in bio-medical engineering must be arranged at both the graduate and undergraduate level with the closest possible cooperation between the life science and engineering faculties. Programs of this type are under development (Table I).

TABLE I

PARTIAL LIST OF PROGRAMS IN BIO-MEDICAL ENGINEERING NOW IN OPERATION OR IN DEVELOPMENT IN THE UNITED STATES

Operating Programs	Programs Under Development
University of California (L.A.)	Bowman Gray School of Medicine
Drexel Institute	University of California (Berkeley)
University of Illinois	Case Institute of Technology
Iowa State University	Duke University
Johns Hopkins University	University of Kentucky
Massachusetts Institute of Technology	Marquette University
University of Minnesota	University of Michigan
Northwestern University	University of Missouri
University of Pennsylvania	University of Nebraska
University of Rochester	New York University
Stanford University	University of North Carolina
University of Washington (Seattle)	University of Wyoming

It is generally agreed that in order to do competent work at a given location in this field in both research and training, a nucleus of several individuals is necessary. The minimum size is generally presumed to be about that of a small basic-science department (4 or 5 people). This presupposes that with the present programs, about 100 individuals at the Ph.D. level could be comfortably used in the departments or groups now in operation.

In addition to the nucleus of trained individuals in the departments directly interested in engineering, there is a steady demand for such people in many other departments of the medical school and in the basic biological and physical sciences. These range from the technician who can devise or repair a minor instrument to the highly trained engineer who can produce mathematical models of biological systems. Demands exist today in departments of surgery, medicine, physiology, biophysics, physics, and radiology, with current estimates indicating that 100 Ph.D. engineers could be placed immediately. Various industrial groups are also on a constant lookout for the trained bioengineer. Most of the companies making biological instruments desire such individuals. Demand also exists for such engineers in aviation, computer facilities, and telephone laboratories. The current estimate is for about 200 men this year. Present estimates of NASA indicate that the space program in the Government will absorb 100 engineers and that these demands will increase. Contractors of NASA will need many more as the space program expands (3.5 billion in 1962). The NASA programs are 5 per cent "in house" and 95 per cent by grant and contract. Conservative estimates indicate that 500 bio-medical engineers could be utilized in 1962. With current plans for expansion the number may be 1500 or many more by 1970. By the most conservative estimates training programs should accommodate approximately 20 times as many graduates as at present in order to meet the current demand. This does not take into account the sudden spurt which may occur (as happened in biophysics) when trained individuals begin to enter the field and influence the future development of the science.

A critical evaluation cannot be made at this time of factors which may affect markedly the demand within the next few years. The newer work in cybernetics and bionics, dealing with the interaction of man and machine, may lead to a technical revolution and a greater demand for workers in the borderland between the two areas. We have now reached the stage where physical devices are necessary to provide extension of sensory manipulative capability in order to observe new phenomena. Only the researcher conversant with the coupling of man and machine can make significant contributions in this new field.

Not only must the increased production of bio-medical engineers be considered, but the type of research which is carried out must be considered. There are several methods of approach to research in this general area:

1) An instrument may be built without a clear understanding of what it is supposed to accomplish. An electronics technician can build a "black box" and build it build better than an engineer, once he has specifications.

2) The biologist may formulate an idea such as "I want to measure blood flow" and the engineer produces an instrument for him to do the precise measurement desired. This is one step higher than the function of the technician and obviously is necessary.

3) The engineer and the biologist may work together to develop a new transducer to measure a parameter in a biological system. This is applied engineering.

4) The bio-medical engineer may develop the concepts of a new physical system, formulate the necessary mathematics or models, design the apparatus for the research, and carry out an independent investigation. This is the highest form of engineering science.

Each of these is necessary and each performs a vital function. If the field is to advance as a whole and not become an ancillary science to medicine operating in much the manner as the clinical laboratory, it must have many of the engineers engaged in true conceptual processes.

The mechanics of organization for such an engineering group are not difficult to imagine. Several types of organization can operate and be successful depending upon the location of the unit. Examples might be:

1) A division within a department in which the group performs a function of bio-medical nature within an electrical engineering, a physiology, or some other department.

2) A department of bio-medical engineering in which an independent department with all rights and privileges within a university is created.

3) An institute for bio-medical engineering where all members of this discipline are brought together for a common purpose in a separate installation.

4) A center where the members of the group are members of independent departments (physiology, engineering, etc.) and come together with a common aim for research and training.

The National Institutes of Health supports about 40 per cent of the health-related research in this country, and it will also support bio-medical engineering. Such support may assume a variety of forms depending upon the needs of the individual and the project:

1) The *Research Grant* consists of a grant to an institution on behalf of an individual and is designed to supply the equipment, technical assistance, supplies, and any other necessities for carrying out a given research aim. Such grants usually are awarded for projects with definite aims and with some indication of past performance on the part of the individual.

2) The *Program Project Grant* is an award made to an institution on behalf of several individuals engaged in a single area of research. Such a grant presupposes the existence of several individuals competent in the general area of research, and further presupposes active research in progress. Such a grant would supply major items for use by an entire group such as an electronics shop, a tube making facility, a machine shop, a computer, and other items necessary for carrying out the research aims of the group.

3) The *Special Resource Grant* will supply a facility for general support of research in an area such as bio-medical engineering to an institution or to a region of the country encompassing several institutions.

4) The *Fellowships Program*. Many fellowships are available for support of individuals engaged in training or in research. Regular Research Fellowships are awarded for the full-time research training of scientists in the fundamental biological and health-related sciences. They are available at the predoctoral and postdoctoral levels and at the special level. These awards are made for periods of from 1 year to 3 or 4 years in the recognized preclinical sciences and also in other rapidly developing fields, such as genetics and developmental sciences, basic endocrinology, biophysical sciences, bio-medical engineering, experimental pathology, immunology and immunochemistry.

Predoctoral Fellowships provide opportunities for full-time training at an early age. This level of training has proven to be a source of stimulation to qualified students interested in a career in research in the health sciences.

Postdoctoral Fellowships are awarded to selected, promising holders of the Ph.D., D.Sc., M.D., D.V.M., D.D.S., and D.P.H. degrees who are interested in undertaking advanced research training in the basic health sciences.

Special Fellowships are awarded to accomplished researchers for from six months to a year who require further specialized training or knowledge of new techniques or disciplines in order to increase their research productivity and to broaden their fields of scientific interest.

The *Career Development Award* is made to young faculty members to allow greater freedom in the development of a career of research.

The *Career Research Award* is made to senior faculty to increase research time.

Each of these has different requirements in that some can be applied for by the individual and others must be directly requested by the institution.

5) The *Training Grant Program* is a grant made to the institution on behalf of a program director to support a program in graduate research training usually leading to an advanced degree. Such programs are usually awarded on the basis of an operating program with several individuals representing various skills within the training area. Such grants will supply funds for stipends, tuition, supplies, modest equipment, faculty for teaching and other items necessary to the program.

Any or all of these sources of support may be utilized by a group interested in the development of biomedical engineering. Further information can be secured from the Division of General Medical Sciences or the Division of Research Grants, National Institutes of Health.

Each grant application from the National Institutes of Health, whether for training or research, is given two independent reviews. The application, submitted on standard forms, first is reviewed for scientific merit by a Study Section or Training Committee composed of a group of individuals capable of judging the scientific merit of the project. These groups recommend the grant application for approval, disapproval, or deferral for further study. If recommended for approval, it is assigned a priority score in accordance with its merit compared to similar grants in the field. The application with its recommendation is then subjected to a second review by the appropriate National Advisory Council which also recommends the application for approval, disapproval, or deferral. Approval at this stage results in a recommendation to the Surgeon Gen-

TABLE II
BIO-MEDICAL ENGINEERING PROGRAMS IN EXISTENCE AT THE PRESENT TIME

Location	Director	Degree	Curriculum	Students	Number of Students
University of California (L.A.)	John Lyman	Ph.D.	Engineering Psychology Human Factors	Engineers Psychologists Basic Scientists	20
Baylor University	L. L. Geddes	M.A. Ph.D.	Largely experimental physiology	Any eligible graduate student	3
Drexel Institute	James Dow	M.S.	$\frac{1}{4}$ biology, anatomy at Drexel, $\frac{3}{4}$ joint courses in control systems, computers, etc.	Engineers, Life scientists (M.D.)	20
Iowa State University	Victor Bolie	M.S. Ph.D.	Special courses in basic sciences and bio-medical engineering taught by group	Any eligible graduate student	12
Johns Hopkins University	S. A. Talbot	Ph.D.	Work in engineering but take special courses in physiology, biochemistry	Engineers (Electrical, Mechanical, Chemical)	6
University of Kentucky	K. O. Lange	M.S.	Largely mechanical engineering. Little physiology. Aeromedical in content	Engineering students	10
Marquette University	Saul Larks	M.S.*	Electrical engineering Fetal physiology	Electrical Engineers	4
University of Minnesota	Otto Schmitt	Ph.D. M.S.	Biophysics and bio-medical engineering	Engineers, Physicists, Biologists, M.D.'s	8
New York University	J. I. Hirsch	Ph.D.	Not formalized	M.D.	1
North Carolina State College	A. R. Eckels	Ph.D.	Routine engineering with biology taken at North Carolina Medical School	Engineers (E.E.)	2
Northwestern University	J. E. Jacobs	Ph.D.	Engineering and medical basic science courses	Mostly E.E. May be biology majors or M.D.	15
University of Pennsylvania	Herman Schwan	Ph.D. None*	Math 11 hrs. Bio-Medical Engineering as joint course. Organic Chemistry, Physiology, Biochemistry	Engineers (Electrical, Mechanical, Chemical)	13
University of Rochester	Daniel Healy	Ph.D. (E.E.)	Seminar in Bio-Medical Engineering. 15 hrs. Chemistry and Biology, 33 hrs. Engineering	E.E.'s	6
University of Washington (Seattle)	R. Rushmer	Ph.D. M.S. None*	Graduate students in physiology take regular courses. Summer courses in bio-medical engineering are short term offerings	Any eligible student may include M.D., Ph.D., Engineers, Graduate students	25

* A nondegree course is also offered.

eral to award the grant. The Surgeon General or his designated official may then decide on the basis of available funds how many of the approved applications can be paid.

It is apparent that most of the programs in the area of bio-medical engineering will be centered largely in universities regardless of the financial arrangements. However, most universities object strongly to instrumentation as a topic for research. The primary function of a university is teaching and research, and most engineering departments consider instrumentation as the straightforward application of known principles, and therefore unsuitable for a doctoral dissertation topic. Such attitudes should be maintained.

From the above discussion, it is apparent that the unit for bio-medical engineering will have to be above a certain size in order to be effective. Rather elaborate equipment and shop facilities are usually required. This presupposes that the operating expenses of such a group will not be small. A countrywide consensus of opinion makes several important points in this regard:

1) Money should not be dissipated on many small projects which are not capable of a direct unified approach to a problem.
2) Money should not be expended primarily on a very few extremely large projects which are less productive in terms of unit cost.
3) Money should be spent on a number of projects which may vary widely in scope but where reasonable return for outlay can be expected.
4) Money should be available to those groups developing a conceptual approach to bio-medical engineering, but should not be given to those interested in instrumentation alone. Too often such instrumentation is of value only to the individual producing it.

Several training programs in bio-medical engineering are now in operation and others are in the planning stage. Table II summarizes information about the current programs which have actually graduated students in the general area. It will be apparent that most of the programs are centered in engineering schools and offer the advanced degree in this framework. The few programs which are not in this framework (Baylor University, University of Washington, and Iowa State University) are centered in departments of physiology. There is no reason why such programs could not be in other engineering departments or in biological frameworks other than those mentioned.

In summary, bio-medical engineering is emerging as a new science in the area between the life sciences and engineering. The National Institutes of Health is prepared to provide support for both research and graduate training to worthy programs in this area. The responsibility for the quality of the research and training rests as squarely upon the shoulders of the engineer as it does upon the doctor. Together they must meet the challenge.

Group Theory and the Energy Band Structure of Semiconductors*

ALLEN NUSSBAUM†, ASSOCIATE, IRE

***Summary*—The purpose of this paper is to present the principles involved in calculating the energy band structures of semiconductors. These calculations can be simplified by the use of group theory, which is a branch of analysis that permits expressing the symmetry properties of crystals in a quantitative manner. Some of the simpler concepts of group theory are explained and then applied to band structure determinations.**

* Received September 13, 1961; revised manuscript received March 15, 1962. This work was supported in part by the U. S. Air Force Office of Scientific Research.

† Department of Electrical Engineering, University of Minnesota, Minneapolis, Minn.

I. Introduction

For a special issue of the Proceedings devoted to solid-state physics, Dr. F. Herman[1] of the RCA Laboratories contributed a paper discussing the electronic band structure of silicon and germanium. In the present paper, we should like to show how these structures are determined and how they are related to the crystal structure of semiconductors. The

[1] F. Herman, "The electronic energy band structure of silicon and germanium," Proc. IRE, vol. 43, pp. 1703–1732; December, 1955.

methods employed for energy band calculations involve taking advantage of the symmetry of the crystal to reduce the quantity of tedious calculations necessary; the branch of mathematics which enables us to express symmetry properties in a quantitative way is called *group theory*. Hence, our first step will be to examine the basic concepts of this subject.

II. Algebra of Groups

A *group* is defined[2] as a collection of elements A, B, C, $\cdots$ which obey the following combinatory laws:

1) The product of any two elements in the collection is also a member of the collection.
2) The collection contains an identity or unit operation E (from the German *einheit*, unity) such that $EA = AE = A$ for every element.
3) The associative law of multiplication holds: $(AB)C = A(BC)$.
4) Every element A has a unique inverse A^{-1} which is a member of the collection. That is, $AA^{-1} = A^{-1}A = E$.

Example: Consider the equilateral triangle of Fig. 1. The operations which leave this triangle congruent to its original position are:

1) E, the identity.
2) A, a reflection in line Aa.
3) B, a reflection in line Bb.
4) C, a reflection in line Cc.
5) D, a 120° clockwise rotation.
6) F, a 120° counterclockwise (or a 240° clockwise) rotation.

It is easily seen that

$$AD = B \tag{1}$$

where the convention is used that operation D is followed by operation A and that the lines Aa, Bb, and Cc remain fixed in the plane. We note that

$$DA = C \neq B.$$

All such products are summarized in Table I, the group multiplication table. The total number of elements g is called the *order* of the group, so that $g = 6$.

A *subgroup* is a portion of a group which obeys the combinatory laws. Table I shows that some subgroups of the group E, A, B, C, D, F are a) E, b) E, A, and c) E, D, F. Note that the order of the subgroups is a factor of the order of the group.

Groups can also be divided into *classes*, which are collections of related operations. Two elements P and Q belong to the same class if

$$Q = X^{-1}PX, \tag{2}$$

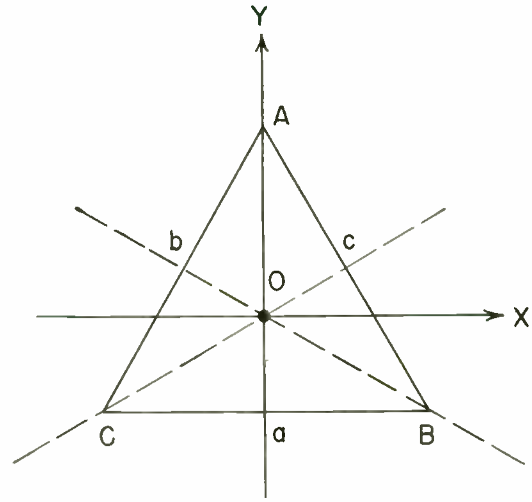

Fig. 1—The symmetry axes of the equilateral triangle.

TABLE I

Multiplication (or Cayley) Table for Symmetry Operations of an Equilateral Triangle

Second Operation \ First Operation	E	A	B	C	D	F
E	E	A	B	C	D	F
A	A	E	D	F	B	C
B	B	F	E	D	C	A
C	C	D	F	E	A	B
D	D	C	A	B	F	E
F	F	B	C	A	E	D

where X is any member of the group. For example

$$A^{-1}DA = A^{-1}C = AC = F,$$
$$A^{-1}FA = AB = D,$$

so that D and F constitute a class. Similarly, so does E and also A, B, C. Hence, the group is broken down into three classes: reflections, rotations, and the identity. For this group, we can separate the operations into classes from physical considerations. However, this does not always work, and it is safer to go through the labor involved in applying definition (2).

III. The Representations of a Group

A *representation* of a group is any collection of elements which obey the group multiplication table. For example, a representation can be obtained by considering the matrices associated with rotations and reflections in a plane. Fig. 2(a) shows the rotation of a vector r through an angle θ, and the two sets of coordinates of

[2] H. Eyring, J. Walter, and G. E. Kimball, "Quantum Chemistry," John Wiley and Sons, Inc., New York, N. Y.; 1944.

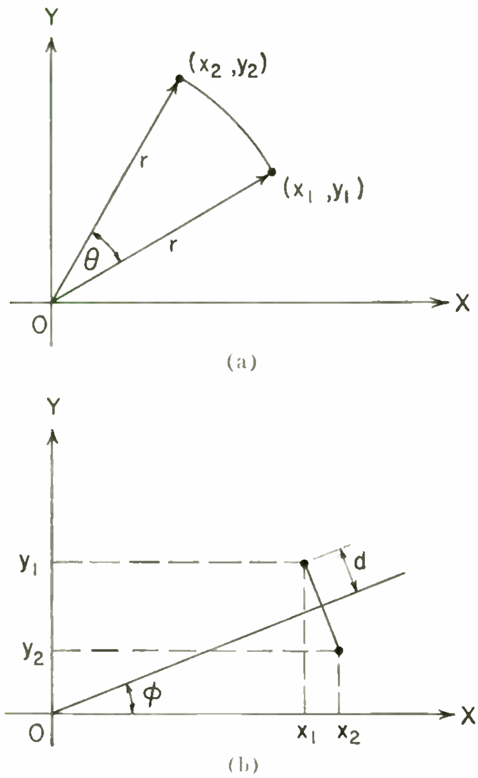

Fig. 2—(a) A rotation. (b) A reflection.

$$\begin{Bmatrix} x_2 \\ y_2 \end{Bmatrix} = \begin{bmatrix} \cos 2\phi & \sin 2\phi \\ \sin 2\phi & -\cos 2\phi \end{bmatrix} \begin{Bmatrix} x_1 \\ y_1 \end{Bmatrix}. \tag{4}$$

Using the matrices given in (3) and (4), we can obtain the representation denoted by Γ_3 in Table II (it is customary to use the symbol Γ to denote some representations). It is left to the reader to verify that the six matrices of Γ_3 multiply as required by Table I. Note that the matrices belonging to Γ_3 are based on the axes XOY being oriented as shown in Fig. 1.

The representation Γ_3 is two-dimensional; that is, it consists of 2×2 matrices. Every group also has a one-dimensional representation of the form $E=A=B=C=D=F=1$, denoted by Γ_1 in Table II. This representation is said to be *unfaithful;* it leads to all the entries of Table I, plus many others which violate the table. Another one-dimensional representation, denoted Γ_2 in Table II, is also unfaithful. We shall show later a systematic method for obtaining these representations, and also explain the notation.

It is also possible to find representations of higher dimensions. Suppose we specify the position of the corners of the equilateral triangle by a pair of coordinates r and α, as shown in Fig. 3. The symmetry operations of Section II can then be represented as 6×6 matrices.

TABLE II

IRREDUCIBLE REPRESENTATIONS FOR THE GROUP OF TABLE I

	E	A	B	C	D	F
Γ_1	1	1	1	1	1	1
Γ_2	1	−1	−1	−1	1	1
Γ_3	$\begin{pmatrix} 1 & 0 \\ 0 & 1 \end{pmatrix}$	$\begin{pmatrix} -1 & 0 \\ 0 & 1 \end{pmatrix}$	$\begin{pmatrix} \frac{1}{2} & -\sqrt{3}/2 \\ -\sqrt{3}/2 & -\frac{1}{2} \end{pmatrix}$	$\begin{pmatrix} \frac{1}{2} & \sqrt{3}/2 \\ \sqrt{3}/2 & -\frac{1}{2} \end{pmatrix}$	$\begin{pmatrix} -\frac{1}{2} & \sqrt{3}/2 \\ -\sqrt{3}/2 & -\frac{1}{2} \end{pmatrix}$	$\begin{pmatrix} -\frac{1}{2} & -\sqrt{3}/2 \\ \sqrt{3}/2 & -\frac{1}{2} \end{pmatrix}$

the vector are related by[3]

$$\begin{Bmatrix} x_2 \\ y_2 \end{Bmatrix} = \begin{bmatrix} \cos\theta & -\sin\theta \\ \sin\theta & \cos\theta \end{bmatrix} \begin{Bmatrix} x_1 \\ y_1 \end{Bmatrix}. \tag{3}$$

Fig. 2(b) shows the reflection of a point (x_1, y_1) in a line making an angle ϕ with the x axis to produce a point (x_2, y_2). The two sets of coordinates are related by

$$x_2 = x_1 + 2d \sin\phi,$$
$$y_2 = y_1 - 2d \cos\phi,$$

from which

For example, the effect of C (a reflection in the line OC) can be denoted by

$$\begin{bmatrix} 0 & 0 & 1 & 0 & 0 & 0 \\ 0 & 1 & 0 & 0 & 0 & 0 \\ 1 & 0 & 0 & 0 & 0 & 0 \\ 0 & 0 & 0 & 0 & 0 & 1 \\ 0 & 0 & 0 & 0 & 1 & 0 \\ 0 & 0 & 0 & 1 & 0 & 0 \end{bmatrix} \begin{Bmatrix} r_1 \\ r_2 \\ r_3 \\ \alpha_1 \\ \alpha_2 \\ \alpha_3 \end{Bmatrix} = \begin{Bmatrix} r_3 \\ r_2 \\ r_1 \\ \alpha_3 \\ \alpha_2 \\ \alpha_1 \end{Bmatrix}. \tag{5}$$

A similar 6×6 matrix can be obtained for the other five operations of the group and it will be found that these six matrices obey the group multiplication table and hence form a representation Γ_4. We shall denote the matrices in Γ_4 by $\Gamma_4(C)$, etc.

[3] An excellent discussion of matrix algebra is given in ch. 6 of R. S. Burington and C. C. Torrance, "Higher Mathematics," McGraw-Hill Book Co., Inc., New York, N. Y.; 1939. The concepts used in this paper are covered more briefly in Appendix A4 of Nussbaum, (reference 4).

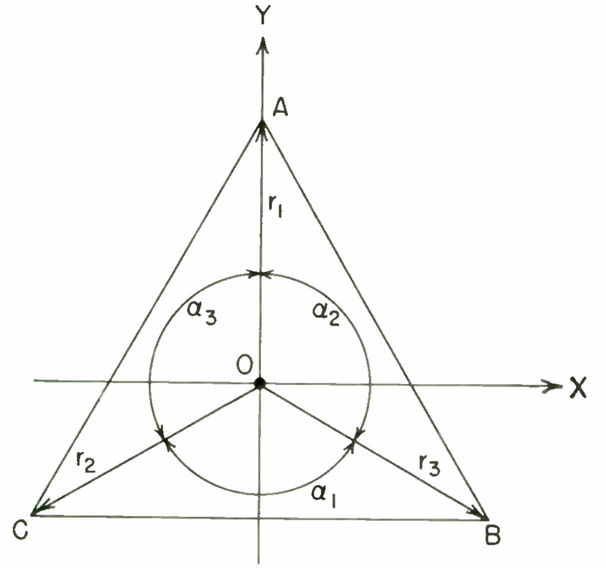

Fig. 3—The coordinates used to establish the reducible representation for the equilateral triangle symmetry group.

Now consider the matrix

$$\mathbf{S} = \begin{bmatrix} 1/\sqrt{3} & 0 & -\sqrt{2}/\sqrt{3} & 0 & 0 & 0 \\ 1/\sqrt{3} & 1/\sqrt{2} & 1/\sqrt{6} & 0 & 0 & 0 \\ 1/\sqrt{3} & -1/\sqrt{2} & 1/\sqrt{6} & 0 & 0 & 0 \\ 0 & 0 & 0 & 1/\sqrt{3} & 0 & -\sqrt{2}/\sqrt{3} \\ 0 & 0 & 0 & 1/\sqrt{3} & 1/\sqrt{2} & 1/\sqrt{6} \\ 0 & 0 & 0 & 1/\sqrt{3} & -1/\sqrt{2} & 1/\sqrt{6} \end{bmatrix} \tag{6}$$

Let us define a new matrix $\Gamma_4'(C)$ obtained from $\Gamma_4(C)$ as follows:

$$\Gamma_4'(C) = \mathbf{S}^{-1}\Gamma_4(C)\mathbf{S} = \begin{bmatrix} 1 & 0 & 0 & 0 & 0 & 0 \\ 0 & 1/2 & \sqrt{3}/2 & 0 & 0 & 0 \\ 0 & \sqrt{3}/2 & -1/2 & 0 & 0 & 0 \\ 0 & 0 & 0 & 1 & 0 & 0 \\ 0 & 0 & 0 & 0 & 1/2 & \sqrt{3}/2 \\ 0 & 0 & 0 & 0 & \sqrt{3}/2 & -1/2 \end{bmatrix} \tag{7}$$

This is of the form

$$\Gamma_4'(C) = \begin{bmatrix} \boxed{\Gamma_3(C)} & & & 0 \\ & \boxed{\Gamma_1(C)} & & \\ & & \boxed{\Gamma_3(C)} & \\ 0 & & & \boxed{\Gamma_1(C)} \end{bmatrix} \tag{8}$$

and the matrix $\Gamma_4(C)$ is said to be *reduced*. The matrix $\Gamma_4'(C)$ is said to *contain* the representations Γ_1 and Γ_3 twice each. It will be found that the same matrix S and its inverse reduces all the 6×6 matrices in Γ_4 to the form of (8). It is not possible to find any other matrix which will further reduce the six matrices in Γ_4' nor further reduce Γ_3 to 1×1 matrices lying on the main diagonal. Hence Γ_1, Γ_2, and Γ_3 are *irreducible representations*, whereas Γ_4 is a reducible representation containing Γ_1 and Γ_3.

IV. The Character System of a Representation

In applying group theory, it is seldom necessary to know the matrices which form a representation. Generally, all that is needed is the *trace* of each matrix (the trace is defined as the sum of the elements on the main diagonal); the set of traces of the matrices in a representation is called the *character* of the representation. Table III is the character table for the four representations we have been considering. The double lines separate the three classes, and we see that all elements in the same class of a given representation have the same character, thus explaining in part the origin of the term. The table illustrates the following very important relation between the characters of reducible and irreducible representations

TABLE III

Characters of the Representations for the Group of Table I

	E	A	B	C	D	F
Γ_1	1	1	1	1	1	1
Γ_2	1	-1	-1	-1	1	1
Γ_3	2	0	0	0	-1	-1
Γ_4	6	2	2	2	0	0

$$n_k = \left[\sum_R \chi(R)\chi_k(R)\right] \Big/ k, \tag{9}$$

where

n_k = number of times the kth irreducible representation is contained in the reducible one,
$\chi(R)$ = character of the matrix R for the reducible representation,
$\chi_k(R)$ = character of kth irreducible representation,
k = dimension of reducible representation.

(We shall not give a proof of theorems like this one, but simply verify them by examples. This will considerably simplify the discussion and allow us to concentrate on physical applications.)

For our example, $k=6$, so that for Γ_1, (9) becomes

$$n_1 = [6(1) + 2(1) + 2(1) + 2(1) + 0(1) + 0(1)]/6 = 2.$$

Similarly

$$n_2 = 0, \qquad n_3 = 2$$

which means that Γ_1 and Γ_3 are each contained in Γ_4 twice, whereas Γ_2 is not contained at all. This agrees with (8) and shows that (9) eliminates the necessity for finding the matrix which reduces a representation.

It can also be seen that

$$\sum_k l_k^2 = g, \tag{10}$$

where

l_k = dimension of kth irreducible representation,
g = order of group.

In our example, $g=6$, so that (10) is verified as follows:

$$1^2 + 1^2 + 2^2 = 6.$$

This theorem then shows that a group with six elements can have only two one-dimensional and one two-dimensional irreducible representation, so that Γ_1, Γ_2, and Γ_3 are the only possible irreducible representations for our example.

V. The Free Electron Approximation

In present-day physics, the electron is considered to be a dual entity, showing characteristics associated with both a wave and a particle. The motion or propagation of the electron is governed by the Schroedinger or wave equation,[4] which is

$$[(-\hbar^2/2m)\nabla^2 + V(r)]\psi(r) = E\psi(r), \tag{11}$$

where

$\hbar$ = Planck's constant divided by 2π,
m = mass of the electron,
E = total energy of the electron,
V = potential energy of the electron,

and the solution ψ is called a wave function.

Referring to Herman's paper,[1] the solution to this equation in a perfectly periodic crystal is

$$\psi_k(r) = e^{i\mathbf{k}\cdot\mathbf{r}}u(\mathbf{r}), \tag{12}$$

where $\mathbf{k}$ is called the propagation constant. The aim of energy band calculations is to determine E as a function of $\mathbf{k}$ in a given range of $\mathbf{k}$ values. Along the cubic axes of silicon and germanium, for example, the range is

$$-2\pi/a \leqq k \leqq 2\pi/a.$$

Substituting (12) into (11) gives

$$\nabla^2 u + 2i\mathbf{k}\cdot\nabla u + (2m/\hbar^2)[E - (\hbar^2 k^2/2m) - V]u = 0. \tag{13}$$

[4] An introductory discussion of the Schroedinger equation will be found in R. L. Sproull, "Modern Physics," John Wiley and Sons, Inc., New York, N. Y.; 1956. A more extended treatment, at an elementary level, is given in A. Nussbaum, "Semiconductor Device Physics," Prentice-Hall, Inc., Englewood Cliffs, N. J.; 1962.

This form of the Schroedinger equation is particularly suited for discussing crystals.

A crystal is a regular arrangement of atoms and the translational pattern of the crystal is called the *direct lattice*. If $\boldsymbol{a}_1$, $\boldsymbol{a}_2$, $\boldsymbol{a}_3$, are three noncoplanar vectors connecting lattice points, and if n_1, n_2, n_3 are an arbitrary set of integers (positive, negative, or zero), then the direct lattice is mapped out by the points $(n_1\boldsymbol{a}_1+n_2\boldsymbol{a}_2+n_3\boldsymbol{a}_3)$. As Jones[5] has pointed out, if the nine components of the three vectors $\boldsymbol{a}_1$, $\boldsymbol{a}_2$, $\boldsymbol{a}_3$ are considered as a matrix $\mathbf{A}$, then the lattice points are determined by the relation

$$\mathbf{A}n = \begin{bmatrix} a_{1x} & a_{2x} & a_{3x} \\ a_{1y} & a_{2y} & a_{3y} \\ a_{1z} & a_{2z} & a_{3z} \end{bmatrix} \begin{Bmatrix} n_1 \\ n_2 \\ n_3 \end{Bmatrix}. \tag{14}$$

The reciprocal lattice is determined by a set of vectors $\boldsymbol{b}_1$, $\boldsymbol{b}_2$, $\boldsymbol{b}_3$ defined by

$$\boldsymbol{a}_i \cdot \boldsymbol{b}_j = 2\pi\delta_{ij} \qquad [i, j = 1, 2, 3], \tag{15}$$

where δ_{ij} is the Kronecker delta. The planes which act as perpendicular bisectors of the nearest-neighbor distances in the reciprocal lattice form the *first Brillouin zone*, which is illustrated in Fig. 4 for the case of germanium and silicon. This zone is also referred to as the *reduced zone in k space*, and the figure shows that along the coordinate axes, for example, the boundaries of the zone are determined by

$$-2\pi/a \leqq k \leqq 2\pi/a, \tag{15a}$$

where a is the lattice constant (for a cubic crystal $a_1=a_2=a_3=a$).

The *reciprocal lattice* can be specified by a matrix $\mathbf{B}$, analogous to $\mathbf{A}$, such that

$$l\mathbf{B} = (l_1, l_2, l_3) \begin{bmatrix} b_{1x} & b_{1y} & b_{1z} \\ b_{2x} & b_{2y} & b_{2z} \\ b_{3x} & b_{3y} & b_{3z} \end{bmatrix} \tag{16}$$

where the l_i are integers. Then it follows from (15) that

$$\mathbf{BA} = 2\pi\mathbf{I} \tag{17}$$

where $\mathbf{I}$ is the unit matrix.

We now introduce the *free electron approximation* by letting $V=0$ in (13). The solution in this case is

$$u = \exp\left[-i(l\mathbf{B})\cdot\boldsymbol{r}\right], \tag{18}$$

and by substituting (18) into (13) for $V=0$, the energy values become

$$E = (\hbar^2/2m)(\boldsymbol{k} - l\mathbf{B})^2. \tag{19}$$

Combining (12) and (18), the wave functions are

$$\psi_k = \exp\left[i(\boldsymbol{k} - l\mathbf{B})\cdot\boldsymbol{r}\right]. \tag{20}$$

[5] H. Jones, "The Theory of Brillouin Zones and Electronic States in Crystals," North-Holland Publishing Co., Amsterdam, The Netherlands; 1960.

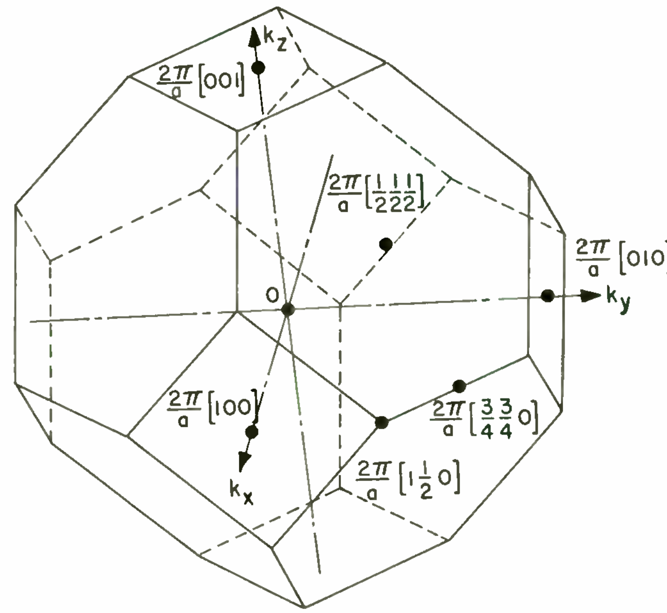

Fig. 4—The Brillouin zone for silicon and germanium.

VI. The Application to Tellurium

Tellurium is a semiconducting element lying in Column VIa of the Periodic Table. The other members of this column are the insulators oxygen and sulfur, the semiconductor selenium, and polonium, a metal. Although tellurium is not of much commercial importance at the moment, it has been studied extensively[6,7] and provides a reasonably simple example of the application of group theory.

The crystal structure and symmetry of tellurium are illustrated in Fig. 5. The atoms are arranged in spiral chains, with three atoms to each turn, so that the fourth atom in Fig. 5 lies directly over the first, the fifth is directly over the second, and so on. The chains are arranged to form hexagons, but the symmetry of the crystal is trigonal because of the threefold nature of the chains. The spiral arrangements are called *screw axes*, since they are generated by combining a 120° rotation with a displacement of $c/3$ along the rotation axis.

The symmetry operations of the tellurium lattice are very similar to the simple example of Section II. They are:

1) E, the identity.
2) C_3, a 120° rotation about the z axis, followed by a translation $c/3$ along the axis.
3) C_3^2.
4) $C_2^{(1)}$, a 180° rotation about the axis $X^{(1)}$ of Fig. 5(b), followed by a translation $c/3$.
5) $C_2^{(2)}$, a 180° rotation about $X^{(2)}$, followed by a translation 0.

[6] J. S. Blakemore, D. Long, K. C. Nomura, and A. Nussbaum, "Tellurium," in "Progress in Semiconductors," A. F. Gibson, Ed., Heywood and Co., London, England, vol. 6; 1962.

[7] A. Nussbaum and R. J. Hager, "Galvanomagnetic coefficients of single-crystal tellurium," *Phys. Rev.*, vol. 123, pp. 1958–1964; September 15, 1961.

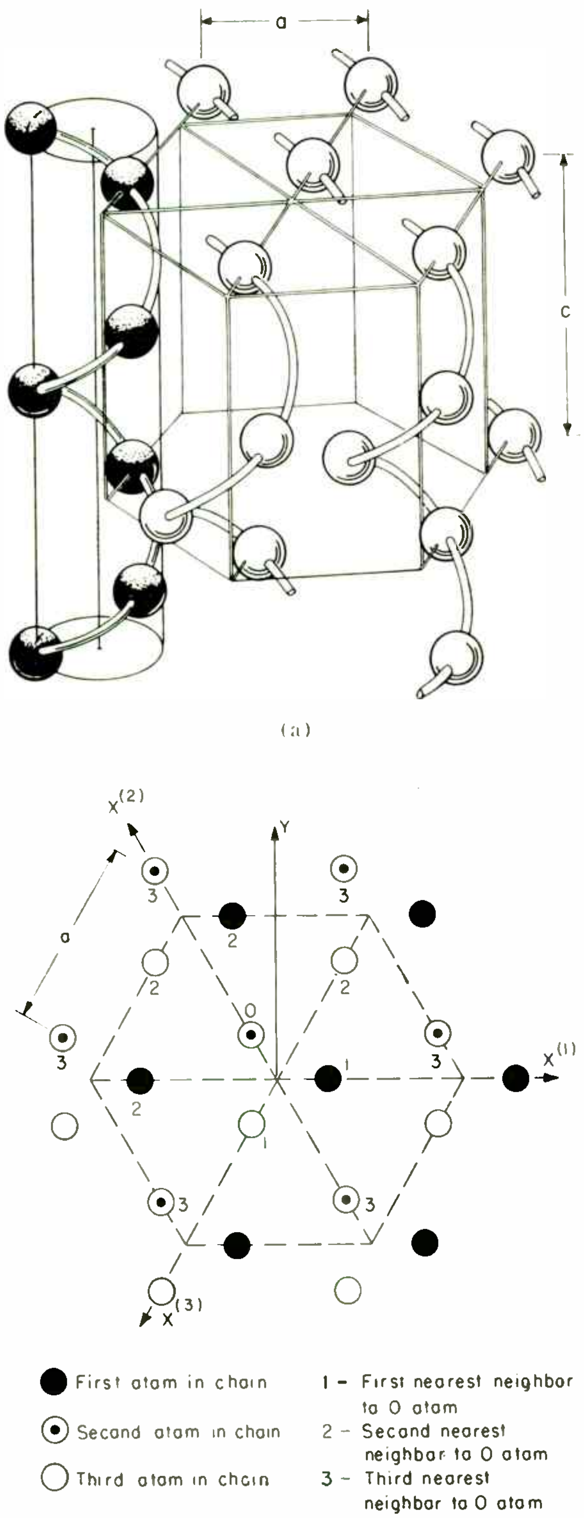

Fig. 5—The crystal lattice of tellurium, showing (a) the lattice in perspective view and (b) an end view.

6) $C_2^{(3)}$, a 180° rotation about $X^{(3)}$, followed by a translation $2c/3$.

These six operations do not form a group, however, because of the screw axes. For example, $C_3C_3^2$ (or $C_3^2C_3$) is equivalent to a pure translation c, which is not listed above. We shall show shortly that group theory may nevertheless be applied.

Using a and c to denote the lattice constants, as shown in Fig. 5, the matrices specifying the direct and reciprocal lattice are

$$\mathbf{A} = \begin{bmatrix} a & -a/2 & 0 \\ 0 & \sqrt{3}a/2 & 0 \\ 0 & 0 & c \end{bmatrix}$$

$$\mathbf{B} = 2\pi \begin{bmatrix} 1/a & 1/\sqrt{3}a & 0 \\ 0 & 2/\sqrt{3}a & 0 \\ 0 & 0 & 1/c \end{bmatrix} \qquad (21)$$

and the Brillouin zone is illustrated in Fig. 6. The center of the zone is customarily labelled Γ, and some other points and axes of symmetry are also labelled. The coordinates of the symmetry points shown are $\Gamma(0, 0, 0)$, $A(0, 0, \pi/c)$, and $M(0, 2\pi/\sqrt{3}\,a, 0)$. Using $\mathbf{B}$ as given by (21), the wave functions and energies become

$$\psi_k = e^{(2\pi i/a)[(\xi - l_1)x + \{\eta - (l_1 + 2l_2)/\sqrt{3}\}y + (a/c)(\zeta - l_3)z]} \qquad (22)$$

$$E_{kl} = (h^2/2ma^2)\left[(\xi - l_1)^2 + \{\eta - (l_1 + 2l_2)/\sqrt{3}\}^2 + (a/c)^2(\zeta - l_3)\right]^2, \qquad (23)$$

where

$$k = (2\pi\xi/a, 2\pi\eta/a, 2\pi\zeta/c).$$

Eq. (23) permits us to plot the E vs $\boldsymbol{k}$ curves for the free electron approximation. For example, along the Δ axis of Fig. 6, $\xi = \eta = 0$ and (23) reduces to

$$E = (h^2/2ma^2)\left[l_1^2 + (l_1 + 2l_2)^2/3 + (a/c)^2(\zeta - l_3)^2\right]. \qquad (24)$$

For tellurium, the value of $(a/c$ is 0.75, and we can plot E vs ξ for various combinations of (l_1, l_2, l_3), as shown in the lower half of Fig. 7. Note that the curve for which $E = 4/3$ at $\zeta = 0$ has six possible sets of l-values, the notation $(0\bar{1}0)$ being used for $l_1 = 0$, $l_2 = -1$, $l_3 = 0$, and this energy curve is therefore *sixfold degenerate*. The valence electrons of tellurium have the configuration $5s^25p^4$, and since there are three nonequivalent atoms in a single turn of the spiral chain, this corresponds to eighteen valence electrons. (These three atoms comprise what is known as a *unit cell;* by placing such an arrangement at each lattice point, we generate the tellurium crystal.) Considering spin allows two electrons per energy level so that the ninth level from the bottom represents the valence band, thus determining the position of the forbidden gap which has been shaded in. A similar calculation gives the E vs $\boldsymbol{k}$ curves along the ΓM direction, shown in the upper half of the figure. The significance of the symbols along the edges will be explained shortly.

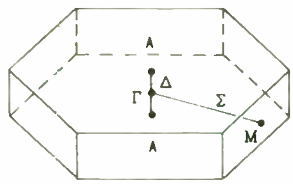

Fig. 6—The Brillouin zone for tellurium.

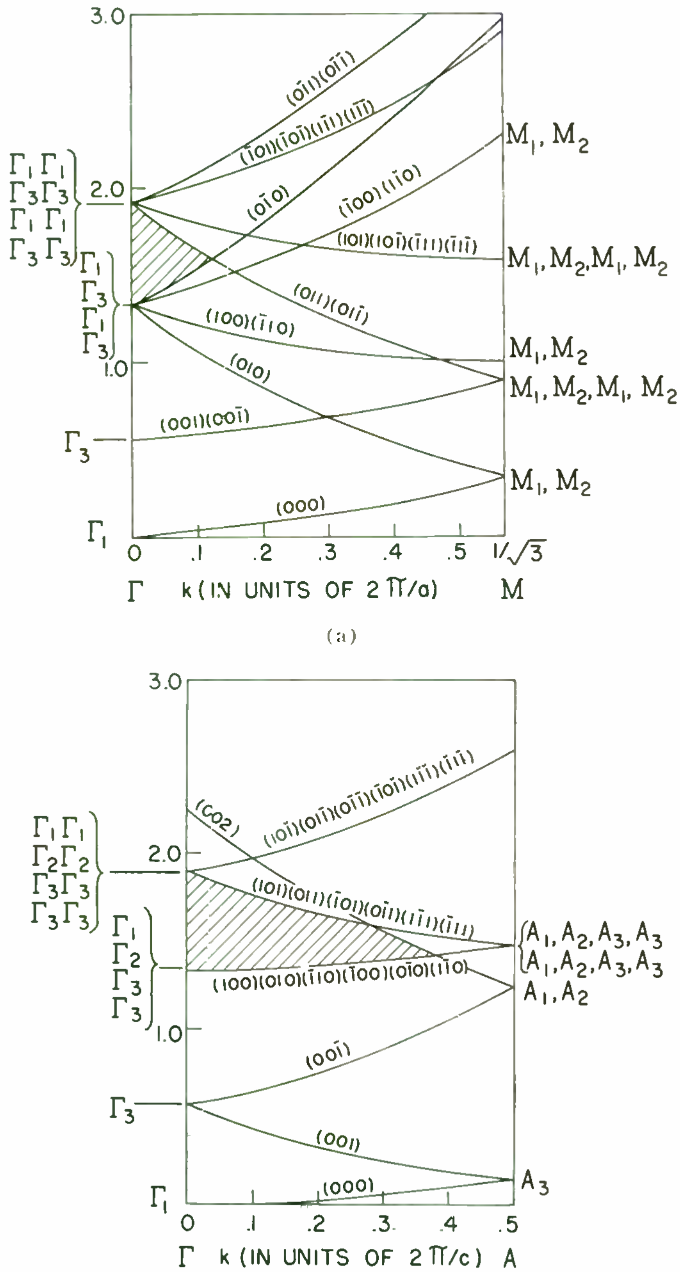

(a)

(b)

Fig. 7—The free electron energy bands for tellurium.

VII. The Tight-Binding Method

One of the earliest methods to be devised for calculating energy bands is the *tight-binding* or *Bloch* method, and group theory has been very useful in simplifying the associated analysis. To briefly explain this procedure, following Dekker,[8] we assume that the atoms in a lattice are so far apart that the behavior of an electron in the vicinity of any one of them is only slightly influenced by the nearest-neighbor atoms. Let a particular atom have a position-vector $\boldsymbol{R}_j$, so that an electron at $\boldsymbol{r}$ will then have a position $(\boldsymbol{r}-\boldsymbol{R}_j)$ with respect to this atom.

It is shown in standard texts[2,4] that the solutions to the Schroedinger equation (11) for a hydrogen atom have the form

$$\psi(r, \theta, \phi) = R_{nl}(r) Y_{lm}(\theta, \phi),$$

where r, θ, and ϕ are spherical coordinates. For multi-electron atoms, the assumption that the potential energy V is a function of r only leads to solutions like these, with the angular part being identical to that of hydrogen. Such solutions are called *atomic orbitals*, and the angular parts of the first few are expressed as follows:

$$\begin{aligned} s &= \text{const} \\ p_1 &\sim \sin\theta e^{i\phi} \\ p_0 &\sim \cos\theta \\ p_{-1} &\sim \sin\theta e^{-i\phi}. \end{aligned} \tag{25}$$

It is convenient at times to replace these p functions by normalized linear combinations, denoted by

$$\begin{aligned} p_x &= (p_1 + p_{-1})/\sqrt{2} \sim \sin\theta\cos\phi \sim x \\ p_y &= -i(p_1 - p_{-1})/\sqrt{2} \sim \sin\theta\sin\phi \sim y \\ p_z &= p_0 \sim \cos\theta \sim z. \end{aligned} \tag{26}$$

The five d functions can also be expressed as the linear combinations d_{xy}, d_{yz}, d_{zx}, $d_{x^2-y^2}$, d_{z^2}, where the subscripts indicate the symmetries in the same way as they do for the p functions. These nine atomic orbitals are illustrated in Fig. 8.

Denoting the atomic orbitals by $\phi(\boldsymbol{r}-\boldsymbol{R}_j)$, we try a general solution

$$\psi_k = \sum_j \exp\{i\boldsymbol{k}\cdot\boldsymbol{R}_j\}\phi(\boldsymbol{r}-\boldsymbol{R}_j), \tag{27}$$

where the sum is taken over all the atoms in the crystal. The form of (27) leads to the alternate name for the method: *linear combination of atomic orbitals* (*LCAO*).

Multiplying (11) by the complex conjugate ψ_k^* and integrating over all space gives

$$\int \psi_k^*[(-\hbar^2/2m)\nabla^2 + V]\psi_k d\tau + E\int \psi_k^*\psi_k d\tau = 0. \tag{28}$$

[8] A. J. Dekker, "Solid State Physics," Prentice-Hall, Inc., New York, N. Y.; 1957.

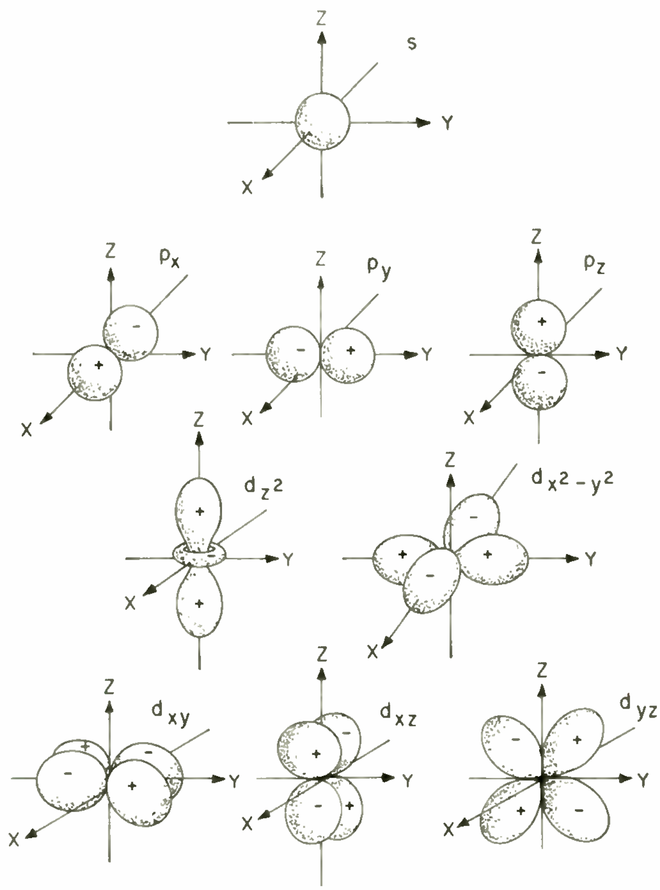

Fig. 8—The s, p, and d atomic orbitals.

We separate V into two terms

$$V(r) = V_a(r - R_j) + V'(r - R_j), \tag{29}$$

where V_a is the potential energy which an electron would have in a single, isolated atom and V' is the additional potential energy it acquires when the atom is incorporated into the crystal. The second integral on the left side of (28) involves the sum of products of atomic orbitals. Using the assumption that the atoms are widely spaced, the integrals involving functions centered around two different atoms will vanish. On the other hand, integrals involving a single atom will reduce to unity if the orbitals are normalized, and since there are N such integrals, where N is the number of atoms, this term becomes EN. Similarly, substituting (29) into (28) gives a term NE_a. This leaves only the integral involving V' to be considered, and here we shall neglect all terms in the summation except those involving nearest neighbors, an inherent feature of the tight-binding method. Define

$$\alpha = -N\int \psi^*(r - R_j)V'\psi(r - R_j)d\tau$$

$$\beta = -N\int \psi^*(r - R_m)V'\psi(r - R_j)d\tau, \tag{30}$$

where j and m are neighbors and where the negative signs are used to make α and β positive. If we assume for the moment that ϕ is spherically symmetric, corresponding to the s function of Fig. 8, then the β integrals are the same for all nearest neighbors. Using (29) and (30), (28) becomes

$$E = E_a - \alpha - \beta \sum_m \exp\{ik\cdot(R_j - R_m)\}, \tag{31}$$

where the sum is over the nearest neighbors of atom j.

As a simple example of the application of this result, consider a square lattice with lattice constant a. The nearest neighbors are then the four points $(\pm a, 0)$, $(0, \pm a)$, and (29) reduces to

$$E = E_a - \alpha - 2\beta(\cos k_x a + \cos k_y a).$$

Since the constants do not affect the form of the relation between E and $\boldsymbol{k}$, we can introduce a reduced energy E_r, given by

$$E_r = (E - E_a + \alpha)/2\beta = -(\cos k_x x + \cos k_y y).$$

Curves of k_x vs k_y for various values of E_r are shown in Fig. 9. These curves are traces in the x, y plane of three-dimensional energy surfaces, and we see that the surfaces close to the origin are spheres.

The tight-binding method has been applied to tellurium by Reitz,[9] who took the p functions as those primarily involved in the valence and conduction bands. For convenience, denote the functions ϕ by $\phi_1 = p_x$, $\phi_2 = p_y$, $\phi_3 = p_z$. Then there are three expressions of the form

$$\psi_{nk} = \sum_j \exp\{ik\cdot R_j\}\phi_n(r - R_j) \qquad [n = 1, 2, 3],$$

and the solution to the Schroedinger equation is taken as

$$\psi_k(r) = \sum_{j,n,s} B_{ns} \exp\{ik\cdot R_{js}\}\phi_n(r - R_{js}), \tag{32}$$

where the B_{ns} are constants to be determined, and the subscript s refers to a summation over the three nonequivalent lattice sites in the unit cell. Again writing V as $V_a + V'$, introducing ψ_k above into the Schroedinger equation, and multiplying it in turn by ϕ_1^*, ϕ_2^*, and ϕ_3^* followed by an integration, we obtain nine homogeneous equations in the unknowns B_{ns}. The condition for a solution to exist is that the determinant of the coefficients vanish, leading to what is known as the *secular equation*. As a first approximation towards solving this 9×9 determinant, Reitz made the simplifying assumption that the interbond angles between ajacent atoms in a chain were 90° instead of the true value 102.6°. Referring to Fig. 10, we label the three atoms in a unit cell as A, B, and C and let $\boldsymbol{R}_\lambda$, $\boldsymbol{R}_\mu$, and $\boldsymbol{R}_\nu$ denote the three nearest-neighbor directions, so that the lattice constant along the trigonal axis can be expressed

$$\boldsymbol{c} = -\boldsymbol{R}_\lambda + \boldsymbol{R}_\mu + \boldsymbol{R}_\nu.$$

[9] J. R. Reitz, "Electronic band structure of selenium and tellurium," *Phys. Rev.*, vol. 105, pp. 1233–1240; February 15, 1957.

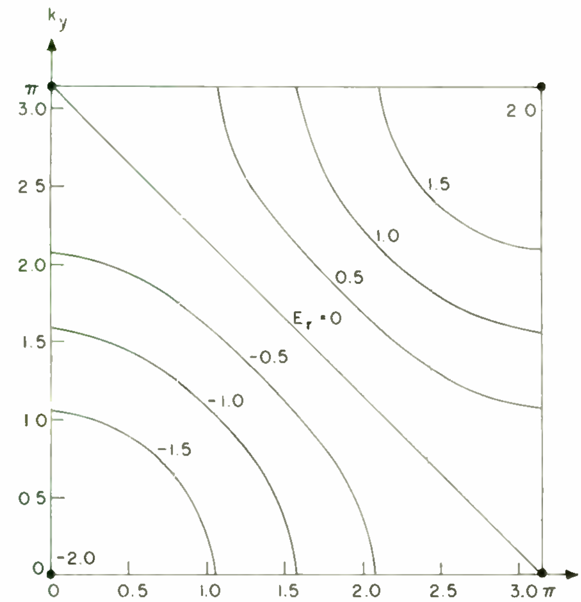

Fig. 9—The constant-energy contours for the tight-binding method applied to the square lattice.

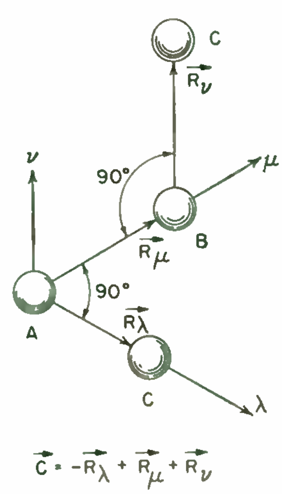

Fig. 10—The tellurium chain assuming 90° bonds.

We then orient the p functions so that they lie along the λ, μ, and ν axes. Because there are so many integrals of the form α and β, above, we use the special symbol

$$(\phi_n^* \mid V' \mid \phi_m) = N \int \phi_n^* V' \phi_m d\tau. \tag{33}$$

Considering only nearest-neighbor integrals and denoting the location of a function by a subscript A, B, or C, the following are the integrals involving p_λ functions:

$$(p_{\lambda A} \mid V' \mid p_{\lambda A}) = (p_{\lambda C} \mid V' \mid p_{\lambda C}) \tag{34a}$$

$$(p_{\lambda B} \mid V' \mid p_{\lambda B}) \tag{34b}$$

$$(p_{\lambda A} \mid V' \mid p_{\lambda B}) = (p_{\lambda B} \mid V' \mid p_{\lambda A})$$

$$= (p_{\lambda B} \mid V' \mid p_{\lambda C}) = (p_{\lambda C} \mid V' \mid p_{\lambda B}) \tag{34c}$$

$$(p_{\lambda C} \mid V' \mid p_{\lambda A}) = (p_{\lambda A} \mid V' \mid p_{\lambda C}). \tag{34d}$$

The relations among these integrals come from the fact that their values depend upon the relative orientation of the two p functions in each integrand. Since two different p functions are orthogonal, all terms of the form $(p_{\lambda A} \mid V' \mid p_{\mu A})$ vanish in this approximation, and the 9×9 determinant reduces to the form

$$\begin{vmatrix} \lambda & 0 & 0 \\ 0 & \mu & 0 \\ 0 & 0 & \nu \end{vmatrix} = 0, \tag{35}$$

where λ denotes a 3×3 block involving p_λ functions only and 0 denotes a 3×3 block composed entirely of zeros.

Equating the λ block separately to zero gives a cubic equation for E, which can be solved by making some further approximations. It is estimated that integrals of the form $(p_{\lambda A} \mid V' \mid p_{\lambda B})$ are about one third the magnitude of those like $(p_{\lambda A} \mid V' \mid p_{\lambda C})$ and we assume that the integrals in (34a) and (34b) are the same. Introducing a relative energy E_R by

$$E_R = E - E_a - (p_{\lambda A} \mid V' \mid p_{\lambda A})$$

and the abbreviation

$$\sigma = (p_{\lambda A} \mid V' \mid p_{\lambda C}),$$

the secular equation becomes

$$-E_R^3 + (11/9) E_R \sigma^2 + (2/9) \sigma^3 \cos k_z c = 0. \tag{36}$$

The dotted curves of Fig. 11 show the three roots of this equation as a function of k_z. The same set of curves will also come from the μ and ν equations and the bands are said to be triply degenerate. This degeneracy can be removed by stretching the bond angles to their true value of 102.6°, which results in the introduction of additional integrals of the form $(p_{\lambda A} \mid V' \mid p_{\mu B})$ into the secular equation. Reitz has solved this 9×9 equation by making further approximations and obtained the solid curves of Fig. 11. In this diagram, we have added the s bands based on the free electron approximation of Section V, and the forbidden gap is located as previously described.

This 9×9 determinant can also be broken down into smaller ones by the methods of group theory, and this has been done by Asendorf,[10] who obtained essentially the same results as Reitz. The method for doing this will be described in Section VIII, using an example which is much easier to handle than tellurium.

[10] R. N. Asendorf, "A Group Theoretical Approach to the Band Structure of Tellurium," Ph.D. dissertation, University of Pennsylvania, Philadelphia, Pa.; 1956.

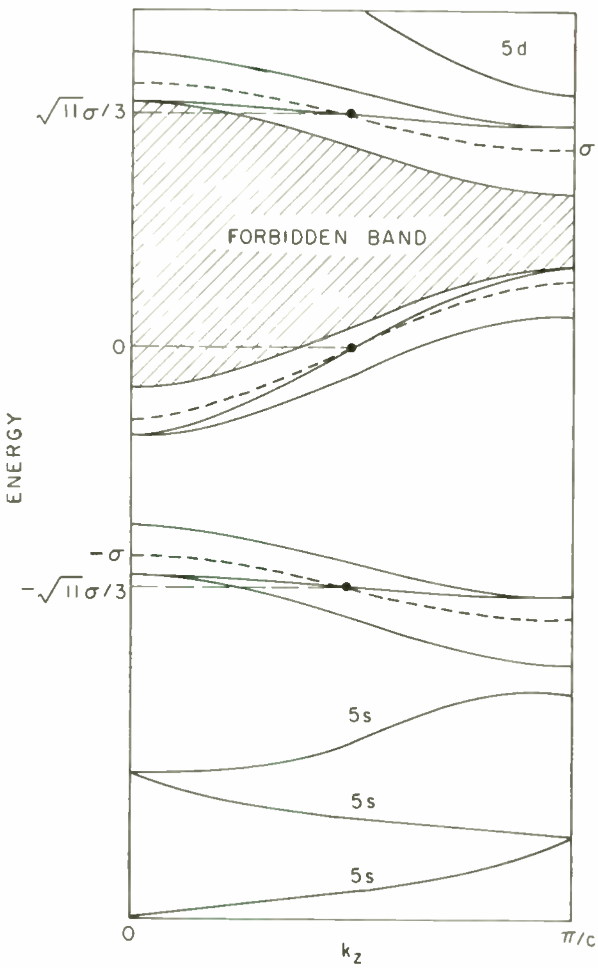

Fig. 11—The energy bands for tellurium based on the tight-binding approximation.

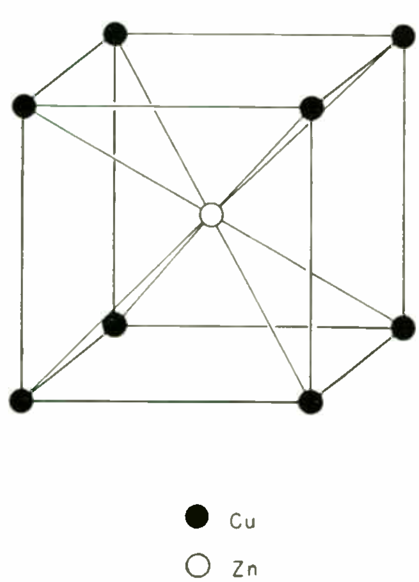

Fig. 12—The beta-brass simple cubic lattice.

VIII. Simplification of the Secular Determinant

Group theory has been applied to the secular determinant arising in a tight-binding calculation for beta-brass by Amsterdam.[11] This alloy in its ideal form consists of equal numbers of copper and zinc atoms, with a unit cell as shown in Fig. 12. Although this particular example is a metal, the method is essentially the same as for semiconductors, and we shall use it because of its simplicity. The unit cell contains one zinc atom and the equivalent of one copper atom, and the lattice is simple cubic, with one atom of each kind assigned to every lattice point.

Consider a cube with its center located at the origin of a set of coordinates $OXYZ$ and its edges parallel to the axes. If we label the eight corners A through H, we can see that the group of symmetry operations has 48 elements, as follows:

Operation	Multiplicity	Description
E	1	The identity
C_4	6	90° rotation about a coordinate axis
C_4^2	3	180° rotation about a coordinate axis
C_2	6	180° rotation about an axis of the type $x=y$, $z=0$
C_3	8	120° rotation about a cube diagonal
J	1	Inversion through the center
JC_4	6	Combination of J and the rotations above.
JC_4^2	3	
JC_2	6	
JC_3	8	

We can set up a multiplication table for these 48 operations like that of Table I and it will be found that each of the ten types listed above constitutes a class. To find the representations and the character table as we did in Section IV is a tedious process, but fortunately it is possible to determine the character system for the irreducible representations without explicitly knowing the matrices in these representations. The method is given by Margenau and Murphy[12] and can be explained by referring to Table I. If we denote the three classes in this group by

$$K_1 = E; \qquad K_2 = A, B, C; \qquad K_3 = D, F$$

then we see, for example, that

[11] M. F. Amsterdam, "The Band Structure of Beta-Brass," Ph.D. dissertation, Temple University, Philadelphia, Pa.; 1958

[12] H. Margenau and G. M. Murphy, "The Mathematics of Physics and Chemistry," D. Van Nostrand Co., Inc., New York, N. Y., 1943; a proof will be found in M. Hamermesh, "Group Theory and Its Applications," Addison-Wesley Publishing Co., Reading, Mass., 1962.

TABLE IV
CHARACTER SYSTEM FOR THE CUBIC GROUP

	E	$3C_4^2$	$6C_4$	$6C_2$	$8C_3$	J	$3JC_4^2$	$6JC_4$	$6JC_2$	$8JC_3$	Associated Functions
Γ_1	1	1	1	1	1	1	1	1	1	1	s
Γ_2	1	1	-1	-1	1	1	1	-1	-1	1	
Γ_{12}	2	2	0	0	-1	2	2	0	0	-1	d_{z^2}, $d_{x^2-y^2}$
Γ_{15}'	3	-1	1	-1	0	3	-1	1	-1	0	
Γ_{25}'	3	-1	-1	1	0	3	-1	-1	1	0	d_{xy}, d_{yz}, d_{zx}
Γ_1'	1	1	1	1	1	-1	-1	-1	-1	-1	
Γ_2'	1	1	-1	-1	1	-1	-1	1	1	-1	
Γ_{12}'	2	2	0	0	-1	-2	-2	0	0	1	
Γ_{15}	3	-1	1	-1	0	-3	1	-1	1	0	p_x, p_y, p_z
Γ_{25}	3	-1	-1	1	0	-3	1	1	-1	0	

$$K_2K_3 = (A, B, C)(D, F)$$
$$= (B, C, A, C, A, B) = 2K_2.$$

Similarly

$$K_2^2 = 3K_1 + 3K_3$$
$$K_3^2 = 2K_1 + K_3$$
etc.,

or, in general

$$K_iK_k = K_kK_i = \sum_j h_{ikj}K_j. \quad (37)$$

Now let χ_k be a character associated with class k and let r_k be the number of elements in this class. Then it can be seen from Table III that

$$r_ir_k\chi_i\chi_k = \chi_1 \sum_j h_{ikj}r_j\chi_j \quad (38)$$

so that

$$3\cdot 3\chi_2^2 = \chi_1[3\cdot 1\cdot \chi_1 + 3\cdot 2\cdot \chi_3]$$
$$4\chi_3^2 = \chi_1[2\chi_1 + 1\chi_3]$$
$$6\chi_2\chi_3 = 6\chi_1\chi_3. \quad (39)$$

The characters χ_1 are 1, 1, and 2. Substituting these values in turn into (37), we find that χ_2 and χ_3 are as given in Table III, thus verifying (38).

We can work in the opposite direction and determine the character system by realizing that the operation E will always be in a class by itself and the characters associated with any matrix representing E will equal the dimensionality l_k of that representation, since E has the form $[\delta_{ij}]$, where δ_{ij} is the Kronecker delta. Hence, from (10), the sum of the squares of the characters χ_1 must equal the order of the group, and the values can be found by trial and error. For example, for the cube, we have ten classes and 48 operations, so that the characters χ_1 for E are determined by

TABLE V
SYMMETRY OPERATIONS OF THE CUBIC GROUP

E	xyz.							
$3C_4^2$	$\bar{x}\bar{y}z$,	$x\bar{y}\bar{z}$,	$\bar{x}y\bar{z}$.					
$6C_4$	$\bar{y}xz$,	$y\bar{x}z$,	$x\bar{z}y$,	$xz\bar{y}$,	$zy\bar{x}$,	$\bar{z}yx$.		
$6C_2$	$yx\bar{z}$,	$z\bar{y}x$,	$\bar{x}zy$,	$\bar{y}\bar{x}\bar{z}$,	$\bar{z}\bar{y}\bar{x}$,	$\bar{x}\bar{z}\bar{y}$.		
$8C_3$	zxy,	yzx,	$z\bar{x}\bar{y}$,	$\bar{y}\bar{z}x$,	$\bar{z}\bar{x}y$,	$\bar{y}z\bar{x}$,	$\bar{z}x\bar{y}$,	$y\bar{z}\bar{x}$.

$$1^2 + 1^2 + 1^2 + 1^2 + 2^2 + 2^2 + 3^2 + 3^2 + 3^2 + 3^2 = 48$$

and this is the only combination of 10 integers whose squares add up to 48. Substituting these in turn into (38) gives the characters of Table IV, as taken from Bouckaert, Smoluchowski, and Wigner.[13] (The peculiar notation for designating the representations will be explained shortly.) An interesting feature of character tables involving the inversion operator is that, if it is divided into four blocks as shown by the dotted lines, three are identical and the fourth one is the negative of the others. This considerably simplifies the computation of the characters.

Some of these representations can have atomic orbitals associated with them. To see how this comes about, we use a line of reasoning given by Jones,[5] and consider the effect of the cubic symmetry operations on an arbitrary point with coordinates x, y, z. For C_4, for example, a 90° rotation about the OZ axis will convert x, y, z into either $-y$, x, z (which we will denote by $\bar{y}xz$) or into $y\bar{x}z$, and the inversion J on xyz gives $\bar{x}$, $\bar{y}$, $\bar{z}$. The results of all 48 operations are summarized in Table V, where the entries for the processes involving J are obtained by simply reversing all three signs.

[13] L. P. Bouckaert, R. Smoluchowski, and E. Wigner, "Theory of Brillouin zones and symmetry properties of wave functions in crystals," *Phys. Rev.*, vol. 50, pp. 58–67; July 1, 1936.

A reducible representation can be generated in terms of xyz, as was done in connection with (5). For example, the matrix E must have a character of 3 and any one of the three matrices for C_4^2 will have a character of -1, since two of the coordinates are converted into their negatives and the third one stays the same, so that the matrix must have the form

$$\begin{pmatrix} 1 & 0 & 0 \\ 0 & -1 & 0 \\ 0 & 0 & -1 \end{pmatrix} \begin{pmatrix} x \\ y \\ z \end{pmatrix} = \begin{pmatrix} x \\ \bar{y} \\ \bar{z} \end{pmatrix} .$$

The full set of reducible characters is then 3, -1, 1, -1, 0, -3, 1, -1, 1, 0, which we see is identical to the representation Γ_{15} of Table IV. Since the orbitals p_x, p_y, p_z are proportional to x, y, z, respectively, we say that the set of triply-degenerate p functions *belongs* to the representation Γ_{15}. Using the same arguments, the completely symmetric s orbital belongs to Γ_1, and by considering the behavior of the products, we can show that d_{xy}, d_{yz}, d_{zx} belong to Γ_{25}, and d_z^2, $d_{x^2-y^2}$ belong to Γ_{12}. This information is summarized in Table IV. The d functions bring up another interesting point: in the free atom they correspond to a fivefold degenerate level, but in a cubic crystal, the d state has been split into a twofold and a threefold state. This phenomenon is known as *crystal field splitting*.

So far, we have been considering the symmetry of the direct lattice. Let us turn now to the Brillouin zone, as shown in Fig. 13, which is also simple cubic. The points and axes of high symmetry are labelled and we shall be interested in the character tables corresponding to the Σ axis. Along this axis, for which $k_x = k_y$ and $k_z = 0$, there are only four symmetry operations in the group, and the associated coordinate transformations are

E	xyz
C_2	$yx\bar{z}$
JC_4^2	$xy\bar{z}$
JC_2	yxz.

The character table (Table VI) can then be determined by the method described above. For the point Γ on the Σ axis, the character table is Table IV, as determined for the cubic group in direct space. The point M at the other end of the Σ axis is of lower symmetry than Γ but higher than the axis; we shall not give its character table since it is not needed here.

Returning now to beta-brass, Amsterdam[11] bases his tight-binding calculation on the use of d functions since both Cu and Zn have ten $3d$ valence electrons. He also neglects Zn−Zn nearest-neighbor interaction, since the distance between these two atoms in the alloy is smaller than between two Cu atoms or between Cu-Zn neighbors. The integrals of the form $(\phi_n^* | V' | \phi_m)$ are more complicated than those in (34), since the lines

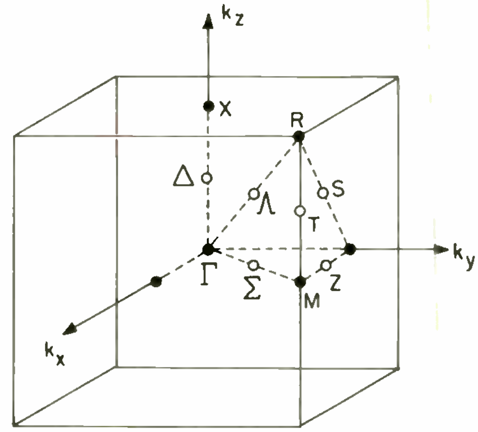

Fig. 13—The Brillouin zone for the simple cubic crystal.

TABLE VI

	E	C_2	JC_4^2	JC_2	Associated d Function
Σ_1	1	1	1	1	xy, z^2
Σ_2	1	1	-1	-1	$yz - xz$
Σ_3	1	-1	-1	1	$yz + xz$
Σ_4	1	-1	1	-1	$x^2 - y^2$

joining two nearest-neighbor atoms do not lie parallel to the coordinate axes. It has been shown by Slater and Koster[14] that some of these integrals vanish for geometric reasons. Applying (27) as we did for the square lattice, it is found that $(xy| V' | yz)$, for example, is converted into an expression involving $\sin k_z a$. Since $k_z = 0$ along the axis $k_x = k_y$, this integral vanishes. (We remind the reader that this example refers to the Σ axis.) Using letters to denote the integrals, the nonvanishing elements in the secular equation are

$$\begin{aligned}
&(xy_C | V' | xy_C) = G \\
&(yz_C | V' | yz_C) = (xz_C | V' | xz_C) = H \\
&(x^2 - y_C^2 | V' | x^2 - y_C^2) = K \\
&(z_C^2 | V' | z_C^2) = L \\
&(xy_Z | V' | xy_Z) = (yz_Z | V' | yz_Z) = (zx_Z | V' | zx_Z) \\
&\qquad = (x^2 - y_Z^2) | V' | x^2 - y_Z^2) = (z_Z^2 | V' | z_Z^2) = D \\
&(xy_C | V' | xy_Z) = (xy_Z | V' | xy_C) = (yz_C | V' | yz_Z) \\
&\qquad = (zx_C | V' | zx_Z) = M \\
&(x^2 - y_C^2 | V' | x^2 - y_Z^2) = (z_C^2 | V' | z_Z^2) = N \\
&(yz_C | V' | zx_Z) = P \\
&(xy_C | V' | z_Z^2) = Q.
\end{aligned} \tag{40}$$

[14] J. C. Slater and G. F. Koster, "Simplified LCAO method for the periodic potential problem," *Phys. Rev.*, vol. 94, pp. 1498–1524; June 15, 1954.

We then set up the secular 10×10 equation as follows:

$$
\begin{array}{cc|ccccc|ccccc|}
 & & \multicolumn{5}{c|}{\mathrm{Cu}} & \multicolumn{5}{c|}{\mathrm{Zn}} \\
 & & xy & yz & zx & x^2-y^2 & z^2 & xy & yz & zx & x^2-y^2 & z^2 \\
\hline
\mathrm{Cu} & xy & G-E & & & & & M & & & & Q \\
 & yz & & H-E & & & & & M & P & & \\
 & zx & & & H-E & & & & P & M & & \\
 & x^2-y^2 & & & & K-E & & & & & N & \\
 & z^2 & & & & & L-E & Q & & & & N \\
\hline
\mathrm{Zn} & xy & M & & & & Q & D-E & & & & \\
 & yz & & M & P & & & & D-E & & & \\
 & zx & & P & M & & & & & D-E & & \\
 & x^2-y^2 & & & & N & & & & & D-E & \\
 & z^2 & Q & & & & N & & & & & D-E \\
\hline
\end{array} = 0, \qquad (41)
$$

where the initial order of the rows and columns is arbitrary, E is the energy with respect to some convenient origin, and all elements not shown are zero. Rearranging rows and columns, this equation becomes

$$
\begin{array}{|cccccccccc|}
xy_C & xy_Z & z_C{}^2 & z_Z{}^2 & x^2-y_C{}^2 & x^2-y_Z{}^2 & yz_C & yz_Z & xz_C & xz_Z \\
\hline
G-E & M & & Q & & & & & & \\
M & D-E & Q & & & & & & & \\
 & Q & L-E & N & & & & & & \\
Q & & N & D-E & & & & & & \\
 & & & & K-E & N & & & & \\
 & & & & N & D-E & & & & \\
 & & & & & & H-E & M & & P \\
 & & & & & & M & D-E & & \\
 & & & & & & & P & H-E & M \\
 & & & & & & P & & M & D-E \\
\hline
\end{array} = 0. \qquad (42)
$$

TABLE VII

SYMMETRY OPERATIONS FOR THE Σ AXIS OF THE SIMPLE CUBIC BRILLOUIN ZONE

E	xyz
C_2	$yx\bar{z}$
JC_4^2	$xy\bar{z}$
JC_2	yxz

TABLE VIII

THE QUANTITIES $R\phi$ FOR THE SIMPLE CUBIC BRILLOUIN ZONE

	E	C_2	JC_4^2	JC_2
xy	xy	yx	xy	yx
yz	yz	$-xz$	$-yz$	xz
xz	xz	$-yz$	$-xz$	yz
x^2-y^2	x^2-y^2	$-(x^2-y^2)$	x^2-y^2	$-(x^2-y^2)$
z^2	z^2	z^2	z^2	z^2

The 4×4 subdeterminant in the lower right-hand corner of this determinant can be further simplified by the use of group theory. To understand the technique, let us return to the arguments leading to the last column of Table IV. It is possible to obtain the same results by using a theorem from group theory which states that the function ϕ_i' associated with the ith irreducible representation can be obtained from the atomic orbitals ϕ by the relation

$$\phi_i' = C\sum_R \chi_i(R)R\phi, \tag{43}$$

where $\chi_i(R)$ is the character associated with the operator R and C is a constant. For example, for p_x, Table V shows

$$\begin{array}{lllll} & E & C_4^2 & C_4^2 & C_4^2 \\ \Gamma_1: \phi' = & 1(p_x) + & 1(-p_x) + & 1(p_x) + & 1(-p_x) + \text{etc.} = 0 \\ \Gamma_{25}: \phi' = & 3(p_x) - & 1(-p_x) - & 1(p_x) - & 1(-p_x) - \text{etc.} = 0 \\ \Gamma_{15}: \phi' = & 3(p_x) - & 1(-p_x) - & 1(p_x) - & 1(-p_x) + \text{etc.} = 8p_x. \end{array}$$

All representations except Γ_{15} give $0(p_x)$, and similar results are obtained with p_y and p_z, verifying Table VI.

Turning now to the operations of Table VI and the five d functions, Table VII gives the results corresponding to Table V, and from this information, we obtain the quantities $R\phi$ of Table VIII. From Tables V and VIII we see that (43) gives for the representation Σ_1

$$xy: \; 1(xy) + 1(yx) + 1(xy) + 1(yx) = 4xy$$

$$yz: \; 1(yz) + 1(-xz) + 1(-yz) + 1(xz) = 0$$

$$xz: \; 1(xz) + 1(-yz) + 1(-xz) + 1(yz) = 0$$

$$x^2-y^2: \; 1(x^2-y^2) + 1(y^2-x^2) + 1(x^2-y^2) + 1(y^2-x^2) = 0$$

$$z^2: \; 1(z^2) + 1(z^2) + 1(z^2) + 1(z^2) = 4z^2.$$

Hence, xy and z^2 belong to Σ_1, but this representation is *not* degenerate (this point will be clarified at the end of this section). Similarly, we find the other results in the last column of Table VI, and we note that group theory has converted our five individual d functions into five linear combinations. Further, the functions belonging to different irreducible representations do not produce any elements in the secular determinant; that is, they are said not to *mix*. To see this, consider for example the integral $(yz - xz_C \mid V' \mid yz + xz_C)$. Then

$$(yz - xz_C \mid V' \mid yz + xz_C) = (yz_C \mid V' \mid yz_C) - (xz_C \mid V' \mid xz_C) + (yz_C \mid V' \mid xz_C) - (xz_C \mid V' \mid yz_C)$$

and by (40), this expression vanishes. On the other hand, by similarly expanding, we see that

$$(yz + xz_C \mid V' \mid yz + xz_C) = 2H$$

and

$$(yz + xz_C \mid V' \mid yz + xz_Z) = 2M + 2P.$$

Dropping the factors of 2, the secular equation now becomes

$$\begin{array}{cccccccccc}
xyc & xyz & zc^2 & zz^2 & x^2-yc^2 & x^2-yz^2 & xz+yzc & xz+yzz & xz-yzc & xz-yzz \\
\hline
G-E & M & & Q & & & & & & \\
M & D-E & Q & & & & & & & \\
 & Q & L-E & N & & & & & & \\
Q & & N & D-E & & & & & & \\
 & & & & K-E & N & & & & \\
 & & & & N & D-E & & & & \\
 & & & & & & H-E & M+P & & \\
 & & & & & & M+P & D-E & & \\
 & & & & & & & & H-E & M-P \\
 & & & & & & & & M-P & D-E \\
\hline
\multicolumn{4}{c}{\longleftarrow \Sigma_1 \longrightarrow} & \multicolumn{2}{c}{\longleftarrow \Sigma_4 \longrightarrow} & \multicolumn{2}{c}{\longleftarrow \Sigma_3 \longrightarrow} & \multicolumn{2}{c}{\longleftarrow \Sigma_2 \longrightarrow}
\end{array} = 0. \quad (44)$$

The application of group theory has thus reduced one of the 4×4 subdeterminants into a pair of 2×2 determinants, and this is as far as the theory takes us in this direction.

We note that this example is in accord with (9). The five d functions form a reducible representation, with characters as follows:

	E	C_2	JC_4^2	JC_2
χ	5	1	1	1

so that

$$n_k = [\sum \chi\chi_k/4]$$

and

$$n_1 = 2, \quad n_2 = 1, \quad n_3 = 1, \quad n_4 = 1,$$

so that the irreducible representation Σ_1 is contained twice in the reducible representation and the other three are contained once. We note that the character for E in any irreducible representation automatically gives the degeneracy, and in the case of Σ_1, we must therefore have two nondegenerate states, rather than a single doubly-degenerate one.

IX. The Nearly-Free Electron Approximation

As we pointed out in the previous section, the presence of a cubic crystalline field splits the fivefold d function level into a twofold and a threefold level. Similarly, if we consider the energies we have determined for the free electron approximation and examine what happens when a crystal field of a given symmetry is applied, we would again expect the removal of some of the degeneracies and perturbations of the original energies. Group theory can tell us what the resultant degeneracies will be and we will return to tellurium as an example.

In our introductory discussion on symmetry, we considered the effect of various operations on the atoms which lie in direct space. In reciprocal space, however, what we are concerned with is the effect of the symmetry operations on the wave functions as well as the atoms. At the top of the Brillouin zone, point A $(0, 0, \pi/c)$ of Fig. 6, a wave function of the form (12) will be

$$\psi_k(z) = e^{ikz}u_k(z). \quad (45)$$

If we now perform the operation C_3 on this function three times, z becomes $z+c$, and

$$\psi_k = e^{ik(z+c)}u_k(z) = -\psi_k$$

since u_k is periodic with period c and

$$e^{i\pi(z+c)/c} = -e^{i\pi z/c}.$$

A second such operation returns ψ_k to its original value, and hence at this point in the Brillouin zone, we have an additional symmetry element T, a displacement of c along the z axis, such that

$$T^2 = E. \quad (46)$$

The operations and classes associated with this special point are then indicated on the top and side of Table IX, which is the multiplication table for this group of twelve elements and six classes. To see how this table is established, consider the two operations T and $C_2^{(1)}$. In Fig. 14(a) there is shown a single turn of a chain with the three levels in the c direction labelled 0, 1, and 2. This denotes their height above the xy plane as 0, $T/3$ and $2T/3$, respectively. The corresponding atoms are labelled A, B, and C. Now consider the effect of the two operations T and $C_2^{(1)}$ on the lattice. The result of T is shown in Fig. 14(b), where the new levels are denoted 3, 4, and 5 to indicate that each atom has moved a distance $3T/3$ along the z axis. Applying $C_2^{(1)}$ to this arrangement gives the result shown in Fig. 14(c). Now, going in reverse order, $C_2^{(1)}$ produces Fig. 14(b′) and the inverse T^{-1} of T once again gives Fig. 14(c) so that

$$C_2^{(1)}T = T^{-1}C_2^{(1)}.$$

From this we may easily show that

$$TC_2^{(1)}T = T^{-1}C_2^{(1)}T^{-1}.$$

This result, however, can also be obtained from the assumption that

$$T^2 = E$$

or

$$T = T^{-1}.$$

This, then, verifies (46).

From the Cayley table we can determine the character table just as we have done before, and this is given by Table X. Before discussing this, consider the function (45) at the origin Γ. Then we have simply

$$\psi_0(z) = u_0(z)$$

TABLE IX

MULTIPLICATION TABLE FOR THE SPACE GROUP OF TELLURIUM

Second Operation		First Operation: K_1	K_2	K_3		K_4		K_5			K_6		
		E	T	C_3	TC_3^2	C_3^2	TC_3	$C_2^{(1)}$	$TC_2^{(2)}$	$TC_2^{(3)}$	$TC_2^{(1)}$	$C_2^{(2)}$	$C_2^{(3)}$
K_1	E	E	T	C_3	TC_3^2	C_3^2	TC_3	$C_2^{(1)}$	$TC_2^{(2)}$	$TC_2^{(3)}$	$TC_2^{(1)}$	$C_2^{(2)}$	$C_2^{(3)}$
K_2	T	T	E	TC_3	C_3^2	TC_3^2	C_3	$TC_2^{(1)}$	$C_2^{(2)}$	$C_2^{(3)}$	$C_2^{(1)}$	$TC_2^{(2)}$	$TC_2^{(3)}$
K_3	C_3	C_3	TC_3	C_3^2	E	T	TC_3^2	$C_2^{(3)}$	$TC_2^{(1)}$	$C_2^{(2)}$	$TC_2^{(3)}$	$C_2^{(1)}$	$TC_2^{(2)}$
	TC_3^2	TC_3^2	C_3^2	E	TC_3	C_3	T	$C_2^{(2)}$	$C_2^{(3)}$	$TC_2^{(1)}$	$TC_2^{(2)}$	$TC_2^{(3)}$	$C_2^{(1)}$
K_4	C_3^2	C_3^2	TC_3^2	T	C_3	TC_3	E	$TC_2^{(2)}$	$TC_2^{(3)}$	$C_2^{(1)}$	$C_2^{(2)}$	$C_2^{(3)}$	$TC_2^{(1)}$
	TC_3	TC_3	C_3	TC_3^2	T	E	C_3^2	$TC_2^{(3)}$	$C_2^{(1)}$	$TC_2^{(2)}$	$C_2^{(3)}$	$TC_2^{(1)}$	$C_2^{(2)}$
K_5	$C_2^{(1)}$	$C_2^{(1)}$	$TC_2^{(1)}$	$C_2^{(2)}$	$C_2^{(3)}$	$TC_2^{(3)}$	$TC_2^{(2)}$	E	TC_3	C_3^2	T	C_3	TC_3^2
	$TC_2^{(2)}$	$TC_2^{(2)}$	$C_2^{(2)}$	$C_2^{(3)}$	$TC_2^{(1)}$	$C_2^{(1)}$	$TC_2^{(3)}$	C_3^2	E	TC_3	TC_3^2	T	C_3
	$TC_2^{(3)}$	$TC_2^{(3)}$	$C_2^{(3)}$	$TC_2^{(1)}$	$C_2^{(2)}$	$TC_2^{(2)}$	$C_2^{(1)}$	TC_3	C_3^2	E	C_3	TC_3^2	T
K_6	$TC_2^{(1)}$	$TC_2^{(1)}$	$C_2^{(1)}$	$TC_2^{(2)}$	$TC_2^{(3)}$	$C_2^{(3)}$	$C_2^{(2)}$	T	C_3	TC_3^2	E	TC_3	C_3^2
	$C_2^{(2)}$	$C_2^{(2)}$	$TC_2^{(2)}$	$TC_2^{(3)}$	$C_2^{(1)}$	$TC_2^{(1)}$	$C_2^{(3)}$	TC_3^2	T	C_3	C_3^2	E	TC_3
	$C_2^{(3)}$	$C_2^{(3)}$	$TC_2^{(3)}$	$C_2^{(1)}$	$TC_2^{(2)}$	$C_2^{(2)}$	$TC_2^{(1)}$	C_3	TC_3^2	T	TC_3	C_3^2	E

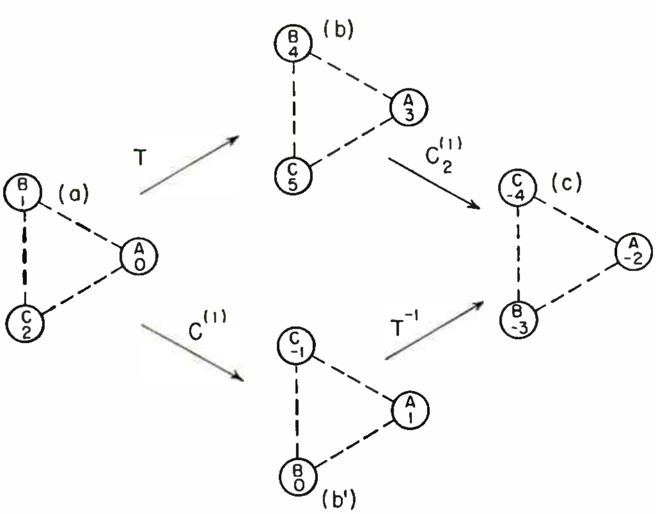

Fig. 14—The geometrical proof that $T^2 = E$.

TABLE X

CHARACTER TABLE FOR THE POINTS A AND Γ

(For the point Γ, the operation T is deleted)

	E	C_3, TC_3^2	$C_2^{(1)}$, $TC_2^{(2)}$, $TC_2^{(3)}$	T	TC_3, C_3^2	$TC_2^{(1)}$, $C_2^{(2)}$, $C_2^{(3)}$
Γ_1	1	1	1	1	1	1
Γ_2	1	1	−1	1	1	−1
Γ_3	2	−1	0	2	−1	0
A_1	1	−1	1	−1	1	−1
A_2	1	−1	−1	−1	1	1
A_3	2	1	0	−2	−1	0

and the operation T is equivalent to E. Therefore, the character table for the point Γ is the upper left-hand corner of the table for the point A and we notice that it has the same structure as Table III. Thus, at the origin of the Brillouin zone, the screw axis does not enter the analysis, whereas at the top, it doubles the size of the group.

Next, let us examine the situation along the Δ axis, excluding the end-points Γ and A. Suppose for the moment that the only symmetry associated with an arbitrary point along this axis is the translational symmetry of the lattice. We can find the characters for the translational operation by considering a one-dimensional chain of N atoms bent into a circle to insure that the lattice is completely periodic. The only symmetry operation is the translation T from one atom to its neighbor, so that the group consists of E, T, $T^2, \cdots, T^{N-1}$, and $T^N=E$. This group is *commutative* or *abelian;* that is, $T^mT^n=T^nT^m$ for every m and n. It is simple to show that for such a group, every element is in a class by itself. Hence, all the representations are one-dimensional and there are N of them. If $D(T)$ denotes the determinants in the representations, they must obey

$$D^N(T) = 1 \tag{47}$$

and the solutions to this equation are

$$D(T) = 1^{l/N} = e\pi^{il/N}, \tag{48}$$

where

$$l = 0, 1, 2, \cdots, N-1.$$

Hence the representations are

	E	T	T^2	$\cdots$	T^{N-1}
Γ_0	1	1	1		1
Γ_1	$\cdot$	$\cdot$	$\cdot$		$\cdot$
$\cdot$	$\cdot$	$\cdot$	$\cdot$		$\cdot$
Γ_l	1	$e^{2\pi il/N}$	$e^{4\pi il/N}$		$e^{(N-1)\pi il/N}$

and this is also the character table, since all the representations are one-dimensional.

The above result shows that all the representations can be expressed in the form $\exp[2\pi il/N]$. This can be rewritten as

$$\exp[2\pi ia(l/Na)] = \exp(ikR) \tag{49}$$

where a is the lattice constant and

$$k = 2\pi l/Na,\ R = la. \tag{50}$$

To see the origin of (50), we apply the condition that the wave function (12) must also obey the cyclic boundary conditions, so that

$$e^{ik(x+Na)}u(x+Na) = e^{ikx}u(x)$$

or

$$e^{ikNa} = 1$$

or

$$k = 2\pi l/Na$$

Using the definition (15) of the reciprocal lattice, $ab=2\pi$, and defining $R=la$ as a typical displacement, verifies (49).

Along the Δ axis of tellurium, we have both translational and rotational symmetry. Considering first the rotational part, the symmetry operations are a 120° rotation, a 240° rotation, and a 360° rotation (equivalent to the unity operation). These three operations form a commutative group and, by the procedure outlined above, we can determine the characters to be the cube roots of unity, which are 1, ω, and ω^2, where $\omega=\exp(2\pi i/3)$. The translational characters, from (49), have the form 1, δ, and δ^2, where $\delta=\exp(ikR)$. It is shown in group theory that the characters for the two types of operations can be combined by direct multiplication, leading to Table XI.

TABLE XI

CHARACTER TABLE FOR THE Δ AXIS

($\omega=e^{2\pi i/3}$, $\delta=e^{ikR}$)

	E	C_3	C_3^2
Δ_1	1	δ	δ^2
Δ_2	1	$\omega\delta$	$\omega\delta^2$
Δ_3	1	$\omega^2\delta$	$\omega^2\delta^2$

In applying this table, we must introduce the additional concept of *compatibility*, which has the following meaning. The symmetry of the wave functions at Γ and at some adjacent point on the Δ axis must bear some relation to one another, since it is necessary that the functions be continuous in the Brillouin zone. The symmetry along the axis should be similar to, but of lower order than, that at the center. The connection between the functions at Γ and along the axis is given by the rule (which we shall not prove) that the sum of the characters of the compatible representations along the axis be equal to the corresponding characters at the center. For example, Tables IV and V show that the characters of Σ_1, Σ_2, and Σ_3 add up to equal the characters of Γ_{25}' for the four operations E, C_2, JC_4^2, and JC_2. This means that the triply-degenerate energy level at Γ is split into three nondegenerate levels as soon as we move out onto the axis. The basis of this rule, as given by Jones,[5] is that a 3×3 irreducible representation at Γ may become reducible along the axis, which is of lower symmetry. However, even though the associated 3×3 matrix can be transformed into three 1×1 matrices, the trace or character is invariant, so that the sum of the new characters must equal the original.

The compatibility relations for tellurium are somewhat complicated to obtain because of the dual nature of the characters. At Γ, the quantity δ in Table XI is unity, so that $\omega+\omega^2=\omega^2+\omega=-1$. It is then seen that $\Delta_2+\Delta_3$ corresponds to Γ_3, which we designate by

$$\Gamma_3 \rightarrow \Delta_2 + \Delta_3.$$

At A, we have $k=\pi/c$ and the translation R corresponds to $c/3$, so that

$$\delta = e^{i(\pi/c)(c/3)} = e^{i2\pi/6}.$$

The character table for this particular point is then

	E	C_3	C_3^2
Δ_1	1	$e^{2\pi i/6}$	$e^{2\pi i/3}$
Δ_2	1	$e^{2\pi i/2}$	$3^{4\pi i/3}$
Δ_3	1	$e^{5\pi i/6}$	$e^{2\pi i}$

It is then easy to verify the compatibility relations of Table XII.

TABLE XII
COMPATIBILITY RELATIONS FOR Δ AND Σ AXES

$\Gamma_1 \rightarrow \Sigma_1 \rightarrow M_1$	
$\Gamma_2 \rightarrow \Sigma_2 \rightarrow M_2$	
$\Gamma_3 \rightarrow \Sigma_1 + \Sigma_2$	
$\Gamma_1 \rightarrow \Delta_1$	$A_1 \rightarrow \Delta_2$
$\Gamma_2 \rightarrow \Delta_1$	$A_2 \rightarrow \Delta_2$
$\Gamma_3 \rightarrow \Delta_2 + \Delta_3$	$A_3 \rightarrow \Delta_1 + \Delta_3$

The functions we shall use for tellurium are those of (22). As an example, consider the functions at Γ for $l=(001)$ or $(00\bar{1})$, which are then

$$\psi = e^{2\pi i z/c}.$$

In applying formula (43) at this point, we need consider only the six symmetry operations of Table I and can ignore the screw displacements, as we have already shown.

However, the twofold degeneracy of Γ_3 makes it necessary to use the complete representations in Table II rather than the characters (this is about the only instance where it is necessary to know the matrices explicitly). Let

$$\begin{aligned}
E\psi &= e^{2\pi i z/c} = \phi_1 \\
C_3\psi &= e^{2\pi i(z+c/3)/c} = \phi_2 = \omega\phi_1 \\
&(\omega = e^{2\pi i/3}) \\
C_3^2\psi &= \phi_3 = \omega^2\phi_1 \\
C_2^{(1)}\psi &= \phi_4 = e^{2\pi i(-z+c/3)} \\
C_2^{(2)}\psi &= \phi_5 = \omega\phi_4 \\
C_2^{(3)}\psi &= \phi_6 = \omega^2\phi_4,
\end{aligned}$$

then

$$\phi_1' = 1\phi_1 + 1\phi_2 + 1\phi_3 + 1\phi_4 + 1\phi_5 - 1\phi_6 = 0$$

so that no function goes with Γ_1. Similarly, nothing goes with Γ_2, and for Γ_3 we find the two linear combinations

$$\phi_3' = \begin{cases} \phi_1 - \phi_2/2 - \phi_3/2 + \phi_4 - \phi_5/2 - \phi_6/2 \\ (\sqrt{3}/2)(-\phi_2 + \phi_3 - \phi_5 + \phi_6). \end{cases}$$

It is interesting to note that, although Table X is obtained from Table IX in the usual fashion (the six classes producing a 6×6 character table), only the last three representations A_1, A_2, A_3 will be found to have associated functions at the point A, and only the first three will have functions at Γ. Hence, the character table for the point Γ is automatically generated when we find the larger one for the point A.

In Fig. 15 we show that the two curves labelled (001) and $(00\bar{1})$ of the free electron approximation (Fig. 7) retain their twofold degeneracy when we apply the crystalline field of tellurium to produce the nearly-free approximation. Note, however, that the crystal field removes the degeneracy at the intersection of the (001) and (002) curve for the point A. The higher-energy curves in Fig. 15 are sketches based on the curves of Fig. 7 plus the use of the compatibility relations. For our example, Table XII shows that $\Gamma_3\rightarrow\Delta_2+\Delta_3$ and $A_3\rightarrow\Delta_1+\Delta_3$, so that the curve joining Γ_3 and A_3 can only belong to Δ_3.

The energy bands for tellurium given in this figure are seen to differ considerably from those of Reitz (Fig. 11). For example, we show the maxima in both the valence and conduction bands as lying about halfway along the Δ axis, rather than at the top. This means, as

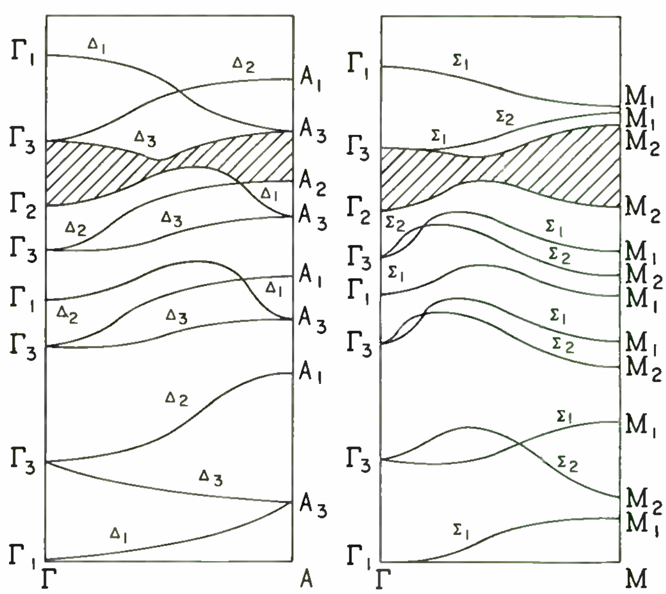

Fig. 15—The band structure of tellurium for the nearly-free electron approximation.

shown by Herman, that the energy surfaces are ellipsoidal and the symmetry of the crystal requires the presence of six ellipsoids per band. The connection between this structure and the electrical and optical properties of tellurium is discussed in detail by Nussbaum and Hager,[7] and similarly, Herman[1] has discussed germanium and silicon.

Finally, we should mention that the band structures calculated by Herman were obtained by a method which is more accurate than those discussed here. In place of using atomic orbitals, the solution which is tried is of the form

$$\psi_k = \sum_{h_1, h_2, h_3} \exp\{i(\boldsymbol{h} + \boldsymbol{k})\cdot \boldsymbol{r}\}.$$

where

$$\boldsymbol{h} = h_1\boldsymbol{b}_1 + h_2\boldsymbol{b}_2 + h_3\boldsymbol{b}_3,$$

and the $\boldsymbol{b}_i$ are the primitive vectors of the reciprocal lattice. These functions have the form of plane waves and the procedure is called the method of *orthogonalized plane waves* (OPW). Once again, group theory is used to determine the linear combinations of proper symmetry and also to simplify the secular determinant. An example of a calculation for the point Γ in the diamond lattice is given by Mariot.[15]

[15] L. Mariot, "Groupes Finis se Symétrie et Recherche de Solutions de L'Equation de Schrödinger," Dunod, Paris, France; 1959.

X. Conclusion

In this paper, we have shown how group theory can be applied to energy band calculations in two different ways:

1) To simplify the evaluation of secular determinants.
2) To determine the degeneracies of energy bands.

On looking back at our discussion, it will be seen that group theory does *not* give quantitative answers; it merely assists in their determination. For the simple example of a secular determinant we have given here, group theory has made only a small contribution towards reducing the labor involved in the calculation. However, in the case of silicon and germanium and for materials still under study, it plays an important role in the band structure determination. Further, for the element tellurium, it has been possible to determine some of the general features of the bands without complex calculations.

XI. Acknowledgment

The author would like to thank Dr. F. Herman, from whom came the suggestion to write this paper, and also Dr. R. H. Asendorf for several long discussions on the subject of group theory. He is also grateful to Dr. C. A. Domenicali, who gave very generously of his time and encouragement, and to Dr. M. F. Amsterdam of the Frankford Arsenal for the gift of a copy of his dissertation and to Dr. M. D. Blue for the sketch of Fig. 5(a).

Injection Currents in Insulators*

MURRAY A. LAMPERT†

Summary—The basic principles of one- and two-carrier, volume-controlled injection currents are reviewed. One-carrier injected currents are necessarily space-charge-limited and are strongly affected by the presence of traps which usually capture and immobilize most of the injected carriers. The trapped carriers are in an effective thermal equilibrium with the free injected carriers. The concepts of "shallow" and "deep" traps are defined and their effects on injected currents studied. It is shown that the presence of "deep" traps leads to a very steep rise of current with voltage, resembling a breakdown curve, at an appropriate voltage. Under double injection, that is, the simultaneous injection into the insulator of electrons from a cathode and holes from an anode, space-charge limitations are at least partially overcome but recombination of injected carriers presents a new limitation on the current flow. In any insulator at sufficiently high injection levels both recombination and space charge contribute to limitation of the current, leading to a dependence of current on the cube of the voltage, for monomolecular recombination processes. For double injection into a semiconductor, the presence of thermally generated free carriers leads to charge neutrality (the so-called ohmic relaxation process) and recombination alone limits the current. In a semiconductor long compared to a diffusion length this leads to a dependence of current on the square of the voltage. In the general case of double injection into an insulator the localized defect states (traps and recombination centers) outnumber the injected free carriers, leading to electron and hole lifetimes which differ greatly and also vary strongly with injection levels. A simple model of an insulator is analyzed in which the hole lifetime increases strongly with injection level. It is shown that this leads to a marked negative resistance.

* Received March 27, 1962; revised manuscript received May 11, 1962. This paper is an expanded version of a talk given at the 1961 Solid State Devices Research Conference, Stanford University, Palo Alto, Calif.
† RCA Laboratories, Princeton, N. J.

I. Introduction

INSULATORS have the vital and pervasive role in electronics of furnishing electrical insulation, that is, of *not* conducting current under an applied voltage. Under the circumstances they would not appear to be promising candidates for the active component in electronic devices.[1] Nonetheless when the modern, or energy-band, theory of the electronic structure of solids emerged from the application of quantum mechanics to solid-state physics, it became clear that, in principle, it should be possible to obtain injection of electrons from a suitable contact into an insulator in a manner closely analogous to their injection from a thermionic cathode into vacuum. One would then expect to observe SCL (space-charge-limited) flow of the injected electrons in the insulator, and, indeed, over the past decade there have been many observations of SCL current flow in many different insulators. Moreover, because of the inevitable presence of chemical impurities and structural defects in materials, the observed behavior of the SCL currents in insulators is much richer in complexity than that of SCL currents flowing out of a thermionic cathode into the "structure-less" vacuum.

In an insulator or semiconductor the positively charged holes are also available as current carriers. With a suitable contact, hole injection into an insulator is possible with concomitant SCL flow of the injected holes. The one-carrier SCL hole currents in an insulator exhibit the same range of behavior as the corresponding one-carrier SCL electron currents.

Current flow in insulators need not be limited to carriers of only one sign of charge. Indeed, suitable contacts to an insulator may be available which favor electron injection into the conduction band at the cathode and, simultaneously, hole injection into the valence band at the anode. In the resulting two-carrier current flow, a major limitation on one-carrier current flow, namely space charge, is to some degree circumvented; the injected electrons and holes can largely neutralize each other.[2] On the other hand an entirely new kind of limitation is introduced—loss of current carriers. The injected electrons and holes can mutually recombine before they complete their respective transits between cathode and anode. Because of these new features, the resultant behavior of two-carrier, or double-injection, currents in insulators is substantially more complex and richer in diversity than the behavior of one-carrier SCL currents.

It is the purpose of this article to review the physical principles underlying the behavior of one- and two-carrier injection currents in insulators. Both the theoretical and the practical state of the insulator have reached the point where we can now be optimistic about the fabrication of active insulator devices based on current injection [1]–[6]. It is the growing interest in insulator devices which, we feel, makes this review of basic principles timely.

The scheme of the paper is as follows: In Section II we review the domain of one-carrier SCL currents. We first discuss the insulator analog to the vacuum diode, namely the trap-free insulator. Next we consider the effect of thermally generated free carriers on the current flow. Then we show how the presence of traps affects the injected current, first for the case of shallow trapping and then for deep trapping. In Section III we consider double-injection currents under conditions where both recombination and space charge limit the current. Such would be the base in any insulator at sufficiently high injection levels. In Section IV we study double injection under semiconductor-like conditions in which the density of free carriers present initially is sufficiently high to permit charge neutralization of the injected carriers (ohmic relaxation). These currents are therefore purely recombination-limited. The discussion in Sections III and IV is confined to those situations in which the injected free carriers exceed the number of defect states in the insulator (the injected plasma case) and in which the free-carrier lifetime is a constant, independent of (or slowly varying with) injection level. Next, in Section V we proceed to the more general double-injection case where the defect states outnumber the injected free carriers and therefore in which the electron and hole lifetimes can differ greatly and also vary strongly with injection level. A simple model of an insulator is analyzed to illustrate this behavior. A particularly interesting result, from the standpoint of device applications, is the presence of a marked negative resistance in the current-voltage characteristic originating in a carrier lifetime which *increases* with injection level.

The discussion throughout is confined to volume-controlled currents, that is, to currents which are in no way constrained at the contacts. Concomitantly we neglect diffusion currents, assuming rather that purely field-driven currents provide an adequate description of the current flow. Since diffusion currents are normally relatively large near the injecting contacts, our analysis presupposes a sufficiently large separation between cathode and anode; just how large is discussed briefly in the text at the appropriate places.

We shall assume on the reader's part at least some

[1] Of course it has been known for many decades that the conductivity of insulators can be drastically increased by illuminating them with light of sufficiently high frequency. We are not concerned here with this photoconductive behavior of materials.

[2] For the vacuum diode, it was shown by I. Langmuir ("The Interaction of Electron and Positive Ion Space Charges in Cathode Sheaths," vol. 33, pp. 954–989; June, 1929) that the simultaneous emission of electrons from the cathode and positive ions from the anode does not lead to a total current I substantially larger than the one-carrier, electron SCL current I_e as given by Child's law. Indeed the maximum possible value of I/I_e, for a planar diode, is 3.7. The reason why only limited space-charge neutralization, and therefore limited current enhancement, are achieved in this case is that in the vacuum diode the carrier drift velocity depends on the potential difference the carrier has traversed. Thus, where carriers of one sign are drifting slowly and therefore have high density, near their emitting electrode, the carriers of opposite sign are drifting at high velocity and have low density. In a solid, on the other hand, carrier drift velocity is proportional to the local electric field intensity. Thus, both electrons *and* holes drift slowly in regions of low field intensity and there is maximum opportunity for mutual neutralization. Correspondingly there can be much greater current enhancement from the presence of carriers of both signs of charge.

familiarity with those concepts of modern solid-state theory which have become working tools of the trade for those engaged in solid-state device work. These concepts include energy bands, localized defect states, trapping, recombination, mobility, Fermi level, etc. We shall not assume any familiarity with the characteristic electronic properties and behavior of insulators. For the purpose of this paper an insulator is distinguished from a semiconductor by virtue of having a relatively small number of free carriers, in thermal equilibrium, compared to its number of localized defect states.

Throughout we shall use mks units, unless otherwise specified. Further, we shall confine our discussion to configurations supporting one-dimensional current flow. Finally we shall discuss only steady, dc current flow. Although ac and transient conditions bring in further complications, they do not change the underlying physical mechanisms which are simpler to think about for steady-state dc currents.

The discussion throughout will employ a minimum of mathematics. Where in a few instances it has seemed convenient to write down the differential equations appropriate to the injection problem, these equations will be solved only in an approximate manner by simple dimensional analysis. That is, derivatives like dn/dx, d^2n/dx^2 will be replaced by $\bar{n}/L$, $\bar{n}/L^2$ respectively, where $\bar{n}$ is a suitable average of n and L is the cathode-anode spacing. Where this procedure has been used, below, the results so obtained have, in each case, been confirmed by rigorous mathematical solution of the differential equations.

II. One-Carrier SCL Currents

For the sake of definiteness we discuss electron currents.

The conceptual basis for carrier injection in solids is easily established by inspection of simple energy-band diagrams. Fig. 1(a) shows a metal-vacuum contact and Fig. 1(b) an electron-injecting, metal-insulator contact, both contacts being in thermal equilibrium (no applied voltage). $\bar{F}$ is the Fermi level, E_{VAC} the lowest vacuum level, and E_c the lowest conduction-band level. Around 1940, Mott and Gurney [7] made the important observation that the metal-vacuum and injecting metal-insulator contact are really very similar, as we see comparing the two figures. Electrons will "boil off" from the metal into the conduction band of the insulator just as they do from the heated cathode into vacuum. Further, the activation energy step Φ at the metal-insulator contact can be substantially smaller than the corresponding work function W for the metal-vacuum contact. As a result, even at room temperature or lower there may be a sufficient number of electrons available at the contact to support SCL current flow in the insulator. Fig. 1(b) depicts a highly idealized model of an insulator, namely one free of electron traps. In 1955 Rose [8] made the important observation that the localized defect states inevitably present in the forbidden gap of any real

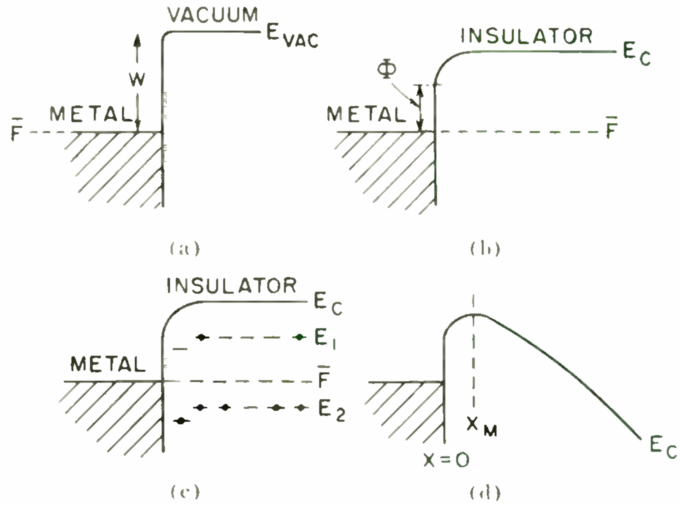

Fig. 1—Schematic energy-band diagrams for injecting contacts: (a) metal-vacuum, (b) metal-insulator (free of traps), (c) Metal-insulator (containing traps), (d) metal-insulator under applied voltage. Diagrams (a)–(c) correspond to thermal equilibrium (no applied voltage).

insulator, for example at levels E_1 and E_2 in Fig. 1(c), may strongly affect the SCL current flow. Those localized states which are initially empty [states at E_1 in Fig. 1(c)], if sufficiently numerous, will capture most of the injected electrons and thereby drastically reduce the current from its trap-free value. Fig. 1(d) shows the contact of Fig. 1(c) under an applied voltage, the contact being negative. Just as in the thermioic vacuum tube under SCL current-flow conditions, there is a potential minimum, or energy maximum (at position x_M), near the contact interface. In both cases this potential minimum is the hallmark of complete space-charge limitation of a one-carrier current.

A. The Perfect Insulator

We first derive the current-voltage characteristic for the simplest possible situation, namely the perfect insulator, free of traps and with no (or negligible) free carriers in thermal equilibrium. This is the closest solid-state analog to the thermionic vacuum diode. All injected electrons remain free and all contribute to space charge, as in the vacuum case. The current density J, which is constant with position, may be written as

$$J = \rho(x)v(x) \simeq \bar{\rho}\bar{v} \tag{1}$$

with $\rho(x)$ the charge density at x, $\bar{\rho}$ the average charge density, $v(x)$ the free-carrier drift velocity at x, and $\bar{v}$ the average drift velocity. As mentioned earlier, diffusion-current flow is neglected.

Total charge Q (per unit area) and applied voltage V are related, in the usual fashion,[3] via the capacitance C

[3] The reader might well question our use of the geometric value ϵ/L for the capacitance C, since the injected space charge is smoothly distributed between cathode and anode rather than concentrated near the cathode. Nonetheless, it has been shown by the author [9] that, under very general conditions including electron trapping, field-dependence of the mobility, etc., an error of at most a factor of two is made through this approximation, for one-dimensional problems.

(per unit area):

$$Q = \bar{\rho}L = CV \simeq \frac{\epsilon}{L} V \tag{2}$$

where L is the cathode-anode spacing and we have taken for C its geometric value ϵ/L, ϵ being the static dielectric constant. Combining (2) and (1), we obtain

$$J \simeq \frac{\epsilon \bar{v} V}{L^2} \cdot \tag{3}$$

The free-carrier drift velocity, dominated by frequent collisions, is given by the product of the free-carrier mobility μ and the electric field intensity $\mathcal{E}$:

$$v(x) = \mu \mathcal{E}(x); \qquad \bar{v} = \mu \bar{\mathcal{E}} = \mu \frac{V}{L} \cdot \tag{4}$$

Combining (3) and (4) we obtain the desired current-voltage characteristic:

$$J \simeq \epsilon\mu \frac{V^2}{L^3} \cdot \tag{5}$$

The more rigorous result, first obtained by Mott and Gurney [7], differs from (5) only through the presence of the multiplicative, numerical factor 9/8. Note that the result (3) is still useful even at high fields where (4) no longer holds, that is, where the mobility is field-dependent. One need only know the functional form of the dependence of $\bar{v}$ on V to obtain, from (3), the J-V characteristic.

Eqs. (1), (2) and (3) are clearly not restricted to current flow in solids. It is instructive to apply these approximate arguments to the thermionic vacuum diode. In this case electrons move freely, without collisions, and their drift velocity at x is related to the potential difference $V(x)$ they have fallen through rather than to the local field at x, as in (4):

$$v(x) = \sqrt{\frac{2eV(x)}{m}}; \qquad \bar{v} \simeq \sqrt{\frac{eV}{m}} \tag{6}$$

where e and m are the charge and mass respectively of the electron, and $V = V(L)$.

Substituting for $\bar{v}$ from (6) into (3), we obtain

$$J \simeq \epsilon_0 \sqrt{\frac{e}{m}} \frac{V^{3/2}}{L^2} \tag{7}$$

where ϵ has been replaced by ϵ_0, the dielectric constant of vacuum.

The correct result, the famous Child's law, differs from (7) only through the presence of the multiplicative, numerical factor $4\sqrt{2}/9 \simeq 0.63$.

The above results, (5) and (7), show the power and usefulness of the simple, approximate arguments introduced by Rose [8], if one is willing to sacrifice some accuracy in a numerical coefficient. The error incurred usually does not exceed a factor of two. In the current state of insulator technology greater accuracy in theoretical results is generally not required.

A further point to be noted is that a theory based on purely field-driven currents, (1), cannot furnish a sensible description of the physical situation near the injecting cathode. For, at the potential minimum (energy maximum), x_M in Fig. 1(d), the field vanishes and the current must therefore be a pure diffusion current. To the left of x_M the actual current J is the difference between opposing diffusion and field-driven currents, the former being dominant. To the right of x_M the two currents add to give J; however the diffusion contribution is negligible beyond $x = 2x_M$. Therefore all of the results of this section are valid only for those situations in which the cathode-anode spacing L substantially exceeds the width $w \approx 2x_M$ of the contact region. In the current state of insulator technology w will generally not exceed 1 μ, its value for a rather pure insulator (impurity state density of about 10^{15} cm^{-3}). The higher the impurity content, the smaller will w be. This limitation on the range of validity of a simple current-flow theory for solids has its analog in vacuum-tube theory. The simple Child's law, (7), for the thermionic diode breaks down when the anode is close to the potential minimum and a more refined treatment taking account of the velocity distribution of the electrons is needed.

B. The Trap-Free Insulator with Free Carriers Present in Thermal Equilibrium

The next step in complexity is the inclusion of the thermally generated free carriers, density n_0, in the problem. Here experience tells us that Ohm's law

$$J = en_0\mu \frac{V}{L}, \tag{8}$$

will be observed at low voltages. This is quite plausible in the light of the injection theory presented above. For although at any voltage V, however small, there will be excess charge injected into the insulator, given by (2), there cannot be significant departures from Ohm's law until the injected, *excess*, free-carrier density n becomes comparable to the thermally generated, hence neutralized, carrier density n_0. Thus the transition from Ohm's law (8) to the Mott-Gurney law (5) will take place, roughly, at the voltage V_{tr} determined by

$$en_0L = Q_{inj} = CV_{tr} = \frac{\epsilon}{L} V_{tr}. \tag{9}$$

Simple algebraic manipulation of (9) gives the significant relation $\epsilon/en_0\mu = L^2/\mu V_{tr}$. Thus the transition is characterized by

$$V_{tr} \simeq \frac{en_0L^2}{\epsilon}, \qquad t_{tr} = t_\Omega \tag{10}$$

where $t_\Omega = \epsilon/en_0\mu$ is the well-known ohmic (or dielectric) relaxation time and $t_{tr} = L^2/\mu V_{tr}$ is the carrier transit time between cathode and anode at voltage V_{tr}. ($L^2/\mu V_{tr} = L/\bar{v}_{tr}$ with $\bar{v}_{tr} = \mu V_{tr}/L$). Thus the injected excess carriers dominate the thermally generated ones when the transit time for the excess carriers is too short for their charge to be relaxed by the thermal carriers.

It is easily checked that the relation (10), derived on the physical basis (9), also corresponds simply to the voltage where Ohm's law (8) crosses the Mott-Gurney law (5).

C. The Insulator with Traps

As pointed out earlier, the presence of traps will generally result in a greatly reduced current since those traps initially empty will capture, and thereby immobilize, most of the injected carriers. This capture of carriers by the traps in the steady state is conveniently analyzed via the concept of the steady-state Fermi level. In thermal equilibrium the free electron density n_0 is given by the familiar expression

$$n_0 = N_c \exp \frac{\overline{F} - E_c}{kT} \tag{11}$$

with N_c the effective density of states in the conduction band, $\overline{F}$ the thermodynamic Fermi level, E_c the bottom conduction-band level, and kT thermal energy. Here we are assuming nondegenerate statistics for the electrons in the conduction band, which is, of course, appropriate for insulators. The occupancy $n_{t,0}$ of the electron traps at level E_t, Fig. 2(a), is given by the familiar Fermi-Dirac expression

$$n_{t,0} = \frac{N_t}{1 + \dfrac{1}{g} \exp \dfrac{E_t - \overline{F}}{kT}} \tag{12}$$

where N_t is the density of traps and g the degeneracy factor for the traps (g is generally a small integer, *e.g.*, $g = 2$ in the simplest case). Clearly this equilibrium trap occupancy results from a balance between capture of electrons into the traps, the downward arrow, and their thermal re-emission into the conduction band, the upward arrow. Now, a very important point for the development of the theory is the fact that the presence of a moderate electric field will not affect these elementary microscopic processes of electron capture and thermal re-emission. Therefore, in the presence of the applied field, if it is not too strong, the balance between free and trapped electrons is altered ***only*** through the change in free-electron density n accompanying injection, as indicated schematically in Fig. 2(b). Therefore, at each position x, *the balance between free and trapped electrons is reached as if the crystal were in thermal equilibrium, only with a free-carrier density $n(x)$ instead of n_0*. The corresponding Fermi level $F_n(x)$ us called the electron steady-state Fermi level, abbreviated ESSFL, and is related to $n(x)$, by definition, exactly as $\overline{F}$ is related to n_0 in (11) namely

$$n(x) = N_c \exp \frac{F_n(x) - E_c}{kT}. \tag{13}$$

$F_n(x)$ now appears in the Fermi-Dirac expression determining trap occupancy $n_t(x)$:

$$n_t(x) = \frac{N_t}{1 + \dfrac{1}{g} \exp \dfrac{E_t - F_n(x)}{kT}} = \frac{N_t}{1 + \dfrac{1}{g}\dfrac{N}{n(x)}}; \qquad N \equiv N_c \exp \frac{E_t - E_c}{kT} \tag{14}$$

and the traps are said to be in quasi-thermal equilibrium with the free carriers. The second expression for $n_t(x)$ in (14) is obtained by simple alegbraic manipulation using (13), the quantity N being introduced as a matter of convenience.

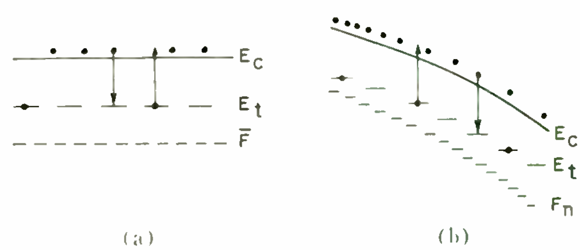

Fig. 2—Fermi levels: (a) thermodynamic equilibrium; the true Fermi level $\overline{F}$. (b) carrier injection under an applied voltage; the ESSFL F_n. Solid circles denote electrons.

Some pertinent elementary properties of the Fermi-Dirac occupation function follow simply upon inspection of (14). First, so long as F_n lies *below* E_t by more than kT, $1 + N/gn(x) \approx N/gn(x)$, the traps are said to be "shallow," and the ratio of free to trapped electron densities is a constant θ independent of $n(x)$:

$$\frac{E_t - F_n(x)}{kT} > 1; \qquad \frac{n(x)}{n_t(x)} = \frac{N}{gN_t} = \theta. \tag{15}$$

Those shallow traps are important for which $\theta \ll 1$, for many more injected electrons are immobilized in such traps than are free. The dominant set of shallow traps is that for which θ is the smallest, $\theta = \theta_S$. Of the total injected charge $Q = CV$, only the small portion $\theta_S Q$ is free to carry current. It is now easily verified, repeating the simplified arguments of Section II-A under this new condition, that the same square-law dependence of current on voltage is obtained as for the trap-free case, (5), only reduced by the constant θ_S:

shallow trapping:

$$J \simeq \theta_S \epsilon \mu \frac{V^2}{L^3} \cdot \tag{16}$$

If there are free carriers, density n_0, in thermal equilibrium, then Ohm's law, (8) will be followed at low voltages. The transition voltage V_{tr} to the square law (16) will now be $1/\theta_S$ times the transition voltage for the trap-free case (10), since in doubling the free-carrier density through injection, the shallow-trapped, excess, injected-electron density must be n_0/θ_S:
shallow trapping:

$$V_{tr} \simeq \frac{e n_0 L^2}{\theta_S \epsilon} \tag{17}$$

If F_n lies *above* E_t by more than kT, $1+N/gn(x) \approx 1$, the traps are said to be "deep," and they are filled with electrons:

deep trapping:

$$\frac{F_n(x) - E_t}{kT} > 1; \qquad n_t(x) \simeq N_t. \tag{18}$$

"Shallow" and "deep" are relative designations which depend on the injection level. As the injection level increases, F_n moves up in the forbidden gap towards the conduction band. When it moves through a trap level, the trap, which had been shallow, becomes deep.

The current-voltage characteristic is profoundly affected by the crossing of a trap level by the SSFL, that is, by the filling of a set of traps. In order to see this, consider, for example, the situation illustrated in Fig. 2(a) where there is a single set of traps at level E_t. Further, assume that the thermodynamic Fermi level $\overline{F}$ lies just below E_t: $E_t - \overline{F} < kT$. The onset of injection occurs, as always, when the applied voltage is sufficient to double the density of free carriers, that is, when $n \simeq 2n_0$. From (13), this corresponds to upward motion of F_n by about kT. Thus F_n has moved through the trap level E_t, and the traps are now full. The corresponding voltage V_{TFL}, determined, as usual, from $Q_{TFL} = eN_tL = CV_{TFL}$, is given by

traps-filled-limit voltage:

$$V_{TFL} \simeq \frac{eN_tL^2}{\epsilon} \cdot \tag{19}$$

In the present case, V_{TFL} coincides with the voltage at which the transition from Ohm's law to SCL current flow takes place, If now the applied voltage is doubled, $V = 2V_{TFL}$, the injected charge must likewise be doubled, $Q(2V_{TFL}) = 2Q_{TFL}$. Since the traps were already filled at the voltage V_{TFL}, the additional injected charge, $Q(2V_{TFL}) - Q(V_{TFL}) = Q(V_{TFL}) \simeq eN_tL$ must all appear in the conduction band. We have then for the ratio of the currents at the two voltages

$$\frac{J(2V_{TFL})}{J(V_{TFL})} \simeq \frac{2n(2V_{TFL})}{n(V_{TFL})} \simeq \frac{N_t}{n_0} \tag{20}$$

where $n(V)$ denotes the total free-electron density, injected plus thermal, at voltage V. Because $E_t - \overline{F} < kT$, $n(V_{TFL}) \simeq 2n_0$ (coincidence here of V_{TFL} and V_{tr}). The additional factor of two appears in the numerator of the middle expression in (20) because the applied field is doubled when the voltage is doubled. The ratio N_t/n_0 may easily be many powers of ten in insulators. We see then that a factor of two change in voltage, following the filling of a set of traps, many produce an enormous change in current.

The complete current-voltage characteristic for this case is shown schematically, curve labelled I, in the log-log plot of Fig. 3. The very steep (near-vertical) portion of the characteristic is called the TFL (traps-filled-limit) law. At voltages $V > 2V_{TFL}$, the total number of injected electrons exceeds the total number of traps and so the J-V curve merges with the trap-free square-law curve as shown.

If, in Fig. 2(a), $\overline{F}$ lies well below E_t, $E_t - \overline{F} \gg kT$, then in the earlier stages of injection the traps are shallow and the modified square law (16) is followed, as indicated schematically by the curve labelled II in Fig. 3. The transition voltage $V_{tr,II}$ for the Ohm's-law/square-law transition for this case is given by (17). At the voltage V_{TFL} the ESSFL crosses E_t, the traps are filled, and curve II merges with the TFL law.

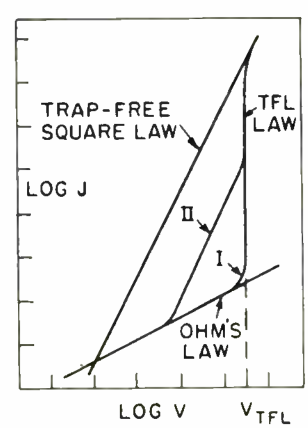

Fig. 3—Prototype current density-voltage characteristics for one-carrier SCL currents.

If the traps are effectively absent in Fig. 2(a), $N_t \leq n_0$, then there are only the two branches: Ohm's law and the Trap-Free square law. The transition voltage for this case is given by (10).

For purposes of illustration we have confined our discussion to the specific case of a single, discrete set of traps. A more detailed treatment of this problem, including the complete analytical solution, is given in a paper by the author [9]. In insulators which are not highly purified it is likely that there will be trap distributions spread out in energy over certain regions of the forbidden gap. The current-voltage characteristics for some typical distributions are derived in the pioneering paper of Rose [8]. One-carrier SCL current flow in depletion regions of semiconductors has been studied, both theoretically [10] and experimentally [11], somewhat earlier. Since our interest is focused on insulators we have not discussed this work here.

Observations of steady-state, one-carrier SCL currents have been made on single crystals [12] and evaporated layers [13] of CdS, single crystals of ZnS [14] and high resistivity GaAs [15], and on amorphous Se [16], [1] with similar results as illustrated in Fig. 3. Recently transient one-carrier SCL currents have been reported in molecular crystals, namely anthracene [17] and iodine [18] and other organic crystals [17b]. A theory for these transient SCL currents has also been presented [17b], [18a] and [19]. Experimental devices based on one-carrier SCL current flow have been reported by several authors [3], [13], [16b], [1], [20].

III. Double-Injection Currents Limited by Recombination and Space Charge

The first double-injection problem we shall study is the relatively simple one illustrated schematically in Fig. 4. The thermally generated free electron and hole densities, n_0 and p_0 respectively, are assumed small enough to be negligible. On the other hand the injected electron and hole densities, n and p respectively, are assumed to exceed greatly the total density of traps and recombination centers, that is of all localized defect (chemical and structural) states N_{def} in the forbidden gap. Under these conditions the injected electrons and holes *approximately* neutralize each other: $n \approx p$, and in effect a plasma of mobile electrons and holes is injected into the insulator. Although the carriers immobilized in the defect states are too few to affect directly the current-voltage characteristic, the defect states—at least the recombination centers—still play a vital role to the extent that they control the recombination of the injected electrons and holes.

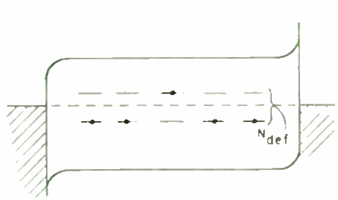

Fig. 4—Double injection into an insulator. N_{def} denotes the total density of localized defect states (chemical and structural) in the forbidden gap.

We proceed to the solution of the problem. For the current density J we have, in place of (1), the contributions of both electrons and holes:

$$J = e(nv_n + pv_p) \sim e\bar{n}(\bar{v}_n + \bar{v}_p) \qquad (21)$$

where a bar over a quantity denotes the value of that quantity evaluated at the mid-plane of the solid, $x = L/2$. This is a representative, or average, value for the quantity. Here and throughout, subscripts n and p refer to electrons and holes respectively. In taking $\bar{n} = \bar{p}$ we are taking cognizance of the *approximate* neutrality of the injected plasma.

The drift velocities $\bar{v}_n$, $\bar{v}_p$ are directly related to the applied voltage; thus at low or moderate fields, $\bar{v}_n = \mu_n \mathcal{E} \simeq \mu_n V/L$, and correspondingly for $\bar{v}_p$. It remains to relate $\bar{n}$ to V. The key to this latter relationship lies in the relatively small departure from charge neutrality over the body of the plasma. The departure must be small when the plasma density $\bar{n}$ is large compared with the space-charge density CV/eL that can be supported by the applied voltage V. Our discussion is restricted to this situation. A reasonable estimate of the fraction f of the total number $e\bar{n}L$ of injected carriers which is unneutralized is $f \approx (\bar{t}_n + \bar{t}_p)/\bar{\tau}$, where $\bar{\tau}$ is the common, average lifetime for the injected electrons and holes, and $\bar{t}_n$, $\bar{t}_p$ are their respective, average transit times. That is, the total space charge Q distributed over the volume of the plasma is $Q \approx e\bar{n}L(\bar{t}_n + \bar{t}_p)/\bar{\tau}$, as the electrons and holes, injected at opposite electrodes, must trasverse a finite distance to reach and neutralize each other. The smaller the lifetime, the greater is the attrition of carriers through mutual recombination, hence the greater will be the departure from neutrality. Conversely, the smaller the transit times, the more carriers can survive in the face of recombination to achieve neutralization. The simplest measure of these opposing, competitive tendencies is just the ratio: transit time/lifetime. Additivity of the ratios $\bar{t}_n/\bar{\tau}$ and $\bar{t}_p/\bar{\tau}$ corresponds to the fact that the electrons and holes are injected at opposite electrodes and drift in opposing senses. This entire picture of an approximately neutral, injected plasma is self-consistent only if $\bar{t}_n/\bar{\tau} \ll 1$ and $\bar{t}_p/\bar{\tau} \ll 1$.

The above argument can be sharpened up a bit by making the reasonable approximation that the attrition of carriers due to recombination can be represented by

$$\left.\begin{aligned} n(x) &\approx \bar{n} \exp \frac{\bar{x} - x}{\bar{v}_n \bar{\tau}} \\ &\approx \bar{n} \left\{ 1 + \bar{\zeta}_n \frac{\bar{x} - x}{L} \right\}; \quad \bar{\zeta}_n = \frac{L}{\bar{v}_n \bar{\tau}} = \frac{\bar{t}_n}{\bar{\tau}} \ll 1 \\ p(x) &\approx \bar{p} \exp \frac{x - \bar{x}}{\bar{v}_p \bar{\tau}} \\ &\approx \bar{n} \left\{ 1 - \bar{\zeta}_p \frac{\bar{x} - x}{L} \right\}; \quad \bar{\zeta}_p = \frac{L}{\bar{v}_p \bar{\tau}} = \frac{\bar{t}_p}{\bar{\tau}} \ll 1 \end{aligned}\right\} \qquad (22)$$

where $\bar{x} = L/2$. The linear variations of n and p with x in (22) are represented by the two dashed straight lines in Fig. 5(a). These straight lines are approximations to presumed variations of n and p represented by the solid lines. From the opposite signs of the slopes of the two lines, it is obvious that where the electrons are in excess, $n > \bar{n}$, the holes are deficient, $p < \bar{n}$, and conversely. For this reason the space charge $Q \propto \bar{t}_n/\bar{\tau} + \bar{t}_p/\bar{\tau}$ as suggested above. From (22) it follows that the uncompensated

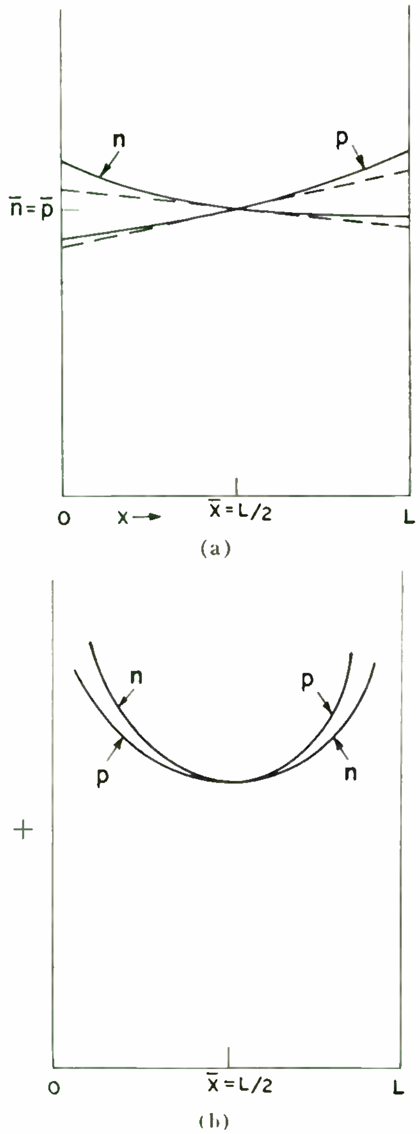

Fig. 5—Injected free-carrier distributions for double injection into an insulator, in the limit of high injection levels: (a) naive approximation, (b) actual distributions (schematic).

charge density over the body of the plasma is given by

$$e(n-p) \approx e\bar n(\xi_n+\xi_p)\frac{\bar x - x}{L}. \qquad (23)$$

The total uncompensated charge of one sign is the integral of (23):

$$|Q_-| = e\int_0^{\bar x}(n-p)dx \approx e\bar n(\xi_n+\xi_p)\frac{L}{8}$$

$$= CV = \frac{\epsilon}{L}V. \qquad (24)$$

The quantity $|Q_-|/e$ is just the triangular area, from $x=0$ to $x=\bar x=L/2$, between the two dashed straight lines in Fig. 5(a). Over-all neutrality of the solid, necessitated by a theory of purely field-driven, double-injection currents if both contacts are idealized, injecting ones ($\mathcal{E}=0$ at both contacts) requires that $|Q_-|=Q_+=e\int_{\bar x}^{L}(p-n)dx$. That is, the left-hand triangular area in Fig. 5(a) must equal the right-hand triangular area. Clearly this requires $\bar x=L/2$, as we have chosen above.

Eq. (24) gives the sought-after relation between $\bar n$ and V:

$$\bar n \approx \frac{8\epsilon\bar\tau V}{eL^3}\left(\frac{\bar v_n\bar v_p}{\bar v_n+\bar v_p}\right). \qquad (25)$$

Combining (21) and (25) we obtain the current-voltage characteristic:

$$J \approx 8\epsilon\bar\tau\bar v_n\bar v_p\frac{V}{L^3} \to 8\epsilon\bar\tau\mu_n\mu_p\frac{V^3}{L^5}. \qquad (26)$$

The second expression in (26) is the "low-field" approximation: $\bar v=\mu V/L$. A special case (equal mobilities) was earlier derived by Rose [21] using similar arguments. A more complete discussion of the problem, along the above lines, has been given by the author [22]. The "low-field" case has been solved rigorously [23], the same result as (26) being obtained except that the numerical coefficient 8 is replaced by $125/18=6.94$. As in the one-carrier SCL current problem, the approximate result obtained by simple, "physical" reasoning is in excellent agreement with the exact solution.

If the average common lifetime $\bar\tau$ is a constant, independent of injection level, the solution is complete. If $\bar\tau$ varies with injection level, $\bar\tau=\bar\tau(\bar n)$, (26) is still useful, that is, approximately correct. However, it still remains to eliminate the density-dependent $\bar\tau$ from the solution. As an interesting illustration, consider the case of bimolecular recombination: $\bar\tau=1/\alpha\bar n$, $\alpha=v_T\sigma_B$ with v_T thermal velocity and σ_B the bimolecular recombination cross section. The lifetime $\bar\tau$ can now be eliminated from (26) using (25), the final result being

$$J \approx 2\epsilon\left\{\frac{\bar v_n\bar v_p(\bar v_n+\bar v_p)}{\mu_0}\right\}^{1/2}\frac{V^{1/2}}{L^{3/2}}$$

$$\to 2\epsilon\left\{\frac{\mu_n\mu_p(\mu_n+\mu_p)}{\mu_0}\right\}^{1/2}\frac{V^2}{L^3} \qquad (27)$$

with $\mu_0=\epsilon\alpha/2e$. The second expression in (27), to which we restrict the further discussion, is the "low-field" approximation, the mobilities μ_n and μ_p being constant and equal to their low-field values.

The quantity μ_0 was first introduced by Parmenter and Ruppel [24] and called by them the "recombination mobility." The conditions $\xi_n \ll 1$, $\xi_p \ll 1$ which must be satisfied if the above treatment is to be valid, are easily shown to be equivalent to the conditions $(\mu_n/\mu_0)^{1/2} \gg 1$ and $(\mu_p/\mu_0)^{1/2} \gg 1$. Since these latter conditions are independent of applied voltage, so likewise must be the transit time-to-lifetime ratios ξ_n and ξ_p. Under these same conditions, Parameter and Ruppel [24] have solved the "low-field" bimolecular-recombination, double-injection problem rigorously, obtaining the same result as (27), only with the numerical factor 2 replaced by $3\sqrt{2\pi}/4=1.89$. The close agreement of (27) with the exact result is particularly significant because it shows that even in a problem where the lifetime varies *explicitly* with free-carrier density, hence with position, the use of just the average lifetime gives excellent results. This is, of course, not fortuitous; rather it is a reflection of the fact that when a plasma is injected into a solid the electric field intensity and therefore other local characteristics and properties of the plasma do not vary strongly with position over the volume of the solid, that is, away from the immediate vicinity of the contacts. When one of the carriers is largely captured by recombination centers, this need no longer be true, as we shall see in Section V.

Assuming for the sake of definiteness that $\mu_n \gtrsim \mu_p$, then (27), for the "low-field" case, can be rewritten as

$$J \simeq 2\epsilon\mu_n \left\{\frac{\mu_p}{\mu_0}\right\}^{1/2} \frac{V^2}{L^3}. \tag{28}$$

Comparing (28) to (5) we see that the double-injection current-voltage characteristic differs from that for one-carrier SCL current flow (traps being negligible in both cases) only through the enhancement factor $2(\mu_p/\mu_0)^{1/2}$. For a reasonable value of σ_B, namely $\sigma_B \approx 10^{-19}$ cm^2, μ_0 is very small, namely $\mu_0 \sim 10^{-5}$ cm^2/volt sec. [This very small value for μ_0 ensures the validity of (27).] In this case, charge neutralization produces a current enhancement on the order of 10^3 to 10^4 over that allowed under the complete space-charge limitation of a one-carrier current.

Having shown that the simplified "physical" arguments give remarkably good results for the currents, it behooves us now to point out that the carrier density distributions given by (22) and the simplified picture of Fig. 5(a) based on them, are not quite correct! The correct free-carrier density distributions are illustrated in Fig. 5(b). The combined requirements of (approximate) charge neutrality and particle conservation do not permit the simple monotonic variations of n and p implied by (22) and shown in Fig. 5(a). The reason that the "physical" argument gives the correct answer is that the *separate* equations in (22) are nowhere used in the derivation! Only the *difference* between these equations, which gives the space-charge density, namely (23), is used, and this latter equation is indeed a good approximation. The triangular areas in Fig. 5(a) quite closely approximate the semilunate areas between the correct n and p curves in Fig. 5(b)! It is easily seen that the approximately correct *space-charge* distribution in Fig. 5(a) actually implies the separate free-carrier distributions as given in Fig. 5(b). From this space-charge distribution it follows that the electric field intensity is a maximum in the center, being zero at both ends. From *approximate* conservation of the separate electron and hole currents, the recombination current being relatively small, the free-carrier densities necessarily follow the inverse of the field intensity and therefore have the distribution pattern of Fig. 5(b).

A final word is in order on the domain of injection levels over which (26) is valid. Since the theory is based on the assumption of an injected plasma, $n \approx p$, it is clearly a high-injection-level theory $n \gg N_{\mathrm{def}}$, as pointed out earlier in this section. Actually, the important role that space charge plays in the derivation, (24), enables us to state more precisely the validity condition, namely $Q = CV \simeq \epsilon V/L > eN_{\mathrm{def}}L$. Thus the onset voltage $V_{\mathrm{tr,high}}$ for this high-injection-level regime is given by

$$V_{\mathrm{tr,high}} \simeq \frac{eN_{\mathrm{def}}L^2}{\epsilon} \tag{29}$$

where N_{def} is the *total* density of electronically active defect states, including shallow donors and acceptors, deeper-lying traps and recombination centers. In using (26) in this high-injection-level regime, it is of course desirable, where the lifetime $\bar{\tau}$ depends on injection level, to eliminate $\bar{\tau}$ from the equation. To do this it is obviously necessary to know the specific functional dependence of $\bar{\tau}$ on $\bar{n}$, as for example, in the bimolecular case discussed above.

We next study the effect of a "large" density of thermally generated free carriers on current flow, under double injection.

IV. Double-Injection Currents Limited Only by Recombination; Space Charge Relaxed Through the Presence of Thermal Free Carriers (Double Injection into a Semiconductor)

Although our primary interest in this article is insulators, it is not only instructive, but also directly useful to study the problem of double injection into a semiconductor. For there are situations in which a high-resistance insulator will be converted into an extrinsic-like semiconductor under double injection. Such is the case, for example, in the insulator problem studied in the following Section V.

The problem we shall study in this section is that illustrated in Fig. 6, namely double injection into an n-type semiconductor. This problem represents the next step in complexity beyond that treated in Section III and differs from the latter problem only through the presence of a large density of thermally generated free carriers. In both problems the free-carrier lifetimes are assumed to be constant, independent of position. In Fig. 6 the contacts shown are an n^+-n junction for the electron-injecting contact and a p-n junction for the hole-injecting contact, as opposed to the metal-insulator contacts in Fig. 4. These differences are inconsequential for a theory of purely field-driven current flow which, in any case, idealizes the contacts.

At very high injection levels, that is, at voltages $V > V_{\mathrm{tr,high}}$ defined by (29), the thermal free carriers can be neglected, and the previous result, (26), correctly describes the dependence of current on voltage. At lower voltages, $V < V_{\mathrm{tr,high}}$, the main physical effect of the thermal free carriers is that of producing neu-

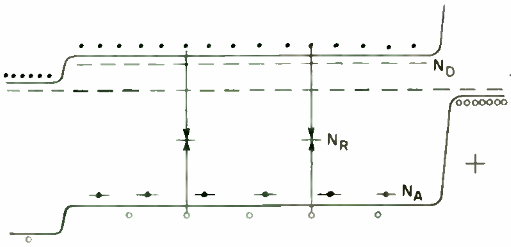

Fig. 6—Double injection into an n-type semiconductor from n^+-n and p-n junction contacts. N_D, N_A, N_R denote donor, acceptor and recombination centers respectively. $\bar{F}$ is the Fermi level.

tralization of injected charge. Consequently space charge plays no role in determining the current-voltage characteristic; the current is purely recombination-limited. Clearly then the effects of recombination on the current must be studied very carefully. Unfortunately, the author has found these effects to be rather subtle and, to date, not amenable to quite so simple, approximate, physical analyses as have worked for the simpler problems discussed up to this point. Indeed it appears to be necessary to write down the differential equations governing the current flow in order to proceed with a sensible discussion. A saving grace, perhaps, is that at least it is not necessary to obtain rigorous solutions of the equations to obtain the desired results; approximate solutions obtained by inspection, using simple dimensional analysis, suffice. The complete equations, including diffusion, which define the problem are: the electron and hole current-flow equations,

$$\left.\begin{aligned} \frac{1}{e} J_n &= \mu_n(n + n_0)\mathcal{E} - D_n \frac{dn}{dx} \quad (30a) \\ \frac{1}{e} J_p &= \mu_p(p + p_0)\mathcal{E} + D_p \frac{dp}{dx} \quad (30b) \end{aligned}\right\} \quad J = J_n + J_p;$$

the Poisson equation (neglecting changes in occupancy of localized, e.g., recombination, centers),

$$\frac{\epsilon}{e} \frac{d\mathcal{E}}{dx} = n - p; \tag{31}$$

and the particle conservation equations,

$$\left.\begin{aligned} -\frac{1}{e} \frac{dJ_n}{dx} &= r \quad (32a) \\ \frac{1}{e} \frac{dJ_p}{dx} &= r \quad (32b) \end{aligned}\right\} \quad r = \frac{n}{\tau_n} = \frac{p}{\tau_p} \cdot$$

Multiplying (32b) by $b = \mu_n/\mu_p$, and adding (32a) to the result using (30a) and (30b) gives

$$\frac{d}{dx}[(p - n)\mathcal{E}] - (n_0 - p_0)\frac{d\mathcal{E}}{dx} + \frac{kT}{e} \frac{d^2}{dx^2}(n + p) = \frac{(b + 1)r}{\mu_n} = \frac{(b + 1)n}{\mu_n \tau_n} = \frac{(b + 1)p}{\mu_p \tau_p} \cdot \tag{33}$$

In the above equations, $J_n J_p$ are the electron and hole current densities respectively; n and p are the injected, excess electrons and holes respectively, n_0 and p_0 the corresponding thermally generated densities; $\mathcal{E}$ is the electric field intensity; μ_n and μ_p are the electron and hole mobilities respectively, D_n and D_p the corresponding diffusion constants, e.g., $D_n = kT\mu_n/e$ with k Boltzmann's constant, T the temperature in degrees Kelvin, e the electronic charge; x is the position coordinate; r is the recombination rate density; τ_n and τ_p are the electron and hole lifetimes respectively.

Eq. (33) is particularly useful for comparison of the different current-flow regimes. Earlier theories of double injection into semiconductors [25]–[28] treated short n-i-p structures in which the current flow is controlled by one or both junctions (contacts) as well as by volume recombination. Of the three terms on the left-hand side of (33) these theories ignore the first two, take $n = p$ in the third term (hence $\tau_n = \tau_p = \tau$), and thereby obtain the well-known diffusion solution, with an effective diffusion length $L_{\text{eff}} = (2D_n\tau/(b+1))^{1/2}$. Note that in obtaining this diffusion solution the field terms are neglected only in (33). The field terms are retained in (30a) and (30b), and indeed these terms are used, in conjunction with the diffusion solution to obtain the field intensity distribution. The diffusion solution, which yields an exponential dependence of current on voltage at low voltages, gives a square-law dependence at higher voltages [27]. This square law is unrelated to that characterizing the semiconductor regime, (38) below.

Although the diffusion term in (33) will generally be dominant near the contacts, in a sample which is many diffusion lengths long the magnitude of this term drops off exponentially, with a characteristic fall-off distance equal to a diffusion length, going away from a contact. Therefore in such a long sample the field terms in (33) will be dominant over most of the sample. Here we simplify the situation somewhat and neglect the diffusion term altogether. Likewise we neglect the diffusion contributions to the separate currents, (30a) and (30b).

In the field-dominated problem defined by the simpler equations neglecting diffusion there will be three separate regimes in the current-voltage characteristic. First, it is obvious that until relatively high injection levels are reached, that is, until $n \approx p > n_0$, p_0, the current-voltage characteristic is simply Ohm's law:

$$J \simeq e(\mu_n n_0 + \mu_p p_0) \frac{V}{L} \cdot \tag{34}$$

At higher injection levels, with $n \approx p > n_0$, p_0, it is permissible to neglect the thermal free-carrier densities n_0, p_0 in the current expressions (30a) and (30b). The total current density J can then be written

$$J \simeq e(b + 1)\mu_p \bar{n} \frac{V}{L} \tag{35}$$

where $\bar{n}$ is the average value of n, hence p, over the volume. Here we have taken cognizance of the fact that any departure from local neutrality, measured by $(n-p)$, will be small compared to n or p.

Comparing the two field terms on the left-hand side of (33) it is evident that until a high enough injection level is reached that $|n-p| \approx |n_0-p_0|$, the second term will be dominant. Here we must keep in mind that even in an intrinsic semiconductor, with $n_0 \approx p_0$, $|n_0-p_0| = |N_D-N_A| \gtrsim 10^{12}/\text{cm}^3$ for the most highly purified semiconductor in the current state of technology. N_D, N_A denote the donor and acceptor impurity densities respectively. Keeping only the second field term on the left-hand side of (33), this equation becomes

$$-(n_0 - p_0)\frac{d\mathcal{E}}{dx} = \frac{(b+1)n}{\mu_n\tau}. \qquad (36)$$

Using simple dimensional analysis we replace $-(d\mathcal{E}/dx)$ by V/L^2 and n by $\bar{n}$, thereby obtaining

$$n_0 > p_0: \qquad (b+1)\bar{n} \simeq \tau\mu_n(n_0 - p_0)\frac{V}{L^2}. \qquad (37)$$

Substitution of (37) into (35) gives the final result

$$n_0 > p_0: \qquad J \simeq e\tau\mu_n\mu_p(n_0 - p_0)\frac{V^2}{L^3}. \qquad (38)$$

We designate this square-law regime of the current-voltage characteristic the "semiconductor regime" because of the decisive role played by the thermal free-carrier densities. The more rigorous, analytically derived result [23] differs from (38) only through the presence of the multiplicative, numerical factor 9/8. Eq. (38) would predict that $J \to 0$ as $p_0 \to n_0$, which is obviously a spurious effect. If p_0 is sufficiently close to n_0 the second field term in (33) is always small compared to the first field term and the correct solution is given by (43) below or (26) above.

The somewhat unexpected dependence of current on the *difference* of the thermal free-carrier densities is a direct consequence of the requirements of particle conservation, that is, of the recombination kinetics. We can see this also by a somewhat different manipulation of the basic equations. For the sake of simplicity consider the case of equal mobilities: $\mu_p = \mu_n = \mu$. From (30a) and (30b), neglecting diffusion, $\mathcal{E} = K/(n_0+p_0+n+p)$ with $K = J/e\mu = \text{constant}$. Putting this result into (32a), we obtain

$$-\frac{d}{dx}\left[\frac{n+n_0}{2(n+n_0)-(n-p)-(n_0-p_0)}\right] = \frac{r}{K\mu}. \qquad (39)$$

Assuming neutrality, $n = p$, we see that it is the presence of the term $n_0 - p_0$ in the denominator which makes possible a nonvanishing divergence, as required if r is not to vanish. Further, expanding the left-hand side of (39) in powers of $(n_0-p_0)/2(n+n_0)$, taking $p-n=0$, the lowest-order nonvanishing term is proportional to (n_0-p_0); thus the recombination rate and hence the current are proportional to (n_0-p_0) as in (38). This dependence of current on (n_0-p_0) has been verified experimentally in studies using Ge [29]. On the other hand in insulators, where n_0 and p_0 are negligible, it is seen from (39) that at least a small departure from neutrality, $n \neq p$, is required if double-injection currents are to be observed. This departure from neutrality is used in obtaining the current-voltage dependence, (23) of Section III and (43) below or (26) above.

An important property of the semiconductor regime as defined by (36), is the monotonic increase of field intensity $\mathcal{E}$ from $\mathcal{E}=0$ at the hole injecting contact, $x=L$ (for double injection into an n-type semiconductor, $n_0 > p_0$) to a maximum $\mathcal{E}_{max}$ at the cathode, $x=0$. Correspondingly, the injected hole density p, hence also n, decrease monotonically from anode to cathode.

A final point of interest is the voltage $V_{tr,\Omega-S}$ at which the transition from Ohm's law to the square law takes place. This voltage is determined from the intersection of the corresponding curves as given by (34) and (38):

$$\tau\mu_p\frac{1-\dfrac{p_0}{n_0}}{1+\dfrac{\mu_p}{\mu_n}\dfrac{p_0}{n_0}}\frac{V_{tr,\Omega-S}}{L^2} = 1. \qquad (40a)$$

Taking $p_0/n_0 \ll 1$, $\mu_p p_0/\mu_n n_0 \ll 1$, (40a) can be rewritten as

$$p_0 \ll n_0: \qquad t_{p,\Omega-S} = \tau, \qquad t_{p,\Omega-S} = \frac{L^2}{\mu_p V_{tr,\Omega-S}}. \qquad (40b)$$

Thus, the onset of double injection occurs at that voltage at which the hole transit time becomes equal to the injected pair lifetime. Note that this same result is obtained from (37) taking $\bar{n} = n_0$, if $b > 1$.

At sufficiently high voltage the first field term on the left-hand side of (33) dominates the second field term. Keeping only this first term and replacing $p-n$ by the corresponding expression in (31), (33) can be rewritten as

$$-\frac{\epsilon}{e}\mu_n\frac{d}{dx}\left(\mathcal{E}\frac{d\mathcal{E}}{dx}\right) = (b+1)\frac{n}{\tau}. \qquad (41)$$

Again a simple dimensional analysis, replacing $-(d/dx)[\mathcal{E}\, d\mathcal{E}/dx]$ by V^2/L^4 and n by its average value $\bar{n}$, gives

$$(b+1)\bar{n} = \frac{\epsilon\tau\mu_n}{e}\frac{V^2}{L^4}. \qquad (42)$$

Substituting this result into (35) gives the final result

$$J \simeq \epsilon\tau\mu_n\mu_p\frac{V^3}{L^5}. \qquad (43)$$

This result is seen to be identical to (26) except for the numerical factor 8. The numerical coefficient in (26), being obtained by a somewhat more refined argument, is closer to the correct value of $125/18=6.94$. Since the thermal free carriers have dropped out of the picture, we refer to this cube-law regime as the "insulator regime."

A final point of interest is the voltage $V_{tr,S-I}$ at which the transition from the semiconductor regime to the insulator regime takes place. This voltage is determined from the intersection of the corresponding curves as given by (38) and (26):

$$\frac{8\epsilon}{e(n_0-p_0)}\frac{V_{tr,S-I}}{L^2}=1. \tag{44}$$

Taking $p_0 \ll n_0$, (44) can be rewritten as

$$p_0 \ll n_0: \qquad t_{n,S-I}=8t_{\Omega n};$$

$$t_{n,S-I}=\frac{L^2}{\mu_n V_{tr,S-I}}, \qquad t_{\Omega n}=\frac{\epsilon}{en_0\mu_n}. \tag{45}$$

Thus, in an n-type semiconductor the transition from the semiconductor regime to the insulator regime takes place at that voltage at which the electron transit time becomes equal to (approximately) eight times the dielectric (ohmic) relaxation time. Except for the numerical factor, this is the same criterion that determines the onset of one-carrier SCL injection currents in an insulator without traps. Finally, we note that (44), for $p_0 \ll n_0$, gives $V_{tr,S-I}=en_0L^2/8\epsilon \simeq eN_DL^2/8\epsilon$ since $n_0 \simeq N_D - N_A \simeq N_D$. Identifying N_D with the defect state density N_{def} we see that $V_{tr,S-I}$ is to be identified with $V_{tr,high}$ as given in (29). The factor of eight in (44a) comes from the more refined analysis. If (43) were used, instead of (26), in obtaining (44) there would have been no numerical discrepancy.

A more complete treatment of the problem discussed in this section has been given by A. Rose and the author [23].

V. Double Injection with Unequal Lifetimes

The double-injection problems analyzed in Sections III and IV are relatively simple in that the injected free electrons and holes exceed the number of defect states and are therefore approximately equal in density and have a common lifetime. True, for any insulator at sufficiently high injection levels these conditions will be realized. However, we have not yet said anything about the double-injection characteristic over the large range of currents for which the injected free-carrier densities n and p are less than the defect density N_{def}. In this case generally $n \neq p$ and accordingly the corresponding lifetimes τ_n and τ_p are also unequal. Further one would expect the double-injection behavior in this realm to depend strongly on the number of defect states and their detailed electronic properties. In the most general case, illustrated in Fig. 7, there are three classes of defect centers. Some, labelled N_{tn} are electron traps, *i.e.*, the electrons in them are in quasi-thermal equilibrium with the free electrons. The occupancy of these traps is determined by the position of the ESSFL as described in Section II. The important trap parameters are the density and energy location in the forbidden gap. Other defect centers, labelled N_{tp}, are hole traps whose occupancies are determined by the H (hole) SSFL. Finally there are the recombination centers, labelled N_R. So long as these centers are deep-lying with respect to both the conduction and valence bands their important properties are their density and their electron and hole capture cross sections.[4] Although the general case is, surprisingly enough, analytically tractable [30],[5] the procedure for obtaining the analytic solution is too unwieldy to be considered here.

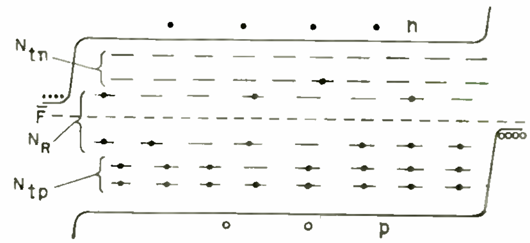

Fig. 7—Double injection into an insulator; general case. N_{tn}, N_{tp}, N_R denote electron traps, hole traps, and recombination centers respectively. $\bar{F}$ is the Fermi level.

In order to illustrate possible double-injection behavior under conditions of unequal electron and hole lifetimes where, further, lifetimes change drastically with injection level, we consider a highly simplified model of an insulator which has these features built into it; this is an insulator without traps and with a single set of recombination centers which are initially filled with electrons, illustrated in Fig. 8. In this model the most interesting case is that for which $\sigma_p \gg \sigma_n$ where $\sigma_p(\sigma_n)$ is the cross section for capture of a hole (electron) by a filled (empty) center. This would be the case if the states N_R were acceptor-like, that is, negatively charged when occupied by an electron. We could then imagine charge neutrality maintained through the presence in the insulator of an equal density of shallow donors $N_D=N_R$. These donors play no further role in the electronic behavior of the insulator and so we have not shown them in Fig. 8.

The double-injection problem for this model has been solved analytically [30] under the assumption that the insulator is everywhere neutral. The resulting double-

[4] For a more precise treatment of defect-state occupancies under steady-state excitation see discussion of "Demarcation Levels" by A. Rose, in "Progress in Semiconductors," vol. 2, Heywood and Co., Ltd., London, Eng., 1957.

[5] The analytic tractability rests on a necessary simplification of the treatment of trapping. This simplification introduces negligible error. See [30].

injection current-voltage characteristic is shown as the solid curve on the log-log plot of Fig. 9. Where the neutrality assumption is in serious error, *i.e.*, where space charge plays an important role, this curve is modified as indicated by the dashed curve. The new and outstanding features of the neutrality-based solution (solid curve) are the voltage threshold for two-carrier current flow and the negative-resistance region in the characteristic.

The voltage threshold has its origin in the "recombination barrier" presented by the filled centers to the passage of holes; that is, the filled recombination centers act as a sink for the injected holes, preventing their free transit across the insulator. Thus, a plasma of injected carriers cannot be built up in the volume until the hole transit time $t_p = L^2/\mu_p V$ becomes comparable to the low-level hole lifetime, $\tau_{p,\mathrm{low}} = 1/\bar{v}_p\sigma_p N_R$. (Generally, the lifetime τ of a free carrier of mean thermal velocity $\bar{v}$ against capture by centers of density N_{capt}, with capture cross section σ_{capt}, is given by $\tau = 1/\bar{v}N_{\mathrm{capt}}\sigma_{\mathrm{capt}}$. At low injection levels the thermal-equilibrium occupancy of the centers N_R by electrons is not much disturbed so that the density of hole-capturing centers is $N_{\mathrm{capt}} = N_R$.)

The existence of the voltage threshold V_{th} determined by $L^2/\mu_p V_{\mathrm{th}} \approx \tau_{p,\mathrm{low}}$ can be convincingly demonstrated by the following simple argument. Assume that two-carrier currents can flow at a substantially lower voltage V, $V \ll V_{\mathrm{th}}$. Define a drift length d as the distance a hole moves in one lifetime $\bar{\tau}_{p,\mathrm{low}}$. Thus $d = v_{\mathrm{drift}}\bar{\tau}_{p,\mathrm{low}} = \mu_p \mathcal{E} \bar{\tau}_{p,\mathrm{low}}$ where $\mathcal{E}$ is the average field intensity over the drift length. Essentially we have assumed that there is more than one drift length between cathode and anode. We now measure off successive drift lengths d_1, d_2, etc. starting from the anode, as illustrated in Fig. 10. At the end of each drift length the free-hole density p decreases by a factor of approximately two. Because of neutrality requirements, the free-electron density n, which everywhere exceeds p, does likewise. In order that the total current remain constant, the field intensity $\mathcal{E}$ must increase by the same factor of roughly two over each drift length. (Variations of p, n and $\mathcal{E}$ with distance are illustrated in Fig. 10.) Thus each drift length is roughly twice as long as the preceding one: $d_2 \simeq 2d_1$, $d_3 \simeq 2d_2 \simeq 4d_1$, etc. It is readily seen that the final drift length d_f equals approximately one half of the total cathode-anode spacing L. It is clear from the plot of $\mathcal{E}$ in Fig. 10 that almost the full applied voltage V appears across the final drift length d_f, so that $(L/2)^2/\mu_p V \approx \bar{\tau}_{p,\mathrm{low}}$, and $V \approx V_{\mathrm{th}}$ as determined by $L^2/\mu_p V_{\mathrm{th}} \approx \tau_{p,\mathrm{low}}$ in contradiction with our starting assumption that $V \ll V_{\mathrm{th}}$. We have therefore verified our assertion. The precise result, given by the analytical solution [30] is $t_{p,\mathrm{th}} = L^2/\mu_p V_{\mathrm{th}} = 2\tau_{p,\mathrm{low}}$.

The negative-resistance regime in Fig. 9 derives from a hole lifetime which *increases* with injection level. We have already noted that at low injection levels the hole lifetime is $\tau_{p,\mathrm{low}} = 1/\bar{v}_p\sigma_p N_R$. At high injection levels, where n and p both greatly exceed N_R, charge neutrality

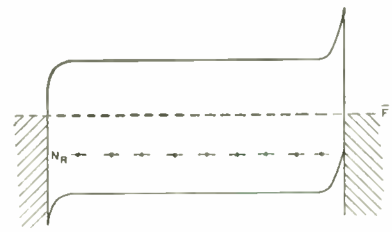

Fig. 8—A theoretician's insulator, free of traps and containing only a single set of recombination centers N_R initially filled with electrons.

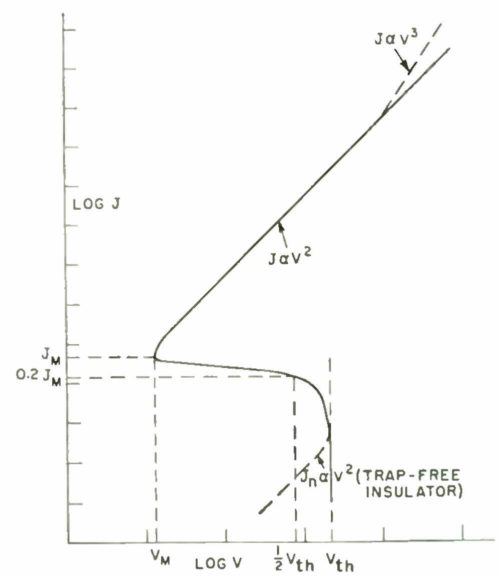

Fig. 9—Current-density-voltage characteristic, on a log-log plot, for the simplified insulator model of Fig. 8. The solid curve represents the solution obtained assuming charge neutrality. The dashed curves, at low and high current densities, are modifications enforced by space charge.

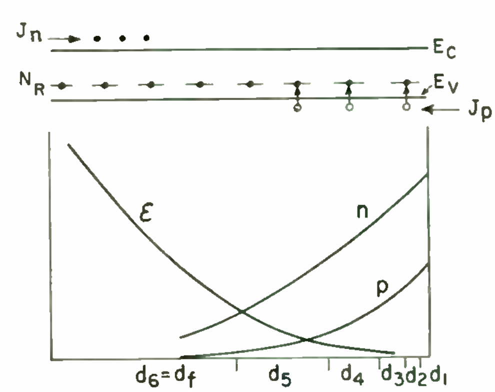

Fig. 10—Diagrammatic proof (see text) of voltage threshold for double injection for the simplified insulator model of Fig. 8.

requires that $n \approx p$. With $\sigma_p \gg \sigma_n$, the electron and hole recombination rates can only be balanced if the recombination centers are largely empty. Thus the density of electron-capturing centers to be used in the lifetime formula to obtain the high-level electron lifetime is $N_{capt} = N_R : \tau_{n,high} = 1/\bar{v}_n\sigma_n N_R$. Since $n \approx p$, this is also the high-level hole lifetime: $\tau_{p,high} = 1/\bar{v}_n\sigma_n N_R$. Comparing the high- and low-level hole lifetimes, $\tau_{p,high}/\tau_{p,low} = \bar{v}_p\sigma_p/\bar{v}_n\sigma_n \approx \sigma_p/\sigma_n$ taking $\bar{v}_p \approx \bar{v}_n$. Since σ_p/σ_n is a large number, exceeding 10^2 when the states N_R are acceptor-like, we see that $\tau_{p,high}/\tau_{p,low} \gg 1$. This drastic increase of hole lifetime with injection level between low and high levels means that, in this region of currents, the more holes injected the easier it is for them to get across the insulator. In fact it is so much easier that the voltage required actually *decreases* as the current *increases*. This is the negative-resistance regime in Fig. 9.

The high-voltage end of this negative-resistance regime is given by the threshold voltage, that is, by $t_{p,th} = L^2/\mu_p V_{th} = 2\tau_{p,low}$. It remains to determine the low-voltage limit V_M. This calculation is facilitated by noting that at the high injection levels, where $n \approx p \gg N_R$ the electrons which were initially in the recombination centers N_R have been transferred to the conduction band. As a result, at high injection levels the insulator behaves exactly like a semiconductor with an equivalent thermal free-carrier density N_R. The insulator has, in a manner of speaking, been electronically converted, through double injection, into a semiconductor. Consequently, in this regime the current-voltage characteristic is identical with that for a semiconductor, (38), except that $(n_0 - p_0)$ must be replaced by N_R and τ by $\tau_{p,high}$: $J \simeq e\tau_{p,high}\mu_n\mu_p N_R V^2/L^3$. This is the square-law regime of Fig. 9.

In the case of the semiconductor problem we saw that the low-voltage limit of the square-law regime, (38), was determined by the relation $t_p = \tau$, (40b), where $t_p = L^2/\mu_p V$, this marking the transition to Ohm's law. In the present insulator regime, the low-voltage end of the square-law regime is determined by the identical criterion: $t_{p,M} = L^2/\mu_p V_M \simeq \tau_{p,high}$, only here the voltage V_M marks the transition to the negative-resistance regime. We have now found the low-voltage end of the negative-resistance regime. Comparing the two voltage limits of the negative-resistance regime, we have $V_{th}/V_M \approx \tau_{p,high}/\tau_{p,low} \approx \sigma_p/\sigma_n$, a large voltage swing. A final point of interest about the negative resistance is the relatively small variation of current with voltage over almost the entire regime: the current increases from 0.2 J_M to J_M between the voltage $V = 0.65\ V_{th}$ and V_M.[6]

The discussion up to this point has dealt only with the neutrality-based solution, the solid line in Fig. 9. We now consider the limits of validity of this solution. First, it is clear that the neutrality-based solution cannot be valid down to arbitrarily low currents. For, associated with the threshold voltage V_{th} is a total space charge $Q_{th} = CV_{th} \simeq \epsilon V_{th}/L$, which is distributed throughout the insulator. Obviously the assumption of charge neutrality cannot be a good approximation until the total number of injected free electrons enL exceeds Q_{th}/e. Corresponding to this injection level there is a lower limiting current at which the neutrality-based current becomes valid. At lower currents the actual current will be the one-carrier, SCL electron current for a trap-free insulator, (5), shown as the lower dashed curve in Fig. 9. (The recombination centers N_R, being filled at the outset, cannot trap the injected electrons.) The transition to the neutrality-based solution obviously takes place where this curve intersects the solid curve.[7]

At sufficiently high voltage the neutrality-based solution is once more not correct due to the role of space charge, and the square-law regime (solid curve) gives way to a cube-law regime (dashed curve). This situation is precisely the same as that discussed in Section IV, (41)–(43), the dashed curve representing the plot of (43) with τ replaced by $\tau_{p,high}$.

Experimentally a current-voltage characteristic such as that of Fig. 9, exhibiting a current-controlled negative resistance, might be exhibited through either of two striking effects: spontaneous oscillations under application of an appropriate dc voltage, or an apparent breakdown at some critical voltage followed by a marked hysteresis in the current going down in voltage after the "breakdown." The oscillations would be due to the dominance of the negative resistance over the external circuit resistance. If the oscillations are suppressed by the external circuit, then the "breakdown" would likely be observed when, at some critical voltage, the current jumps from the lower branch of the characteristic in Fig. 2 to some point on the upper branch as voltage is lowered down to some other critical voltage, where the current will drop sharply down to the lower branch, extinguishing the "breakdown."

Both types of phenomena have been observed in high-resistivity germanium at liquid nitrogen temperature, spontaneous oscillations in gold-doped samples [31], [28b], and "breakdown" and hysteresis in iron-doped samples [32]. In neither case is sufficient data furnished by the authors to make a quantitative comparison of the observations with our theory. However, in both cases [31b], [32] the authors attribute the observed phenomena to double injection with hole capture

[6] The entire lower branch of the neutrality-based solution (solid line) in Fig. 9, between V_{th} and V_M is given, to a high degree of accuracy, by the simple quadratic voltage-current dependence: $V = V_M(J/J_M)^2 + V_{th}(1 - J/J_M)^2$. The derivation of this result will be presented elsewhere.

[7] It is important to note that this intersection *may* occur at a voltage V_{th}' which is substantially smaller than V_{th}. In this case the observed "threshold" for the negative resistance will be V_{th}', not V_{th}.

by the deep-lying acceptors. In the studies with the iron-doped samples this interpretation is further supported by optical experiments.

Hysteresis in the dc current-voltage characteristic is a common observation in insulator studies. The effect has been seen in CdSe powders [33a] and attributed [33b] to double injection accompanied by changing carrier lifetime; however for this material the model is necessarily more complicated than the simple one of Fig. 9. In single crystals of CdS, frequent observations [34] have been made of a hysteresis associated with steeply rising and falling double-injection currents. In these experiments the double injection is verified directly by observation of the green bandgap light emitted through the radiative recombination of electrons and holes.

VI. Concluding Remarks

The field of injection currents in insulators is relatively new, particularly the study of double-injection currents. Undoubtedly far more of interest remains to be discovered than is known at present. The author and his colleagues at RCA have concerned themselves to date almost exclusively with steady-state, dc injection currents; on the theoretical side our investigations have been mainly restricted to one-dimensional configurations. The usefulness of transient, namely pulsed dc, measurements has recently been demonstrated in the study of molecular crystals [17], [18], and we may anticipate a considerable expansion of activity along this line. (In this connection the transient behavior of the injecting contact [35] must certainly be taken into account.) The field of ac injection currents is largely unexplored.

This brief review has been confined to discussion of the underlying physical principles of injection current flow. Although rigorous solutions have been obtained for a number of single- and double-injection problems, under the assumption that the current flow is field-controlled, rather than diffusion-controlled, in every case the formal solution is too unwieldy to lend, by itself, much insight into the phenomena. On the other hand, in each instance, with a relatively small sacrifice in accuracy, the main results can be obtained by the simple methods outlined in this review.

Acknowledgment

The author is very much indebted to his colleague Dr. A. Rose for illuminating conversations and a very fruitful collaboration over a period of many years. Dr. Rose not only has pioneered the field of injection currents in insulators but, even more, has been a most effective champion of the view that one can solve the problems in this field simply through understanding the underlying principles. For this alone the author would be in considerable debt to Dr. Rose.

The author would also like to acknowledge helpful conversations with his colleagues D. O. North and R. H. Parmenter on the theoretical aspects of the field, and with his colleagues R. H. Bube, J. Dresner, W. Ruppel, F. V. Shallcross, R. W. Smith and P. K. Weimer on their experimental work in this field.

References

[1] P. K. Weimer and A. D. Cope, "Photoconductivity in amorphous selenium," *RCA Rev.*, vol. 12, pp. 314–334; September, 1951.

[2] W. Shockley, "Transistor electronics: imperfections, unipolar and analog transistors," Proc. IRE, vol. 40, pp. 1289–1313; November, 1952.

[3] W. Ruppel and R. W. Smith, "A CdS analog diode and triode," *RCA Rev.*, vol. 20, pp. 702–714; December, 1959.

[4] G. T. Wright, "A proposed space-charge-limited dielectric triode," *J. Brit. IRE*, vol. 20, pp. 337–355; May, 1960.

[5] A. Fischer, "Injection electroluminescence," *Solid State Electronics*, vol. 2, pp. 232–246; 1961.

[6] P. K. Weimer, "An Evaporated Thin-Film Triode," presented at the Solid State Devices Res. Conf., Stanford University, Palo Alto, Calif.; June 26–28, 1961.
———, "The 'TFT'—a new thin-film transistor," Proc. IRE, vol. 50, pp. 1462–1469; June, 1962.

[7] N. F. Mott and R. W. Gurney, "Electronic Processes in Ionic Crystals," Oxford University Press, New York, N. Y., 1st ed., p. 172; 1940.

[8] A. Rose, "Space-charge-limited currents in solids," *Phys. Rev.*, vol. 97, pp. 1538–1544; March, 1955.

[9] M. A. Lampert, "Simplified theory of space-charge-limited currents in an insulator with traps," *Phys. Rev.*, vol. 103, pp. 1648–1656; September, 1956.

[10] W. Shockley and R. C. Prim, "Space-charge-limited emission in semiconductors," *Phys. Rev.*, vol. 90, pp. 753–758; June, 1953.

[11] G. C. Dacey, "Space-charged-limited hole current in germanium," *Phys. Rev.*, vol. 90, pp. 759–763; June, 1953.

[12] R. W. Smith and A. Rose, "Space-charge-limited currents in single crystals of cadmium sulfide," *Phys. Rev.*, vol. 97, pp. 1531–1537; March, 1955.
R. W. Smith, "Properties of deep traps derived from space-charge-current flow and photoconductcive decay," *RCA Rev.*, vol. 20, pp. 69–78; December, 1959.

[13] J. Dresner and F. V. Shallcross, "Preparation and Electrical Properties of Evaporated CdS Diodes," presented at Solid State Devices Res. Conf., Stanford University, Palo Alto, Calif.; June 26–28, 1961.

[14] G. F. Alfrey and I. Cooke, "Electric contact to zinc sulphide crystals," *Proc. Phys. Soc. (London)*, vol. 70B, pp. 1096–1098; November, 1957.
W. Ruppel, "Space-charge-limited currents in ZnS single crystals," *Helv. Phys. Acta*, vol. 31, pp. 311–313; July, 1958.

[15] J. W. Allen and R. J. Cherry, "Space-charge currents in gallium arsenide," *Space Electronics Res. Labs. Tech. J.*, vol. 11, pp. 60–62; March, 1961.

[16] a) W. E. Spear and A. P. D. Lanyon, "Carrier mobility and trapping centres in selenium," in "Proc. Internat'l Conf. on Semiconductor Physics" (Prague, Czechoslovakia, August, 1960), Academic Press, Inc., New York, N. Y.; pp. 987–989; 1962.
b) J. Dresner, "Quenching effects and negative photoconductivity in amorphous selenium," *J. Chem. Phys.*, vol. 35, pp. 1628–1635; November, 1961.

[17] a) P. Mark, "Raumladungsbeschränkte Ströme in organischen Kristallen," presented at the Bavarian Phys. Soc. Meeting, Würzburg, Germany; April days, 1961.
b) W. Helfrich and P. Mark, "Raumladungsbeschränkte Ströme in Anthrazen als Mittel zur Bestimmung der Beweglichkeit von Defektelektronen," *Z. Physik*, vol. 166, pp. 370–385; January, 1962.
P. Mark and W. Helfrich, "Space-charge-limited currents in organic crystals," *J. Appl. Phys.*, vol. 33, pp. 205–215; January, 1962.
c) M. Silver, M. Swicord, R. C. Jarnigan, A. Many, S. Z. Weizz, and M. Simhony, "Transient space-charge-limited photocurrents in anthracene," *J. Phys. Chem. Solids*, (In press)

[18] a) A. Many, M. Simhony, A. Z. Weizz, and J. Levinson, "Studies of photoconductivity in iodine single crystals," in "Photoconductivity, Proc. of Internat'l Conf." (Cornell University, Ithaca, N. Y., August, 1961), H. Levinstein, Ed., Pergamon Inc., New York, N. Y.; pp. 285–292; 1962.

b) A. Many, S. Z. Weizz, and M. Simhony, "Space-charge-limited currents in iodine single crystals," to be published in *Phys. Rev.*, 1962.

[19] A. Many and G. Rakavy, "Theory of transient space-charge-limited currents in solids in the presence of trapping," to be published in *Phys. Rev.*, 1962.

[20] G. T. Wright, "A Comparison of Diffusion Limited Semiconductor Junction Diodes and the Space Charge Limited Dielectric Diode," presented at the Internat'l Solid State Circuit Conf., Philadelphia, Pa.; February, 1961.

[21] A. Rose, unpublished notes; 1955.

[22] M. A. Lampert, "A simplified theory of two-carrier, space-charge-limited carrier flow in solids," *RCA Rev.*, vol. 20, pp. 682–701; December, 1959.

[23] M. A. Lampert and A. Rose, "Volume-controlled, two-carrier currents in solids: the injected plasma case," *Phys. Rev.*, vol. 121, pp. 26–37; January, 1961.

[24] R. H. Parmenter and W. Ruppel, "Two-carrier space-charge-limited current in trap-free insulator," *J. Appl. Phys.*, vol. 30, pp. 1548–1558; October, 1959.

[25] R. N. Hall, "Power rectifiers and transistors," Proc. IRE, vol. 40, pp. 1512–1518; November, 1952.

[26] A. Herlet and E. Spenke, "Gleichrichter mit p-i-n bezw. mit p-s-n Struktur unter Gleichstrombelastung," *Z. angew. Phys.*, vol. 7, pp. 99–107, and pp. 149–163; 1956.

A. Herlet, "Die Abhängigkeit der Stromdichte eines p-i-n Gleichrichters von der Breite seiner Mittelzone," *Z. Physik*, vol. 141, pp. 335–345; July, 1955.

[27] D. A. Kleinman, "The forward characteristics of the PIN diode," *Bell Sys. Tech. J.*, vol. 35, pp. 685–706; 1956.

[28] a) V. I. Stafeev, "Effect of the resistance of the bulk of a semiconductor on the form of the current-voltage characteristic of a diode," *J. Tech. Phys. (USSR)*, vol. 28, pp. 1631–1641; August, 1958. (Translation: *Soviet Phys. (Tech. Phys.)*, vol. 3, pp. 1502–1512; 1958.)

——, "Modulation of diffusion length as a new principle of operation of semiconductor devices," *J. Solid State Phys., Acad. Sci. USSR*, vol. 1, pp. 841–848; August, 1959. (Translation: *Soviet Phys. (Solid State)*, vol. 1, pp. 763–769; December, 1959.)

[29] R. D. Larrabee, "Current-voltage characteristics of forward biased long p-i-n structures," *Phys. Rev.*, vol. 121, pp. 37–39; January, 1961.

[30] M. A. Lampert, "Double injection in insulators," *Phys. Rev.*, vol. 125, pp. 126–141; January, 1962.

[31] A. A. Lebedev, V. I. Stafeev, and V. M. Tuchkevich, "Some properties of gold-doped germanium diodes," *J. Tech. Phys. (USSR)*, vol. 26, pp. 2131–2141 1956. (Translation: *Soviet Phys. (Tech. Phys.)*, vol. 1, pp. 2071–2080; October, 1956.)

[32] W. W. Tyler, "Injection breakdown in iron-doped germanium diodes," *Phys. Rev.*, vol. 96, pp. 226–227; October, 1954.

[33] a) F. H. Nicoll, "A hysteresis effect in cadmium selenide and its use in a solid-state image storage device," *RCA Rev.*, vol. 19, pp. 77–85; March, 1958.

b) R. H. Bube, "Mechanism of photoconductivity in microcrystalline powders," *J. Appl. Phys.*, vol. 31, pp. 2239–2254; December, 1960.

[34] R. W. Smith, "Low-field electroluminescence in insulating crystals of cadmium sulfide," *Phys. Rev.*, vol. 105, pp. 900–904; February, 1957. Also private communication.

[35] M. A. Lampert and A. Rose, "Transient behavior of the ohmic contact," *Phys. Rev.*, vol. 113, pp. 1236–1239; March, 1959.

Theoretical Considerations on Millimeter Wave Generation by Optical Frequency Mixing*

J. R. FONTANA†, MEMBER, IRE, AND R. H. PANTELL†, MEMBER, IRE

Summary—**The generation of radiation by mixing optical maser signals is one possible method for closing the gap between microwaves and infrared. The conversion efficiency attainable with different types of nonlinear media is considered. It is shown that lossless nonlinear media, such as dielectrics, have very low conversion efficiency properties, regardless of the way they are used. Nonlinear resistive media, on the other hand, have efficiencies up to 25 per cent, independently of the frequency conversion ratio. Consequently, in order to generate wavelengths in the millimeter range by mixing optical maser outputs, the materials used should involve nonlinear dissipative processes.**

Introduction

There are as yet no practical oscillators available between wavelengths of 1 to 0.01 millimeter. At somewhat longer wavelengths, microwave tube techniques can be used to design tubes similar to those for centimeter waves, and in the optical and near infrared region, maser devices can now provide considerable power, but the region between them is devoid of sources of energy.

One approach for generating signals in this range would consist of starting from other frequencies and using nonlinear elements to synthesize the outputs desired. Until now, this has meant harmonic generation using the large microwave powers available at centimeter and subcentimeter wavelengths. The efficiencies obtainable in this way, however, are acceptable only for frequency doubling or tripling and become small for higher harmonics.

The alternative solution of mixing two signals of shorter wavelengths can now be considered, due to the advance of optical and near infrared masers. These oscillators are capable of pulsed outputs of many kilowatts, and their frequency stability is quite sufficient to produce monochromatic beats at wavelengths thousands of times larger.

The problem considered in this paper is the mixing

* Received February 9, 1962; revised manuscript received May 9, 1962. The research in this document was supported jointly by the U. S. Army Signal Corps, the U. S. Air Force, and the U. S. Navy (Office of Naval Research).

† Microwave Laboratory of Physics, Stanford University, Stanford, Calif.

of two strong signals relatively close in frequency to produce an output at the difference frequency. To achieve this result, a nonlinear element or medium must be used, and the question is to determine its desirable properties and the best way of using them. Lossless elements (reactors) are considered first. It is seen that, contrary to the situation in harmonic generators, they can only give low efficiencies. Nonlinear resistors are studied next, and the results of the analysis indicate that efficiencies up to 25 per cent are possible if elements with appropriate current-voltage characteristics are used.

The discussion is centered around the problem of generating signals near 1 mm from optical maser outputs, but all the considerations also apply to the mixing of signals in other frequency ranges, both for power generation and for detection.

The general method followed consists in expanding the voltage $v(t)$ and the current $i(t)$ of the nonlinear element in series involving all linear combinations of two applied frequencies ω_1 and ω_2:

$$i = \sum_{m=-\infty}^{\infty} \sum_{n=-\infty}^{\infty} I_{m,n} e^{j(mx+ny)} \tag{1}$$

$$v = \sum_{m=-\infty}^{\infty} \sum_{n=-\infty}^{\infty} V_{m,n} e^{j(mx+ny)}, \tag{2}$$

where $x=\omega_1 t$ and $y=\omega_2 t$.

Since i and v are real, we have

$$I_{-m,-n} = I_{m,n}{}^* \quad \text{and} \quad V_{-m,-n} = V_{m,n}{}^*,$$

where asterisks indicate complex conjugates. This is the same approach used by Manley and Rowe[1] and by Pantell[2] to derive general power relations for the lossless and for the resistive cases, respectively. In the case of the mixing of the frequencies ω_1 and ω_2 to produce an output $\omega_1-\omega_2$ only, all the series terms are zero except those involving the exponentials $\pm x$, $\pm y$, and $\pm(x-y)$. The situation may be described by means of the equivalent circuit of Fig. 1, in which the boxes associated with the two sources and the load are open circuits at the frequencies shown and are short circuits otherwise. The validity of using a lumped equivalent for a distributed nonlinear system has been considered by Haus,[3] and his results indicate that the power relationships obtained from the lumped equivalent are the same as those obtained from a solution of the field problem.

The average input powers contributed by the sources, and the average output power flowing into the load

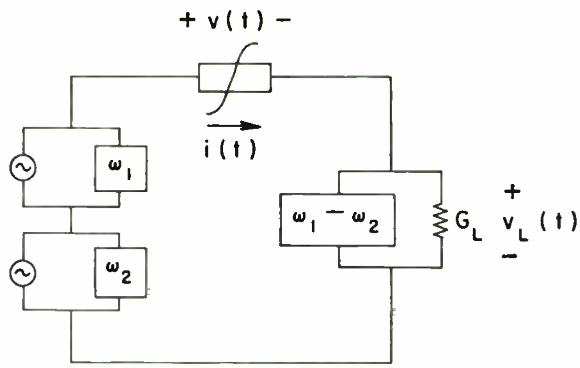

Fig. 1—The nonlinear element circuit, with resonant tanks at the two drive frequencies and the difference frequency.

G_L, are given by

$$P_{in} = W_{1,0} + W_{0,1} = (V_{1,0}I^*_{1,0} + V^*_{1,0}I_{1,0}) + (V_{0,1}I^*_{0,1} + I^*_{0,1}I_{0,1}) \tag{3}$$

and

$$P_{out} = -W_{1,-1} = -(V_{1,-1}I^*_{1,-1} + V^*_{1,-1}I_{1,-1}). \tag{4}$$

Nonlinear Reactors

The powers W_{mn} into any reactor without hystereris, regardless of the specific form of the nonlinear characteristic, must fit the Manley-Rowe[1] relations:

$$\sum_{m=0}^{\infty} \sum_{n=-\infty}^{\infty} \frac{mW_{m,n}}{m\omega_1 + n\omega_2} = 0 \tag{5}$$

and

$$\sum_{m=-\infty}^{\infty} \sum_{n=0}^{\infty} \frac{nW_{m,n}}{m\omega_1 + n\omega_2} = 0. \tag{6}$$

In the case only involving powers at ω_1, ω_2, and the difference frequency, these equations reduce to

$$W_{1,0} + W_{0,1} + W_{1,-1} = 0 \tag{7}$$

and

$$\frac{W_{1,0}}{\omega_1} = -\frac{W_{0,1}}{\omega_2} = -\frac{W_{1,-1}}{\omega_1 - \omega_2}. \tag{8}$$

Eq. (7) restates the lossless character of the nonlinear reactor by equating input and output power. The conversion efficiency is 100 per cent:

$$\eta = \frac{P_{out}}{P_{in}} = 1. \tag{9}$$

Eq. (8), however, shows that, in order to have positive output power at $\omega_1-\omega_2$, the lower frequency source at ω_2 must absorb positive power rather than produce it. As the three powers are proportional in magnitude to their respective frequencies, if $\omega_1-\omega_2$ is very much smaller than ω_1, most of the power supplied by the source at ω_1 is extracted by the source at ω_2, and so only a small remnant reaches the load. Fig. 2 is a diagram

[1] J. M. Manley and H. E. Rowe, "Some general properties of nonlinear elements, Part I. General energy relations," Proc. IRE, vol. 44, pp. 904–913; July, 1956.

[2] R. H. Pantell, "General power relationship for positive and negative nonlinear resistive elements," Proc. IRE, vol. 46, pp. 1910–1913; December, 1958.

[3] H. A. Haus, "Power-flow relations in lossless nonlinear media," IRE Trans. on Microwave Theory and Techniques, vol. MTT-6, pp. 317–324; July, 1958.

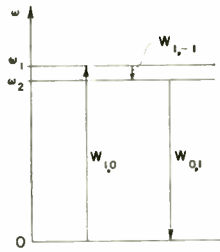

Fig. 2—The energy diagram for the nonlinear reactive element.

showing the frequencies ω_1, ω_2, and $\omega_1-\omega_2$. Symbolizing positive power by upward and negative powers by downward arrows, respectively, it can be seen how most of the power generated is at the useless frequency ω_2, rather than at $\omega_1-\omega_2$.

This result shows that nonlinear reactors operated in this fashion are, in fact, parameteric oscillators pumped at ω_1 and producing frequencies ω_2 and $\omega_1-\omega_2$, rather than mixers with two inputs and a single output. The significant efficiency is the one defined in terms of the output at the difference frequency rather than total output:

$$\eta' = \frac{W_{1,-1}}{W_{1,0}} = \frac{\omega_1 - \omega_2}{\omega_1}. \tag{10}$$

It thus becomes apparent that if millimeter waves are to be produced from optical signals in lossless media, very poor efficiencies are to be expected, since the frequency ratio given by (10) is small.

Nonlinear Resistors

For a nonlinear resistor without hysteresis, that is to say, for an element entirely specified by a characteristic $i(v)$ which is single-valued, the relationship between powers is given by the Pantell[2] equations.

$$\sum_{m=0}^{\infty}\sum_{n=-\infty}^{\infty} m^2 W_{m,n} = \frac{1}{4\pi^2}\int_0^{2\pi} dy \int_0^{2\pi} dx\, \frac{di}{dv}\left(\frac{\partial v}{\partial x}\right)^2, \tag{11}$$

and

$$\sum_{m=-\infty}^{\infty}\sum_{n=0}^{\infty} n^2 W_{m,n} = \frac{1}{4\pi^2}\int_0^{2\pi} dx \int_0^{2\pi} dy\, \frac{di}{dv}\left(\frac{\partial v}{\partial y}\right)^2. \tag{12}$$

A significant difference between these expressions and the Manley-Rowe relations for the reactive case is that they involve the nonlinear element characteristic. Consequently, the conversion efficiency will be dependent on the type of resistor used.

Another important distinction is that (11) and (12) do not involve frequency if the nonlinear characteristic of the resistor is frequency-independent. In the latter case, efficiency will not depend upon the frequency ratio of input to output.

To calculate conversion efficiency, it is necessary to obtain expressions for input and output powers from (11) and (12). By adding (11) and (12), we find that

$$W_{1,0} + W_{0,1} + 2W_{1,-1} = P_{in} - 2P_{out} = \frac{1}{2\pi^2}\int_0^{2\pi}\int_0^{2\pi} dxdy\, \frac{di}{dv}\left[\left(\frac{\partial v}{\partial x}\right)^2 + \left(\frac{\partial v}{\partial y}\right)^2\right]. \tag{13}$$

The output power is the average value of the product of the load voltage v_L, and the current. From Fig. 2, the total voltage is

$$v = V_{1,0}e^{jx} + V_{-1,0}e^{-jx} + V_{1,-1}e^{j(x-y)} + V_{-1,1}e^{-j(x-y)} + V_{0,1}e^{jy} + V_{0,-1}e^{-jy}.$$

Therefore the load voltage, which is

$$v_L = -\left[V_{1,-1}e^{j(x-y)} + V_{-1,1}e^{-j(x-y)}\right],$$

can be written as

$$v_L = -\frac{\partial^2 v}{\partial y \partial x}. \tag{14}$$

Hence, we have

$$P_{out} = \frac{1}{4\pi^2}\int_0^{2\pi}\int_0^{2\pi} dxdy(iv_L) = -\frac{1}{4\pi^2}\int_0^{2\pi}\int_0^{2\pi} dxdy\left[i\frac{\partial^2 v}{\partial y\partial x}\right]. \tag{15}$$

Upon integrating (15) by parts, the output power is

$$P_{out} = \frac{1}{4\pi^2}\int_0^{2\pi}\int_0^{2\pi} dxdy\, \frac{di}{dv}\left(\frac{\partial v}{\partial x}\frac{\partial v}{\partial y}\right). \tag{16}$$

Combining (13) and (16) results in

$$P_{in} = \frac{1}{4\pi^2}\int_0^{2\pi}\int_0^{2\pi} dxdy\, \frac{di}{dv}\left(\frac{\partial v}{\partial x} + \frac{\partial v}{\partial y}\right)^2. \tag{17}$$

The ratio of (16) and (17) gives

$$\eta = \frac{P_{out}}{P_{in}} = \frac{\int_0^{2\pi}\int_0^{2\pi} dxdy\, \frac{di}{dv}\left(\frac{\partial v}{\partial x}\frac{\partial v}{\partial y}\right)}{\int_0^{2\pi}\int_0^{2\pi} dxdy\, \frac{di}{dv}\left(\frac{\partial v}{\partial x} + \frac{\partial v}{\partial y}\right)^2}. \tag{18}$$

To determine the maximum value for η, (18) can be rewritten as

$$\eta = \frac{1}{4} - \frac{1}{4}\,\frac{\int_0^{2\pi}\int_0^{2\pi} dxdy\, \frac{di}{dv}\left(\frac{\partial v}{\partial x} - \frac{\partial v}{\partial y}\right)^2}{\int_0^{2\pi}\int_0^{2\pi} dxdy\, \frac{di}{dv}\left(\frac{\partial v}{\partial x} + \frac{\partial y}{\partial y}\right)^2}. \tag{19}$$

For a positive nonlinear resistor, that is for $(di/dv) \geq 0$, it is seen from (19) that $\eta \leq \frac{1}{4}$. The restriction of having a positive nonlinear resistor means that the mixing is accomplished by a passive element. To obtain 25 per cent efficiency it is necessary that $di/dv = 0$ except at those instants of time for which $\partial v/\partial x = \partial v/\partial y$. The maximum conversion efficiency for a passive nondispersive, nonlinear resistor is 25 per cent.

Examples with Nonlinear Resistors

A. The Diode

Fig. 3 shows a diode characteristic with a voltage cutoff at $v=V_c$. This diode will have 25 per cent efficiency mixing if the source voltages are chosen to be

$$V_{1,0} = V^*_{1,0} = V_{0,1} = V^*_{0,1} = \frac{V_c}{3}, \tag{20}$$

and the load conductance, G_L, is adjusted so that the load voltage is

$$V_{1,-1} = V^*_{1,-1} = -\frac{V_c}{6}. \tag{21}$$

For these values of voltages, the total voltage applied to the diode is

$$v = \tfrac{2}{3}V_c \cos x + \tfrac{2}{3}V_c \cos y - \tfrac{1}{3}V_c \cos (x-y).$$

Only at $t=0$ the voltage v reaches the value V_c and produces current flow, and at any other time of the cycle there is no current. The efficiency can be calculated from (18). For this case, we have that $dv/dv=0$ except in the vicinity of $x=y=0$, at which point

$$\frac{\partial v}{\partial x} \simeq -\frac{2}{3} V_c \sin x$$

$$\frac{\partial v}{\partial y} \simeq -\frac{2}{3} V_c \sin y.$$

Since $\sin x \simeq \sin y$ near $t=0$, the efficiency is 25 per cent.

B. The Square-Law Resistor

Fig. 4 illustrates a resistor characteristic given by

$$i = av + v^2. \tag{22}$$

It is assumed that the resistor is passive ($di/dv \geq 0$), so that the voltage is constrained by

$$v \geq -\frac{a}{2}, \tag{23}$$

thereby satisfying the requirement for having a passive element. The relationship between load current and load voltage is specified by the load conductance:

$$I_{1,-1} = -G_L V_{1,-1}. \tag{24}$$

From (18), (22), and (24) the efficiency is

$$\eta = \frac{G_L |V_{1,-1}|^2}{a[|V_{1,0}|^2 + |V_{0,1}|^2] + 2V_{1,-1}V_{-1,0}V_{0,1} + 2V_{-1,1}V_{1,0}V_{0,-1}}. \tag{25}$$

The voltage $V_{1,-1}$ is determined from (22) and (24) to be

$$V_{1,-1} = -\frac{2V_{1,0}V_{0,-1}}{(a+G_L)}. \tag{26}$$

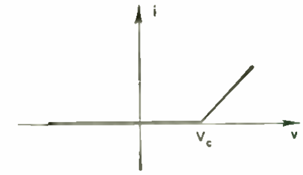

Fig. 3—A diode characteristic with cutoff at $v=V_c$.

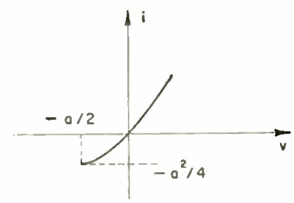

Fig. 4—A nonlinear resistor characteristic given by $i=v^2+av$.

Substituting this expression for $V_{1,-1}$ into (25) and neglecting terms in $V_{1,-1}$ in the denominator of (25) gives

$$\eta \simeq \frac{4G_L |V_{1,0}{}^2|^2 |V_{0,1}|^2}{a(a+G_L)^2[|V_{1,0}|^2 + |V_{0,1}|^2]}. \tag{27}$$

To maximize η,

$$|V_{1,0}|^2 = |V_{0,1}|^2 \quad \text{and} \quad G_L = a.$$

Thus, the result is

$$\eta_{\max} = \frac{|V_{1,0}|^2}{2a^2}. \tag{28}$$

The maximum value for $|V_{1,0}|^2/2a^2$ is given by (23):

$$\frac{|V_{1,0}|^2}{2a^2} \leq \frac{1}{128}, \tag{29}$$

so that

$$\eta_{\max} = \frac{1}{128}.$$

To include a correction for having neglected the $V_{1,-1}$ terms in the denominator of (25), we write

$$\eta = \frac{\dfrac{|V_{1,0}|^2}{2a^2}}{1 - 4\dfrac{|V_{1,0}|^2}{2a^2}} \leq \frac{1}{124}.$$

Therefore, the maximum conversion efficiency for a passive, nonlinear resistor that can be represented by (22) over the region of operation is 0.81 per cent.

Conclusion

The problem of generating wavelengths of the order of 1 mm by mixing optical or near infrared signals involves the quest for a type of material and a mode of operation capable of yielding good efficiencies. By applying the general relations of passive nonlinear element theory, it is shown that lossless media, such as nonlinear dielectrics, are necessarily poor because their maximum efficiency is given by the ratio of output to input frequency. Nonlinear passive resistive elements, on the other hand, may be up to 25 per cent efficient regardless of the frequency ratio. Consequently, efficient mixing will require the use of materials involving nonlinear power absorption processes. The type of nonlinearity of the resistive element is of importance, and maximum efficiency can be obtained with the use of a diode.

Electron Guns for Forming Solid Beams of High Perveance and High Convergence*

R. D. FROST†, MEMBER, IRE, O. T. PURL†, SENIOR MEMBER, IRE, AND H. R. JOHNSON†, FELLOW, IRE

Summary—**A new method has been employed for the design of solid-beam electron guns of high perveance and area convergence. This has resulted in designs with perveance 2.2×10^{-6} a/v$^{3/2}$ and convergence ratio 300; and perveance 5×10^{-6} a/v$^{3/2}$ and area convergence 6. Using conventional methods, a design with perveance 0.1×10^{-6}a/v$^{3/2}$ and area convergence ratio 1000 has been obtained. Each of these guns has yielded over 95 per cent transmission through a drift tube, in most cases with less than 1.5 times theoretical Brillouin focusing magnetic field. The design method consists of 1) paper design following earlier workers; 2) construction of a model using the design cathode and anode, but with the focus electrode replaced by a series of annular disk electrodes; 3) measurement, in pulsed bell-jar beam tester, of the beam leaving this gun, by means of a pinhole aperture followed by a split collector, yielding data on current density and trajectory angle as a function of radius and axial position; 4) modifications of annular disk potentials and cathode surface shape to improve beam quality; 5) electrolytic tank determination of the shape of a single electrode to replace the annular disks; and 6) test of the final design in a sealed-off, shielded-cathode, pulsed beam tester in which the beam flows through a drift tube in a uniform magnetic field. These methods are relatively exact and rapid. Drawings are presented for some specific designs.**

Introduction

Klystrons, traveling-wave tubes and backward-wave oscillators are generally based upon interaction between a long cylindrical beam of electrons and a slow-wave circuit. Efficiency and bandwidth of these devices generally increases with the current density and with the perveance, or ratio of current in the beam to the 3/2 power of the potential of the beam relative to the cathode. Total power input increases with the product of this potential and total beam current. But the life of the device decreases as the current density at the cathode increases, and also is limited by heating of the circuit by intercepted electrons and by arcing between elements of the electron gun. When an attempt is made to make these devices work at shorter and shorter wavelengths, there finally arrives a wavelength so short that the device is no longer feasible with available electron beams. The subject of this paper is the electron gun, the arrangement for converging and focusing the electrons emitted from the cathode into a cylindrical beam in which all electron trajectories are as parallel as possible to the beam axis. The electron emission is space-charge limited in all gun designs discussed. This paper is further limited to consideration of solid beams.

Much work has been done on this subject in the past. A definitive work is Pierce's book.[1] Pierce is the inventor of the "Pierce gun," a convergent gun based upon the known analytical solution of the problem of electron flow between coaxial spheres. The analysis of an actual gun is complicated by the fact that the electrons are emitted from the cathode with random thermal velocities, as discussed by Pierce[1] and by Cutler and Hines;[2] it is further extremely complicated by the presence of the

* Received January 22, 1962; revised manuscript received, April 30, 1962. This work was supported in part by the USAF, Aeronautical Systems Division, Electronic Technology Laboratory, under Contract No. AF 33(616)-6441.

† Watkins-Johnson Company, Palo Alto, Calif.

[1] J. R. Pierce, "Theory and Design of Electron Beams," D. Van Nostrand Co., Inc., New York, N. Y.; 1949.

[2] C. C. Cutler and M. E. Hines, "Thermal effects in electron guns," Proc. IRE, vol. 43, pp. 307–315; March, 1955.

TABLE I

Results of pulsed tests of guns designed by the methods of this paper. Tests were made in sealed-off shielded-cathode beam testers with drift tube diameter d_{drift} and length l_{drift}. Magnetic focusing field was B, and Brillouin field B_{br} was calculated using measured beam diameter d_{beam}. The gridded gun 2DG2 was operated at three different ratios of anode voltage V_a to grid voltage V_g.

Gun \ Quan.	Perveance $\times 10^6$	Area Conv.	Transm. %	B/B_{br}	Spacing* / d_{beam}	Va/Vg On	Va/Vg Off	d_{beam}/d_{drift}	l_{drift}/d_{drift}
5B	2.2	300	99.9	1.4	2.0	—	—	0.44	44.4
9	0.1	1000	95.5	3.5†	16.0	—	—	0.57	14.3
7	5.1	6	97.7	1.0	0.2	—	—	0.64	6.4
2DG2	1.0	60	95.5	1.5	2.6	140	140	0.47	23.5
4A	1.9	29	99.5	1.3	1.21	−250‡	—	0.64	22.2
2D	1.2	52	98.2	1.24	1.44	—	—	0.55	19.2

* Ratio of minimum interelectrode spacing to beam diameter.
† Preliminary result. It is believed that this will be reduced substantially by better magnetic shielding of the cathode. In addition, this gun was designed by the method of Pierce—it did not require the methods of this paper.
‡ A negative potential of 1/250 of the anode voltage was applied to the focus electrode.

anode hole[3–9] in cases in which both high perveance and high area convergence are desired simultaneously.

Approximations are not sufficiently accurate to produce guns of optimum design with perveances greater than about 1×10^{-6}. The analog computer methods so far used have been expensive, cumbersome, and may have insufficient accuracy. The design method to be presented here utilizes the actual electron beam and is relatively rapid and effective.

In this paper some specific beam-tester results are given first. It is believed that these represent a significant step forward in the achievement of perveances in the region 0.1–6×10^{-6} and area convergences up to 1000:1. These results are presented because they (in some cases) illustrate the power of the design method described later, and because they may prove useful in themselves, especially since they can be scaled linearly by any desired factor and still show good performance over a range of voltages limited by thermal velocities on the low side and by cathode current density or arcing on the high side. Next, the method by which these designs were evolved is presented, followed by experimental details and recommendations for future work.

[3] M. Müller, "New points of view in the design of electron guns for cylindrical beams of high space charge," *J. Brit. IRE*, vol. 16, pp. 83–94; February, 1956.
[4] W. E. Danielson, J. L. Rosenfeld, and J. A. Saloom, "A detailed analysis of beam formation with electron guns of the Pierce type," *Bell Sys. Tech. J.*, vol. 35, pp. 375–420; March, 1956.
[5] G. R. Brewer, "Formation of high-density electron beams," *J. Appl. Phys.*, vol. 28, pp. 7–15; June, 1957.
[6] L. E. S. Mathias and P. G. R. King, "On the performance of high perveance electron guns," IRE TRANS. ON ELECTRON DEVICES, vol. ED-4, pp. 280–287; July, 1957.
[7] R. Hechtel, "Elektronenkanonen hoher Perveanz," *Arch. der Elektrischen Übertragung*, vol. 10, pp. 535–540; December, 1956.
[8] M. R. Barber and K. F. Sander, "The calculation of electrostatic electron gun performance," *J. Electronics and Control*, vol. 7, pp. 465–481; December, 1959.
[9] J. E. Piquendar, O. Cahen, and P. Lapostelle, "Les effets de la charge d'éspace dans les canons à électrons," Compagnie Françaíse de Thomson-Houston, Paris, France; 1956.

RESULTS

Following completion of the design of a new gun using the method to be described in the next section, a test of the gun is performed in a sealed-off beam tester consisting of the gun under test (with its cathode shielded from magnetic field), followed by a magnetic iron pole piece, followed by a copper drift tube, followed by a pole piece and collector operated at a potential slightly higher than that of the drift tube in order to collect most of the secondary electrons. Measurements on this beam tester are conducted on a pulsed basis with pulses of approximately 2 μsec duration with pressure less than 10^{-6} mm Hg so that ions will not be a factor in focusing, and at a voltage high enough so there is little effect due to thermal velocities. Results of such tests on six representative guns are presented in Table I.

DESIGN TECHNIQUE

A basic problem in the synthesis of an electron gun through the use of an analog computer is that the computer is a tool for analysis of a given design. Following completion of the analysis of an interim design, the design must be modified and the new design analyzed. Past work using analog computers has involved a great deal of time to accomplish this feedback cycle. Another problem is that the analog computer must be of extreme accuracy for use with very high convergence guns.

As a result of these considerations, the following plan was evolved for the design of electron guns:

1) Make a paper design of the gun based upon the references cited.
2) Construct an actual working model of the gun, including cathode and anode as actually designed, but replacing the focus electrode by a series of about five annular disk electrodes between cathode and anode (see Fig. 1).

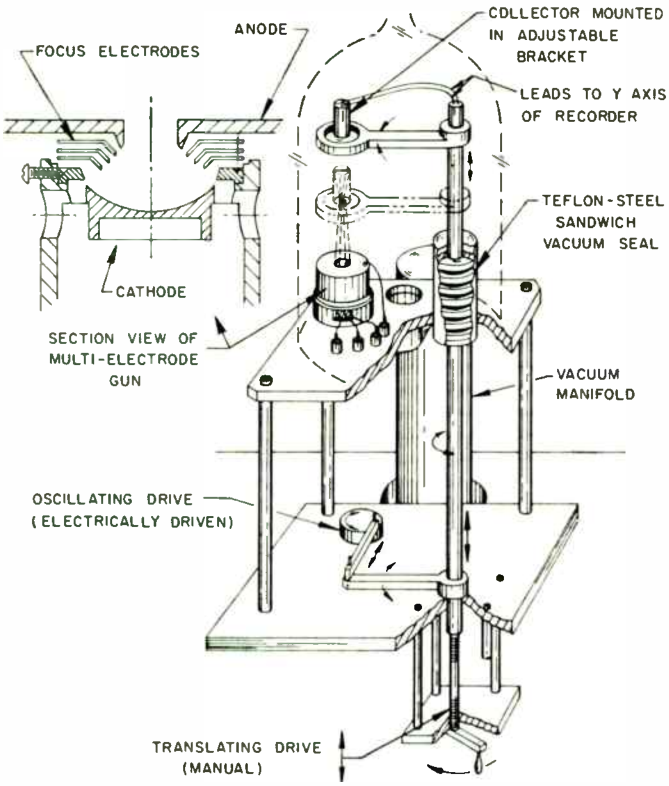

Fig. 1—Schematic drawing of bell-jar test setup which includes a multielectrode electron gun and beam analyzer.

3) Test this actual working model with short pulses (for negligible ion formation) in a bell jar-test setup. Probe the beam with a pinhole-camera collector to measure the beam current density as a function of radius. At each point, measure the transverse velocity of the beam through the use of a split collector following the pinhole.
4) Experimentally adjust the potentials of the electrodes between cathode and anode to produce a beam of uniform current density and minimum transverse velocities at the beam minimum.
5) Realizing that all electrostatic lenses have spherical aberrations of the same sign, try different cathode shapes, starting at 2) above and repeating the work. First, try spherical cathodes of different radii. Then try nonspherical cathodes.[10,11] (All of the guns listed in Table I have spherical cathodes.)
6) Make an analog experiment in an electrolytic tank to determine the shape of a single focus electrode which will be equivalent to the best multi-electrode potential distribution determined in step 5) above.
7) Construct a working model of the single focus electrode version and test it in the bell jar with pulsed voltage to verify that it is equivalent to the multi-electrode version.

[10] O. Heil and J. J. Ebers, "A new wide-range, high-frequency oscillator," Proc. IRE, vol. 38, pp. 645–650; June, 1950.
[11] E. D. Reed, "A mm-wave reflex klystron," *Bell. Sys. Tech. J.*, vol. 34, pp. 563–599; May, 1955.

8) Construct a working sealed-off model of the single-focus-electrode gun, shielded against magnetic field, followed by a magnetic pole piece, drift tube, another magnetic pole piece, and collector. Measure per cent beam transmission of this device as a function of magnetic field with pulsed cathode voltage as parameter.

Experimental Technique

The first innovation which has been used is to determine the beam edge potential distribution which actually does optimize the beam formation without making any assumption in regard to space charge or anode aperture geometry. This is accomplished by setting up a simulated gun with the desired anode and cathode design to give the desired perveance and area convergence. The focus electrode is simulated by a series of insulated disk electrodes placed along the beam boundary between the cathode and anode. This configuration is shown in Fig. 1 (section view). The remainder of the equipment shown is to analyze the resulting beam to provide information on current density and radial velocity as a function of radial position across the beam cross section and axial position along the beam path. A photograph of the actual experimental setup is shown in Fig. 2.

The voltage on each electrode can be altered to any arbitrary value to obtain a wide range of potential distributions. Initially, however, the potentials on each electrode are adjusted to obtain the theoretical beam boundary potential calculated as described by Brewer.[5] Then the potentials of these electrodes are adjusted, while observing the beam in the analyzer, to the values which produce the most laminar beam. Even for high-convergence guns of perveances between 1×10^{-6} and 3×10^{-6}, the beam boundary potential near the cathode can usually be maintained near the theoretical value, thus preserving rectilinear flow in that region.

Once the desired beam is obtained, the geometry and potentials are transferred to an electrolytic tank where the optimum beam edge potential distribution (obtained in the beam analyzer) is measured. A dielectric strip which is perpendicular to the cathode and which extends approximately half the distance to the anode along the beam edge is used during the measurements. Once the beam-edge potential is known, a single electrode can be designed to replace the multielectrode stack for simplicity of construction and operation.

The above procedure is justified because the flow near the cathode is rectilinear. A further justification is that a gun designed using these procedures produced a beam of perveance 2.2×10^{-6} and area convergence 300:1. Both of these numbers are quite close to the results obtained from its multielectrode equivalent. These guns are described later.

The demountable beam analyzer in which the essential characteristics of a beam can be analyzed rapidly is shown schematically in Fig. 1. The device used con-

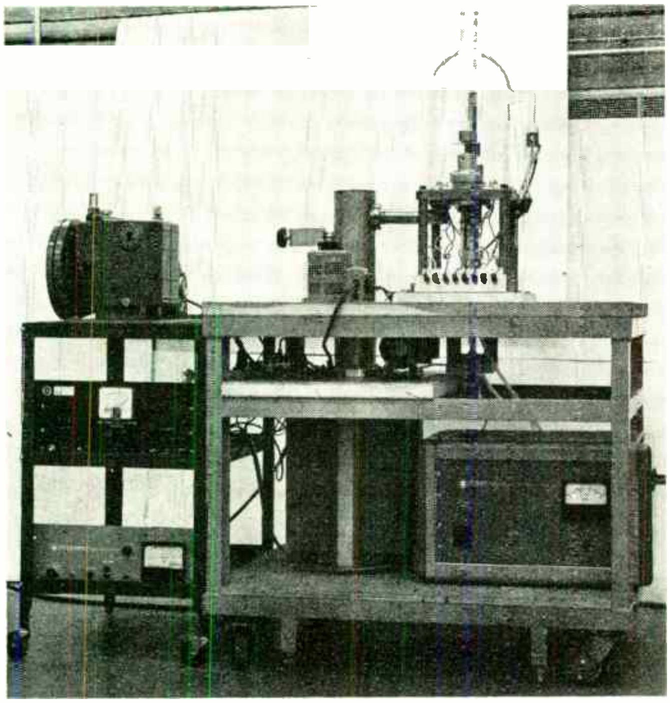

Fig. 2—Photograph of the actual bell-jar test setup.

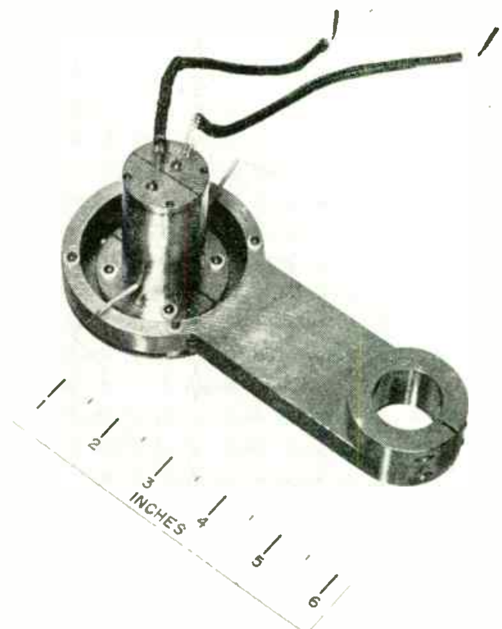

Fig. 3—Photograph of split collector.

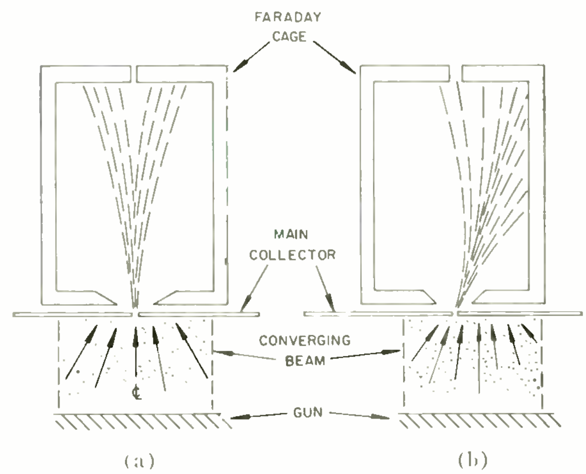

Fig. 4—Schematic illustrating the operation of a radial velocity measuring system. (a) At a point in the beam where radial velocity is zero, current distributes equally between the two halves. (b) At a point where radial velocity is not zero, current distributes unequally.

sists of a demountable bell-jar type vacuum system, a gun mount, a main collector plate with sampling pinhole capable of both radial and axial motion, a split Faraday cage mounted directly behind the main collector sampling hole, and the various measuring equipment necessary for observing and recording data.

One feature of the vacuum equipment is the ion pump used which eliminates the need for oil diffusion pumps and liquid nitrogen traps. The capacity of the pump is 140 liters per second; it can bring the system from air to operating conditions in a few hours. Considerable care is required in the seals with a demountable system of this kind. Ordinary "O-rings" are not suitable; a special vacuum neoprene, CMC-57, is used which has been vacuum baked prior to usage. The sliding seal around the movable shaft is made of a teflon-steel sandwich and, as all other seals in the system, is operated dry, free from any lubricant. With the cathode hot, the pressure at the ion gauge on the bell jar is less than 1.0×10^{-5} mm Hg.

The main collector consists of a copper plate with a pinhole of diameter 0.006 inch which is insulated from all other electrodes. The split Faraday cage collects the beam sample that passes through the hole. When the two halves of the cage are electrically connected, the total current to them is a measure of the current density at the position of the pinhole. When the two halves are insulated from each other, the radial velocity content of the beam can be determined. Fig. 3 is a photograph of the Faraday cage mounted on the main collector. As shown in Fig. 4(a), when no radial velocities are present in the beam segment, the beam sample will distribute equally between the two collector halves. If, on the other hand, a radial velocity component is present, as shown in Fig. 4(b), the current to the two halves will be unequal. Secondary electrons inside the collector are suppressed by means of carbon on the inside surface of the split collector bucket.

Carbon has also been used on the main collector plate to reduce secondaries from this electrode. No significant difference was observed in the beam profiles due to the presence or absence of these secondaries, so long as the outside of the Faraday cage and the leads to the cage are shielded from the secondaries.

In Fig. 5(a)–(c) the upper curves are current density as a function of radial position for an ideal beam. The two lower traces below the total current density pro-

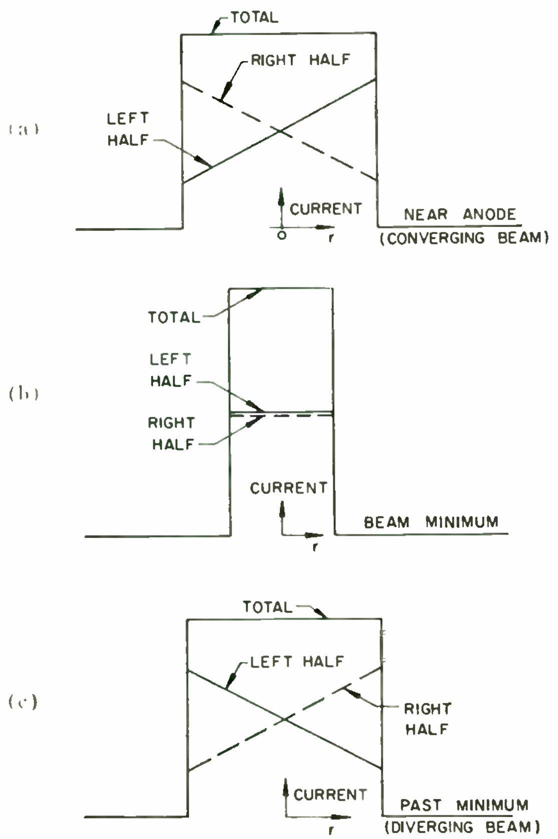

Fig. 5—Current density vs radial distance r of sampling pinhole from the gun axis for various axial positions (a)–(c) along an ideal beam. Position (a) is near the anode, where the beam is converging; position (b) is that at which the beam has a minimum diameter and is parallel to the axis; position (c) is past the minimum, where the beam is diverging. For each position the upper solid curve is the sum of the currents collected on both halves of the split collector; the solid lower curve is the portion of the current collected on the left half of the split collector; and the dashed lower curve is the portion collected on the right half. Superposition of the lower curves, as in axial position (b), indicates no radial velocities at any radial position. Note that radial velocities at a given radius are in opposite directions at axial positions (a) and (c).

files are currents to each half of the split Faraday cage. When there are no radial velocities, the two smaller traces superimpose. This null gives a precise determination of ideal parallel flow at the beam minimum. Where the beam is converging (radial velocity component toward axis) near the gun, the solid trace is greater than the dashed traces to right of the centerline. Where the beam is diverging, far out from the gun, the dashed trace will be greater than the solid trace to right of the centerline. These latter figures are somewhat qualitative since the spread of the beam sample in the Faraday cage, due to space charge and thermal velocities, must be known in order to compute the radial velocity component at any point in the beam.

The data can be taken manually with an x-y recorder or presented in visual form in a swept display on an oscilloscope. In either case a potentiometer is driven by the radial motion of the collector assembly and the resulting voltage is used to drive the X axis. The current collected in the Faraday cage is amplified and used to drive the Y axis.

The cathode is driven with 2-μsec pulses at a duty cycle of about 0.001, hence minimizing the effect of ions.

Another powerful method for reducing nonlaminarity in beams from high perveance guns, caused by anode lens aberrations, is to alter the cathode shape. For example, to obtain a perveance 2×10^{-6} gun, having only a moderate convergence, one would use the methods described by Brewer[5] or Müller[3] to obtain the desired perveance and to compensate partially for the distortion of the anode hole. The beam from such a gun would normally have a very nonuniform current density distribution and be too nonlaminar to focus well.

This beam is improved by reducing the spherical radius of the cathode to the value which optimizes beam laminarity. Any slight aberration remaining in the beam can be reduced to an insignificant magnitude by slight adjustments in the focus electrode as will be illustrated later. In addition to reducing the aberrations in the beam, the technique of reducing the cathode spherical radius also results in a beam with increased area convergence and a nearly uniform current density distribution outside the acceleration region.

Decreasing the spherical radius of the cathode does not materially affect the uniformity of the cathode emission density. This statement has been verified by placing a grid very near the cathode which was concentric with the cathode of the perveance 1.2×10^{-6} gun described later. The beam shape changed very little, indicating that the cathode loading of the ungridded gun was substantially uniform.

These two techniques have been used to design a series of guns from perveance 1.0×10^{-6} to 6×10^{-6} and area convergence of 5 to over 300:1. The remainder of this paper will describe these results in some detail.

Detailed Results

High-convergence, perveance 2.2×10^{-6} gun, type 5B

A gun of area convergence 300:1 and perveance 2.2×10^{-6} was obtained using a combination of the two techniques described above. Using a cathode curvature which would normally be used with a typical modified Pierce design, a laminar beam could be obtained using a multielectrode simulator but the area convergence was limited to 85 to 1 with perveance of 1.6×10^{-6}. By decreasing the radius of curvature of the cathode and reoptimizing the beam edge potential, laminar flow could be obtained at markedly higher values of area convergence and perveance. The design thus obtained was reproduced in the electrolytic tank and a single electrode focus electrode was thereby obtained to replace the multielectrode structure. This design yielded the 300:1 convergence[12] and 2.2×10^{-6} perveance values

[12] The beam diameter is arbitrarily defined as the diameter of the cylinder enclosing 95 per cent of the beam current.

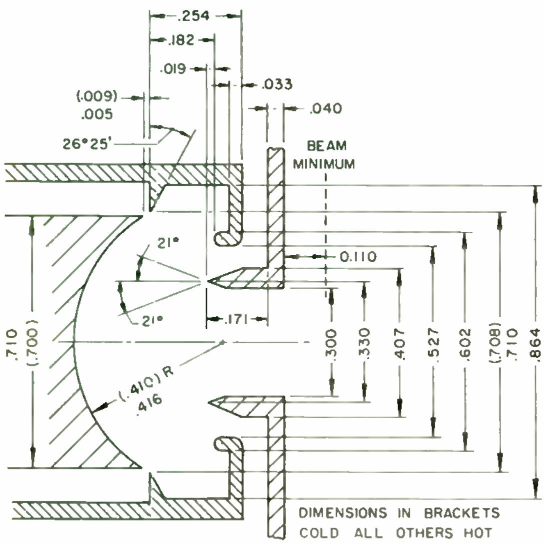

Fig. 6—Configuration of the perveance 2.2×10^{-6} (convergence 300:1) gun (type 5B). This gun was developed using multielectrodes to optimize the beam boundary potential after the cathode was reshaped. Multielectrodes were then replaced by single electrode shown.

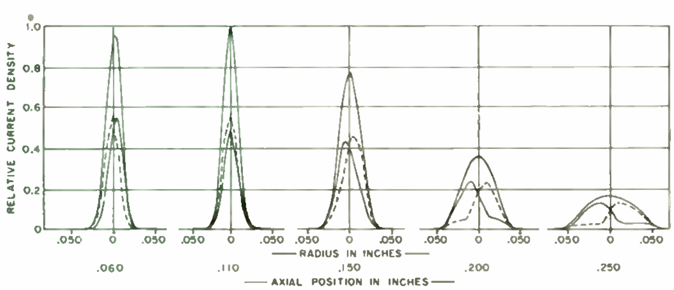

Fig. 7—Beam current density profiles taken at various axial positions for the perveance 2.2×10^{-6} gun (area convergence over 300:1) (type 5B). The number under each figure indicates the distance between the anode outer face and the position where the profile was taken. The amplitude difference of the two radial velocity profiles is a measurement error and not a property of the beam.

quoted above. The gun configuration is shown in Fig. 6 and the beam profiles are shown in Fig. 7. A 10 to 15 per cent change in convergence and perveance was noted in translating from the multielectrode to single electrode geometry but an error in scaling was later detected which accounted for approximately half of this discrepancy.

The measured current density profile at beam minimum and one computed for this gun using the method described by Cutler and Hines[2] are quite similar. The ideal shape and degree of laminarity in this beam indicate that it should focus well. This is shown to be the case in Fig. 8. At a magnetic field of 1.4 Brillouin, 99 per cent transmission is obtained.

Perveance 1.9×10^{-6} gun designed using cathode shaping, type 4A

The gun shown in Fig. 9 (next page) was designed using the method described by Brewer partially compensate for the effect of the large anode hole.[5] As shown

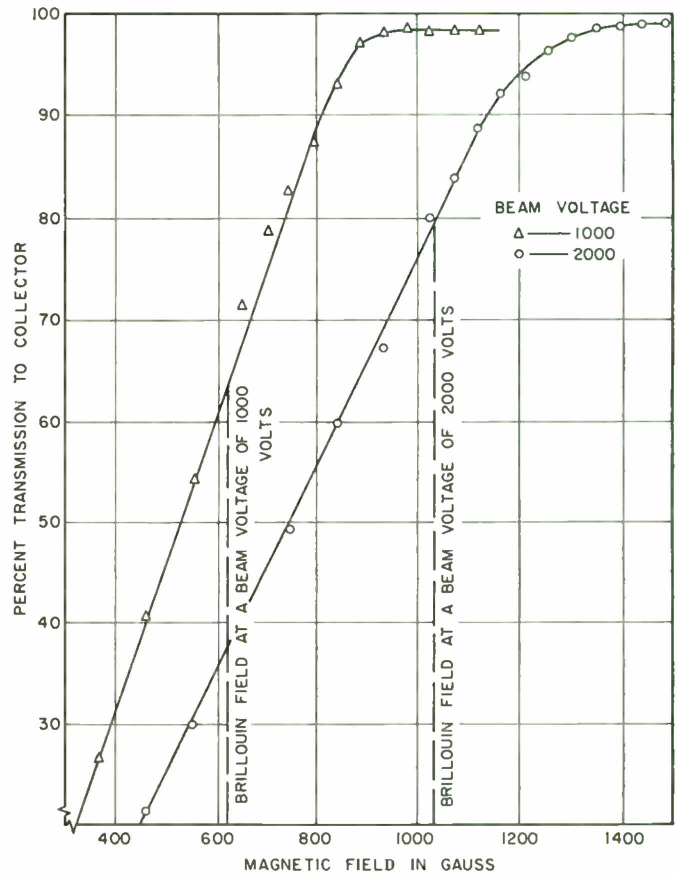

Fig. 8—Per cent transmission of the beam from the perveance 2.2×10^{-6} (area convergence 300:1) (type 5B) gun, through a drift tube 0.090 inch in diameter, as a function of magnetic field. An anode interception of 4 per cent was measured during this test because the anode was placed 0.010 inch too close to the cathode. In later tests with the anode in the proper position, focusing was not degraded and anode interception was less than 0.5 per cent.

in Fig. 10, the beam from this gun has a nonuniform current density distribution. Furthermore, the beam is quite non-laminar since the radial velocity content of the beam is high even at the beam minimum, where radial velocity content would be zero in a laminar beam.

In Fig. 9, shown in dashed lines, is a cathode having a reduced spherical radius. The beam resulting from this gun (type 4A) is shown in Fig. 11. Note that in contrast to the beam shown in Fig. 10, this beam has a nearly uniform current density distribution which is well maintained at every axial position, and this beam has nearly zero radial velocity content at beam minimum. Also the diameter of the beam at the minimum point is now much smaller than in the original beam. The slight aberration remaining in this beam can be eliminated by a slight adjustment of the focus electrode. This is demonstrated by Fig. 12, which was obtained from the gun shown in Fig. 9 by placing −8 volts (with respect to the cathode) on the focus electrode when the anode was operated at 2000 volts. This information can be used in the electrolytic tank to reform the focus electrode such that it can be operated at cathode potential.

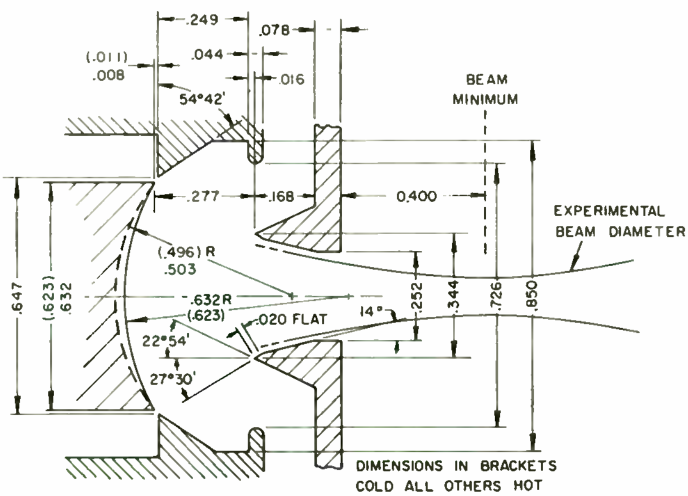

Fig. 9—Perveance 1.9×10^{-6} gun designed using the method of Brewer and Müller to compensate partially for the anode aperture. Shown as a dashed line is the reshaped cathode used to obtain complete anode hole compensation (type 4A) and an area convergence of 27:1 at 1 kv.

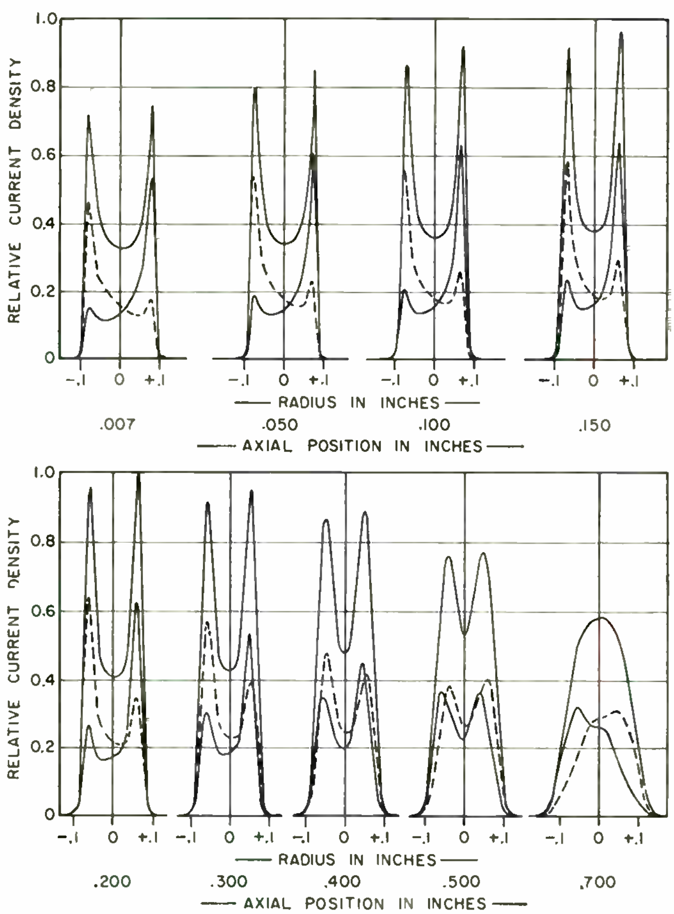

Fig. 10—Beam current density profiles taken at various axial positions for the perveance 1.9×10^{-6} gun (Fig. 9, cathode spherical radius 0.632 inch). The number under each figure indicates the distance between the anode outer face and the position where the profile was taken.

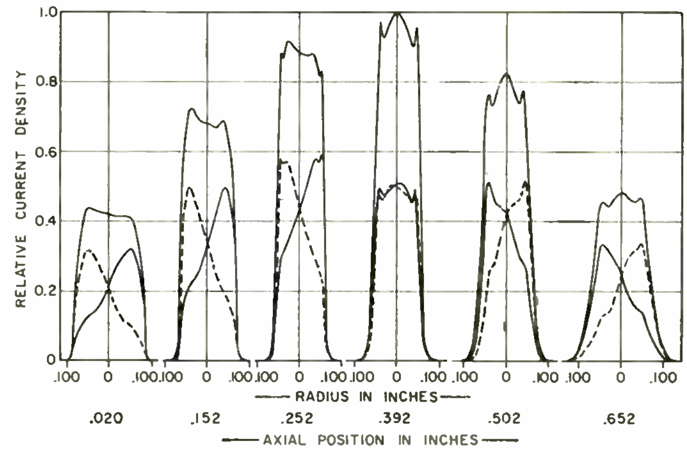

Fig. 11—Beam current density profiles taken at various axial positions for the perveance 1.9×10^{-6} gun (type 4A) (Fig. 9, cathode spherical radius 0.496 inch). The number under each figure indicates the distance between the anode outer face and the position where the profile was obtained.

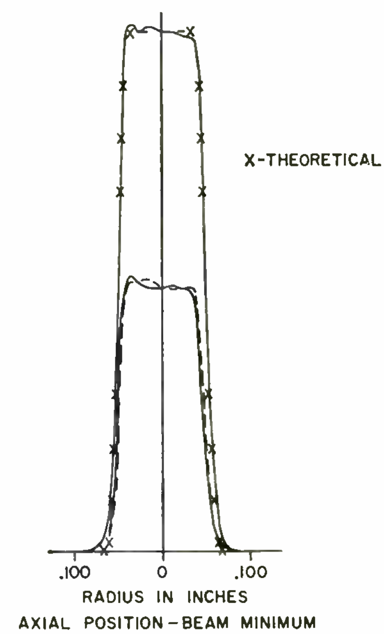

Fig. 12—Comparison of the current density distribution at beam minimum of the ideal and experimental beam obtained from the (type 4A) gun shown in Fig. 9. The anode was at 2000 volts and the focus electrode was at −8 volts with respect to the cathode.

Also shown in Fig. 12 is the current density distribution of an ideal laminar beam having the same perveance and convergence as the above gun operated at the same beam voltage. The ideal beam shape was computed from (32) and Fig. 6 in the paper by Cutler and Hines[2] which predicts the effect of thermal velocities on the beam current density distribution of ideal beams.

The most conclusive test for the quality of a beam is a focusing test wherein the beam is injected into a Brillouin type magnetic field. This was done by enclosing the gun in a vacuum envelope containing a drift tube of length 4 inches and inside diameter 0.180 inch. The per cent current transmission through the drift tube as a function of magnetic field is shown in Fig. 13. Data are included for the beams in Figs. 11 and 12.

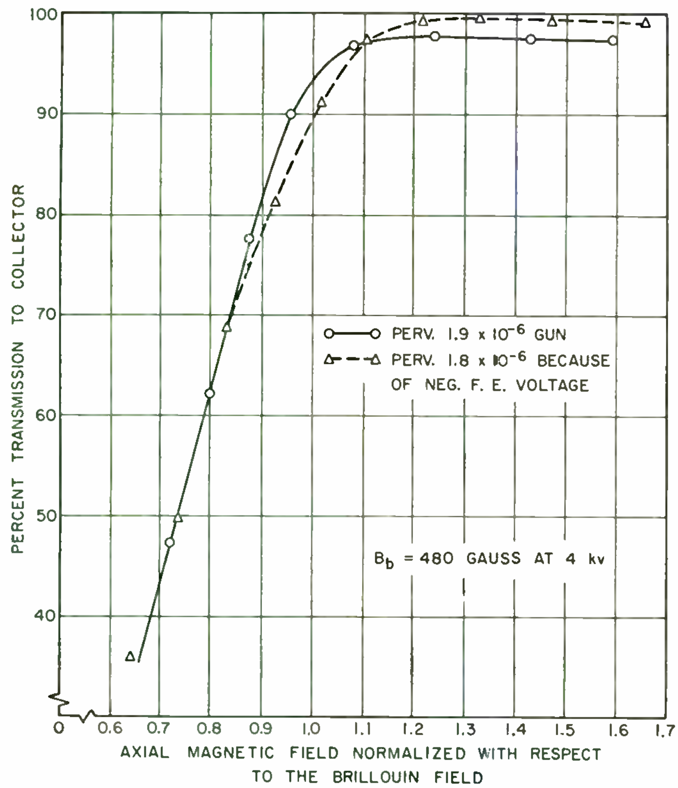

Fig. 13—Per cent transmission of the beam from the perveance 1.9×10^{-6} gun (type 4A), through a drift tube 0.180 inch in diameter, as a function of magnetic field.

Perveance 1.2×10^{-6} gun designed using cathode shaping, type 2D

A perveance 1.2×10^{-6} gun having a cone half angle of 30° and a cathode spherical radius of 0.623 inch was also designed, first by using the Brewer techniques, followed by shortening the cathode spherical radius to 0.535 inch. The result was again an improvement in beam laminarity and current density distribution, and an increase in convergence. The area convergence was over 50:1 at a beam voltage of 2000 volts. Transmission through a drift tube having an inside diameter 1.5 times the beam diameter was 98.2 per cent at a magnetic field of 1.24 Brillouin.

Range of effectiveness

The two new techniques described herein have provided the best results in the range between perveance 1.0×10^{-6} and about perveance 3×10^{-6}. The use of these two methods resulted in the three designs which have been described. Other guns have been designed at this laboratory ranging from a perveance 6×10^{-6} gun having an area convergence of 6:1 to a perveance 0.1×10^{-6} gun having an area convergence of 1000:1 and higher. At a perveance as high as 6×10^{-6}, the anode aperture compensation problem becomes so severe that laminarity was extremely difficult to obtain. With the two new techniques described, it has been possible to design a perveance 6×10^{-6} gun which has a beam that can be focused with a magnetic field reasonably near the Brillouin field. However, the beam from this gun is not truly laminar, but is relatively easily focused because of its low convergence.

On the other hand, guns having extremely high area convergence, but low perveance, can be designed which are quite laminar at high operating voltages (where the effect of thermal velocities is small) without the use of the new techniques described. For example, the perveance 0.1×10^{-6} gun having a 1000:1 area convergence mentioned above was designed using the theory described by Pierce.[1] The primary difficulty with this gun, as with all highly convergent guns, is in obtaining proper entrance conditions into the focusing field and is not in matching internal beam boundary potentials.

Conclusions

Two new methods useful in the design of high-perveance, high-convergence guns have been described. One of these consists of using a multielectrode focus electrode for finding the optimum beam boundary potential in a gun. The other is based on experimentally adjusting the cathode shape. Three guns developed using these techniques have also been described. One of these has a 300:1 area convergence at a perveance of 2.2×10^{-6}. Proper shaping of the cathode and the use of a multielectrode structure, in place of the usual focus electrode, to optimize the beam edge potential were necessary to obtain this novel gun design. Cathode shaping was the most important method used for designing the moderately convergent guns described.

All of the guns shown have been thoroughly analyzed and have been successfully focused (greater than 98 per cent beam transmission with near Brillouin fields on most guns) in sealed-off drift tube beam testers. Although extreme care must be exercised in the focusing of very highly convergent beams, the practicality of these new guns has been demonstrated.

Recommendations for Future Work

It is believed that the methods presented here can be used to design a family of solid-beam guns of convergence ratios in the range 2–2000 and perveances in the range 0.1–7.0×10^{-6} a/v$^{3/2}$. Little or no change in Pierce's design method is necessary below perveance 1×10^{-6}. Use of a nonspherical cathode should allow these limits to be increased greatly. Furthermore, the technique could easily be applied to hollow electron beams as produced by the several versions of hollow-beam guns which have been suggested in the literature.

Acknowledgment

We acknowledge considerable help from many people in this work, including R. W. Peter, J. W. Sedin, K. W. Slocum, and D. A. Watkins; C. E. Hildebrand, who constructed many of the guns and experimental apparatus; and T. L. Durgans, J. J. Enright, and W. R. Knecht.

Thermal Noise in Field-Effect Transistors*

A. VAN DER ZIEL†, FELLOW, IRE

Summary—**The limiting noise mechanism in field-effect transistors is thermal noise of the conducting channel. The noise can be represented by a current generator $\sqrt{\overline{i^2}}$ in parallel to the output. The value of $\overline{i^2}$ is calculated; for zero drain voltage the noise corresponds to thermal noise of the drain conductance, and for other bias conditions the noise at a given gate voltage depends only slightly upon the drain voltage. Because of modulation effects in the channel, $\overline{i^2}$ is somewhat larger than the thermal noise of the dc drain conductance, except for zero drain bias and beyond saturation. The noise resistance of the device is approximately equal to g_{max}/g_m^2, where g_m is the transconductance of the transistor and g_{max} its maximum value. The approximation becomes even closer if feedback due to the series resistances of the channel must be taken into account.**

Introduction

Shockley[1] has given a theory of the field-effect transistor. This paper aims at applying his model for calculating the noise of the device, caused by thermal noise generated in the conducting channel.

Let the field-effect transistor be a planar transistor made on p-type material and let it be provided with two gate contacts G, a source contact S and a drain contact D (Fig. 1). Let the transistor have unit width, let $2a$ be the distance between the gate contacts and L the length of the conducting channel. Let, for a given bias W between the gate and the channel, the width of the channel be $2b$, and let W_{00} be the bias needed for cutoff ($b=0$). Then, according to Shockley,

$$W = W_{00}(1 - b/a)^2; \quad \text{or} \quad b/a = [1 - (W/W_{00})^{1/2}]. \tag{1}$$

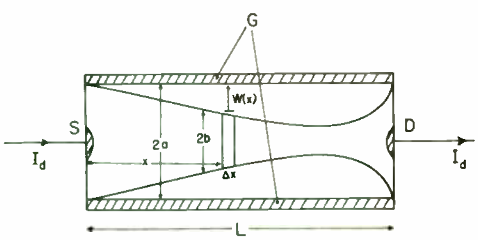

Fig. 1—Cross section of a planar field-effect transistor showing the source S, the gate G, the drain D, the conducting channel of width $2b$ and the space-charge regions of width $(b-a)$. $W(x)$ is the bias between the conducting channel and the gate.

Here W and b are slow functions of the distance x to the source. If V_g is the potential of the gate with respect to the source, V_d the potential of the drain and V_{dif} the diffusion potential, then $W = W_s = (V_g + V_{dif})$ at the source and $W = W_d = (V_g + V_{dif} - V_d)$ at the drain.

For a given gate voltage the field strength component E_x in the X direction is

$$E_x = \frac{dW}{dx}. \tag{2}$$

If σ_0 is the conductivity of the p-type channel, then the dc current is

$$I = 2\sigma_0 b \frac{dW}{dx} = g(W)\frac{dW}{dx} \tag{3}$$

where

$$g(W) = 2\sigma_0 b = g_0\left[1 - \left(\frac{W}{W_{00}}\right)^{1/2}\right], \quad \text{and} \quad g_0 = 2\sigma_0 a. \tag{3a}$$

Consequently, the current is

$$I = \frac{1}{L}\int_{W_s}^{W_d} g(W)\,dW = \frac{g_0}{L}\left[W_d - W_s - \frac{2}{3}\,\frac{(W_d^{3/2} - W_s^{3/2})}{W_{00}^{1/2}}\right]. \tag{4}$$

The transconductance g_m of the device is

$$g_m = -\frac{\partial I}{\partial V_g} = \frac{g_0}{L}\left[\left(\frac{W_d}{W_{00}}\right)^{1/2} - \left(\frac{W_s}{W_{00}}\right)^{1/2}\right], \tag{5}$$

and the output conductance g_d of the device is

$$g_d = -\frac{\partial I}{\partial V_d} = \frac{g_0}{L}\left[1 - \left(\frac{W_d}{W_{00}}\right)^{1/2}\right]. \tag{6}$$

At $V_d = 0$, $W_d = W_s = (V_g + V_{dif})$, which is the smallest value W_d can take for given V_g. In that case $I = 0$ and $g_m = 0$ and

$$g_d = g_{d0} = \frac{g_0}{L}\left[1 - \left(\frac{W_s}{W_{00}}\right)^{1/2}\right]. \tag{6a}$$

For $W_d \to W_{00}$, $g_d \to 0$, the (I, V) characteristic becomes saturated and

$$g_m \to g_{max} = \frac{g_0}{L}\left[1 - \left(\frac{W_s}{W_{00}}\right)^{1/2}\right] = g_{d0} \tag{5a}$$

attains its maximum value. Adding (5) and (6) one obtains the general relationship

$$g_m + g_d = g_{max} = g_{d0}. \tag{5b}$$

If the drain voltage is more negative than is needed for saturation, the current I is practically independent of voltage and Shockley's solution does not hold.

* Received February 26, 1962; revised manuscript received, April 20, 1962. This work was supported by a U. S. Signal Corps Contract.
† Electrical Engineering Department, University of Minnesota, Minneapolis, Minn.
[1] W. Shockley, "A unipolar field-effect transistor," Proc. IRE, vol. 40, pp. 1365–1376; November, 1952.

Calculation of the Noise in Field-Effect Transistors

Let it now be assumed that the dc current is kept constant at the value I. A thermal noise voltage developed between x and $(x+\Delta x)$ will then modulate the width of the channel between x and the drain and give an amplified noise voltage at the drain. By integrating over all sections Δx one obtains the total output noise voltage.

To take this into account, one puts $W(x)=W_0+\Delta W$ and $b(x)=b_0+\Delta b$, where W_0 and b_0 are the dc values and ΔW and Δb are the fluctuations induced by the thermal noise developed between x and $(x+\Delta x)$.

Eq. (1) thus gives

$$W_0 = W_{00}\left(1-\frac{b_0}{a}\right)^2;$$

$$(W_0+\Delta W) = W_{00}\left[1-\left(\frac{b_0+\Delta b}{a}\right)\right]^2. \quad (7)$$

Hence, neglecting the term in Δb^2,

$$\Delta W = -2\frac{W_{00}}{a}\left(1-\frac{b_0}{a}\right)\Delta b = -\frac{2}{a}(W_{00}W_0)^{1/2}\Delta b. \quad (7a)$$

Eq. (3) gives

$$I = 2\sigma_0 b_0\frac{dW}{dx} = 2\sigma_0(b_0+\Delta b)\left(\frac{dW_0}{dx}+\frac{d\Delta W}{dx}\right)$$

$$= 2\sigma_0 b_0\frac{dW_0}{dx}, \quad (8)$$

since I is kept constant. Neglecting second-order terms yields

$$\Delta b\frac{dW_0}{dx}+b_0\frac{d\Delta W}{dx}=0. \quad (8a)$$

Substituting (7a) into (8a) yields

$$\frac{d\Delta W}{\Delta W} = \frac{1}{2}\,\frac{d(W_0/W_{00})}{(W_0/W_{00})^{1/2}[1-(W_0/W_{00})^{1/2}]} = \frac{du}{1-u} \quad (9)$$

where $u=(W_0/W_{00})^{1/2}$. Integrating between the limits x and L, one obtains

$$\frac{\Delta W_d}{\Delta W_x} = \frac{1-u_x}{1-u_L} = \frac{1-[W_0(x)/W_{00}]^{1/2}}{1-(W_d/W_{00})^{1/2}} \quad (10)$$

where ΔW_x is the fluctuation in the section Δx and ΔW_d is the resulting fluctuation at the drain; $W_0(x)$ is the value of W_0 at the point x where the fluctuation occurs. Since ΔW_x is caused by thermal noise, its mean square value is

$$\overline{\Delta W_x^2} = 4kT\Delta f\frac{\Delta x}{g(W_0)} = \frac{4kT\Delta f\Delta W_0}{g(W_0)dW_0/dx}$$

$$= \frac{4kT\Delta f}{I}\Delta W_0. \quad (11)$$

Hence we have

$$\overline{\Delta W_d^2} = \frac{4kT\Delta f}{I}\left[\frac{1-(W_0/W_{00})^{1/2}}{1-(W_d/W_{00})^{1/2}}\right]^2\Delta W_0. \quad (12)$$

The total mean square open-circuit noise voltage is obtained by integrating over the length of the sample, that is, between the limits W_s and W_d. This yields

$$\overline{e^2} = \frac{4kT\Delta f}{I}\,\frac{\left[(W_d-W_s)-\frac{4}{3}(W_d^{3/2}-W_s^{3/2})/W_{00}^{1/2}+\frac{1}{2}(W_d^2-W_s^2)/W_{00}\right]}{[1-(W_d/W_{00})^{1/2}]^2}. \quad (13)$$

The short-circuit noise current has the mean square value

$$\overline{i^2} = \overline{e^2}g_d^2 = 4kT\frac{g_0}{L}\Delta f\;\frac{\left[(x-y)-\frac{4}{3}(x^{3/2}-y^{3/2})+\frac{1}{2}(x^2-y^2)\right]}{\left[(x-y)-\frac{2}{3}(x^{3/2}-y^{3/2})\right]} \quad (14)$$

as is found by substituting for I and g_d and putting $x=W_d/W_{00}$ and $y=W_s/W_{00}$. The equation holds for $0\leq W_s/W_{00}\leq W_d/W_{00}\leq 1$, but does not hold in the saturated region of the characteristic.

For zero drain bias ($V_d=0$), $x=y$ and the expression (14) can be written

$$\overline{i^2} = 4kT\frac{g_0}{L}\Delta f(1-y^{1/2}) = 4kTg_{d0}\Delta f, \quad (14a)$$

as is found by taking the limit $x\to y$ in (14). Since g_{d0} is the ac output conductance for zero drain bias, (14) indicates that the device gives thermal noise for zero bias, as expected.

Since the dc conductance $g_{dc}=I/(V_s-V_d)$ approaches g_{d0} for $V_d\to V_s$, the device gives also thermal noise of the dc conductance for zero drain bias. If $V_d\neq V_s$ this is no longer the case, but it is still worth while to compare (14) with the thermal noise of the conductance g_{dc}. To that end one writes

$$\overline{i^2} = 4kTg_{dc}\Delta fP(x,y). \quad (15)$$

Substituting for $\overline{i^2}$ and I, putting $(V_s-V_d)=(W_d-W_s)$ and writing again $x=W_d/W_{00}$ and $y=W_s/W_{00}$, one obtains for the factor $P(x,y)$

$$P(x, y) = \frac{(x - y)\left[(x - y) - \frac{4}{3}(x^{3/2} - y^{3/2}) + \frac{1}{2}(x^2 - y^2)\right]}{\left[(x - y) - \frac{2}{3}(x^{3/2} - y^{3/2})\right]^2}. \tag{15a}$$

For $0 \leqq y \leqq x \leqq 1$, the function $P(x, y)$ is a monotonically *increasing* function of x for fixed values of y and a monotonically *decreasing* function of y for fixed values of x. $P(x, y)$ has the value 1.00 for $x = y$ (zero drain voltage), the value 3/2 for $x = 1$, $y = 0$ and the value 4/3 for $x = 1$, $y = 1$.

It can thus be concluded that the noise is nearly equal to the thermal noise of the dc conductance g_{de} of the channel for all values of W_s and W_d, as long as the device is not operating on the saturated region of the characteristic.

Other Expressions for the Noise

It is convenient to write the expression for $\overline{i^2}$ in a different form by putting

$$\overline{i^2} = 4kTg_{\max}\Delta f Q(W_d, W_d) \tag{16}$$

where

$$Q(W_d, W_s) = Q(x, y) = \frac{\left[(x - y) - \frac{4}{3}(x^{3/2} - y^{3/2}) + \frac{1}{2}(x^2 - y^2)\right]}{(1 - y^{1/2})\left[(x - y) - \frac{2}{3}(x^{3/2} - y^{3/2})\right]} \tag{16a}$$

as is found by substituting (14) and introducing the expression (5a) for $g_{\max}$.

For $0 \leqq y \leqq x \leqq 1$ the function $Q(x, y)$ is a monotonically *decreasing* function of x for fixed values of y and a monotonically *increasing* function of y for fixed values of x. $Q(x, y)$ has the value 1.00 for $x = y$ (zero drain voltage), the value 1/2 for $x = 1$, $y = 0$ and the value 2/3 for $x = 1$, $y = 1$. Since W_s/W_{00} cannot be smaller than V_{dif}/W_{00} for positive gate bias, at least for the type of field-effect transistor under discussion, the smallest value of $Q(x, y)$ is always somewhat larger than 1/2.

In the saturated condition $x = 1$ and

$$\overline{i^2} = 4kTg_{\max}\Delta f Q(1, y). \tag{16b}$$

The theory does not hold beyond saturation, but it is found experimentally that (16b) is nearly correct in the saturated part of the characteristic as long as the field strength in the cutoff part of the channel is not too large. Eq. (16b) may thus be applied under saturated condition.

It is often convenient to introduce the noise resistance, R_n of the device by the equation

$$\overline{i^2} = 4kTR_n\Delta f g_m^2. \tag{17}$$

Substituting for $\overline{i^2}$, one obtains for R_n

$$R_n = \frac{g_{\max}}{g_m^2} Q(x, y). \tag{18}$$

Since $Q(x, y)$ has a value close to unity, R_n may be approximated as

$$R_n \simeq \frac{g_{\max}}{g_m^2}. \tag{18a}$$

For a more accurate evaluation of R_n one has to determine the value of $Q(x, y)$.

At saturation $g_m = g_{\max}$ and $x = 1$, hence

$$R_n = \frac{Q(1, y)}{g_{\max}}. \tag{18b}$$

The theory does not hold beyond saturation, but in view of what was said about $\overline{i^2}$, (18b) remains valid in good approximation in the saturated region of the characteristic, as long as the field strength in the cutoff part of the channel is not too large. The value of $Q(1, y)$ usually lies between 0.60 and 0.67.

Influence of the Series Resistances in the Channel

If the gate contacts cover only part of the channel, one has to take into account the series resistance r_s at the source side of the channel and the resistance r_d at the drain side of the channel. The corresponding equivalent circuit is now as shown in Fig. 2.

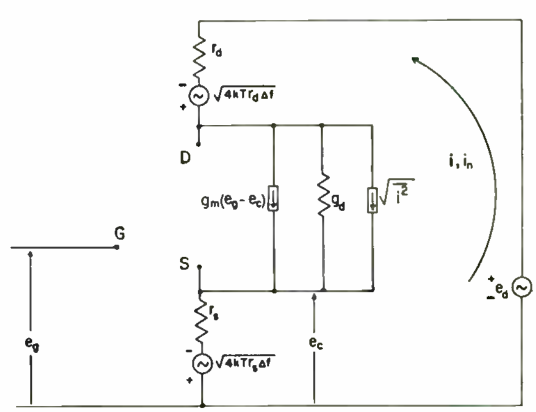

Fig. 2—Equivalent circuit of a field-effect transistor including the thermal noise of the two series resistances r_s and r_d of the channel.

It is easily demonstrated that the "apparent" transconductance g_m' of the device is given by

$$g_m' = \frac{g_m}{1 + r_s g_{\max} + r_d g_d}, \tag{19}$$

and that the "apparent" output conductance g_d' of the device is

$$g_d' = \frac{g_d}{1 + r_s g_{\max} + r_d g_d}. \tag{20}$$

At saturation $g_d = 0$ and the apparent maximum transconductance $g_{\max}'$ is

$$g_{\max}' = \frac{g_{\max}}{1 + r_s g_{\max}}. \tag{19a}$$

For zero drain bias $g_d = g_{d0} = g_{\max}$ and g_d' has the value g_{d0}'

$$g_{d0}' = \frac{g_{\max}}{1 + r_s g_{\max} + r_d g_{\max}}. \tag{20a}$$

Hence it is now no longer true that $g_{d0}' = g_{\max}'$; this might be used as a means for demonstrating series resistance effects.

The mean square value $\overline{i_n^2}$ of the noise current in the short-circuited output is found to be

$$\overline{i_n^2} = 4kT\Delta f \frac{[g_{\max}^2 r_s + g_{\max} Q(x, y) + g_d^2 r_d]}{(1 + g_{\max} r_s + r_d g_d)^2}$$
$$= 4kT g_{\max}' \Delta f Q'(x, y) \tag{21}$$

where

$$Q'(x, y) = \frac{[Q(x, y) + g_{\max} r_s + g_d^2 r_d / g_{\max}](1 + g_{\max} r_s)}{(1 + g_{\max} r_s + r_d g_d)^2}. \tag{22}$$

Since $Q(y, y) = 1$ for zero drain bias and $g_d = g_{\max}$ in that condition, one finds for $Q'(y, y)$

$$Q'(y, y) = \frac{1 + g_{\max} r_s}{(1 + g_{\max} r_s + g_{\max} r_d)} < 1. \tag{22a}$$

Under saturated conditions $x = 1$ and $g_d = 0$, so that

$$Q'(1, y) = \frac{Q(1, y) + g_{\max} r_s}{1 + g_{\max} r_s}. \tag{22b}$$

Since $Q(1, y) < 1$, (22b) indicates that

$$Q(1, y) \leq Q'(1, y) < 1. \tag{22c}$$

The effect of the series resistances is thus to make the factor $Q'(x, y)$ more nearly independent of the drain voltage. If the device is completely cut off, $Q(1, y) \to Q(1, 1) = 2/3$ and $g_{\max} \to 0$. Consequently $Q'(1, 1) = Q(1, 1) = 2/3$.

Introducing the total noise resistance R_n' of the device, by putting

$$\overline{i_n^2} = 4kTR_n' \Delta f g_m'^2 \tag{23}$$

yields

$$R_n' = \frac{g_{\max}'}{g_m'^2} Q'(x, y) \tag{24}$$

so that the total noise resistance can be approximated by $(g_{\max}'/g_m'^2)$ in good approximation in many applications. For a more accurate calculation of R_n' the factor $Q'(x, y)$ must be evaluated.

The resulting noise resistance is quite low. For example, in a field-effect transistor in or near the saturated region with attainable values as $g_m' = g_{\max} = 1000$ μmho and with $Q(1, y) = 0.75$, which is a typical value, gives $R_n = 750$ ohms. This is about a factor four better than the shot noise resistance of a vacuum tube with comparable transconductance and considerably better than the noise resistance of transistor circuits at high input impedance levels.

Other Noise Sources

It has been suggested[2] that the observed noise can be interpreted as suppressed shot noise. There is no physical basis for such a suggestion. For evidently the field-effect transistor operates on the principle of true conductance modulation, as Shockley's theory indicates. Generally one associates *thermal* noise with a true conductance and *not* shot noise. It is hard to see how shot noise could ever be generated and, if generated, how it could be partly suppressed. As this paper indicates, the assumption of thermal noise allows a straightforward explanation of the observed noise.

Even the cutoff portion of the channel behaves as a true resistor, though perhaps a nonlinear one, and thus should have thermal noise associated with it. This does not deny, of course, the possibility of an additional noise source. Present experimental evidence does not seem to indicate that this noise is important.[3,4]

Generation and recombination of carriers in the conducting channel would be another possible source of noise. This effect has been observed[3,4] in CdS field-effect phototransistors, where the carriers in the conducting channel are generated by the absorption of light. Noise due to deep lying traps would also belong to this category.

Besides the thermal noise of the conducting channel, field-effect transistors should also show shot noise of the gate current and $1/f$ noise of the gate and the channel currents.[2,3]

The shot noise of the gate current can be described as follows. Let the gate current I_g consist of a part $-I_{g1}$ due to holes arriving at the gate and electrons leaving the gate and a part $+I_{g2}$ due to holes leaving the gate and electrons arriving at the gate, then

$$I_g = -I_{g1} + I_{g2}. \tag{25}$$

The noise can then be represented by a current generator $\sqrt{\overline{i_g^2}}$ between the gate and the source

$$\overline{i_g^2} = 2e(I_{g1} + I_{g2})\Delta f. \tag{26}$$

[2] P. O. Lauritzen, "Field effect transistors as low-noise amplifiers," 1962 Internatl. Solid-State Circuits Conf., Philadelphia, Pa., February 14-16, 1962, *Digest of Technical Papers*, pp. 62-63; February, 1962.

[3] E. R. Chenette, to be published.

[4] W. C. Bruncke, to be published.

For low-noise operation the currents I_{g1} and I_{g2} should be kept as small as possible. Because of the location of the current generator $\sqrt{i_g^2}$, its effect will be especially pronounced for large values of the impedance in the gate circuit.

Some $1/f$ noise should be present at low frequencies, both in the gate current and in the channel current. The latter is most pronounced for low impedances in the gate circuit whereas the former will show up for large impedances in the gate circuit. As is well known, the magnitude of these $1/f$ noises can be substantially reduced by appropriate surface treatment, so that it need not be bothersome above a few hundred cycles.

At high frequencies the effect of the thermal noise in the conducting channel will also show up in the gate circuit. This comes about because of the capacitive coupling between the channel and the gate; as a consequence, a capacitive noise current will flow to the gate at high frequencies. This noise should be partly correlated with the channel noise and might thus be used to eliminate part of the latter.[2] It can be represented by a current generator $\sqrt{i_c^2}$ between the gate and the source; because of the capacitive coupling, $\overline{i_c^2}$ should be proportional to the square of the frequency over a wide frequency range. Though it resembles induced grid noise in vacuum tubes in this respect, its interpretation is different, as the above discussion shows.

The shot noise of the gate current and the $1/f$ noises can be reduced by the choice of the transistor material, by improved construction of the device and by proper treatment of the finished product. The thermal noise of the conducting channel and the capacitive gate current resulting from it are always present; however, they determine the lowest noise figure that can be obtained with field-effect transistors.

Conclusions

The theoretical discussion shows that the basic limitation of the noise figure of field-effect transistors is the thermal noise of the conducting channel. Expressions are derived for the equivalent output noise current generator and for the equivalent noise resistance of the device that can be easily checked with experiment.

The theoretical predictions of this paper have been verified experimentally by Dr. E. R. Chenette[3] and W. C. Bruncke,[4] both of the Electrical Engineering Department of the University of Minnesota. The author is indebted to these investigators for several stimulating discussions about the interpretation of their experimental results, which led to the development of the theory presented in this paper.

Higher-Order Temperature Coefficients of the Elastic Stiffnesses and Compliances of Alpha-Quartz*

R. BECHMANN†, FELLOW, IRE, A. D. BALLATO†, MEMBER, IRE, AND T. J. LUKASZEK†, MEMBER, IRE

Summary—**The first-, second-, and third-order temperature coefficients of the elastic stiffnesses and compliances of alpha-quartz have been derived from thickness mode resonances of doublerotated quartz plates employing Christoffel's theory of wave propagation. The temperature dependence of all possible thickness modes can be calculated from the values of the elastic stiffnesses and their temperature coefficients as derived during this investigation. A curve showing the locus of the first-order zero temperature coefficient of frequency of thickness-shear modes has been calculated and compared with experiments. The second- and third-order temperature coefficients of frequency of the first-order zero quartz cuts are given. Applications to AT, BT, CT, and DT cuts are made by comparing the calculated with the experimental values which characterize the temperature behavior of frequencies and new useful piezoelectric cuts of quartz are indicated.**

* Received February 7, 1962; revised manuscript received April 10, 1962.

† U. S. Army Signal Res. and Dev. Lab., Fort Monmouth, N. J.

Introduction

The frequency-temperature behavior of the various quartz cuts and consequently the behavior of the elastic constants, *i.e.*, the stiffnesses $c_{\lambda\mu}$ determining the thickness modes and the compliances $s_{\lambda\mu}$ determining the contour modes, is in general a nonlinear function of temperature. Therefore higher-order temperature coefficients have to be taken into consideration for these quantities, *e.g.*, by use of a power series.

The Christoffel theory [1] of propagation of plane waves governs the thickness modes of piezoelectric crystals. The six so-called Christoffel moduli $\Gamma_{ik}=\Gamma_{ki}$ $(i, k=1, 2, 3)$ which are combinations of the 21 stiffnesses $c_{\lambda\mu}$ $(\lambda, \mu=1, 2, \cdots, 6)$ and the direction cosines of the wave propagation were thereby introduced.

Christoffel's equation results in three possible types of plane waves for any direction of propagation, each wave having a different velocity and the three directions of vibration being mutually perpendicular.

The solution of the three second-order differential equations derived by Christoffel leads to three resulting stiffnesses c_m $(m=1, 2, 3)$ which are related to the velocities of wave propagation and the directions of the displacements which are generally neither parallel nor perpendicular to the direction of the wave propagation. Assuming infinitely extended plates, Koga [2] derived in closed form a solution for the three thickness modes corresponding to the three wave velocities, the direction of the propagation being parallel to the normal of the plate. These three frequency equations form the basis for consideration of the influence of temperature on frequency by applying a power series. Satisfactory agreement between measurements and calculations was obtained when the first three orders of the temperature coefficients of the frequencies and stiffnesses were applied. The first-order temperature coeffiicents of the stiffnesses and compliances of alpha-quartz were originally derived by Bechmann [3] using measured values for the temperature coefficient of frequency of thickness modes of plates and extensional modes of bars. The new determination of the values of the first- to third-order temperature coefficients of the elastic constants of quartz is based on measurements of various double-rotated thickness modes of plates.

A modified theory of elasticity was considered by Laval [4] in 1951, and later by others, proposing that the asymmetrical part of the stress tensor enters into the constitutive relations, thereby increasing the number of elastic constants compared with the classical theory. According to Laval's theory of elasticity the number of elastic constants for the crystal class D_3 is increased by $c_{55} \neq c_{44}$ and c_{17}. Zubov and Firsova [5] carried out a new determination of the elastic stiffnesses of quartz using the increased number of elastic stiffnesses. Their values fall within the limits of accuracy of measurements. The experimental values for quartz, which have been used for determination of the elastic stiffnesses given by Bechmann [6], have been recalculated with respect to the new theory. He found that the values for c_{44} and c_{55}, c_{14} and c_{17} are so close and so critical that from an experimental point of view no support for the Laval theory is provided. Recent studies by Mindlin [7] show that the principles of conservation of momentum and energy are not fulfilled by Laval's theory. In the following, the determination of the temperature coefficients of the stiffnesses is based on the classical theory of elasticity, which is defined by six independent elastic constants for quartz.

Christoffel's Theory of Plane Elastic Waves in Crystals

Christoffel's theory of the propagation of plane elastic waves in crystals is well known and treated in many papers and textbooks [8]. It is therefore unnecessary to repeat this theory.

The differential equation for plane waves in anisotropic media is written considering one dimension, that of the propagation s with the direction cosines $\alpha_1, \alpha_2, \alpha_3$ in the form

$$\rho \frac{\partial^2 \xi}{\partial t^2} - c \frac{\partial^2 \xi}{\partial s^2} = 0, \tag{1}$$

where ξ is the direction of the displacement, c is

$$c = \Gamma_{11}p^2 + \Gamma_{22}q^2 + \Gamma_{33}r^2 + \Gamma_{23}qr + \Gamma_{31}rp + \Gamma_{12}pq \tag{2}$$

and

$$\Gamma_{ik} = \sum_{jl}^{3} c_{ij,kl}\alpha_j\alpha_l, \tag{3}$$

the Christoffel stiffnesses, a combination of the stiffnesses c_{ik} and the direction cosines for the direction s of the propagation. The constants p, q, r, when normalized by $p^2+q^2+r^2=1$, are the direction cosines for the displacement ξ_i. To solve (1) for an infinitely extended plate, the boundary conditions for the free plate

$$\frac{\partial \xi}{\partial s} = 0 \text{ for } s = 0 \text{ and } s = e \text{ (}e\text{ is the thickness of the plate)}$$

have to be introduced.

When considering the propagation of elastic waves in a piezoelectric material, an additional piezoelectric stress due to the electric field E must be introduced. Therefore a slight modification of the elastic stiffnesses $c_{\lambda\mu} = c_{\lambda\mu}{}^E$ occurs, resulting in $c_{\lambda\mu}{}^D$ where D_s refers to constant normal displacement. For infinite plates, on the basis of Maxwell's equation, $D_{\text{normal}}(=D_s)$ and E_{tangent} must be continuous and therefore the related coefficients $c_{\lambda\mu}$ and Γ_{ik} are mixed with $D=0$ normal to, $E=0$ parallel to, the wave front. Consequently $\Gamma_{ik}{}^E$ becomes $\Gamma_{ik}{}^D$, the direction cosines of the displacement change, and the resulting stiffnesses $c_m{}^E$ becomes $c_m{}^D$.

The secular equation defining the three resulting stiffnesses c_m of a piezoelectric material is given by

$$\begin{vmatrix} \Gamma_{11}{}^{D_s} - c^{D_s} & \Gamma_{12}{}^{D_s} & \Gamma_{13}{}^{D_s} \\ \Gamma_{12}{}^{D_s} & \Gamma_{22}{}^{D_s} - c^{D_s} & \Gamma_{23}{}^{D_s} \\ \Gamma_{13}{}^{D_s} & \Gamma_{23}{}^{D_s} & \Gamma_{33}{}^{D_s} - c^{D_s} \end{vmatrix} \equiv \begin{vmatrix} \Gamma_{11}{}^E - c^{D_s} & \Gamma_{12}{}^E & \Gamma_{13}{}^E & \Xi_1 \\ \Gamma_{12}{}^E & \Gamma_{22}{}^E - c^{D_s} & \Gamma_{23}{}^E & \Xi_2 \\ \Gamma_{13}{}^E & \Gamma_{23}{}^E & \Gamma_{33}{}^E - c^{D_s} & \Xi_3 \\ \Xi_1 & \Xi_2 & \Xi_3 & -\epsilon_s \end{vmatrix} = 0. \tag{4}$$

The expressions for $\Gamma_{ik}{}^E$ and $\Gamma_{ik}{}^{D_s}$ at constant electric field and constant displacement, respectively, in these equations are related by

$$\Gamma_{ik}{}^{D_s} = \Gamma_{ik}{}^E + \frac{1}{\epsilon_s}\Xi_i\Xi_k. \tag{5}$$

The expressions for Christoffel's stiffnesses

$$\Gamma_{ik}(i, k = 1, 2, 3),$$

the piezoelectric stress constants Ξ_l $(l=1, 2, 3)$, and the dielectric constant ϵ_s of alpha-quartz belonging to the trigonal crystal class D_3, as displayed in (4), follow from Table I.

TABLE I

Expressions for the Christoffel Stiffnesses Γ_{ik}, the Piezoelectric Stress Constants Ξ_l and the Dielectric Permittivity ϵ_s for the Trigonal Crystal Class D_3, e.g., Alpha-Quartz

	α_1^2	α_2^2	α_3^2	$\alpha_2\alpha_3$	$\alpha_3\alpha_1$	$\alpha_1\alpha_2$
Γ_{11}	c_{11}	c_{66}	c_{44}	$2c_{14}$	0	0
Γ_{22}	c_{66}	c_{11}	c_{44}	$-2c_{14}$	0	0
Γ_{33}	c_{44}	c_{44}	c_{33}	0	0	0
Γ_{23}	c_{14}	$-c_{14}$	0	$c_{13}+c_{44}$	0	0
Γ_{31}	0	0	0	0	$c_{13}+c_{44}$	$2c_{14}$
Γ_{12}	0	0	0	0	$2c_{14}$	$c_{12}+c_{66}$
Ξ_1	e_{11}	$-e_{11}$	0	$-e_{14}$	0	0
Ξ_2	0	0	0	0	e_{14}	$-2e_{11}$
Ξ_3	0	0	0	0	0	0
ϵ_s	ϵ_{11}	ϵ_{11}	ϵ_{33}	0	0	0

Considering the eigenfrequencies $\omega = 2\pi f$ of an infinitely extended plate vibrating in thickness modes, introducing $c = \rho\omega^2/k^2$, and taking into account the boundary conditions $\cos ke/2 = 0$ having the solution $ke/2 = n\pi/2$, the frequency in first approximation is

$$f_m^{(n)} = \frac{n}{2e}\sqrt{\frac{c_m^{D_s}}{\rho}}, \qquad (m = 1, 2, 3) \tag{6}$$

where n is an odd integer. Eq. (6) is rigorous for resonators having a large electrode gap or vibrating at high overtones. When these conditions are not fulfilled, as in the case of plated crystals vibrating at fundamental modes, a small correction term has to be considered. The frequency $f_m^{(n)}$ for the nth overtone for mode m is determined by the eigenvalue $c_m^{D_s}$, the thickness of the plate e, and the density ρ. Generally, three solutions for the frequency $f_m (m=1, 2, 3)$ of the thickness vibrations and their overtones exist for each individual plate and in the following are designated as modes A, B, and C. Mode A is essentially the thickness-extensional mode while modes B and C are essentially thickness-shear modes. The frequencies for each plate always follow in the sequence $f_A > f_B > f_C$.

The equation for the temperature behavior of the frequency can be developed in the power series

$$\frac{f - f_0}{f_0} = \frac{\Delta f}{f_0} = \sum_{n=1}^{3} Tf^{(n)}(T - T_0)^n \tag{7}$$

where

$$Tf^{(n)} = \frac{1}{n!f_0}\left(\frac{\partial^n f}{\partial T^n}\right)_{T=T_0}, \tag{8}$$

$Tf^{(n)}$ $(n=1, 2, 3)$ being designated a, b, and c respectively. T is the variable temperature and T_0 is the reference temperature.

The relationships between the first-order temperature coefficients of frequency $Tf^{(1)}$ and the first-order temperature coefficients of the stiffnesses $Tc_{\lambda\mu}^{(1)}$ are given by

$$2Tf^{(1)} = Tc^{(1)} - T\rho^{(1)} - 2Te^{(1)}; \tag{9}$$

the relations for the second-order temperature coefficients of frequency and stiffnesses are

$$\begin{aligned} 2[Tf^{(2)} - \tfrac{1}{2}(Tf^{(1)})^2] &= Tc^{(2)} - T\rho^{(2)} - 2Te^{(2)} \\ &\quad - \tfrac{1}{2}[(Tc^{(1)})^2 - (T\rho^{(1)})^2 - 2(Te^{(1)})^2]; \end{aligned} \tag{10}$$

and for the third order

$$\begin{aligned} 2[Tf^{(3)} - Tf^{(2)}Tf^{(1)} + 1/3(Tf^{(1)})^3] &= Tc^{(3)} - T\rho^{(3)} - 2Te^{(3)} \\ &\quad - [Tc^{(2)}Tc^{(1)} - T\rho^{(2)}T\rho^{(1)} - 2Te^{(2)}Te^{(1)}] \\ &\quad + 1/3[(Tc^{(1)})^3 - (T\rho^{(1)})^3 - 2(Te^{(1)})^3], \end{aligned} \tag{11}$$

where $T\rho = -(2\alpha_x + \alpha_z)$ and α_x and α_z are the expansion coefficients. Te is the temperature coefficient of the thickness of the plate. The essential term in these equations is the temperature coefficient of the eigenvalue Tc; however, the terms resulting from dimensions of the plate are also taken into consideration.

Methods and Equipment for Measurements

The measurements carried out included: 1) frequency measurements of the three modes of vibration at room temperature, and 2) frequency-temperature dependence of these three modes in an extended temperature range.

The frequency range for these three modes of vibration were approximately 4 to 8 Mc with $f_A > f_B > f_C$. Most of the crystals were excited in a CI Meter Type TS 330/TSM. A Heegner oscillator [9] was used sometimes to excite modes whose activity was too low for excitation in the CI Meter. The frequencies were determined with a Hewlett-Packard Counter, Model 524B.

The apparatus used for measuring the dependence of crystal frequency on temperature included: 1) a small aluminum cylinder having two cavities, with a canned crystal unit inserted in one of the cavities and a thermocouple in the other; 2) a calibrated precision bridge to determine the temperature; 3) a wire heating element which was wound around the aluminum cylinder; and 4) a well-insulated Dewar flask containing liquid nitrogen.

Measurements of the frequency-temperature behavior were conducted as follows: in order to obtain a very low initial temperature, the cylinder containing the crystal and a thermocouple was lowered into the flask containing liquid nitrogen. After the temperature within the two cavities approximated the temperature of liquid nitrogen, the liquid nitrogen was removed and the flask containing the cylinder was sealed to stabilize the temperature within the flask at the desired temperature. By means of the heating element described above and controlled by a variac, the temperature was gradually increased and frequency readings were taken at 5°C intervals over the temperature range of approximately −196°C to +170°C.

Determination of the Temperature Coefficients of the Stiffnesses and Compliances of Alpha-Quartz

A large number of crystals vibrating in the fundamental thickness modes, cut at various orientation angles,[1] were investigated with respect to their temperature behavior. The crystals were divided into three groups:

1) Crystals oriented at negative Θ angles and various Φ angles. These plates were square and had a length and width of 0.5 in, their edges were bevelled, and the plates were mounted in HC-6 holders. The plate thicknesses were adjusted so that mode B was calibrated at a frequency of about 5 Mc. These crystals were fabricated by McCoy Electronics Company, Mount Holly Springs, Pa. The accuracy of the orientation angles was better than 10′ for the angle Φ and better than 5′ for the angle Θ according to the manufacturer.
2) Some crystals oriented at positive angles of Θ. Plates vibrating in the mode C and oriented at about $\Phi=20°$, $\Theta=34°20'$, are known as IT-cuts and were furnished through the courtesy of Scientific Radio Products, Inc., Loveland, Colo.
3) Several crystal plates having the orientation angle $(xyl)\Theta$ in the range $\Theta=0°$ to $60°$ at $10°$ intervals (rotated X-cuts). These crystals were fabricated at the U. S. Army Signal Research and Development Laboratory, Fort Monmouth, N. J.

The values for the frequency constant $N=f\cdot e$ of the three fundamental modes A, B, and C were calculated using (4) and the recently published values for $c_{\lambda\mu}$ for quartz [6]. The elastic stiffnesses used are given in Table II which also includes a new determination of the stiffnesses by Mindlin and Gazis [12]. The values derived by Mindlin agree closely with the values for the stiffnesses given by Bechmann [6].

The frequencies of the crystals in Group 1 were measured having a large electrode separation. The agreement between the calculated frequency constant and the measured frequency constant is then much closer, as (6) is rigorous for crystals having a large electrode separation. Results for the measurements of the frequency constants N of the three modes together with the calculated values are shown in Table III. Agreement between calculated and measured values is better than 1 per cent.

The values for the temperature coefficients of the elastic stiffnesses $Tc_{\lambda\mu}$ are dependent on the accuracy of the measurements of the temperature coefficients of frequency Tf. It is well known that the temperature coefficients of frequency depend slightly on the state of the plate measured, *e.g.*, the form of the plate (circular or square), the electrode size (ratio Φ_e/e where Φ_e is the diameter of the electrode and e is the thickness of the plate), the electrode separation (whether an air gap or plated blank is used), the order of overtone which changes the zero angles for the first-order zero temperature coefficients $Tf^{(1)}$, the bevelling of the plate which is necessary to avoid coupling with other modes which gives rise to errors, and the drive level of the resonator. Further, there are slight differences between the temperature coefficients of natural and synthetic quartz. Finally, the temperature coefficients of the stiffnesses are dependent on the approximation of the solution of the equations on which the determination is based.

Some previous investigations of the frequency-temperature behavior of double-rotated quartz crystals were conducted by Saunders and Hammond [13] based on the earlier calculation by Bechmann [3].

The frequency-temperature dependence of the quartz blanks mentioned was measured in the temperature range −196°C to +170°C. All blanks used for frequency-temperature measurements were plated. The resulting frequency curve was developed in a power series with respect to the reference temperature $T_0=25°C$ up to the third order. The first-, second-, and third-order temperature coefficients of frequency a, b, and c of a number of these crystals, which were used for determination of the temperature coefficients of the stiffnesses, are also listed in Table III, together with values calculated from the newly determined temperature coefficients. The values for $Tc_{\lambda\mu}^{(n)}(n=1, 2, 3)$ follow from (4) by differentiation with respect to the temperature.

The newly determined first-order temperature coefficients of the stiffnesses $Tc_{44}^{(1)}$, $Tc_{66}^{(1)}$, and $Tc_{14}^{(1)}$ are considered very accurate, as the values follow from rotated plates $(yxl)\Theta$. The behavior of the AT and BT cuts, their orientation angles for the zero temperature coefficient of frequency and the change of their temperature coefficients with respect to the angle Θ are very well known [14] (see Table III). In addition, the Y cut (yx) which has a first-order temperature coefficient of frequency of $92.5\cdot10^{-6}/°C$ has also been used.

The values for $Tc_{44}^{(1)}$, $Tc_{66}^{(1)}$, and $Tc_{14}^{(1)}$, as shown in the left-hand column of Table IV, are obtained for the

[1] The IRE rotational symbol [10] is used throughout this paper.

TABLE II

ELASTIC STIFFNESSES $c_{\lambda\mu}$ IN $10^9 Nm^{-2}$ FOR ALPHA-QUARTZ AT 20°C

$\lambda\mu$	Stiffnesses of Quartz Bechmann [6]		Stiffnesses of Quartz Mindlin and Gazis [12]
	$c_{\lambda\mu}{}^{E\sigma}$	$c_{\lambda\mu}{}^{D\sigma}$	$c_{\lambda\mu}$
11	86.74	87.49	86.75
33	107.2	107.2	107.2
12	6.99	6.23	5.95
13	11.91	11.91	11.91
44	57.94	57.98	57.8
66	39.88	40.63	40.4
14	−17.91	−18.09	−17.8

and using again $\partial a/\partial\Theta = -5.15\cdot 10^{-6}$ for the slope of the AT cut, the values listed on the right-hand side of Table IV are obtained. These latter values occur in the case of the AT and BT cuts when high overtones [15] are used or large electrode gaps are employed. The difference Δ between these values are also listed in Table IV, and the accuracy for determination of the temperature coefficients of the elastic stiffnesses $Tc_{44}{}^{(1)}$, $Tc_{66}{}^{(1)}$, and $Tc_{14}{}^{(1)}$ falls within this order of magnitude.

$Tc_{11}{}^{(1)}$ follows from the X cut (xy) which has a value for the first-order temperature coefficient of frequency $Tf^{(1)} = -20.5^{-6}/°C$. $Tc_{33}{}^{(1)}$ was determined using the

TABLE III

MEASURED AND CALCULATED FREQUENCY CONSTANTS N AND FIRST-, SECOND- AND THIRD-ORDER TEMPERATURE COEFFICIENTS OF FREQUENCY a, b, c FOR THE THICKNESS MODES A, B, AND C OF SOME SELECTED QUARTZ PLATES

Cut	Orientation Angle		Mode	N kc·mm Observed	N kc·mm Calculated	Observed			Calculated		
	Φ	Θ				a $10^{-6}/°C$	b $10^{-9}/(°C)^2$	c $10^{-12}/(°C)^3$	a $10^{-6}/°C$	b $10^{-9}/(°C)^2$	c $10^{-12}/(°C)^3$
X	30°	0°	A	2845	2873	−20.5	− 53.2	− 36.6	−20.5	−52.0	− 36.9
	30°	10°	A	2890	2980	−29.3	− 67.0	− 58.3	−29.8	−64.3	− 68.6
	30°	20°	A		3135	−42.0	− 86.0	− 92.7	−41.4	−80.7	− 95.4
	30°	30°	A		3254	−54.8	−105.5	−119.5	−51.7	−96.0	−113.0
BT	0°	−49°13′	B	2540	2530	0	− 40	−128	0	−39.6	−128
	5°	−47°	B	2519	2515	− 0.9	− 41.0	−118.0	1.7	−39.8	−127
	5°	−48°	B		2521	− 1.5	− 43.0	−123.0	− 0.2	−41.5	−128
	10°	−38°	B	2347	2388	1.1	− 39.0	− 91.0	6.8	−40.7	−120
	10°	−40°	B		2410	− 2.4	− 42.0	−115.0	4.3	−42.2	−122
	15°	−34°30′	B		2264	− 7.4	− 28.1	− 40.0	− 0.67	−47.4	−105
	15°	−35°	B	2208	2270	− 7.45	− 33.5	− 59	− 0.98	−47.7	−106
	30°	20°	B		2220	− 9.3	− 21.8	− 34.4	− 9.3	−20.4	− 37.6
	30°	30°	B	2048	2050	−19.1	− 24.5	− 28.9	−18.2	−27.0	− 33.9
Y	0°	0°	C	1946	1957	92.5			92.5	57.5	5.8
AT	0°	35°15′	C	1660	1660	0	0.40	109	0	− 0.6	109
	10°	−32°	C	2106	2120	0.26	− 9.8	− 32.4	− 1.5	−13	− 29.3
	10°	−33°	C	2158	2100	− 0.87	− 7.8	− 21.5	− 1.9	−12.5	− 25
	12.5°	−33°	C	2101	2088	0.8	− 7.6	− 19.6	− 1.62	−12.1	− 20.7
	12.5°	−33°30′	C		2079	− 0.4	− 7.4	− 14.0	− 2.07	−11.9	− 18.8
RT	15°	−34°30′	C	2040	2047	1.3	− 7.3	− 6.6	− 2.9	−10.6	− 10.5
	15°	−35°	C		2038	− 0.2	− 7.02	− 2.6	− 3.5	−10.5	− 8.8
IT	20°	34°20′	C	1693	1783	− 0.06	− 8.9	52.0	− 0.5	−10.5	62
	30°	34°	C		1911	0.75	− 13.0	17.4	0.26	−14.3	32.0
	30°	36°	C		1897	− 4.55	− 14.3	20.6	− 5.4	−14.4	34.4

TABLE IV

VALUES FOR $Tc_{44}{}^{(1)}$, $Tc_{66}{}^{(1)}$, $Tc_{14}{}^{(1)}$ IN $10^{-6}/°C$ USING TWO DIFFERENT ZERO ANGLES OF THE AT AND BT CUTS

	Zero Angle AT: $\Theta =$ 35°15′ BT: $\Theta =$ −49°13′	Zero Angle AT: $\Theta =$ 35°22′ BT: $\Theta =$ −49°40′	Δ Per Cent
$Tc_{44}{}^{(1)}$	−177.4	−175.6	1.02
$Tc_{66}{}^{(1)}$	177.6	179.3	0.96
$Tc_{14}{}^{(1)}$	101.3	103.9	2.55

first-order zero temperature coefficient of frequency when

Θ = 35°15′ for the AT cut, − 49°13′ for the BT cut,

and $\partial a/\partial\Theta = -5.15\cdot 10^{-6}$ for the slope of the AT cut. When the zero angle Θ is shifted to

Θ = 35°22′ for the AT cut, − 49°40′ for the BT cut,

zero angles for the double-rotated plates $(yxwl)\Phi\Theta$ listed in Table III.

The second- and third-order temperature coefficients of the elastic stiffnesses were determined using the experimental values for the AT and BT cuts [14] and the newly observed values for the frequency dependence of the double-rotated plates (Group 1).

Table V enumerates the newly determined values for the first-, second-, and third-order temperature coefficients of the elastic stiffnesses for alpha-quartz. For comparison, corresponding values determined by Mason [16] are given in Table VI, and the values calculated from Koga, *et al.* [17] using the expressions

$$\hat{c} = \frac{c}{4\rho}, \quad \frac{\partial \hat{c}}{\partial T}, \quad \frac{1}{2}\frac{\partial^2 \hat{c}}{\partial T^2}, \quad \text{and} \quad \frac{1}{6}\frac{\partial^3 \hat{c}}{\partial T^3}, \tag{12}$$

are given in Table VII.

In addition to the values listed in Tables VI and

TABLE V

New Values for the Temperature Coefficients of the Stiffnesses for Alpha-Quartz at 25°C

	$Tc_{\lambda\mu}^{(1)}$	$Tc_{\lambda\mu}^{(2)}$	$Tc_{\lambda\mu}^{(3)}$
$\lambda\mu$	10^{-6}/°C	10^{-9}/(°C)^2	10^{-12}/(°C)^3
11	− 48.5	− 107	− 70
33	− 160	− 275	− 250
12	−3000	−3050	−1260
13	− 550	−1150	− 750
44	− 177	− 216	− 216
66	178	118	21
14	101	− 48	− 590

TABLE VI

Values for the Temperature Coefficients of the Stiffnesses for Alpha-Quartz at 50°C According to Mason [16], 1951

	$Tc_{\lambda\mu}^{(1)}$	$Tc_{\lambda\mu}^{(2)}$	$Tc_{\lambda\mu}^{(3)}$
$\lambda\mu$	10^{-6}/°C	10^{-9}/(°C)^2	10^{-12}/(°C)^3
11	− 48.5	− 75	− 15
33	− 153	− 182	410
12	−2703	−1500	1910
13	− 583	−2000	600
44	− 158	− 212	− 65
66	169	− 5	− 167
14	105	− 270	− 630

TABLE VII

Values for the Temperature Coefficients of the Stiffnesses for Alpha-Quartz at 20°C According to Koga, et al. [17], 1958

	$Tc_{\lambda\mu}^{(1)}$	$Tc_{\lambda\mu}^{(2)}$	$Tc_{\lambda\mu}^{(3)}$
$\lambda\mu$	10^{-6}/°C	10^{-9}/(°C)^2	10^{-12}/(°C)^3
11	− 44.3	− 407	− 371
33	− 188	−1412	− 243
12	−2930	−7245	4195
13	− 492	− 596	−5559
44	− 172	− 225	− 190
66	180	201	− 777
14	98	− 13	− 625

TABLE VIII

Elastic Compliances $s_{\lambda\mu}$ for Alpha-Quartz at 20°C in $10^{-11}m^2N^{-1}$

	Compliances of Quartz According to Bechmann [6]		Compliances of Quartz Calculated from Mindlin and Gazis [12] Using Their Values $c_{\lambda\mu}$
$\lambda\mu$	$s_{\lambda\mu}^{E\sigma}$	$s_{\lambda\mu}^{D\sigma}$	$s_{\lambda\mu}$
11	12.77	12.64	12.71
33	9.60	9.60	9.60
12	−1.79	−1.66	−1.61
13	−1.22	−1.22	−1.23
44	20.04	20.03	20.017
66	29.12	28.58	28.64
14	4.50	4.46	4.41

TABLE IX

New Values for the Temperature Coefficients of the Compliances for Alpha-Quartz at 25°C

	$Ts_{\lambda\mu}^{(1)}$	$Ts_{\lambda\mu}^{(2)}$	$Ts_{\lambda\mu}^{(3)}$
$\lambda\mu$	10^{-6}/°C	10^{-9}/(°C)^2	10^{-12}/(°C)^3
11	15.5	85.3	147
33	140	247	300
12	−1370	−1385	−2287
13	− 166	− 718	− 823
44	210	262	162
66	− 145	− 85	− 135
14	134	93	− 465

TABLE X

Values for the Temperature Coefficients of the Compliances for Alpha-Quartz at 50°C According to Mason [16], 1951

	$Ts_{\lambda\mu}^{(1)}$	$Ts_{\lambda\mu}^{(2)}$	$Ts_{\lambda\mu}^{(3)}$
$\lambda\mu$	10^{-6}/°C	10^{-9}/(°C)^2	10^{-12}/(°C)^3
11	16.5	58.5	33
33	134.5	144	570
12	−1270	− 575	−215
13	− 678	−2100	610
44	201	200	− 26
66	− 138	− 18	3
14	139.5	40	− 54

VII, the first-order temperature coefficients of the stiffnesses were determined by Bechmann [3], Mason [18], and Atanasoff and Hart [19]. The second-order temperature coefficients were also derived by Mason [18]. Values for the first- and second-order temperature coefficients for Tc_{44}, Tc_{66}, and Tc_{11} have been determined by Bechmann and Ayers [20].

The compliances $s_{\lambda\mu}$ and their first-, second-, and third-order temperature coefficients $Ts_{\lambda\mu}^{(n)}$ were calculated from the values of the stiffnesses $c_{\lambda\mu}$ and their temperature coefficients $Tc_{\lambda\mu}^{(n)}$ using the well-known relationships between the stiffnesses and compliances. The values for the compliances $s_{\lambda\mu}$ given by Bechmann [6] are listed in Table VIII together with values calculated from the stiffnesses $c_{\lambda\mu}$ given by Mindlin and Gazis [12]. The newly determined first-, second-, and third-order temperature coefficients of the elastic compliances $Ts_{\lambda\mu}^{(n)}$ are listed in Table IX. All new values for the temperature coefficients of the stiffnesses and compliances refer to 25°C. For comparison, values are shown in Table X for the temperature coefficients of the compliances $Ts_{\lambda\mu}^{(n)}$ by Mason [16]. Additional determinations for the first-order temperature coefficients of the compliances have been made by Bechmann [3], Giebe and Blechschmidt [21], and Mason [18]; the second-order temperature coefficients were also given by Giebe and Blechschmidt [21]. The first- and second-order temperature coefficient values for s_{11}, s_{66}, and s_{14} can also be found in [20].

All new values for the temperature coefficients of the stiffnesses $Tc_{\lambda\mu}^{(n)}$ obtained from measurements of thickness modes and those of the compliances $Ts_{\lambda\mu}^{(n)}$ calculated from the temperature coefficients of the stiffnesses $Tc_{\lambda\mu}^{(n)}$ are in close proximity to the values at constant normal displacement D_s. The values would

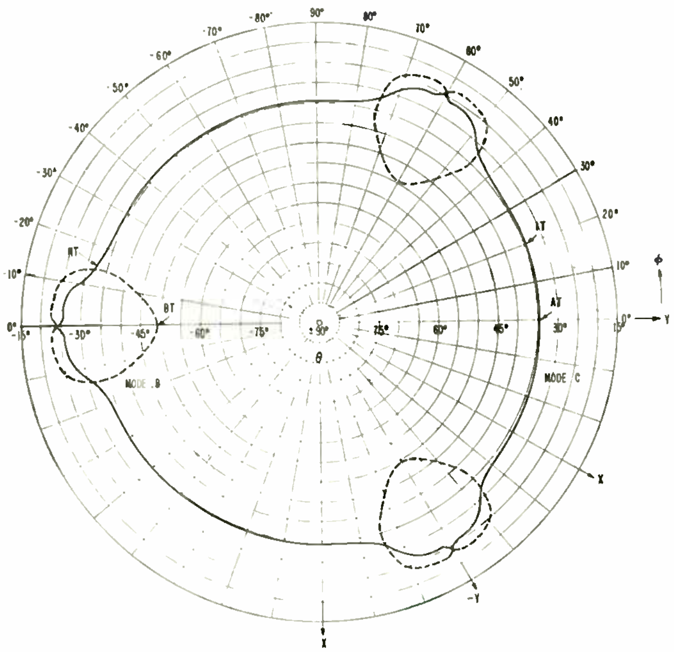

Fig. 1—Locus of $Tf^{(1)}=0$ for the thickness modes B and C of quartz plates as function of the angles Θ and Φ in a polar coordinate system.

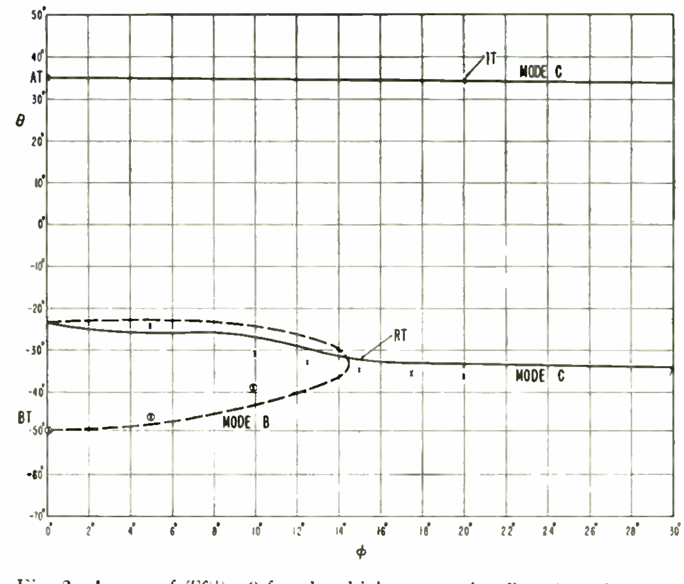

Fig. 2—Locus of $Tf^{(1)}=0$ for the thickness modes B and C of quartz plates as function of the angles Θ and Φ in a rectangular coordinate system.

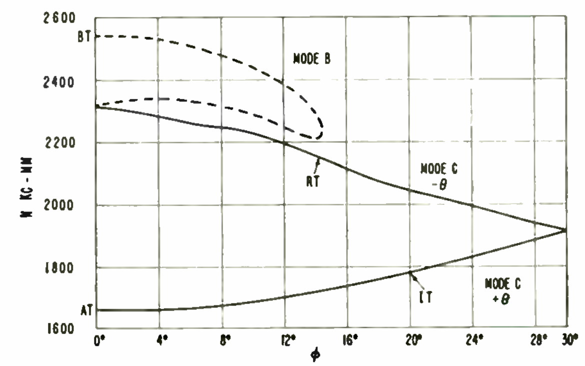

Fig. 3—Frequency constant N of the thickness modes B and C, for alpha-quartz when $Tf^{(1)}=0$, as function of the angles Φ and Θ.

agree exactly with values at constant displacement D_x if high overtones or large gaps were used. However, as mentioned before, plated blanks were used requiring a small correction in the frequency equation, (6). This correction is not taken into consideration as it would have made the calculation unduly complicated. This error, which has been neglected, is considered within the limits of accuracy of measurements of the temperature dependence of the plates.

Applications to Double-Rotated Quartz Plates

Since the temperature coefficients of the stiffnesses are known, the temperature behavior of thickness modes of any orientation can be calculated from these values. Mode A, essentially a longitudinal mode, has a negative temperature coefficient of frequency for all orientations while shear mode B has a first-order zero temperature coefficient of frequency in the range $\Phi=0°$ to $13°$ at two angles of Θ, both on the negative side adjoining the BT cut at $\Phi=0°$ and $\Theta=-49°$. The shear mode C has zero temperature coefficients of frequency for all values of $\Phi(0°$ to $30°)$ at both positive and negative angles and adjoining the AT cut at $\Phi=0°$ and $\Theta=35°$.

Fig. 1 represents the locus of the first-order zero temperature coefficients of frequency for modes B and C in a polar coordinate system illustrating the three-fold symmetry of quartz showing that, at an angle $\Phi+n\,120°$ $(n=0, 1, 2)$, the elastic properties of quartz are identical with those of the angle Φ.

Fig. 2 shows the calculated locus of the first-order zero temperature coefficients of frequency for modes B and C in a rectangular coordinate system compared with some measured results. The values for the mode C are indicated by X, those for the mode B by ⊗. The agreement between the calculated and measured zero angles is better than 3 per cent and, taking into account the uncertainties mentioned above, the agreement is considered very satisfactory.

Fig. 3 shows the frequency constants $N=e\cdot f$ for modes B and C when the first-order temperature coefficient of frequency is zero as function of the angle Φ. Figs. 4 and 5 give the second- and third-order temperature coefficients of frequency when the first-order temperature coefficient of frequency is zero for negative and positive angles of Θ, respectively.

For mode C the second-order temperature coefficient of frequency is always negative and reaches for negative Θ angles a minimum value of about $-7\cdot10^{-9}/(°C)^2$ at $\Phi=15°$. The third-order temperature coefficient changes its sign as function of the angle Φ at negative Θ angles but the zero angles for the first- and third-order temperature coefficients of frequency do not coincide.

At the angle $\Phi=15°$, $\Theta=-34°30'$, the C mode shows a first-order zero temperature coefficient of frequency, a

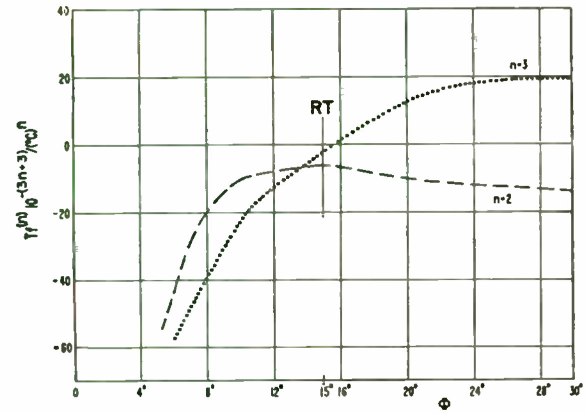

Fig. 4—Values for the second- and third-order temperature coefficients of frequency for the thickness mode C, negative angle Θ when $Tf^{(1)}=0$.

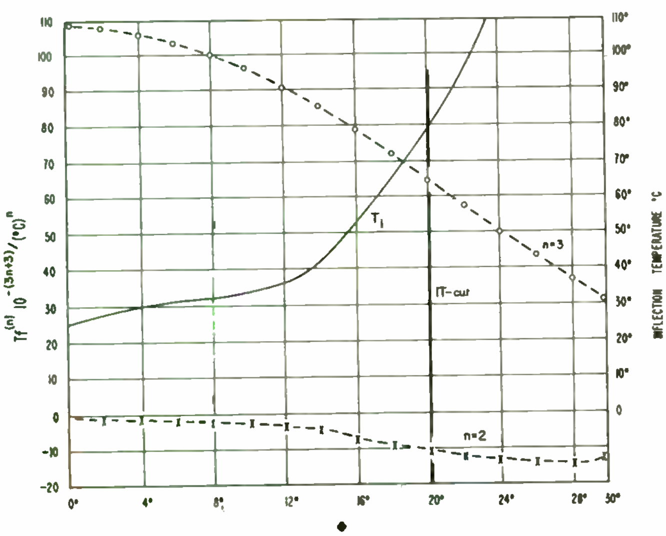

Fig. 5—Values for the second- and third-order temperature coefficients of frequency for the thickness mode C, positive angle Θ when $Tf^{(1)}=0$, and the inflection temperature T_i.

second-order temperature coefficient of frequency of $-6.5\cdot 10^{-9}/(°C)^2$, and a third-order temperature coefficient of $-2\cdot 10^{-12}/(°C)^3$ (see Table IV). This cut has been proposed for practical applications and designated the RT cut [22]. Other double-rotated cuts may be useful for application at low temperatures. For example, the C mode of the cut $\Phi=10°$, $\Theta=-33°$ shows a very small frequency change with temperature in the range $-160°$ to 0°C. The first-, second-, and third-order temperature coefficients of these cuts over this range compensate (see Table IV). An experimental frequency-temperature curve is shown in Fig. 6. The disadvantage of the double-rotated cuts is that all three modes are excitable, modes B and C being rather close together. The separation between these modes is in the order of 7 per cent for the RT cut and in the order of 10 per cent for the IT cut. The B mode displays a large negative second-order temperature coefficient of frequency for all zero temperature coefficient cuts, including the BT cut, which for practical purposes makes mode B less useful than mode C.

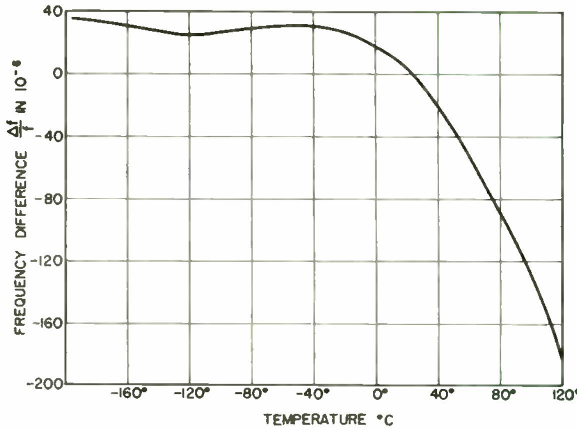

Fig. 6—Quartz cut ($yxwl$) 10°, $-33°$ having a small temperature dependence in the temperature range $-200°C$ to 0°C.

The inflection temperature T_i is defined by

$$\frac{\partial Tf}{\partial T}=\frac{\partial^2 f}{\partial T^2}=0. \tag{13}$$

The inflection temperature for the double-rotated plates of positive angles of Θ when the first-order temperature coefficient of frequency is zero is also shown in Fig. 5. The inflection temperature for the AT cut is about 25°C and is increased by increasing the angle Φ, reaching about 80°C for IT cut at an angle of $\Phi=20°$.

Applications to AT- and BT-Cut Quartz Crystals in an Extended Temperature Range

The temperature behavior of the so-called rotated Y cuts (yxl)Θ is shown in Figs. 7 and 8 which give the first-, second-, and third-order temperature coefficients, respectively, calculated from the values given in Table V using (9)–(11). The values for the rotated stiffnesses as function of the angle Θ are

$$c_{66}' = c_{44}\sin^2\Theta + c_{66}\cos^2\Theta + 2c_{14}\cos\Theta\sin\Theta. \tag{14}$$

The AT cut is described by the angle $\Theta=35°15'$, the BT cut by the angle $\Theta=-49°13'$. The AT cut belongs to mode C while the BT cut belongs to mode B. The jump from mode B to mode C occurs at the angle $\Theta=-23°50'$. This discontinuity is not apparent in (14) but follows from (4).

Considering the AT and BT cuts, a maximum and minimum for the frequency-temperature curve exists as function of the orientation angle Θ following from (7) and (8). The behavior of the maximum and minimum can be represented by a parabola having the parabola constant b_μ ($\mu=$ max or min) for the angle considered. The calculated and observed values for T_{max} and T_{min} vs the orientation angle Θ for the AT cut in the range $\Theta=35°$ to 41° and for the BT cut in the range $\Theta=-46°$ to $-52°$ are given in Figs. 9 and 10, respectively [14], [23]. The inflection temperatures for the AT and BT cuts, as function of the angle Θ, are also shown in Figs. 9 and 10.

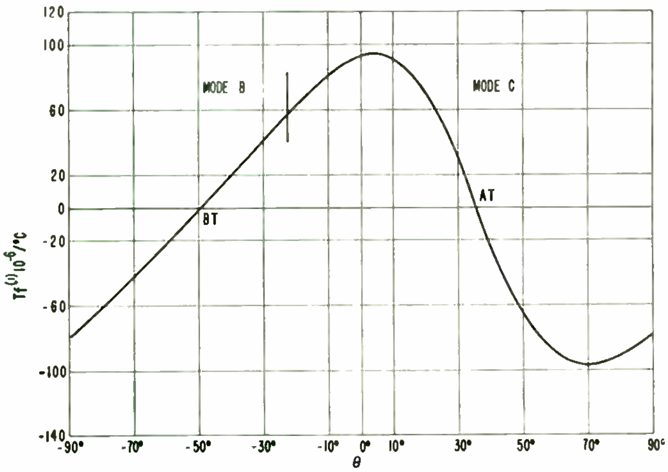

Fig. 7—First-order temperature coefficient of frequency for the plates $(yxl)\Theta$ vibrating in thickness modes as function of the angle Θ.

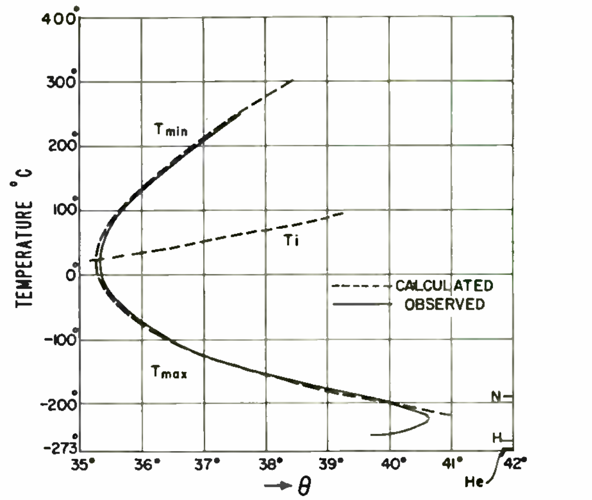

Fig. 9—Calculated and observed temperature of zero first-order temperature coefficient of frequency vs the orientation angle Θ for the AT cut.

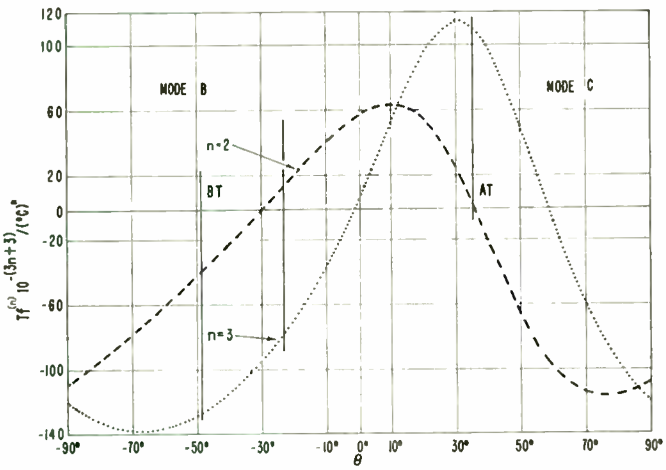

Fig. 8—Second- and third-order temperature coefficients of frequency for the plates $(yxl)\Theta$ vibrating in thickness modes as function of the angle Θ.

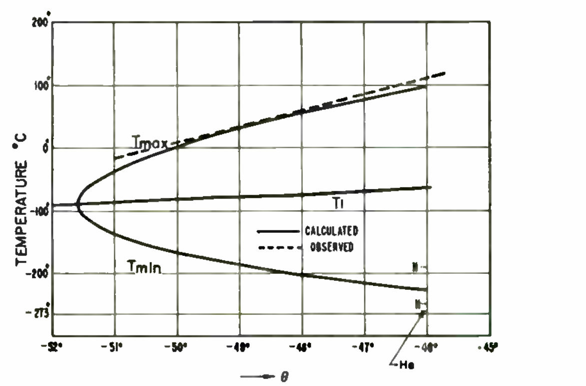

Fig. 10—Calculated and observed temperature of zero first-order temperature coefficient of frequency vs the orientation angle Θ for the BT cut.

Applications to Quartz Cuts Vibrating in Contour Modes

The frequencies and their temperature behavior are determined for contour modes of plates and extensional modes of bars by the elastic compliances and their temperature coefficients. Two cuts of interest exist for square plates which have one side parallel to and are rotated around the X axis at angle Θ, *i.e.*, cuts of the orientation $(yxl)\Theta$, where the first-order temperature coefficient of frequency is zero, the CT cut with an orientation angle of approximately $\Theta=38°$, and the DT cut with an angle of approximately $\Theta=-51°$. There are three types of these cuts:

1) Square plates with one side parallel to the X axis, $Y_{\Theta 0°}\equiv(yxl)\Theta$.
2) Square plates with the X axis diagonal,

$$Y_{\Theta 45°}\equiv(yxle)\Theta 45°.$$

Contour-extensional mode I of square plates [24]. (e = thickness of the plates.)

3) Circular plates $Y_{\Theta°}$.

The frequencies for these three modes are given by the equation

$$f=\frac{F}{2h}\sqrt{\frac{2}{\rho s_{55}'}} \tag{15}$$

where h is the length l of square plates or the diameter Φ of circular plates. The expressions for F for plates $Y_{\Theta 0°}$ and plates $Y_{\Theta 45°}$ can be found in [24], while for circular plates $Y_{\Theta°}$ no solution has been derived. However, the value obtained experimentally on circular quartz plates is $F=1.055\pm 1$ per cent.

The values for the rotated compliances as function of the angle Θ are

$$s_{55}'=s_{44}'=s_{44}\cos^2\Theta+s_{66}\sin^2\Theta-4s_{14}\cos\Theta\sin\Theta. \tag{16}$$

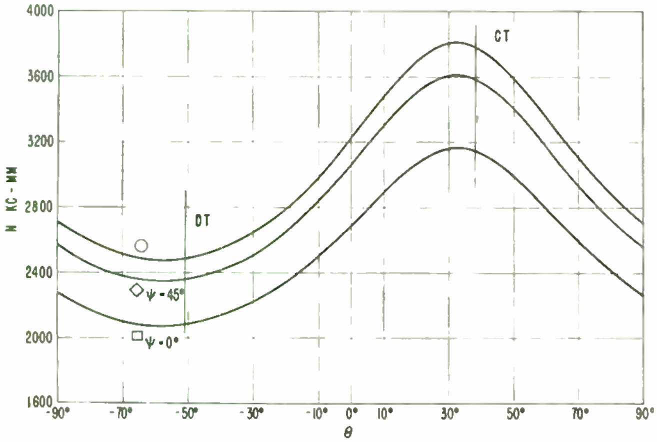

Fig. 11—Frequency constants N for the contour modes $F_{\Theta 0°}$, $F_{\Theta 45°}$, $F_{\Theta°}$ for plates $(yxl)\Theta$ as function of the angle Θ.

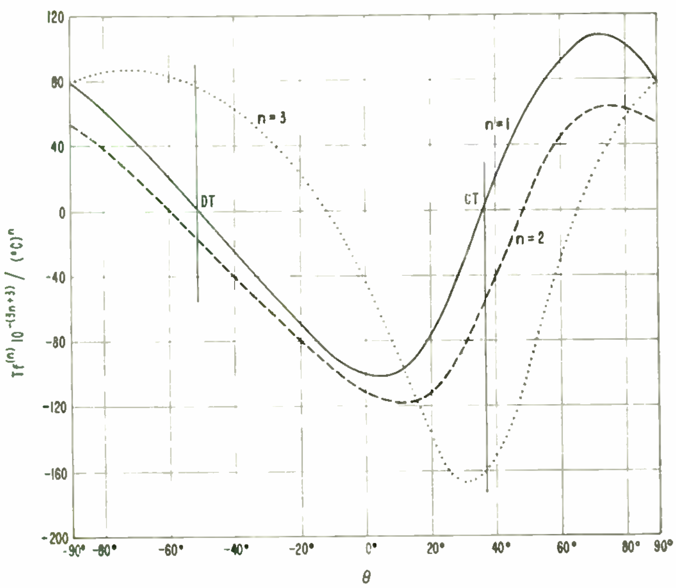

Fig. 12—First-, second-, and third-order temperature coefficients of frequency of the plates $(yxl)\Theta$ as function of the angle Θ vibrating in contour modes.

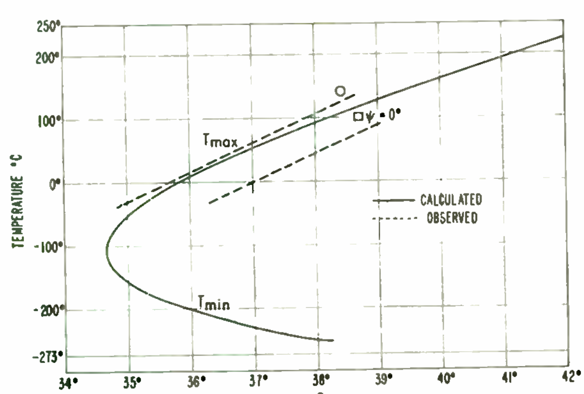

Fig. 13—Calculated and observed temperature of first-order zero temperature coefficient of frequency vs the orientation angle Θ for the CT cut.

Fig. 11 shows the frequency constants N in the range $\Theta = -90°$ to $+90°$ for the three modes $F_{\Theta 0°}$, $F_{\Theta 45°}$, and $F_{\Theta°}$. Fig. 12 gives the first-, second-, and third-order temperature coefficients of frequency calculated from the new values given in Table IX.

According to (15), the values for the temperature coefficients of frequency of the three modes are equal, as F is a constant determined by boundary conditions and therefore all three modes should have identical angles for their first-order zero temperature coefficients of frequency.

The calculated maximum and minimum for the frequency-temperature curve as a function of the orientation angle Θ is shown in Fig. 13 for the CT cut. In this curve the experimental values for $T_{\min}$, assumed to be linear in [25], are also presented by dashed lines. The theoretical and experimental values are in very good agreement.

Appendix

In order to determine the values for $Tc_{\lambda\mu}^{(n)}$, $Ts_{\lambda\mu}^{(n)}$ $(n=1, 2, 3)$, the following values for the material constants of alpha-quartz have been used in the course of this investigation:

1) Elastic stiffnesses $c_{\lambda\mu}$ of alpha-quartz are given in Table II. Elastic compliances $s_{\lambda\mu}$ of alpha-quartz are given in Table VIII.

2)
$$e_{11} = 0.171$$
$$e_{14} = 0.0403$$

Piezoelectric stress constants in C m^{-2} of alpha-quartz [6].

3)
$$\epsilon_{11}^{T} = \epsilon_{22}^{T} = 39.97 \qquad \epsilon_{11}^{S} - \epsilon_{11}^{T} = -0.76$$
$$\epsilon_{33}^{T} = 41.03 \qquad \epsilon_{33}^{S} - \epsilon_{33}^{T} = 0$$

Dielectric constants in 10^{-12} F m^{-1} of alpha-quartz.

4)
$$\alpha_{11}^{(1)} = \alpha_{22}^{(1)} = 13.71 \ 10^{-6}/°\text{C}$$
$$\alpha_{33}^{(1)} = 7.48$$
$$\alpha_{11}^{(2)} = \alpha_{22}^{(2)} = 6.5 \ 10^{-9}/(°\text{C})^2$$
$$\alpha_{33}^{(2)} = 2.9$$
$$\alpha_{11}^{(3)} = \alpha_{22}^{(3)} = -1.9 \ 10^{-12}/(°\text{C})^3$$
$$\alpha_{33}^{(3)} = -1.5.$$

Coefficients of thermal expansion of alpha-quartz.

5)
$$\rho = 2.65 \ 10^{3}\text{N m}^{-4}\text{s}^{2}$$
$$T\rho^{(1)} = -34.92 \ 10^{-6}/(°\text{C})$$
$$T\rho^{(2)} = -15.9 \ 10^{-9}/(°\text{C})^2$$
$$T\rho^{(3)} = 5.30 \ 10^{-12}/(°\text{C})^3.$$

Density and its temperature coefficients of alpha-quartz.

REFERENCES

[1] E. B. Christoffel, "Ueber die Fortpflanzung von Stössen durch elastische feste Körper," *Ann. di Matematica Milano*, vol. 8, pp. 193–243; 1877.

[2] I. Koga, "Thickness vibrations of piezoelectric oscillating crystals," *Physics*, vol. 3, pp. 70–80; August, 1932.

[3] R. Bechmann, "Über die Temperatur-Koeffizienten der Eigenschwingungen piezoelektrischer Quarzplatten und Stäbe," *Hochfrequenz. und Elektroak.*, vol. 44, pp. 145–160; November, 1934.

[4] J. Laval, "Élasticité des cristaux," *Compt. rend. Acad. Sci., (Paris)*, vol. 232, pp. 1947–1948; May 21, 1951.
——, "Sur l'élasticité du milieu cristallin, L'état solide," Congres Solvay, Stoops, Bruxelles, pp. 273–313; 1952.

[5] V. G. Zubov and M. M. Firsova, "On the measurement and new computation of the dynamic elastic constants of quartz," *Kristallografiya*, vol. 1, pp. 546–556; May, 1956. (In Russian.)

[6] R. Bechmann, "Elastic and piezoelectric constants of alpha-quartz," *Phys. Rev.*, vol. 110, pp. 1060–1061; June 1, 1958.

[7] R. D. Mindlin, Letter-type Rept., U. S. Signal Corps Contract DA 36-039 SC-87414; March 29, 1961. (Unpublished.)

[8] W. G. Cady, "Piezoelectricity," McGraw-Hill Book Co., New York, N. Y., London, England; 1946.
J. A. Schouten, "Tensor Analysis for Physicists," Clarendon Press, Oxford, England; 1951.
J. P. Musgrave, "The Propagation of Elastic Waves in Crystals and Other Anisotropic Media," *Repts. Progr. Phys.*, vol. 22, pp. 74–96, 1959, Physical Soc., London, England; 1959.

[9] K. Heegner, "Gekoppelte selbsterregte elektrische Kreise und Kristalloszillatoren," *Elektr. Nachrichtentech.*, vol. 15, pp. 359–368; December, 1938.

[10] "IRE standards on piezoelectric crystals, 1949," PROC. IRE, vol. 37, pp. 1378–1395; December, 1949.

[11] W. R. Ives, "A New Zero Temperature Coefficient Quartz Oscillator Plate," M.S. thesis, Colorado A & M College, Ft. Collins, Colo.; March, 1951.

[12] R. D. Mindlin and D. C. Gazis, "Strong Resonances of Rectangular AT-cut Quartz Plates," Rept., U. S. Signal Corps Contract DA 36-039 SC-87414; July, 1961.

[13] J. L. Saunders and D. L. Hammond, "Design and Development of Extended Temperature Range CR-(XA-21)/U Crystal Units," Wright Air Dev. Ctr., Wright Patterson AF Base, Ohio, Final Rept. AF 33(600)33889, September 16, 1956–June 26, 1959.

[14] R. Bechmann, "Frequency-temperature-angle characteristics of AT- and BT-type quartz oscillators in an extended temperature range," PROC. IRE, vol. 48, p. 1494; August, 1960.

[15] ——, "Influence of the order of overtone on the temperature coefficient of frequency of AT-type quartz resonators," PROC. IRE, vol. 43, pp. 1667–1668; November, 1955.

[16] W. P. Mason, "Zero temperature coefficient quartz-crystals for very high temperatures," *Bell Sys. Tech. J.*, vol. 30, pp. 366–380; April, 1951.

[17] I. Koga, M. Aruga and Y. Yoshinaka, "Theory of plane elastic waves in a piezoelectric crystalline medium and determination of elastic and piezoelectric constants of quartz," *Phys. Rev.*, vol. 109, pp. 1467–1473; March, 1958.

[18] W. P. Mason, "Low temperature coefficient quartz crystals," *Bell Sys. Tech. J.*, vol. 19, pp. 74–93; January, 1940.

[19] J. V. Atanasoff and P. J. Hart, "Dynamical determination of the elastic constants and their temperature coefficients for quartz," *Phys. Rev.*, vol. 59, pp. 85–96; January 1, 1941.

[20] R. Bechmann and S. Ayers, "The Shear Elastic Constants of Quartz and their Behaviour with Temperature," Post Office Res. Sta., Engrg. Dept. London, Dollis Hill, England, Res. Rept. No. 13524; December, 1951.

[21] E. Giebe and E. Blechschmidt, "Über Drillungsschwingungen von Quarzstäben und ihre Benützung für Frequenznormale," *Hochfrequenz. und Elektroak.*, vol. 56, pp. 65–87; March, 1940.

[22] R. Bechmann, "Thickness-shear mode quartz cut with small second- and third-order temperature coefficients of frequency (RT-cut)," PROC. IRE, vol. 49, p. 1454; September, 1961.

[23] P. A. Simpson, C. Barclay and F. P. Phelps, U. S. Patent No. 2,931,924; April 5, 1960.

[24] "IRE standards on piezoelectric crystals: determination of the elastic, piezoelectric, and dielectric constants—the electromechanical coupling factor, 1958," PROC. IRE, vol. 46, pp. 764–778; April, 1958.

[25] R. Bechmann, "Quarzoszillatoren und Resonatoren im Bereich von 50 bis 300 kHz.," *Hochfrequenz. und Elektroak.*, vol. 61, pp. 1–12; January, 1943.

Correspondence

Recombination Radiation Emitted by Gallium Arsenide*

When appropriately diffused GaAs diodes are biased in the forward direction they emit intense line radiation corresponding to gap transitions. Absolute measurements of the emitted radiation intensity indicate that at 77°K these diodes may be as high as 85 per cent efficient in the conversion of injected holes into photons of the gap energy. Data pertaining to the spectral distribution and speed of response of the emitted radiation is presented, and also the high conversion efficiency of the diode and its implications are discussed.

The diodes were fabricated from single-crystal *n*-type GaAs. A *p*-type layer was formed by diffusing in a sealed evacuated quartz tube zinc from a dilute solution of zinc in gallium. The wafers were lapped to 0.003 inch and diced. The die was then alloyed to a Au-Sn plated Mo tab [as shown in Fig. 1(a)] to form the base contact after which an InZn sphere was alloyed to the *p*-type layer in a position above the hole in the base tab to form the other ohmic contact. The diode was then etched to define a junction area of about 7.5×10^{-4} cm². The forward current-voltage characteristics of this diode at 298°K and 77°K are shown in Fig. 1. At 298°K the current varies as exp $(qV/2kT)$ up to about 0.1 a. At 77°K the current also varies as exp $(qV/2kT)$ between 10^{-3} and 3×10^{-2} a and below 10^{-10} a with an intermediate region in which it varies between exp $(qV/2kT)$ and exp $(qV/8kT)$.

Fig. 2 shows the relative intensity of the emitted photons as a function of photon energy. Two peaks in the radiation distribution are observed at room temperature. The photon energies at which the peaks occur agree approximately with those observed by Pankove,[1] but the relative intensities of the two peaks are diametrically opposed to those he reported. At room temperature our diodes emit an approximately equal number of photons in each line while at 77°K about 90 per cent of the emitted energy appears in the 1.44 ev band. From measurements of the absolute value of the emitted flux and its angular dependence, calculations which take into account the photon loss due to refraction and internal reflection at the GaAs surface indicate that at 300°K approximately 40 per cent of the holes injected at the *p-n* junction produce photons in the 1.33 ev band. A similar calculation based on the measurements at 77° would give 5 photons in the 1.44 ev band produced per injected hole. However, this result is in error because when the efficiency of producing 1.44 ev photons is close to unity, many photons which would normally not reach the measuring apparatus because of refraction and internal reflection are absorbed and re-emitted until they ultimately emerge from the crystal. By completely neglecting all refraction and internal reflection losses, a lower limit of 0.48 photon in the 1.44 ev band produced per injected hole can be established. On the other hand, if one as-

* Received May 25, 1962.

[1] J. I. Pankove and M. Massoulie, "Recombination Radiation in a Gallium Arsenide P-N Junction," The Electrochem. Soc., Electronics Div. (*Abstracts*), vol. 11, pp. 71–75, Spring Meeting, Los Angeles, Calif.; May 6–10, 1962.

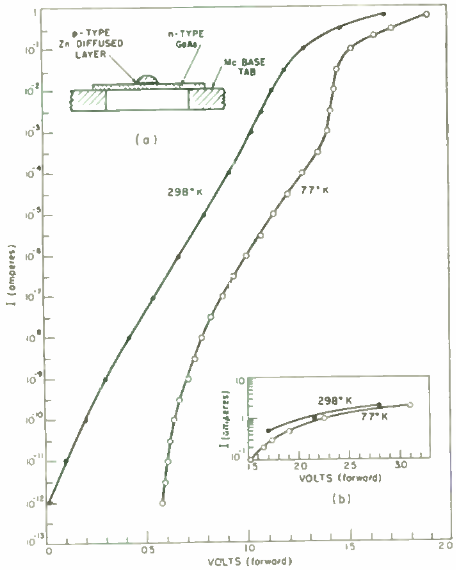

Fig. 1—Current-voltage characteristics for a zinc diffused GaAs diode. Pulse techniques were used for measurements above 10⁻¹ a; all other measurements were dc. Higher current measurements are shown in inset (b) and a cross section of diode structure is shown in inset (a).

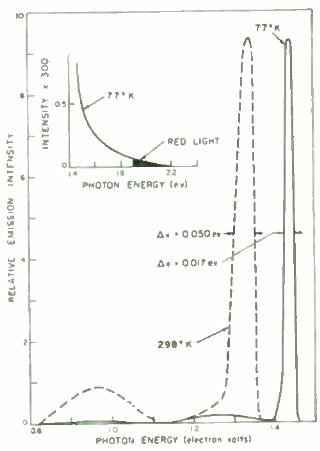

Fig. 2—Relative diode emission intensity as a function of photon energy at 298°K and 77°K. The emission intensity scale is relative and is not the same for both temperature plots. Inset shows the high energy tail at 77°K on an expanded scale.

sumes that the over-all quantum efficiency (photons per injected hole) is unity, one can determine from Fig. 2 that as an upper limit 0.85 photon in the 1.44 ev band are produced per injected hole.

Also shown in an inset in Fig. 2 is the high energy distribution of emitted photons. One sees that there is a small but finite tail which extends into the visible region of the spectrum. This is the source of the "red glow" reported by Mayburg and is quite visible at low temperatures. It is believed that this tail is due to recombination radiation of high energy electrons in the conduction band.

Measurements of emitted radiation at various injection currents above 30 a/cm² show that the radiation increases linearly with current up to current densities of 2.5 $\times 10^3$ a/cm² at which point the radiation tends to saturate with increased current density. When the injection was performed with a current pulse with a decay time of about 2 μsec it was found that the emitted radiation had the same decay time. Measurements of the switching time for similar diodes (2×10^{-9} sec) indicate that the emission can be modulated in excess of 100 mc.

The above results indicate that it may be possible to fabricate diodes in which for every injected hole a photon of energy close to the band-gap is emitted from the diode. If such diodes are possible, they will, when forward-biased, extract heat from the surroundings. This is because the holes that are injected are from the high energy tail of the Fermi distribution, and the full band-gap energy is not necessary to inject them into the n-region. The heat extracted per unit time will be

$$-\frac{dQ}{dt} = I\left(\frac{h\nu}{q} - V\right)$$

where V is the applied voltage in volts and $h\nu/q$ is the average photon energy also in volts. It is evident from the above equation and Fig. 1 that diodes in which each injected carrier produces a photon of energy close to the band-gap can act as refrigerators.

The authors express their thanks to Dr. R. H. Rediker for many helpful discussions and suggestions, to F. M. Sullivan for the diode fabrication, and to D. H. Bates for assistance in taking the measurements.

R. J. Keyes
T. M. Quist
Lincoln Laboratory[2]
Mass. Inst. Tech.
Lexington, Mass.

[2] Operated with support by the U. S. Army, Navy and Air Force.

Microwave Photomixing of Optical Maser Outputs with a *PIN*-Junction Photodiode*

This paper reports the possibility of using a PIN-junction photodiode as a mixer in an optical superheterodyne system employing microwave-modulated light. With such a diode, we have detected signals from UHF through X band produced by photomixing[1,2] between axial-mode components of ruby lasers. The observations were made by exposing the laser beam onto a silicon PIN photodiode, so that the photocurrent included signals corresponding to differences between the simultaneous, discrete optical frequencies in the laser output. These heterodyned signals are then detected with high signal-to-noise ratio.

The experimental setup is like that employed by McMurtry and Siegman,[2] with the photodiode replacing the microwave phototube. The photodiode is a point-contact PIN-junction type, the P region consisting of a GaAu dot ~10 mils diameter deposited on an epitaxial I region ~10 μ thick (fabricated by Prof. J. F. Gibbons of Stanford). Reverse breakdown voltage is >150 volts. The ceramic-diode cartridge was partly cut away and the diode inserted in the center conductor of a coaxial line, with a small hole in the outer conductor to admit the laser light. One end of the diode holder was connected to the receiving system via coaxial cables and tuners; the other end was connected to a movable short. A break in the outer conductor, insulated by a Mylar sheet, allowed a dc bias voltage to be applied across the diode. Receivers with 10 Mc/sec IF bandwidth were used in the frequency ranges from UHF through X-band. The laser light output was pointed directly at the junction from approximately one foot away, without focusing. Back-bias voltages were generally between 50 v and 100 v.

The top trace of Fig. 1 shows typical microwave photo-beats from the diode as detected with a superheterodyne receiver tuned to the fundamental frequency spacing between adjacent axial optical resonances in

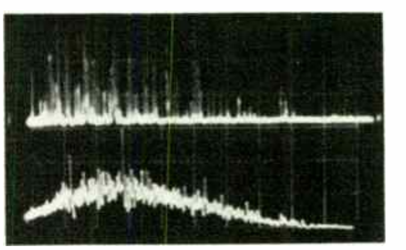

Fig. 1—Lower trace: photocurrent from PIN-junction photodiode with 50 v of back-biased voltage. Upper trace: simultaneous microwave output at 2135 Mc sec. Sweep speed: 50 μsec div. Sweep triggers at start of laser action.

the laser rod. The bottom trace shows the simultaneous spikes of photocurrent from the same diode. Observations like Fig. 1 have been made with several ruby rods of different lengths, at their fundamental frequencies and also at higher mode intervals. With a 122-mm long rod, we have detected beats at the first through sixteenth mode intervals, from 691 to 11,050 Mc/sec. A 39-mm long sapphire clad rod yielded beats up to the fifth mode interval, from 2135 to 10,675 Mc/sec. No outputs are observed except at these discrete frequencies.

The higher frequency outputs might possibly represent not higher mode intervals as claimed here, but rather harmonics of the fundamental frequency, generated by nonlinearities in the diode or receiver. To eliminate this possibility, we measured the harmonic generation in the photodiode itself,

* Received May 21, 1962; revised manuscript received June 11, 1962. This work was supported by the Signal Engineering Laboratories of the U. S. Army Signal Corps.

[1] A. T. Forrester, "Photoelectric mixing as a spectroscopic tool," *J. Opt. Soc. Am.*, vol. 51, pp. 253–259; March, 1961.

[2] B. J. McMurtry and A. E. Siegman, "Photomixing experiments with a ruby optical maser and a travelling-wave microwave phototube," *Appl. Optics*, vol. 1, pp. 51–53; January, 1962.

by inserting pulsed signals into the diode at the fundamental frequency and looking for harmonics. The conversion loss for harmonic generation was found to be large enough to eliminate this possibility.

In principle, the frequency at which the *PIN* photodiode can give substantial output is limited by the transit time through the intrinsic region of junction. For our diode, the expected value for the transit time is $\sim 10^{-10}$ sec, consistent with the experimental results presented here.

This method of optical heterodyning between simultaneous optical modes is a simple but powerful means for studying optical masers. The *PIN* photodiode serves as an optical-frequency mixer which is compact, simple, capable of fairly wide frequency range (when retuned at each frequency), and possessed of good infrared response. It requires, however, a separate amplifier or more sensitive receiver following it. By contrast, the microwave phototube offers the advantage of very wide instantaneous bandwidths ($>3:1$ in a single device), together with substantial internal amplification of the detected signal. For various reasons, the phototube may be more promising at higher beat frequencies, from 10 kMc/sec upwards.

These experiments were first stimulated by reports of Reisz's work[3] on similar diodes; we have more recently learned of similar work at frequencies up to 4200 Mc/sec by workers at the Philco Scientific Laboratories.[4]

H. Inaba†
A. E. Siegman
Stanford Electronics Labs.
Stanford University
Stanford, Calif.

[3] R. P. Riesz, "High-Speed Semiconductor Photodiodes," to be published.
[4] G. Lucovsky, M. E. Lasser, and R. B. Emmons, "Coherent Light Detection in Solid State Photodiodes," to be published.
† On leave of absence from Tohoku University, Sendai, Japan.

Silicon Field-Effect Transistor with Internal Epitaxial Channel*

Many techniques have been applied to the fabrication of field-effect devices since Shockley's detailed presentation of the principles.[1] These have included alloying, diffusion, etching, and mechanical cutting, for example.[2,3] But field-effect device channels must be regions of high sheet resistivity, typically about 4000 Ω/square, and with these techniques it is difficult to generate such layers reproducibly. Epitaxial techniques, however, have been able to meet the requirement in a highly satisfactory manner.

We have employed a *p*-type silicon substrate having two epitaxial layers. A high sheet resistivity *n* layer which will serve as a low pinch-off voltage channel is first deposited onto the *p*-type substrate. A surface *p* layer is then deposited by switching dopant during the growing process. Thus a *pnp* structure is grown continuously. All resistivities are made equal, about 0.5 Ω cm. Typical dimensions are given in Fig. 1(a).

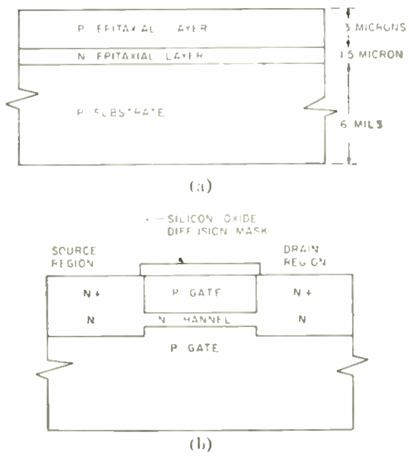

Fig. 1—(a) Epitaxial starting material. (b) Structure completed by means of single diffusion.

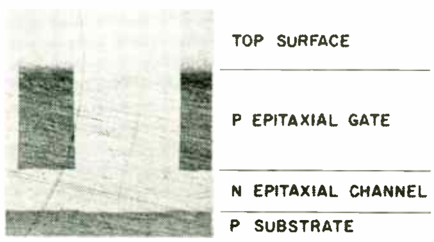

Fig. 2—Beveled and stained specimen showing final structure.

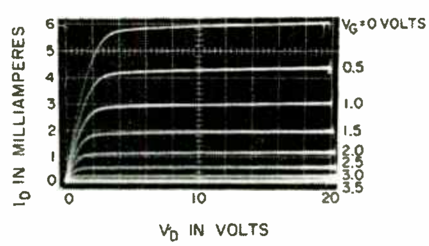

Fig. 3—Output characteristics of epitaxial field effect transistor.

A conventional photoresist procedure is used to produce an oxide diffusion mask forming a compact, convoluted pattern on the surface. A phosphorus diffusion then defines the channel and forms the source and drain contact regions, as shown in Fig. 1(b). This represents a section through any portion of the pattern mentioned above; note that vertical dimensions are exaggerated for clarity, just as they are exaggerated in the beveled and stained section, Fig. 2. Diffusion depth is very noncritical. The depth must merely exceed 3 microns, the thickness of the *p* layer, and make contact with the *n* layer. Overshooting by a few microns has a trifling effect on channel length, which is of the order of 60 microns. Hence this approach to field-effect device fabrication assigns the necessary lateral geometry control to the diffusion operation, which is easy with conventional masking techniques, and it assigns sheet resistivity control to the epitaxial process, which is well adapted to meeting this requirement.

Excellent devices have been made in a passivated planar configuration. In addition, unpassivated mesa devices have exhibited good characteristics and a high degree of electrical stability. The present devices are being assembled in the TO-5 package. Fig. 3 shows an example of the output characteristics.

The same structure principles of lateral geometry control by oxide masked diffusion and sheet resistivity control by epitaxial deposition will of course be applicable to field-effect transistors with *p*-type channels.

Contacts can be applied to either or both of the gates, as desired. By connecting the gates electrically to the source, one obtains an efficient current limiter.[3]

G. C. Onodera
W. J. Corrigan
R. M. Warner, Jr.
Motorola
Semiconductor Products Div.
Phoenix, Ariz.

* Received May 17, 1962.
[1] W. Shockley, "A unipolar 'field-effect' transistor," Proc. IRE, vol. 40, pp. 1365–1376; November, 1952.
[2] G. C. Dacey and I. M. Ross, "The field-effect transistor," *Bell Sys. Tech. J.*, vol. 34, pp. 1149–1189; November, 1955.
[3] R. M. Warner, Jr., W. H. Jackson, E. I. Doucette, and H. A. Stone, Jr., "A semiconductor current limiter," Proc. IRE, vol. 47, pp. 44–56; January, 1959.

Optical Harmonic Frequency Ratio Measurements*

Generation of optical harmonics with high intensity ruby masers has been reported by several workers.[1–3] Tentative reports[4] of discrepancies in the expected ratio of 2:1 between the harmonic and fundamental frequencies as well as the possibility of observing phonon effects have led to the high resolution study discussed below.

The harmonics were generated by focussing the output of a cooled pulsed-ruby source, estimated at several joules, onto a KDP crystal, at 45° to $X-Y$ axes and normal to the Z axis. Since as a result of thermal tuning,[5] the output wavelength of the ruby may be different on consecutive pulses, it was essential to make simultaneous observations on both the fundamental and second harmonic. In order to accomplish this, the light in the forward direction was

* Received May 29, 1962. Work supported in part by a grant from the U. S. Air Force, monitored by the Air Force Office of Scientific Research.
[1] P. A. Franklin, A. E. Hill, C. W. Peters and G. Weinreich, "Generation of optical harmonics," *Phys. Rev. Lett.*, vol. 7, pp. 118–119; August, 1961.
[2] J. Giordmaine, "Mixing of light beams in crystals," *Phys. Rev. Lett.*, vol. 8, pp. 19–20; January, 1962.
[3] P. D. Maker, R. W. Terhune, M. Nisenoff and C. M. Savage, "Effects of dispersion and focussing on the production of optical harmonics," *Phys. Rev. Lett.*, vol. 8, pp. 21–22; January, 1962.
[4] H. S. Boyne, private communication.
[5] I. D. Abella and H. Z. Cummins, "Thermal tuning of ruby optical maser," *J. Appl. Phys.*, vol. 32, pp. 1177–1178; June, 1961.

passed through a collimating system, incident on a direct-view prism, then refocused onto the slit of a 3.4-meter Jarrell-Ash Ebert Spectrograph with a resolving power of about 250,000 in the eighth-order red. The direct-view prism displaces the red and ultraviolet images along the length of the slit by several millimeters. This serves to separate the images on the film, thus preventing superposition and possible confusion. With this arrangement it was possible to obtain single-flash images on Kodak 103-O plates in the eighth-order red and sixteenth-order ultraviolet. The separation of images was further aided by dispersion of air which caused a sensible relative displacement of the ultraviolet image to shorter wavelength. The focused spots were carefully centered on the entrance slit by photographing them with a separate camera and making the necessary alignment of external optics.

The plates were measured with a traveling microscope comparator, and corrections due to dispersion of air were applied.[6] Near threshold the expected 2:1 frequency ratio was found to hold to within the instrumental uncertainty of about 1.5 ppm (0.043 cm^{-1} at the second harmonic). At higher intensities the harmonic line appeared to be displaced toward the blue by as much as 10 ppm. This apparent shift is consistent with the effects to be expected from thermal tuning[5] during single high-power pulses. As a result of heating, the ruby output shifts toward the red during the pulse, producing a smeared image on the film. The red power output rises rapidly to a maximum, then decays slowly in time. The second harmonic output, proportional to the square of the input power, is produced most efficiently at the early part of the pulse before appreciable tuning occurs. The result of this is that the center of gravity of the ultraviolet line is displaced from the center of gravity of the red line. This effect is further complicated by the differential response of the 103-O emulsion to red and ultraviolet. One concludes from the threshold observations that to within the experimental uncertainty of 1.5 ppm the expected 2:1 ratio obtains.[7] The apparent shifts observed with high power are believed to be purely instrumental for the reasons given.

Mention should be made of the occasional appearance of fine structure in the ultraviolet images, consistent with the operation of several longitudinal modes in the ruby source.[8] The structure was not, however, visible in the red image in this experiment. We believe that the apparent absence of these lines results from the poor red contrast and sensitivity of the emulsion used which gives rise instead to a broadened image.

Some estimates of linewidths were made although the arrangement was not best suited for this. In a few clear cases close to threshold the width of the second harmonic line was essentially twice the fundamental width of 0.1 cm^{-1}. Phonon effects in the ultraviolet generating crystal which could cause line broadening are quite weak, and none were observed here.

The author is indebted to Prof. C. H. Townes and H. S. Boyne for useful discussions, and to Prof. R. Novick for his critical reading of the text.

I. D. Abella
Columbia Radiation Lab.
Columbia University
New York, N. Y.

[6] B. Edlen, "Dispersion of standard air," *J. Opt. Soc. Am.*, vol. 43, pp. 339–344; May, 1953.
[7] Similar results were found by H. S. Boyne and W. C. Martin, *J. Opt. Soc. Am.* (to be published), and J. Giordmaine, private communication.
[8] I. D. Abella and C. H. Townes, "Mode characteristics and coherence in optical ruby masers," *Nature*, vol. 192, pp. 957–959; December, 1961.

Highly Sensitive Static Magnetic Field Detector*

A simple and high sensitive scheme has been developed for the detection and measurement of small static magnetic fields. The scheme utilizes the diamagnetic properties of superconductors. The detector consists of a tin gate lying on top of, and insulated from, a lead ground plane. While the devices tested consisted of thin, vapor-deposited films, no doubt this device would be constructed of foils. The device is cooled to a temperature sufficiently low to allow the lead and tin to become superconducting. The approximate geometry of a simple device is shown in Fig. 1(a). The cross section shown in Fig. 1(b) has been greatly exaggerated for clarity.

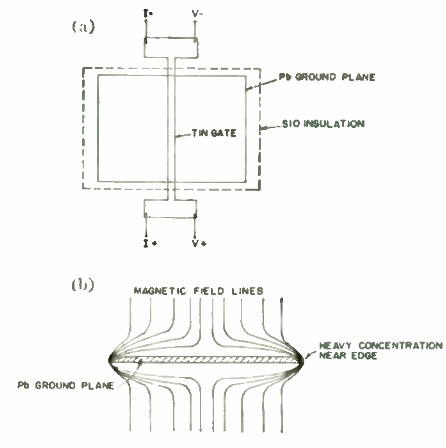

Fig. 1—(a) Geometry of a sample device. (b) Cross section showing concentration of flux lines.

The critical current of the tin gate is a marked function of the field applied to the sample. Fig. 2 shows a typical plot of the critical current of the tin as a function of angle, when the device is rotated in the stray field within a test dewar. The critical current varied from 205 ma to 8 ma. In some samples the magnification has been sufficient to produce an orientation in which the gate is held resistive.

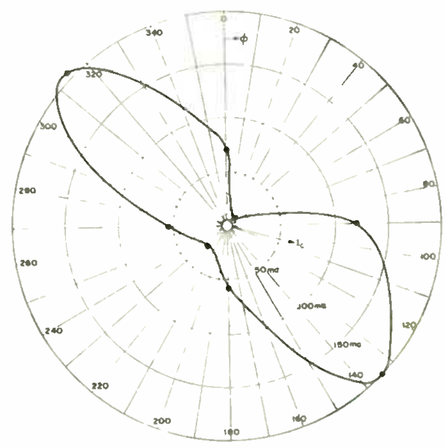

Fig. 2—Critical current of the tin gate vs angle in the dewar.

Operation of the detector can be understood by noting that the field in the vicinity of the edge of an ellipsoid is approximately given by[1]

$$H_e = H_a\left(1 + \frac{a}{b}\right)$$

where

$H_e = H$ at the edge of the ellipsoid
$H_a = H$ applied normal to the major axis of the ellipsoid
a — length of major axis
b — length of minor axis.

This equation is valid for $H_e < H_c$, the critical field of the ellipsoid.

For the sample shown in Fig. 1, $a = 1$ cm, $b = 5000$ Å, $a/b = 20{,}000$. If, for example, the component of earth's field normal to the sample is 0.001 oersted, the edge field will be about 20 oersted. It is precisely this magnification that caused the orientation sensitivity shown in Fig. 2. The symmetry is expected since the edge field and the field due to current in the tin gate add in quadrature.

A slight orientation sensitivity observed in open field cryotrons has been attributed to this effect.[2] Here the control acts as the magnifier. The device is also sensitive to initial orientation in the dewar. The field trapped when the ground plane becomes superconducting manifests itself as an edge field.

This device is extremely useful for detection of small static magnetic fields. When a "field free" region is produced using Helmholtz coils, this detector is superb for detecting the null field. The device can also be used to accurately detect and map anomalies in the earth's magnetic field. In order to measure the field, it is only necessary to provide a null field and then accurately calibrate critical current of the tin gate vs applied field.

David J. Dumin
Applied Electronics Labs.
Stanford University
Stanford, Calif.
formerly at
IBM Labs.
Yorktown Heights, N. Y

* Received June 5, 1962.
[1] See, for example, D. Shoenberg, "Superconductivity," Cambridge University Press, London, Eng.; pp. 164–171, 1952.

[2] A. Brenemann, private communication.

Light and Gravitation*

The frequency shift experienced by photons in falling through a gravitational field, as measured by Pound and Rebka,[1] can be explained in a simple and nonrelativistic way. If the effective weight of the photon is taken as $m=E/c^2=h\nu$, the energy gained in falling the distance l in the earth's field will be mgl and the momentum gained will be mgl/c. If m and c are the mass and velocity at the higher point, and m' and c' are the corresponding quantities at the lower point, then we have, from conservation of momentum, $m'c'=mc+mgl/c$, and from conservation of mass-energy, $m'c'^2=mc^2+mgl$. Solving these equations, we obtain $c'=c$ and $m'=m(1+gl/c^2)$. If λ and λ' are the wavelengths at the two points, and ν and ν' are the frequencies, we also have $\lambda'=\lambda(1-gl/c^2)$ and $\nu'=\nu(1+gl/c^2)$.

If we visualize a photon as consisting of a wave packet of length Δx containing N cycles, then $\Delta x=N\lambda$. From quantum mechanics the spatial extension of a wave packet is inversely proportional to its momentum. Hence $\Delta x'=N\lambda'$ with N, the number of cycles, remaining constant.

We now see rather clearly what happens to a photon as it gains energy in falling through a gravity field. The wave packet shrinks in both total length and wavelength, the velocity and number of cycles remaining constant. The decrease in wavelength at constant velocity accounts for the increase in frequency.

A further crucial test for any theory of light and gravitation is to predict the observed deflection of star images close to the sun during a solar eclipse.[2] In this case the photon is moving transverse to the direction of the gravity field; and if one calculates, as for example in Bohm,[3] the deflection of a photon, assuming it to be a particle of mass $m=E/c^2$ and velocity c, the resulting deflection will only be about half the observed value. However, the photon will have an extension in the direction of the field, and, as we have seen, the wavelength decreases in this direction. Thus the wavefronts of the photon will be tilted in the direction of the field, and this will cause a further deflection of the photon since it will follow the direction of its wavenormals. If this additional deflection is calculated, it turns out to be the missing half of the observed value.

Since we have seen that in the interaction of light and gravity the light velocity remains constant, it is tempting to revive an old idea, due originally to Faraday, that the gravity field is the medium for the propagation of electromagnetic radiation. Without inquiring into the question of how this comes about, let us make the assumption that the velocity of light is constant relative to the structure of a *local* gravity field and see how far this assumption will take us.

Planets, stars, galaxies, clusters of galaxies, all of the ascending hierarchy of assemblages of matter in the universe, possess local gravity fields. In gravitational terms, we may describe the universe in terms of relatively moving local gravity fields. We should then expect the phenomena of stellar aberration and Doppler shift to be explainable in terms of these relatively moving fields plus the assumption that the velocity of light is always equal to c relative to whatever local gravity field it is traversing.

Space in this communication does not permit a detailed description of how these accommodations take place, but it is possible to rough them in briefly. If we consider the Doppler shift from a moving stellar source, for example, we find the following. The star will have a local gravity field which is moving with respect to the galactic gravity field, for instance. Since the velocity of propagation must be the same in both fields, light originating on the star, on crossing the transition between the two fields, must have its wavelength increased or decreased depending on the relative motion of the two fields. If this light is finally observed on the earth, and the earth is moving with respect to the galactic field, another change in wavelength will occur on entering the earth's gravity field. The final wavelength observed will depend only on the relative motion of the star and earth.

In the case of stellar aberration we have to consider the behavior of a spherical wave crossing the boundary between two local gravity fields which are moving relative to each other in a direction at right angles to the direction of propagation. In this case a simple Huyghens construction will show that the pattern of waves in the second gravity field will be distorted in such a manner that the waves entering a telescope in the second field will be tilted and will appear to come from a source which is displaced from its true position by an amount depending on the relative motion of the two fields.

More interesting questions present themselves when we consider the rotating earth. To what extent does the structure of its gravity field that determines light velocity rotate with the earth? To determine this requires the measurement of an "ether drift" of 0.3 km/sec or less in temperate latitudes. The Michelson-Morley experiment and its later refinement by Joos,[1] in a 360° rotation of the apparatus, found no drift greater than about 1.0 km/sec, and it is clear that a precision of at least an order of magnitude better than this will be required to reach the actual rotational velocity. The Cedarholm-Townes ammonia maser experiment[5] which currently reports no drift greater than 0.015 km/sec is actually of no value in this measurement, because on rotation of the apparatus a considerable positive effect was observed which was ascribed to an unavoidable change in local magnetic conditions. The Michelson-Gale experiment[6] is consistent with the view that the earth rotates with respect to the propagation medium but since this experiment can be explained, though tortuously, by general relativity, a verification by a refined Michelson-Morley type of experiment is urgently desired. Techniques using microwaves and atomic frequency standards for the rotational experiment will be the subject of a future communication.

C. W. CARNAHAN
120 Fawn Lane
Menlo Park, Calif.

* Received December 28, 1961.

[1] R. V. Pound and G. A. Rebka, Jr., "Apparent weight of photons," *Phys. Rev. Lett.*, vol. 4, pp. 337–341; April 1, 1960.

[2] H. von Kluber, "The determination of Einstein's light-deflection in the gravitational field of the Sun," in "Vistas in Astronomy," Pergamon Press, New York, N. Y., vol. 3, pp. 47–77; 1960.

[3] D. Bohm, "Quantum Theory," Prentice-Hall, Inc., New York, N. Y., pp. 517–519; 1951.

[1] G. Joos, "Theoretical Physics," Hafner Publishing Co., New York, N. Y., 2nd ed., pp. 235–237; 1950.

[5] J. P. Cedarholm, G. F. Bland, B. L. Havens, and C. H. Townes, "New experimental test of special relativity," *Phys. Rev. Lett.*, vol. 1, p. 342; November, 1958.

[6] Joos, *op. cit.*, pp. 471–473.

Modes in Rectangular Guides Loaded with Magnetized Ferrite*

In previous works[1,2] the exact investigation of propagating modes of any order in a rectangular guide partially filled with a transversely magnetized lossless ferrite slab situated against one side wall has been carried out. The numerical calculations showed the existence of structures for which the first and second order modes have a unidirectional character.

Seidel and Fletcher published a paper[3] on an approximate solution of the same problem. They have considered the asymptotic case of vanishingly small waveguides. They found, besides the zero order ferrite-dielectric modes, three types of higher order modes, which they called FM (ferrite-metal), FAI (ferrite-air I) and FAII (ferrite-air II). The propagation constants of the FM and FAI modes are equal and opposite, and therefore from the Seidel and Fletcher analysis it appears that in the asymptotic case the structure cannot be unidirectional for modes of order higher than zero and for a certain range of the ferrite tensor permeability components.

This result seemed to be somehow in contrast with our numerical calculations since, although for guides of finite cross section, we found, for the same range of the ferrite tensor permeability components considered by Seidel and Fletcher, unidirectional higher order propagating modes.

We have therefore made the vanishingly small waveguide approximation in our characteristic equation [(11) of the above men-

* Received, February 5, 1962; revised manuscript received, February 23, 1962. The research reported in this document has been sponsored by the Electronics Research Directorate, AF Cambridge Res. Lab., AFRD (Air Research and Development Command) through its European Office, under Contract AF 61(052)-101.

[1] G. Barzilai and G. Gerosa, "Modes in rectangular guides filled with magnetized ferrite," *L'Onde électrique*, vol. 38, pp. 612–617, *Supplément Spécial, Congrès International Circuits et Antennes Hyperfréquences*, Paris; October 21–26, 1957.

[2] G. Barzilai and G. Gerosa, "Modes in rectangular guides partially filled with transversely magnetized ferrite," IRE TRANS. ON ANTENNAS AND PROPAGATION, vol. AP-7, special supplement, pp. S471–S474; December, 1959.

[3] H. Seidel and R. C. Fletcher, "Gyromagnetic modes in waveguide partially loaded with ferrite," *Bell Sys. Tech. J.*, vol. 38, pp. 1427–1456; November, 1959.

tioned work[1]] to see if the bidirectional character of the higher order modes was peculiar to the asymptotic structure. However, from our characteristic equation we obtained the FM and FAII modes, but we did not find the FAI set. Therefore the asymptotic analysis of our characteristic equation was consistent with our previously obtained results, since the lack of the FAI modes makes possible structures with unidirectional higher order modes even in the asymptotic case.

We have investigated the reasons for the discrepancy between our asymptotic analysis and the one carried out by Seidel and Fletcher, and we have found that the Seidel and Fletcher FAI modes are trivial solutions with zero amplitude. The arguments supporting this conclusion are reported below.

Apart from the asymptotic approximation, the method of attacking the problem we have used and the one used by Seidel and Fletcher differ for the expression of the e.m. field in the vacuum region. We have expressed such a field as a superposition of a TE wave and a TM wave, while Seidel and Fletcher used two waves, one of which has the tangential electric field parallel at the vacuum-ferrite interface to the tangential electric field of one mode in the ferrite region, and the other has the tangential magnetic field parallel to the tangential magnetic field of the other mode in the ferrite region.

If we introduce into Maxwell's equations for a vacuum region a wave solution of the following form:

$$\begin{Bmatrix} E \\ H \end{Bmatrix} = \begin{Bmatrix} \sqrt{\mu_0/\epsilon_0}\,\mathbf{e} \\ \boldsymbol{h} \end{Bmatrix} B \cdot \exp\left[j(k_x x + k_y y + k_z z)\right] \qquad (1)$$

(time dependence $\exp j\omega t$ is assumed), we obtain a system of six linear algebraic homogeneous equations in the six components $e_x, e_y, e_z, h_x, h_y, h_z$ of the two constant adimensional vectors $\mathbf{e}$ and $\boldsymbol{h}$. By setting equal to zero the determinant of the coefficients, we obtain (by normalizing the propagation constants with respect to $\omega\sqrt{\mu_0\epsilon_0}$):

$$k_x^2 + k_y^2 + k_z^2 = 1. \qquad (2)$$

If (2) is satisfied, by computing all the 5-order minors of the 6-order determinant, it is found that they are all equal to zero, while there are 4-order minors different from zero; therefore, the 6-order determinant of the coefficients becomes a 4-rank determinant. This means that from Maxwell's equations we obtain only four independent equations for the six field components.

We can obtain a solution with only one arbitrary amplitude by adding to four of the six Maxwell's equations a fifth linear homogeneous relation among the six field components. This fifth linear relation must of course be independent from Maxwell's equations.

If we separately pick up two different linear homogeneous relations we can obtain two different wave solutions having the same form (1). However in order to obtain two independent waves it is necessary that four of the six Maxwell's equations and the two different additional linear homogeneous conditions are altogether six independent conditions. This is so if the 8×6 matrix, obtained by adding to the six Maxwell's equations the two additional linear homogeneous conditions for the two waves, is a 6-rank matrix, *i.e.*, at least one 6-order minor is different from zero. If, on the contrary, the rank of the above mentioned 8×6 matrix is less than 6, the two waves obtained are not independent.

In our work[1] we have chosen for the two waves used to express the e.m. field in the vacuum region the following additional linear equations (x axis = longitudinal axis of the guide):

$$e_x = 0 \quad \text{(TE wave);} \qquad (3)$$

$$h_x = 0 \quad \text{(TM wave),} \qquad (4)$$

while Seidel and Fletcher chose

$$e_{zf1}e_x - e_{xf1}e_z = 0 \quad \text{(parallelism between the tangential electric fields);} \qquad (5)$$

$$h_{zf11}h_x - h_{xf11}h_z = 0 \quad \text{(parallelism between the tangential magnetic fields)} \qquad (6)$$

where the subscript f refers to the ferrite region.

Under conditions (3) and (4) the 6-order minors of the above mentioned 8×6 matrix are all equal to zero if

$$1 - k_x^2 = 0, \qquad (7)$$

while under (5) and (6) this happens if:

$$k_x e_{zf1}\left[(k_x - 1/k_x)h_{zf11} - k_z h_{xf11}\right] - k_z e_{xf1}\left[k_x h_{zf11} - (k_z - 1/k_z)h_{xf11}\right] = 0. \qquad (8)$$

Eqs. (7) and (8) represent, therefore, for the two different expressions of the e.m. field in the vacuum region, the no-independence condition for the two waves. It can be verified that if (7) is satisfied all components of the TE and the TM waves become proportional, reducing the two waves to TEM waves, and if (8) is satisfied all components of the two waves obtained under conditions (5) and (6) become proportional.

Consider now the boundary value problem considered by Seidel and Fletcher,[3] *i.e.*, a vacuum-ferrite interface. We can express the e.m. field in the vacuum and in the ferrite region as a superposition of two waves. If however we choose for the vacuum region two waves having all components proportional, it can be shown that the characteristic equation obtained from the boundary conditions is automatically satisfied, but the corresponding e.m. field is everywhere equal to zero.

Therefore the no-independence condition for the two waves used to express the e.m. field in the vacuum region always corresponds to a trivial solution for the boundary value problem considered by Seidel and Fletcher.[3] The same happens in the more complicated boundary value problem considered by us,[1] and in fact our characteristic equation also contains the trivial solution (7), which, however, we have neglected.

Under asymptotic approximation, condition (8) becomes:

$$k_x e_{zf1} - k_z e_{xf1} = 0 \qquad (9)$$

or

$$k_x h_{zf11} - k_z h_{xf11} = 0. \qquad (10)$$

Eq. (9) is identical to the characteristic equation for the FAI modes found by Seidel and Fletcher. Therefore the FAI modes are modes of zero amplitude and the relative characteristic equation is only the expression for the no-independence condition discussed above.

We note that if we compute the e.m. field corresponding to the characteristic equation for the FAI modes by using the asymptotic approximation we do not obtain zero, since the approximate expressions for the field components of the two waves in the vacuum region are not exactly proportional. This is perhaps the reason why Seidel and Fletcher, who started directly with the approximate expressions, did not realize that the FAI modes are solutions of zero amplitude.

From the preceding analysis it can be concluded that the FAI modes found by Seidel and Fletcher do not exist; therefore, even in the asymptotic case they have considered, undirectional higher order modes can be found.

The author wishes to express his thanks to Prof. G. Barzilai for encouragements and helpful suggestions and discussions in the course of this investigation.

GIORGIO GEROSA
Istituto di Elettronica dell' Università di Roma
Rome, Italy

Single-Sideband Suppressed-Carrier Modulation of Coherent Light Beams*

A method for producing single-sideband suppressed-carrier modulation at optical frequencies was recently devised and tested in our Laboratories with a coherent carrier obtained from a helium-neon gas laser. This type of modulation is of interest for improving signal-to-noise ratio and conserving bandwidth. It is also important in that it provides a solution to the problem of shifting the inherently fixed frequency of a laser beam to another frequency without introducing additional frequency components, thus making possible a variety of new communications and physics applications of the laser.

The principle of the modulator is that a rotating birefringent plate, or a system that simulates the action of such a plate, will act upon a circularly polarized light beam to produce a separable component shifted in frequency. The rotation is accomplished by the use of the Pockels electro-optic effect in a pair of potassium dihydrogen phosphate (KDP) crystals. This rotation can transform a left-circularly polarized light beam to produce a right-circularly polarized component at one of the modulation sideband frequencies. The displacement of this frequency is limited only to the maximum frequency at which the electro-optic effect can

* Received May 14, 1962; revised manuscript received May 21, 1962.

be produced, which has been shown to extend into the microwave range.[1]

A diagram of the single-sideband suppressed-carrier optical modulator (SSBSCOM), is shown in Fig. 1. Incoming light is passed through a combination of a plane polarizer and a quarter-wave birefringent plate that functions as a left-handed circular polarizer. This polarized light is passed through the two electro-optic crystals along their optic axes (or c directions) and then through a right-handed circular analyzer (the mirror image of the polarizer), which extracts the desired r.h. component and blocks the l.h. component. A modulating electric field is applied to each crystal in the c-axis direction by means of transparent electrodes. The effect of a rotating birefringent plate is obtained by having the b axes of the two crystals oriented 45 degrees apart, as shown, and applying the modulation voltages in phase quadrature. It can be shown that the output light consists of a l.h. component of one fixed amplitude and a r.h. component of a second fixed amplitude. The l.h. component rotates in synchronism with the input left-polarized light. However, the r.h. component executes one additional r.h. cycle of rotation during each modulation cycle, and therefore the frequency of this component is the sum of the input light frequency and the modulation frequency, *i.e.*, the upper sideband frequency.

The SSBSCOM has been tested at audio frequencies by using it to modulate light from a General Telephone & Electronics Laboratories gas laser. The crystals used were a pair of potassium dihydrogen phosphate bars 7 mm long and 10 mm square, with peak modulating voltages of about 2000 volts. The occurrence of SSBSC modulation was established by using the two-tone test that is employed for this same purpose at ordinary radio frequencies. Two modulating frequencies were applied, and the modulated light was detected with an RCA 7102 multiplier phototube. The modulation envelope was then displayed on an oscilloscope and examined for beat frequencies. Fig. 2 shows oscillograms obtained under four different conditions of operation. Tones of 1 and 1.5 kc were used, and the circuitry was arranged so that upper sideband output could be obtained for either tone alone [Figs. 2(a) and 2(b)] or for both tones together [Fig. 2(c)]; alternatively, upper sideband output could be obtained for one tone and lower sideband output for the other [Fig. 2(d)]. The upper traces are the waveforms of the voltage on the first crystal, the middle traces are the modulation envelopes, and the lower traces are base lines obtained with the light turned off. The envelopes of Figs. 2(a) and 2(b) are horizontal lines with a slight ripple at the modulation frequency, indicating extinction of the lower sideband and almost complete suppression of the carrier. The envelope of Fig. 2(c) displays the beat frequency of 0.5 kc between the two upper sideband frequencies. The envelope of Fig. 2(d) displays the beat frequency of 2.5 kc between the upper and lower sideband frequencies.

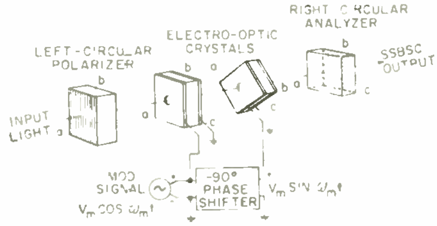

Fig. 1—Single-sideband suppressed-carrier optical modulator (SSBSCOM).

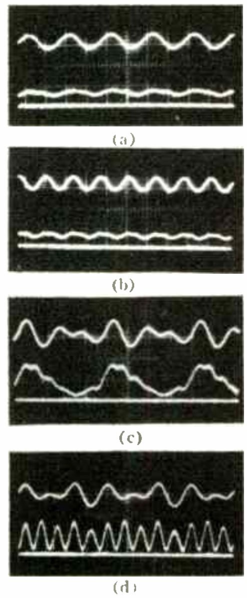

Fig. 2—Two-tone test of SSBSCOM. (a) 1-kc upper sideband output. (b) 1.5-kc upper sideband output. (c) 1-kc upper sideband output and 1.5-kc upper sideband output. (d) 1-kc upper sideband output and 1.5-kc lower sideband output.

Detailed mathematical analysis of the SSBSCOM reveals that the l.h. component at the output of the second crystal consists of a carrier of frequency f_c and a series of even-ordered double-sideband terms at frequencies $f_c + nf_m$, where f_m is the modulation frequency. The amplitudes of these l.h. frequency components are

$$L_n = \begin{cases} AJ_n(kV_m) & \text{(for } n \text{ even or zero)} \\ 0 & \text{(for } n \text{ add)} \end{cases} \tag{1}$$

where $k = 2\frac{1}{2}\pi n^3 r/\lambda$ n is the index of refraction, r is the appropriate electro-optic constant, λ is the light wavelength, A is the amplitude of the input light, V_m is the peak modulation voltage, and J_n are nth order Bessel functions of the first kind. All of these terms are eliminated by passing the light through the r.h. circular analyzer. The r.h. component at the output is a series of odd-ordered single-sideband terms at frequencies $f_c + nf_m$. The amplitudes of these terms are

$$R_n = \begin{cases} \sqrt{2}AJ_n(kV_m) \\ \quad \text{(for } n = n = +1, -3, +5, -7, \cdots) \\ 0 \text{ (for all other values of } n) \end{cases} \tag{2}$$

The modulation transfer characteristic is R_1, which is nearly linear for rV_m up to about $\pi/2$ radian. At this value the incident light power has been divided as follows: 51 per cent carrier (suppressed) 45 per cent upper sideband fundamental, 3.9 per cent double sideband second harmonic (suppressed), and 0.1 per cent lower sideband third harmonic.

The writers acknowledge with thanks the help given by Dr. E. M. Conwell in this work.

C. F. Buhrer
V. J. Fowler
L. R. Bloom
General Telephone & Electronics Labs., Inc.
Bayside, N. Y.

[1] I. P. Kaminow, "Microwave modulation of the electro-optic effect in KH_2PO_4," *Phys. Rev. Lett.*, vol. 6, p. 528; May 15, 1961.

Inductance from a Field-Effect Tetrode*

In their paper[1] on the field-effect tetrode Stone and Warner show that suitable biasing will cause this device to display transfer admittances of opposite sign and thus to behave as a gyrator. Of chief interest is the gyrator's ability to simulate inductances by inverting capacitive admittances. In practice attempts to find bias conditions which give a useable inductance combined with a high Q at a reasonable operating frequency usually prove abortive. It is suggested here that biasing the tetrode to produce negative self-admittance may well result in interesting combinations of these three parameters. The model, terminology and basic assumptions are similar to those of Stone and Warner.

The following criteria were applied to calculated results in order to determine which were of practical importance:

a) Results which involve working frequencies outside the range 1 kc to 100 Mc were rejected.
b) A range of 1 pf to 0.1 μf was imposed on both the load capacitance and the capacitance which would be needed to tune the inductance produced. (This is approximately the range for capacitors realizable by microminiature techniques used in the production of thin film circuits and solid circuits.)

The fact that negative self-admittance can be obtained for the field-effect tetrode suggests that it should be employed to cancel, or nearly cancel, real components of the input admittance of the gyrator-capacitor combination to yield inductance of very high Q. Two possible arrangements present themselves for this treatment.

First Quadrant, Case I where $y_{11} < 0$,
Third Quadrant, Case II where $y_{22} < 0$.

* Received April 24, 1962; revised manuscript received May 7, 1962.

[1] H. A. Stone and R. M. Warner, "The field-effect tetrode," Proc. IRE, vol. 49, pp. 1170–1184; July, 1961.

The load capacitor is assumed to be of infinite Q to keep the analysis simple, *i.e.*, $y_c = j\omega C$.

First Quadrant, Case I

The input admittance of the combination is given by

$$Y_{IN} = y_{11} - y_{12}y_{21}/y_{22} + y_c \qquad (1)$$

and the condition that the real part of Y_{IN} is zero, to give an infinite Q emerges as

$$\omega^2 C^2 = y_{22}(y_{12}y_{21} - y_{11}y_{22}). \qquad (2)$$

The imaginary part of Y_{IN} is

$$-1/j \frac{(y_{22}^2 + \omega^2 C^2)}{\omega C y_{12}y_{21}}. \qquad (3)$$

As $y_{12}y_{21} < 0$ this quantity is positive and equivalent to $1/j\omega L$, the admittance of an inductance L. For the condition imposed by (2) the product ωC is constant for any chosen G_1 so that the inductance is completely defined by

$$\frac{L}{C} = (y_{22}^2 + \omega^2 C^2)/\omega^2 C^2 y_{12}y_{21}. \qquad (4)$$

Choose bias conditions $V_1 = 1.2W_p$, $V_3 = W_p$ and $G_1 = 10^{-2}$ mho. These quantities determine the admittance parameters of the tetrode and hence fix ω^2C^2 and L/C for the combination. In Table I C_1 is the capacitance needed to tune the inductance produced. Results for $G_1 = 10^{-1}$ mho are also included.

TABLE I

	$C(pf)$	$f(Q=\infty)$	L	$C_1(pf)$
$G_1 = 10^{-2}$ mho	10^4	142 Kc	0.6 mh	2100
	10^3	1.42 Mc	60 μh	210
	10^2	14.2 Mc	6.0 μh	21
	10	142 Mc	0.6 μh	2.1
$G_1 = 10^{-1}$ mho	10^4	1.42 Mc	6.0 μh	2100
	10^3	14.2 Mc	0.6 μh	210
	10^2	142 Mc	60 mμh	21

The stability of the device under these bias conditions needs further investigation in applications to amplifiers, oscillators and mixers.

Third Quadrant, Case II

A similar analysis performed for this case with a choice of $V_1 = -W_p$, $V_3 = -1.2W_p$ and $G_1 = 10^{-2}$ mho allows Table II to be constructed.

TABLE II

$C(pf)$	$f(Q=\infty)$	L	$C_1(pf)$
10^4	422 kc	0.55 mh	260
10^3	4.22 Mc	55 μh	26
10^2	42.2 Mc	5.5 μh	2.6
10	422 Mc	0.55 μh	0.26

Thus it would seem that there is sufficient theoretical evidence to justify building some devices with small initial conductance and attempting to measure them while biased in this particular manner.

Gyrator Design

The limitations of pinch-off in both channels together with the requirements on initial conductance suggest the following design for a silicon gyrator.

A 5 Ω cm n-type channel should be combined with a 12 Ω cm p-type channel having a common channel thickness of 3 microns. The pinch-off voltage then becomes 14.5 v and the bias voltages suggested become 14.5 v and 17.5 v, respectively. A reverse bias of 3 v should not put the junction in danger of breakdown. For the n-type channel an initial conductance $G_1 = 2.5 \times 10^{-3}$ mho (400 Ω) would be obtained with an aspect ratio of 0.01 (see Fig. 1).

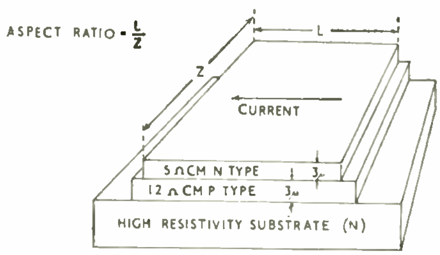

Fig. 1—Proposed construction for a gyrator.

Epitaxial techniques should be ideally suited for the fabrication of these otherwise delicate structures. The n-type floating substrate imposes no additional frequency limit as the capacitance of the junction it forms can be made small compared with that between the epitaxial layers.

The authors wish to thank the directors of the Plessey Company Ltd. for permission to publish this note and also the Ministry of Aviation for their support.

P. J. Etter
B. L. H. Wilson
The Plessey Company Ltd.
Caswell, Towchester
Northants, England

Generation and Radiation of Ultramicrowaves by Optical Mixing*

The presence of small nonlinearity in the dielectric constant of optically transparent materials has recently[1,2,3] been used for generation of harmonics and optical mixing of focused pulsed laser beams producing intense electric fields of the order of 10^5 volts/cm and above. The wavelength of the monochromatic light emitted by two lasers operating at different temperatures is separated a few angstroms apart with the frequency difference on the order of 500 to 2000 kMc. By using the nonlinearity of the medium it should be possible to generate this ultramicrowave beat frequency. The nonlinearity coefficient α in the dielectric constant expression $\epsilon = \bar{\epsilon}(1 + \alpha E)$ is usually quite small ($\sim 10^{-13}$ to 10^{-12} cm/volt) for optical harmonic mixing, but may be considerably larger for beat frequency generation, because ionic displacements play a larger role due to $f_1 - f_2$ being below the infrared absorption band of the material (between 3 to 10 teracycles/second for materials of interest).

The two input frequencies f_1 and f_2 (phase constants β_1, β_2, respectively) beating in the nonlinear dielectric medium cause a displacement current with phase constant $\beta_1 - \beta_2$ at the submillimeter beat frequency. This phase constant is, in general, different from the propagation constant

$$\left(\beta = \frac{\omega_1 - \omega_2}{c} \sqrt{\epsilon_{f_1 - f_2}}\right)$$

of waves at frequency $f_1 - f_2$. Due to the fact that the permittivity at ultramicrowaves is either larger or equal to that at optical wavelengths, *i.e.*, $\beta > \beta_1 - \beta_2$, radiation at submillimeter wavelengths from the displacement current at these frequencies is possible at an angle $\psi = \sin^{-1}(\beta_1 - \beta_2)/\beta$. In fact, the radiation pattern can be obtained from the theory of long-wire antennas,[4] and can be shown to have a polar coefficient of the form

$$\sin \theta \frac{\sin \left[\frac{\beta L}{2} (\sin \theta - \sin \psi)\right]}{\sin \theta - \sin \psi}.$$

Since a few centimeter lengths L of the medium provide a radiation path several hundred wavelengths long, extremely narrow radiated beams may be obtained at submillimeter frequencies (angular width of the major lobe $= (2\lambda/L)1/\cos \psi \sim 0.5$ to $1°$). The power level at the maximum of the first sidelobe at $\psi \pm (3\lambda/L)1/\cos \psi$ is about 13.5 db below the principal maximum, independently of the actual value of L/λ as long as it is large. Since the nonlinear medium used is by definition transparent to the optical frequencies, use can be made of the multiple reflections of the input signals from the two end boundaries. In other words, the medium can be so dimensioned ($\beta_1 L = n_1\pi$, $\beta_2 L = n_2\pi$; where n_1 and n_2 are integers) and strongly reflecting end boundaries are provided to create a high Q resonator at the two incoming wavelengths. Under these conditions, the electric field strength E_{opt} at optical wavelengths is increased by a factor $1/(1-R)^{1/2}$, where R is the power reflection coefficient of the end boundaries at optical wavelengths (assumed equal for the two end boundaries, without any loss of generality). Since the displacement current at submillimeter frequencies is proportional to $(E_{opt})^2$ and the radiated power is equal to (displacement current)$^2 \times$ radiation resistance R_r, an improvement of $1/(1-R)^2$ may be achieved in the radiated power by this means.

* Received June 8, 1962.

[1] P. A. Franken, *et al.*, "Generation of optical harmonics," *Phys. Rev. Lett.*, vol. 7, pp. 118; August, 1961.

[2] M. Bass, *et al.*, "Optical mixing," *Phys. Rev. Lett.*, vol. 8, pp. 18; January, 1962.

[3] J. A. Giordmaine, "Mixing of light beams in crystals," *Phys. Rev. Lett.*, vol. 8, pp. 19; January, 1962.

[4] S. A. Schelkunoff, "Electromagnetic Waves," D. Van Nostrand Co., Inc., New York, N. Y.; 1948.

The total radiated power is given by

$$P_0 = \frac{1}{(1-R)^2}\,\frac{\eta}{2\pi}\left(2(\omega_1-\omega_2)\bar{\epsilon}\alpha P_{in}\,\frac{\eta}{\sin\psi}\right)^2 \cdot \int_0^{\pi/2} G^2(\theta)\sin\theta\, d\theta$$

where η is the characteristic impedance of the medium at frequency $f_1 - f_2$, $\bar{\epsilon}$ the permittivity of the medium and $G(\theta)$ the polar coefficient of radiation for the above arrangement of multiple reflections.

$$G(\theta) = \sin\theta\left[\frac{\sin\left(\frac{\beta L}{2}(\sin\psi - \sin\theta)\right)}{\sin\psi - \sin\theta} + \frac{\sin\left(\frac{\beta L}{2}(\sin\psi + \sin\theta)\right)}{\sin\psi + \sin\theta}\right]$$

The dimensions of the medium are assumed much larger than the wavelength $\lambda = 2\pi/\beta$ to neglect the induction field in the field expressions. In order to form an idea of the order of magnitude involved, let us assume the following parameters:

$f_1 - f_2 = 10^{12}$ c/s
$P_{in} = 6$ Kw (3 Joule, $\frac{1}{2}$ msec. pulse)
$\alpha = 10^{-10}$ cm/volt
$R = 0.99$
$R_r = 200$ ohms.

The radiated power P_0 is calculated to be 45 mw. The value of α at these frequencies is not known at present and may be somewhat lower than the value assumed. The above presented scheme of nonlinear mixing provides a simultaneous generator and highly directional radiator at ultramicrowaves. The edge boundaries of the medium are shaped so as to allow the radiation out of the system.

The author is grateful to Dr. S. K. Ghandhi for his interest and encouragement during the course of this work.

OM P. GANDHI
Philco Scientific Laboratory
Blue Bell, Pa.

Tunnel Diode Loaded by a Shorted Transmission Line*

Nagumo and Shimura[1] have made a thorough analysis of the tunnel diode loaded by a shorted transmission line. Unfortunately, some readers may have trouble following this worthy paper in one place due to an equation that appears to have suffered a misprint and in other places due to apparent errors in some of the figures.

Since $\Delta t = T = 2l/v$, the next to last equation in column one of page 1287 should read

* Received September 18, 1961.

[1] J. Nagumo and M. Shimura, "Self-oscillation in a transmission line with a tunnel diode," PROC. IRE, vol. 49, pp. 1281–1291; August, 1961.

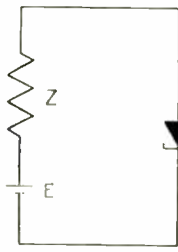

Fig. A—The equivalent circuit.

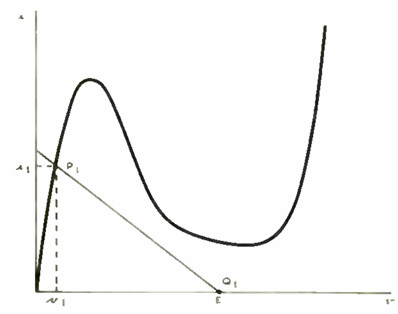

Fig. B—Determination of the first operation point, P_1.

$$\Delta t = T = 2l\sqrt{LC}.$$

The following equation is correct as it stands indicating that this error is only an unfortunate misprint.

More serious is the confusion created by some of the figures, of which Fig. 21 is a good example. In order to see that the path indicated is incorrect, let us repeat the analysis in more physical terms than used by Nagumo and Shimura. Consider, as an initial condition, that the transmission line in Fig. 1 is completely discharged. Then an equivalent circuit is that shown in Fig. A, where Z is purely resistive since the line is assumed lossless. The resulting operation point P_1 can be determined by drawing a load line corresponding to Z and E on the characteristic curve of the tunnel diode as shown in Fig. B. (The problem of bistability has been side-stepped for the time being by choosing a monostable load line for the first example.)

Operation at P_1 is obtained by impressing a negative voltage $(v_1 - E)$ and a positive current (i_1) on the line. These polarities are consistent with a wave traveling away from the diode. When this wave reaches the shorted end of the line, it is reflected with inverted voltage and travels back to the diode. Now, in general, there will be a reflection at the diode, and a third wave will travel down the line toward the short. This third wave is determined by the fact that the sum of the three waves must be consistent in voltage and current with the characteristic of the diode. Considering at first only the first two waves plus E, the combined voltage will be E, and the combined current will be $i_1 + (i_1 - 0) = 2i_1$. In addition to this there will be the voltage and current of the third wave which have the ratio $-Z$. The second operating point P_2 can then be found by drawing a second load line through point Q_2 as shown in Fig. C. Now, as before, the third wave, having a positive voltage $(v_2 - E)$ and

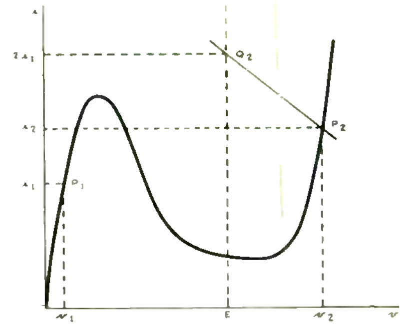

Fig. C—Determination of the second operation point, P_2.

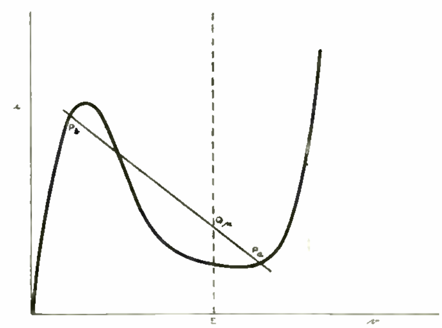

Fig. D—A load line showing bistability.

a negative current $(i_2 - 2i_1)$, will be reflected at the shorted end of the line, reversing its voltage to become a fourth wave, and the fourth wave is reflected at the diode creating a fifth wave. The third operating point P_3 can be found by drawing a third load line through the point Q_3 whose coordinates are $v = E$, $i = i_2 + (i_2 - 2i_1) = 2i_2 - 2i_1$. The process may be continued indefinitely to trace the action of the circuit through as many cycles as may be desired.

Before taking up the question of bistability, let us compare the results so far with those of Nagumo and Shimura. We find that we have drawn a set of load lines Q_nP_n having slopes $-1/Z$ in the v, i plane and with all the points Q_n lying on the line $v = E$. We can also draw in connectives P_nQ_{n+1} having slopes $+1/Z$, in which case we find that $Q_nP_nQ_{n+1}$ always forms a half diamond. If we take the trouble to normalize the variables in the manner of Nagumo and Shimura, we find that in the ξ, η plane the above lines have slopes of ± 1 (45°) and the points Q_n all lie on the η axis in agreement with Nagumo and Shimura.

Now consider a point Q_n and load line as shown in Fig. D. Do we take P_a or P_b to be P_n? So far we have considered the tunnel diode to be an ideal diode having no capacitance. Let us be more realistic and consider that there is a capacitance but that it is too small to make the rise times appreciable. Now if Q_n lies above the diode characteristic, as shown, the sum of the $2n-2$ waves considered thus far have more current flowing toward the diode than at that instant (before the reflection) is taken by the diode. The difference must flow into the capacitance, raising the voltage, and the circuit moves to point P_a. If Q_n had been below the diode

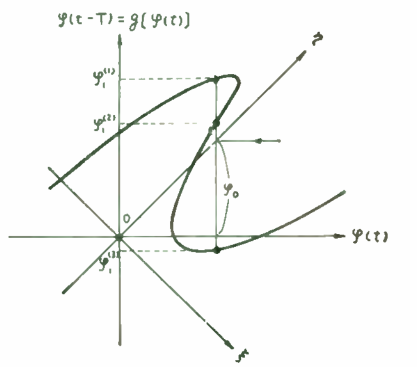

Fig. 1—The three roots of the equation $G(\Phi, \phi_0, 0) = 0$ are $\Phi = \phi_1^{(1)}$, $\phi_1^{(2)}$ and $\phi_1^{(3)}$.

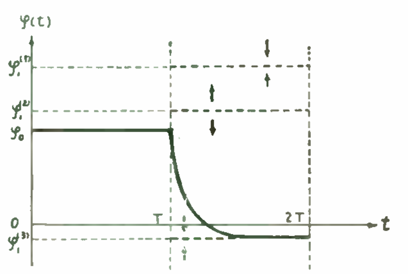

Fig. 2—$\phi(t+T)$ for $0 \leq t \leq T$ approaches to $\phi_1^{(1)}$ if $\phi_0 > \phi_1^{(2)}$, and to $\phi_1^{(3)}$ if $\phi_0 < \phi_1^{(3)}$.

characteristic, the circuit would have had to move in the direction of lower voltage coming to a point such as P_b. Thus the (geometric) reflection (of the construction lines) at Q_n is to the right if Q_n lies above the diode characteristic and to the left if Q_n is below the diode characteristic. Examining Fig. 21 we find that the reflection is incorrect at the next to bottom such point. Similar mistakes can be found in several other figures.

MALCOLM H. STEWARD
Westwood Division
Houston Fearless Corp.
Los Angeles, Calif.

Authors' Comment[2]

The first point which is indicated by Steward is apparently our careless mistake. The next to last equation in column one of page 1287 should read

$$\Delta t = T = 2l\sqrt{LC}$$

as pointed out by Steward.

Concerning the second point, which is more serious, Steward's conclusion seems to be incorrect. The reason is as follows.

Let us consider the differential-difference equation (38) in the case where the function g is triple valued. Let the three roots of the equation of Φ

$$G(\Phi, \phi_0, 0) = 0$$

[2] Received October 9, 1961.

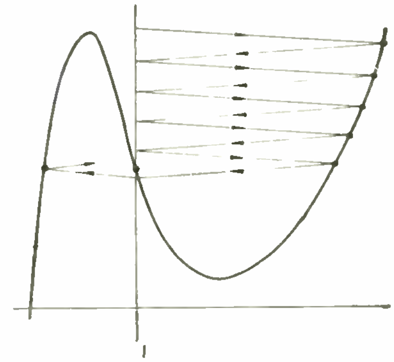

Fig. 3—If Steward's conclusion is correct, the operating points ought to behave as shown in this figure.

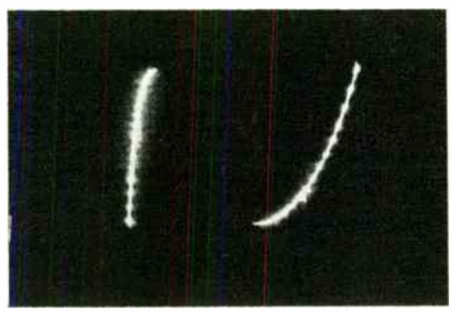

(a)

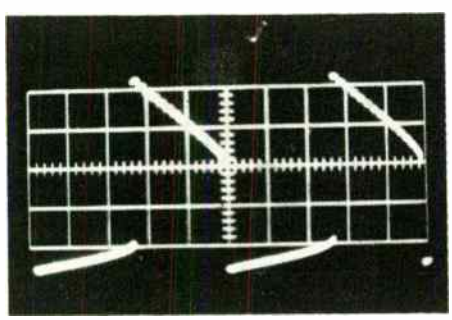

(b)

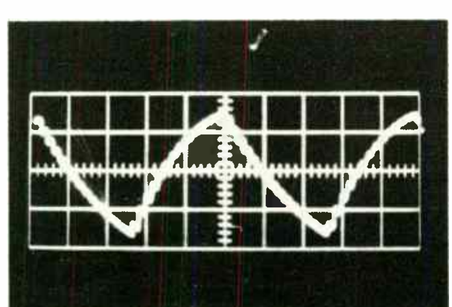

(c)

Fig. 4—The case $m=16$, $n=15$. $Z=1$ kΩ, $T/2=100$ μsec, $E=0.14$ volt. (a) The V-I characteristic. (b) The voltage waveform. 0.05 volt/division (vertical), 1.2 msec/division (horizontal). (c) The current waveform. 1m amp/division (vertical), 1.2 msec/division (horizontal).

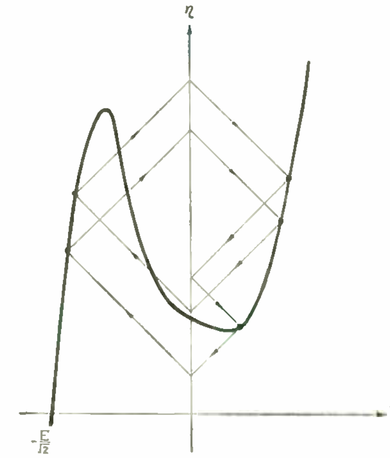

Fig. 5—Fig. 21 must be replaced by this figure.

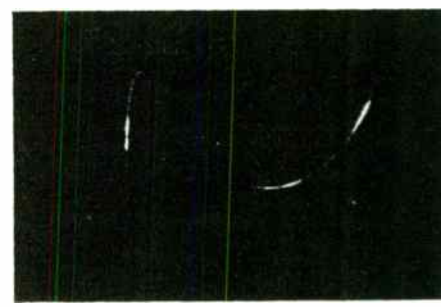

(a)

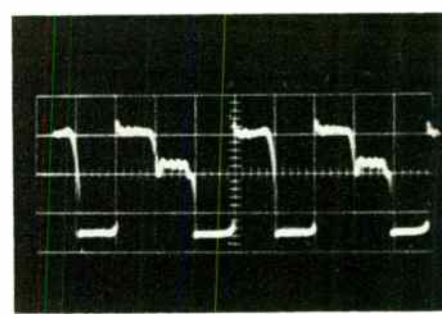

(b)

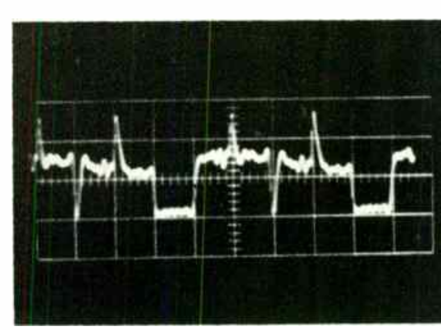

(c)

Fig. 6—The case $m=2$, $n=3$ [$(1:1) \rightleftarrows (1:2)$] $Z=220$ Ω, $T/2=450$ μsec, $E=0.28$ volt. (a) The V-I characteristic. (b) The voltage waveform. 0.1 volt/division (vertical), 900 μsec/division (horizontal). (c) The current waveform. 2m amp/division (vertical), 900 μsec/division (horizontal).

be $\Phi=\phi_1^{(1)}$, $\phi_1^{(2)}$ and $\phi_1^{(3)}$ $(\phi_1^{(1)}>\phi_1^{(2)}>\phi_1^{(3)})$, where ϕ_0 is a constant (see Fig. 1).

If the initial condition of the differential-difference equation (38) is assumed as

$$\phi_0(t) = \phi_0\text{: constant} \qquad \text{for } 0 \leq t \leq T,$$

(38) reduces to a differential equation of the first order:

$$C_0 \frac{d\phi(t+T)}{dt} = G(\phi(t+T), \phi_0, 0) \qquad \text{for } 0 \leq t \leq T. \quad \text{(a)}$$

Since $G(\phi_1^{(i)}, \phi_0, 0)=0$ for $i=1$, 2 and 3, this differential equation has three constant solutions:

$$\phi(t+T) = \phi_1^{(1)}, \phi_1^{(2)}, \phi_1^{(3)}, \quad \text{for } 0 \leq t \leq T.$$

From the fact that $G(\Phi, \phi_0, 0)<0$ for $\Phi>\phi_1^{(1)}$, $\phi_1^{(2)}>\Phi>\phi_1^{(3)}$ and $G(\Phi, \phi_0, 0)>0$ for $\phi_1^{(1)}>\Phi>\phi_1^{(2)}$, $\Phi<\phi_1^{(3)}$, we know that the solutions $\phi_1^{(1)}$ and $\phi_1^{(3)}$ are stable, while $\phi_1^{(2)}$ is unstable. Therefore, we can conclude that the solution of (a), $\phi(t+T)$ for $0\leq t\leq T$, approaches to $\phi_0^{(1)}$ if $\phi_0>\phi_1^{(2)}$, and to $\phi_1^{(3)}$ if $\phi_0<\phi_1^{(2)}$. It is easily seen that this conclusion is equivalent to Steward's (see Fig. 2).

It must be pointed out, however, that this conclusion is based on the assumption that "$\phi_0(t)$ is constant for $0\leq t\leq T$," which is implicitly assumed in Steward's physical discussion too. If $\phi_0(t)$ is not constant for $0\leq t\leq T$, the above-mentioned conclusion does not necessarily hold. Even if the initial condition is assumed to be constant for the first period, we cannot make such an assumption for the next period because of the parallel capacitance C_0 of the tunnel diode. The effect of the term $C_0(d\phi(t)/dt)$ in (38) cannot easily be estimated as done in Steward's discussion.

To make this situation definite, let us consider the case where Z is large. If Steward's conclusion is assumed to be correct, the operating points ought to behave as shown in Fig. 3, which is obviously not true, as Fig. 4 of our experimental result shows.

However, Fig. 21 is our mistake by itself and we must replace it by Fig. 5 below. An experimental result which corresponds to it it shown in Fig. 6.

J. Nagumo
M. Shimura
Dept. of Applied Physics
Faculty of Engineering
University of Tokyo
Tokyo, Japan

Mr. Steward's Reply[3]

In reply to the authors' comment I must maintain that my conclusions are not incorrect for the case assumed, which was that there is no capacitance across the tunnel diode. My wording was, ". . . there is a capacitance but that it is too small to make the rise times appreciable." In other words, the concept of capacitance was introduced only to the point of determining the choice between P_a and P_b. It was still to be considered that the voltages and currents were step functions. Nagumo and Shimura seem to alternately agree and disagree with my conclusions. The reason for that is that they are not always clear as to whether capacitance is being neglected or not, and the presence of capacitance in non-negligible amounts can make impressive differences in the results.

In their original paper (4) implicitly states that capacitance is to be neglected, and nothing in the text changes this assumption until the beginning of Section VI. All figures up to and including Fig. 29 are presumed by the reader to be based on the assumption of no capacitance, and on the basis of this assumption, many of them, including the revision shown in Fig. 5 of their comment, are incorrect. Toward the end of their comment, the authors reveal the cause of the confusion. Without ever stating the amount of capacitance involved, they have been drawing their figures so as to agree as far as possible with experimental results. The large number of discrepancies obtained indicate the strong effects of practical amounts of capacitance.

In Section VI of their original paper the authors state the equations governing the case in which capacitance is considered, but do not explain the effects of this capacitance on the results. I must confess I had not given this much thought either, until I read their comment. In order to get a qualitative feel for the importance of practical amounts of capacitance, let us study Fig. E below.

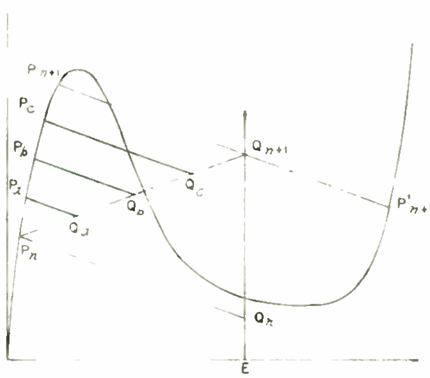

Fig. E—A moving loadline as when rise time is non-negligible.

Suppose we have arrived at P_n, and the next wave coming toward the diode takes us to Q_{n+1}. If the rise time of this wave is negligible, the next operation point must be P_{n+1}'. However, if, as a result of smoothing introduced in previous periods, the rise time is appreciable, we may think of the voltage and current applied to the diode as moving gradually from P_n through Q_a, Q_b, and Q_c to Q_{n+1}. During this time the diode capacitance will be charged by the difference between the diode and line currents. If the applied voltage and current jumped from P_n to Q_a and then stopped, the effect of the charging would be to move the operating point from Q_a along the road line Q_aP_a toward P_a. It can therefore be seen that the actual operation point will follow some curve from P_n to a point on Q_aP_a, to a point on Q_bP_b, to a point on Q_cP_c, to, finally, either P_{n+1} or P_{n+1}'. If the capacitance charges rapidly enough, compared to the rise time of the applied wave, to keep the operating point under the diode characteristic, the end point will be P_{n+1}. If not, the changing current will reverse part way through the process, and the end point will be P_{n+1}'. The motion of the operating point away from P_nQ_{n+1} generates a new wave on the transmission line traveling away from the diode to continue the process of oscillation. The rise time of this wave will correspond to the charging time of the diode capacitance.

If, as assumed above, the charging time is similar to the rise time (of the applied wave, not the new wave), it appears that the operation point will stay on the same branch of the diode characteristic until this is no longer possible because of passing the peak point or the valley point. Since both times are determined by the same capacitance, it appears that this might be a common condition and explains most of the figures shown by Nagumo and Shimura. On the other hand, if the inductance in series with the diode becomes appreciable, the result could be the other way around again. The situation can obviously get quite complicated. If a prediction of circuit performance is required, the best approach is to add the effect of inductance to (34) and (35) and then solve using the actual circuit values. These equations become

$$i(l,t) = f\left(E + v(l,t) - L\frac{\partial i(l,t)}{\partial t}\right) + C_0\frac{\partial v(l,t)}{\partial t}$$

$$\phi_1\left(t-\frac{T}{2}\right) + \phi_1\left(t+\frac{T}{2}\right) = Zf\left(E + \phi_1\left(t-\frac{T}{2}\right) - \phi_1\left(t+\frac{T}{2}\right) - L\phi_1'\left(t-\frac{T}{2}\right) - L\phi_1'\left(t+\frac{T}{2}\right)\right) + ZC_0\phi_1'\left(t-\frac{T}{2}\right) - ZC_0\phi_1'\left(t+\frac{T}{2}\right).$$

In conclusion, it appears that the figures shown by Nagumo and Shimura are probably correct in real life, but not for the simplified case assumed in most of their paper. In spite of this, their paper is very enlightening and draws many interesting conclusions of practical importance.

Authors' Reply[4]

In case the reactance of the tunnel diode is completely neglected, the circuit behavior is governed by and only by the difference equation (18) and the stability condition (25). If there exist many solutions which satisfy (18) and (25), therefore, it is impossible to decide which one of them is actually chosen to occur.

Nevertheless, only one circuit behavior is observed in actual fact. To give a theoretical explanation of this fact, it is necessary to consider the reactance of the tunnel diode. As the first step toward the attempt, we considered the parallel capacitance of the tunnel diode. We thus obtained the differen-

[3] Received December 4, 1961.

[4] Received January 8, 1962.

tial-difference equation (38) and defined the stability condition mentioned in our paper (Section VI). To our regret, we can not give complete discussion on this problem now.

Many figures displayed in our paper are drawn to show solutions of the difference equation (18) satisfying the stability condition (25), which coincide with our experimental results. It is expected, however, that the occurrence of these solutions displayed in our paper will be theoretically confirmed when the full treatment of the differential-difference equation (38) is accomplished.

Furthermore, it will be necessary in some cases to consider not only the parallel capacitance but also the series inductance of the tunnel diode, as pointed out by Steward.

Eventually, Steward's conclusion mentioned in his Reply does not seem to be in discord with our opinion. We express sincere thanks to Steward for his valuable discussions.

J. Nagumo
M. Shimura

A Total-Reflection Solid-State Optical-Maser Resonator*

Various schemes for solid-state optical maser oscillators have been proposed and are being tested in a number of laboratories.[1–6] Initially only pulsed operation was possible. More recently, attempts to set up continuously operating solid-state optical masers using special pumping techniques and cooling have been successful.[7,8]

In this communication a novel resonator and output coupling configuration for an optical maser is described. This configuration differs from others in current use in that it uses total internal reflection to reflect the light beam and frustrated total reflection for output coupling.

One possible configuration of the total reflection resonator is shown in Fig. 1. As the figure shows, the adjacent end walls of the resonator are at right angles to each other. If the resonator is placed in an optically rarer medium such that the ratio of the refractive indexes of the resonator medium and the external medium is greater than $\sqrt{2}$, a light beam in a direction parallel to the side walls will be totally reflected from the end walls and confined within the crystal. This eliminates the need for dissipative metallic or multilayer dielectric coatings. Power is abstracted from the resonator through frustrated total reflection, that is, by coupling to the rapidly decaying fields in the optically rarer medium associated with the phenomenon of internal reflection. This can be achieved by placing the hypotenuse of a right-angle prism parallel to and in close proximity of one of the totally reflecting end walls. The arrangement is shown schematically in Fig. 2. Frustrated total reflection will occur if the refractive indexes of the coupling prism and the coupling medium (relative to that of the resonator medium) are properly chosen. (It is readily found that for frustrated total reflection to occur, $n_2 < n_1 \sin \alpha_1 < n_3$, where n_1, n_2 and n_3 are the refractive indexes of the resonator, coupling medium and coupling prism, respectively, and α_1 is the angle of incidence.) The amount transmitted power depends on the angle of incidence α_1, on the ratio of the refractive indices n_2 and n_3 of the couping medium and the coupling prism, respectively, to the refractive index n_1 of the resonator, and on the thickness d of the coupling layer. It should be clear that the medium of the coupling layer need not be the same as the medium surrounding the other reflecting surfaces of the resonator.

Fig. 1—The total reflection optical-maser resonator.

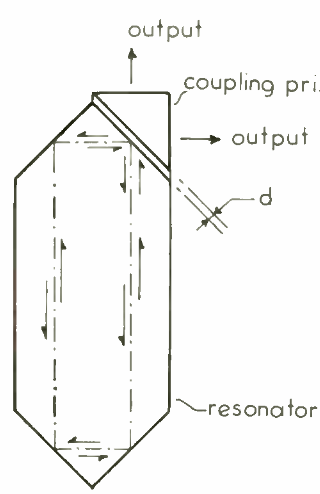

Fig. 2—The total reflection optical-maser resonator with coupling prism.

The threshold requirements for optical-maser oscillation are determined by the requirement that the amplification by stimulated emission be sufficient to compensate for the losses.[9] Thus, both the threshold concentration of active atoms in the host crystal and the pumping power required to maintain the threshold number of excited atoms are determined primarily by the losses. These consist of the scattering by the inhomogeneities in the rod material, the end-wall absorption, diffraction and scattering losses, and the useful output. In the total reflection resonator the end-wall losses are substantially eliminated. As a result the threshold pumping power is reduced and the available output is increased.

Another, perhaps more important, aspect of the reduced losses lies in the lower threshold concentration of active atoms. Since the light quanta emitted either by spontaneous or induced emission are necessarily smaller than the input pumping quanta, a substantial fraction of the pumping power is dissipated as heat within the host material. This dissipated heat is proportional to the concentration of active atoms. A lower concentration will thus result in a lower heat dissipation so that continuous operation without elaborate cooling and pumping techniques becomes feasible.

The total-reflection resonator exhibits another interesting property. All the other optical-maser resonator cavities use either metallic or multi-layer dielectric coating of the end walls to normally reflect the light beam. As a result a definite phase relationship exists between the two contradirectionally traveling wave systems. No such relationship is established by the boundary conditions existing in the total reflection resonator. It would therefore appear that this configuration can support two mutually independent contradirectionally traveling resonant wave systems. The only process that might couple these two wave systems is the emission process. It would therefore be of interest to determine if any correlation exists between these wave systems. Since power from the two contradirectionally traveling wave systems can be brought out separately from the two different faces of the coupling prism such an experiment can be readily performed.

L. Bergstein
W. Kahn
Polytechnic Institute of Brooklyn,
Brooklyn, N. Y.
C. Shulman
Polytechnic Institute of Brooklyn, and
The School of Technology,
The City University
New York, N. Y.

* Received June 22, 1962. The work reported herein was sponsored by the U. S. Army Signal Research and Development Labs., Office of Naval Research and the Air Force Office of Scientific Research, under Contract No. AF-18 (600)-1505.

[1] A. L. Schawlow and C. H. Townes, "Infrared and optical masers," *Phys. Rev.*, vol. 112, pp. 1940–1949; December, 1958.

[2] T. H. Maiman, "Stimulated optical radiation in ruby," *Nature*, vol. 187, pp. 493–484; August, 1960.

[3] R. J. Collins, D. F. Nelson, A. L. Schawlow, W. Bond, C. G. B. Garret, and W. Kaiser, "Coherence, narrowing, directionality, and relaxation oscillations in the light emission from ruby," *Phys. Rev. Lett.*, vol. 5, pp. 303–305; October, 1960.

[4] G. E. Devlin, J. McKenna, A. D. May, and A. L. Schawlow, "Composite rod optical masers," *Appl. Optics*, vol. 1, pp. 11–15; January, 1962.

[5] L. F. Johnson, G. D. Boyd, and K. Nassau, "Optical maser characteristics of Tm^{+3} in $CaWO_4$," Proc. IRE (*Correspondence*), vol. 50, pp. 86–87; January, 1962.

[6] L. F. Johnson, G. D. Boyd, and K. Nassau, "Optical maser characteristics of Ho^{+3} in $CaWO_4$," Proc. IRE (*Correspondence*), vol. 50, pp. 87–88; January, 1962.

[7] L. F. Johnson, G. D. Boyd, K. Nassau, and R. R. Soden, "Continuous operation of the $CaWO_4:Nd^{+3}$ optical maser," Proc. IRE (*Correspondence*), vol. 50, p. 213; February, 1962.

[8] D. F. Nelson and W. S. Boyle, "A continuously operating ruby optical maser," *Appl. Optics*, vol. 1, pp. 181–183; March, 1962.

[9] A. L. Schawlow, "Optical and infrared masers," *Solid State J.*, vol. 2, pp. 21–29; June, 1961.

Current-Voltage Characteristic of Tunnel Junctions*

Tunneling through thin insulating films, discovered some thirty years ago, has been studied extensively in connection with tunnel diodes.[1] Recently, it has been pointed out[2] that, in addition to tunneling, there are other modes of electron transport through thin films. We have been studying symmetrical current-voltage characteristics of metal-insulator-metal junctions, of the type illustrated in Fig. 1, which was made with an Al-Al_2O_3-Cu junction at room temperature and atmospheric pressure. The natural oxide coating of commercial Al foil was used in this case, but similar characteristics are observed with thicker oxide films formed by anodizing. The slope at the origin is that of a 1330-ohm resistor, and an empirical formula $I=(V+0.625V^3)/1330$ represents the curve, apart from the "hysteresis."

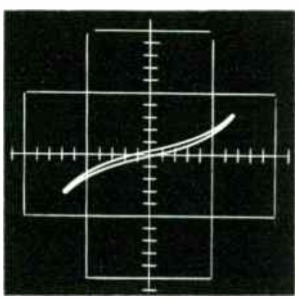

Fig. 1—Current voltage characteristic of metal-insulator metal tunneling. Maximum current, 1.59 ma, maximum voltage, 1.15; slope at origin indicates 1330 ohms; frequency, 10 kc.

There is no known theory for the hysteresis displayed. It is not attributable to capacitance in the usual sense, as shown by varying the frequency of the applied alternating voltage. We have observed curves enclosing more area, and curves with less are common. Open loops, with less included area, have been observed at 0.05 cps by Handy,[3] who formed junctions by air oxidation of evaporated Al films, on which various other metals were subsequently deposited by evaporation. No theory has been proposed to account for the hysteresis.

Our junctions are quite unstable, being formed by pressing the oxide-coated foil lightly against a flattened wire of Cu, Al or Au.

By tapping the support, an initially open junction is brought into the tunneling mode; an open or a short circuit may occur suddenly by further jarring or apparently spontaneously.

We are attempting to form more stable structures, to distinguish between different modes of transport, and to investigate the observed hysteresis.

H. P. Knauss
R. A. Breslow
Department of Physics
The University of Connecticut
Storrs, Conn.

* Received June 11, 1962. This work was supported in part by a grant from the Research Corporation.

[1] N. Holonyak, Jr., and I. A. Lesk, "Gallium arsenide tunnel diodes," Proc. IRE, vol. 48, pp. 1405–1409; August, 1960.

[2] P. R. Emtage and W. Tantraporn, "Schottky emission through thin insulating films," *Phys. Rev. Lett.*, vol. 8, pp. 267–268; April 1, 1962.

[3] Robert M. Handy, "Electrode effects on aluminum oxide tunnel junctions," *Phys. Rev.*, vol. 126, p. 1968; June, 1962. The authors are also indebted to Dr. Handy for a copy of his Ph.D. dissertation, Northwestern University, Evanston, Ill., 1961, unpublished.

A High-Speed Point Contact Photodiode*

Proposed optical communication systems require photodetectors capable of broad-band operation to frequencies in excess of 10^9 cps. A germanium formed point contact photodetector[1] that responds to the beat frequencies of the He-Ne gas maser up to 900 Mc has been constructed. The device should be capable of operation at frequencies up to 50 Gc.

This germanium photodetector was constructed using a P^+ body with an epitaxially grown π layer. The π layer is approximately 8 microns thick. A 2-mil diameter mesa was chemically etched. 0.6-mil arsenic doped gold foil was pointed and brought into contact with the π region in the center of the mesa. A short-current pulse was used to alloy the point material into the π layer. The alloyed region is approximately 4 microns in diameter and penetrates the π layer to a depth of 4 to 5 microns. The diode structure is shown in an expanded scale in Fig. 1.

Light is incident at the side of the π region as indicated in Fig. 1. The V-I characteristics of a typical diode are indicated in Fig. 2.

The operation of this type of photodetector was discussed by Gaertner.[2] The device is basically a PIN structure. With reverse bias the depletion layer of the junctions (P-I and I-N) spread out to occupy the entire I or in our case π region. This π region becomes a region of high and nearly constant electric field. Photons of sufficient energy to excite hole-electron pairs are incident on the π region. The generated carriers move with terminal velocity across the swept π region and are collected at the P^+ and N^+ regions. Since the carrier lifetimes in the P^+ and alloyed N region or N^+ region are quite small, typically 10^{-10} sec or less, these collected charges recombine quickly. The terminal velocity in the π region is approximately 10^7 cm/sec under a reverse bias condition of 3 volts or more.

An estimate of the ultimate performance can be obtained. The active π region (Fig. 1) is about 4 microns thick. With the terminal velocity of 10^7 cm/sec, photon excited carriers will transit this region in times less than 4×10^{-11} sec. The capacity can be estimated by considering the device as a parallel plate condenser. With a π layer of 4-micron thickness and a 4-micron diameter point region, the capacity is 4.5×10^{-3} pf (ϵ for germanium is 1.42×10^{-10} farad/m). The measured series resistance of a typical diode is about 10 ohms. The RC cutoff frequency will be on the order of 10^{13} cps. The transit time will thus limit the frequency response of the detected output to the 25- to 50-Gc region.

Tests were conducted with this diode mounted without encapsulation across the coaxial structure shown in Fig. 3. The output of the HE-NE gas maser at a wavelength of 1.153 microns was focused through the small hole in the side of the coaxial structure onto the π region in the vicinity of the point. A reverse bias of 3 to 4 volts was used. Both short-circuit and open-circuit tuning stubs

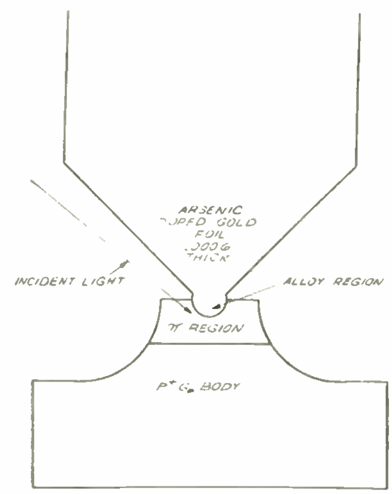

Fig. 1—Point contact photodiode structure.

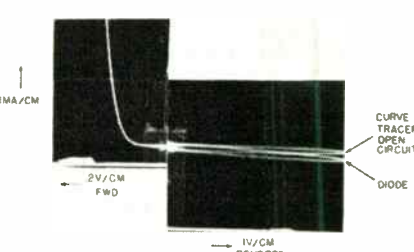

Fig. 2—Photodiode I-V characteristics.

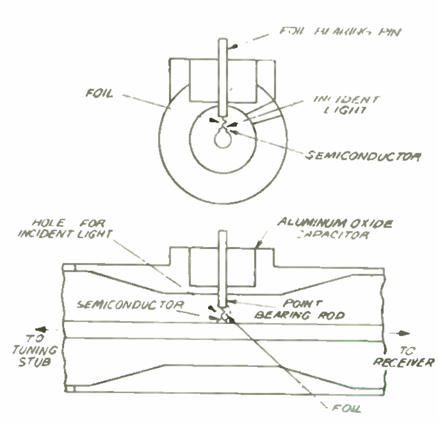

Fig. 3—Coaxial photodiode mount.

* Received June 15, 1962.

[1] R. P. Riesz of the Bell Telephone Labs. has submitted a report for publication to the *Journal of Applied Physics* detailing the construction and operations of a P-I-N junction photodetector.

[2] W. W. Gaertner, *Phys. Rev.*, vol. 116, no. 84, 1959.

were placed on one coaxial terminal. The second terminal was connected to a conventional microwave receiver consisting of a tuned preselector and a single diode mixer followed by a 30-Mc IF amplifier.

The several modes present in the maser output were mixed in the diode to produce RF beat frequencies at 117 Mc. Beat frequencies as high as 936 Mc were detected. The output level of the 117-Mc beat frequency with proper adjustment of the RF tuning stub was comparable with that obtained from a 7102 photomultiplier. This high speed photomultiplier has a cathode response peaked near 8500 Å.

The author wishes to express his thanks to A. Kuper who supplied the germanium and to acknowledge the helpful discussion with R. P. Riesz of the Bell Telephone Laboratories.

L. U. Kibler
Bell Telephone Labs., Inc.
Holmdel, N. J.

A Method for Calibration of Laser Energy Output*

The development of pulsed high power ruby lasers has been hampered by the lack of accurate power level measurements. A calorimetric method has been reported on.[1] The following is a description of a method for calibrating the energy output of a laser; this method is especially applicable at low energy output, *i.e.*, near threshold.

The laser energy output is calibrated by attenuating the laser beam with neutral filters, directing it into a phototube (with S-1 spectral response), and integrating the current produced. This charge is directly dependent on the number of light quanta, and therefore the light energy.

The filters are calibrated by dividing the laser beam in two using a semireflective mirror (Fig. 1). The two beams are directed into separate phototube sensors. A dual-beam oscilloscope displays both signals; the display is then photographed, the camera shutter being appropriately synchronized with the firing of the laser. A series of photographs is taken, with various attenuating filters in one of the paths of the laser beam. The two displays are equalized by adjusting the oscilloscope preamplifier gains [Fig. 2(a)]. The ratio of these gains is then compared to the ratio obtained with no filters in the beams [Fig. 2(b)]. The resultant is the attenuation of each neutral filter. The filters are thus calibrated with a laser beam at the color at which they are to be used.

The laser beam is allowed to enter one phototube with intensity peaks yielding more than 200 μa while the reflected beam is attenuated to less than 10 μa. The output signals have the same complex shape, indicating linearity of phototube and associated circuitry.

Fig. 2(c) indicates the output of the laser beam beyond the mirror. The detailed waveforms of each pulse appear different. Investigations indicate that this is due to the fact that each pulse is differently polarized. The beam-splitting mirror favors certain polarizations for transmission and reflection. In order to achieve identical signals in both channels, it was found necessary to remove this polarization effect. By inserting a polarizing filter[2] after the laser, linearly polarized light is available to the mirror. The ratio of intensities of the two beams is determined by subtracting the signals in a differential amplifier. By varying the angle of the polaroid and mirror, the ratio of intensity of the split signals is adjusted, the difference signal being nulled out. Apparently the polarization of the laser beam is dependent on the output intensity since the nulled-out condition changes with input energy.

The sensor is a RCA 917 phototube whose load impedance is 4.0 K ohms. The signal is amplified, integrated by a capacitor, followed by a peak detector.

The calibration of the integrator is dependent on the sensitivity of the photo cathode surface. The integrator design is such that a pulse of 0.60 v amplitude and 120 μsec length is integrated to 4 v. A current of 0.15 ma through 4.0 K will yield 0.60 v. This current for 120×10^{-6} sec determines a charge flow of 1.8×10^{-8} coulombs. The sensitivity of the S-1 cathode is approximately 1.5×10^{-3} coulombs/joule;[3] thus 1.2×10^{-5} joules yields a 4-v integrated output.

Fig. 3 indicates the results of calibration of an early Raytheon laser design, Model LH-1, using two different ruby rods.

Alvin L. Glick
Raytheon Company
Wayland, Mass.

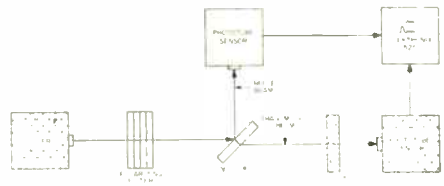

Fig. 1—Filter calibration. Laser output measurement uses only cross-hatched items.

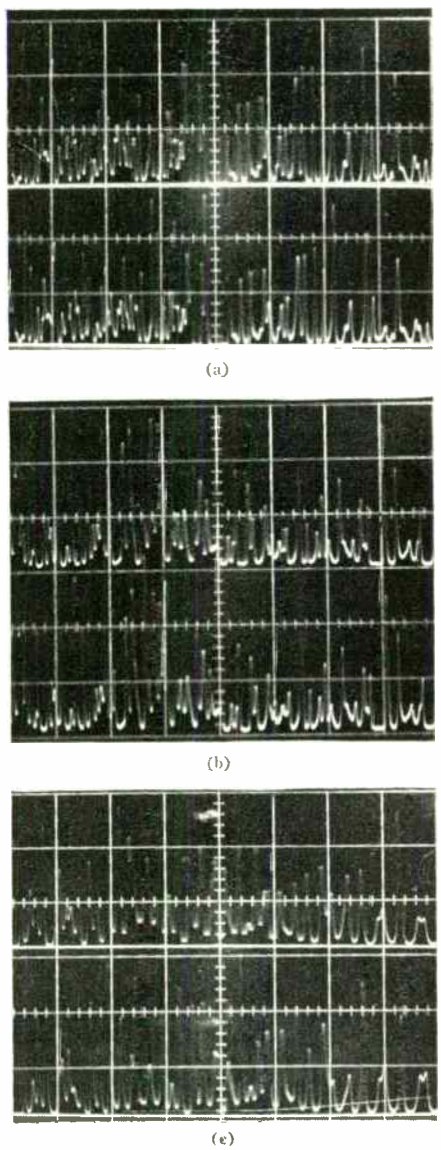

Fig. 2—Reflected and transmitted laser beams, 20 μsec/cm. (a) Polarized; upper, transmitted, 100 mv cm; lower, reflected, 50 mv cm. (b) Polarized; upper, transmitted through B filter, 50 mv cm; lower, reflected, 100 mv/cm. (c) Unpolarized; upper, relected, 50 mv/cm; lower, transmitted, 50 mv cm.

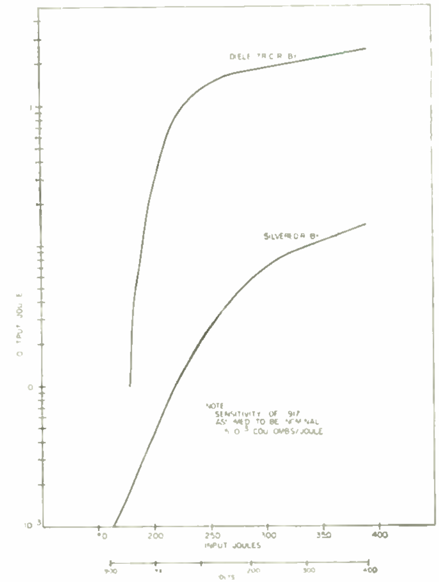

Fig. 3—Output energy curves.

* Received May 11, 1962; revised manuscript received, May 21, 1962.

[1] S. Koozekanani, P. P. Debye, A. Krutchkoff and M. Cifran, "Measurements of the laser output," Proc. IRE (*Correspondence*), vol. 50, p. 207; February, 1962.

[2] Four "Polaroid" filters in line, No. KN-36.

[3] The sensitivity range for the 917 is 0.90 to 3.0 μa/w at 7000 A°, a typical value being 1.5 μa w. Correspondence from R. C. Park, RCA Electron Tube Div.

For absolute calibration of phototube see R. W. Engstrom, "Absolute spectral response characteristics of photosensitive devices," *RCA Rev.*, vol. 21, p. 184; June, 1960.

On a Random Failure Mechanism*

When Lusser[1] was Reliability Coordinator at Redstone Arsenal, he suggested that random failures of components were caused by random stresses. In the course of an unsuccessful search (unsuccessful in that the hypothesis of random stresses was found insufficient and unnecessary) for a mathematical connection between random failures and random stresses, the following results were found which may be of interest.

Assume that a stress X varies randomly with time with unvarying statistics. Then the fraction of time the stress spends in a stress interval dx is

$$f_X(x)dx = \frac{dt}{T}, \tag{1}$$

where T is an observation interval and $f_X(x)$ is the probability frequency function of the stress distribution.

Assume a simplified linear stress-failure mechanism wherein a parameter p degrades as a function of only the applied stress,

$$\frac{dp}{dt} = h(X).$$

In a time T the degradation Δp is

$$\Delta p = \int_0^T h(X)dt. \tag{2}$$

Substitution of (1) into (2) yields

$$\Delta p = T\int_{-\infty}^{\infty} h(x)f_X(x)dx = kT \tag{3}$$

where k is a constant defined by the integral. This result is essentially independent of the random nature of the stress contrary to Lusser's suggestion. If X is a constant stress of value S,

$$f_X(x) = \delta(x - S) \tag{4}$$

where δ is the Dirac delta function. Substitution of (4) into (3) yields

$$\Delta p = Th(S) \tag{5}$$

which describes the classical stress-failure curves which have been published, for example, for circuit breakers. Eq. (5) enables one to determine $h(X)$ experimentally.

Returning to (3), assume that a component fails when $\Delta p > \phi$ and that k and ϕ are distributed in a component population with frequency functions $f_k(x)$ and $f_\phi(x)$. We have by a change of variable.

$$P(x < kT \leq x + dx) = \frac{1}{T}f_k\left(\frac{x}{T}\right)dx.$$

If k and ϕ are independent random variables, their joint distribution is given by

$$P(x < kT \leq x + dx, y < \phi \leq y + dy) = \frac{1}{T}f_k\left(\frac{x}{T}\right)f_\phi(y)dxdy$$

Hence,

$$P(\Delta p < \phi) = \frac{1}{T}\int_{x=y}^{x=\infty}\int_{y=-\infty}^{\infty} f_k\left(\frac{x}{T}\right)f_\phi(y)dxdy.$$

Let $z = x - y$. Then,

$$P(\Delta p > \phi) = \frac{1}{T}\int_0^T\int_{-\infty}^{\infty} f_k\left(\frac{x}{T}\right)f_\phi(x - z)dxdz. \tag{6}$$

P in (6) can be interpreted as the fraction of components in the population that have failed at time T. Its derivative is the failure rate at that time.

Let us evaluate (6) for the case when T is small or when k has a unique value $\bar{k}$. Then,

$$\frac{1}{T}f_k\left(\frac{x}{T}\right) = \delta(x - \bar{k}T). \tag{7}$$

Substitution of (7) into (6) yields, after integration,

$$P(\Delta p > \phi) = \int_{-\infty}^{\bar{k}T} f_\phi(u)du.$$

Differentiation yields the failure rate r at time T,

$$r = \frac{dP}{dT} = f_\phi(\bar{k}T). \tag{8}$$

The shape of a typical stress-failure distribution for components produced without any kind of testing or screening is shown in Fig. 1. Such distributions have been seen, for example, in the case of germanium diodes where the stress was mechanical acceleration. The "tail" extending down to very low values of stress seems to be characteristic of such distributions.

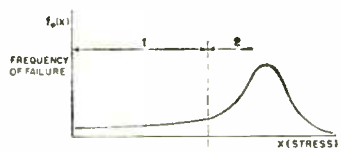

Fig. 1—Typical stress-failure distribution.

By (8), the failure rate as a function of time may be obtained by replacing the abscissa x in Fig. 1 by $\bar{k}T$. Such a time history of failure rates has the characteristics of the classical curve wherein there is a period 1 in which the failure rate is approximately constant ("random" failures) followed by a rising failure rate period 2 ascribed to wear-out failures.

This suggests the following procedure for reducing (if not eliminating) "random" failures:

1) Determine the stresses that cause component failures.
2) Determine the mechanism by means of which the stress causes the component failures.
3) Modify the component manufacturing process and/or the environmental conditions in which the component is used so that the desired reliability can be achieved.
4) Test (100 per cent) to weed out all components having excessive degradation rates k and inadequate stress margins ϕ.

Essentially, such procedures seem to have been developed by various people (*e.g.*, Remington Rand[2,3]) resulting in very low random failure rates. These procedures appear to have been developed on the basis of experience rather than from any mathematical insight. Incidentally, an examination of Reid and Raymond[3] suggests that the electronic component failures in the Athena computer are a highly probable result of maintenance procedures rather than a fault of the components.

HARRY J. GRAY
The Moore School of Electrical Engineering
University of Pennsylvania
Philadelphia, Pa.

* Received by the IRE, December 20, 1961.

[1] Robert M. Lusser (22 pamphlets on the reliability of missiles), Army Rocket and Guided Missile Agency, Redstone Arsenal, Ala.

[2] N. S. Prywes, H. Lukoff, and J. Schwarz, "UNIVAC-LARC high-speed circuitry: case history in circuit optimization," IRE TRANS. ON ELECTRONIC COMPUTERS, vol. EC-10, pp. 428–429, 437–438; September, 1961.

[3] L. W. Reid and G. A. Raymond, "The Athena computer, a reliability report," *Proc. Eastern Joint Computer Conf.*, Philadelphia, Pa. AIEE Publication T114, pp. 20–24; December 3–5, 1958; July, 1959.

WWV and WWVH Standard Frequency and Time Transmissions*

The frequencies of the National Bureau of Standards radio stations WWV and WWVH are kept in agreement with respect to each other and have been maintained as constant as possible since December 1, 1957, with respect to an improved United States Frequency Standard (USFS).[1] The corrections reported here were arrived at by means of improved measurement methods based on transmissions from the NBS stations WWVB (60 kc) and WWVL (20 kc). The values given in the table are 5-day running averages of the daily 24-hour values for the period beginning at 1800 UT of each day listed.

The time signals of WWV and WWVH are also kept in agreement with each other. Since these signals are locked to the frequency of the transmissions, a continuous departure from UT2 may occur. Corrections are determined and published by the U. S. Naval Observatory. The time signals are maintained in close agreement with UT2 by properly offsetting the broadcast frequency from the USFS at the beginning of each year when necessary. This new system was commenced on January 1, 1960.

Subsequent changes were as follows:

FREQUENCY OFFSET, WITH REFERENCE TO THE USFS

January 1, 1960, —150 parts in 10^{10}
January 1, 1962, —130 parts in 10^{10}

TIME ADJUSTMENTS, WITH REFERENCE TO THE TIME SCALE UT2

December 16, 1959, retardation, 20 milliseconds
January 1, 1961, retardation, 5 milliseconds
August 1, 1961, advancement, 50 milliseconds

* Received June 21, 1962.

[1] Refer to "National Standards of Time and Frequency in the United States," PROC. IRE, vol. 48, pp. 105–106; January, 1960.

Adjustments were made at 0000 UT on the foregoing dates; an advancement means that the signals were adjusted to occur at an earlier time than before.

WWV Frequency
With Respect to U. S. Frequency Standard

1962		Parts in 10^{10}†
May	1	−130.1
	2	−130.0
	3	−129.9
	4	−129.8
	5	−129.7
	6	−129.6
	7	−129.5
	8	−129.4
	9‡	−129.4
	10	−129.9
	11	−129.8
	12	−129.7
	13	−129.7
	14	−129.7
	15	−129.6
	16	−129.5
	17‡	−129.5
	18	−130.3
	19	−130.2
	20	−130.3
	21	−130.4
	22	−130.4
	23	−130.3
	24	−130.4
	25	−130.4
	26	−130.4
	27	−130.4
	28	−130.4
	29	−130.4
	30	−130.3
	31	−130.3

† A minus sign indicates that the broadcast frequency was below nominal. The uncertainty associated with these values is $\pm 5\times10^{-11}$.
‡ WWV frequency adjusted or interrupted as follows:
May 9, -0.5×10^{-10} adjustment, 1900 UT
May 17, -0.7×10^{-10} adjustment, 1900 UT

National Bureau of Standards
Boulder, Colo.

Electromagnetic Scattering from Radially Inhomogeneous Spheres*

Although the analysis of electromagnetic wave propagation through planar media having a varying index of refraction along the direction of propagation has received considerable attention in both the classic and more recent literature, comparatively little work has been directed at the similar problem of propagation through media which are spherically symmetric and have a varying refractive index in the radial direction. The chief work on this latter problem is that of Tai,[1] who derived the equations in the radial variable for the TE (m-type) and TM (e-type) modes. Using these equations as a basis, a method of obtaining the scattering from radially inhomogeneous spheres has been formulated for high-speed computer calculation.

* Received by the IRE, December 11, 1961. The research reported here was sponsored in part by Aeronautical Systems Div., AF Systems Command, U. S. Air Force, Wright-Patterson AFB, Dayton, Ohio, under Contract No. AF 33 (616)-8039.

[1] C. T. Tai, "The electromagnetic theory of the spherical Luneberg lens," *Appl. Sci. Res.*, sec. B, vol. 7, pp. 113–130; 1959.

The far electric fields scattered from the sphere of Fig. 1 are given by

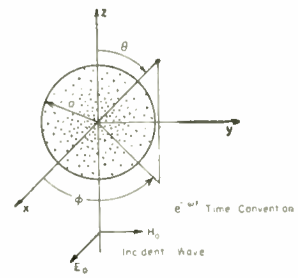

Fig. 1.

$$E_\theta^s = \frac{-iE_0e^{ikr}}{kr}\cos\phi\sum_{n=1}^{\infty}\frac{2n+1}{n(n+1)} \cdot\left[a_n^s\frac{P_n^1(\cos\theta)}{\sin\theta}+b_n^s\frac{\partial P_n^1(\cos\theta)}{\partial\theta}\right], \quad (1)$$

$$E_\phi^s = \frac{+iE_0e^{ikr}}{kr}\sin\phi\sum_{n=1}^{\infty}\frac{2n+1}{n(n+1)} \cdot\left[a_n^s\frac{\partial P_n^1(\cos\theta)}{\partial\theta}+b_n^s\frac{P_n^1(\cos\theta)}{\sin\theta}\right], \quad (2)$$

where a_n^s and b_n^s are, respectively, the magnetic and electric scattering coefficients of the sphere under investigation and $k=\omega\sqrt{\mu_0\epsilon_0}$ is the wavenumber in the ambient medium. The scattering coefficients are calculated from

$$a_n^s = -\frac{kaj_n(ka)-z_n^{(m)}(ka)[kaj_n(ka)]'}{kah_n^{(1)}(ka)-z_n^{(m)}(ka)[kah_n^{(1)}(ka)]'}, \quad (3)$$

$$b_n^s = -\frac{kaj_n(ka)-y_n^{(e)}(ka)[kaj_n(ka)]'}{kah_n^{(1)}(ka)-y_n^{(e)}(ka)[kah_n^{(1)}(ka)]'}, \quad (4)$$

where the symbol (′) means d/dkr and the quantities $z_n^{(m)}(kr)$ and $y_n^{(e)}(kr)$ satisfy the following Riccati equations:

$$\frac{dz_n^{(m)}}{dkr} = \tau(r)+\left[\kappa(r)-\frac{n(n+1)}{(kr)^2\tau(r)}\right][z_n^{(m)}]^2 \quad (5)$$

$$\frac{dy_n^{(e)}}{dkr} = \kappa(r)+\left[\tau(r)-\frac{n(n+1)}{(kr)^2\kappa(r)}\right][y_n^{(e)}]^2, \quad (6)$$

when $\mu(r)=\tau(r)\mu_0$ and $\epsilon(r)=\kappa(r)\epsilon_0$ are the constitutive parameters of the sphere. The quantity $-iz_n^{(m)}$ is defined to be the TE modal surface impedance at radius r, normalized to the intrinsic impedance of the ambient medium, and the quantity $-iy_n^{(e)}$ is defined to be the TM modal surface admittance at radius r, normalized to the intrinsic admittance of the ambient medium. An IBM 704 computer has been programmed to numerically integrate (5) and (6) under appropriate end conditions for arbitrary complex functions $\kappa(r)$ and $\tau(r)$. As examples, normalized E- and H-plane scattering patterns, given by

$$\sigma_E = \lim_{r\to\infty} 4\pi r^2\frac{|E_\theta^s|^2_{\phi=0°}}{|E_0|^2}, \quad (7)$$

$$\sigma_H = \lim_{r\to\infty} 4\pi r^2\frac{|E_\phi^s|^2_{\phi=90°}}{|E_0|^2}, \quad (8)$$

have been calculated using this program with two real permittivity distributions, known in the literature as the Luneberg lens and the Eaton-Lippmann lens. These distributions and corresponding patterns appear in Figs. 2 and 3. Further details are presented in an Antenna Laboratory memorandum.[2]

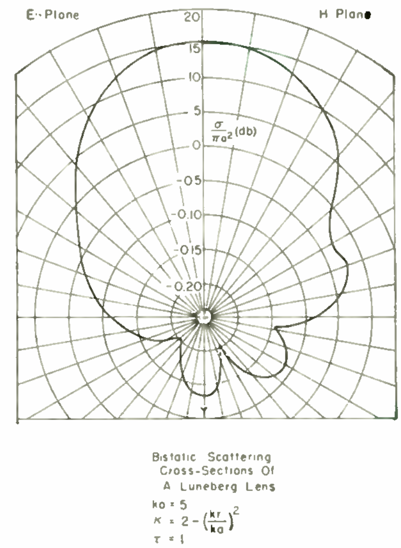

Fig. 2.

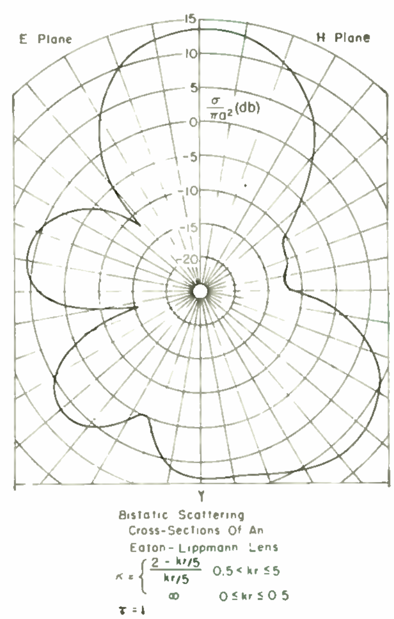

Fig. 3.

The work of D. Call and L. Du in programming the IBM 704 computer is acknowledged with gratitude.

R. J. Garbacz
Antenna Lab.
Dept. of Electrical Engineering
Ohio State University
Columbus, Ohio

[2] R. J. Garbacz, "Electromagnetic Scattering by Radially Inhomogeneous Spheres," Antenna Lab., Ohio State University, Columbus, Rept. No. 1223-3 (in process).

Space-Charge-Layer Width and Capacitance of Symmetrical Step Junctions*

The behavior of semiconductor p-n junction under large forward bias has received much attention in the recent years. Due to the effect of conductivity modulation and/or generation-recombination current in the space-charge region, it was found that the current varies as $\exp(qV/2kT)$ in the high forward-bias region, where V is the applied voltage less the ohmic drop in the neutral regions.[1] However, an inductive effect, which was observed at some high voltages, is not as yet satisfactorily explained. In junction capacitance calculation, it is usually assumed that the difference in quasi-Fermi levels across the junction is constant and is equal to the applied voltage, leading to a capacitance which increases with applied voltage, and is in contrast to the observed finite maximum capacitance at some high forward bias. It is the purpose of this correspondence to show that, for step junctions, the inductance effect is associated with drop of quasi-Fermi levels in the neutral regions in which the corresponding carriers are majority carriers.

For step junctions at thermal equilibrium Adirovich, *et al.*,[2] showed that the Poisson equation can always be put into a closed integral form. If a transition-layer width is defined as the distance between points, between which the electrostatic potential difference equals 95 per cent of the built-in voltage between p- and n-regions, it was found that the transition-layer width thus obtained agrees with the result from space-charge approximation. The agreement is within 2 per cent for bulk impurity densities ranging from 10^{13} to 10^{19}. Fig. 1 shows the normalized potential distribution across a symmetrical step junction with various impurity doping on both sides of a symmetrical junction.

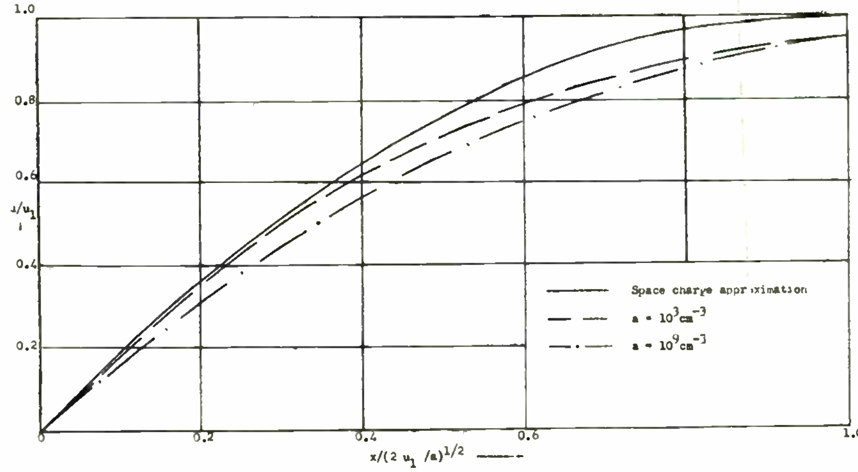

Fig. 1—Potential distribution in one side of the space-charge region. u_1 is the electrostatic potential in the neutral region.

To calculate the capacitance of the junction under bias, one has to solve the normalized Poisson equation

$$\frac{d^2u}{dy^2} = e^{(u_p-u_n)/2}\sinh\left(u - \frac{u_p+u_n}{2}\right) - \frac{a}{2}, \qquad y > 0, \tag{1}$$

where $y = x/L_D$ is the distance in units of Debye length, u, u_p, and u_n are, respectively, the electrostatic potential, quasi-Fermi levels for holes and electrons, multiplied by q/kT, and a is the doping density divided by the intrinsic carrier density. Eq. (1) can be solved only if the variations in u_p and u_n are known. We shall therefore try to find an approximate solution by defining a transition region, bounded by two planes at $y = \pm w$, by the following conditions:

$$u''(y) = u'(y) = 0, \; y > w; \qquad u(0) = 0. \tag{2}$$

We shall assume that the quasi-Fermi levels remain approximately constant throughout the transition region and, therefore, that u' and u'' are identical with u_0' and u_0'' in the transition region, where $u_0 = u - (u_p + u_n)/2$. This approximation is evidently valid under a forward-bias condition and a moderate reverse-bias condition.[1] Inasmuch as the ohmic drops are negligible, $u_p - u_n$ across the junction is equal to the applied voltage. As the forward bias is increased, however, the ohmic drops are no longer negligible; as a result, only a fraction of the applied voltage appears across the junction and $u_p - u_n$ becomes less than v, where $v = qV/kT$. Assuming predominance of minority-diffusion current, these drops can be approximately expressed as $\delta u_p = \alpha e^{v/2}$ with similar expression for δu_n. Here α is a parameter characteristic of a particular junction device and is a measure of the effective resistivity of, and effective diffusion length of minority carriers in, the respective neutral regions. An approximate form of $(u_p - u_n)$ across the junction at high forward bias is, therefore,

$$u_p - u_n = 2\alpha e^{v/2}. \tag{3}$$

It is seen that α is usually small, of the order of e^{-v_D}, there v_D is the built-in voltage. Clearly (3) is not valid in the extreme case in which v is much higher than the built-in voltage so that the electrostatic potential across the junction diminishes to zero and the current varies linearly with the applied voltage. With the above, (1) can be integrated once to read

$$\frac{du_0}{dy} = \sqrt{2}\, e^{v/2 - \alpha e^{v/2}}\left[u_1\sinh u_1 - \cosh u_1 + \cosh u - u\sinh u_1\right]^{1/2}, \tag{4}$$

where u_1 is the value of u_0 evaluated at edge of the transition layer.

Introducing a normalizing capacitance $C_0 = q^2 n_i L_D/kT (= 256\ \mu\mu f/\text{cm}^2$ for Si), the normalized capacitance

$$c = \frac{d}{dv}\int_{-l}^{+l} p\, dy.$$

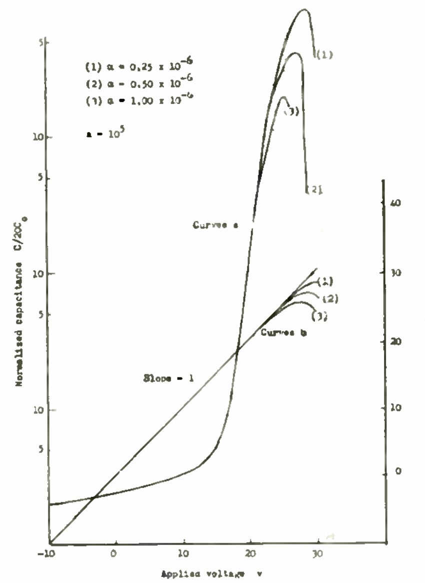

Fig. 2—(a) Capacitance of a symmetrical step junction. (b) Drop of quasi-Fermi levels across a symmetrical step junction.

can be written as the sum of three capacitances: 1) diffusion capacitance c_d; 2) space-charge capacitance c_t; 3) transition-region-carrier capacitance c_s, where

$$c_d = \int_{-l}^{w}\frac{dn}{dv}dy + \int_{w}^{l}\frac{dp}{dv}dy,$$

$$c_s = -2\frac{du_0'(0)}{dv}, \qquad c_t = 2\int_0^{w}\frac{dp}{dv}dy.$$

The diffusion capacitance can be obtained by assuming that minority-carrier densities decay exponentially in the neutral regions with appropriate diffusion lengths, whereas the other two can be put into closed integral form using (4). A numerical evaluation of the capacitances was obtained and the result is shown in Fig. 2, together with the variations of $u_p - u_n$ across the junction. Observe that the capacitance increases to a maximum at some voltage beyond v_D; at still higher voltage, the capacitance decreases and would tend to zero in the limit as the junction de-

* Received December 22, 1961; revised manuscript received January 5, 1962.

[1] C. T. Sah, R. N. Noyce, and W. Shockley, "Carrier generation and recombination in p-n junctions and p-n junction characteristics," Proc. IRE, vol. 45, pp. 1228–1243; September, 1957.

[2] E. I. Adirovich, Iu. S. Riabinkin, and K. V. Temko, "Equilibrium distribution of potential, field and concentration of current carriers in fused junctions," *Soviet J. Tech. Phys.*, vol. 3, pp. 49–59; January, 1958. (Translation.)

vice under consideration becomes a resistive element. Note also that the deviation of $u_p - u_n$ from v is small even at very high bias, whereas the resulting decrease in capacitance is large. This perhaps explains why the usual assumption of $u_p - u_n = v$ across the junction has not been able to detect the obvious inductance effect in *p-n* junctions. Since the impedance associated with majority-current flow increases with frequency and bulk resistivity, it appears that the voltage at which the inductive effect occurs is lowered with increase in either bulk resistivity or the frequency of the applied voltage, in general agreement with the result of Sah for linearly graded junctions.[3]

The author wishes to acknowledge the help of H. Golde in programming for numerical solution.

C. C. Wang
Dept. of Electrical Engineering
University of Washington
Seattle, Wash.

[3] C. T. Sah, "Effects of electrons and holes on the transition layer characteristics of linearly graded *p-n* junctions," Proc. IRE, vol. 49, pp. 603–618; March, 1961.

Power Carried by the Helitron Waves on an *E*-Type Filamentary Electron Beam*

Waves on an *E*-type filamentary electron beam in a transverse-field circuit have been pointed out by Pantell,[1] who found the existence of the fast and slow space charge waves, but did not analyze the kinetic power flow of each wave. It is the purpose of this paper to show that the kinetic power flow on the *E*-type filamentary electron beam can be expressed in a normal mode form as well. These waves are named "fast helitron waves" and "slow helitron waves," respectively. It is found that similar expressions for the power of each wave component to those of *O*- and *M*-type electron beams can be obtained by this analysis.

In a drift space of the *E*-type beam as shown in Fig. 1, the following equations are obtained from the force equation for electrons which are traveling to the z-direction with dc velocity u_0, under the conditions of electrostatic focusing. It is assumed that the electron traces the path of a helix and all electrons form a right circular hollow cylinder which is thin in the radial dimension.

$$\frac{d^2x}{dt^2} = \eta V_0 \frac{x}{x^2+y^2}$$
$$\frac{d^2y}{dt^2} = \eta V_0 \frac{y}{x^2+y^2}$$
$$\frac{dz}{dt} = \sqrt{\eta V_0}\tan\phi \qquad (1)$$

where the definitions of quantities are given as follows:

$\eta = 1.759 \times 10^{11}$ c/kg,
$V_0 = (V_c - V_s)/\ln(s/c)$, $V_c > V_s$,
V_s = voltage between outer cylinder and ground,
V_c = voltage between inner cylinder and ground,
ϕ = electron pitch angle.

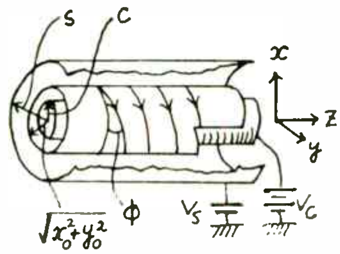

Fig. 1—Electrons form a right circular hollow beam that is thin in the radial direction and the electron traces the path of a helix between coaxial cylinders.

Under a small signal theory, the motion of the electron is given as a sum of a dc quantity and an RF disturbance.

$$x = x_0 + x_1,$$
$$y = y_0 + y_1,$$
$$z = z_0. \qquad (2)$$

The subscript 0 refers to the dc quantity and the subscript 1 refers to the RF motion.

Using (2), (1) becomes

$$\frac{dv_{1x}}{dt} + 2\omega_h^2 x_1 = 0,$$
$$\frac{dv_{1y}}{dt} + 2\omega_h^2 y_1 = 0,$$
$$\frac{dx_1}{dt} = v_{1x},$$
$$\frac{dy_1}{dt} = v_{1y} \qquad (3)$$

where ω_h is named "helitron angular frequency,"

$$\omega_h = \sqrt{\eta V_0/(x_0^2+y_0^2)}.$$

Now, we introduce the effective transverse current[2] K, as well as Chu's kinetic voltage U.

$$2U = U_x + jU_y,$$
$$2K = K_x + jK_y,$$
$$U_x = -u_0 v_{1x}/\eta,$$
$$U_y = -u_0 v_{1y}/\eta,$$
$$K_x = j\omega\sigma_0 x_1,$$
$$K_y = j\omega\sigma_0 y_1, \qquad (4)$$

where σ_0 is the total charge of the electron beam per transverse unit area. The subscript x denotes an x component and the subscript y denotes a y component. From (3) and (4), the following space charge wave equations are obtained:

$$\left(\frac{d}{dz} + j\beta_e\right) U = -j\frac{2\omega_h^2}{\omega q \sigma_0} K,$$
$$\left(\frac{d}{dz} + j\beta_e\right) K = -j\frac{\omega q\sigma_0}{u_0^2} U. \qquad (5)$$

These expressions are very similar to those for the longitudinal beam[3] (one dimensional).

Next, we define the helitron normal mode $a_\pm$ using U and K:

$$a_\pm = \frac{1}{4\sqrt{Z_0}}(U \pm Z_0 K) \qquad (6)$$

where z_0 is the characteristic beam impedance for the small-signal quantities of the helitron waves,

$$Z_0 = \frac{2V_0}{|I_0|}\frac{\sqrt{2}\beta_h}{\beta_e} \qquad (7)$$

where I_0 is the dc beam current ($|I_0| = -\sigma_0 u_0$), $\beta_h = \omega_h/u_0$ and $\beta_e = \omega/u_0$.

Using (6) and (7), (5) then becomes

$$\left(\frac{d}{dz} + j(\beta_e \mp \sqrt{2}\beta_h)\right) a_\pm = 0. \qquad (8)$$

These are the normal mode forms of the helitron waves. Accordingly, for an arbitrary excitation in terms of the mode amplitudes at the input plane $z=0$, the solution of (8) are,

$$a_{\pm(z)} = a_{\pm(0)} e^{-j(\beta_e \mp \sqrt{2}\beta_h)z}. \qquad (9)$$

It is easy to see that from (9) the a_+ mode, the fast helitron wave, travels with a phase velocity slightly greater than the dc velocity, whereas the a_- mode, the slow helitron wave, travels with a phase velocity slightly less than u_0. By $\omega = \sqrt{2}\omega_h$, it is possible to have an infinite phase velocity associated with fast helitron waves.

From (9), K and u may be expressed as follows:

$$U = 2\,\mathrm{Re}\left\{\sqrt{Z_0}\left[a_{+(z)} + a_{-(z)}\right] e^{j\omega t}\right\},$$
$$K = 2\,\mathrm{Re}\left\{\frac{1}{\sqrt{Z_0}}\left[a_{+(z)} - a_{-(z)}\right] e^{j\omega t}\right\} \qquad (10)$$

The power carried by helitron waves can be given by the generalized Chu's power theorem as follows:

$$P = \tfrac{1}{2}\,\mathrm{Re}\,(UK^*) = 2(|a_+|^2 - |a_-|^2). \qquad (11)$$

In order to show that P is independent z, we differentiate (10) with z and (8) and their complex conjugate substitute into this expression. It then follows immediately that $dP/dz = 0$.

In conclusion, the power flow on the *E*-type filamentary electron beam in the drift space discussed here is given as (10) and it is seen that the fast helitron wave carries positive power, whereas the slow helitron wave carries negative power.

Ichiro Sakuraba
Faculty of Engineering
Hokkaido University
Hokkaido, Japan

* Received by the IRE, December 11, 1961.
[1] R. H. Pantell, "Electrostatic electron beam coupler," IRE Trans. on Electron Devices, vol. ED-8, pp. 39–43; January, 1961.
[2] S. Saito, "Power carried by the cyclotron waves and the synchronous waves on a filamentary electron beam," Proc. IRE, vol. 49, pp. 969–970; May, 1961.
[3] W. H. Louisell, "Coupled Mode and Parametric Electronics," John Wiley and Sons, Inc., New York, N. Y.; 1960.

A Technique for Equalizing Parabolic Group Delay*

It can be shown[1] that the phase shift in a band-pass filter that is a minimum phase-shift network is

$$\theta = -\sum_{b=1}^{n} \tan^{-1}\frac{X - X_{bi}}{X_{br}} \tag{1}$$

when X = normalized frequency variable, X_{bi} and X_{br} are real and imaginary components of the pole positions (*i.e.*, poles of filter transfer function), n = number of resonant circuits.

If group delay is defined as the derivative of the phase shift with respect to frequency

$$d = \frac{1}{\pi\Delta f}\sum_{b=1}^{n}\frac{B_b}{1 + (A_b + B_b X)^2} \tag{2}$$

where

$$A_b = \frac{1}{X_{br}} \quad \text{and} \quad B_b = -\frac{X_{bi}}{X_{br}}$$

and d = absolute group delay of the filter, Δf = 3-db bandwidth of the filter. At the band center

$$(x = 0)$$

then

$$d_0 = \frac{1}{\pi\Delta f}\sum_{b=1}^{n}\frac{B_b}{1 + A_b^2}. \tag{3}$$

Letting Δd = the differential group delay at any normalized frequency X, then

$$\Delta d = d - d_0. \tag{4}$$

Parabolic group delay which occurs in the pass band centers of maximally flat band-pass filters can be equalized using the conventional all-pass network which provides compensating group delay and no amplitude discrimination. All-pass equalizers usually are lattice or bridged-T networks which are often difficult to physically realize. This paper considers a technique for equalization that does not use all-pass networks as equalizers.

For a maximally flat band-pass filter with *two or more* resonant circuits it can be shown that

$$\Delta d_f \cong \frac{C X_f^2}{\pi\Delta f_f} \qquad (0 < X_f < 0.4). \tag{5}$$

where

Δd_f = differential group delay of filter
X_f = normalized frequency variable of filter
f = frequency
f_0 = center (*i.e.*, resonant) frequency of filter
Δf_f = 3-db bandwidth of filter.

For narrow bandwidth filters

$$\left(\frac{\Delta f_f}{f_0} \leqq 2\%\right)$$

$$X_f \cong \frac{2|f - f_0|}{\Delta f_f} \tag{6}$$

then

$$\Delta d_f = \frac{4C|f - f_0|^2}{\pi(\Delta f_f)^3}. \tag{7}$$

This is a parabolic differential group-delay function that is concave upward. For a single-tuned circuit (*i.e.*, maximally flat filter with one resonator)

$$\Delta d_e \cong \frac{-X_e^2}{\pi\Delta f_e} \tag{8}$$

where

Δd_e = differential group delay of equalizer
X_e = normalized frequency variable of equalizer
f = frequency
f_0 = center (*i.e.*, resonant) frequency of equalizer
Δf_e = 3-db bandwidth of equalizer.

For narrow bandwidth equalizers

$$\left(\frac{\Delta f_e}{f_0} \leqq 2\%\right)$$

$$X_e \cong \frac{2|f - f_0|}{\Delta f_e} \tag{9}$$

then

$$\Delta d_e = \frac{-4|f - f_0|^2}{\pi(\Delta f_e)^3}. \tag{10}$$

This is a parabolic differential group-delay function that is concave downward. For equalization

$$\Delta d_f + \Delta d_e = 0 \quad \text{and} \quad \Delta d_f = -\Delta d_e$$

$$\frac{4C|f - f_0|^2}{\pi(\Delta f_f)^3} = \frac{4|f - f_0|^2}{\pi(\Delta f_e)^3} \tag{11}$$

$$\therefore\ (\Delta f_e)^3 = \frac{1}{C}(\Delta f_f)^3$$

$$\Delta f_e = C^{-1/3}\Delta f_f. \tag{12}$$

For maximally flat band-pass filters, (2) becomes

$$d = \frac{1}{\pi\Delta f}\sum_{r=1}^{n}\frac{B_r}{1 + (A_r + B_r X)^2} \tag{13}$$

where

$$A_r = \csc\left(\frac{2r - 1}{2n}\right)\pi$$

and

$$B_r = -\operatorname{ctn}\left(\frac{2r - 1}{2n}\right)\pi$$

$$d_0 = \frac{1}{\pi\Delta f}\sum_{r=1}^{n}\frac{B_r}{1 + A_r^2} = \frac{D_0}{\pi\Delta f}. \tag{14}$$

Using a parabolic approximation for differential group delay

$$\frac{CX^2}{\pi\Delta f} \cong d - d_0. \tag{15}$$

The constant C is selected at a value of $X = 0.2$. A table of values of C and D_0 for n from two to eight resonators follows:

n	C	D_0
2	1.414	1.414
3	1	2.000
4	1.083	2.613
5	1.236	3.236
6	1.414	3.864
7	1.604	4.494
8	1.799	5.126

This technique should be applicable to RF and IF amplifier chains in which single-tuned and double-tuned circuits can be readily used in alternate coupling networks.

R. M. KURZROK
RCA Surface Commun. Sys. Lab.
New York, N. Y.

* Received December 12, 1961.

[1] M. Dishal, "Dissipative band-pass filters," PROC. IRE, vol. 37, pp. 1058–1060; September, 1949.

A Useful Technique for Treatment of Certain Statistical Sampled-Data Control Systems*

In any statistical treatment of control systems the first- or second-order statistic, namely the average value and mean-square value, has special significance. Two theorems appeared in Ku and Wolf,[1] and Wolf,[2] which are given below.

Theorem 1: Given a random process $g(t)$ with known statistical quantities and a deterministic operator L such that if $G(q)$ is the resulting transform-random process according to the relation $G(q) = L\{g(t)\}$ where q is the transform-random variable corresponding to the original random t, then $\langle G(q)\rangle_G = L[\langle g(t)\rangle_g]$ where $\langle\ \rangle_G$ is the ensemble average with respect to G and $\langle\ \rangle_g$ is the ensemble average with respect to g and these are commutative with respect to each other and the deterministic operator L.

Theorem 2: Given a random process $g(t)$ and its transform $G(q)$, the mean nth ensemble average of the given process is $\langle g^n(t)\rangle_g = L^{-1}[\langle C^{n-1}\{G(q)\}\rangle_G]$ where $C^k\{\ \}$ is the convolution transform of the kth order.

Second-order statistic is specifically obtained for a continuous case using Laplace transform.[2] This seems to be quite useful. This technique can now be developed for sampled-data case using z transforms. Closed-form solution can be immediately obtained.

In this short note we will use above theorems to obtain specific results for the sampled-data case. Let the system consist

* Received by the IRE, December 28, 1961; revised manuscript received, January 15, 1962.

[1] Ku, Y. H. and Wolf, A. A., "Transform ensemble method for the analysis of linear and non-linear systems with random inputs," *Proc. Natl. Electronics Conf.*, Chicago, Ill., 1960, Natl. Electronics Conf. Inc., Chicago, Ill., vol. 15, pp. 441–455; 1960.

[2] Wolf, A. A., "On poles and zeros of a random process in linear and nonlinear systems," *Proc. Natl. Electronics Conf.*, Chicago, Ill., Natl. Electronics Conf. Inc., Chicago, Ill., vol. 15; 1960.

of a sampler, hold circuit $H(s)$ and linear element $G(s)$. Let the input be $x(t)$ and the output be $y(t)$ (sampled output $y(nT)$). For this system we can write using z transform $Y(z)=GH(z)X(z)$ which gives

$$y(nT) = z^{-1}\{GH(z)X(z)\}$$

or using Theorem 1, we get

$$\langle y(nT)\rangle = z^{-1}\{GH(z)\cdot\langle X(z)\rangle_X\}.$$

Hence, this gives us a way of getting the mean value of the output at sampling instants, knowing the mean value of the input using z transforms.

In statistical work we are usually concerned with the mean-square values; then let us try to find mean-square value of output first at sampling instants.

Using Theorem 2 we can write

$$\langle y^2(nT)\rangle_y = z^{-1}[\langle C\{Y(z)\}\rangle_y,$$

where $C\{Y(z)\}$ is the convolution of $Y(z)$ *i.e.*,[3]

$$C[Y(z)] = Y(z) * Y(z) = \frac{1}{2\pi j}\int_\Gamma p^{-1}Y(p)Y\left(\frac{z}{p}\right)dp.$$

In our case $Y(z)=GH(z)X(z)$

$$\therefore [CY(z)] = \frac{1}{2\pi j}\int_\Gamma p^{-1}GH(p)X(p)GH\left(\frac{z}{p}\right)X\left(\frac{z}{p}\right)dp$$

$$= \frac{1}{2\pi j}\int_\Gamma p^{-1}GH(p)GH\left(\frac{z}{p}\right)X(p)X\left(\frac{z}{p}\right)dp$$

or

$$\langle C[Y(z)]\rangle_Y = \frac{1}{2\pi j}\int_\Gamma p^{-1}GH(p)GH\left(\frac{z}{p}\right)\cdot\left\langle X(p)X\left(\frac{z}{p}\right)\right\rangle_X dp.$$

Hence, we can write that

$$\langle y^2(nT)\rangle_y = z^{-1}\left[\frac{1}{2\pi j}\int_\Gamma p^{-1}GH(p)GH\left(\frac{z}{p}\right)\cdot\left\langle X(p)X\left(\frac{z}{p}\right)\right\rangle_X dp\right]. \quad (1)$$

Now we must define what we mean by $\langle X(p)X(z/p)\rangle_X$. Consider $\langle x(t)x(t+\tau)\rangle_x$. It can be easily shown

$$L_{(t)}^{(s)}L_{(\tau)}^{(k)}[x(t)x(t+\tau)] = X(k)X(s-k),$$

where

$L_{(t)}^{(s)}$ is defined as the Laplace transform w.r.t.t with new variable s.

and

$L_{(\tau)}^{(k)}$ is defined as the Laplace transform w.r.t.τ with new variable k.

Now

$$z_{(k)}^{(p)}z_{(s)}^{(z)}[X(k)X(s-k)] = X(p)X\left(\frac{z}{p}\right),$$

where

$z_{(k)}^{(p)}$ is defined as the z transform w.r.t.k with new variable p,

and

$z_{(s)}^{(z)}$ is defined as the z transform w.r.t.s with new variable z.

By Theorem 1 we can write

$$z^{(p)}z^{(z)}[\langle x(t)x(t+\tau)\rangle_x] = \left\langle X(p)X\left(\frac{z}{p}\right)\right\rangle_X.$$

Hence we can find $\langle X(p)X(z/p)\rangle_X$ as follows:

1) Find $\langle x(t)x(t+\tau)\rangle_x$, which by definition is $\phi_{xx}(\tau)$, the autocorrelation function of the input.
2) Then find
$$L_{(t)}^{(s)}L_{(\tau)}^{(k)}\langle x(t)x(t+\tau)\rangle_x,$$
which will be of the form
$$\langle X(k)X(s-k)\rangle_X.$$
3) Then find
$$z_{(k)}^{(p)}z_{(s)}^{(z)}\langle X(k)X(s-k)\rangle_X,$$
which will give
$$\left\langle X(p)X\left(\frac{z}{p}\right)\right\rangle_X.$$

Substituting in integral (1), we have the complex integral which can be easily evaluated by complex integration,[3] giving us the mean-square value at sampling instants in a closed form. Closed-loop system causes no more difficulty.

If we are interested in obtaining the mean-square value in general and not only at sampling instants, we consider the modified z-transform approach.

For the system considered above, we can write $Y(z, m)=GH(z, m)X(z)$ which can be written by Theorem 1 as

$$\langle y(nT, m)\rangle_y = Z_m^{-1}[GH(z, m)\langle X(z)\rangle_X]$$

where

$$0 < m < 1.$$

Now

$$\overline{y(t)} = \int_0^1 \langle y(nt, m)\rangle_y dm.$$

In order to get the mean-square value at the output we again apply Theorem 2. Applying the same reasoning as above, we can write $\langle y^2(nT, m)\rangle_y$

$$= Z_m^{-1}\left[\frac{1}{2\pi j}\int_\Gamma p^{-1}GH(p, m)GH\left(\frac{z}{p}, m\right)\cdot\left\langle X(p)X\left(\frac{z}{p}\right)\right\rangle_X dp\right] \quad (2)$$

where $\langle X(p)X(z/p)\rangle_X$ has already been defined above. The integral can be evaluated by usual techniques.[3] Now

$$\overline{y^2(t)} = \tau\int_0^1 \langle y^2(nT, m)\rangle dm.$$

Then (1) and (2) give us the closed-form mean-square values at the output for sampling instants and in general, respectively, when the input-correlation function is known. Other methods to get these results are known and are equivalent to this,[3] but it seems that for the study of sampled-data systems this point of view proves to be quite handy. The major advantage of this technique is that we can apply Theorem 2 continuously to get higher moments without any greater difficulty and this helps us to construct the probability distribution at the output because this probability density function can be expressed in terms of moments of the output.

S. C. Gupta
Dept. of Electrical Engineering
University of California
Berkeley, Calif.

[3] E. I. Jury, Class Notes in "Applications of z-Transform Theory," University of California, Berkeley, Fall, 1961 (to be published).

Duration and Spacing of Sferic Pulses*

Distributions of durations and the spacing between sferic pulses were obtained from a limited sample of sferics recorded simultaneously at two stations. About 9000 sferic waveforms from the 35-mm film records were analyzed to provide preliminary information for a receiver development project. The duration of a sferic was arbitrarily defined as the length of time (after the sweep was triggered) that the amplitude exceeded 10 mv/m. A total oscilloscope sweep of 500 μsec was used for these recordings, and when the amplitude still exceeded 10 mv/m at the end of the trace, the duration was tabulated as >500 μsec. The frequency response of the recording equipment was approximately 1 to 150 kc. The triggering circuits had a 60 per cent bandwidth centered at 10 kc and were calibrated to the peak-to-peak amplitude of an equivalent CW signal which would just produce a trigger. The triggering sensitivity was set at various levels during the recording periods.

Fig. 1 shows the duration distributions for a period on May 27, 1960 when a large thunderstorm was located from 10 to 30 miles from the omnidirectional station at Goodland, Kansas.[1] The Brighton, Colorado station (near Denver) employed an Ephi directional system[2] which permitted the selection of sferics from pre-selected azimuths, in this case a 6° sector centered over Goodland (102° azimuth). During the recording interval the storm near Goodland was also the storm nearest Brighton (distance 160–180 miles), although there were clouds beyond Goodland which could also have produced some sferics. The Goodland station was operated at a high triggering level (324 mv/m) to avoid saturation or overlapping of waveforms on the film resulting from the sferics of the nearby storm.

Observations at Leoti, Kansas and Brighton, Colorado on May 19, 1960 indi-

* Received December 29, 1961; revised manuscript received, January 29, 1962.

[1] Time references are in Mountain Standard Time (105th meridian).

[2] G. Heney, R. F. Linfield and T. L. Davis, "The Ephi system for VLF direction finding," *J. Res. NBS*, vol. 65C, pp. 42–49; January–March, 1961.

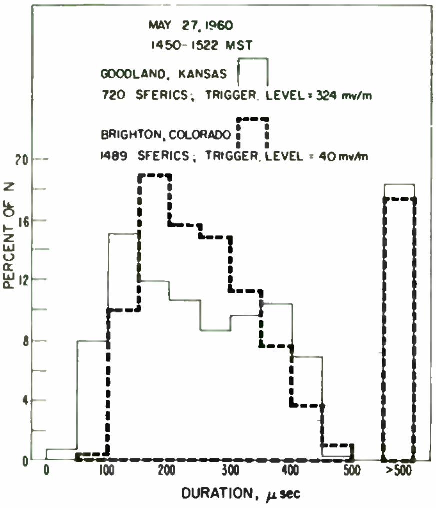

Fig. 1—Comparative duration distributions (N = total sferics).

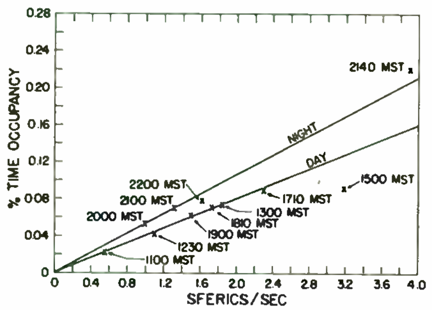

Fig. 2—Percentage of sample interval occupied by sferics—Leoti, Kansas, May 19, 1960.

cated a considerable shift in the duration peak as weather and propagation factors varied during the course of the day. Sferic durations were longer at night or when the source was at a great distance, and there were indications of a shift toward shorter durations coincident with tornado occurrences.[3]

The percentage of the sample interval occupied by sferics was calculated for a series of observations made at Leoti with the same omnidirectional equipment later used at Goodland. Sferics tabulated as ">500 μsec" were arbitrarily assigned a duration of 750 μsec for this part of the study. The total time occupancy is shown as a function of sferic rate in Fig. 2 for both day and night conditions. An extension of the two curves to higher sferic rates would indicate sferic time occupancy of about 4 to 5 per cent at 100 sferics/sec, and 12 to 15 per cent at a rate of 300 sferics/sec. However, this assumption of a linear relationship between rate and time occupancy may not be justified, and direct observation at the higher rates is needed. A change in the gating sensitivity (triggering level) will of course change the relative time occupancy.

Observations of the rate-vs-triggering level relationship were made at Brighton

[3] C. A. Samson and R. F. Linfield, "Sferic observations of the severe weather on May 19, 1961," *J. Geophys. Res.*, February, 1962.

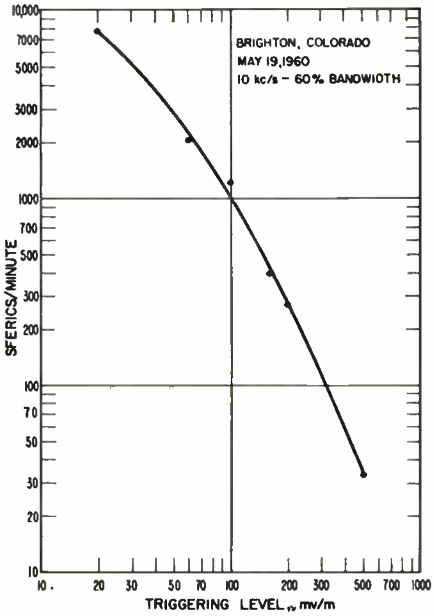

Fig. 3—Rate-vs-triggering level relationship.

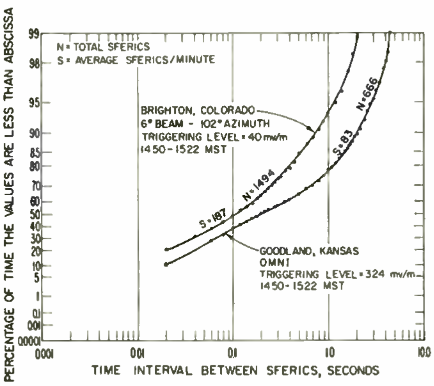

Fig. 4—Distribution of intervals between sferics, May 27, 1960.

over a period of about 9 hours on May 19, 1960, using an omnidirectional antenna. The average curve for this relationship is shown in Fig. 3. There was widespread storm activity in the midwest on this date, but no storms within several hundred miles of Brighton. Observations of this type indicate that some limiting value of sferic rate is approached as the sensitivity of the receiver is increased. The highest rate actually observed on May 19 was at about 2200 MST, when 12,880 sferics were recorded in one minute at a triggering level of 20 mv/m. The average rate during this interval was 215 sferics/sec, at a time when the major storm activity was 500–700 miles distant.

Fig. 4 shows the distribution of the time interval between sferics for the data used in Fig. 1. Other data indicate that the interval distribution varies as the sferic rate changes, regardless of variations in storm location.

R. F. Linfield
DECO Electronics, Inc.
Boulder, Colo.
C. A. Samson
Central Radio Propagation Lab.
National Bureau of Standards
Boulder, Colo.

RMS Currents in Variable-Width Pulse (VWP) Power Supply Circuits*

The use of "chopping techniques" employing variable-width pulse (VWP) methods for controlling and regulating dc power is becoming increasingly common in electronic applications. An important parameter in a VWP circuit is the rms current flowing. Herein is described a simple method for determining rms currents by means of measuring certain dc currents only.

In Fig. 1 is shown a common embodiment of the basic VWP circuit, employing a variable-width pulse for output-voltage control and regulation. The dc input E_1 is greater than the required dc output E_2. Power transistor Q_1 is turned on and off at a fixed frequency corresponding to a period T. The time t that the transistor is turned on is varied to give pulses of variable widths. Similar action may be obtained with SCR's, but turn-on turn-off circuits are more complicated than with transistors.

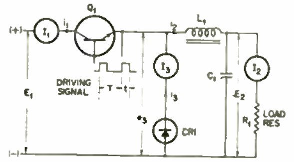

Fig. 1—Basic VWP circuit.

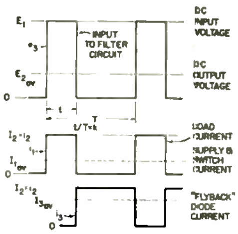

Fig. 2—Voltage and current waveforms of VWP circuit.

Fig. 2 shows major voltage waveforms and the corresponding current waveforms. It is assumed that L_1 of Fig. 1 is large, the load current ripple is small, and essentially constant current flows through L_1. Accordingly,

$$i_2 = I_2 = I_2\,\text{av} = I_2\,\text{peak}. \qquad (1)$$

Under these conditions, the average dc value of the voltage wave e_3 appears across the output capacitor C_1. Therefore, the output voltage is equal to the average of the variable-width rectangular wave shown in Fig. 2. Hence,

$$E_2 = E_2\,\text{av} = kE_1, \qquad (2)$$

where

$$k = t/T. \qquad (3)$$

By varying k, the output voltage can be controlled and regulated.

* Received January 8, 1962; revised manuscript received March 2, 1962.

Normally, instrumentation is not readily available for accurate rms measurements over wide ranges of pulsed currents, operating frequencies, etc; further, when the instruments are available, they are usually of the thermocouple type, and sensitive to damage if overloaded.

For rectangular pulses of current, as shown in Fig. 2, rms measurements need NOT be made; dc average current measurements will suffice. The rms current in Q_1 is given by

$$I_1 = \sqrt{I_1 \text{ av} \times I_2 \text{ av}}, \qquad (4)$$

i.e., the value of the duty cycle also need NOT be measured.

This is proved as follows:

From Fig. 2 it is apparent that

$$I_1 \text{ av} = kI_2. \qquad (5)$$

However, the rms value of a rectangular wave is given by

$$\text{Irms} = I = \sqrt{k}\, I \text{ peak}. \qquad (6)$$

But from (5) it is determined that

$$k = \frac{I_1 \text{ av}}{I_2}. \qquad (7)$$

Using (1), and substituting (7) into (6) gives:

$$I_1 = \sqrt{\frac{I_1 \text{ av}}{I_2 \text{ av}}} \times I_2 \text{ av}$$

$$= \sqrt{I_1 \text{ av} \times I_2 \text{ av}}, \text{ Q.E.D.} \qquad (8)$$

The average value of the current in CR1 is given by

$$I_3 \text{ av} = I_2(1 - k). \qquad (9)$$

This *average value* is determined from Kirchhoff's Law, that the algebraic sum of all currents at a point must be equal to 0.

The rms current is similarly determined, and is given by, using (1) and (8),

$$I_3 = \sqrt{I_2^2 - I_1^2} = \sqrt{I_2^2 - I_1 \text{ av} \times I_2 \text{ av}}$$

$$= \sqrt{I_2(I_2 - I_1 \text{ av})}. \qquad (10)$$

In higher power circuits, and in circuits requiring isolation between the output and input and/or a higher output voltage than input voltage, a transformer must be employed, as shown in Fig. 3. If N is the ratio of secondary voltage to primary voltage, then the following relationships can be shown to exist:

$$I_1 \text{ av} = kNI_2. \qquad (11)$$

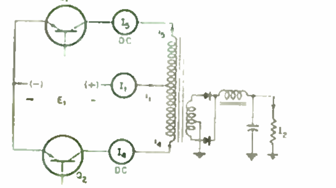

Fig. 3—VWP circuit with output transformer.

For the rms current from the dc source

$$I_1 = \sqrt{I_1 \text{ av} \times I_2 \times N}. \qquad (12)$$

For the rms switching devices' currents, assuming balanced conditions,

$$I_4 = I_5 = \sqrt{\frac{I_1 \text{ av} \times I_2 \times N}{2}}. \qquad (13)$$

V. Wouk
E. Poss
Electronic Energy Conversion Corp.
New York, N. Y.

Gain of Multisampler Systems*

Two recent notes[1,2] have presented methods for obtaining the output of multisampler systems. I believe the method presented here is simpler than the preceding two since it consists of only one step—writing the answer.

Given the system block diagram, first imagine that all samplers are closed (or that the system is continuous). Since block diagrams are only trivially different from signal flow graphs, Mason's technique may be applied directly to the block diagram. Each path is traversed in the normal manner set down by Mason. The multisampled character of the system is accounted for by writing an asterisk each time a sampler is traversed. If desired, a viniculum can be placed above all terms between this asterisk and the one preceding it to indicate that the sampler operates on the product of these terms. In writing a loop gain, the starting point must be the output of a sampler.

This simple technique is applicable under the following conditions. If interest is centered on the system's loop subgraph, two conditions are of interest in evaluating the gain of these isolated "subsystems." 1) The "subsystem" contains no loops which possess continuous (unsampled) paths from the output of a sampler in a feedback path to the output node of the "subsystem." 2) There exist such paths, but the samplers in question operate on the output of the "subsystem."

If condition 1) applies, the discrete and continuous output of the system can be written as explained above. The last example given by Lendaris[2] satisfies this requirement and can therefore be solved by inspection. If condition 2) applies, only the discrete system output can be found in this manner. However the continuous output can still be determined by inspection using Tou's results as follows:

First open all samplers which violate condition 1). Apply Mason's rules to determine the output response due to input signals. To this result add a term of the form GB^*/Δ^* where G is the sum of the continuous gains from the output of each opened sampler to the "subsystem" output, B^* is the sum of the Z-transforms of the signals appearing at these open samplers due to the various inputs, and Δ^* is the sampled determinant found from the loop gains involving the open samplers. (It is assumed that all samplers in the feedback path have a common node.)

For a system having many loops with all of the above conditions violated, the technique proposed in this note would provide a graph reduction process for arriving at a solution.

George C. Reis
Dept. of Electrical Engineering
Drexel Institute of Technology
Philadelphia, Pa.

* Received February 20, 1962.

[1] J. T. Tou, "A simplified technique for the determination of output transforms of multiloop, multisampler, variable-rate discrete data systems," Proc. IRE (*Correspondence*), vol. 49, pp. 646–647; March, 1961.

[2] G. C. Lendaris, "Input-output relationships for multisampled loop systems," Proc. IRE (*Correspondence*), vol. 49, p. 1709; November, 1961.

A Theorem for the Construction of Root Loci*

Theorem: Given any two polynomials in s with real coefficients: $D(s)$ and $N(s)$ and a constant K. Let $z_1 z_2 \cdots z_n$ denote all the roots of $N(s)$, and $p_1 p_2 \cdots p_m$ denote all the roots of $D(s)+KN(s)$. The degree of $D(s)$ is higher than that of $N(s)$, $m>n$. Then

$$\prod_{i=1}^{i=m} (z_j - p_i) = C_j \qquad j = 1, 2 \cdots n \qquad (1)$$

where $C_1 C_2 \cdots C_n$ are constants independent of K.

Proof: Let A_0 denote the coefficient of s^m in $D(s)$. Then

$$D(s) + KN(s) = A_0 \prod_{i=1}^{i=m} (s - p_i). \qquad (2)$$

Substituting z_j for s in the above equation gives

$$D(z_j) + KN(z_j) = A_0 \prod_{i=1}^{i=m} (z_j - p_i). \qquad (3)$$

Because $N(z_j)=0$ by definition of z_j, (3) is reduced to (1) with $C_j = D(z_j)/A_0$.

The practical significance of the above theorem is that using (1) and other known rules of root-loci plot, a complete set of poles for a given gain can usually be determined directly from the root loci without making extensive algebraic calculations.

A special case of application is to evaluate the vector separation of a closed-loop pole-zero pair. Control systems usually have zeros closer to the origin than the "control poles," and invariably these zeros draw closed-loop poles to their vicinity to form pole-zero pairs. As the latter poles are in the near zone of origin, they are liable to introduce long error tails in the transient response of the closed-loop system. The magnitude of an error tail is directly proportional to the separation of the zero from the pole which gives rise to it.

Another special application is in the synthesis of optimum systems satisfying a quadratic criterion (least mean-square error with limited mean-square control effort, etc.). It

* Received by the IRE, January 15, 1962.

has been shown that the optimum closed-loop system function is related to the transfer function of the controlled plant by a root-square locus plot (root-locus plot in the ω^2 plane).[1] The above theorem helps to reduce the most difficult part of the synthesis procedure (finding the optimum closed-loop system function) to a completely graphical basis.

S. S. L. CHANG
New York University
New York, N. Y.

[1] S. S. L. Chang, "Synthesis of Optimum Control Systems," McGraw-Hill Book Co., Inc., New York, N. Y.; ch. 2; 1961.

Noise Figure of Moody and Wacker's Broad-Band Tunnel Diode Amplifier*

It is the aim of this note to determine the noise figure of Moody and Wacker's broad-band tunnel diode amplifier.[1] An n-stage amplifier is shown in Fig. 1. A tunnel diode of negative resistance $-R_n$ is connected between each two adjacent filter sections. The characteristic impedance of the ith filter section is chosen such that[2]

$$\frac{1}{R_{0i}} = \frac{1}{R_{01}} + \frac{(i-1)}{R_n} \quad (i = 1 \cdots n+1). \quad (1)$$

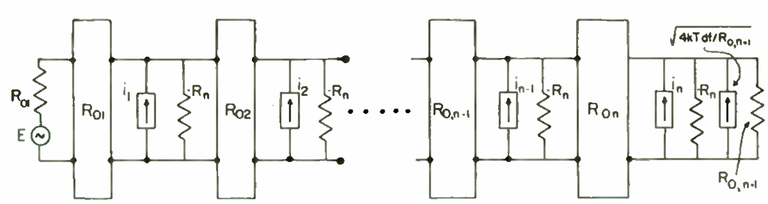

Fig. 1.

The mean-square noise output due to the source is

$$kTdfR_{01}. \quad (2)$$

Let the noise of the diodes be represented by current generators $i_1 \cdots i_n$. If all diodes are identical, have a current I_d, and show full shot noise, then

$$\overline{i_1^2} = \overline{i_2^2} = \cdots = \overline{i_n^2} = 2eI_d df. \quad (3)$$

The ith diode looks into an impedance consisting of the resistances R_{0i}, $-R_n$ and $R_{0,i+1}$ connected in parallel and hence it sees the total resistance $\frac{1}{2}R_{0i}(i=1, \cdots, n)$. Each diode gives instantaneously a voltage $\frac{1}{2}i_iR_{0i}$ at its location in the filter chain and hence a voltage wave $\frac{1}{2}i_iR_{0i}$ flows from the left to the right. There is also a voltage wave flowing from the right to the left and that wave is partially reflected at all the interconnections between the ith diode and the source.

The reflection coefficient at the ith interconnection is

$$\frac{(1/R_{0,i+1}) - (1/R_{0,i} - 1/R_n)}{(1/R_{0,i+1}) + (1/R_{0,i} - 1/R_n)} = \frac{R_{0i}}{R_n} \quad (4)$$

and hence a wave $\frac{1}{2}i_iR_{0i}$ generated at the ith interconnection gives rise to a reflected wave $\frac{1}{2}i_iR_{0i}(R_{0,i-1}/R_n)$ at the previous interconnection and to a wave $\frac{1}{2}i_iR_{0i}(1+R_{0,i-1}/R_n)$ continuing to the left. The total wave coming back to the load, if ϕ is the phase angle due to the travel back and forth along one filter section, is therefore

$$\begin{aligned}
&\frac{1}{2}i_iR_{0,i} + \frac{1}{2}i_iR_{0i}\left(\frac{R_{0,i-1}}{R_n}\right)\cos\phi \\
&+ \frac{1}{2}i_iR_{0i}\left(1+\frac{R_{0,i-1}}{R_n}\right)\left(\frac{R_{0,i-2}}{R_n}\right)\cos 2\phi + \cdots \\
&\quad \frac{1}{2}i_nR_{0i}\left(1+\frac{R_{0,i-1}}{R_n}\right)\left(1+\frac{R_{0,i-2}}{R_n}\right)\cdots \\
&\quad \cdot\left(1+\frac{R_{02}}{R_n}\right)\frac{R_{01}}{R_n}\cos(i-1)\phi \\
&= \frac{1}{2}i_iR_n\left[\frac{R_{0i}}{R_n} + \frac{R_{0i}}{R_n}\frac{R_{0,i-1}}{R_n}\cos\phi\right. \\
&\quad + \frac{R_{0,i-1}}{R_n}\frac{R_{0,i-2}}{R_n}\cos 2\phi + \cdots \\
&\quad \left.+ \frac{R_{02}}{R_n}\frac{R_{01}}{R_n}\cos(i-1)\phi\right] \qquad (5)
\end{aligned}$$

since $(1+R_{0i}/R_n) = R_{0i}/R_{0,i+1}$.

Hence the noise figure F is:

$$\begin{aligned}
F = 1 &+ \frac{e}{2kT}I_dR_n\left(\frac{R_n}{R_{01}}\right)\left[\left(\frac{R_{01}}{R_n}\right)^2\right. \\
&+ \left(\frac{R_{02}}{R_n} + \frac{R_{02}}{R_n}\frac{R_{01}}{R_n}\cos\phi\right)^2 + \cdots \\
&+ \left(\frac{R_{0n}}{R_n} + \frac{R_{0n}}{R_n}\frac{R_{0,n-1}}{R_n}\cos\phi + \cdots\right. \\
&\left.\left.+ \frac{R_{02}}{R_n}\frac{R_{01}}{R_n}\cos(n-1)\phi\right)^2\right] \qquad (6)
\end{aligned}$$

If the noise contribution of the load resistance $R_{0,n+1}$ is taken into account, one obtains a noise figure

$$\begin{aligned}
F_L = F &+ \frac{T_L}{T}\frac{R_n^2}{R_{0,n+1}R_{01}} \\
&\cdot\left[\frac{R_{0n}}{R_n} + \frac{R_{0n}}{R_n}\frac{R_{0,n-1}}{R_n}\cos\phi + \cdots\right. \\
&\left.+ \frac{R_{02}}{R_n}\frac{R_{01}}{R_n}\cos(n+1)\phi\right]^2 \qquad (7)
\end{aligned}$$

where T_L is the noise temperature of the load.

At low frequencies $\phi=0$, and F_L may be written

$$\begin{aligned}
F_L &= (F_L)_{l.f.} \\
&= 1 + Mn\frac{R_{01}}{R_n} + \frac{T_L}{T}\left(1+n\frac{R_{01}}{R_n}\right) \qquad (7a)
\end{aligned}$$

where $M = eI_dR_n/(2kT)$ is the noise measure of the tunnel diode.

The low-frequency noise figure thus increases linearly with n and is quite large. The high-frequency noise figure is somewhat better, because of the destructive interference of waves coming from the same noise source.

A. VAN DER ZIEL
Elec. Engrg. Dept.
University of Minnesota
Minneapolis, Minn.

* Received by the IRE, December 22, 1962; revised manuscript received, January 8, 1962.

[1] N. F. Moody and A. G. Wacker, "Broad-band tunnel diode amplifier," PROC. IRE, vol. 49, p. 835; April, 1961.

[2] This means that the line is matched at all interconnections for waves going from the left to the right.

Parametric Machines*

It seems that Stockman has rediscovered the reluctance motor[1] and its dual, the electrostatic motor.[2] These elementary machine types are used to introduce the subject of electromechanical energy conversion in at least one modern text book.[3]

Insofar as an electromechanical machine or transducer can be viewed from its electrical terminals as composed of circuit parameters R, L, and C, every case of electromechanical energy conversion may be explained by the time variation of L or C. (Though in the case of the homopolar machine, a stretch of the imagination is necessary.) Variation of the particular parameter is due to motion of one portion of the device with respect to another. Variation of a reactive (energy storage) element is required because the mechanical and electrical systems are coupled by an electric or magnetic field, the energy of which is the medium of exchange. Thus, all electromechanical machinery may be termed "parametric." This circuit viewpoint is not the most fundamental, but it is most convenient for the sake of analysis.

D. J. HANRAHAN
Energy Conversion Branch
U. S. Naval Res. Lab.
Washington, D. C.

Author's Comment[4]

As will be evident from the following, I have not "rediscovered" the reluctance and electrostatic motors, and I shall be glad to explain the difference between my parametric time-constant motors and the motor types described in the Fitzgerald and Kingsley textbook.[3] Actually, my motors have

* Received January 8, 1962.

[1] H. E. Stockman, "Parametric oscillatory and rotary motion," PROC. IRE (*Correspondence*), vol. 48, pp. 1157–1158; June, 1960.

[2] H. E. Stockman, "Parametric variable-capacitor motor," *ibid.*, vol. 49, pp. 970–971; May, 1961.

[3] A. E. Fitzgerald and C. Kingsley, Jr., "Electric Machinery," McGraw-Hill Book Co., Inc., New York, N. Y.; 1952.

[4] Received January 19, 1962.

very little in common with the old motor types as far as basic theory goes. This becomes apparent from a study of the instantaneous torque equation for the old motor,

$$T = -\,\text{const.}\,\phi^2 \frac{d\mathcal{R}}{d\alpha}\cdot \tag{1}$$

where ϕ is the instantaneous flux, $\mathcal{R}$ the reluctance, and α associated with rotor angular deviation. T switches sign with the derivative, so that synchronous operation with $\omega_{\text{lines}} = \omega_{\text{rotor}}$ is the only possibility in the basic case. No average torque is produced at any other speed (except for harmonic effects). Eq. (1) also shows that the old motor lacks dc torque and therefore is not self-starting. The maximum average torque expression

$$T_{\max} = \text{const.}\,\phi^2_{\max}(\mathcal{R}_Q - \mathcal{R}_D) \tag{2}$$

spells out the unfortunate limitation of the old motor that if $T_{\max}$ is exceeded by the torque requirement of the mechanical loading, loss of motor action and shutdown results. My time-constant motor behaves quite differently since it is an *ASYNCHRONOUS* motor, not intended for operation in a synchronous state. Accordingly, the reluctance rate of change is largely independent of ω_{line}, and if the lines frequency were to be suddenly increased from 60 to 70 cps, as an experiment of thought, the old motor would fall out of synch, while my motor merely would slow down, and then continue at constant speed. Similarly, mechanical overload makes my motor slow down, while in accordance with (2), it makes the old motor fall out of synch. Further, my motor is self-starting, except for one peculiar position of the rotor; a defect that can be remedied. These striking differences are logical in view of the fact that the quoted textbook, on page 89, claims that it is discussing a synchronous machine of reluctance type, while my motor is an asynchronous machine of time-constant type. In essence, the time-constant motor is a brushless dc motor, using an ac carrier supply as dc substitute in about the same fashion as a magnetic amplifier. It extracts its driving torque from the double-valued force-function established by the time constant; a phenomena totally different from that causing the torque in the old motor. Any suspicion that my motor is a rediscovery of an old motor is unfounded, at least as far as a comparison with the old reluctance motor goes. The same is true in a comparison of my electric field version asynchronous motor with the electric field synchronous motor described in the quoted textbook, which correctly claims that the analysis of its electrostatic machine parallels that of its electromagnetic machine.

Within the ramifications of his note, Hanrahan states without any verification that every case of electromagnetic energy conversion may be explained by the time variation of L and C, that variation of a reactive element is required, and that all electromechanical machinery may be termed "parametric." That these opinions are unjustified is indicated by the fact that if a fundamental law were to be formulated, it would be just the opposite of what is claimed by Hanrahan: "Parametric action is *NOT* a necessary requirement for energy conversion." This is amply demonstrated by a commercially available motor, shown in principle with its equivalent two-terminal network in Fig. 1.[5] This motor is parametric in a quantity not even included as a possibility in Hanrahan's statement, namely R. It consists of a spinning magnet NS, which via a smaller magnet ns activates the variational resistance device M, which functions like a carbon mike. The produced ac drives via the inductor L the nonsalient pole magnetic disk D. There is no intended or essential change in any storage element, but still the device converts electrical energy to mechanical energy, and quite successfully, too. If the variational resistance device M is replaced by a brush and a contact element, a nonparametric motor results, demonstrating the most fundamental fact that we can do without parametric action in energy conversion, if we so wish.

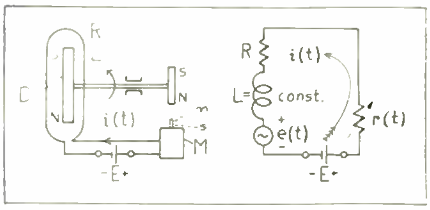

Fig. 1.

HARRY E. STOCKMAN
Lowell Tech. Inst.
Lowell, Mass.

[5] Made by SINE-SER Co., Waltham, Mass.

Dependence of Parametric Element Nonlinearity on Tuning Circuit*

In a recent letter on the behavior of the nonlinearity in a parametric device employing a capacitor, Helgesson[1] states that the difference produced by series and parallel tuning affects only the second and higher order nonlinear terms and leaves the first unchanged. This is correct only for low-level pumping in which the diode is swept through a small portion of its characteristic. Helgesson's Eq. (5), which compares the proportional reactance sweep in the series tuned circuit with the proportional susceptance sweep in the parallel tuned circuit, assumes an approximate linear relation between charge and voltage which is invalid for high-level pumping. It will be shown below that under these conditions considerable advantage can be obtained by using a series tuned high-impedance terminated circuit.

The standard method of analyzing each of the dual arrangements is identical but for the interchange of δq, the incremental charge on the nonlinear capacitor, and δv, the incremental voltage, and starts from a power series of δq in terms of δv for the parallel tuning and δv in terms of δq for the series tuning. These series can be conveniently compared if they are expressed in terms of the dimensionless quantities $\delta q/q_0$ and $\delta v/v_0$, the charge q_0 and the voltage v_0 corresponding to the operating point and being measured with respect to the point of infinite ac capacitance.

Assuming the static characteristic to be of the form

$$q = kv^{(1-n)}, \tag{1}$$

one obtains

$$\delta q/q_0 = (1-n)\{\delta v/v_0 + (n/2!)(\delta v/v_0)^2 + \cdots\} \tag{2}$$

$$\delta v/v_0 = (1-n)\{dq/q_0 - \frac{n}{2!(1-n)}(\delta q/q_0)^2 + \cdots\} \tag{3}$$

for the series and parallel tuning respectively. With these variables the second expansion has the greater nonlinearity. In each case the maximum gain-bandwidth gB of the amplifier is given by the ratio of the second to the first term. Thus

$$gB = (n/2)(\delta v/v_0) \tag{4}$$

for parallel tuning, and

$$gB = \frac{n}{2(1-n)}\frac{(\delta q)}{(q_0)} \tag{5}$$

for series tuning.

Hence, provided $\delta q_{\max}/q_0$, the maximum fractional charge excursion, is not less than $(1-n)\delta v_{\max}/v_0$ the series tuning will be preferable. This can be shown to be true as follows.

A typical voltage charge characteristic is shown in Fig. 1, upper and lower limits of satisfactory operating voltage, v_2 and v_1, being indicated. These might correspond to the points of reverse breakdown and forward conduction respectively. The whole range between v_1 and v_2 may be utilized if the parallel tuned amplifier is biased to a voltage $(v_1+v_2)/2$ and the series tuned amplifier to a charge of $(q_1+q_2)/2$. The corresponding maximum voltage and charge excursions are given by

$$\delta v_{\max}/v_0 = (1 - v_1/v_2)/(1 + v_1/v_2) \tag{6}$$

$$\begin{aligned}\delta q_{\max}/q_0 &= (1 - q_1/q_2)/(1 + q_1/q_2)\\ &= \{1 - (v_1/v_2)^{1-n}\}/\{1 + (v_1/v_2)^{1-n}\}.\end{aligned} \tag{7}$$

Investigation of these shows that as v_1/v_2 varies from unity (small allowable capacitance variation) to zero (maximum allowable capacitance variation) $(\delta q_{\max}/q_0)/(\delta v_{\max}/v_0)$ varies from $1-n$ to unity. Hence from (4) and (5), the ratio of the gain bandwidth of the two amplifier arrange-

* Received January 15, 1962.

[1] A. L. Helgesson, "Nonsymmetrical properties of nonlinear elements in low- and high-impedance circuits," PROC. IRE (*Correspondence*), vol. 49, p. 1569; October, 1961.

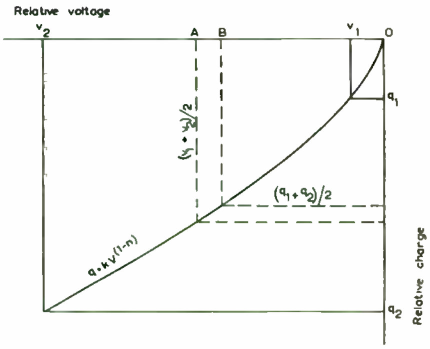

Fig. 1—Voltage-charge characteristic of nonlinear capacitance showing limits of operation and biasing points.

ments varies from unity for small pumping to $1-n$ for large pumping always in favor of the series tuned layout.

G. H. B. THOMPSON
Standard Telecommun. Labs., Inc.
Harlow, Essex, England

Author's Reply[2]

Thompson has raised a very good point, with which the author fully agrees. Series and parallel tuning are compared for equal bias conditions,[1] but as Thompson shows, optimum pumping is achieved in each case for different bias points. For $0<n<1$, the optimum bias point for series tuning is always in a region of higher nonlinearity, resulting in larger gain-bandwidth product.

It is interesting to compare the maximum pumping obtainable from abrupt and graded junction varactors in series and parallel resonant circuits. In parallel tuning, $\Delta C_B/C_B$ is determined from (4) of Helgesson[1] with $|\nu(t)| = \phi - V_B$, and $\Delta S_B/S_B$ for series tuning is computed from this by using Thompson's improvement factor of $1/(1-n)$.

	$n=\frac{1}{2}$	$n=\frac{1}{3}$
Parallel Tuning $(\Delta C_B/C_B)_{\max}$	$\frac{1}{4}$	$\frac{1}{6}$
Series Tuning $(\Delta S_B/S_B)_{\max}$	$\frac{1}{2}$	$\frac{1}{4}$

Of the four combinations, the series tuned circuit with an abrupt junction varactor has the highest gain-bandwidth capability in addition to the elimination of the higher order perturbations mentioned previously. Series tuning has the additional advantage that in the frequency regions of greatest interest at present, the source of loss in the varactor is series resistance, and the second harmonics and other mixing products are prevented from dissipating power in this resistance because of the high impedance termination at these frequencies. For parallel tuning, these frequencies cannot be completely short circuited, and they develop some voltage across the capacitance and dissipate some loss in the series resistance.

There is, however, one minor disadvantage of series tuning that has not been mentioned to date. When the charge voltage expansions are derived with the dc terms included,[3] it can be seen that average elastance is a function of the magnitudes of the ac charges. This has two effects in the circuit. The first is that the optimum bias voltage is not determined, as might be incorrectly inferred from point B of Thompson's diagram, by taking the voltage corresponding to the average charge. Because of the shift in bias charge due to the pumping, the average charge is not uniquely determined by the bias voltage. In Thompson's notation, if $V_1=0$ and $n=\frac{1}{2}$, point A is $V_2/2$ and point B is $V_2/4$. It can be shown that the optimum bias voltage for series tuning is $\frac{3}{8}V_2$.

The second effect produced by the average-charge shift is that the average elastance is a function of the signal amplitude. This produces a slight phase distortion which may be important in systems that require phase coherence. However, this perturbation can be shown to be about a factor of 3 less than that produced by the third-order term for parallel tuning, as calculated from (6) of Helgesson.[1] [Eqs. (6) and (7) of this reference are in error. The right-hand sides of both should be multiplied by ω_i.]

In summary, the case for series tuning appears to be well established.

ALAN L. HELGESSON
Sylvania Elec. Products, Inc.
Waltham, Mass.

[2] Received January 30, 1962.

[3] A. L. Helgesson, "Varactor charge-voltage expansions for large pumping conditions," this issue, same page.

Varactor Charge-Voltage Expansions for Large Pumping Conditions*

In a previous correspondence,[1] charge-voltage expansions for a varactor were derived for small ac variations about a fixed bias point. The purpose of this correspondence is to extend these results to the large pumping case by deriving the complete expansions with the inclusion of the dc terms. It will be shown that (2) of Helgesson is valid under large-pumping conditions, but that (3) must be modified. From these new expansions, the dependence of the average charge and the average elastance on the magnitudes of the ac variations is calculated.

The expression for the derivative of the total charge as a function of the total voltage,

$$\frac{dQ}{dV} = C_0\left[1 - \frac{V}{\phi}\right]^{-n}, \tag{1}$$

is integrated, and the boundary condition that Q is zero when V is zero is imposed, giving

$$Q = \frac{C_0\phi^n}{1-n}\left[\phi^{1-n} - (\phi - V)^{1-n}\right]. \tag{2}$$

This is the fundamental equation relating charge and voltage on the varactor.

CHARGE EXPANSION

We are now separate dc and ac components and define

$$Q(t) = Q_{\text{ave}} + q(t)$$
$$V(t) = V_{\text{ave}} + v(t) \tag{3}$$

where $q(t)$ and $v(t)$ have zero mean. For the first expansion, we will consider the case in which the circuitry external to the varactor restricts the average voltage to be equal to that of a bias supply

$$V_{\text{ave}} = V_B, \tag{4}$$

and allows $v(t)$ to consist of only a small finite number of sinusoidal components

$$v(t) = \sum_{k=1}^{K} |V_k| \cos(\omega_k t + \theta_k). \tag{5}$$

For this case we write (2) in the form

$$Q_{\text{ave}} + q(t) = \frac{C_0\phi^n(\phi - V_B)^{1-n}}{1-n} \cdot\left[\left(\frac{\phi}{\phi - V_B}\right)^{1-n} - \left(1 - \frac{v(t)}{\phi - V_B}\right)^{1-n}\right] \tag{6}$$

and expand into the series

$$\begin{aligned} Q_{\text{ave}} + q(t) &= \frac{C_0\phi^n}{1-n}\left[\phi^{1-n} - (\phi - V_B)^{1-n}\right] \\ &+ C_B\left[v(t) + \frac{nv^2(t)}{2!(\phi - V_B)} + \frac{n(n+1)v^3(t)}{3!(\phi - V_B)^2} + \frac{n(n+1)(n+2)v^4(t)}{4!(\phi - V_B)^3} + \cdots\right] \\ &= Q_B + C_B v(t) + \mathfrak{C}_a v^2(t) + \mathfrak{C}_b v^3(t) + \cdots \end{aligned} \tag{7}$$

where the average capacitance as determined by the bias voltage is

$$C_B = \frac{C_0\phi^n}{(\phi - V_B)^n}. \tag{8}$$

Inspection of (7) shows that average charge is not completely determined by the bias voltage, but has a component dependent upon the magnitides of the ac voltages. Writing

$$Q_{\text{ave}} = Q_B + Q_{\text{ac}} \tag{9}$$

the first term in (7) gives the charge due to the bias voltage

$$Q_B = \frac{C_0\phi^n}{1-n}\left[\phi^{1-n} - (\phi - V_B)^{1-n}\right] \tag{10}$$

and the contribution from the ac voltages is

$$Q_{\text{ac}} = C_B\left[\frac{n}{2!(\phi - V_B)}\,\frac{1}{2}\sum_{k=1}^{K} V_k^2 + \frac{n(n+1)(n+2)}{4!(\phi - V_B)^3}\,\frac{3}{8}\sum_{k=1}^{K} V_k^4 + \cdots\right]. \tag{11}$$

In this case the fact that the average charge changes with the magnitudes of the ac voltages is only of academic interest, since all constants multiplying powers of $v(t)$ in (7) are determined by the bias voltage, and the circuit properties of the device are independent of the average charge. Eq. (2) of Helgesson[1] is therefore valid for large pumping, except that it contains the additional average charge Q_{ac}.

* Received January 30, 1962.

[1] A. L. Helgesson, "Nonsymmetrical properties of nonlinear elements in low- and high-impedance circuits," PROC. IRE (*Correspondence*), vol. 49, pp. 1569–1570; October, 1961.

Voltage Expansion

For the second expansion we consider the case in which the ac charge variation is restricted to consist of a small finite number of sinusoidal components.

$$q(t) = \sum_{k=1}^{K} |Q_k| \cos(\omega_k t + \theta_k). \tag{12}$$

It would be most desirable if we could simultaneously impose a restriction on the average charge, but unfortunately, dc charge sources are not available. Instead, biasing of the device must be done with a voltage source and the constraint on the average value is again given by (4).

Solving (2) for V in terms of Q gives

$$V = \phi - \left[\phi^{1-n} - \frac{Q(1-n)}{C_0\phi^n}\right]^{1/(1-n)}. \tag{13}$$

There are several expansions that can be made in this mixed system of constraints. The one that leads to the most convenient form for the circuit equations is obtained by writing (13) in the form

$$V_B + v(t) = \phi - \left[\left(\phi^{1-n} - \frac{Q_B(1-n)}{C_0\phi^n}\right) - \frac{[Q_{ac} + q(t)](1-n)}{C_0\phi^n}\right]^{1/(1-n)}, \tag{14}$$

recognizing from (10) that

$$\phi^{1-n} - \frac{Q_B(1-n)}{C_0\phi^n} = (\phi - V_B)^{1-n}, \tag{15}$$

and expanding as

$$\begin{aligned} V_B + v(t) &= V_B + \frac{Q_{ac} + q(t)}{C_B} - \frac{n[Q_{ac} + q(t)]^2}{2!(\phi - V_B)C_B^2} \\ &\quad - \frac{(1-2n)n[Q_{ac} + q(t)]^3}{3!(\phi - V_B)^2 C_B^3} - \cdots \\ &= V_B + S_B[Q_{ac} + q(t)] - S_a[Q_{ac} + q(t)]^2 \\ &\quad - S_b[Q_{ac} + q(t)]^3 - \cdots. \end{aligned} \tag{16}$$

This is the complete form for (3) of Helgesson.[1] The solution for Q_{ac} may be made by noting that $v(t)$ has zero average value so that

$$\frac{Q_{ac}}{C_B} - \frac{n\left[Q_{ac}^2 + \frac{1}{2}\sum_{k=1}^{K}|Q_k|^2\right]}{2!(\phi - V_B)C_B^2} - \frac{(1-2n)nQ_{ac}^3}{3!(\phi - V_B)^2 C_B^3} - \cdots = 0. \tag{17}$$

In general, the solution of this equation is difficult because it is of high order in Q_{ac}. However, the case of greatest practical interest is fortunately that for which $n=\frac{1}{2}$, for which the equation reduces to a quadratic. The average charge contributed by the ac variations is then

$$Q_{ac} = 2(\phi - V_B)C_B \cdot \left[1 - \sqrt{1 - \frac{1}{8(\phi - V_B)^2 C_B^2}\sum_{k=1}^{K}|Q_k|^2}\right]. \tag{18}$$

For an example of the effect of Q_{ac}, let us consider a three frequency device in which

$$q(t) = \frac{Q_1 e^{j\omega_1 t} + Q_1^* e^{-j\omega_1 t}}{2} + \frac{Q_2 e^{j\omega_2 t} + Q_2^* e^{-j\omega_2 t}}{2} + \frac{Q_3 e^{j\omega_3 t} + Q_3^* e^{-j\omega_3 t}}{2} \tag{19}$$

and

$$\omega_1 + \omega_2 = \omega_3. \tag{20}$$

The voltage component produced at $+\omega_1$, for example, is from (16)

$$\begin{aligned} V_1 &= \frac{Q_1}{C_B} - \frac{Q_{ac}Q_1}{2(\phi - V_B)C_B^2} - \frac{Q_2^* Q_3}{4(\phi - V_B)C_B^2} \\ &= \frac{Q_1}{C_B}\sqrt{1 - \frac{|Q_1|^2 + |Q_2|^2 + |Q_3|^2}{8(\phi - V_B)^2 C_B^2}} \\ &\quad - \frac{Q_2^* Q_3}{4(\phi - V_B)C_B^2}. \end{aligned} \tag{21}$$

The magnitudes of the ac charges change the average elastance of the varactor in each of the three circuits to the value

$$S_{ave} = S_B\sqrt{1 - \frac{|Q_1|^2 + |Q_2|^2 + |Q_3|^2}{8(\phi - V_B)^2 C_B^2}}. \tag{22}$$

The term producing power conversion is unaffected and is determined only by the bias voltage. The elastance shift due to the fixed pump magnitude may be accounted for by proper design, but a small perturbation dependent upon the magnitudes of signal and idler charges will always exist.

To compute the maximum pumping obtainable, we assume that the pump charge is large in comparison to that of the signal and idler, and that the varactor is driven to the point of forward conduction. Setting $V_B + v(t) = \phi$ and $q(t) = |Q_p|_{max}$ in (16) we solve for the pump charge with the help of (18). For $n=\frac{1}{2}$ the result is

$$|Q_p|_{max} = \sqrt{\frac{8}{3}}(\phi - V_B)C_B. \tag{23}$$

The relative elastance change for maximum pumping is

$$\frac{\Delta S_{ave}}{S_{ave}} = \frac{S_a|Q_p|_{max}}{S_{ave}} = \frac{S_B\sqrt{\frac{1}{6}}}{S_B\sqrt{\frac{2}{3}}} = \frac{1}{2}, \tag{24}$$

which is twice the maximum $\Delta C_B/C_B$ obtainable in a parallel-tuned configuration.

If the varactor is not pumped to its maximum value, but is to be driven between a specified upper voltage V_u and a lower voltage V_l, the pumping charge and the proper bias voltage may again be computed from (16) and (18). The general solution is algebraically cumbersome, but if we assume $\phi \approx 0$ the bias voltage is given by the simpler form

$$V_B = \frac{3[V_l + V_u] - 2\sqrt{V_l V_u}}{8}. \tag{25}$$

In addition to presenting the complete forms of the charge-voltage expansions, the important conclusions to be drawn from this analysis are that in the charge controlled configuration, the average charge and average elastance are functions of the ac charge magnitudes, and that more percentage pumping may be obtained than in the voltage controlled circuit.

Alan L. Helgesson
Sylvania Elec. Products Inc.
Waltham, Mass.

A Broad-Band Ku-Crystal Diode Switch*

A broad-band diode switch which can be made to operate over the 12.0 to 17.0 Gc frequency range with a minimum bandwidth of 2 Gc is described in this note. This bandwidth is described here to be an isolation greater than 20 db and insertion loss less than or equal to 1.5 db. The results shown here were taken with a D4151A diode, although from the data it appears that other germanium point contact diodes in suitable packages would work equally well. The D4151A was purposely designed to have the lead inductance and package capacitance one half the value normally found in commercial glass-package germanium diodes. A pill-type package should work equally well in this band.

Because the 1N283 glass diode worked extremely well in waveguide at X band, we initially tried extending the switching action to Ku band with this type diode. Although we obtained definite switching action, it was not too successful. The difference between the isolation and insertion states was only on the order of 5 db above 13 Gc with insertion losses of 4 to 6 db. Obviously this is not a good device for systems applications. Since the 1N283 worked extremely well from 5 Gc to 12.5 Gc, we thought that since the lead inductance and package capacitance were lowered by a factor of two, if the switching states were somehow a function of these parameters, combined with the junction capacitance, switching might be made to occur at higher frequencies with the D4151A diode used as the switching elements.

Studies made at this laboratory on waveguide semiconductor switches from 5 Gc to 12 Gc indicated quite strongly that by reactively loading the diodes, better switching results are obtained. The reason for this appears to be that the diode and the reactive structures act together as a band-pass filter element where the reactive element is sized for the particular frequency range under consideration.

In this frequency range, a single diode element, suitably loaded, gives a 0.9 Gc bandwidth. However, two diode elements suitably loaded and spaced one quarter wavelength apart give substantially better results. The bandwidth is much larger and the switching ratio is improved over the band. Switching ratio is defined as the difference between the isolation and insertion losses in db. The isolation is due to the reactive structure and diode presenting a large reactive impedance which results in the energy being reflected back toward the source. Normally this reflected energy is 1 db down from the incident power, where the 1 db is dissipated across the resistances within the diode.

Fig. 1 shows the results obtained from a one-diode reactive loaded switch. Here the peak occurs at 13.9 Gc, although this peak can be shifted up and down in frequency by suitably changing the reactive loading on the diode. Fig. 2 shows the characteristics of a two-diode switch which is

* Received by the IRE, January 5, 1962.

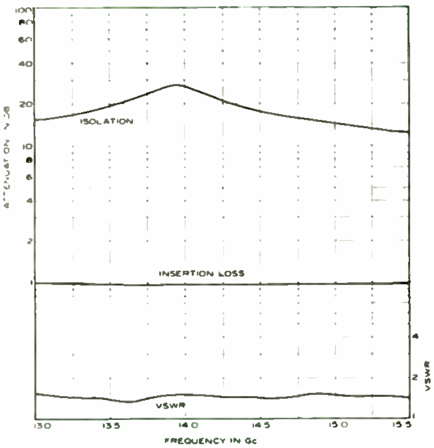

Fig. 1—Characteristics of a single-diode Ku-band switch.

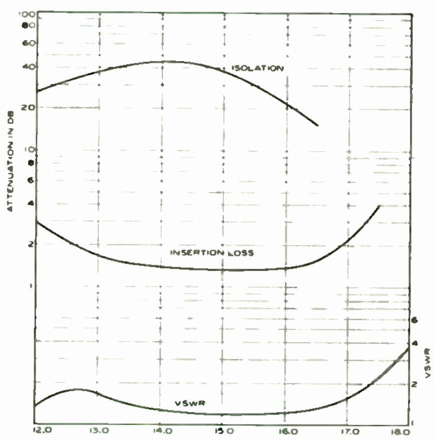

Fig. 2—Characteristics of a two-diode Ku-band switch.

improved over the one-diode switch. The first apparent factor is the increase in the bandwidth which is larger by a factor greater than two. The isolation also increased greatly while the insertion loss increased by a factor somewhat less than two. The insertion losses shown in Figs. 1 and 2 can be greatly reduced because our biasing arrangements are not ideal and some energy is being dissipated in the dc input. For the Ku-band switch reported here, the reactive loading took the form of capacitive elements at the diode position. This loading will vary appreciably with frequency at X and C band for a gold-bonded germanium 1N283, the loading becomes inductive.

The isolation condition shown in Figs. 1 and 2 occurred with the diode biased in the reversed direction at -50 v. At -10-v bias, the isolation is nearly 90 per cent of the value recorded at -50 v. In the insertion direction, the loss is inversely proportional to the forward current; the larger the forward current, the smaller the insertion loss. It is the ability of the diode to handle current that limits the insertion loss since the forward resistance of the diode is the one source of dissipative losses in the diode.

We have not made power tests on this switch, but we expect the switch to propagate an average power of 1 w and a peak power of 150 w at 001 duty cycles. These estimates are derived from an examination of the diode's dc characteristics. These, however, need to be verified. But the feasibility of the switch for low-power receiver applications is obvious where relatively large bandwidths are required We also feel that crystal switches can be extended to higher frequency ranges if careful attention is paid to package design and reactive loading.

The authors would like to acknowledge the assistance of M. Groll of Sylvania, Waltham, Mass., for supplying many diodes.

K. W. Beck
J. J. Rowley
Sylvania Electric Products, Inc.
Microwave Device Division
Mountain View, Calif.

Radiation from a Magnetic Line Dipole Source of Finite Width*

The problem of radiation from a magnetic line dipole source lying in a lossy plane is of great interest since, in addition to radiating components, a surface wave is also launched. What is of importance in this problem is the fact that if the line dipole source is of finite width the surface-wave component can be either reduced to zero, or it can be maximized.

Assume a line dipole source lying in the $y=0$ plane, extending from $z=-\infty$ to $z=+\infty$. For $y>0$, let the medium be characterized by μ_0, ϵ_0, and the medium for $y\leq 0$ by μ, ϵ such that the wave number at the surface $y=0$ is given by $k_s=i\omega\epsilon_0(R_s+iX_s)$ $=2\pi/\lambda_s$. The solution of this problem, normalized for a point source, is given by[1]

$$u(x,y) = -i\pi\left[H_0^{(2)}(kr) - k_s e^{-k_s y}\int_{-\infty}^{y} e^{k_s\eta}H_0^{(2)}(k\rho)d\eta + \frac{2k_s\exp(-k_s y)\exp(-i\sqrt{k^2+k_s^2}\,|x|)}{(k^2+k_s^2)^{1/2}}\right] \quad (1)$$

for harmonic time dependence $e^{i\omega t}$; $u(x,y)=H_z$, and $\partial/\partial z$ was assumed zero; $k^2=\omega^2\mu_0\epsilon_0=(2\pi/\lambda_0)^2$; $H_0^{(2)}(kr)$ are Hankel functions of second kind, and order zero and $r^2=x^2+y^2$, and $\rho^2=x^2+\eta^2$.

The first and second term of (1) represent the source and secondary contribution to the cylindrically radiated field; the last term represents the surface wave. Let us, for the moment, consider this last term alone, and extend the solution to a number of line dipole sources distributed from $x=-d/2$ to $x=d/2$. Assuming that there is no interaction between the sources, and that the sources are in phase, the total contribution to the surface-wave field will be given by

$$U_s = \sum_n u_{sn}[(x - nx_0), y], \quad (2)$$

where x_0 is the distance between neighboring line dipole sources. If there are N sources distributed uniformly over a distance d, (2) can be written as

$$U_s = \sum_{n=-N/2}^{N/2} u_{sn}\left[\left(x-\frac{nd}{N}\right), y\right] \rightarrow \int_{-N/2}^{N/2} u_{sn}\left[\left(x-\frac{nd}{N}\right),\right] y\,dn \quad (3)$$

for large N.

Substitution of the expression for u_{sn}, from (1)

$$u_{sn} = A\exp\left[-i\sqrt{k^2+k_s^2}\left|x-\frac{nd}{N}\right|\right], \quad (4)$$

where

$$A = -\frac{2\pi i k_s}{(k^2+k_s^2)^{1/2}}\exp(-k_s y),$$

and integration between the indicated limits results in

$$U_s\Big|_{|x|>\frac{d}{2}} = NA\frac{\sin B}{B}\exp(-i\sqrt{k^2+k_s^2}\,|x|) \quad (5)$$

$$U_s\Big|_{|x|\leq\frac{d}{2}} = -\frac{NA}{B}\left[1-\cos\left(\frac{2B}{d}x\right)\exp(-iB)\right] \quad (6)$$

where $2B=d(k^2+k_s^2)^{1/2}$. In the limit as $B\rightarrow 0$, (6) reduces to zero, and (5) to the surface wave term due to one line dipole source at (0, 0).

It is evident that for $x>d/2$ the surface-wave term will vanish if $B=\pm m\pi$, $m=1, 2, \cdots$, in which case k_s must be pure real or pure imaginary. There is no value of B for which (5) can be equal to zero in the case of complex k_s. Assuming, then, that k_s is either pure real or pure imaginary,

$$d = \pm\frac{2m\pi}{(k^2\pm k_s^2)^{1/2}} = \pm\frac{m\lambda_0\lambda_s}{(\lambda_s^2\pm\lambda_0^2)^{1/2}} \quad (7)$$

for elimination of the surface-wave term for all values of $x>d/2$. It follows from (1) and (7) that for k_s pure imaginary we actually have a "leaky" surface wave,[2] whereas for k_s pure real we have a "true" surface wave. This must be so, since for $k_s^2<0$ real values of d require $\lambda_s>\lambda_0$, i.e., the phase velocity along the surface will exceed c, the speed of light.

When (7) is satisfied, we obtain from (6)

* Received by the IRE, January 10, 1962.

[1] S. N. Karp, F. Karal, "Surface Waves on a Right Angled Wedge," AF Cambridge Res. Ctr., Bedford, Mass., Tech. Rept. No. AFCRC-58-368; August, 1958.

[2] F. J. Zucker, "The guiding and radiation of surface waves," *Proc. Symp. on Modern Advances in Microwave Techniques*, Polytechnic Inst. of Brooklyn, Brooklyn, N. Y.; November 8-10, 1954.

$$U_s|_{|x|\leq \frac{d}{2}} = -\frac{2NA}{m\pi}\cos^2\left(\frac{m\pi}{d}x\right) \quad (8)$$

representing a standing wave with nodes at $x=\pm d/2m$.

Somewhat similar results are obtained if the individual sources are not fed in phase. If a phase shift

$$\beta_n = \beta_0\left(\frac{d}{2}+\frac{nd}{N}\right)$$

is assumed from source to source

$$U_s|_{|x|>\frac{d}{2}} = NA\frac{\sin D}{D}\exp\left[-i\sqrt{k^2+k_s^2}\,|x|+\frac{\beta_0 d}{2}\right] \quad (9)$$

with $2D=d(\sqrt{k^2+k_s^2}+\beta_0)$. As in the preceding case, the surface wave for $x>d/2$ will disappear for $D=\pm m\pi$, $m=1, 2, \cdots$.

In both cases, the surface-wave term will be a maximum when $d\to 0$. Consequently, it can be concluded that for maximum efficiency in launching a surface wave a source of infinitesimal thickness is required. Furthermore, since in this case k_s must be pure real, a purely inductive surface impedance is required, in agreement with conditions for support of surface waves derived by Barlow and Cullen.[3] When the surface impedance is complex, or pure real, a "leaky" surface wave is obtained. The surface-wave term can be eliminated only if the surface impedance is not complex.

Leon W. Zelby
The Moore School of Electrical Engineering
University of Pennsylvania
Philadelphia, Pa.

[3] H. E. M. Barlow, A. L. Cullen, "Surface waves," *Proc. IEE*, vol. 100, pt. 3, pp. 329–347; November, 1953.

Sensitivity of a Magneto-resistance Wattmeter*

As reported previously,[1,2] it was proved that the magnetoresistance effect in a semiconductor could be used as a wattmeter. Here, the theory has been developed in connection with a Hall-effect wattmeter.

The resistance of a rectangular semiconductor specimen of length l, width w, thickness t under a high magnetic field B as shown in Fig. 1(a) is approximately expressed by

$$R(B) = R(0)\frac{\rho(B)}{\rho(0)}\left\{1+\frac{w}{l}\left(\mu B-\frac{4}{\pi}\ln 2\right)\right\}, \quad (1)$$

* Received by the IRE, January 2, 1962.
[1] S. Kataoka, "Magneto-resistance multiplier with higher gain," Proc. IRE, to be published.
[2] S. Kataoka and S. Kobayashi, "The application of the magnetoresistance effect in an intermetallic semiconductor to the measurement of electric power (Part I. Fundamental)," *Bull. Electrotech. Lab.*, vol. 25, pp. 827–834; November, 1961.

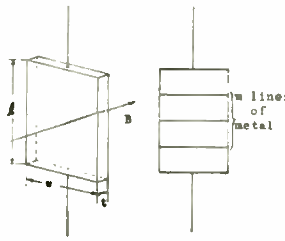

Fig. 1—Semiconductor element. (a) Without metal line. (b) With m metal lines.

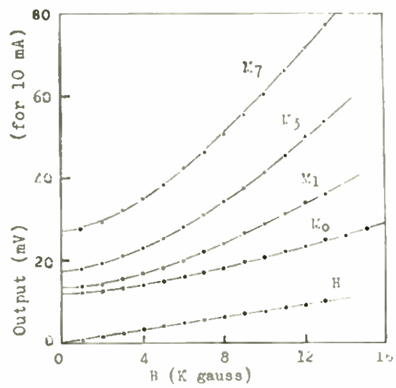

Fig. 2—Galvanomagnetic characteristics of an InAs crystal. H: Hall effect. Mm: Magnetoresistance with m lines of metal.

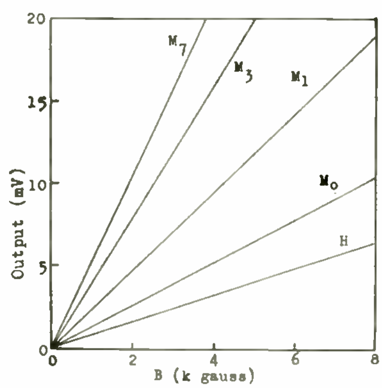

Fig. 3—Output characteristics of a magnetoresistance wattmeter. H: Hall effect. Mm: Magnetoresistance with m lines of metal.

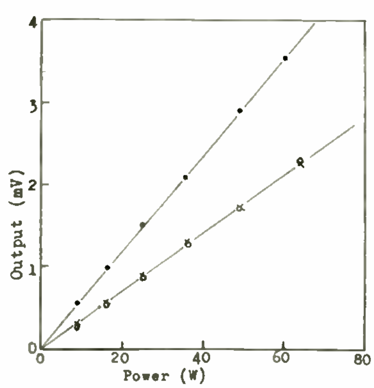

Fig. 4—Output characteristics of a Halltron wattmeter; ○=Hall output, ×=magnetoresistance output (Hall terminals opened), ●=magnetoresistance output (Hall terminals shorted).

where

$R(B)$ = resistance in a magnetic flux density B,

$R(0)$ = resistance without magnetic field,

$\rho(B)$ = resistivity in a magnetic flux density B,

$\rho(0)$ = resistivity without magnetic field,

μ = mobility of charge carriers.

The first term $\rho(B)/\rho(0)$ increases with B^2 and reaches a saturation at high value of B. The second term $\{1+w/l(\mu B-4/\pi\ln 2)\}$ is obtained by analyzing an electric field distortion employing the Schwarz-Christoffel conformal transformation.[3]

Thus, $R(B)$ increases linearly with B at high magnetic field and a voltage drop variation across the semiconductor is proportional to a product of a current I passed through it and a magnetic field variation B', if the semiconductor is biased magnetically at a relatively high magnetic field B_0. At ac, the time-average voltage of the semiconductor is proportional to the active product of B' and I, that is $\bar{v}=KB'I\cos\phi$, to be used as a wattmeter. Here, K, a proportionality constant, represents a sensitivity of the device and can be found by differentiating (1), in considering $R(0)=\rho(0)l/wt$ and $\rho\mu=\Re_H$.

$$K = \frac{dR(B)}{dB} = R(0)\frac{\rho(B)}{\rho(0)}\frac{w}{l}\mu = \frac{\Re_H}{t}, \quad (2)$$

where $\Re_H$ is a Hall coefficient of the semiconductor.

It is quite interesting to note that the sensitivity of a magnetoresistance wattmeter is exactly the same as a Hall-effect wattmeter in so far as the semiconductor element remains the same.

Next, let us consider a case where m lines of metal are attached onto the semiconductor plate as shown in Fig. 1(b). The resistance of such an element is

$$Rm(B) = Rm(0)\frac{\rho(B)}{\rho(0)}\cdot\left\{1+\frac{(m+1)w}{l}\left(\mu B-\frac{4}{\pi}\ln 2\right)\right\}, \quad (3)$$

and the sensitivity of a wattmeter

$$Km = \frac{dRm(B)}{dB} = \frac{(m+1)\Re_H}{t}. \quad (4)$$

This relation leads to a conclusion that the output would be increased by a factor of $(m+1)$.

Fig. 2 shows experimental results of the magnetoresistance and the Hall-effect characteristics of an InAs polycrystal specimen of 8×4×0.1 mm and Fig. 3 the deduced output characteristics of both kinds of wattmeter. Fig. 4 shows the results on output characteristics of a Halltron wattmeter[1,2] in both ways of use.

[3] V. H. J. Lipmann and F. Kuhrt, "Der Geometrieeinfluss auf den transversalen magnetischen Widerstandseffekt bei rechteckförmigen Halbleiterplatten," *Z. Naturforsch.*, Band 13a, pp. 462–474; June, 1958.

All these experimental results seem to verify the above theoretical considerations. The considerable deviation from the theory for large m may be due to the facts that the metallic line has a width of 0.2 mm and that these were soldered on only one side of the specimen.

Shoei Kataoka
Electrotechnical Lab.
Nagata-cho, Chiyoda-ku
Tokyo, Japan

A Tunnel-Diode Wide-Band Frequency Doubling Circuit*

A recent note[1] describes an elegant wide-band frequency doubling circuit which makes use of the fact that the volt-ampere characteristic of a tunnel diode closely approximates a parabola in the region of the peak point. The circuit as described is of limited usefulness because of sensitivity to variations in ambient temperature. The operating point of the tunnel diode is set by the base biasing network of the transistor (Fig. 1). However, the tunnel diode is in the emitter circuit so its bias will change if the emitter-base voltage of the transistor changes. For a silicon transistor V_{eb} has a temperature dependence of approximately -2 mv/°C. Since the peak point of the diode occurs at approximately 55 mv, this shifts the bias of the tunnel diode by -3 per cent/°C. With a signal of 25 mv peak, this shift is approximately 8 per cent of peak swing per °C. Therefore a 1°C temperature change will cause alternate peaks of the output wave to differ in amplitude by as much as 16 per cent (see Fig. 2).

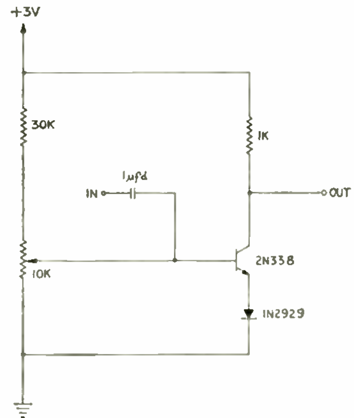

Fig. 1—Neu's frequency doubling circuit.

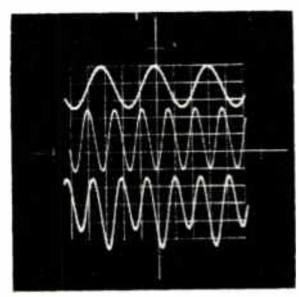

Fig. 2—Top: 800 cps input. Center: 1600 cps output, bias correct. Bottom: 1600 cps output, bias 5 mv offset. Vertical sensitivity: 50 mv/div.

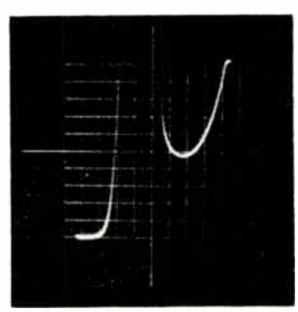

Fig. 3—Transfer characteristic of transistor-tunnel diode combination (peak point is off scale). Horizontal (input): 75 mv/div. Vertical (output): 200 mv/div.

By using forward biased silicon diodes in the bias network to compensate for the temperature dependence of V_{eb}, considerable reduction in temperature sensitivity can be achieved. The biasing diodes should, of course, be in close thermal contact with the transistor. This lowers the input impedance, but not to such an extent as to cause any difficulty in driving the circuit.

Further stabilization can be realized by biasing at the valley point of the tunnel diode. While the tunnel diode characteristic alone is not a good approximation of a parabola at this point, the transfer characteristic of the transistor-tunnel diode combination is (Fig. 3). The gain of the squaring portion of the circuit is lower, but since the quiescent current is lower by a larger factor, slightly more voltage gain is available from the circuit as a whole. An improvement of about a factor of six (=valley point voltage/peak point voltage) in temperature stability results.

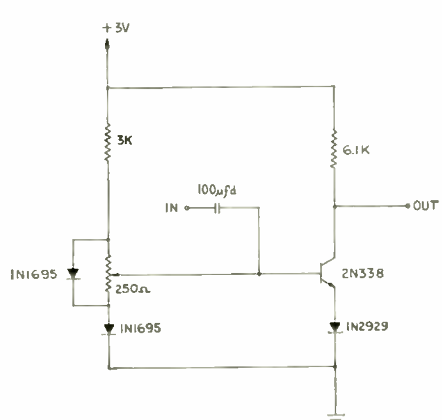

Fig. 4—Improved frequency doubler.

The resulting circuit (Fig. 4), while still not suitable for wide temperature ranges, can be used in many applications where temperature changes are reasonably small and the bias can be checked and adjusted occasionally if necessary. It has been operated for eight hours at a time in a non air-conditioned laboratory without noticeable bias drift after a short warm-up period.

J. H. Burbo
Instrumentation Lab.
Mass. Inst. Tech.
Concord, Mass.

* Received by the IRE, January 3, 1962.
[1] F. D. Neu, "A tunnel diode wide-band frequency doubling circuit," Proc. IRE, vol. 49, pp. 1963–1964; December, 1961.

Graphical Expressions of Synchronous Conditions in the Transverse-Type Electron Beam Parametric Amplifier*

There are several types of pumping in the transverse-type electron beam parametric amplifier, each of which has a different synchronous condition. This condition is explained physically by deriving it from a geometrical sum of the signal and idler waves.

The case of amplification by the coupling of two fast cyclotron waves is shown in Fig. 1, where ω_s, ω_i and ω_p represent signal, idler and pump frequency, respectively. In both waves the electron rotates by $\omega_c t$ in time t while it proceeds axially at $v_0 t$, where ω_c is cyclotron frequency and v_0 is the axial mean velocity of electron. From a simple geometrical consideration the following phase velocities are obtained:

$$v_s = v_0/1 - \frac{\omega_c}{\omega_s}, \qquad v_i = v_0/1 - \frac{\omega_c}{\omega_i}$$

where the subscripts s and i refer to signal and idler. Summing up the displacement of these waves, a new wave pattern is obtained, where the relation $\omega_s + \omega_i = \omega_p$ holds at the initial plane and the rate of rotation observed from a moving electron becomes $2\omega_c t$. From the new pattern the following relation is given:

$$\omega_p\left(1 - \frac{v_0}{v_p}\right) = 2\omega_c$$

This is nothing but a synchronous condition, needed for the pump wave, so that the Doppler frequency is equal to two times cyclotron frequency.

Fig. 2 shows the case of amplification by the coupling of two synchronous waves in quadrupole amplifier. In this case the phase velocity of pump wave remains equal to the electron velocity. Then the synchronous condition is given by

$$\omega_p\left(1 - \frac{v_0}{v_p}\right) = 0,$$

showing that Doppler frequency equals zero.

Fig. 3 shows the case where amplification occurs by the coupling of the fast cyclotron and slow synchronous waves in the axially

* Received January 3, 1962; revised manuscript received, February 23, 1962.

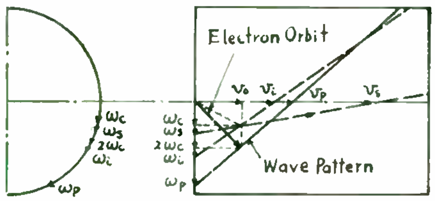

Fig. 1—Amplification by the coupling of fast cyclotron waves (quadrupole pump).

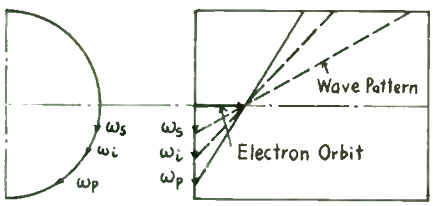

Fig. 2—Amplification by the coupling of synchronous waves (quadrupole pump).

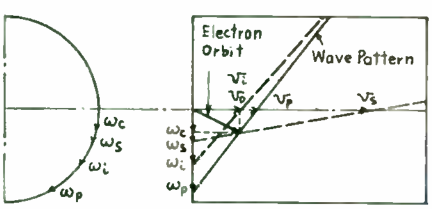

Fig. 3—Amplification by the coupling of fast and slow synchronous waves (axially symmetric field pump).

symmetric field pump. By means of a similar process the synchronous condition is found as follows:

$$\omega_p\left(1-\frac{v_0}{v_p}\right)=\omega_c.$$

Here, the Doppler frequency equals the cyclotron frequency.

In conclusion it may be stated that the number of $2\omega_c$, 0 and ω_c, included in the above equations, corresponds to the number of cyclotron waves related to the amplification process.

K. Kakizaki
Central Research Laboratory
Tokyo Shibaura Electric Co., Ltd.
Kawasaki, Japan

Symmetrical DC Converter Using Tunnel Diodes*

A possibly useful application of the tunnel diode is in a dc converter circuit to raise the output level of a low voltage source such as a thermoelectric generator. The symmetrical converter circuit shown in Fig. 1 is

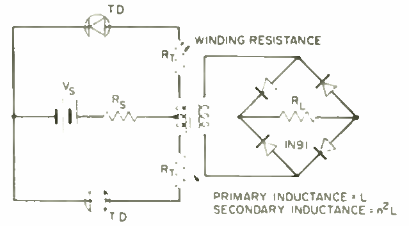

Fig. 1—Symmetrical tunnel diode converter circuit.

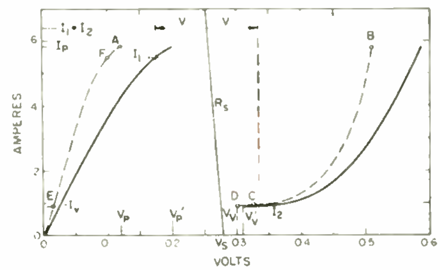

Fig. 2—Dashed line: $v-i$ characteristic of tunnel diode. Solid line: $v-i$ characteristic of tunnel diode in series with transformer primary resistance R_T.

particularly interesting because it allows a relatively steady current to be drawn from the source.[1] This results in a higher efficiency (ratio of output power to *available* power at the input) than is possible with a single diode circuit.[2,3]

The operation of this circuit has been analyzed and examined experimentally for the antisymmetric mode of oscillation. The voltage-current trajectory for one diode can be traced on Fig. 2. Starting at point A the diode switches *very* quickly (in the constant current switching time) to B and quickly (in the order of the time to charge the transformer leakage inductance) to C. It then relaxes *slowly* (in the order of L/R time constants) to D, very quickly to E, quickly to F, and slowly back to A. The locations of points C and F depend upon the loading. For no load F coincides with E and C with B; while under maximum loading (minimum R_L) F coincides with A and C with D.

Under maximum loading, therefore, the diodes effectively switch back and forth between their peak and valley points. The power output is

$$P_{out} = \tfrac{1}{2}(V_v' - V_p')(I_p - I_v) \qquad (1)$$

where $V_v' = V_v + R_T I_v$ and $V_p' = V_p + R_T I_p$ as indicated in Fig. 2. The efficiency is

$$\epsilon \approx \frac{4m}{(1+m)^2}\left(\frac{V_v' - V_p'}{V_v' + V_p'}\right)\left(\frac{I_p - I_v}{I_p + I_v}\right). \qquad (2)$$

where $m = R_s/R$ and $R_s = \frac{1}{2}(V_v' + V_p')/(I_p + I_v)$ is the resistance which the circuit presents to the source. The source resistance R_s must be less than $\frac{1}{2}(V_v' - V_p')/(I_p - I_v)$ to insure stable biasing of the circuit. Therefore

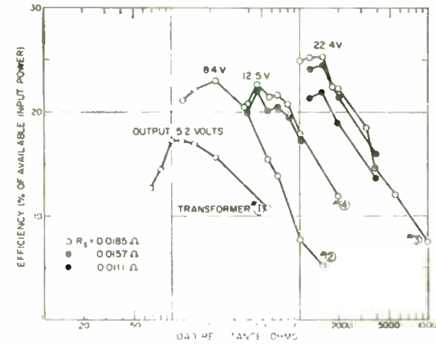

Fig. 3—Efficiency vs load resistance and source resistance for various transformers. Transformer #1 R_T=0.125 ohm, #2 0.004 ohm, #3 0.0018 ohm, #4 0.0042 ohms.

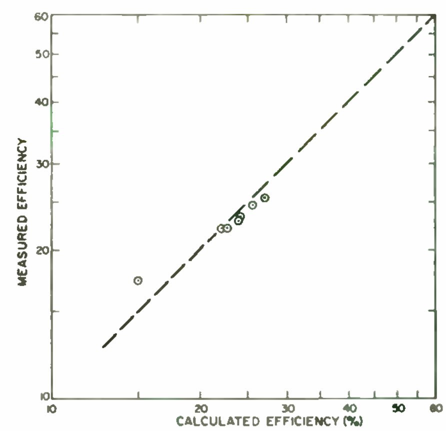

Fig. 4—Comparison of measured and calculated efficiencies.

$$m > \left(\frac{V_v' + V_p'}{V_v' - V_p'}\right)\left(\frac{I_p - I_v}{I_p + I_v}\right). \qquad (3)$$

Thus for maximum efficiency it is desirable to have V_v'/V_p' and I_p/I_v as large as possible and $V_v'/V_p' \geq I_p/I_v$.

Efficiency has been measured in a circuit using two "solution grown" germanium diodes with matched v-i characteristics as shown in Fig. 2.[4] Efficiency vs load resistance is plotted for several values of source resistance and for various transformers in Fig. 3. In Fig. 4 maximum efficiency is compared with that calculated from (2). Output power is between 300 and 400 mw.

If the load resistance is made less than

$$R_L < 2n^2\frac{V_v' - V_p'}{I_p - I_v}, \qquad (4)$$

the diodes relax quickly from B to D and from E to A. The transformer flux does not have time to become equal in the windings and the antisymmetric mode is no longer favored by the winding polarity. A symmetric mode then obtains which is characterized by a much higher frequency and which does not couple to the load.

A. C. Scott
Dept. of Elec. Engrg.
Massachusetts Institute of Technology,
Cambridge, Mass.

* Received January 31, 1962. This note is based on a thesis submitted in partial fulfillment of the requirements of the degree of Doctor of Science in the Department of Electrical Engineering at the Massachusetts Institute of Technology, Cambridge, on August 21, 1961.

[1] This circuit was suggested to the author by Dr. Paul Pittman of the Westinghouse Res. Labs., Pittsburgh, Pa.

[2] H. F. Storm and D. P. Shattuck, "Tunnel Diode D-C Power Converter," presented at AIEE Winter General Meeting, New York, N. Y.; January 29–February 3, 1961.

[3] S. Wang, "Converter efficiency and power output of a tunnel diode relaxation oscillator," Proc. IRE, vol. 49, pp. 1219–1220; July, 1961.

[4] The author is indebted to the staff of the Bell Telephone Labs., Murray Hill, N. J., for the opportunity to fabricate these diodes during the summer of 1960.

Magneto-Ionic Duct Propagation Time (Whistler-Mode) vs Geomagnetic Latitude at 4 KC*

When the transmitted frequency f is well below the plasma frequency f_p in ionospheric propagation, the extraordinary ray direction is approximately that of the earth's magnetic field lines. At increasing geomagnetic latitudes of origination, the propagation time from the originating point to the conjugate point should increase with the path length. Correspondingly, the group velocity is lessened in varying degree with height in the ionosphere, and for different lengths of time dependent upon the ray path length in the ionosphere. Thus, it seems reasonable to assume that on a graph of the propagation time vs geomagnetic origination latitude, some portion of the curve may be quite flat or perhaps have a negative slope. A simplified analysis follows to show that this situation is quite possible, if the ray follows the field line closely.

The assumptions employed are listed below:

1) Energy travels in the direction of the earth's magnetic field.
2) Circular polarization with the right-hand sense for propagation from south to north is assumed (these first assumptions are completely equivalent to assuming a longitudinal extraordinary mode.
3) The earth's magnetic field is represented by an earth-centered magnetic dipole.
4) The collisional frequency μ is zero.

The group velocity v_g is given by[1]

$$v_g = \frac{c}{n + f\,dn/df}$$

$$= \frac{2c(f_H - f)^{3/2}[f^2(f_H - f) + ff_p^2]^{1/2}}{2f^3 - 4f^2 f_H + 2ff_H^2 + f_p^2 f_H}$$

where

$$n^2 = 1 + \frac{f_p^2}{f(f_H - f)},$$

f_p = plasma frequency $= 9\sqrt{N} \times 10^3$ c/s,

f_H = gyro frequency $= 2.8 \times 10^6 B$ c/s,

n = the refractive index,

N = the electron concentration electrons/cm³,

B = the magnetic field flux density, gauss,

f = wave frequency, cps.

The conventional first- and second-order approximations are given by

$$v_g \doteq 2c\frac{f^{1/2}(f_H - f)^{3/2}}{f_H f_p}, \qquad f_p^2 \gg ff_H$$

$$v_g \doteq \frac{2c(ff_H)^{1/2}}{f_p}, \qquad f_p^2 \gg ff_H,\ f \ll f_H.$$

The propagation time T is to be evaluated graphically from

$$T = \int_{\text{path}} \frac{ds}{v_g} \triangleq \frac{D}{\sqrt{f}}$$

which defines D, the dispersion. The magnetic path length s is

$$s = \frac{R_0}{2}\left\{(1 + 3\sin^2\lambda)^{1/2}\sin\lambda + \frac{1}{\sqrt{3}}\ln\left[\sin\lambda + \frac{(1 + 3\sin^2\lambda)^{1/2}}{\sqrt{3}}\right]\right\}_{\lambda_1}^{\lambda_0}$$

where

λ_0 = the originating latitude, degrees,

λ_1 = the latitude to which path length is desired,

R_0 = the maximum radius of the magnetic dipole path, in units of earth radii, $\sec^2\lambda_0$.

The height h above the earth's surface is

$$h = (R_0\cos\lambda - 1)a$$

where a is the earth's radius. Assuming symmetry of the dipole field above and below the geomagnetic equator, only one-half the path need be considered for integration purposes.

Due to evident approximations in the foregoing, computations were run by hand at a single frequency of 4 kc. The results are given in Fig. 1 for a one-way path. In Table I the one-way dispersion as a function of originating latitude is given.

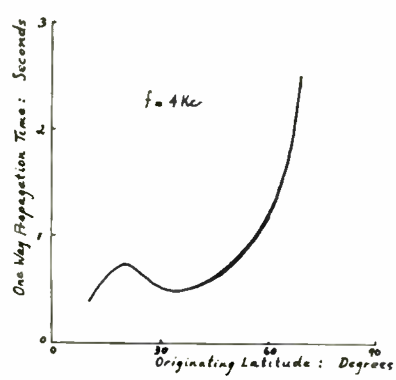

Fig. 1—Propagation time vs originating geomagnetic latitude.

TABLE I

DISPERSION VS ORIGINATING LATITUDE

λ_0 (degrees)	$D = Tf^{1/2}$ (seconds)$^{1/2}$
10	24.5
20	46.3
30	32.2
40	32.2
50	47.7
60	159.8

Granted that the foregoing is an approximate analysis, the phenomenon demonstrated by Fig. 1 is very interesting. A more elaborate investigation is certainly warranted at other frequencies and for other parameter models. The models used in this analysis were those of a dipole magnetic field for the earth and an electron density profile compiled from Penn State data, NRL rocket data, USSR data (rocket, February 21, 1958), USSR satellite data, and "whistler" estimates.

CHARLES V. GREENMAN
RCA
Camden, N. J.

* Received January 29, 1962.

[1] G. R. Ellis, "On the propagation of whistling atmospherics," *J. Atmospheric and Terrestrial Phys.*, vol. 8, pp. 338–344; June, 1956.

A Two-Term Analytical Approximation of Tunnel-Diode Static Characteristics*

In the articles previously published on tunnel-diode circuitry design, either a polynomial expression[1] or sectional straight-line approximations are used to represent the tunnel-diode static current-voltage characteristics. This paper will present a simple two-term exponential approximation. The accuracy of this approximation compared with actual tunnel-diode characteristics will also be discussed.

The static I-V characteristic of a tunnel

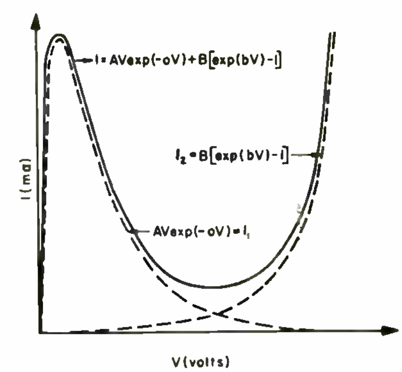

Fig. 1—Tunnel-diode static I-V characteristics and the two current components.

diode is shown as the solid curve in Fig. 1. It is found that a plot of the natural logarithm of (I/V) vs the applied voltage gives a straight line in the negative resistance region. This suggests that the total tunnel-diode current may be expressed as[2]

$$I = I_1 + I_2$$
$$= AV\exp(-aV) + B[\exp(bV) - 1]. \quad (1)$$

The first term is the tunnel current and the second term is the ordinary diode current. They are shown as the dotted curves in Fig. 1. The constants a, A, b, and B are determined as follows:

For voltages less than the valley voltage, the second term of (1) can be neglected giving

$$I_1 = AV\exp(-aV) \quad (2)$$

which can be written as

$$\ln(I_1/V) = \ln A - aV. \quad (3)$$

In the straight line plot of $\ln(I_1/V)$ vs the applied voltage, the slope is equal to $(-a)$, and the zero voltage intercept is equal to $\ln A$, as shown in Fig. 2.

For large values of forward bias, the first term of (1) can be neglected and since $\exp(bV) \gg 1$, (1) reduces to

$$I_2 \approx B\exp(bV), \quad (4)$$

* Received January 31, 1962; revised manuscript received, February 15, 1962.

[1] M. Schuller and W. W. Gartner, "Large-signal circuit theory for negative-resistance diodes, in particular tunnel diodes," PROC. IRE, vol. 49, pp. 1268–1278; August, 1961.

[2] A. Ferendeci, "A Study of Tunnel Diode Characteristics," M.S. thesis, Case Institute of Technology, Cleveland, Ohio; 1961.

which can be written as

$$\ln I_2 = \ln B + bV. \tag{5}$$

The plot of $\ln I_2$ vs the applied voltage should give a straight line with a slope equal to b and the zero voltage intercept equal to $\ln B$, as is shown in Fig. 2.

If (2) and (4) are plotted, then the sum of the two curves should approximate the actual tunnel-diode curve. This approximation has been applied to germanium, silicon and Ga-As tunnel diodes with results better than ± 10 per cent accuracy over the complete curve. A typical germanium tunnel diode (1N-2941), is used to illustrate the results of this two-term approximation as shown in Fig. 3. The actual diode curves are obtained from a photograph taken from a curve tracer oscilloscope. From the graphs of $\ln (I/V)$ vs V and $\ln I$ vs V, the constants a, b, A, and B are calculated giving the approximation as:

$$I = 0.044V \exp(-16.8V) + 5.4 \times 10^{-7}[\exp(15.4V) - 1] \text{(amperes)}. \tag{6}$$

Using (6) the currents for corresponding voltages are calculated and the results are plotted on the same graph paper with the actual tunnel-diode curves for comparison. The current difference between the actual and the calculated curves is normalized with respect to the peak current and plotted on the lower portion of the graphs. It is seen that the approximation is accurate to ± 6 per cent or better.

For engineering purposes the four constants may be determined by measuring four sets of current and voltage values at four pilot points to be fitted accurately. Two of the pilot points should be in the tunnel current region and the other points in the ordinary diode current region. By substituting these I-V values into (3) or (5), the constants may be found. The peak point corresponds to the first $dI/dV = 0$ point; therefore, if the peak point is selected to be one of the pilot points, then the constant $a = (1/V_p)$.

It is not surprising to find that for the simple approximations, the constants a and b are not multiples of (e/kT), especially the ordinary diode constant b. This is possibly due to the valley current which effects the ordinary diode current considerably within the regions of interest.

A. Ferendeci
W. H. Ko
Engrg. Div.
Case Inst. Tech.
Cleveland, Ohio

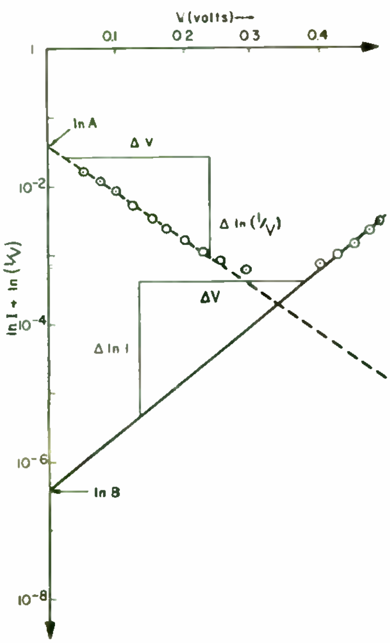

Fig. 2—ln (I/V) vs V and ln (I) vs V curves.

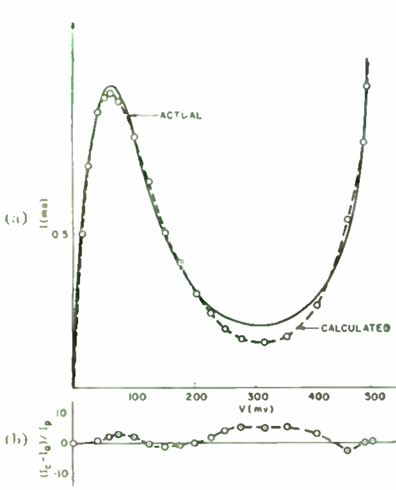

Fig. 3—1N-2941 Germanium tunnel diode. (a) Actual and calculated characteristics. (b) Per cent error between actual and calculated characteristics.

Nonlinear Distortion in Tunnel-Diode Amplifiers*

An important performance characteristic of tunnel-diode amplifiers is dynamic range. The upper limit imposed upon the dynamic range of a tunnel-diode amplifier is usually due to nonlinear distortion. In this paper, an approximate theoretical analysis of the nonlinear distortion within tunnel-diode amplifiers will be presented.

The current-vs-voltage characteristic of a typical tunnel diode is shown in Fig. 1. In the negative resistance region this i-e curve can be approximated by an exponential function:

$$i = A\epsilon^{ae} \tag{1}$$

where

i = tunnel-diode current,
e = tunnel-diode voltage,
A and a are constants.

Letting $X = e - e_b$ = tunnel-diode ac voltage, where e_b = voltage at operating point of the tunnel-diode amplifier

$$i = A\epsilon^{a(x+e_b)} \cong A\epsilon^{ae_b}\left[1 + ax + \frac{a^2}{2!}x^2 + \frac{a^3}{3!}x^3 + \cdots\right]. \tag{2}$$

At the operating point

$X = 0$ and $e = e_b$, then

$$a = \frac{\left.\dfrac{di}{de}\right|_{e=e_b}}{i}. \tag{3}$$

$$A = i_b\epsilon^{-ae_b}. \tag{4}$$

Constants a and A can be evaluated using (3) and (4) for an operating point within the negative resistance region of a particular tunnel diode.

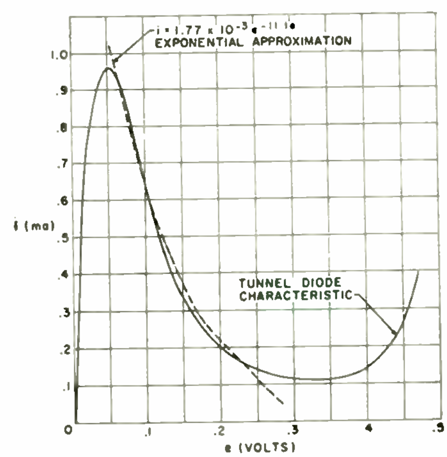

Fig. 1—Typical current-vs-voltage characteristic of tunnel diode and exponential approximation in the negative resistance region.

To determine the second- and third-order harmonic and intermodulation distortion the first four terms of (2) are employed:

$$i = A\epsilon^{ae_b}\left[1 + ax + \frac{a^2}{2}x^2 + \frac{a^3}{6}x^3\right]. \tag{5}$$

Assuming two equilevel signals of peak voltage E and angular frequencies ω_1 and ω_2,

$$x = E\cos\omega_1 t + E\cos\omega_2 t. \tag{6}$$

Substituting (6) into (5) and expanding, it can be shown that

$$\begin{aligned} i = A\epsilon^{ae_b}\Big\{&\left(1 + \frac{a^2E^2}{2}\right) \\ &+ (aE + \tfrac{3}{8}a^3E^3)(\cos\omega_1 t + \cos\omega_2 t) \\ &+ \frac{a^2E^2}{4}(\cos 2\omega_1 t + \cos 2\omega_2 t) \\ &+ \frac{a^2E^2}{2}\cos(\omega_1 + \omega_2)t + \frac{a^2E^2}{2}\cos(\omega_1 - \omega_2) \\ &+ \frac{a^3E^3}{24}(\cos 3\omega_1 t + \cos 3\omega_2 t) \\ &+ \frac{a^3E^3}{8}[\cos(2\omega_1 + \omega_2)t + \cos(2\omega_2 + \omega_1)t \\ &+ \cos(2\omega_1 - \omega_2)t + \cos(2\omega_2 - \omega_1)t]\Big\}. \end{aligned} \tag{7}$$

* Received January 26, 1962.

Then

$$\frac{\text{Signal}}{\text{2nd Harmonic}} = \frac{4(1+\frac{3}{8}a^2E^2)}{aE} \qquad (8)$$

$$\frac{\text{Signal}}{\text{2nd Order Intermodulation}} = \frac{2(1+\frac{3}{8}a^2E^2)}{aE} \qquad (9)$$

$$\frac{\text{Signal}}{\text{3rd Harmonic}} = \frac{24(1+\frac{3}{8}a^2E^2)}{a^2E^2} \qquad (10)$$

$$\frac{\text{Signal}}{\text{3rd Order Intermodulation}} = \frac{8(1+\frac{3}{8}a^2E^2)}{a^2E^2}. \qquad (11)$$

The ratios of signal-to-harmonic distortion and signal-to-intermodulation distortion are given in (8)–(11). Although these ratios appear to be independent of bias voltage, they are functions of the constant a which is evaluated for a particular value of bias voltage. At different operating points, a different value of a would generally yield a better fit of the exponential approximating function.

This theoretical analysis is of limited accuracy. Higher-order curvatures have been neglected and possible mismatches seen by the tunnel diode at the distortion frequencies have not been considered. The exponential approximation obviously breaks down for ac voltage magnitudes that are large enough to swing into the tunnel-diode positive resistance region. Nevertheless the exponential approximating function provides simple equations that can be used to obtain "ballpark" estimates of the various signal-to-distortion ratios.

Because of the different sources of error previously mentioned, it is seldom profitable to employ the more exact representation of the tunnel-diode characteristics and experimental techniques are more expedient.

R. M. Kurzrok
A. Newton
RCA Surface Commun. Sys. Lab.
New York, N. Y.

Capacitance and Charge Coefficients for Varactor Diodes*

It has been shown desirable to know the Fourier coefficients of the charge and capacity of a varactor diode driven by a single frequency voltage.[1,2] These coefficients have been previously calculated either in approximate series form or in terms of untabulated functions. It is possible to express them in an elegant and simple functional form.

In the back-biased diode, the capacity as a function of voltage is taken to be

$$C = C_0\left(1 - \frac{V}{\phi_0}\right)^\nu. \qquad (1)$$

We impose

$$V = V_0 + 2V_1 \cos \omega t. \qquad (2)$$

Hence

$$C = C_0\left\{\left(1 - \frac{V_0}{\phi_0}\right) - \frac{2V_1}{\phi_0}\cos \omega t\right\}^\nu \qquad (3)$$

$$C = C_d\left\{1 - \frac{2V_1}{\phi_0 - V_0}\cos \omega t\right\}^\nu, \qquad (4)$$

where

$$C_d = C_0\left(1 - \frac{V_0}{\phi_0}\right)^\nu, \qquad (5)$$

C_d is the capacity of the varactor at voltage V_0.

We want the complex Fourier coefficient

$$C_n = \frac{1}{\pi}\int_0^\pi C_d\left\{1 - \frac{2V_1}{\phi_0 - V_0}\cos \omega t\right\}^\nu \cdot \cos n\omega t d(\omega t) \qquad (6)$$

$$C_n = C_d\frac{(-1)^n}{\pi}\int_0^\pi (1 + \alpha\cos\theta)^\nu \cos n\theta d\theta, \qquad (7)$$

where we have set

$$\theta = (\omega t + \pi) \qquad (8)$$

and

$$\alpha = \frac{2V_1}{\phi_0 - V_0}. \qquad (9)$$

The integral (7) may now be related to a known integral, known as the Laplace integral.

From Erdelyi:[3]

$$\frac{1}{\pi}\int_0^\pi (z + \sqrt{z^2-1}\cos\theta)^\nu \cos n\theta\, d\theta = \frac{\Gamma(\nu+1)}{\Gamma(\nu+n+1)}P_\nu^n(z), \qquad (10)$$

where $P_\nu^n(z)$ is the associated Legendre function.

Multiplying and dividing by z^ν, we have

$$\frac{1}{\pi}\int_0^\pi \left(1 + \frac{\sqrt{z^2-1}}{z}\cos\theta\right)^\nu z^\nu \cos n\theta d\theta = \frac{z^\nu}{\pi}\int_0^\pi (1+\alpha\cos\theta)^\nu \cos n\theta d\theta, \qquad (11)$$

with

$$\alpha = \frac{\sqrt{z^2-1}}{z} \quad \text{or} \quad z = \frac{1}{\sqrt{1-\alpha^2}}. \qquad (12)$$

Thus

$$C_n = C_d\frac{(-1)^n}{\pi}\int_0^\pi (1+\alpha\cos\theta)^\nu \cos n\theta d\theta = C_d(-1)^n\frac{\Gamma(\nu+1)}{\Gamma(\nu+n+1)}z^{-\nu}P_\nu^n(z). \qquad (13)$$

$P_\nu^n(z)$ is tabulated[4] for non-integral values of ν, and we may evaluate any Fourier coefficient of capacity simply, and with no approximations at any drive level.

The same procedure is used in the calculation of the Fourier coefficients of the charge Q. We find Q as a function of V by integrating (1)

$$Q = \frac{-C_0\phi_0}{\nu+1}\left(1 - \frac{V}{\phi_0}\right)^{\nu+1}. \qquad (14)$$

The Fourier integral is of the same form as before

$$Q_n = -Q_d\frac{(-1)^n}{\pi}\int_0^\pi (1+\alpha\cos\theta)^{\nu+1} \cdot \cos n\theta d\theta, \qquad (15)$$

where

$$Q_d = \frac{C_0\phi_0}{(\nu+1)}\left(1 - \frac{V_0}{\phi_0}\right)^{\nu+1} = \frac{C_d(\phi_0 - V_0)}{(\nu+1)}. \qquad (16)$$

Using (10) we have

$$Q_n = Q_d(-1)^{n+1}\frac{\Gamma(\nu+2)}{\Gamma(\nu+n+2)}z^{-(\nu+1)}P_{\nu+1}^n(z) \qquad (17)$$

$$C_n = C_d(-1)^n\frac{\Gamma(\nu+1)}{\Gamma(\nu+n+1)}z^{-\nu}P_\nu^n(z), \qquad (13)$$

where

$$z = \frac{1}{\sqrt{1-\alpha^2}}. \qquad (12)$$

Eqs. (12) and (13) are repeated here to summarize the results.

D. B. Leeson
Dept. Elec. Engrg.
Stanford Univ.
Stanford, Calif.

* Received January 22, 1962.

[1] S. Sensiper, and R. D. Weglein, "Capacitance and charge coefficients for parametric diode devices," Proc. IRE, vol. 48, pp. 1482–1483; August, 1960.

[2] —, "Capacitance coefficients for varactor diodes," Proc. IRE (*Correspondence*), vol. 49, p. 810; April, 1961.

[3] A. Erdelyi, "Note on Heine's integral representation of associated Legendre functions," *Philos. Mag.*, ser. 7, vol. 32, pp. 351–352; October, 1941.

[4] A. Lowan, "Tables of Associated Legendre Functions," Natl. Bur. Standards, Columbia Univ. Press, New York, N. Y., pp. 230 ff.; 1945.

Invariant Stability Parameters*

In a recent paper,[1] it is shown that there exists an invariant stability factor k defined by

$$k = \frac{2\rho_{11}\rho_{22} - \mathrm{Re}(\gamma_{12}\gamma_{21})}{|\gamma_{12}\gamma_{21}|} \qquad (1)$$

where the γ may be any of the conventional z, y, h, g twoport matrix parameters, and $\rho_{11} = \mathrm{Re}(\gamma_{11})$, etc. The quantity k is invariant under arbitrary lossless terminations, under interchange of input and output, and under "immittance substitution," a transformation group involving the arbitrary interchanging of impedance and admittance formulations at both ports (replacing any set of the z, y, h, g parameters by any other). These transformations are associated with stability,[1] and provided $\rho_{11}, \rho_{22} \geq 0$, k is a unique measure of the degree of conditional $(-1 \leq k < 1)$ or unconditional $(k > 1)$ stability of the twoport. This means that k is a measure of what would happen in the worst possible case (as regards stability) of arbitrary passive terminations.

There is, however, a need for a stability parameter which will indicate the degree of

* Received January 23, 1962.

[1] J. M. Rollett, "Stability and power gain invariants of linear two-ports," IRE Trans. on Circuit Theory, vol. CT-9, pp. 29–32; March, 1962.

stability of a twoport in a particular situation of interest, and not only in an "idealized" worst possible case. Such a parameter (if it exists) must take account of source (Γ_1) and load (Γ_2) immittances, and will be invariant under interchange of input and output (including terminations) and under immittance substitution.

Instability occurs when the total immittance at either port is zero, *i.e.*, when

$$\Gamma_1 + \Gamma_{in} = \frac{(\Gamma_1 + \gamma_{11})(\Gamma_2 + \gamma_{22}) - \gamma_{12}\gamma_{21}}{(\Gamma_2 + \gamma_{22})} = 0 \qquad (2)$$

and similarly for $(\Gamma_2 + \Gamma_{out})$. The zeros of this expression[2] are the zeros of $(\Gamma_1 + \gamma_{11})(\Gamma_2 + \gamma_{22}) - \gamma_{12}\gamma_{21}$, provided that the source immittance is passive (and similarly for the load immittance), and provided that the characteristic frequencies of the twoport with infinite immittances are left half-plane. Consequently,

$$(\Gamma_1 + \gamma_{11})(\Gamma_2 + \gamma_{22}) - \gamma_{12}\gamma_{21} = 0 \qquad (3)$$

is called the characteristic equation[3,4] of the system.

Now the characteristic function of (3) is invariant under interchange of input and output, but not under immittance substitution. A search for suitably invariant functions of the characteristic function has unearthed a quantity

$$\chi = \frac{(\Gamma_1 + \gamma_{11})(\Gamma_2 + \gamma_{22}) - \gamma_{12}\gamma_{21}}{\sqrt{(\Gamma_1\Gamma_2\gamma_{12}\gamma_{21})}} \qquad (4)$$

which is "semi"-invariant under immittance substitution, *i.e.*, invariant except for an ambiguity in phase of $m\pi/2$ (m integral). This ambiguity may be removed by forming such functions as $|\chi|$, χ^4 or $\chi \exp jm\pi/2$, etc.

The properties of χ may be briefly summarized.

1) χ is invariant under interchange of input and output and semi-invariant under immittance substitution.
2) The zeros of χ are the zeros of the characteristic function of (3), with the provisos mentioned above.
3) The generalized signal gain (*i.e.*, ratio of an output current/voltage to a signal current/voltage) is given by

$$A = \frac{(-1)^n}{\chi}\sqrt{\left(\frac{\gamma_{21}}{\gamma_{12}}\right)}\sqrt{\left(\frac{\Gamma_2'}{\Gamma_1'}\right)} \qquad (5)$$

where the immittance representations of Γ_1', Γ_2' are chosen (independently of the choice of matrix parameters γ) according to the particular ratio required, *i.e.*, impedance for voltage, admittance for current; n is taken as 0 if Γ_2, Γ_2' are equal, and 1 if they are reciprocal, to preserve conventional phase relations.

Thus, for example, voltage gain is given by

$$A_v = \frac{v_2}{v_g} = \frac{(-1)^n}{\chi}\sqrt{\left(\frac{\gamma_{21}}{\gamma_{12}}\right)}\sqrt{\left(\frac{Z_2}{Z_1}\right)} \qquad (6)$$

in general, or in particular

$$A_v = \frac{-y_{21}Z_2}{(Y_1 + y_{11})(Y_2 + y_{22}) - y_{12}y_{21}}; \qquad (7)$$

while transadmittance is given by

$$Y_m = \frac{i_2}{v_g} = \frac{(-1)^n}{\chi}\sqrt{\left(\frac{\gamma_{21}}{\gamma_{12}}\right)}\sqrt{\left(\frac{Y_2}{Z_1}\right)}. \qquad (8)$$

The quantity[5] $\sqrt{(\gamma_{21}/\gamma_{12})}$ is also semi-invariant under immittance substitution.

4) The transducer gain G_T is given by

$$G_T = \frac{4}{|\chi|^2}\cdot\left|\frac{\gamma_{21}}{\gamma_{12}}\right|\cdot\frac{P_1P_2}{|\Gamma_1\Gamma_2|} \qquad (9)$$

where $P_1 = \text{Re}(\Gamma_1)$, etc.; $P_1P_2/|\Gamma_1\Gamma_2|$ is invariant under immittance substitution.

The usefulness of χ lies in the fact that it is an invariant measure of stability, or in effect, an invariant return difference.[1,6] The size and shape of the plot of χ as a function of frequency in the complex plane is unique, apart from rotations of $m\pi/2$. Thus the shape of the locus can be examined, as in the Nyquist test, to provide information about the zeros;[3,6] while the distance of χ from the critical point, the origin, is proportional to the stability of the system at real frequencies. In simple cases, a knowledge of the magnitude of χ provides sufficient information for the circuit designer, in the form of a plot of $|\chi|$ or $|\chi|^2$ against frequency.

The stability parameter χ or its magnitude may be measured by making use of the properties given in paragraphs 3) and 4) above. Thus

5) If the reverse generalized signal gain, found by interchanging input and output, is denoted by A^r then

$$\chi = 1/\sqrt{(A \cdot A^r)} \text{ or } |\chi|^2 = 1/|A \cdot A^r|. \qquad (10)$$

6) If the reverse transducer gain is denoted by G_T^r then

$$|\chi|^2 = \frac{4}{\sqrt{(G_T \cdot G_T^r)}}\cdot\frac{P_1P_2}{|\Gamma_1\Gamma_2|}. \qquad (11)$$

Since $P_1P_2/|\Gamma_1\Gamma_2|$ is invariant, there is no need to include it as a factor. If power measurements are made, it is more convenient to plot a reduced stability parameter $|\chi'|^2$ where[7]

$$|\chi'|^2 = \frac{1}{\sqrt{(G_T \cdot G_T^r)}} = \frac{|(\Gamma_1 + \gamma_{11})(\Gamma_2 + \gamma_{22}) - \gamma_{12}\gamma_{21}|^2}{4P_1P_2|\gamma_{12}\gamma_{21}|}. \qquad (12)$$

The product of the transducer gain G_T and the stability parameter $|\chi'|^2$ is the invariant maximum stable power gain,[8,1] $|\gamma_{21}/\gamma_{12}|$, of the twoport. Thus $1/|\chi'|^2$ is the efficiency of the reciprocal part of the twoport, so that $|\chi'|^2$ may be called the "reciprocal attenuation";[1] the transducer gain is then given by dividing the maximum stable power gain by the reciprocal attenuation. By analogy, χ may be called the (complex) reciprocal signal attenuation. It is the main suggestion of this letter that these invariant reciprocal attenuation parameters are closely connected with stability.

J. M. Rollett
British Telecommun. Res., Ltd.
Taplow Court, Taplow
Nr. Maidenhead, Berks.
England

[2] The condition that the real part of the total port immittance be positive with arbitrary lossless terminations is that the over-all stability factor of Rollett[1] be greater than unity.

[3] F. B. Llewellyn, "Some fundamental properties of transmission systems," Proc. IRE, vol. 40, pp. 271–283; March, 1952.

[4] J. G. Linvill and J. F. Gibbons, "Transistors and Active Circuits," McGraw-Hill Book Co., Inc., New York, N. Y.; 1961.

[5] C. G. Aurell, "Representation of the general linear four-terminal network and some of its properties," *Ericsson Technics*, vol. 11, pp. 155–179; 1955.

[6] H. W. Bode, "Network Analysis and Feedback Amplifier Design," D. Van Nostrand Co., Inc., Princeton, N. J., pp. 151, 166; 1945.

[7] L. G. Cripps and J. A. G. Slatter, "Amplifier gain and stability," *J. Brit. IRE*, vol. 22, p. 417; November, 1961.

[8] M. A. Karp, "Power gain and stability," IRE Trans. on Circuit Theory (*Correspondence*), vol. CT-4, pp. 339–340; December, 1957.

Demodulators*

In the detection of a signal ensemble which is a sample of white Gaussian noise, an approximation to the optimum receiver consists of a full-wave square law demodulator followed by an integrator, or summer.[1,2] If a full-wave linear demodulator is used in place of the "optimum" demodulator, the degree of suboptimality is of interest.

Using the notation of Peterson, Birdsall, and Fox,[1] the parameter d is seen to be a convenient measure of the reliability of detection.

$$d = \frac{2E}{N_0} = \frac{(M_{SN} - M_N)^2}{\sigma_N^2}. \qquad (1)$$

where

E = signal energy in a record of length T
N_0 = noise spectral density
M_{SN} = mean value at demodulator output (signal plus noise)
M_N = mean value of demodulator output (noise alone)
σ_N^2 = variance of noise.
σ_{SN}^2 = variance of signal plus noise.

The performance of the receiver, regardless of the decision criteria used, is conveniently represented by the Receiver Operating Characteristic (ROC) curves; the parameter d serves to identify individual members of such a family of curves. A convenient meth-

* Received January 22, 1962.

[1] W. W. Peterson, T. G. Birdsall, and W. C. Fox, "The theory of signal detectability," IRE Trans. on Information Theory, vol. IT-4, pp. 171–212; September, 1954.

[2] J. J. Bussgang and W. L. Mudgett, "A note of caution on square-law approximation to an optimum detector," IRE Trans. on Information Theory (*Correspondence*), vol. IT-10, p. 504; September, 1960.

od of computing the effect of the suboptimum (linear) demodulator is to form the ratio

$$\mu = \frac{d_{\text{square-law}}}{d_{\text{linear}}} = \frac{\left[\dfrac{\sigma_{SN}{}^2 - \sigma_N{}^2}{\sqrt{2}\sigma_N{}^2}\right]^2}{\left[\dfrac{\sqrt{\dfrac{2}{\pi}}\,(\sigma_{SN} - \sigma_N)}{\sqrt{1 - \dfrac{2}{\pi}}\,\sigma_N}\right]^2}$$

$$= \frac{(\pi - 2)}{4}\left[1 + 2\left(\frac{\sigma_{SN}}{\sigma_N}\right) + \frac{\sigma_{SN}{}^2}{\sigma_N{}^2}\right]. \qquad (2)$$

In the small signal case $\sigma_N \simeq \sigma_{SN}$, and $\mu = 1.14$. Since E is proportional to the length of record T, the factor μ indicates that, for equivalent receiver performance, the record length T must be increased by 14 per cent when the suboptimum linear demodulator is used.

J. Knudson
Western Dev. Labs.
Philco Corp.
Palo Alto, Calif.

The Dielectric Constant of a Semiconductor as Related to the Intrinsic Activation Energy*

A general equation which shows the relationship, for a semiconductor, between impurity activation energy, dielectric constant and the effective mass is shown as

$$E = \frac{E_h}{\epsilon_s{}^2}\left(\frac{m_\phi}{m_0}\right) \qquad (1)$$

Here E is the activation energy of the impurity, m_ϕ is the effective mass, and ϵ_s is the dielectric constant of the semiconductor. E_h is the first ionization potential of hydrogen, and m_0 is the rest mass of an electron. Eq. (1) gives the basic relationship between the effective mass and the dielectric constant.

The energy gap or intrinsic activation energy is related to the square of the optical dielectric constant. This concept was first given by Moss in 1952.[1] The equation showing the connection between the two parameters is given by:

$$E_g\epsilon^2 = \text{constant} \qquad (2)$$

where E_g is the intrinsic activation energy between the valence band and the conduction band. ϵ is the optical dielectric constant.

A relationship between the impurity activation energy and the carrier effective mass may be found from the theory of Brillouin zones of one dimension. If we consider the effective mass as determined by one dimensional K-space, Brilloiun zone theory gives an equation of the form that is shown in the following:[2]

$$m_\phi = \frac{h^2}{4\pi^2}\left(1 \Big/ \frac{d^2E}{dK^2}\right). \qquad (3)$$

Substituting the equation for the effective mass (1) and rearranging terms to form a differential equation, we have for this new expression

$$\frac{d^2E}{dK^2} = \frac{E_h h^2}{4\pi^2\epsilon^2 m_0 E}. \qquad (4)$$

Multiplying both sides of (4) by $2dE$ and integrating will give

$$\left(\frac{dE}{dK}\right)^2 = \frac{E_h h^2}{2\pi^2\epsilon^2 m_0}\ln E. \qquad (5)$$

This equation is equivalent to that obtained by Moss from his investigation of photoconductivity. The approximate value of ($\ln E$) is found by plotting a curve of the ratio E_g/E_h vs $1/\epsilon^2$. Here ($\ln E$) is found from the curve made up of the parameters for several semiconductors. This curve and the value of its slope, $\ln E$, are shown in Fig. 1. The slope of this curve was found to be equal to a value of 11.7. Therefore, the product of the first ionization potential of hydrogen and the slope of the curve (11.7) is equal to the constant given in (2). The approximate value of this constant was found to be 159 ev. The energy gap or intrinsic activation energy is approximated by

$$E_g = \frac{159 \text{ ev}}{\epsilon^2}. \qquad (10)$$

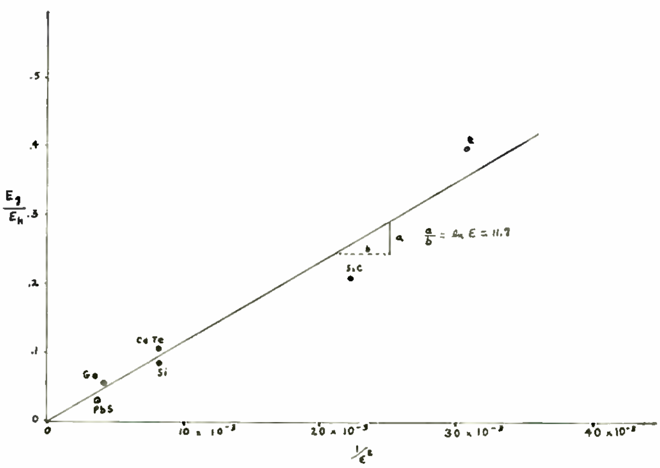

Fig. 1.

This equation relates the energy of an electron or hole to the wave number. An electron's wave energy in one dimensional K-space is shown by

$$E = \frac{h^2K^2}{8\pi^2 m_\phi}. \qquad (6)$$

The derivative of this equation for energy with respect to the wave number, K, results in

$$\frac{dE}{dK} = \frac{h^2K}{4\pi^2 m_\phi}. \qquad (7)$$

If this derivative is substituted into (5), then the energy relationship becomes:

$$\frac{h^2K^2 m_0}{8\pi^2 m_\phi{}^2} = \frac{E_h}{\epsilon^2}\ln E. \qquad (8)$$

Here $K = 1, 2, 3, 4, \cdots, n$.

The left-hand side of (8) will represent the intrinsic activation energy for the allowed wave number K. Eq. (8) now becomes

$$E_g = \frac{E_h}{\epsilon^2}\ln E. \quad T = \text{constant in } ^\circ\text{Kelvin}. \qquad (9)$$

Moss has indicated that indium antimonide and indium arsenide would not follow the relationship of (2). Calculated values of the dielectric constant ϵ_c, as given in Table I, show this to be correct for the above equation. Table I has values of measured energy gap or intrinsic activation energy E_g and dielectric constant ϵ_m taken from Moss.[1] ϵ_c is the calculated value of the dielectric constant from (10).

TABLE I

$T = 300°K$

Element	E_g	E_m	E_c
C (diamond)	5.40 ev	5.7	5.4
Si	1.12 ev	11.7	11.8
Ge	0.65 ev	16.0	15.6
Sn (Grey)	0.09 ev	?	42.0
PbS	0.40 ev	16.8	19.9
CdTe	1.43 ev	11.0	10.5
SiC	2.80 ev	6.7	7.5
PbTe	0.32 ev	28.6	22.3
PbSe	0.26 ev	21.0	24.7
CdS	1.30 ev	11.6	11.1
InSb	0.18 ev	15.7	29.7
InAs	0.33 ev	12.2	21.9
InP	1.26 ev	9.6	11.0
GaAs	1.35 ev	11.5	10.9
GaSb	0.70 ev	14.5	15.0
GaP	2.24 ev	8.4	8.4
AlSb	1.60 ev	10.2	9.9
AlAs	2.16 ev	?	8.0

C. F. Cole, Jr.
Box 233
Clear, Alaska

* Received January 29, 1962; revised manuscript received, February 13, 1962.

[1] T. S. Moss, "The Optical Properties of Semi-conductors," Academic Press Inc., New York, N. Y., pp. 48–49; 1959.

[2] C. Kittel, "Introduction to Solid State Physics," John Wiley and Sons, Inc., New York, N. Y., 2nd ed., p. 289; 1956.

Contributors

Arthur D. Ballato (S'55–M'59) was born in Astoria, N. Y., on October 15, 1936. He received the B.S. degree in electrical engineering from Massachusetts Institute of Technology, Cambridge, in 1958. He is presently a candidate for the M.S. degree in electrical engineering at Rutgers University, New Brunswick, N. J.

In 1958 he joined the Piezoelectric Crystal and Circuitry Branch, Solid State and Frequency Control Division of the U. S. Army Signal Research and Development Laboratory, Fort Monmouth, N. J., working in the areas of pressure and thermal effects in vibrating crystals.

❖

Rudolf Bechmann (SM'54–F'60) was born in Nuremberg, Germany, on July 22, 1902. He received the Ph.D. degree in theoretical physics from the University of Munich, Germany, in 1927.

From 1927 to 1945 he was employed by Telefunken Company for Wireless Telegraphy, Ltd., Berlin, Germany. He was particularly concerned at first with antenna problems, especially with questions of radiation resistance and radiation characteristics of composite antennas. In 1931 he developed the so-called EMF method. Later he turned his full attention to piezoelectric quartz crystals and developed this field in all directions during the following decade. In 1933 he discovered, independently, several quartz cuts having zero frequency temperature coefficients—the AT-, BT-, CT- and DT-type resonators. He made many contributions, practical and theoretical, to the field of elasticity and piezoelectricity and its application to quartz. By joining the production of oscillators and resonators to his scientific laboratory activities, he became involved in all questions related to quartz crystals. During World War II he directed several agencies covering the quartz industry as a whole, in addition to his specified activities with Telefunken.

After the war he joined the Oberspree Company in Berlin and directed it from 1946 to 1948. Moving to England in 1948, he was Principal Scientific Officer at the British Post Office Research Station, Dollis Hill, London. Here he studied the properties of several water-soluble piezoelectric materials and developed methods for determining the elastic and piezoelectric constants, using the resonance method applied to various modes of plates. The results of this research are compiled in "Piezoelectricity," General Post Office, Selected Engineering Reports, H. M. Stationery Office, London, 1957. In 1953 he became associated with the Brush Laboratories Company, now the Clevite Research Center, Cleveland, Ohio, as head of the Dielectric Phenomena Section of the Electrophysical Research Department. He extended his studies on methods of determining the elastic and piezoelectric constants into the field of ferroelectric ceramics. His chief activity, however, was the investigation of properties of synthetic quartz resonators. In 1956 he joined the U. S. Army Signal Research and Development Laboratory, Fort Monmouth, N. J., as a Consultant Physicist.

Dr. Bechmann is a Fellow of the American Physical Society, a member of the Piezoelectric Crystals Committee of the IRE, and a Corresponding Member of the German Committee for Standards on Piezoelectric Crystals.

❖

Jack Harold U. Brown (SM'61) was born in San Antonio, Tex., on November 16, 1918. He received the B.S. degree from the Southwest Texas State College, San Marcos, in 1939, and the Ph.D. degree from Rutgers University, New Brunswick, N.J., in 1948.

He served as Instructor in Physics at Southwest Texas State College in 1944, Instructor in Physical Chemistry at Rutgers in 1945, and as Radio Engineer for the Air Force during World War II. Following the war, he entered physiology and biophysics and was a Fellow of the Institute and Director of the Physiology Laboratory at Mellon Institute, Pittsburgh, Pa., and Lecturer at the University of Pittsburgh. He served as a member of the staff of the Oak Ridge Institute of Nuclear Studies, Oak Ridge, Tenn., in 1949 while also serving as Assistant Professor of Physiology at the University of North Carolina, Chapel Hill. After moving to Emory University, Emory University, Ga., in 1952, he became successively Associate Professor, Professor, and Acting Chairman of the Department of Physiology. In 1961 he joined the National Institutes of Health, Bethesda, Md., as Executive Secretary in charge of Biomedical Engineering Training Programs.

Dr. Brown is the author of more than 60 papers in various aspects of engineering and physiology, holds 6 patents or descriptions of biological apparatus, and is the author of two books including one on "Man in Space." He won the Sigma Xi research award in 1961. He is a member of Sigma Xi, Pi Kappa Delta, Phi Lambda Upsilon, Alpha Chi, the ACS, the New York Academy of Science, the American Physiological Society, the Society for Experimental Biology and Medicine, and the Endocrine Society, and is a Fellow of the AAAS.

❖

Jorge R. Fontana (A'53–M'58) was born in Barcelona, Spain, on April 1, 1925. He received the degree of Industrial Engineer from the University of Buenos Aires, Argentina, the B.S. and M.S. degrees in electrical engineering from Massachusetts Institute of Technology, Cambridge, in 1952, and the Ph.D. degree in the same field from Stanford University, Calif., in 1960.

His research interests include microwave tubes, particularly millimeter and submillimeter wave devices. In this connection, he has studied the applications of field emission cathodes and the nonlinear properties of quantized systems for harmonic generation and parametric amplification. At the present time, he is a Research Associate at the Microwave Laboratory of Stanford University and Acting Assistant Professor in the Electrical Engineering Department.

❖

Robert D. Frost (M'57) was born in Portland, Ore., on February 15, 1934. He received the B.S.E.E. degree from Oregon State College, Corvallis, in 1956, and the M.S.E.E. degree from the University of Washington, Seattle, in 1960.

From 1956 to 1958 he was an officer in the U. S. Coast and Geodetic Survey in charge of position control radar and sonic equipment aboard the ship *Pathfinder*. Since 1960 he has been a Member of the Technical Staff at Watkins-Johnson Company, Palo Alto, Calif., and is presently engaged in the development of electron guns and microwave tubes.

❖

H. Richard Johnson (S'45–A'51–SM'55–F'62) was born in Jersey City, N. J., on April 26, 1926. He received the B.E.E. degree from Cornell University, Ithaca, N. Y., in 1946, and the Ph.D. degree in physics from Massachusetts Institute of

Technology, Cambridge, in 1952.

While at MIT he held a Research Laboratory of Electronics Fellowship, and did work in electromagnetic wave propagation and microwave spectroscopy. From 1952 to 1957 he was with the Hughes Aircraft Company in Culver City, Calif., where he was engaged in research and development of microwave devices and became Head of the Microwave Tube Department. He was also a Lecturer in Engineering at the University of California at Los Angeles. He is presently Vice President of Watkins-Johnson Company, Palo Alto, Calif., and Lecturer in Electrical Engineering at Stanford University, Calif.

Dr. Johnson is a member of the American Physical Society, Past Chairman of the Los Angeles IRE Professional Group on Electron Devices, and a member of Tau Beta Pi, Eta Kappa Nu, Phi Kappa Phi, Sigma Xi, and RESA.

❖

Murray A. Lampert was born in New York, N. Y., on November 29, 1921. He received the B.A. degree from Harvard College in 1942, and the M.A. degree in physics from Harvard University, in 1945.

He was a Teaching Fellow in Physics at Harvard from 1942 to 1943 and an Instructor in Electronics at the Harvard Electronics Training School (for Armed Services Personnel) from 1943 to 1945. During 1945 he was in charge of the Lens Design Group at the Optical Research Laboratory of the Harvard Observatory. From 1946 to 1948 he was a member of the Theoretical Group of the Radiation Laboratory of the University of California at Berkeley, where he worked on high-energy problems in nuclear physics. He was at the Federal Telecommunication Laboratories (now the IT&T Laboratories), Nutley, N. J., from 1949 to 1952, where he worked on traveling-wave tubes and on the interaction of microwaves with plasmas. He joined the RCA Laboratories, Princeton, N. J., in 1952, where he has worked primarily in theoretical solid-state physics, particularly the electronic physics of insulators. From August, 1961 to April, 1962 he was the Acting Head of the General Solid-State Research Group.

Mr. Lampert is a member of Phi Beta Kappa, Sigma Xi and the American Physics Society.

❖

Theodore J. Lukaszek (S'61–M'62) was born in Perth Amboy, N. J. on March 8, 1935. He received the B.S. degree in physics from Monmouth College, West Long Branch, N. J., in 1960. He has also done postgraduate work in the Electronic Engineering

Department at Monmouth College and is presently enrolled to specialize in Solid-State Physics at the Graduate School of Fairleigh Dickinson University.

From 1953 to 1956 he served in the U. S. Marine Corps. In 1960 he joined the Solid-State and Frequency Control Division, U. S. Army Signal Research and Development Laboratory, Fort Monmouth, N. J., where he has been engaged primarily in environmental studies on the double-rotated piezoelectric quartz resonator and the design and construction of high-frequency quartz crystals for filter use.

❖

Allen Nussbaum (A'54) was born in Philadelphia, Pa., on August 22, 1919. He received the B.A. degree in chemistry, in 1939, the M.A. degree in physics, in 1940, and the Ph.D. degree in semiconductor physics, in 1953, all from the University of Pennsylvania, Philadelphia.

He entered the service in 1941, serving as a Radio Engineer with the Signal Corps in Italy and with the Air Force in Germany from 1947 to 1949. He was a Research Physicist and Supervisor in solid-state physics at the Honeywell Research Center, Hopkins, Minn., from 1952 to 1961. He was principal investigator on the tellurium program supported by the Air Force Office of Scientific Research. Since September, 1961, he has been Solid-State Division Head at American Electronic Laboratories, Inc., Lansdale, Pa. His fields of interest include basic semiconductor physics and device development.

❖

Richard H. Pantell (S'54–A'55–M'60) was born in New York, N. Y., on December 25, 1927. He received the B.S. and M.S. degrees from Massachusetts Institute of Technology, Cambridge, in 1950. His studies at M.I.T. were performed within the electrical engineering cooperative course, with four semesters spent in the General Electric Company test program. He received the Ph.D. degree in electrical engineering from Stanford University, Calif., in 1954.

During 1950–1951 he taught electrical engineering at the Polytechnic Institute of Brooklyn, N. Y., and from 1951 to 1954, he was a Research Assistant at the Stanford Electronics Research Laboratory, investigating new techniques for network synthesis. For the next two years, he was Assistant Professor of Electrical Engineering at Stanford University, and Research Associate in the Microwave Laboratory. He taught a graduate course in network synthesis, and did research on the development of a high-power traveling-wave tube. He was granted a leave of absence from Stanford to become a Visiting Assistant Professor at the University of Illinois, Urbana, during 1956–1957. There he worked on the generation of millimeter and microwave measurements. He has resumed his position at Stanford as an Associate Professor and is continuing his research into the generation of microwave energy.

❖

O. Thomas Purl (S'50–A'54–SM'58) was born in East St. Louis, Ill., on June 5, 1924. He received the B.S. degree in general engineering from the University of Illinois, Urbana, in 1948, and the B.S.E.E., M.S.E.E., and Ph.D. degrees, in 1951, 1952, and 1955, respectively, from the same institution.

He was a meteorologist with the Air Force from 1943 to 1946; from 1948 to 1949 he was engaged in microwave tube work at the Collins Radio Company; from 1955 to 1958 he was associated with the Hughes Electron Tube Laboratory, where he was Head of the Power Traveling-Wave Tube section and Senior Member of the Technical Staff. Since 1958 he has been a Member of the Technical Staff at Watkins-Johnson Co., Palo Alto, Calif., where he has been engaged in research and development on electron guns and microwave tubes.

Dr. Purl is a member of Sigma Xi, Eta Kappa Nu, Phi Kappa Phi, and Sigma Tau.

❖

Aldert van der Ziel (SM'49–F'56) was born in Zandeweer, the Netherlands, on December 12, 1910. From 1928 to 1934 he studied physics at the University of Groningen, The Netherlands, where he received the Ph.D. degree in 1934.

He was a Member of the Research Staff of the Physics Laboratory of N. V. Philips' Gloeilampenfabrieken, Eindhoven, The Netherlands, from 1934 to 1947. At that time he became an Associate Professor of Physics at the University of British Columbia, Vancouver, Canada. He has been Professor of Electrical Engineering at the University of Minnesota, Minneapolis, since 1950.

Dr. van der Ziel is a member of the American Physical Society and Sigma Xi.

Books

Subminiature Electron Tube Life Factors, by M. W. Edwards, D. E. Lammers, and J. A. Zoellner

Published (1961) by Engineering Publishers, P.O. Box 2, Elizabeth, N. J. 158 pages+xv pages+15 appendix pages. Illus. 8¾×11¼. $9.50.

The book reviewed here deals with a product—the electron tube—which is now reaching full maturity, at a time when another product—the transistor—is making rapid progress toward acceptance as the electron tube's replacement. In fact, many people already think that information pertaining to tubes is obsolete and uninteresting.

Is this book then useless, and should we bypass it in our race toward new inventions? Certainly not. We should, on the contrary, pause and study the carefully planned experiments which the authors describe. If progress is to be made, the techniques and methods developed in these experiments for vacuum tube improvement must be used, with the necessary changes, to improve and perfect the application of transistors or other devices that will replace tubes. The valuable guidance provided by past experience is sufficient justification for a book of this kind at this late period of tube technology.

The authors have diligently organized and presented the highlights of a very large investigation sponsored by the U. S. Army Signal Research and Development Laboratories on the life behavior of subminiature tubes. They show the "Percent Characteristic Survival" of transconductance or operating current values for eight tube types, under the effect of variation of five different parameters (heater voltage, heater-cathode bias, plate dissipation, plate voltage, and bulb temperature), and in three modes of operation (direct current, pulse, and vibration conditions).

The results confirm previously observed findings, in particular, that rated heater voltage is not conducive to long life, that high bulb temperature produces electrolysis, and that interelectrode leakage is reduced by high bulb temperature. The importance of these confirmations is enhanced by the solid statistical basis of the experiments which produced them.

The authors' aim is to provide information of value in the design of high-reliability electronic circuits using subminiature tubes. Following the presentation of the data, they recommend operating conditions that will yield maximum reliability for each tube type. The book should not be considered, however, as the answer to all problems of unreliability or as a blueprint for "super-reliability" (a Madison Avenue word that does not belong in a technical book).

The large quantity of data presented in this volume requires serious study for proper interpretation, and it should be considered only as contributing to better understanding of a few factors, as the title implies. The results are somewhat limited by the consideration of a single characteristic per tube type; yet the recommendations cover other characteristics. For instance, there is no data on the rate of formation of leakage as a function of the heater voltage nor on the variability of characteristics within the samples at low heater voltage as compared to the variability at higher heater voltage. These variabilities cannot be estimated from the data as presented because only minimum values are given.

These are but minor flaws in an otherwise well organized presentation. A few designers of tube circuits may still use this book. This reviewer hopes, however, that many other design engineers will be inspired to obtain similar data on variability of characteristics under expected operating conditions for other devices as an aid to design of circuits leading to high reliability.

E. R. Jervis
ARINC Research Co.
Washington, D. C.

Signals and Systems in Electrical Engineering, by W. A. Lynch and J. F. Truxal

Published (1962) by McGraw-Hill Book Co., Inc., 330 W. 42 St., New York 36, N. Y. 820 pages+xvii pages+11 index pages. Illus. 6¼×9¼. $12.50.

This book presents the fundamental concepts underlying the subjects of linear systems analysis and instrumentation. Although it was developed primarily for an introductory electrical engineering course for nonelectrical majors, it has evidently also served well for majors in electrical engineering when the book is supplemented by additional classroom notes which develop certain selected topics in greater detail.

The first half of the book introduces the viewpoints and methods of the electrical engineer. A unified systems point of view is employed, utilizing a wide variety of modern electrical engineering approaches and techniques. The model concept and the transfer function concept are continually emphasized and applied. That the approach is unusual is evident from the chapter titles titles for Part 1 which are: "Introductory System Analysis: The Language of Signals and Systems;" "Signals;" "Models for Mechanical Systems;" "Electrical Systems;" "The Response of Simple Electrical Circuits;" "The Transfer Function;" "The Elements of Analog Simulation and Analog Computers;" "Summary Illustrative Examples."

The second half of the book considers a variety of specific engineering problems which are drawn from such areas as analog simulation and computation, electronic instrumentation, communications, automatic control, electrical machinery, and vehicle guidance and control. Part 2, entitled, "Principles of Electronic Instrumentation," contains the following chapters: "Networks with Controlled Sources;" "Determination of Models for Physical Devices;" "Electronic Amplifiers;" "Feedback Systems;" "Instrumentation Systems and Communication;" "Electromechanical Transduction Systems;" "Systems for Automatic Navigation."

On the whole, this is a rather remarkable book in both coverage and presentation. Despite the fact that it is written at a level suitable for the sophomore student, it does so with a sophistication which goes far beyond that ordinarily attempted for these students. There is a wealth of material here, and the reader who has not had previous contact with the important modern topics in systems analysis will find the presentation highly readable and a rewarding effort. It will provide a discussion of many topics which previously might have been considered available only to the more advanced student. The discussion is limited largely to linear systems. The book is recommended for formal classroom study as a modern view of electrical engineering. It will also provide an excellent vehicle for home study for those who wish an introduction to the methods and results of modern linear systems analysis.

Samuel Seely
National Science Foundation
Washington, D. C.

Electromagnetic Waveguides and Cavities, by George Goubau

Published (1961) by Pergamon Press Inc., 122 E. 55 St., New York 22, N. Y. 652 pages+4 index pages +xvii pages. Illus. 7¼×10. $13.50.

This is an English version of a book that was completed in 1947 and published in German in 1955. It is an advanced and detailed mathematical treatment of important aspects of the subject.

Chapter I was written by Professor Richard Honerjäger. It is entitled "Theory of Electromagnetic Waves," is relatively short, and serves to introduce the notation and carry out the familiar analysis of cylindrical waveguides in terms of TE, TM, and TEM modes. The excitation of these modes by surface distributions in the transverse plane and by line sources is also treated, as are reflections at plane interfaces between different media and at diaphragms.

Chapter II, by Professor Rolf Muller, is concerned with the "Theory of Cavity Resonators." It contains a thorough formulation and solution of the eigenvalue problem. A perturbation method for obtaining the solution of a slightly perturbed problem from a known solution is discussed and illustrated. The excitation of a cavity and the application of the general theory to cavities of simple shapes are treated.

Chapter III, by Professor Georg Goubau, is by far the longest chapter. Entitled "Theory of Systems Coupled by Wave Guides," this is a very detailed and thorough study of the theory of networks composed of elements that are interconnected by hollow guides or coaxial lines. Based on appropriate definitions of current and voltage in the waveguides, the elements are treated as $2n$-poles and characterized by impedances. Alternatively, the more physical approach based on incoming and outgoing waves is also developed quite fully. Chapter IV, also by Professor Goubau, treats the network theory of cavities and the coupling of cavities with lines, with the assumption that mutual coupling is quasi-stationary.

Within a somewhat limited scope, this book by three outstanding authorities is well integrated and very complete. However, since it includes only work done in Germany until 1947, it naturally contains no account of the extensive research carried out in the United States during and since the war. For example, variational techniques in the analysis of obstacles in waveguides are not mentioned. A more concise, more complete, and more useful book could have been prepared if a new and completely revised and modernized edition had been planned instead of translation of a manuscript written fifteen years ago. Nevertheless, the book contains much useful material for the specialist in the field.

A general criticism of the book is the uneven quality of the printing. Presumably, in the interest of economy, the English text was simply typewritten between the equations taken from the German edition, and the combination reproduced by offset. In spite of heavy inking, which makes many of the German letters in the equations somewhat blurred, the fine lines in fractions, parentheses, certain symbols, and some figures are quite often very faint and occasionally invisible. For the reader not accustomed to the use of foreign language texts, the German terminology and symbolism such as "Lecher waves" for TEM waves, "rot" for curl, "Sin" for sinh, "Tg" for tanh, etc., may be somewhat disconcerting.

RONOLD W. P. KING
Harvard University
Cambridge, Mass.

Management Models and Industrial Applications of Linear Programming, Vol. 2, by A. Charnes and W. W. Cooper

Published (1961) by John Wiley and Sons, Inc., 440 Park Ave. S., New York 16, N. Y. 390 pages+xxi pages+32 bibliography pages+2 index pages+17 appendix pages. Illus. 6¼×10¼. $11.75.

Although the simplex and revised simplex algorithms are capable of solving any linear programming problem, their use involves a great deal of computation when we have a large number of variables and constraints. It often happens that large problems have a structure which permits the development of special algorithms, thus transforming a problem which is economically unfeasible into one where the solution may be found within the computing resources available. The transportation and assignment problems are well-known examples. It also happens that problems, which are not linear at first sight, can be made linear, with suitable ingenuity. In this book Charnes and Cooper develop methods for handling a very wide range of problems, and without doubt it will become a standard reference for the specialist linear programmer. However, the authors "have resisted the temptation to report . . . until . . . precision could be achieved at least to some extent." This means that in many cases the mathematical structure of problems is clearly implied in the verbal descriptions. Any experienced management scientist knows that he never receives problems in this way. It is up to the scientist to build his own mathematical structure, and this is frequently the hardest part of his task. It would have been of interest to read about problems as originally presented, before their structure was apparent.

While the authors have written the book for readers without much mathematical sophistication, the nature of their topic inevitably makes the ability to think rapidly in matrix-algebraic terms a highly desirable background.

Failing such ability the book requires a great deal of sustained concentration to follow its well-developed arguments. This of course is no fault of the authors; the subject matter could not be discussed with economy in any other way. However, now that so many writers are rushing into print with books which are merely their own wording of standard algorithms it is a pleasure to report that two of the experts have collected the results of their research in a worth-while volume.

M. W. SASIENI
Case Inst. of Technology
Cleveland, Ohio

Synthesis of Optimum Control Systems, by Sheldon S. L. Chang

Published (1961) by McGraw-Hill Book Co., Inc., 330 W. 42 St., New York 36, N. Y. 324 pages+5 index pages+xii pages+7 bibliography pages+21 appendix pages+21 pages of problems. Illus. 6¼×9¼. $11.75.

This book is a graduate text in control theory to be used after a senior course which covers the now classical material in Truxal's "Control System Synthesis," or its equivalent. The first part of the book is concerned with the least squares design of linear control systems, and treats both continuous and sampled data cases. The stationary system results are derived in the frequency (or z plane) domain, rather than the time domain. A knowledge of the Laplace transform and of the z transform is assumed. The principal results known or linear filtering and control of time variable systems are included.

Two chapters are devoted to adaptive or self-optimizing systems. These chapters summarize in unified notation many publications in this field. In particular, readable and self-contained accounts are given of the optimalizing control of Draper and Li, and of the stochastic approximations of Robbins and Munro. The optimization of the adaptive or surface searching loop for discrete systems with a parameter perturbation method of gradient measurement, is discussed at length.

Nonlinear optimal control problems are discussed in two chapters, one of which treats the minimal time problem with the maximum principle. The other introduces dynamic programming and the maximum principle for discrete systems. A sizable number of problems are included with each chapter.

Professor Chang has written a transition text which stands on the bridge between classical control theory—based mainly on operational calculus methods and designed for hand calculation—and the "modern" theory based on nonlinear differential equations and designed with computer assistance in mind.

GENE F. FRANKLIN
Stanford University
Stanford, Calif.

Electronic Equipment Design and Construction, by G. Dummer, C. Brunetti, and L. Lee

Published (1961) by McGraw-Hill Book Co., Inc., 330 W. 42 St., New York 36, N. Y. 241 pages+3 index pages+vii pages+2 bibliography pages. Illus. 6×9. $8.50.

Designing equipment that will withstand the severe environmental conditions encountered today, while achieving maximum reliability, can be attained if one has plenty of time and money, to test, alter, and at times completely redesign it where weaknesses show up. However, with the ever-shortening of the time between the starting and delivery dates, it is desirable that as many of the physical and mechanical constructional details as possible be considered at early stages.

Recommended constructional techniques are rarely touched upon in engineering courses, so that they, and indeed the very reasons behind the precautions are puzzles to some of the designers on the job who handle the basic concepts and the circuitry involved—the initial phases of the project.

While this book may contain little new information for seasoned production engineers, it does contain a wealth of background information relating to all phases of construction and production: climatic environments, mechanical ruggedness, the handling of temperature and nuclear radiation effects, the reduction of radio interference, to name but a few. The various chapters cover details for designing the apparatus to be reliable and easy to produce, operate and maintain.

Attention (roughly half the subject matter) is given to recent production techniques, covering both manual and automatic processes, and new design concepts required for modular packaging and miniaturization.

The book should be required reading for everyone concerned with equipment designing, whether the product be headed for military, industrial or commercial uses.

RALPH R. BATCHER
Design Consultant
Douglaston, N. Y.

An Introduction to Information Theory, by Fazollah M. Reza

Published (1961) by McGraw-Hill Book Co., Inc., 330 W. 42 St., New York 36, N. Y. 449 pages+6 index pages+xxi pages+10 bibliography pages+31 appendix pages. Illus. 6¼×9¼. $13.50.

Despite the appearance of several recent books relating to various aspects of information theory, it appears that it is still possible for a new book to appear which does not duplicate any of the existing books. Although the author does not so specifically state, the present book appears to be designed for a graduate level course. Like most books on the subject, it assumes that the student has had no prior exposure to probability theory. Unlike a number of them, however, it does assume the student to be familiar with Fourier integrals and series.

The book is devoted primarily to problems of coding and the transmission of information. It does not devote more than a couple of paragraphs to the problem of detecting a radar target or the problem of optimum filtering. On the other hand, it does allot considerable space to fairly recent developments in coding theory, including three distinct proofs of Shannon's fundamental theorem for the noisy channel, and a fairly extensive discussion of group codes, including such subjects as Hadamard matrices and Bose-Chaudhuri codes.

The book is divided into an introduction and four parts. Part 1 discusses discrete systems without memory. Part 2 is devoted to the continuum without memory, and Part 3 is concerned with problems in stochastic regimes. Each of these first three parts starts with a discussion of the pertinent probability principles and then proceeds to a treatment of the related communication problems. Part 4 is in the nature of an addendum consisting of two chapters. The first gives the three rigorous proofs of Shannon's fundamental theorem which was mentioned earlier. The second is a treatment of modern group code concepts.

In choosing a textbook, the instructor must be governed by factors such as the maturity and background of his students and the goals of the course. It is believed that the present book is somewhat advanced to be considered as an undergraduate text even in today's accelerated curricula. Further, it is felt that, even at the graduate level, it is probably unwise to go so deeply into coding theory concepts with no mention at all of optimum filters, radar detection problems, etc. On the other hand, a one-year course consisting of one semester with a text such as Davenport and Root[1] and one semester with the present book could be counted on to give the graduate student a complete and solid background. The book is well written and liberally provided with examples and problems to be solved by the student. In addition to its use as a text it will also serve as a convenient reference work for the practicing engineer who wishes to update his knowledge of modern development in the field. Not the least of its features is a group of tables, including tables of entropy, logarithms to the base two, etc.

Warren D. White
Airborne Instruments Laboratory
Melville, N. Y.

[1] W. B. Davenport and W. L. Root, "An Introduction to the Theory of Random Signals and Noise," McGraw-Hill Book Co., Inc., New York, N. Y., 1958.

Introduction to Feedback Systems, by L. Dale Harris

Published (1961) by John Wiley and Sons, Inc., 440 Park Ave. S., New York 16, N. Y. 325 pages+3 index pages+xi pages+34 appendix pages. Illus. 6×9¼. $10.50.

In the Preface, the author states that "this book was written with the intent of meeting the need for teaching some basic concepts of feedback at a point in the undergraduate program so that dependent areas such as feedback in electronics and control systems can be built on this common foundation." It is assumed that the student have as a prerequisite, "a modest background in elementary differential equations and in elementary Laplace transforms."

In accordance with his stated objective, the author logically develops principles of feedback theory, using examples from the fields of electronics and control systems.

Following the brief introductory Chapter 1, the reader is presented, in Chapter 2, with an elementary mathematical analysis of a number of simple physical systems, both open and closed loop. Concepts of transfer function and of stability are introduced in a rather simplified fashion.

Chapter 3 gives a fairly complete discussion of techniques for plotting the root locus. These techniques are introduced informally by means of increasingly difficult examples. Chapters 4 and 5 deal with elementary analysis and synthesis problems of various systems using the s-plane approach. First, the relationship between responses to standard inputs (*i.e.*, step, ramp and sinusoids) and the pole-zero configuration of the transfer function is examined, and then methods of controlling the pole-zero configurations by means of feedback are indicated. Chapters 6 and 7 are devoted to particular problems connected with amplifiers and control systems respectively, and Chapter 8 is again of a general nature dealing with feedback from the point of view of the frequency domain. Topics discussed in this chapter include the polar and rectangular plots, the Nyquist Criterion, M-circles, etc. Chapter 9 is devoted to a brief discussion of sinusoidal oscillators.

The four appendices in this book include an elementary review of Laplace transform methods, methods of finding the roots of higher order equations using the root-locus derivation of transfer functions for a number of simple devices, and an additional technique for finding the real-axis departure points of root-locus branches.

The principal merit of the book is the large number of examples and problems which are interwoven into the text and which logically follow each section. The main weakness is the lack of rigor and detail which, however, does not detract from its possible use as a text for an elementary undergraduate course in general feedback principles. The lucid style and the clear exposition should make this book popular among practicing engineers who wish to learn about feedback.

G. M. Kranc
Electrical Engineering Dept.
Columbia University
New York, N. Y.

Recent Books

Carroll, John M. *Electron Devices and Circuits.* McGraw-Hill Book Co., Inc., 330 W. 42 St., New York 36, N. Y. $8.75. Textbook for junior colleges, technical institutes, and industrial technician training programs. Covers the structure and operation of electron devices and their application in electronic circuits, presented from the electron physics point of view.

Ellis, David O. and Ludwig, Fred J. *Systems Philosophy.* Prentice-Hall, Inc., Englewood Cliffs, N. J. $13.00. An examination and study of a diversity of systems from a common viewpoint, in language comprehensible to management and the public as well as engineers and scientists.

Romanowitz, H. Alex. *Fundamentals of Semiconductor and Tube Electronics.* John Wiley and Sons, Inc., 440 Park Ave. S., New York 16, N. Y. $8.25. A textbook of fundamental concepts and principles in electronics, including both tube and semiconductor theory.

Scanning the Transactions

Microminiaturization is a broad term which can almost be considered obsolescent, primarily because it has been in use for several years during which research has been far from barren. Previously it was felt necessary to solicit the aid of the qualifying prefix to show progress over *miniaturized* circuits. The next step could be to resort to *picominiaturization* as circuits become increasingly minute, a development which is assured because of an impressive amount of research being conducted with just that in mind.

Terminology aside, the results from work in this area are sometimes quite amazing, often exciting, and certainly suggestive of future trends in electronic circuitry. With the wrist-watch radio a possibility if not a reality, one wonders when the day of the tie-clasp computer or the diamond-ring radio beacon will arrive. Keeping up with the fast-and-furious developments in miniaturization can be a tall order unless a reliable survey is resorted to. A recent example covers all types of microminiaturization: 1) assembly of specially designed, miniaturized component parts; 2) printing or vapor deposition of multicomponent assemblies on flat, insulating substrates; and 3) preparation of complete circuits from solid blocks of semiconductor material. The first technique is already in active commercial use. The second is in the initial stages of commercial exploitation; although devices with two-dimensional passive parts and attached conventional active parts are available, realization of the full commercial potentialities awaits reduction of the active parts to two dimensions. The third technique is also in the initial stages of commercial production. (E. F. Horsey and P. J. Franklin, "Status of Microminiaturization," IRE TRANS. ON COMPONENT PARTS, March 1962.)

Electric Power Generation. At first blush this phrase still brings to mind flux-cutting conductors, sparking brushes, and the left-hand rule. Today "it ain't necessarily true" that things must move in order that electric power be generated. Direct-energy methods are concerned with the conversion of solar, chemical, or nuclear energy to electricity by direct processes which bypass rotating machinery completely.

Electrochemistry, photoelectricity, thermoelectricity, thermionics, and magnetohydrodynamics are not new terms, but the multi-million dollar research effort being conducted in these areas is. New energy sources for new applications—and old ones too—are the goal. Fuel cells promise to extend the application of electrochemical processes to a broad realm ranging from submarine propulsion to energy-storage devices for space vehicles. Photovoltaic solar cells in combination with nickel-cadmium batteries are providing the electrical power for satellites now in orbit and are expected to do so with improved weight, cost, and reliability factors for several years. The thermoelectric effect, known for a century and a half, awaited the recent developments in semiconductors to be exploited as a power source. Both the thermionic and MHD processes, although having great potential, have been prevented from making significant practical contributions to date because of their dependence on high-temperature heat sources with concomitant materials and engineering problems. (G. B. Wareham, "Direct Energy Conversion," and entire issue of IRE TRANS. ON MILITARY ELECTRONICS, January 1962.)

The Non-National Character of the IRE was emphasized recently by the establishment of Region 9, which encompasses Europe and certain bordering countries. That this internationality is not token only is attested to by the March, 1962 issue of the IRE TRANSACTIONS ON CIRCUIT THEORY, in which there are contributors from nine countries other than the United States: Belgium, Canada, The Congo, England, Israel, Italy, The Netherlands, Poland, and Rumania.

Antennas Incognito. You may not be able to tell a book by its cover, but at least you can tell that it's a book. In the olden days (*viz.*, several years ago), roughly the same statement could be made about antennas: a glance at a parabolic dish, a horn, or an array of helices left no doubt about what the object was. Nowadays only a specialist can infallibly recognize an antenna as an antenna.

One new antenna is made up of an array of dielectric-loaded rectangular waveguides with common narrow walls. Longitudinal slots, which are cut in the center of each wall, are covered with a slab of dielectric. The array radiates a pencil beam, which is directed up from the aperture at an angle equal to the arc cosine of the velocity of light divided by the slotted-waveguide phase velocity. An approximate theory for this device has been developed, and measurements have been made on an antenna designed for 10 kMc. At the design frequency the beamwidth was 5.4° by 8.0°. Good radiation patterns were obtained from 8–11 kMc. (E. D. Sharp and E. M. T. Jones, "An Antenna Array of Longitudinally-Slotted Dielectric-Loaded Waveguides," IRE TRANS. ON ANTENNAS AND PROPAGATION, March 1962.)

A Gigawatt is a lot of power. Designing a precision piece of equipment operating in that power range is bound to offer some unique problems.

A 1000-megawatt peak-power linear electron accelerator is required for the injection of electrons into a thermonuclear fusion experimental device, called the Astron, which is now under construction at the Lawrence Radiation Laboratory. An electron gun having a cathode with a ten-inch diameter is used; although spectacular, this size is not entirely unexpected when it is learned that a beam current of 200 amperes must be supplied. The accelerator is of the induction type using 400 large ferromagnetic cores. The modulating circuits for pulsing the cores required special considerations. The details of the design and development of the accelerator and associated circuitry are discussed in two recent papers. (W. A. S. Lamb, "Design Features of a High-Current Pulsed Electron Accelerator," and V. L. Smith, "Development of 36-Megawatt Modulators for the Astron 1000-Megawatt Electron Accelerator," IRE TRANS. ON NUCLEAR SCIENCE, April 1962.)

Biological Simulation. Much of the credibility of modern biochemistry is derived from a relatively few chemical reactions which can be isolated and thoroughly analyzed by standard means in a laboratory. The analysis of large chemical systems requires new tools and methods. A recent paper discusses a method for simulating a large biological system, the respiratory function of the blood in the human lung, by constructing a mathematical model and utilizing an analog computer. The simulation is not considered complete but rather the first of a series of models which will successively incorporate more of the essential chemical reactions. Although the digital computer gives results which are more accurate and reproducible, the data obtained from the much faster analog computer indicate that the accuracy and stability are sufficient for analysis within the laboratory experimental accuracy. (E. C. DeLand, "Simulation of a Biological System on an Analog Computer," IRE TRANS. on ELECTRONIC COMPUTERS, February 1962.)

Abstracts of IRE Transactions

The following issues of TRANSACTIONS have recently been published, and are now available from the Institute of Radio Engineers, Inc., 1 East 79 Street, New York 21, N. Y., at the following prices. The contents of each issue and, where available, abstracts of technical papers are given below.

Sponsoring Group	Publication	IRE Members	Libraries and Colleges	Non-Members
Antennas and Propagation	AP-10, No. 3	$2.25	$3.25	$ 4.50
Audio	AU-10, No. 2	2.25	3.25	4.50
Bio-Medical Electronics	BME-9, No. 2	2.25	3.25	4.50
Communications Systems	CS-9, No. 4	5.00	7.50	10.00
Component Parts	CP-9, No. 2	2.25	3.25	4.50
Electron Devices	ED-9, No. 3	2.25	3.25	4.50
Industrial Electronics	IE-9, No. 1	2.25	3.25	4.50
Microwave Theory and Techniques	MTT-10, No. 3	2.25	3.25	4.50
Military Electronics	MIL-6, No. 2	2.25	3.25	4.50
Radio Frequency Interference	RFI-4, No. 2	2.25	3.25	4.50
Reliability and Quality Control	RQC-11, No. 1	2.25	3.25	4.50

Antennas and Propagation

Vol. AP-10, No. 3, May, 1962

The Transient Response of Linear Antennas and Loops—R. W. P. King and H. J. Schmitt (p. 222)

The transient response of straight wires and circular loops when short pulses are applied is studied experimentally and theoretically. It is shown that the initial response is always that of an infinitely long antenna at a frequency near the upper limit of the frequencies contained in the pulse provided this is sufficiently short so that the first reflection from the end of the wire or loop is not superimposed on it.

A Method for Synthesis of Optimum Directional Patterns From Nonplanar Apertures—J. H. Harris and H. E. Shanks (p. 228)

The scalar radiation problem is considered for sources lying on a surface of arbitrary shape. An optimum directional pattern is specified and the source distribution which gives rise to the optimum pattern is determined in terms of the Green's function for the surface. The optimum source distribution is found to be proportional to the complex conjugate of the Green's function evaluated at the beam pointing coordinates and to lie in a region enclosed by an equimagnitude curve of this function.

Examples are included for sources on planes and spheres.

A Study of Tracking Accuracy in Monopulse Phased Arrays—William H. Nester (p. 237)

The requirements for high-data rates in modern weapons systems favor the use of phased arrays for monopulse tracking antennas. A discussion is presented of the tracking errors produced by the phase and amplitude errors in the excitation function of a phased array. Both systematic and random phase errors are considered. The effects of both scan and aperture correlation of the random errors is discussed. Even when off-boresight tracking is performed, boresight errors were found to be the predominant tracking error.

Surface-Wave Propagation on Coated or Uncoated Metal Wires at Millimeter Wavelengths—M. J. King and J. C. Wiltse (p. 246)

The properties of surface waves guided by an uncoated cylinder of finite conductivity (Sommerfeld wave) or by a perfectly conducting cylinder with a dielectric coating (Goubau wave) have been analyzed theoretically for frequencies in the millimeter and submillimeter wavelength regions. Previous analysis by Goubau for lower frequencies provided the primary basis for this investigation. For wire sizes which provide low loss propagation above about 100 kMc, the approximations used by earlier workers are not sufficiently accurate to provide useful results. More accurate solutions for some of the properties have been obtained for wires of circular cross section by the use of fewer or different approximations. Numerical values have been calculated for attenuation, power-handling ability, and radial extent of the region of principal power flow. The results show that above 70 kMc the significant field extent is reasonable and the attenuation may be orders of magnitude smaller than for rectangular waveguide. Consideration was also given to the problem of surface-wave propagation on wires of elliptical cross section, but in this case the solutions for the field components must normally be expressed in the form of infinite series of products of the radial and angular Mathieu functions. Numerical results are therefore extremely difficult to obtain for elliptical wires.

A New Approach to the Evaluation of HF Aircraft Antennas—J. F. Cline and R. L. Tanner (p. 254)

An improved method is described for establishing a factor of merit for an airborne HF transmitting system, taking into account both the transmitter power and the antenna radiation patterns at different frequencies. A large number of communication events are postulated, having different path lengths, directions, geographic locations, and times of occurrence. Some of these events are successful while others are not, depending on the calculated SNR at the receiver sites. The factor of merit is defined as the ratio of the number of successful events to the total number of events postulated. A graph of the factor of merit of a particular system as a function of the transmitter power can be used as a guide in effecting a reasonable compromise between power economy and system performance. Graphs based on two or more antennas can be used to compare the antennas in terms of the relative powers required for a given system factor of merit or in terms of the relative factors of merit obtained with a given power.

Excitation of a Conducting Cylindrical Surface of Large Radius of Curvature—G. Hasserjian and A. Ishimaru (p. 264)

Approximate expressions are obtained for the magnetic field induced by slots on conducting circular cylinders of infinite length and of radius large compared to the signal wavelength. The approximations are derived from the formal solution of the cylinder problem and are valid for all distances from the slot. The expression for a short slot dipole, at any orientation, is expressed in terms of the field of the slot on a flat conducting sheet multiplied by a curvature term. The latter is a function of the "ray path" length and radius of curvature, making the results applicable to other convex surfaces. Corresponding expressions for half wavelength axis and transverse slots are also obtained and the results compared with experimental measurements.

Scattering Error in a Radio Interferometer—Charles W. Harrison, Jr. (p. 273)

Scattering error in an interferometer-angle-measuring system is investigated theoretically and numerically. The model employed consists of four identical base-loaded vertical antennas erected at the corners of a square. The assumption is made that the earth is a perfectly conducting plane of infinite extent. Curves are supplied for the error angle as a function of antenna spacing, with azimuth angle of wave arrival as parameter. The incident electric field is vertically polarized. These data were computed for quarter-wave vertical elements having a length-to-radius ratio of 122.35 and for base-load resistors of 12.5, 50, 200 and 500 ohms. A brief résumé of the theory of the two-element ratio interferometer is presented, together with a numerical analysis when quarter-wave antennas are employed having a length-to-radius ratio of 74.21 and for the same values of base loads.

The Determination of Noise Temperatures of Large Paraboloidal Antennas—D. Schuster, C. T. Stelzried, and G. S. Levy (p. 286)

A maser receiving system may have higher noise contributions from the antenna and transmission line than from the amplifier. To develop lower-noise receiving systems, it therefore is important to know the antenna and transmission-line noise temperature as well as the receiver noise temperature. Several techniques for the measurement of absolute antenna noise temperature have been tested at the Jet Propulsion Laboratory (JPL). Experiments have been conducted at 960 and 2388 Mc using an 85-ft paraboloidal reflector with several antenna feed configurations. At 2388 Mc, an antenna noise temperature of 15°K has been attained with an efficient antenna feed.

Use of a High-Speed Computer for Ground-Wave Calculations—I. H. Gerks (p. 292)

Procedures for calculating the propagation loss between antennas located near the surface of a smooth spherical earth of finite conductivity in the absence of an atmosphere have been known for many years. The increasing availability of high-speed computers suggests that the drudgery of such calculations can be eliminated, and more accurate and voluminous data made available. The equations and graphical aids developed in the past generally are not well adapted for use with computers. This report outlines methods whereby the field strength relative to free space can be calculated for the cases where the ionosphere is neglected and refraction in the troposphere is approximated by assuming an appropriate constant gradient of refractive index. Plane-earth methods are employed to determine the solution for short distances, and the residue series is used under conditions where the surface curvature is important. The input parameters are the horizontal distance, the antenna heights, the equivalent radius of the earth, the wavelength, and the dielectric constant and conductivity of the earth.

Transmission Through Inhomogeneous Plane Layers—J. H. Richmond (p. 300)

A plane wave is considered to be incident obliquely on a dielectric layer whose permittivity is a function of distance from the plane surface. The field distribution and the transmission coefficient are obtained from step-by-step numerical integration.

Since the calculations are simple and repetitive, the technique is suitable for both manual and automatic calculations. The method has been used successfully for lossy and lossless layers with perpendicular and parallel polarization. Some of the calculated field distributions are presented graphically. Only ten steps are required in the numerical integration for a typical half-wave inhomogeneous radome wall to obtain results accurate to within one per cent.

Charts for Computing the Refractive Indexes of a Magneto-Ionic Medium—G. A. Deschamps and W. L. Weeks (p. 305)

The complex refractive index of a magneto-ionic medium for various directions of propagation is evaluated graphically. Most of the constructions make use of a Smith Chart on which the scales have been suitably relabeled. When the directions of propagation are longitudinal or transverse with respect to the applied magnetic field, the constructions take the losses into account. The energy transferred to the medium is characterized by conductivity coefficients that are also evaluated graphically. An overlay converts the refractive index into the reflection coefficient at a plane boundary of the medium. The indexes for propagation at an arbitrary angle with respect to the magnetic field are evaluated similarly, provided the collision frequency is very low.

The Reflection of Microwaves by a Refractive Layer Perturbed by Waves—Earl E. Gossard (p. 317)

The power spectra of amplitude and slope for several cases of internal waves on a radio refractive layer are shown and the implication of these waves for radio and radar coverage is discussed. The angular reflection patterns are derived for rough layers and the beamwidths in elevation and azimuth are obtained. The amplitude, frequency, wavelength and velocity of atmospheric waves are described, and the possibility of such waves acting as very rapidly moving reflectors is discussed. It is concluded on the basis of present observations of wavelength, amplitude, and phase velocity of atmospheric internal waves that they are not likely to be a source of very rapidly moving reflections such as were observed by Waterman at microwave frequencies.

Optimum HF Prediction—H. Greenberg, S. Krevsky, and G. B. Bumiller (p. 325)

The usual HF prediction is based on MUF, maximum usable frequencies, alone. More detailed predictions include LUF, lowest usable high frequency, calculations which indicate the lowest frequency at which the receiver threshold is exceeded at least 50 per cent of the time. The optimum HF prediction presented in this paper provides contours of the probability of successful HF transmission as a function of frequency and time of day. This contour presentation now provides a detailed means for efficient HF spectrum utilization, giving a probability number to any assigned frequency at a given time of day which can be compared to any other available channel probability.

DC Signaling in Conducting Media—Charles R. Burrows (p. 328)

The electric field produced by the dc current between two spheres is calculated and expressed in terms of input power.

The attenuation between these spheres and a pair of receiving spheres considered as a four terminal network is found to be $P_2/P_1 = l_1^2 l_2^2 a_1 a_2 / 16r^6$, where a_1 is the radius of the transmitting spheres separated by a distance l_1 apart, a_2 is the radius of the receiving spheres separated by a distance l_2, and r is the distance between transmitter and receiver all in the same units. This equation applies when the line joining the receiving spheres is parallel to the line joining the transmitting spheres and perpendicular to the direction of propagation.

For colinear spheres, P_2/P_1 is four times as great but other factors combine to counteract this apparent advantage.

The transient responses to a unit step and a unit pulse are calculated and presented as curves. The minimum practical pulse duration for the former configuration is $t_0 = \sigma\mu r^2/8$, where σ is the conductivity and μ the permeability all in mks units. A pulse of the same length is more smeared in the colinear direction and reduced in amplitude by a factor of approximately three, and power by a factor of nine more than counteracting the favorable factor of four for the steady-state condition for colinear spheres.

A Selective Survey of Soviet Bloc Scatter Development—John H. Barton (p. 335)

Results of a study of the Soviet Bloc literature on the various forms of scatter propagation are presented. Backscatter and meteor scatter are included along with tropospheric and ionospheric scatter. The theoretical work is emphasized, since it is presented more fully in the available literature, and since hardware development appears to be lagging behind theoretical study. It is concluded that the Soviet Bloc has a vigorous well-organized program to explore the potentialities of these forms of propagation.

Log-Periodic-Slotted Cylinder Antenna—G. A. Jackson and W. R. Wheeler (p. 341)

Comments on "Aperture Fields"—W. H. Nester and R. Plonsey (p. 342)

Monopulse Difference Slope and Gain Standards—Richard R. Kinsey (p. 343)

Comments on "Diffraction of a Plane Wave by a Perfectly Conducting Sphere with a Concentric Shell"—R. J. Garbacz and M. A. Plonus (p. 345)

Equatorial Plane Radiation Fields Produced by a Circumferential Slot on a Large Circular Cylinder—N. A. Logan, R. L. Mason, and K. S. Yee (p. 345)

Lateral Waves on an Anisotropic Plasma Interface—L. B. Felsen (p. 347)

Higher Modes in Guided Electromagnetic-Wave Beams—J. B. Beyer and E. H. Scheibe (p. 349)

A Relationship Between Slope Functions for Array and Aperture Monopulse Antennas—George M. Kirkpatrick (p. 350)

Scattering Pattern of a Plane Wave from a Magneto-Plasma Cylinder—S. Adachi (p. 350)

Resolution of Angular Ambiguities in Radar Array Antennas with Widely-Spaced Elements and Grating Lobes—Merrill I. Skolnik (p. 351)

Contributors (p. 353)

Papers to be Published in Future Issues (Inside Back Cover)

Audio

VOL. AU-10, NO. 2, MARCH-APRIL, 1962

The Editor's Corner—Marvin Camras (p. 29)

PGA News (p. 32)

Signal-to-Noise Ratio and Equalization of Magnetic-Tape Recording—Hanswerner Pieplow (p. 34)

Future tape recorders running at a speed of $1\frac{7}{8}$ ips must achieve an upper frequency limit of 15 kc on a quarter track recording, with better SNR than presently obtained with commercial recorders. This means that the subjective quality of present full track machines at 15 ips must be maintained in spite of a fifty-fold increase of information density.

It is obvious that such an improvement cannot be obtained only by changes to the electronic circuitry and the like. In fact, the future requirement would be impossible to meet if improvements in tape and heads were not made. Such improvements must include new knowledge of head construction, tape-to-head contact problems, and optimum balancing of recording parameters. But once these improvements are effected, it is then necessary to check carefully if the most thorough use is being made of all available technical possibilities.

It will be shown that recording techniques have advanced to a stage where a change in the standardization characteristics is advantageous and even necessary, though they may be more complicated than the existing standards.

Design Aspects of FM Stereo Tuners and Adaptors—D. R. von Recklinghausen and H. H. Scott (p. 38)

The stereophonic composite signal may be decoded in adaptor circuitry by time multiplex or sum-and-difference approaches. To obtain suppression of SCA (background music) signals while maintaining adequate separation of the two stereophonic audio signals double, single, or residual sideband demodulation of the stereo subcarrier can be employed. Satisfactory reception of FM stereo signals requires tuner circuitry of higher performance than for equal monophonic performance. Calculated and measured stereophonic separation, distortion, and signal-to-noise ratio are shown with major causes of these performance aspects.

A Versatile Phonograph Preamplifier-Equalizer—Harold Fristoe (p. 41)

A phonograph preamplifier-equalizer system has been developed which permits continuous equalization adjustment over a wide frequency range. The playback contour can therefore be "fitted" to accommodate any recording characteristic normally encountered in practice.

Musical Transfer Functions and Processed Music—Andrew G. Pilker (p. 47)

Increasing complexity in the combinations of music and electronic technology suggests a general model of the musical transfer function. Conventional transfer includes: 1) universe of tones, 2) composer, 3) score, 4) performer, 5) musical instrument, 6) audience. Recording, broadcast, electronic synthesis and composing music by the computer either extend or modify the conventional transfer. Under "processed music," alternating and synchronous applications of live and mechanical music, time-processed music and the more visionary polyphonic separation are described. The method of juxtaposition described permits automatic scoring of ensemble performances.

Automatic Measurement of Phonograph Reproducers—B. B. Bauer (p. 52)

A stereophonic test record has been designed for measurement of pickup response on a curve recorder. The principles of stereophonic disk recording which have governed the design of this record are reviewed. The new test record contains two sweep-frequency bands for the left and right channels, the signal frequency varying logarithmically with time at a rate of 1 decade each 24 seconds covering a range of 40–20,000 cps. Left and right spot-frequency tones with voice announcements have also been provided covering a range of 20–20,000 cps. Automatic recording of pickup response has been estimated to save ½ to ⅓ of manpower used in pickup and phonograph development. For automatic measurement of preamplifier characteristics, an RC RIAA generating network has been designed. A circuit for automatic starting of recorder by keying tones on the record is described.

Additional Comments on "Enhanced Stereo"—R. W. Benson and H. H. Heller (p. 56)

Contributors (p. 58)

Bio-Medical Electronics

Vol. BME-9, No. 2, April, 1962

Editorial—Edward F. MacNichol, Jr. (p. 72)

Guest Editorial—John E. Jacobs (p. 73)

Sound and Pressure Signals Obtained from a Single Intracardiac Transducer—E. M. Allard (p. 74)

The Reaction of Luminous Bacteria to Microwave Radiation Exposures in the Frequency Range of 2608.7–3082.3 Mc—Donald E. Barber (p. 77)

Suspensions of luminous bacteria were used to investigate the response of this biological system to microwave exposures in the stated frequency range at power levels up to 16.7 w. The merits of the biological system for this work are presented. The experimental arrangement, method of exposure and results are presented. Nonthermal effects in the test organism are found not to occur under the conditions of the investigation. The significance of this finding with respect to man is discussed.

An Automatic Scanning and Printing Analog-to-Digital Densitometer—H. F. Gatzek, E. Gordy, and P. Hasenpusch (p. 81)

Probability Methods in the Study of Bioelectrical Brain Reactions—V. A. Kozhevnikov (p. 85)

Phase Detection Electromagnetic Flowmeter—Design and Use—Frederick Olmsted (p. 88)

Two types of gated sine-wave electromagnetic flowmeter are examined critically, and found to be sensitive to phase shift in the transducer signal. This phase shift is always found in a sine-wave flow transducer because of imperfection in construction, particularly in those used for physiology and medicine. A flowmeter design that discards amplitude modulation and is sensitive to phase change only is described. Advantages over other types of electromagnetic flowmeter are discussed. Results obtained with the phase detection flowmeter are illustrated.

Electrical Properties of the Cytoplasmic Membrane and the Cytoplasm of Bacteria and of Protoplasts—Helmut Pauly (p. 93)

Electronic Summation of Small Amplitude Biopotentials—R. J. Plaszczynski, C. A. Milleret, and P. McLeod (p. 96)

Effects ot Chronic Microwave Irradiation on Mice—S. Prausnitz and C. Susskind (p. 104)

An experiment has been carried out to determine pathological and longevity effects caused by chronic microwave irradiation of mice. Two hundred males were exposed daily for 59 weeks to 0.109 w cm² for 4.5 minutes. This treatment produced an average body temperature rise of 3.3°C. Histopathology was performed on all dead mice in both irradiated and control groups. Changes in body weight, body temperature response to heating and in the blood picture were not evident. Testicular degeneration in the form of tubule atrophy and neoplasms of the white cells were indicated. Longevity of the mice did not appear to be affected under the prevailing conditions.

Multifunction Instaneous Display Counter—R. L. Schoenfeld and L. Eisenberg (p. 108)

A two-channel, three-decade counter incorporating digital logic for selecting nerve impulses by amplitude and time interval of occurrence is discussed. The count of the number of selected impulses, their time interval or time of occurrence, is printed out photographically superimposed on the oscilloscope trace of the impulses.

Printed circuit logic modules facilitate construction, maintenance, change of function or expansion of capacity.

Electro-Oculography in a Pilot Study of Cerebral Palsied Children—B. Shackel, J. R. Davis, and M. L. J. Abercrombie (p. 112)

The technique of electro-oculography has been used to record the saccadic and the pursuit eye movements of normal and cerebral palsied children under simple task conditions. Performance significantly worse by about 50 per cent among the cerebral palsied children, a correlation between performance and chronological age amongst all subjects, and unexpected discrepancies between performance on the saccadic and the pursuit tasks, have been found. These findings are relevant to the study of the oculo-motor system as one of the control systems in the body.

Blood Pressure Measuring Methods—Hampton W. Shirer (p. 116)

Blood pressure can be measured directly or indirectly. While direct methods provide the maximum quantity of reliable information from probes inserted into the blood stream, indirect methods produce much less disturbance to the subject. Indirect methods are based on the adjustment of a known external pressure to equal the vascular pressure. Systolic and diastolic pressure can be determined intermittently from the pressure that will just collapse the vessel; an approximation of the instantaneous pressure level is obtained from a surrounding chamber adjusted to remove all vessel wall tension. Direct methods can provide continuous, high fidelity recordings of the absolute vascular pressure via a catheter either to transmit the blood pressure through liquid to an external sensor or to carry the signal leads from a miniature internal sensor. External sensors require careful adjustment of the catheter dimensions to obtain optimum dynamic response. Internal sensors provide the maximum dynamic response and avoid acceleration artifacts. Convenience of electrical signal manipulation, display and recording have made electrical transducers increasingly popular.

Nonlinear Computations in the Human Controller—Otto J. M. Smith (p. 125)

The response of the human forearm following random input step commands was observed to approach at its best the same kind of response as that of a maximum-effort minimum-time optimum bang-bang servo in which the magnitude of the error is compared with a nonlinear function of the stored energy in the load. Tests were made which required the hand to move both small and large inertias, small and large friction coefficients, and small and large springs, with combinations of these. The muscle force was calculated and plotted as a function of time for a great many tests on different individuals. This paper will not describe the average response, but the best response which any individual is capable of achieving. The muscle forces were relatively constant for each individual regardless of the dynamics of the load or the magnitude of the command.

Electrogastrographics—M. A. Sobakin, I. P. Smirnov, and L. N. Mishin (p. 129)

A Compensated Dichromatic Densitometer for Indocyanine Green—W. F. Sutterer and E. H. Wood (p. 133)

A Compensation Circuit for Coaxial and Double-Barreled Microelectrodes—Tsuneo Tomita (p. 138)

In both the coaxial and double-barrelled micropipet electrodes, capacitative interference occurs across the wall that makes the boundary between the two pipets. Report will be made on a device which compensates this interference as well as the capacitance of each pipet. A combination of vacuum tubes and transistors was found useful.

Behavior of Thermistors at Biological Temperatures—H. W. Trolander and J. J. Sterling (p. 142)

The U. S. Focoscan Method—H. C. von Ardenne and R. Millner (p. 145)

This paper describes a supersonic-impulse-echo method employing double-focusing for selective depiction of certain internal body layers. By employing the impulse echo principle, a point supersonic source is focused on the object element to be examined by means of a sound-optical system; the echo reflected by the object element is focused by the same sound-optics on the identical effectively point-shaped sound receiver and is transformed into a voltage impulse that serves for the production of an image. First results of experiments confirm an essential improvement in SNR as was expected.

Limitations of Combined Image Amplifier—Television Systems for Medical Fluoroscopy—E. W. Webster and R. Wipfelder (p. 150)

Evaluation of Simple Computer for Cardiac Output Measurements Based on Thermal Dilution—H. U. Wessel, J. E. Jacobs, O. D. Despe, and P. Kezdi (p. 155)

Television Ophthalmoscopy—S. S. West, A. M. Potts, and J. R. Shearer (p. 159)

A Critical Appraisal of Methods of Blood Flow Determination in Animals and Man—E. Wetterer (p. 165)

Classification of the various procedures of blood flow measurement is presented. The discussion is confined to the recording of pulsatile flow and its rapid fluctuations. The hydromechanical, electromagnetical and sonic types are particularly considered. It is concluded that, by now, the electromagnetic methods are the most superior procedures since they possess almost all the properties of an ideal direct method. Especially, their calibration in terms of the flow rate is independent of the velocity profile. Besides, the sonic flowmeters seem to very promising.

Letter to the Editor—Quartz Crystal Tonometer—R. S. Mackay, E. Marg, and R. Oechsli (p. 174)

Communications Systems

Vol. CS-9, No. 4, December, 1961

Editorial (p. 327)

Link Error Control and Network Route Selection—R. C. Amara, H. Lindgren, and M. Pollack (p. 328)

Military networks must deliver messages during periods of high noise. On a link basis, character reliabiltiy can be increased during decision feedback for error control. Two specific decision feedback schemes are described in detail. The improved reliabilities and the reduced capacities for information transfer are computed. A method is then given for determining the optimal message route between each origin and destination—that is, the route whose capacity is maximum such that the route character reliability is adequate. Using a typical military network as an example, and typical jamming noise, optimal routes are determined from a station to each of six stations. The routes thus chosen are compared with routes chosen by another criterion.

An Automatic Computer-to-Computer Digital Communications System—R. L. Ellsworth and D. N. Lytle (p. 335)

This paper discusses the design of an automatic on-line computer-to-computer intercommunications system with locations at several data processing centers throughout the world. The solution to the problem is developed in logical order starting with the selection of a transmission medium. Leased private wire telephone facilities were found to be the best worldwide common denominator for economically meeting reliability and speed (1200, 2400 and 600 bit/sec) criteria. Pertinent statistical information characterized the transmission environment with short periods of high burst noise and long periods of error-free transmission. A statistically related burst "error model" of 48 successive bits subject to error was derived. Several available error detecting and correcting codes were considered, and the limitations of each explored. A geometric block code combined with a Hamming cyclical code was found to possess excellent burst error detection capability (343 consecutive bits subject to error or an error correction capacity of one "error model" of 48 bits). When this forward acting code is combined with decision feedback the probability of undetected error entering the system is reduced to less than that in computer systems. Implementation of the code structure is uniquely suitable to time sharing and linear-feedback shift-register techniques.

Analysis of a PCM System Employing a PPM Vernier—Walter H. Lob (p. 342)

The upper limit to the output SNR of sampled-data PCM systems is set by the quantization noise. The present study is concerned with a method of overcoming this limitation by employing time shifting of the PCM pulse groups so as to constitute an analog encoding of the difference between the sample amplitude and the nearest quantization level. Thus PCM is introduced to serve as a vernier to PPM.

For this Vernier system the optimum values are found of 1) the number of pulses per pulse group for a given time-bandwidth per pulse group and 2) the detection threshold. An SNR analysis is then carried out, comparing this system with conventional double-polarity PCM and with conventional single-polarity PPM. This comparison is made on the basis of equal energy and time-bandwidth per pulse group and a simplified model of the channel and detection scheme.

The analysis shows that the Vernier system's threshold of channel SNR required for reliable detection is about 6 db higher than that for pure PCM, but that, near and beyond this threshold, the Vernier system's performance exceeds that of pure PCM and of pure PPM consistently and considerably. This improvement in performance can be realized as an increase in output SNR, as a decrease in time-bandwidth occupancy, or as a combination of these advantages.

Linear Reconstruction of Quantized and Sampled Random Signals—D. S. Ruchkin (p. 350)

Techniques for optimal mean-square linear reconstruction from quantized samples of a random signal and the resulting errors are discussed in this paper. The signal is assumed to be wide-sense stationary with Gaussian statistics. The shape of the sample pulse is arbitrary. It is shown that the pulse shape has no effect upon the minimum mean-square error.

An optimal linear filter for reconstruction from quantized samples and the resulting error are obtained. The mean-square error that arises when the optimal filter for unquantized samples reconstructs from quantized samples is also obtained.

The errors of the above-mentioned filters are then compared. It is shown that, for sufficiently high sampling rates, the filter that takes quantizing into account can achieve a significant reduction in quantizing error relative to the filter for unquantized samples. However, when a constraint of constant channel capacity is imposed, there is essentially no difference between the optimal performances of the two filters.

Effects of Impulse Noise on Digital Data Transmission—Andrew B. Bodonyi (p. 355)

This paper presents the basic characteristics of impulse noise and its effects on various types of binary data transmission systems. The sources and properties of such impulsive noise, in contrast to Gaussian noise, are discussed. A method is described for the experimental comparative evaluation of bit error rates in the presence of additive impulse noise. The method is shown to permit unique comparison among the three modulation schemes tested, namely, on off carrier, frequency shift, and phase reversal keying.

On the Potential Advantage of a Smearing, Desmearing Filter Technique in Overcoming Impulse-Noise Problems in Data Systems—Richard A. Wainwright (p. 362)

It has long been recognized that impulse noises or even very short duration line interruptions are the most vicious form of interference affecting data communications over wire lines. These noises, while annoying, are not catastrophic in voice communications because of the inherent redundancy in speech sounds. If a degree of apparent redundancy can be inserted into a data stream, the serious degradation caused by these noises can be materially reduced. Data signals which require a sizable bandwidth can be transmitted by modifying the real time placement of their frequency components (smearing) before transmission through a channel corrupted by impulse noises. A reversal of the time-vs-energy frequency modification before detection (desmear) reconstructs the data signal but "smears" the impulse or line interruption into a time-energy distribution form considerable different from that of the signal.

Effects of Terrestrial Electromagnetic Storms on Wireline Communications—R. Sanders (p. 367)

Effects of natural electromagnetic phenomena on wireline circuits are discussed. An important factor causing degradation of system operation or damage to equipment is the occurrence of earth currents, or geoelectric variations, associated with electromagnetic storms. Three to six earth-current storms occur yearly, during and after the maximum of the sunspot cycle. Peak disturbances last 10 to 30 minutes and return to normal within 6 to 48 hours. Typical disturbances are 3 to 20 v/km in the auroral zones, 0.5 to 5.0 v/km in middle latitudes, and less than 100 mv/km near the equator. Current flow is generally N-S, except near the geomagnetic equator where it is E-W. Undisturbed diurnal variations exhibit the same general characteristics, but attain values in the range of 5 to 300 mv/km. Cases are cited of adverse effects on commercial circuits; open wire, buried cable, and submarine cable systems are compared. Geophysical processes underlying geoelectric variations are discussed briefly.

Statistics of Hyperbolic Error Distribution in Data Transmission—Pierre Mertz (p. 377)

Error bursts in data transmission systems do not usually occur completely at random. It has been found that often they follow a hyperbolic rather than a Poisson distribution. Several statistical quantities consistent with the hyperbolic distribution have been developed. These are compared with the corresponding quantities for a Poisson distribution. Specifically the quantities are the probability of exactly c bursts in a time interval for which the long-time average is a, the cumulative probability of at least c bursts in this time interval, and the cumulative probability of burst-free stretches of n time intervals or longer.

A Long Range Digital Communication System—A. J. Strassman and A. C. Chapman (p. 383)

With the arrival of digital data-processing techniques, it becomes necessary both to increase the speed of communication between the data-processing and automatic control equipments and to increase the reliability with which the data are transmitted—particularly over comparatively long ranges. With the immense number of systems that must be developed to provide the ever-increasing amount of data processing required by modern technology and modern business, a reliable digital data transmission technique for use over long ranges becomes critically important. This paper describes a high-frequency, digital data communication system using the quantized frequency-modulation (QFM) technique and the quantized phase-modulation (QPM) technique. QFM is a synchronous frequency shifting technique that can provide a predetermined amount of gap protection between successively transmitted pulses on the same subchannel frequency. The combination of these two techniques (defined below) provides a system with the capability of combating propagation anomalies found in the HF spectrum. The design of the system provides for a basic bit rate of 1000 bits/sec and is capable of expansion to 8000 bits/sec. System peripheral equipments provide digital inputs from facsimile and voice (Vocoder), as well as from multispeed teletype. Highly miniaturized modular construction is used throughout for all equipments and installations.

The Long Range Subsurface Communication System—Rabindra N. Ghose (p. 390)

Discussed herein is a point-to-point communication system for ranges in the order of hundreds of miles where the transmitting and receiving equipment, including radiating devices, can be buried deep underground. Results of theoretical analyses and subsequent experimental verifications of various aspects of the communication system have been presented in this paper. Problems on the optimization of system parameters for different geo-electromagnetic conditions of the ground, noise environment, and for various system constraints are discussed. Also presented in the paper are the solutions of some of the above problems suitable for engineering uses.

Long Line Systems for Global Communications—A. W. Montgomery (p. 396)

Some aspects of the entire global telecommunication system are considered with emphasis on transmission delay and circuit instabilities. Some calculations are made using CCITT recommendations. Attention is then focused on the local networks and terminal equipment and their relation to the entire system.

The Dwindling High-Frequency Spectrum—G. Jacobs and E. T. Martin (p. 399)

The bulk of the world's long-distance communications presently takes place in the high-frequency radio spectrum (between approximately 3 and 30 Mc), by means of ionospheric reflection. The ionosphere is formed mainly by ultraviolet radiation emitted from the sun, and its capability to reflect HF radio waves varies diurnally, seasonally, geographically and throughout the sunspot cycle.

While the physical nature of sunspots and the cause of the 11-year sunspot cycle are not yet clearly understood, it is known that solar activity is a reliable index of the total available bandwidth, or propagationally useful capacity of the HF radio spectrum. During periods or high solar activity, as occurred between 1957 and 1959, the ionosphere is capable of reflecting radio waves over a very wide range of frequencies between approximately 3 and 50 Mc; when the solar cycle declines to low levels, frequencies above 20 Mc may seldom be reflected.

This paper points out that the present sunspot cycle, which climbed to an unprecedented peak during early 1958, is now declining. This decline is expected to continue until the cycle reaches a minimum sometime during 1965. There are also indications that the present cycle may be followed by three cycles of relatively low maxima, which could result in unusually low solar activity for the remainder of the century.

Such a drastic reduction in solar activity would be accompanied by a similar reduction in the amount of propagationally useful HF spectrum. The spectrum will be compressed more or less linearly towards the lower frequency end as the solar cycle declines. During the forthcoming years of low solar activity the HF spectrum may be reduced by more than one-half that available during the recent years of high sunspot count (1957–1959).

Such a reduction in the traffic handling capability of the HF spectrum, coupled with the ever increasing world-wide demands for additional HF circuits, leads to the conclusion that the HF radio spectrum will become progessively less useful for communications during the years ahead, and that the amount of available useful spectrum will fall far short of meeting the anticipated demands.

To avoid communications chaos which could easily result from such a condition, this paper concludes by urging that space satellite communication systems, intercontinental microwave links and expanded underwater multichannel cables as well as other communication systems not dependent upon the vagaries of the ionosphere, be developed at an accelerated pace.

Frequency Division Multiplexing on Transoceanic Cables—Walter Lyons (p. 408)

Heretofore cable, land-line telegraph, and microwave channeling has been limited to approximately 1100 bits per second (bauds), utilizing 22 subcarriers spaced 120 cps apart. Frequency shift keying, together with more sophisticated filter design has enabled this capacity to be doubled.

High data transmission speeds require frequency division multiplexing in order to reduce the distortion in the received signal. A certain degree of time division multiplexing is desirable although it is more economical and otherwise required to utilize frequency division multiplexing to a greater degree.

This paper describes means for accommodation of traffic over the transatlantic telephone cable voice channels at a speed of more than 2200 bits per second with reasonably low error rates. Techniques for this utilize sine wave keying pulses at the fundamental keying rate over subcarriers spaced every 120 cps from 420 cps to 2940 cps, and time division multiplex of the slower input information channels. Cable outages required adequate, not necessarily 100 per cent, backup by independent sideband HF radio circuits using similar subcarrier modulation with tones spaced at 170-cps intervals instead of 120-cps by reason of the additional distortion-due multipath delay.

Examples of filter characteristics for reception and transmission to accomplish this are shown, as well as typical equipment for each tone channel. Curves presented give distortion at various speeds per subcarrier and illustrate the effects of cross-talk and tone jitter as per cent distortion vs keying rate.

A New Frequency-Division Radiotelegraph Multiplex System (MADFAS)—A. Niutta (p. 412)

A frequency-division multiplex system (MADFAS) is described for operation at HF with less bandwidth than is commonly allowed. The reduction in required bandwidth is achieved by using oscillators with greater frequency stability, and signaling by FSK with the minimum frequency shift compatible with the keying speed. Details on the design and operational characteristics of the system are presented.

Some Design and Application Considerations of a 600-Channel Military Multiplex System—R. C. Benoit, Jr., D. B. Nowakoski, T. F. Mayne, and T. J. Wortman (p. 417)

An applications review is presented of a single-sideband suppressed-carrier 600-channel all-transistorized multiplex system for use on cable, and line-of-sight or tropospheric scatter radio circuits. System flexibility provides for growth in 12-channel increments up to the full channel complement. Highly ruggedized modular construction, and miniaturized printed-circuit techniques are employed throughout. System design accommodates voice, data, teletype, and graphic services.

Certain features of the system that aid in the alignment and maintenance of the equipment by personnel with limited specialized training, are discussed.

Equipment Configuration and Performance Criteria for Fully Optimized Tropospheric-Scatter Systems—Charles A. Parry (p. 427)

The "optimum" system is examined with the aid of a basic equation related to channel SNR. Expressions are then developed which show that for equal channel loading and capacity, FM systems are likely to be superior to SSB systems for normal voice channel operation. Further improvement in FM performance may be achieved with "phase-locked" receivers. Performance equations for such receivers are used in basic expressions for optimized scatter circuits to express channel capacity as a function of maximum distance for minimum power. From this equipment configurations for various performance capabilities are developed. These data then give the maximum capability of the tropospheric scatter system when all relevant design parameters are optimized.

It is suggested that long-haul toll performance criteria should be based on six tandem links. This leads to a per-link requirement for channel signal-to-weighted thermal noise ratio with quadruple diversity operation of 45.7 db, and 53 db for the channel signal-to-weighted nonlinear noise ratio. Difficulties in the measurement of thermal noise are discussed. It is believed that a suitable approach is to specify single-link performance in terms of a distribution obtained with one-to-two minute averaged samples. Data are also developed for the minimum permissible system bandwidth and the transmitted spectrum as a function of channel capacity.

Finally, it is considered that the performance in multilink multichannel circuits may be limited by nonlinear noise introduced by multipath effects related to selective fading. In this respect, further research is necessary in order to obtain reliable computational techniques for the intermodulation noise associated with the multichannel system.

Results of Bandwidth Tests on the 185-Mile Florida-Cuba Tropospheric Scatter Radio System—C. E. Clutts, R. N. Kennedy, and J. M. Trecker (p. 434)

Some proposed tropospheric scatter paths are several hundred miles long, and their geometry suggests the possibility that the increased relative delays of signal components traveling the higher-altitude paths could result in significant interchannel modulation interference in an FM system. Therefore, a program of experimental investigation has been undertaken by Bell Telephone Laboratories to determine the extent of the intermodulation problem. Tone amplitude stability tests have been included as part of the study.

The first in a planned series of tests was conducted during March, 1960, over the 185-mile FM system between Florida City, Fla. and Guanabo, Cuba. The system was loaded with random noise of various bandwidths up to 2.5 Mc. and peak deviations up to ±8 Mc were used. Tests were made with no diversity and with dual diversity.

It was found that intermodulation resulting from multipath propagation can limit system performance. Both deviation and base bandwidth are important and have an influence on intermodulation and tone stability. Diversity has little effect on intermodulation but improves tone stability appreciably. The paper presents numerical results of the measurements of average intermodulation and some information on cumulative probability distributions for various combinations of base bandwidth, deviation, and diversity.

Path Loss Measurements vs Prediction for Long Distance Tropospheric Scatter Circuits—A. F. Barghausen and C. F. Peterson (p. 439)

Before any communications circuit can be established between two points whether it be by wire lines or by tropospheric or ionospheric radio propagation, a thorough knowledge of the intended path should be obtained so that an efficient and economical installation can be made. Each system should have as high a reliability as is required for its intended use. Tropospheric forward scatter circuits have established their place in the world-wide communications network of the military and it is the intent of this paper to illustrate by a specific example how the performance of a circuit of this type may be predicted with adequate accuracy without making costly transmission loss measurements over the intended path.

Interdependence Between Hourly Median Transmission Loss and Surface Refractivity Index Observed at 900 Mc on a 232-Mile Far-Beyond-the-Horizon Path—I. Benoliel and J. B. Potts (p. 445)

A detailed analysis is made of propagation data obtained from the North Atlantic Scatter System installed in Iceland. In particular the correlation of the transmission loss and meteorological observations on a long path is analyzed in detail. By separating the data into various time periods it is shown that for periods of time during which the received field is lowest the correlation between transmission loss and surface refractivity is very high. The ability to establish a strong correlation between transmission loss and surface refractivity for this period allows the system designer to make more accurate predictions of the lower expected received fields and thus is able to calculate the minimum required transmitter with greater accuracy.

Parametric Converter Performance on a Beyond-the-Horizon Microwave Link—J. Harvey (p. 451)

Experimental parametric converters were installed on a quadruple-diversity link of the White Alice system. Two parametric receivers with noise figures of 1.5 db were operated simultaneously with two normal receivers of 8.8-db noise figures. Comparative measurements showed improvements of 7 db in telephone-channel noise and 10-fold in teletype error-rates.

An 11,000-Mc Radio System Across Chesapeake Bay—Arthur G. Miller (p. 455)

This paper describes briefly the Western Electric type TJ microwave Radio System designed for operation in the 10.7 to 11.7-kMc frequency allocation and covers the performance of this system since it was placed in service across Chesapeake Bay on February 1, 1959. This is the first TJ system to be placed in service in the territory of The Chesapeake and Potomac Telephone Company of Virginia, and operates between Hampton and Kiptopeke, Va., a distance of 22.5 statute miles. The overwater portion of this path has a length of 18.5 miles.

Coexistence of Celestial and Terrestrial Communications—F. A. Losee and S. G. Lutz (p. 460)

Artificial satellite repeaters will revolutionize radio communication by permitting the use of microwaves over long paths. There will also be a continuing and mounting need for terrestrial applications of microwave services over relatively short distances. Achieving coexistence between these long- and short-distance systems will conserve and enhance the utilization of the microwave spectrum. Extensions of prior interference coordination techniques, such as use of three-dimensional antenna directivity, can cause the desired signal to override interfering signals and thus permit most satellite communication systems to share frequencies with most terrestrial microwave communication systems. Even though satellite communication may not need such a large fraction of the microwave spectrum for some years, focusing prompt attention on the needs and probable problems of frequency sharing can help guide its evolution around subsequent difficulties.

Mutual Interference in Communication Equipment Can Be Reduced—Francis H. Yonker (p. 462)

The application of well-known techniques in the re-examination of existing systems, aided by interference charts to identify areas of greatest vulnerability, will prolong the useful life of present equipment and guide designers of future systems to meet advancements in the state of the art.

Contributors (p. 470)

Announcement (p. 477)

Annual Index 1961 (Follows page 477)

Component Parts

Vol. CP-9, No. 2, June, 1962

Information for Authors (p. 51)

Who's Who in PGCP—Vincent J. Kublin (p. 52)

Solid Aluminum Electrolytic Capacitors with Etched Aluminum Foil—Wolfgang Post (p. 53)

Some suggestions are made for further developments in the field of electrolytic capacitors using etched aluminum foils and solid electrolytes.

Various laboratory-tested construction procedures are discussed in detail. The behavior of capacity, dissipation factor, and leakage is illustrated as the function of temperature and frequency during storage with and without current. It is shown that the production of aluminum electrolytic capacitors with commercially available etched foils and solid electrolytes will be entirely feasible in the near future.

In conclusion, the optimal data found so far in a series of experiments are reported, pointing the way toward results that may reasonably be expected from further investigations.

Reducing Size of Radar Pulse Transformers—Reuben Lee (p. 58)

With today's high performance magnetic materials, the pulse transformer designer has advantages not previously obtainable for reducing size. These advantages are further implemented by improved methods of dissipating losses, which hitherto have prevented substantial size reductions. In order to employ these advantages to their fullest, toroidal cores with reset bias are used. For example, at 7.5 megawatts peak power, or 15 kilowatts average power, it is possible to reduce transformer weight from 105 pounds to 22 pounds. This is achieved by using the best known core material, the most efficient cooling and a reset core together. Proportionate size reduction is possible in smaller ratings, and is of particular importance in transportable radar: on land, sea or in space.

Solid-State Physical Phenomena and Effects—Part III—Edwin J. Scheibner (p. 61)

This is the third in a series of four articles describing solid-state phenomena. Twelve solid-state phenomena and physical effects are provided. All of the twelve phenomena belong to a group which includes effects related to the dielectric properties of materials and transport phenomena for particles other than electrons or holes.

Optimization of the Dynamic Parameters of the Controlled Superconductor—V. A. Marsocci and P. M. Chirlian (p. 74)

The theory of the operation of the controlled superconductor as a linear amplifier is briefly described. The relationship between constants which describe the physical operation of the controlled superconductor and the small-signal parameters of the device are developed, and the optimization of the small-signal parameters in terms of the geometry of the device is discussed. The current gain expressions of linear amplifiers in two circuit connections are presented and the conditions necessary for the optimization of these gains are also derived.

Nonreciprocal Behavior in Passive Systems—Jerome H. Silverman (p. 77)

The nonreciprocal behavior of certain types of linear passive systems is explained by employing the ideal gyrator as a network element. The pertinent network properties of passive nonreciprocal systems are developed, with particular attention being paid to the passive isolator.

Actual examples of passive low-frequency gyrators and isolators are shown in the form of Hall effect devices and magneto-electrodynamic transducers.

The Electromechanical Circulator—Jerome H. Silverman (p. 81)

Three-channel passive circulators may be constructed about antireciprocal two-ports whose parameters obey the restriction $(\mathrm{Re}\ Y_{11})(\mathrm{Re}\ Y_{22})<(\mathrm{Re}\ Y_{12})^2$. The characteristics of such circulators are derived in terms of the network parameters of the antireciprocal twoport.

Expressions are presented for the required terminations, the driving-point admittances, and the transducer gain of the circulator.

Experimental data is presented on circulators constructed about the electromechanical gyrator. The agreement between the calculated and the experimental performance is very good. The electromechanical circulator, an inexpensive and readily fabricated device, has applications in communications and in various instrumentation.

Contributors (p. 86)

Electron Devices

Vol. ED-9, No. 3, May, 1962

The Multiple-Beam Klystron—M. R. Boyd, R. A. Dehn, J. S. Hickey, and T. G. Mihran (p. 247)

The multiple-beam klystron (MBK) is a device for extending klystron power generation capability at a given frequency by a factor of ten or more. The MBK utilizes a multiplicity of electron beams in conjunction with multiwavelength waveguide circuits. These circuits are periodically loaded and operate in the $\pi/2$-mode. The efficiency, bandwidth, gain and stability of the MBK are equal to or better than that of the single-beam prototype klystron. Furthermore, the MBK permits generation of a given power level at an unusually low voltage, thus minimizing insulation, X-radiation, and modulator problems.

An MBK utilizing ten external-circuit klystrons has been built for 750-Mc operation to demonstrate the principle of the device. A single main magnetic circuit is used to focus all beams simultaneously. An RF power output ten times that of one klystron was measured, corresponding to an efficiency of 44 per cent. Bandwidth and gain were identical with single-beam prototype operation. Individual beam drop-out tests were made which showed no disruption of operation in case of the failure of one or more beams. Limited tests tend to confirm the conclusion that the harmonic content of an MBK can be lower than that of a single-beam klystron.

Analysis of a Frequency-Modulated Reflex Klystron With Minimum Incidental Amplitude Modulation—Walter R. Day, Jr. (p. 253)

Simultaneous modulation of the reflector and beam voltages of a reflex klystron will produce frequency modulation with minimum incidental amplitude modulation. The required variation of reflector voltage with beam voltage, for constant output power, is derived from the fundamental equations of the reflex klystron. Experimental verification of this analysis is presented. Reflex klystron oscillators which can be frequency modulated with minimum incidental amplitude modulation find application in FM Doppler radars, communications systems, and as signal sources for microwave testing.

Phase Focusing in Linear-Beam Devices—J. G. Meeker and J. E. Rowe (p. 257)

The phenomenon of phase focusing in linear-beam devices is investigated theoretically by modifying the nonlinear interaction equations for devices such as the traveling-wave amplifier (TWA) to accommodate spatially-varying parameters and then investigating their use under a variety of operating conditions. Phase focusing can be accomplished either by tapering the RF circuit phase velocity or by applying a dc voltage gradient along the beam or structure. Both approximate analytical solutions and general computer solutions are presented for each of the phase-focusing techniques. The analytic solutions yield profiles which are explicit functions of tube length and these are compared with more general computer solutions where space-charge effects are included.

An experimental S-band high-power TWA was constructed with a variable-pitch helix designed on the basis of the hard-kernel-bunch theory. Experimental data indicate an efficiency improvement from 18 per cent to 35 per cent and an improvement in the gain-frequency characteristics.

Glow Discharge Indicator Tube for Small Signals—H. Omi, Y. Fukukawa and T. Nakajo (p. 266)

A new glow discharge indicator tube was developed for the purpose of obtaining a visible indication of the small-signal voltage obtained from transistors or other small-signal sources.

The principle of operation is based upon the current transfer between two adjacent cathodes. In this indicator tube about 60 Mw (200 v 300 μa) of power dissipation is required to keep the glow on the sustaining cathode, and only a few volts of negative potential are required to transfer the glow to the indicator cathode.

In addition to its ability to indicate very small signals, this tube has several other outstanding features. These are 1) small size, 2) small power dissipation, 3) stable characteristics, and 4) long life compared with other types of indicators (*e.g.*, a lamp or a gas-filled tube indicator). This paper describes in detail the principle of operation, construction, electrical characteristics and applications of a new type of indicator for small signals.

Low-Voltage Mercury-Alkali Metal Arc—Gilbert H. Reiling (p. 271)

Measurements of the arc voltage and electron temperature were made on low-pressure arcs utilizing a mercury-pool cathode containing various concentrations of alkali metals. The arc-burning voltage was substantially lower than the pure mercury arc and the minimum arc voltage depended on the concentration of the alkali metal and ambient tube temperature. The measurements suggest that there are three processes which collectively are responsible for the arc behavior. These are a lower anode work function, a Penning two-stage ionization process of alkali metal atoms by mercury metastables and an improved electron emission by reliable anchoring of the cathode spot. With the addition of small amounts of alkali metal the cathode spot emission zone was stable on a molybdenum anchor at currents as high as 200 a. The cathode fall potential was the order of 4 v. It is shown that the voltage reduction is mainly in the cathode fall region and that it is lower for rubidium than cesium, potassium or sodium in the preceding order.

A Microspot Tube with Very High Resolution—Kurt Schlesinger (p. 281)

A 5-inch microspot tube with a spot size of 8 to 9 microns and a beam current of 1.5 μa is described. The neck of this tube uses an accelerating spiral anode, in combination with a decelerating prefocus lens. This combination stretches the 6-inch neck structure to an effective length of 13 to 16 inches.

The resulting demagnification of 0.6 permits realizing the above spot size as an electron image of a 1/2 mil object-aperture. The latter is illuminated with a current density of 20 a/cm² by a microgun, which uses an impregnated cathode at 2a/cm².

The microgun operates by the FRM principle ("Focus Reflex Modulation"). An improved vapor-reacted screen is employed, whose light output is more than tripled from previous types of transparent phosphors.

An Investigation of the Magnetic Transverse Waves on an Electron Beam—Curtis C. Johnson (p. 288)

An electron beam in the presence of an axial magnetic field supports four transverse waves; two cyclotron waves, and two synchronous waves. A general coupling theory is developed from an electronic equation and a circuit equation to describe how these waves can be coupled to traveling-wave circuits. The polarization and power flow characteristics of the waves are derived. The theory is applied to the bifilar helix, a circuit which can couple selectively to each of the four modes. A bifilar helix traveling-wave tube was used to investigate experimentally the four beam modes and provide a quantitative check of the coupling theory.

Noise Performance of Transistors—Don G. Peterson (p. 296)

The accuracy with which the Beatie lumped model represents transistor noise performance is experimentally verified. The noise model consists of three statistically independent shot-noise generators connected across the lumped elements representing the generation-recombination and diffusion mechanisms of the transistor. In addition a thermal-noise generator is used to represent the noise contributed by the base spreading resistance. By comparing measurements with calculations based on the model, not only is good over-all agreement obtained, but it becomes evident that certain bias and source conditions allow separate confirmation of the internally postulated noise generators. The statistical properties of transistor noise are studied using a laboratory-constructed amplitude-probability density analyzer. The results show that the first-order amplitude distribution function of transistors is indeed Gaussian.

Thermal Stress and Fracture in Shear-Constrained Semiconductor Device Structures—T. C. Taylor and F. L. Yuan (p. 303)

The construction of semiconductor devices as well as other electron devices, often requires the utilization of brittle materials, such as the semiconductor itself, as part of a larger structure. Thermal stress, caused by cooling from high temperature bonding operations, can cause fracture of the brittle part, due to thermal expansivity mismatch with other parts of the structure. This paper considers a widely used type of bond, consisting of a nonpenetrating butt-joint, wherein the parts develop thermal stresses by reason of shear constraint in a solder layer. This type of joint is therefore called a shear-constrained bond.

A one-dimensional, elastic analytical model is presented, which predicts the location and orientation of the principal tensile stress in a shear-constrained brittle strip. The tensile stress required for brittle fracture is shown to be induced, primarily, by shear tractions in the solder layer which are applied to one face of the strip. Extended to a real structure, the model would predict the highest tensile stress at the outer periphery of a bond, and oriented at 45° with the plane of the bond interface. This prediction is found to be in agreement with the bulk of fracture experience in shear-constrained semiconductors.

Low-Frequency Noise Figure and Its Application to the Measurement of Certain Transistor Parameters—J. F. Gibbons (p. 308)

Low-frequency noise measurements are shown to provide a convenient and reasonably accurate (±10 per cent) means of measuring $r_{b'}$. Their application to the measurement of the factor n in the function law $p_e = p_n(e^{qV/nkT} - 1)$ is also described, though the values of n obtained from noise measurements do not check accurately with the values of n determined by other methods.

Experimental determinations of the variation of low-frequency noise figure with emitter-bias current are also presented for several transistor types. The observed behavior suggests that the principal source of $1/f$ noise in low-noise transistors may be in the emitter-base transition region instead of on the base surfaces where it is placed in presently accepted noise models.

Noise and the Potential Minimum at High Frequencies—Martin A. Pollack (p. 316)

Contributors (p. 317)

Industrial Electronics

Vol. IE-9, No. 1, May, 1962

Noncontact Dimensional Measurements by Optical and Electronic Techniques—Charles D. Bryant (p. 1)

Accurate dimensional measurements of products during processing are a major requirement in many industries. Because of high heat radiation, rapid motion, or other factors a noncontact measurement system is desirable. Systems have been developed using a combination of closed-circuit television and special optical techniques together with special purpose computers and associated readout devices. A typical application is a system for measuring the length of red hot steel I-beam blanks.

Moisture Measurement in Industry—Harold W. Gebele (p. 7)

Through a specialized capacitor we can achieve a device capable of being employed by commercial paper mills to measure and control the amount of moisture contained in a moving sheet of paper. By such control a mill can achieve dollar savings by producing more paper to exact specifications, and with less down time from paper breaks. Continuous monitoring of the moisture content of a fast moving web of paper can be made by using a spray or fringe field capacitor and a compatible electronic system. The basic principle involved is that the area and spacing factors of the capacitor have been held rigidly constant so that one variable is the dielectric. This dielectric is a web of paper that travels across a stationary capacitance measuring device.

As the paper varies from a relatively dry to a wet condition the basic capacitance will change as the dielectric changes. If this varying capacitor is connected into a special voltage bridge circuit and the bridge is excited with 5000 cycles, the use of an amplifier, a 5000 cycle phase detector, and a mechanical feedback loop to a variable capacitor will rebalance the bridge to a null condition. With the rebalanced variable capacitor position connected to a pen the per cent moisture deviation of a web of paper can be read on a chart.

Analytical Instrumentation for Process Monitoring and Control—Helmut J. Maier (p. 11)

Automatic analytical instrumentation may be classified into three broad categories: instruments which measure physical properties of chemical compounds, instruments which automate procedures of analytical chemistry, instruments which perform a quantitative separation of the constituents of a mixture. Each of these categories will be discussed. The process gas chromatograph will be discussed in considerable detail.

Electronic Devices for Measuring Flow—Douglas R. Lynch (p. 22)

This paper presents evidence of the mounting interest in electronics as a means for measuring flow by reviewing several of the more recent developments in this area. The review helps to indicate which of the electronic measurement techniques have immediate application and which hold promise of application in the foreseeable future.

Educating Engineers for Careers in Industrial Electronics—J. Frank Reintjes (p. 31)

From a small beginning only a few decades ago, the electronics industry has grown to a place of first importance in our national economy. Electrical engineering education has not only adapted to reflect this growth but continually altered its approach in order to provide leadership for further expansion of the field. In this paper the process of educating engineers for careers in industrial electronics is discussed, with emphasis upon the kinds of educational experiences engineering students should now have in order that they may be prepared to cope with the many challenges the industry will face in the future.

Digital Control Techniques Applied to Automatic Weighing Processes—D. W. Kennedy and C. W. Hibscher (p. 35)

The weighing industry is perhaps more cognizant of accuracy than any other instrumentation industry. Basic scale accuracies of $\frac{1}{10}$ of 1 per cent are, generally speaking, minimum, with over-all system accuracies in this vicinity desirable. The two digital devices described in this paper are unique in that they are an integral part of the weighing instrument and as a result, the accuracy of conversion from weight indication to a digital signal is absolute (no error encountered). Therefore, the system accuracy is virtually the same as the basic instrument accuracy.

Analog Computer Systems in Blending Processes—Harold H. Roth (p. 42)

Analog computers especially engineered to program and control specific blending processes, are establishing themselves as practical solutions to scores of industrial blending problems. They reduce production costs, eliminate raw material waste and multiply product output many times over. An important consideration is that non-technical personnel can be quickly trained to a high degree of operational proficiency.

DC-to-AC Power Conversion by Semiconductor Inverters—Edward J. Duckett (p. 48)

The rapid improvement in semiconductor

power devices and in inverter circuits has given rise to an accelerated introduction of new equipment for the conversion of electrical power in military, industrial, and commercial applications. Increased power handling capability and improved operating characteristics have made it possible to perform many functions effectively which, until recently, were achieved only by nonstatic apparatus. The ability to convert from dc to ac efficiently and reliably has received special emphasis during the past several years. Developmental models of semiconductor inverters have been constructed, and a number of potential applications have been investigated. These new types of power conversion apparatus should be of use in a wide variety of application areas, including emergency power supplies, controlled frequency sources, and frequency converters. Predictions of future applications and capabilities indicate that the semiconductor power inverter and allied apparatus should be a significant factor in the design concepts for future electrical systems.

A 50-KVA Adjustable-Frequency 24-Phase-Controlled Rectifier Inverter—C. W. Flairty (p. 56)

This paper describes a multiphase 50-kva silicon-controlled rectifier inverter that uses phase displacement of the outputs from four 3-phase bridge inverters to generate a 3-phase output waveform with low harmonic content. The output voltage is controlled over a wide range by simply changing the phase position of controlled rectifier gate signals. Low harmonic content is maintained in the unfiltered output wave over the complete voltage range. At one phase position the lowest harmonic of consequence present in the output waveform is the 23rd. Frequency of the inverter output is smoothly adjustable over the range of 50 to 500 cps.

The static inverter offers this adjustable frequency, and adjustable voltage power supply with electronic precision. Frequency regulation is independent of supply voltage or load variations and only dependent upon a low power timing oscillator.

Thermoelectric Applications to Industrial Problems—John C. R. Kelly, Jr. (p. 61)

The efficiency and durability of thermocouples have been improved by recent research and development. This has led to a number of prototype applications for both cooling and power generating devices. The inherent characteristic of a thermoelectric system that lends itself to easy modular design and adaptation is the thermocouple itself. Each couple may be rated by watts of power produced or consumed. Examples of a number of different applications will be given.

Panel Discussion of Manufacturer-User Problems (p. 66)

Microwave Theory and Techniques

Vol. MTT-10, No. 3, May, 1962

Magnetically Tunable Nonreciprocal Band-pass Filters Using Ferrimagnetic Resonators—C. N. Patel (p. 152)

Possibilities of a small-bandwidth, small-insertion loss, magnetically tunable band-pass filters with nonreciprocal characteristics have been studied. The unloaded $Q(Q_u)$ for a ferrimagnetic sample has been derived, considering the fundamental definition of Q for a resonator. Theoretical analysis is given for coupling due to ferrimagnetic resonance, between two RF transmission circuits when the RF magnetic fields due to the two circuits are circularly polarized or, in general, elliptically polarized. The analysis gives the open-circuit impedance parameters for the equivalent circuit representing the ferrimagnetic coupling mechanism, from which the external-loading Q's (Q_{e1} and Q_{e2}) are obtained. This analysis, applied to the case of the waveguides, shows that the behavior of the Q_e vs frequency characteristic depends upon the ellipticity of the RF magnetic field, and hence, upon the location of the off-axis position of the ferrimagnetic resonator. Also, the nonreciprocity depends upon the ellipticity of the RF magnetic field the nonreciprocal behavior being optimum when the RF magnetic field is circularly polarized. Thus, again, for the case of waveguide circuits, the off-axis position determines the reverse-coupling-vs-frequency characteristic. The measurements on the experimental filters, tunable from 8.2 to 12.4 kMc, verify the results obtained from the theory. The forward and the reverse directions of the operation of these filters can be interchanged by reversing the dc magnetic field. Power limiting with these filters is briefly described.

Propagation on Modulated Corrugated Rods—C. C. Wang and E. T. Kornhauser (p. 161)

The velocity of surface-wave propagation on two types of axially modulated corrugated rods has been measured experimentally. Type A has a constant outer diameter and sinusoidally varying slot depth, while in type B the slot depth varies in virtue of a modulated outer diameter. In both cases the measured phase velocity is about ten per cent less than that for a uniformly corrugated rod with the average slot depth and outer diameter, but agrees within two per cent over the frequency range used with the value calculated from an analysis based on the Mathieu equation.

Small Resonant Scatterers and Their Use for Field Measurements—Roger F. Harrington (p. 165)

A general formulation for the back-scattered field from loaded objects is given. It is shown that small resonant objects produce a much greater back-scattered field than small nonresonant ones. The theory is applied to short dipoles and small loops. The use of small resonant scatterers to measure electric and magnetic fields by scattering techniques is discussed. Resonant scatterers are found to have several advantages over nonresonant scatterers when used for field measurements.

Wide-Band Matching of Lossless Wave-guide Two-Ports—Darko Kaifez (p. 171)

A new procedure of matching is presented, based in the equations which transform the output reflection coefficient of a lossless two-port network into the input reflection coefficient. The parameters of the equations are the residual reflection coefficients which can be easily measured. The optimum reflection coefficients which have the minimum frequency variation are computed for the specific case when the frequency variation of the residual reflection coefficients can be approximated by a circular arc in the Smith diagram. An illustrative example is given to explain the determination of the position and the size of the inductive obstacles that match a waveguide two-port structure within a wide frequency band.

An *X*-Band Ferroelectric Phase Shifter—M. DiDomenico, Jr. and R. H. Pantell (p. 179)

An *X*-band electrically-tunable ferroelectric phase shifter has been constructed. The phase shifter is reciprocal and consists of a thin ferroelectric slab completely filling the transverse plane of a rectangular waveguide with suitable dielectric matching sections placed symmetrically about the slab forming a band-pass filter. Phase shift is controlled by applying a dc electric field to the ferroelectric. The measured characteristics of this device indicate that incremental phase shifts of 40° to 50° are attainable over a bandwidth of 400 Mc centered about 9.3 kMc with insertion losses ranging from 2 to 6 db. Since the phase shifter does not require a magnetic field for operation, the device can be biased with inexpensive, light-weight equipment requiring negligible dc control power, and the response time can be expected to be fast.

A Balanced-Type Parametric Amplifier—S. Hayasi and T. Kurokawa (p. 185)

A balanced-type diode amplifier is reported, in which the cutoff mode of the pumping waveguide resonating with the diode capacitances, is used as a signal circuit and a series connected diode loop is used as an idler. Theoretical noise-figure and gain-bandwidth product are derived after calculating the equivalent susceptance matrix of two diodes which are parallel-connected for the signal input and series-connected for the idler. This reveals that 1) the noise figure of the balanced-type amplifier can be expressed in the same form as that of the single diode amplifier, and 2) the gain-bandwidth product is identical to that of the single diode amplifier. In the experiment at 1900 Mc, a bandwidth of more than 200 Mc is obtained at the power gain of more than 10 db. A single-channel noise-figure of 2.5 db is measured at the pump power of 100 Mw.

A Survey of the Theory of Wire Grids—Tove Larsen (p. 191)

The paper gives a survey of the literature concerning the electromagnetic properties of wire grids. As an introduction to the literature survey, a short description of the properties and applications of wire grids is given. Finally some particular grid configurations are mentioned.

Propagation of TE Modes in Nonuniform Waveguides—H. Zucker and G. I. Cohn (p. 202)

The conditions for TE mode propagation in rectangular waveguides with nonuniform dielectric media are established. An equation is derived for determining the capacitivity functions which have equivalent curved waveguides with uniform dielectric media. The types of variable dielectric waveguides which have equivalent curved wall waveguides and a separable wave equation are determined.

An Investigation of a Feedback Control System for Stabilization of Microwave Radiometers—Theodore V. Seling (p. 209)

A method of stabilizing receivers for radio telescopes is discussed and shown to be capable of substantially reducing sensitivity to gain fluctuations. The system employs a variable noise source as a controlled feedback element.

Such a system does not require long warm-up times since the output is dependent only upon the stability of the variable noise source and reaches stabilization very rapidly.

Investigations were made of a number of variable noise sources for use in the system, including: gas discharge tubes with variable attenuators, crystal diodes, and gas discharge tubes with variable duty cycles. Several crystal diodes were measured and the noise output was found to be linear with current for temperatures up to approximately 5000°K. A variable noise source using a gas discharge tube with variable duty cycles to adjust the average temperature of the comparison termination of the radiometer is also discussed.

Results are given for an experimental *X*-band system using a crystal diode as a variable noise source. For this system, a reduction of gain by 5 db had no measurable effect on the accuracy of measurement.

Surface Current Measurements with an Electric Probe—Robert Plonsey (p. 214)

The use of an electric probe for measurement of induced surface currents on obstacles in a parallel plate region is described. An analysis of the sources of error, and in particular the interaction of the probe with the obstacle, is examined theoretically and experimentally. It is concluded that the technique is capable of yielding measurements of good accuracy.

Direct Coupled Coaxial and Waveguide

Military Electronics

Vol. MIL-6, No. 2, April, 1962

Some Early Developments in Synthetic Aperture Radar Systems—C. W. Sherwin, J. P. Ruina and R. D. Rawcliffe (p. 111)

This paper describes some of the early developments in the synthetic aperture technique for radar application. The basic principle and later extensions to the theory are described. The results of the first experimental verification at the University of Illinois are given as well as the results of subsequent experiments. The paper also includes a section comparing some of the important features of real and synthetic aperture systems.

The Equivalence Among Three Approaches to Deriving Synthetic Array Patterns and Analyzing Processing Techniques—H. L. McCord (p. 116)

The equivalence of the vector addition, cross-correlation, and filtering approaches to deriving synthetic array patterns and analyzing processing techniques is demonstrated here. A mathematical model is defined which establishes a geometry, a transmitted and received signal, and a general synthetic array weighting function. A preliminary analysis of this model derives the signals received at the flight-path points where radar pulse transmission and reception occurred, and the effects at these flight-path points of the synthetic array weighting function. The weighted, received signal expression is then summed over the array, and the resultant shown to be a vector addition, a cross-correlation integral, or a filtering operation depending on the changes of variable and formal manipulations employed.

A Comparison of Techniques for Achieving Fine Azimuth Resolution—L. J. Cutrona and G. O. Hall (p. 119)

In the discussion of techniques for achieving azimuth resolution, it is instructive to compare the achievable resolution for three cases:

1) the conventional case for which

$$\text{Res} = k\,\frac{\lambda R}{D}$$

2) the unfocused synthetic antenna case for which

$$\text{Res} = k\sqrt{R\lambda}$$

3) the focused synthetic antenna case for which

$$\text{Res} = kD$$

where λ is wavelength, D is aperture of physical antenna used and R is range, and the k's are constants of proportionality.

These cases are compared. It is shown for unfocussed synthetic antennas that there is a maximum length which depends on range and wavelength. This restriction on length can be removed by focussing.

A number of degrees of freedom exist for the design of a synthetic antenna which are not available for a real linear array. Among these is the ability to focus simultaneously at all ranges.

Theory and Evaluation of Gain Patterns of Synthetic Arrays—R. C. Heimiller (p. 122)

The results of an analysis of synthetic array gain patterns, including sidelobe response, are summarized. Both focused and unfocused arrays are examined. The phase time history of echoes from reflectors on the ground as a function of position is used to modify the equations for the broadside synthetic array for application to forward-looking antenna arrays. The dependence of the "optimal" length and resolution of an unfocused array on the look angle is derived. The gain patterns of unfocused synthetic arrays are presented for arrays of various lengths with both rectangular and exponential amplitude weighting.

Calculations are made showing that the physical antenna gain pattern acts as amplitude weighting with resultant sidelobe suppression and illustrating that the final gain pattern *cannot* be expressed as the product of the space factor of the array time the real antenna gain pattern. However, unless the length of the synthetic array is about equal to or greater than the real antenna beamwidth times the range, the product approximation error is negligible in the region near the main lobe and amounts to a reduction in gain.

The results of this analysis are then put in the form of design curves from which such parameters as the maximum resolution of an unfocused array and the length of array necessary for a given resolution at a given frequency can be obtained.

The Effect of Normally Distributed Random Phase Errors on Synthetic Array Gain Patterns—C. A. Greene and R. T. Moller (p. 130)

In the practical formation of synthetic array patterns the individual signals which are integrated to form the array will sustain uncompensated phase shifts. If these uncompensated phase shifts are deterministic, the evaluation of their effect on the synthetic array radiation pattern is straightforward. On the other hand, if the uncompensated phase shifts are random, such as would be produced by propagation anomalies, a statistical study must be made to determine statistical measures of the effects on the radiation pattern.

Part I describes an analytical study of the effects of normally distributed random phase errors on synthetic array performance. The statistical measures of performance derived include expected beam broadening, rms beam canting, and expected loss in peak gain. The analysis is limited to the case of small rms difference in phase error across the array.

Part II describes a Monte Carlo simulation study which removed the restriction of small rms phase error difference. In addition, the simulated radiation patterns generated in the simulation study allowed the computation of the statistics of the ratio of main lobe to integrated sidelobe power. This performance parameter is, in general, the most sensitive of all the performance measures to residual uncompensated phase errors.

Phase-Amplitude Monopulse System—W. Hausz and R. A. Zachary (p. 140)

Phase monopulse, amplitude monopulse, and phase-amplitude monopulse are compared. The latter uses only two antenna feeds and by controlling the aperture illumination from these feeds has a separation of the illumination phase centers in one axis and opposed tilts of the phase fronts, or squint, in the other axis. It is described as more fundamental or less redundant than fourhorn or other multihorn monopulse designs. In lacking redundancy it is less complex, but has fewer degrees of freedom to optimize performance. The earliest example of phase-amplitude monopulse, the AN/APG-25 (XN-2), is described and its performance given.

SCAMP—A Single-Channel Monopulse Radar Signal Processing Technique—W. L. Rubin and S. K. Kamen (p. 146)

A new monopulse radar signal processing technique is described, which requires only a single IF amplifier channel to instantaneously process the returns from all targets within a beamwidth. The basic signal processor consists of a wide-band amplifier-hard limiter, followed by appropriate band-pass filtering. The mathematical basis for its operation is developed and corroborating experimental results are given. Angle accuracy curves for a sum and difference monopulse system are derived as a function of input SNR.

Continuous-Wave Radar with High Range Resolution and Unambiguous Velocity Determination—S. E. Craig, W. Fishbein and O. E. Rittenbach (p. 153)

The conventional pulse radar has two shortcomings. First, since the pulse width and pulse repetition frequency are constrained by resolution and maximum range requirements, the average transmitter power can be increased only by increasing the peak transmitter power. Second, the limitation imposed by the sampling theorem prevents unambiguous measurement of Doppler frequencies higher than one half the pulse repetition frequency.

These disadvantages can be circumvented by operating with continuous transmission, suitably modulating the transmitter power and correlating returned echoes with a delayed replica of the modulating signal.

An excellent waveform for modulating the transmitter is the pseudo-random code generated by a shift register with multiple feedback paths. The autocorrelation function of the code has a single narrow peak each code length and low sidelobes. The code is easy to generate. Long delays are possible, since it is necessary only to memorize the code generation logic and not the code itself. The binary nature of the code makes it easy to perform such operations as multiplication.

Realization of the desirable properties of the pseudo-random code depends on the manner in which the radio frequency carrier is modulated and demodulated. It is shown that phase-reversal modulation results in little distortion of the code, while frequency modulation can give rise to false range indications.

Sidelobe Suppression in a Range-Channel Pulse-Compression Radar—C. L. Temes (p. 162)

A model range-channel pulse-compression system is postulated and the problem of suppressing sidelobes in the compressed pulse is discussed. It is concluded that amplitude-weighting in the time domain (at IF) is a convenient method of suppressing sidelobes. An integration loss factor is defined which characterizes the decrease in signal-to-noise ratio (SNR) resulting from the inclusion of weighting. For a radar system which is peak-power-limited, it is shown that the integration loss is less if the amplitude-weighting is accomplished entirely at the receiver while "mismatching" the system, rather than weighting at both transmitter and receiver while preserving a "matched" system. Some common amplitude-weighting functions are compared in terms of integration loss, main-lobe broadening, and sidelobe structure. The Hamming weighting is shown to be a good compromise among the above factors and, in addition, it is relatively easy to implement. The effect of a time-mismatch between the Hamming amplitude-weighting function and an echo pulse is considered for the special case of linear-frequency modulation.

A Large Time-Bandwidth Product Pulse-Compression Technique—R. C. Thor (p. 169)

A pulse-compression radar system which utilizes a linear FM waveform has a theoretical upper limit to the magnitude of its compression ratio or time-bandwidth product. This limit is a function of the observed target's relative radial velocity, and the effect on the return signal is characterized by both a pulse stretching and amplitude reduction if the limit is exceeded. The use of a logarithmic phase-modulation signal waveform and a corresponding "matched" receiver possesses the desirable characteristics of the linear FM and in addition has no upper limit to the magnitude of the compression ratio. A single receive pulse-compression filter is matched for all target velocities. A linear FM signal can be thought of as a very good approximation to a logarithmic phase-modulation signal for compression ratios less than the maximum limit. A general method of implementing a variety of systems employing pulse-compression ratios up to 10^5 and utilizing logarithmic phase modulation is presented.

Optical Processing of Simulated IF Pulse-Doppler Signals—W. G. Hoefer (p. 174)

The potentially wide bandwidth and large storage capacity of optical recording and processing systems leads naturally to consideration of direct IF recording. A method of recording and processing IF pulse-Doppler signals is presented and it is shown how ambiguities are reduced, compared to video processing, in the manner expected from sampling theory. Processing of a linearly varying Doppler frequency is also discussed. Experimental results with simulated constant frequency and linearly varying frequency recordings are shown.

An RF Multiple Beam-Forming Technique—William P. Delaney (p. 179)

An RF beam-forming matrix is described which forms "*n*" simultaneous beams from an "*n*" element array in a passive and theoretically lossless manner. The principle of operation is explained using some simple matrix configuration. A general expression for the far-field pattern of any beam is derived and then used to study the positions of beam peaks, the position of beam nulls, the crossover level between beams and the frequency sensitivity of beam positions. This matrix provides a uniform illumination of the array aperture; however, simple beam combining techniques will yield tapered illuminations. An experimental 16-element beam-forming matrix which operates at 900 Mcps is described, and results of RF and antenna measurements on the matrix are presented.

Theory of Coherent Systems—W. M. Brown and C. J. Palermo (p. 187)

A circuit theory model is derived for coherent radar, communication, sonar and antenna systems. The model involves linear time invariant operators and hence can be thought of as cascaded filters. The model provides insight for such systems not previously available, and it provides a unified approach to the analysis of all the above systems.

The analysis is concerned with continuously distributed target fields and point targets, perturbed by both additive noise and random phase errors. The model in general consists of two filters, a pre-filter and a post-filter. For radar, sonar, and antenna systems the input is the reflectivity of the target field to be sensed. For the radar and sonar case the impulse response of the pre-filter is the transmitted pulse while for antenna systems the impulse response is the current distribution. For communications, radar, and sonar the post-filter is the receiver while for antennas the post-filter is a combination of the receiver and the receiving antenna. Additive receiver noise is accounted for at the input of the post-filter. Lack of perfect coherence or phase errors can be due to many causes, *e.g.*, atmosphere or ocean inhomogeneities. To account for the various sources of phase errors, one must consider both the pre-filter and post-filter as random parameter systems and include a multiplicative error at the input of the post-filter. This also accounts for fading.

Optimum detection has been considered extensively in the literature; in this report we emphasize two other related criteria, namely resolution and mean-square error. Even for the case where there is no interfering phenomenon, one can optimize a system for resolution. The definition one uses for resolution may be motivated at least in part by the fact that there will always be noise present. Optimum systems are derived for various constraints and definitions of resolution in the noiseless case. Such considerations provide a simple philosophy for system design. These simple results on resolution are applied to pulse compression radars and to antenna design.

The second section of the paper deals with least-squares optimization. The problem in the radar case is to estimate the reflectivity of a continuous target field in the least-squares sense. An optimum receiver is first derived in the presence of both phase errors and additive noise. Then the best pre-filter is derived in presence of only additive noise. This determines the best transmitted pulse. Also, phase modulated communications systems are discussed briefly; it is shown that rather elaborate complex filtering provides improvement. Even when the signal is a real function the best receiver is still a complex parameter system rather than a real parameter system.

In the last section, the case of point targets is discussed. Primary emphasis is placed on estimating resolution in the presence of phase errors. For the case of point targets, we examine the effect of phase errors on the ambiguity function. It is shown that two effects are present due to phase errors. The first is a degradation of resolution in both dimensions and the second is a degradation in the ability to detect the targets against additive noise.

The resolution in the frequency variable is derived for an arbitrary transmitted pulse and the resolution in time, or position, is derived for a linear FM (chirp) pulse. In the presence of random phase errors, the resolution of the expected response is found. For the special case of LF phase errors, the displacement of the peak of the ambiguity function and the increase in its width (resolution degradation) caused by phase errors are calculated. Also, for LF phase errors it is shown that the same data processing maximizes SNR while optimizing resolution.

Radar Resolution of Closely Spaced Targets—W. L. Root (p. 197)

This paper presents an analysis of the problem of the resolvability of two radar targets which are located close together, in the sense that any parameters of the targets being measured (*e.g.*, range, range rate, range acceleration, azimuth, azimuth rate, etc.) are close together. Arbitrary sets of parameters are allowed, and it is assumed there is additive noise of arbitrary but known spectral shape. A criterion of resolvability is formulated, and in terms of this criterion equations are derived for the general case to show whether neighboring targets are resolvable. The results are specialized for the case of white-noise interference and the measurement of range and range rate.

Signal Fidelity in Radar Processing—W. A. Penn (p. 204)

Usually in a radar signal-processing scheme, the primary consideration is the geometrical resolution of the system, or, if a particular measurement is desired, the accuracy of the system. Thus a given signal-to-noise ratio may be sought in order to meet a simple detection requirement or a desired accuracy. Usually, beyond these simple criteria, the matter of signal amplitude fidelity is not particularly stressed. In many processes, however, signal fidelity can be an important consideration in evaluating the over-all effect on the observer.

In this paper the loss of information caused by signal interference in correlation or matched filter techniques is evaluated in an approximate manner. This is related to the invariance of the total integral of the Woodward ambiguity function. Degradation of the desired signal due to the statistical fluctuation of the signal itself is also considered. The distinction between pre-detection integration, which is involved in the correlation process, and post-detection integration is made. How these fluctuations can be reduced by post-detection integration is discussed and the resulting probability distributions of the signal are evaluated.

Finally some brief comments are made on the philosophy of providing adequate gray-level rendition in radar displays. Attention is given to reconciling the dynamic ranges of the display and the signal, and to the number of resolvable gray levels available in the signal.

A good example of these principles is the problem of recognition of objects in maps obtained from high-resolution radars. A ground-mapping system, using a coherent digital correlator and a pseudo-random code is analyzed in order to demonstrate a particular application. Several photographic simulations are shown which graphically illustrate the effects of correlation noise and post-detection integration.

Analysis of Signal Processing Distortion in Radar Systems—J. V. DiFranco and W. L. Rubin (p. 219)

Signal processing distortion degrades radar performance with respect to target data accuracy, ambiguity and resolution. A measure of the loss in performance is obtained by the development of a modified radar "uncertainty function" which results from the presence of time- and frequency-domain distortions in the system. Losses due to the major sources of distortion are evaluated and several compensation techniques discussed.

Contributors (p. 228)

Radio Frequency Interference

Vol. RFI-4, No. 2, May, 1962

The Issue in Brief (p. i)

A Few Words from Your National Chairman—H. E. Dinger (p. iii)

Control of Interference Between Surface Microwave and Satellite Communication Systems—W. L. Firestone, S. G. Lutz, and J. Smith (p. 1)

Satellite technology can expand global communication by orders of magnitude, but only by sharing frequencies with surface services now occupying the spectrum. Feasibility of frequency sharing with fixed microwave systems is discussed here. Such systems occupy a useful fraction of the spectrum and employ horizontally-beamed low power. Passive and active, stationary and low orbit satellite point-to-point systems are considered.

Interference may be "surface" (earth terminal to or from microwave) or "orbital" (to, from, or via satellites). Surface coordination is eased by the minimum elevation angles of terminal antennas, but still requires beyond-horizon separations or topographically protected sites. Interference from satellites is inconsequential. Main-beam interference to satellites can come only from a tangential belt.

Radio Interference—Suicide or Challenge—G. Jacobs (p. 21)

The reduction and ultimate prevention of radio frequency interference, and the solution of the broader problem of radio spectrum conservation, are among the greatest technical challenges to be faced in the decade of the 1960's. To meet this challenge successfully, it is stressed that close cooperation must exist between the engineer and the diplomat, between telecommunication planners, managers, and policy makers, both nationally and internationally. To help accomplish this, the suggestion is made that the PGRFI broaden its responsibilities to cover the entire field of radio spectrum conservation.

Recent Developments in RF Interference—O. M. Salati (p. 24)

Present trends in the design of transmitters, receivers, and antennas for use in communications and radar are reviewed to assess their impact on interference, interference measurement techniques, shielding and prediction methods. It is shown that transmitter power output and antenna size have increased by a factor of 10 in the last decade and that similar increases are anticipated in the next five to ten years. Transmitter spurious outputs are now frequently greater than the desired outputs of transmitters a few years ago. It is also shown that receiver sensitivity improvement, as a result of new techniques (masers, parametric, amplifiers, etc.), may not be realizable unless antenna side- and backlobes are drastically reduced. It is further shown that the sensitivity and frequency range of field intensity meters must be increased to permit meaningful measurements in the light of these developments. It is suggested that the performance of filters for transmitters must be developed for receivers to reduce interference.

Contributors (p. 34)

Reliability and Quality Control

Vol. RQC-11, No. 1, May, 1962

System Evaluation or Reliability in Economic Perspective—E. S. Winlund (p. 1)

KEWB—A Radiation Burst Test Facility—J. W. Flora and R. K. Stitt (p. 4)

It is a well-established fact that brief pulses of intense radiation, such as those produced during a nuclear detonation, can disable, or cause serious malfunction of, most electronic systems even though they are located outside the thermal and shock destruction zones. This fact has given rise to the need for a device which can simulate the radiation environment accompanying a nuclear detonation. Coincidental with the evolution of this need, a family of nuclear reactors has been demonstrated as being capable of producing radiation bursts which, in all important respects, adequately simulate a nuclear weapon. These devices offer additional advantages over field tests involving actual detonation in that they may be operated on a routine repetitive basis at a much reduced cost and under carefully controlled laboratory conditions.

The Kinetic Experiments on Water Boiler (KEWB) reactor has a demonstrated ability to perform in the capacity of a weapon simulator. This reactor is located in the Los Angeles area and is operated by Atomics International for the Atomic Energy Commission. Organizations executing Government contracts can take advantage of its availability if transient radiation resistance requirements are encountered during execution of their contract. The reactor is of the aqueous homogeneous type and produces the shortest duration pulse of any of the the thermal neutron reactors operating today. Radiation pulses of varying widths down to 3.0 msec can be obtained with the assembly together with peak neutron and gamma intensities of 3×10^{16} neutrons/cm²-sec and operating today. Radiation pulses of varying widths down to 3.0 msec can be obtained with the assembly together with peak neutron and gamma intensities of 3×10^{16} neutrons/cm²-sec and 3×10^{7} R/sec, respectively. Equipment occupying several cubic feet can be located in the immediate vicinity of the reactor core and exposed to these intense radiations.

A Computer Application to Reliable Circuit Design—L. Hellerman (p. 9)

The problem of reliable electronic circuit design by statistical methods is described. After a brief account of the history of this problem, we give the principle of one successful method—Monte Carlo. Two implementations of this method, as digital-computer programs, are given. The first program analyzes the reliability of a given circuit. The second program picks component values to optimize the circuit behavior with respect to several performance aspects. Examples illustrating the nature of the input and output information are included.

> " . . . Civilization advances by extending the number of important operations which we can perform without thinking about them. . . . "
>
> —A. N. Whitehead

A Survey of Applications of Radioactivity to Electronics—A. J. Moses (p. 19)

After a review of the nature of radioactivity and its detection, typical applications of radioactivity are presented in research, development and quality control with emphasis on the field of electronics.

Topics discussed include the efficiency of cleaning operations, determination of impurities in semiconductor materials, detection of leakage of air into sealed units, wear of relay contacts, isotopic dating of products, preionization of gases, dissipation of electrostatic charges, location of hidden splices, and verification of installation of small components.

Which Road to Satellite Reliability—R. H. Myers (p. 24)

Unless exceptionally high levels of reliability are achieved in long mission satellite systems such as those required for navigation, weather, ICBM warning, or communication purposes, the operating costs become prohibitive in terms of satellites needed to keep the system going and multimillion dollar costs per launch.

This paper outlines and discusses the technical reliability approach and the related reliability program plan needed to meet the severe reliability requirements of satellite systems.

On Models for Reliability Prediction—R. S. Robins (p. 33)

The paper presents a review and commentary on various mathematical models which have been proposed and used for analytical prediction of reliability. Attention is given to the physical interpretation of some of the mathematical postulates on which particular models are built. A rough classification of models for long-term life quality analyses as distinct from short-term success at any instant predictions are made. Based on the considerations presented, a summary commentary is made on the present status of reliability prediction theories.

Improving the Reliability of Digital Devices with Redundancy: An Application of Decision Theory—E. J. Farrell (p. 44)

The reliability of complex digital systems can be increased by increasing the reliability of the components of the system or by inserting redundant components into the system. Since it is often prohibitively expensive to obtain successively higher levels of component reliability, inserting redundant components may be the only reasonable way to satisfy future digital system requirements.

The reliability of a given computer subsystem may be improved by adding redundant subsystems of the same sort having the same inputs, and entering the several outputs into a decision element designed to produce the most probably, correct final output. This paper deals with designing the decision element.

The optimum design is obtained for several different types of systems. The decision element that maximizes the "reliability" is derived when the a priori probabilities of various outputs are known and when they are unknown. The optimum element is unique when the a priori probability is unknown.

Call for Papers—9th National Symposium (p. 53)

Abstracts and References

Compiled by the Radio Research Organization of the Department of Scientific and Industrial Research, London, England, and Published by Arrangement with that Department and *Electronic Technology*, Dorset House, Stamford St., London S.E. 1, England

NOTE: The Institute of Radio Engineers does not have available copies of the publications mentioned in these pages, nor does it have reprints of the articles abstracted. Correspondence regarding these articles and requests for their procurement should be addressed to the individual publications, not to the IRE.

The Index to the Abstracts and References published in the PROC. IRE from February, 1961 through January, 1962 is published by the PROC. IRE, June, 1962, Part II. It is also published by *Electronic Technology* and appears in the March, 1962, issue of that Journal. Included with the Index is a selected list of journals scanned for abstracting with publishers' addresses.

The number in heavy type at the upper left of each Abstract is its Universal Decimal Classification number. The number in heavy type at the top right is the serial number of the Abstract. DC numbers marked with a dagger (†) must be regarded as provisional.

UDC NUMBERS

Certain changes and extensions in UDC numbers, as published in PE Notes up to and including PE 666, will be introduced in this and subsequent issues. The main changes are:

Artificial satellites:	551.507.362.2	(PE 657)
Semiconductor devices:	621.382	(PE 657)
Velocity-control tubes, klystrons, etc.:	621.385.6	(PE 634)
Quality of received signal, propagation conditions, etc.:	621.391.8	(PE 651)
Color television:	621.397.132	(PE 650)

The "Extension and Corrections to the UDC," Ser. 3, No. 6, August, 1959, contains details of PE Notes 598–658. This and other UDC publications, including individual PE Notes, are obtainable from The International Federation for Documentation, Willem Witsenplein 6, The Hague, Netherlands or from The British Standards Institution, 2 Park Street, London, W. 1, England.

A list of organizations which have available English translations of Russian journals in the electronics and allied fields appears each June and December at the end of the Abstracts and References section.

ACOUSTICS AND AUDIO FREQUENCIES

534.232 **2137**

Active Load Impedance—R. J. Bobber. (*J. Acoust. Soc. Am.*, vol. 34, pp. 282 288; March, 1962.) Theory is developed for the operation of a load impedance of any magnitude and phase, including negative resistance. The load impedance of a generator or the radiation impedance of a transducer is controlled by a second generator coupled to the first by a transmission line. The theory is applicable to underwater sound transducers.

534.232 **2138**

Preloading of Acoustic Transducers for High-Pressure Operation—A. D. Brickman. (*J. Acoust. Soc. Am.* vol. 34, pp. 305 311; March, 1962.) By preloading a piston-type transducer mechanically, high-pressure performance is improved. The advantages of conical disk springs as isolators are discussed.

534.232 **2139**

Theory of a Passive, Reversible, Distributed-Coupling Transducer—W. J. Trott. (*J. Acoust. Soc. Am.*, vol. 34, pp. 333–337; March, 1962.) Equations are derived for a low-Q, high-efficiency, underwater sound transducer with constant resistive impedance. It consists of an acoustic transmission line coupled to a low-pass electrical transmission line. Theory and four proposed designs are given.

534.232 **2140**

Low-Resonant-Frequency Barium Titanate Transducer—L. W. Dean, III, and N. A. Ball. (*J. Acoust. Soc. Am.*, vol. 34, p. 347; March, 1962.) The transducer, which is a bilaminate strip of $BaTiO_3$ mass-loaded at its ends, has a resonance frequency in the range 200–1700 cps.

534.232-8 **2141**

Ultrasonic Intensity Gain by Composite Transducers—W. J. Fry and F. Dunn. (*J. Acoust. Soc. Am.*, vol. 34, pp. 188 192; February, 1962.) An analytic description of the action of a composite layered transducer is given. The increase in acoustic intensity over that obtained by direct coupling is considered quantitatively and the results are presented graphically. Intensities as high as 10^{8} w/cm may be attained.

534.24 **2142**

Reflection and Transmission of Sound by Elastic Spherical Shells—R. R. Goodman and R. Stern. (*J. Acoust. Soc. Am.*, vol. 34, pp. 338 344; March, 1962.)

534.522.1 **2143**

Optical Measurement of the Sound-Pressure Amplitude and Waveform of Ultrasonic Pulses—W. W. Lester and E. A. Hiedemann. (*J. Acoust. Soc. Am.*, vol. 34, pp. 265–268; March, 1962.) The use of light diffraction for measuring the sound-pressure amplitude and waveform of ultrasonic waves [*e.g.*, 1467 of 1960 (Hargrove, *et al.*)] is extended to pulses. The method has been used for transducer calibration in water at 5 Mc for pulses of 3–12-μs duration. Results are in agreement with those obtained by CW technique.

534.522.1 **2144**

Optical Method for Ultrasonic Velocity Measurements at Liquid-Solid Boundaries—W. G. Mayer and J. F. Kelsey. (*J. Acoust. Soc. Am.*, vol. 34, pp. 269 270; March, 1962.) "An optical method is used to measure the energy ratio of reflected and incident ultrasonic waves at a liquid-solid interface. The ultrasonic velocities in the solid are calculated from the angles of maximum reflection in the liquid."

534.61-14 **2145**

Sound Sources and Probes for the Measurement of Pulsed Acoustical Waves in Water—W. G. Neubauer. (*J. Acoust. Soc. Am.*, vol. 34, pp. 312 318; March, 1962.)

534.63-8 **2146**

Precise Determination of Wavelength with an Ultrasonic Interferometer—I. Ikeda. (*J. Acoust. Soc. Am.*, vol. 34, pp 351 352; March, 1962). An interferometer operating at 15 Mc and capable of detecting an adjustment of 0.2μ in the length of an acoustic path is described.

534.79 **2147**

The Loudness of Diffuse Sound Fields—D. W. Robinson, L. S. Whittle and J. M. Bowsher. (*Acustica*, vol. 11, no. 6, pp. 397–404; 1961.) Description of subjective tests in which the loudness of diffuse sound fields was compared with the loudness of normally incident progressive waves. Results are compared with those of investigations using different experimental arrangements. The form of the equal-loudness contours for diffuse fields is derived. For measurements on directional sound fields see 1713 of 1961 (Robinson and Whittle).

534.84 **2148**

The Influence of the Surface of the Test Material on the Diffusivity of the Sound Field in the Echo Chamber and on the Sound Absorption Coefficient—F. Kolmer and M. Kršňák.

(*Acoustica*, vol. 11, no. 6, pp. 405–413; in German.) Continuation of earlier investigations of sound-field diffusivity. [*Acoustica*, vol. 10, nos. 5/6, pp. 357–371; 1960 (Kolmer, *et al.*)]

534.843.3 2149
Variations of the Level of Acoustic Pressure in an Enclosed Space—H. Š. Kurtović. (*Ann. Télécommun.*, vol. 16, pp. 254–267; November/December, 1961.) The laws of variation of acoustic intensity in rooms are examined for widely varied acoustic conditions.

534.861:621.391.827 2150
Radio-Frequency Screened Equipment for Audio-Frequency Circuits—H. Schiesser. (*Rundfunktech. Mitt.*, vol. 6, pp. 42–46; February, 1962.) The problem of shielding studio equipment from RF fields is discussed with reference to measurements of coupling resistance on various cable systems. A new type of seven-pole screened coupler is described.

534.88 2151
Optimum Signal Processing of Three-Dimensional Arrays Operating on Gaussian Signals and Noise—F. Bryn. (*J. Acoust. Soc. Am.*, vol. 34, pp. 289–297; March, 1962.) The elements required for design of an optimum detector are deduced and numerical examples are presented.

534.88 2152
Effect of Rough Surfaces on the Resolution of Acoustic Rays in the Ocean—A. Berman. (*J. Acoust. Soc. Am.*, vol. 34, pp. 298–304; March, 1962.) The effect of boundary scattering at frequencies below 1 kc on the resolution of ray paths is investigated.

534.88 2153
Scanned Line Hydrophone Method of Determining Angle of Arrival of Sound in Water—M. T. Pigott, D. C. Whitmarsh, and J. L. Brown, Jr. (*J. Acoust. Soc. Am.*, vol. 34, pp. 319–328; March, 1962.) By rapid electronic sequential scanning of a group of hydrophones closely spaced in a straight line, an output effectively that of a rapidly moving single receiver is produced. The Doppler effect observed at the output determines the bearing of the received signal.

534.88 2154
Problems Associated with the Measurement of Ambient-Noise Directivity by means of Linear Additive Arrays—J. Stone. (*J. Acoust Soc. Am.*, vol. 34, pp. 328–333; March, 1962.) Limitations in frequency response and smoothing caused by sidelobe responses reduce the reliability of measurements made with the array.

621.395.61.089.6 2155
Problems in the Testing of Pressure-Gradient and Velocity Microphones—G. Kaszynski and W. Ortmeyer. (*Hochfrequenz. und Elektroak.*, vol. 71, pp. 29–34; February, 1962.) The calibration of microphones in anechoic chambers is discussed with particular regard to the importance of establishing the correct sound field.

ANTENNAS AND TRANSMISSION LINES

621.372.8 2156
Demonstration of Higher Modes of Oscillation in Waveguides with the Aid of the Radiation Field—K. E. Müller. (*Nachrtech.*, vol. 12, pp. 18–24; January, 1962.) The radiation characteristics of circular and rectangular waveguide are investigated and used as a means for analyzing the modes present in the waveguide.

621.372.8:537.527 2157
Gaseous Breakdown in Pressurized Microwave Components—R. M. White and R. H. Stone. (*Electronics*, vol. 35, pp. 45–47; April 20, 1962.) Factors that cause electric breakdown in waveguides and other microwave components are discussed. Means of preventing this type of breakdown are considered.

621.372.81+538.566 2158
The Propagation of Electromagnetic Waves in a Parallel-Plate Medium whose Plates are Arbitrarily Thick and Lossy—Thust. (See 2251.

621.372.823:537.226 2159
Propagation along Unbounded and Bounded Dielectric Rods: Parts 1 & 2—P. J. B. Clarricoats. (*Proc. IEE*, vol. 108, pp. 170–176, and 177–186; March, 1961.) The propagation constants of a rod are derived and its behavior inside a circular waveguide is studied. Expressions are given for power distribution and attenuation.

621.372.825 2160
The Theory of a Diaphragm-Loaded Waveguide of Rectangular Cross-Section—E. S. Kovalenko and V. S. Kovalenko. (*Izv. vyssh. uch. Zav., Radiotekhnika*, vol. 4, pp. 11–25; January/February, 1961.) An infinite system of algebraic equations occurring in the theory of ridge waveguides is considered and a method of solution is given. Numerical calculations are made relating to the harmonics and cutoff frequencies of LE and LM waves.

621.372.826:621.396.677.7 2161
The Launching of Surface Waves by a Magnetic Line Source—C. M. Angulo and W. S. C. Chang. (*Proc. IEE*, vol. 108, pt. C, pp. 187–196; March, 1961.) The excitation of surface waves along parallel dielectric slabs is found by modal analysis. Radiation field, the power of the waves and conditions for optimum launching efficiency are obtained.

621.372.852.15 2162
Microwave Filter Design Techniques—E. Tahan. (*Microwave J.*, vol. 5, pp. 111–116; March, 1962.) Design data are given to enable filters to be built up of uniform tunable cavities and irises, the required pass bands being obtained by moving the irises and tuning the cavities.

621.372.852.32:621.396.43:551.507.362.2 2163
A Temperature-Stabilized Microwave Power Limiter for Communication Satellite Use—R. L. Comstock, W. A. Dean and L. J. Varnerin. (*Proc. IRE*, vol. 50, pt. 1, pp. 470–471; April, 1962.) The limiter comprises a spherical crystal of Y-Fe garnet in a microwave cavity. Operation is stable from 55° to 120°F.

621.372.852.323 2164
A Magnetless Millimetre-Wave Isolator using Strontium Ferrite—P. Vilmur, K. Ishii, and F. F. Y. Wang. (*Microwave J.*, vol. 5, pp. 106–110; March, 1962.) Design information is presented for the range 57–59.5 Gc, for various mounting positions and dimensions of ferrite and polystyrene strips.

621.372.852.34+621.372.855.4 2165
Investigations on Waveguide Attenuators and Terminations with Curved Resistive Layers—C. Stäger. (*Tech. Mitt. PTT*, vol. 39, pp. 297–305; September, 1961.) In the devices described the layer of resistive material is carried on an elastic support strip whose curvature and penetration into the waveguide can be varied. Good wide-band characteristics at low reflection are obtained as indicated by the test results given.

621.372.852.4 2166
Relation between Normal Waves in Waveguides with Ferrites—Yu. Ya. Yurov. (*Izv. vyssh. uch. Zav., Radiotekhnika*, vol. 4, pp. 26–36; January/February, 1961.) Expressions are derived for the propagation constant and wave amplitude in a ferrite-loaded waveguide. A new principle for the transformation of axially symmetric waves into linearly polarized waves by means of ferrite is suggested.

621.372.853:537.56 2167
A Backward Wave in Plasma Waveguide—S. F. Paik. (Proc. IRE, vol. 50, pt. 1, pp. 462–463; April, 1962.) A cylindrical rod on the axis of a cylindrical plasma column has pronounced backward-wave properties. A thin dielectr c cylinder around the plasma tends to enhance the backward wave.

621.372.835.1 2168
Lined Waveguide—H. G. Unger. (*Bell Sys. Tech. J.*, vol. 41, pp. 745–768; March, 1962.) A more exact analysis is presented for straight and curved waveguides and for all practical linings.

621.396.67:621.318.57:621.387 2169
Duplexing and Switching with Multipactor Discharges—M. P. Forrer and C. Milazzo. (Proc. IRE, vol. 50, pt. 1, pp. 442–450; April, 1962.) The devices described handle peak powers up to 5.5 mw at nanosecond switching speeds. Practical S-band switches are described, and the theory is surveyed.

621.396.67:621.396.621.22 2170
Progress in the Construction of Common Aeria s using New Components—H. Licht. (*Rundfunktech. Mitt.*, vol. 6, pp. 21–25; February, 1962.) Distribution equipment for use in communal antenna installations is described which has particularly good characteristics for operation in bands *IV/V*.

621.396.67:624.97.042 2171
Wind Pressure on Aerial Supports at Great Heights above Sea Level—F. Staiger. (*Rundfunktech. Mitt.*, vol. 6, pp. 39–41; February, 1962.) Design factors allowing for wind pressure on antenna towers and masts are considered. For previous investigations of the loading of antenna structures due to ice formation see 2850 of 1961.

621.396.678.424 2172
A Survey of the Very-Wide-Band and Frequency-Independent Antennas—1945 to the Present—J. D. Dyson. (*J. Res. NBS*, vol. 66D, pp. 1–6; January/February, 1962.) An illustrated review of spiral and log-periodic antennas. For another version with additional references see *Electronics*, vol. 35, pp. 39–47; April, 1962.

621.396.67.095 2173
Current on and Input Impedance of a Cylindrical Antenna—Y. M. Chen and J. B. Keller. (*J. Res. NBS*, vol. 66D, pp. 15–21; January/February, 1962.) The current is expressed as the sum of a current emanating from the gap and two currents reflected from the ends.

621.396.673 2174
The E-Field and H-Field Losses around Antennas with a Radial Ground Wire System—T. Larsen. (*J. Phys. NBS*, vol. 66D, pp. 189–204; March/April, 1962.) The antennas used in the investigation were $\lambda/2$ and $\lambda/4$ monopoles, and electrically short monopoles, some top-loaded.

621.396.673 2175
The Electric Field at the Ground Plate near a Disk-Loaded Monopole—J. Hansen and T. Larsen. (*J. Res. NBS*, vol. 66D, pp. 205–210; March/April, 1962.) A knowledge of the electric and magnetic fields near such an antenna is necessary for the calculation of ground losses.

621.396.677.4 2176
Theory of the Infinite Cylindrical Antenna including the Feedpoint Singularity in Antenna Current—R. H. Duncan. (*J. Res. NBS*, vol. 66D, pp. 181–188; March/April, 1962.) A theoretical study of the feedpoint singularity.

621.396.677.5 2177
A Note on the Radiation Resistance and Field Strength of Large Loop Antennas—K. S. Imrie. (PROC. IRE, vol. 50, pt. 1, p. 477; April, 1962.) Expressions are derived using a power-series expansion which shows more clearly the relation between different types of loops.

621.396.677.7 2178
Ferrite-Loaded Microwave Radiators—R. Kühn and G. Teske. (*Nachrtech.*, vol. 12, pp. 9–12; January, 1962.) A survey of various types of microwave radiator with facilities for beam scanning, including a reciprocal phase shifter in rectangular waveguide.

621.396.677.73 2179
The Diagonal Horn Antenna—A. W. Love. (*Microwave J.*, vol. 5, pp. 117–122; March, 1962.) All horn cross sections are square and for small flare angles the electric vector is parallel to one of the diagonals. The far field has almost perfect circular symmetry. With an aperture five inches square operating at 16.5 Gc, half-power beamwidth is 8.5°; sidelobes in the principal planes are 33 db down.

621.396.677.832:621.396.969.3 2180
Radar Corner Reflectors for Linear or Circular Polarization—Latmiral and Sposito. (See 2334.)

621.396.677.833 2181
Horn-Parabola Aerial—H. K. Neske. (*Nachrtech.*, vol. 12, pp. 13–17; January, 1962.) Design and construction problems are discussed and the characteristics of an antenna using a honeycomb type of structural material are given.

621.396.679 2182
Numerical Investigation of the Equivalent Impedance of a Wire Grid Parallel to the Interface between Two Media—T. Larsen. (*J. Res. NBS*, vol. 66D, pp. 7–14; January/February, 1962.) Curves showing the impedance of a grid parallel to a ground/air interface are plotted as a function of grid dimensions and parameters of the ground. See 3273 of 1957 (Wait).

621.396.679 2183
Impedance of a Monopole Antenna with a Radial-Wire Ground System on an Imperfectly Conducting Half-Space: Part 1—S. W. Maley and R. H. King. (*J. Res. NBS*, vol. 66D, pp. 175–180; March/April, 1962.) The effectiveness of a radial wire system as an approximation to a radial conducting disk is investigated.

AUTOMATIC COMPUTERS

681.142 2184
Tunnel-Diode Shift Register—B. Rabinovici. (PROC. IRE, vol. 50, pt. 1, p. 473; April, 1962.) Circuit and performance details are given of a simple register with low power consumption and capable of high-speed operation.

681.142 2185
A Directly Coupled Serial Adder Designed for Use in a Digital Differential Analyser—B. A. Boulter. (*J. Brit. IRE*, vol. 23, pp. 243–252; April, 1962.) A single type of transistor and a single tube of collector load resistor are used throughout equipment for maximum economy and optimum operational reliability.

681.142:621.375.4.018.756 2186
Nonsaturated Semiconductor Pulse Amplifier for Digital Computers—Filippov. (See 2223.)

681.142:621.376.5 2187
Accurate Analogue Computation with Pulse-Time Modulation—W. R. Seegmiller. (*Electronics*, vol. 35, pp. 54–57; March, 1962.) A technique is described for performing analog multiplication using a magnetic pulse-time modulator and transistors with a special feedback circuit.

681.142:621.382.23 2188
Multiplication and Division using Silicon Diodes—H. L. Kahn. (*Rev. Sci. Instr.*, vol. 33, pp. 235–238; February, 1962.) The logarithmic characteristic of a silicon diode is used to perform division, multiplication and the extraction of square roots. Curves of results are given, showing an accuracy within 2 per cent in division and within about 3 per cnt in multiplication, over a range in excess of two decades. Applications of the principles to an AGC circuit and to a system for controlling scanning speed of a recorder are presented.

681.142:621.382.3 2189
Transistors as Function Generators—J. K. Sen. (PROC. IRE, vol. 50, pt. 1, pp. 478–479; April, 1962.) A design procedure is outlined for transistor circuits which give square, square-root and logarithmic responses.

681.142:621.395.625.3 2190
High-Density Storage of Wide-Band Analogue Data—M. H. Damon and F. J. Messina. (*Electronics*, vol. 35, pp. 45–49; March, 1962.) A time-division multiplex system is used with a two-track video tape recorder to record and reproduce fifty-two separate channels.

CIRCUITS AND CIRCUIT ELEMENTS

621.318.4.042.1:621.318.134 2191
Disaccommodation and its Relation to the Stability of Inductors having Manganese-Zinc Ferrite Cores—E. C. Snelling. (*Mullard Tech. Commun.*, vol. 6, pp. 207–215; March, 1962.) Results show the time variation in permeability produced by temperature changes.

621.318.57:621.382.3 2192
Temperature Characteristics and Examples of Application of Electronic Switches with Complementary Transistors—A. E. Bachmann. (*Tech. Mitt. PTT*, vol. 39, pp. 401–416; December, 1961; vol. 40, pp. 19–28; January, 1962.) The operation of circuits based on the combination of *p-n-p-* and *n-p-n*-type transistors is investigated with regard to the effect of temperature variations. Applications discussed are mainly concerned with telephony equipment. 31 references.

621.372.412 2193
A New Type of Piezoelectric Flexural Vibrator in the Form of Balanced Cantilevers—S. Ayers. (PROC. IRE, vol. 108, pt. C, pp. 35–49; March, 1961.) The theory of various forms of vibrator is considered. The theoretical frequencies, temperature characteristics, Q factors and displacement patterns are compared with experimental values.

621.372.44 2194
Conjunctors, another New Class of Nonenergic Nonlinear Network Elements—S. Duinker. (*Philips Res. Repts.*, vol. 17, pp. 1–19; February, 1962.) This new device is a locally active but parametrically passive nonlinear three-port element defined by a set of algebraic equations between voltages and currents.

621.372.5 2195
Continuous Formation of Mean Values with the aid of Passive Networks—H. J. Langer. (*Frequenz*, vol. 16, pp. 15–24; January, 1962.) Passive *RCL* networks are used to form the arithmetic mean over time intervals ranging from a few μs to several secons.

621.372.5:512.23 2196
Connection Matrices and Networks Algebra—M. Boisvert. (*Ann. Télécommun.*, vol. 16, pp. 268–287; November/December, 1961.) An algebra of passive linear reciprocal networks is described.

621.372.5:621.3.049.75 2197
Synthesis of Distributed-Parameter *RC* Networks—W. W. Happ. (PROC. IRE, vol. 50, pt. 1, pp. 483–484; April, 1962.) Improvements in design and operational characteristics of thin-film distributed parameter networks are described.

621.372.5:621.391.822 2198
Noise Figure Calculation based on the Admittance Matrix of the Network—E. L. Rotholz. (PROC. IRE, vol. 50, pt. 1, pp. 477–478; April 1962.) A method of calculating the noise voltages and noise figure of a network is described. The network is assumed to be linear, passive and time-invariant.

621.372.512:621.372.543.2 2199
The Frequency-Dependent Properties of Two Coupled Loss-Free Oscillatory Circuits—K. H. R. Weber. (*Tech. Mitt. BRF, Berlin*, vol. 5, pp. 166–173; December, 1961.) The characteristics of capacitively and inductively coupled loss-free parallel-tuned circuits are compared as a basis for investigating the performance of a two-circuit high-frequency band filter.

621.372.54 2200
Conditionally Equivalent Circuits for Bridge Circuits—W. Herzog. (*Frequenz*, vol. 15, pp. 391–404; December, 1961.) The substitution of bridge circuits by direct circuits eliminating transformers or differential transformers is investigated. A survey of double-bridge double-T networks indicates many possible bridge-equivalent circuits. See also 1473 of May.

621.372.54 2201
Transmission Factors with Tchebysheff-Type Approximation of Constant Group Delay—T. A. Abele. (*Arch. elekt. Übertragung*, vol. 16, pp. 9–18; January, 1962.) A filter design method is given and the polynomials used are tabulated. For a different method based on the same type of approximation see 2877 of 1961 (Ulbrich and Piloty).

621.372.54 2202
Diagonalizing Quadratic Filters—A. D. Hause. (PROC. IRE, vol. 50, pt. 1, p. 484; April, 1962.) Interpretation of quadratic filter operation can be simplified by using a diagonalizing transformation.

621.372.54 2203
A New Symmetrical Ladder Filter: the Parametric Band-Pass Filter—J. E. Colin. (*Cables & Trans.* (Paris), vol. 16, pp. 39–40; January, 1962.) An additional degree of freedom is provided to that of normal ladder filters by which one element can be suppressed, the group-delay characteristic improved, attenuation in one of the rejection bands increased, or the values of some elements of the filter modified. See also 1833 of June (Watanabe).

621.372.54 2204
High-Pass and Low-Pass Antimetric Ladder Filters with Tchebycheff Behaviour in both the Transmission and Attenuation Bands—

J. E. Colin and P. Allemandou. (*Cables & Trans.* (*Paris*), vol., 16, pp. 51–62; January, 1962.) By means of the transformations described antimetric filters can be designed by methods applicable to symmetric filters having similar characteristics.

621.372.6 2205
Matrix Analysis of Constrained Networks—A. Nathan. (Proc. IRE, vol. 108, pt. C, pp. 98–106; March 1961.) Applications included are a computing network difference amplifiers, a dc amplifier, and signal-flow graphs.

621.372.6:[512+513.83 2206
The Algebra and Topology of Electrical Networks—P. R. Bryant. (*Proc. IEE*, vol. 108, pt. C, pp. 215–229; March, 1961.) A review and development of three methods of network analysis. 53 references.

621.372.6:519 2207
A New Approach to Kron's Method of Analysing Large Systems—R. Onodera. (*Proc. IEE*, vol. 108, pt. C, pp. 122–129; March, 1961.) A simplification of Kron's diakoptics is attempted, and a dual method using the operations of open circuiting and short circuiting is introduced. See 289 of 1961 (Weinzweig).

621.372.632:621.382.23 2208
Theory of the Esaki-Diode Frequency Converter—R. A. Pucel. (*Solid-State Electronics*, vol. 3, pp. 167–207; November/December, 1961.) A matrix is formed whose elements are coefficients of the time-dependent diode conductance produced by the local oscillator. Expressions for minimum noise, *etc.*, are derived from this and the results compared with an experimental Esaki characteristic.

621.372.632:621.382.23 2209
Stable Low-Noise Tunnel-Diode Frequency Converters—F. Sterzer and A. Presser. (*RCA Rev.*, vol. 23, pp. 3–28; March, 1962.) Experimental UHF and microwave converters that are stable with input voltage SWR's exceeding 10:1 are described. Conversion losses and noise figures are lower than those of conventional crystal-diode converters. The Fourier coefficients of the conductance and of the equivalent shot-noise currents of a Ge-diode unit are given for a wide range of bias voltages and local-oscillator amplitudes. See 3668 of 1961.

621.372.632:621.382.23 2210
Some Characteristics of Tunnel-Diode U.H.F. Mixers—J. Klapper, A. Newton, and B. Rabinovici. (Proc. IRE, vol. 50, pt. 1, p. 479; April, 1962.) Further data on tunnel-diode mixers are given together with a description of a tunnel-diode down converter which requires no external bias.

621.372.632:621.385.63 2211
Frequency Changing by means of a Travelling-Wave Tube—W. Rudolph. (*Nachrtech.*, vol. 12, pp. 6–9; January, 1962.) A PM system of frequency translation for a radio link changing the incoming frequency of 3.6 Gc by 213 Mc is described.

621.373.42.072.7 2212
Variational Techniques applied to Capture in Phase-Controlled Oscillators—R. D. Barnard. (*Bell Sys. Tech. J.*, vol. 41, pp. 227–256; January, 1962.) An analytical procedure for obtaining bounds on the capture range is developed and applied to systems involving symmetric comparators and simple lag *RC* filters.

621.373.42.072.7 2213
Properties and Design of the Phase-Controlled Oscillator with a Sawtooth Comparator—C. J. Byrne. (*Bell Sys. Tech. J.*, vol. 41, pp. 559–692; March, 1962.) Properties of the circuit relating to many applications of the device are presented in a manner convenient for design. New data on the effects of fast jitter and noise are included.

621.373.42.072.7 2214
Analysis of the Phase-Controlled Loop with a Sawtooth Comparator—A. J. Goldstein. (*Bell Sys. Tech. J.*, vol. 41, pp. 603–633; March, 1962.) A detailed analysis concerned primarily with finding the pull-in range of the loop.

621.373.421:621.382.23 2215
Current-Tuned *RC* Oscillator—U. S. Ganguly. (*Electronic Tech.*, vol. 39, pp. 192–198; May, 1962.) Description of the design of an *RC* oscillator in which forward-biased Si junction diodes are used as current-variable resistive elements in the frequency-determining network.

621.373.43:621.382.3 2216
A Transistorized Voltage-Controlled Variable-Pulse-Rate Generator—C. D. Clarke. *Electronic Eng.*, vol. 34, pp. 322–325; May, 1962.) Output frequencies from 0.5 to 1000 pulses/sec are covered in a single range, the input/output characteristics being substantially linear over the major portion of the range.

621.373.431.4 2217
Forced Oscillation in an Oscillator with Two Degrees of Freedom—B. R. Nag. (*Proc. IEE*, vol. 108, pt. C, pp. 93–97; March, 1961.) Resonance characteristics determined theoretically agree to within 1 per cent with those obtained using a differential analyzer. Characteristics of oscillations outside the zone of synchronization are also described.

621.374.33:621.382.23 2218
Tunnel-Diode Gate has Subnanoseconed Rise Time—F. W. Kantor. (*Electronics*, vol. 35, pp. 62–64; April, 1962.) Operation depends on the small-signal impedance in the two stable states being significantly different. The principle should be applicable to other negative-resistance devices.

621.374.4:538.569.4 2219
Harmonic Generation using the Ammonia Inversion Transition—J. R. Fontana, R. H. Pantell, and R. G. Smith. (Proc. IRE, vol. 50, pt. 1, pp. 469–470; April, 1962.) A third-harmonic output of 10 mw may be obtained for an input of about 1 kw at a pressure of 2000 mm Hg.

621.375.121 2220
Limitations on Realizable Response Shapes for Certain Wide-Band Band-Pass Amplifier Circuits—R. A. Woodrow. (*Proc. IEE*, vol. 108, pt. C, pp. 107–114; March, 1961.) Either stagger-tuned stages or a chain of feedback pairs are used to realize Chebychev or Butterworth response shapes.

621.375.2 2221
Circuits for Difference Amplifiers: Parts 1 & 2—G. Klein and J. J. Zaalberg van Zelst. (*Philips Tech. Rev.*, vol. 23, pp. 142–150 and 173–180; February 7, and March 13, 1962.) The design of circuits to give high rejection factors is discussed and efficient methods of using difference amplifiers are examined.

621.375.4 2222
A Transmitter Preamplifier for Fast Transients—B. J. Elliott. (Proc. IRE, vol. 50, p. 476; April, 1962.) A small pulse preamplifier is described with a gain of 27 db and noise figure 8 db.

621.375.4.018.756:681.142 2223
Nonsaturated Semiconductor Pulse Amplifier for Digital Computers—A. G. Filippov. (*Izv. vyssh. uch. Zav., Radiotekhnika*, vol. 4, pp. 77–83; January/February, 1961.) The special feature of the circuit is an arrangement for switching-in the nonlinear feedback by means of an auto-transformer in the transistor output. Experimental data are given and the circuit performance is compared with that of a cascaded pulse amplifier.

621.375.9:621.372.44 2224
On the Use of Passive-Circuit Measurements for the Adjustment of Variable-Capacitance Amplifier—K. Kurokawa. (*Bell Sys. Tech. J.*, vol. 41, pp. 361–381; January, 1962.) The important circuit parameters and conditions for optimum performance are derived from measurements of impedance loci with the pump inoperative. Experimental confirmation with a 6-Gc degenerate amplifier is quoted.

621.375.9:621.372.44 2225
Parametric Amplification at Ultra High Frequencies—G. Pircher and M. Chaussedoux. (*Ann. Télécommun.*, vol. 16, pp. 296–307; November/December, 1961.) The operation and characteristics of a parametric system are analyzed on the basis of propagation concepts and the laws of black-body radiation. The Manley-Rowe relations are derived from energy considerations and an expression for gain is given in terms of measurable parameters.

621.375.9:621.372.44 2226
Isolated Parametric Amplifier has Low Noise Figure—L. D. Baldwin. (*Electronics*, vol. 35, pp. 58–59; March, 1962.) The input of the amplifier is isolated from the output by using two time-varying reactances. As ferrite circulators are not needed, insertion loss and amplifier noise are reduced. See also 2900 of 1961.

621.375.9:621.372.44:537.227 2227
Ferroelectric Parametric Amplifier—E. Fatuzzo and H. Roetshi. (Proc. IRE, vol. 50, pt. 1, p. 462; April, 1962.) The amplifier is based on a property of ferroelectric materials by which the small-signal dielectric constant increases during switching. The frequency range of the device extends from dc to about 50 kc.

621.375.9:621.372.44:621.372.8 2228
The Equivalent Circuit, Gain and Bandwidth of Travelling-Wave Parametric Amplifiers with Controlled Capacitors—W. Heinlein. (*Arch. elekt. Übertragung*, vol. 15, pp. 547–554; December, 1961.) Analysis of the operation of parametric amplifiers comprising a waveguide with band-pass characteristics, and variable-capacitance semiconductor diodes.

621.375.9:621.372.44:621.385.6 2229
Subharmonic Parametric Pumping of a Quadrupole Amplifier—Carroll. (See 2502).

621.375.9:621.372.44:621.387 2230
A Note on the Parametric Amplifier Theory for Plasmas—S. F. Paik. (*J. Appl. Phys.*, vol. 33, pp. 1017–1018; March, 1962.) An apparent inconsistency in the theory of Kino (4159 of 1960) is pointed out and a consistent expression is derived.

621.376.22:538.632 2231
An Improved Radio-Frequency Hall-Effect Modulator—E. Cohen. (*Electronic Eng.*, vol. 34, pp. 316–319; May, 1962.) The improvements consist in the attenuation, by means of simple compensating circuits, of residual and parasitic voltages normally present in Hall effect multipliers, and in the reduction of size compared to an earlier model.

621.376.32:621.395.625.3 2232
Frequency Modulation in Magnetic Storage—H. Völz. (*Nachrtech.*, vol. 11, pp. 553–557;

December, 1961; vol. 12, pp. 36-40; January, 1962.) The problems of FM signal recording on magnetic tape are examined on the basis of information theory. The design of modulators with a large frequency swing is discussed.

GENERAL PHYSICS

537.311.3 2233
Electrical Conduction Phenomena in Anisotropic Media: Part 2—The Electrical Resistance of Elliptically Anisotropic Media—D. Langbein. (*Z. Phys.*, vol. 166; pp. 22-41; December, 1961.) Part 1: 65 of January.

537.311.3 2234
Degenerate Fermi Surfaces and Electrical Resistance—E. Gerlach. (*Z. Phys.*, vol. 166, pp. 81-92; December, 1961.) Electrical resistance is calculated with the aid of Bloch's integral equation, and the results obtained are applied to the case of graphite.

537.312.62 2235
Theory of Superconductivity—S. H. Liu. (*Phys. Rev.*, vol. 125, pp. 1244-1248; February, 1962.) The differences between the theories of Eliashberg, Bogoliubov and Bardeen, Cooper, and Schrieffer are discussed.

537.312.63 2236
Calculation of the Superconducting State Parameters with Retarded Electron-Phonon Interaction—P. Morel and P. W. Anderson. (*Phys. Rev.*, vol. 125, pp. 1263-1271; February, 1962.)

537.533 2237
Experimental Evidence of Landau Damping in Electron Beams—M. Caulton, B. Hershenov, and F. Paschke. (*J. Appl. Phys.*, vol. 33, pp. 800-803; March, 1962.) Measurements have been made of the convection current in a velocity-modulated slowly drifting electron beam. Under conditions of appreciable velocity spread the fast space-charge wave is damped. This confirms qualitatively the theory of Berghammer (to published).

537.533 2238
Generalized Brillouin Flows—K. Pöschl and W. Veith. (*J. Appl. Phys.*, vol. 33, pp. 1013-1014; March, 1962.) The behavior of laminar electron flow including space charge in the presence of an axial magnetic field and an electric quadrupole field transverse to the direction of flow is investigated.

537.533 2239
Electron-Optical Field Distribution with Specified Imaging Propert'es—H. Hänsel. (*Optik, Stuttgart*, vol. 19, pp. 67-75; January, 1962.) Calculations are based on a method proposed by Picht (1361 of 1956).

537.533:538.3 2240
The Phase Shift of Electron Waves by Potentials in Field-Free Space—F. Lenz. (*Naturwiss.*, vol. 49, p. 82; February, 1962.) Discussion of the dependence of electron-beam interference on a magnetic vector potential, as demonstrated, *e.g.*, in 2407 below.

537.56:538.566:537.311.33 2241
Observation of Critical Fluctuations associated with Plasma-Wave Instabilities—S. Ichimaru, D. Pines, and N. Rostoker. (*Phys. Rev. Lett.*, vol. 8, pp. 231-233; March, 1962.) It should be possible to detect drift instabilities in an ionized plasma by the increased scattering cross section for EM waves. Results of calculations relating to electron-hole plasma in InSb are summarized.

537.56:538.63 2242
Plasma Oscillations in a Magnetic Field as an Initial-Value Problem—N. Anderson. (*J. Electronics and Control*, vol. 12, pp. 119-124; February, 1962.) An expression is obtained for the Laplace transform of the electric potential of the field which arises due to the oscillations. It is used to derive the dispersion relation between the oscillation frequency and wave number.

537.56:538.63 2243
Viscosity Coefficient of a Plasma in a Magnetic Field—S. Kaneko. (*J. Phys. Soc. Japan*, vol. 17, pp. 390-392; February, 1962.) The convergence of Chapman-Enskog's approximation to the viscosity coefficient of a plasma is calculated up to the fourth approximation. The viscosity coefficient in the second approximation, accurate for practical purposes, has an error of 5 per cent.

537.56:621.374.4 2244
Microwave Generation of the Second Harmonic in a Plasma—M. Moriyama and M. Sumi. (*J. Phys. Soc. Japan*, vol. 17, p. 397; February, 1962.) The second-harmonic current density is calculated taking into account the time-dependence of the plasma electron density.

537.56.08 2245
Comparison of Microwave and Langmuir Probe Measurements on a Gaseous Plasma—G. R. Nicoll and J. Basu. (*J. Electronics and Control*, vol. 12, pp. 23-29; January, 1962.) Values of average electron density and collision frequency obtained by the two methods are compared.

537.56.08 2246
Effects of Finite Probe Size in the Determination of Electron Energy Distribution Functions—J. D. Swift. (*Proc. Phys. Soc.* (*London*), *A*, vol. 79, pp. 697-701; April, 1962.) The principal effect considered is the disturbance produced by the drain of electrons to the probe.

538.26 2247
Magnetic Shielding Factors of a System of Concentric Spherical Shells—F. Schweizer. (*J. Appl. Phys.*, vol. 33, pp. 1001-1003; March, 1962.) General expressions are developed for the shielding factors of concentric spherical shells of linear isotropic magnetic material. Approximate results are given for shells of highly permeable material which are thin compared to their radii.

538.26:537.312.62 2248
Approach to the Ideal Magnetic Circuit Concept through Superconductivity—P. P. Cioffi. (*J. Appl. Phys.*, vol. 33, pp. 875-879; March, 1962.)

538.561:539.124 2249
Cherenkov Effect under the Influence of an External Magnetic Field—A. M. Sayied. (*Proc. Phys. Soc.* (*London*), *A*, vol. 79, pp. 816-818; April, 1962.) The field confines the particle to a circular orbit.

538.561:539.124 2250
The Radiation of Electromagnetic Waves and the Instability of Electrons Moving at Super-light Velocity in a Medium—V. L. Ginzburg, V. V. Zheleznyakov, and V. Ya. Eidman. (*Phil. Mag.*, vol. 7, pp. 451-458; March, 1962.) At super-light velocities, the radiation reaction force on a particle can change sign, with resultant instabilities; this follows from both simple quantum and classical theories.

538.566+621.372.81 2251
The Propagation of Electromagnetic Waves in a Parallel-Plate Medium whose Plates are Arbitrarily Thick and Lossy—P. Thust. (*Arch. elekt. Übertragung*, vol. 16, pp. 42-50; January, 1962.) Calculations based on exact theory and carried out for the case in which the electric field is parallel to the plates and perpendicular to the direction of propagation. Approximations are derived for different frequency ranges and sets of dimensions.

538.566 2252
Reiterative Wave Beams of Rectangular Symmetry—F. Schwering. (*Arch. elekt. Übertragung*, vol. 15, pp. 555-564; December, 1961. In English.) The wave beams considered are of rectangular symmetry and have passed through a structure of equally spaced phase-correction devices. For a study of the case of cylindrical symmetry see IRE TRANSACTIONS ON ANTENNAS AND PROPAGATION, vol. AP-9, pp. 248-256; May, 1961 (Goubau and Schwering).

538.566:535.42 2253
Derivation of Three-Dimensional Diffraction Solutions for Plane Electromagnetic Waves from Two-Dimensional Solutions—H. Stöckel. (*Optik, Stuttgart*, vol. 19, pp. 3-7; January, 1962.) The diffraction of a plane EM wave at a cylinder is considered.

538.566:537.56 2254
Effects of Electron Random Motion on Microwave Propagation through a Plasma Parallel to a Magnetic Field—J. E. Willett. (*J. Appl. Phys.*, vol. 33, pp. 898-906; March, 1962.) Expressions for the propagation of a circularly polarized microwave through a plasma parallel to a uniform static magnetic field are derived by two methods. The predicted effects of the random motion of electrons result from a) Doppler shift, b) electron free paths extending over distances significant compared to the attenuation length, c) variation of collision frequency with electron velocity.

538.566:537.56 2255
Nonlinear Interaction of an Electromagnetic Wave with a Plasma Layer in the Presence of a Static Field: Part 2—Higher Harmonics and a Nonlinear Propagation Theory—R. F. Whitmer and E. B. Barrett. (*Phys. Rev.*, vol. 125, pp. 1478-1484; March, 1962.) The properties of the third and fourth harmonics are discussed, the *h*th harmonic conversion loss is deducted, and a method is presented for reiterating the general solution for the *h*th harmonic field. Part 1: 2167 of 1961.

538.566:537.56 2256
The Passage of Microwaves through Plane Plasma Layers—K. Hain and M. Tutter. (*Z. Naturforsch.*, vol. 17a, pp. 59-64; January, 1962.) Calculations of the reflection and transmission coefficients for a plane EM wave propagating through a plasma slab with and without a static magnetic field.

538.567.4:621.391.63 2257
Design of a Microwave-Frequency Light Modulator—R. H. Blumenthal. (PROC. IRE, vol. 50, pt. 1, pp. 452-546; April, 1962.) The modulator is a uniaxial ADP crystal in a coaxial-line resonator. The electric field of the wave alters the propagation of light in the crystal.

538.569.4:535.853 2258
Spectrometers for Electron Paramagnetic Resonance—S. Koepp. (*Hochfrequenz. und Elektroak.*, vol. 71, pp. 1-27; February, 1962.)

Part 1: Microwave Networks and Limiting Sensitivity of Spectrometers (pp. 1-14).

Part 2: Methods of Signal Modulation and

of Stabilization of the Operating Point (pp. 15–27).
A detailed review with 82 references.

538.569.4:535.853 2259
The Effect of a Second Radio-Frequency Field on High-Resolution Proton Magnetic Resonance Spectra—R. Freeman and D. H. Whiffen. (*Proc. Phys. Soc.* (*London*), *A*, vol. 79, pp. 594–807; April, 1962.) "Field sweep" and "frequency sweep" methods of investigating decoupled resonance patterns are discussed.

538.569.4:537.29 2260
Electrically Induced Transitions between Spin Levels—G. W. Ludwig and F. S. Ham. (*Phys. Rev. Lett.*, vol. 8, pp. 210–212; March, 1962.) Experimental observations of electrically induced transitions between energy levels of Mn^+ ions in Si are reported. Their relative intensity with respect to magnetically induced transitions is discussed.

538.569.4:538.222 2261
Spin Diffusion in Inhomogeneously Broadened Systems—A. Kiel (*Phys. Rev.*, vol. 125, pp. 1451–1455; March, 1962.) Theoretical treatment of cross-relaxation within inhomogeneous spin systems.

538.569.4:538.222 2262
Classical Microscopic Model for Magnetic Resonance including Relaxation Effects—R. K. Waring, Jr. (*Phys. Rev.*, vol. 125, pp. 1218–1226; February, 1962.)

538.569.4:621.375.9:535.61–2 2263
Discrimination against Unwanted Orders in the Fabry-Perot Resonator—D. A. Kleinman and P. P. Kisliuk. (*Bell. Sys. Tech. J.*, vol. 41, pp. 453–462; March, 1962.) A modification to the interferometer structure of an optical maser is proposed, in which another reflecting plate is suitably positioned outside the maser to increase the losses of certain orders. A simplified analysis of the effect is given and numerical results are presented for a practical case.

538.569.4:621.375.9:535.61–2 2264
Giant Optical Pulsations from Ruby—F. J. McClung and R. W. Hellwarth. (*J. Appl. Phys.*, vol. 33, pp. 828–829; March, 1962.) By varying the effective reflectivity of the reflecting surfaces at the ends of the ruby rod through a Kerr-cell switching technique, pulses several orders of magnitude greater than the normal level are observed.

538.569.4:621.375.9:535.61–2 2265
Observations on the Pump Light Intensity Distribution of a Ruby Optical Maser with Different Pumping Schemes—T. Li and S. D. Sims. (PROC. IRE, vol. 50, pt. 1, pp. 464–465; April, 1962.) The helical lamp in a circular cylindrical reflector and the linear lamp in an elliptical cylindrical reflector are studied. The helical lamp appears more suitable for giving a high-energy maser beam.

538.569.4:621.375.9:535.61–2 2266
Parametric Amplification and Oscillation at Optical Frequencies—R. H. Kingston. (PROC. IRE, vol. 50, pt. 1, p. 472; April, 1962.) The generation of coherent optical energy at subfrequencies is proposed using a simple cavity, a nonlinear dielectric material and an optical maser pump.

538.569.4.029.6:547.6 2267
Absorption Measurements on Diphenyl Compounds in the Microwave Range—F. Hufnagel, G. Klages, and P. Knobloch. (*Z. Naturforsch.*, vol. 17a, pp. 96–98; January, 1962.)

538.569.4.029.65:535.853 2268
Dispersion Measurements on CsBr and CaF_2 in the Far Infrared and with Millimetre Waves—H. Happ, H. W. Hofmann, E. Lux, and G. Seger. (*Z. Phys.*, vol. 166, pp. 510–518; February, 1962.) Report on investigations in the range 0.4–3.5 mm λ by means of a grating spectrometer described in 114 of 1960. (Genzel, *et al.*)

538.63+538.66 2269
The Two-Band Theory of Galvano- and Thermo-magnetic Transverse Effects—F. Dannhäuser. (*Z. Phys.*, vol. 166, pp. 519–543; February, 1962.) Formulas for the coefficients of electrical and thermal conductivity and of the Hall, Ettingshausen, Nernst and Righi-Leduc effects are derived on the basis of the two-band model. Anomalies are discussed.

539.2:537.226 2270
Electric Dipoles due to Trapped Electrons—J. A. Sussmann. (*Proc. Phys. Soc.* (*London*), *A*, vol. 79, pp. 758–774; April, 1962.) An electron trapped at a vacancy or impurity center with three or four (tetrahedral) nearest neighbors can give an electric dipole with directional degeneracy, even with no lattice deformation. Such a dipole leads to a Debye type of dielectric loss and piezoelectricity.

GEOPHYSICAL AND EXTRA-TERRESTRIAL PHENOMENA

523.12 2271
Cosmic Electrical Discharges or 'Gobs of Anti-matter'—C. E. R. Bruce. (*Engineer* (*London*), vol. 212, pp. 946–950; December, 1961.) New developments of the electrical-discharge theory of the universe (see also 1488 of 1961) are discussed, and several galactic and stellar phenomena are interpreted on the basis of this theory.

523.152.3 2272
Semi-empirical Model of the Interplanetary Medium—J. C. Brandt and R. W. Michie. (*Phys. Rev. Lett.*, vol. 8, pp. 195–196; March, 1962.) A model giving the expansion velocity and density of the interplanetary medium up to a radius of five astronomical units is presented.

523.16+55]:629.19 2273
Some Geophysical and Astronomical Aspects of Soviet Space Research—V. I. Krassovsky (Krasovskii). (*Endeavour*, vol. 21, pp. 65–72; April, 1962.) Review of the main results of investigations carried out in support of manned space flight. 42 references to Russian literature.

523.164 2274
Spectra of Discrete Sources of Radio Emission Observed with the 22-Metre Radio Telescope—A. D. Kuzmin. (*Astron. Zhur.*, vol. 39, pp. 22–28; January–February, 1962.) Observations of discrete sources on 9.6 and 3.2 cm λ are compared with results of other authors. Spectra of thermal and nonthermal sources are given.

523.164 2275
A High-Accuracy Radio Interferometer—A. W. L. Carter. (*Observatory*, vol. 82, pp. 9–12; February, 1962.) A method of combining the signals from a 2- or 4-element linear antenna array that eliminates the need for calibrating the system without appreciable loss of sensitivity.

523.164:551.507.362.1/2 2276
Radio-Astronomy Investigations using Artificial Satellites and Space Rockets—E. A. Benediktov, G. G. Getmantsev, and V. L. Ginzburg.—(*Isk. Sput. Zemli*, no. 7, pp. 3–22; 1961, English Translation, *Planet-Space Sci.*, vol. 9, pp. 109–127; March, 1962.) Advantages of making observations from above the atmosphere and the measurement principles for investigating the interplanetary medium and the radiation from the sun and from cosmic and discrete sources are discussed.

523.164.3 2277
The Radio Emission Spectrum of Cassiopeia-A at Frequencies Below 30 Mc/s—S. Ya. Braude, A. V. Men', I. N. Zhuk, and K. A. Babenkov. (*Astron. Zhur.*, vol. 39, pp. 163–165; January/February, 1962.) A note on flux density measurements in the range 19.5–31 Mc.

523.164.3 2278
A Model of the Orion Nebula from Radio Observations—Yu. N. Parilskii. (*Astron. Zhur.*, vol. 38, pp. 798–808; September/October, 1961.)

523.164.3 2279
On the Selection of a Standard Discrete Source of Cosmic Radio Emission—S. Ya. Braude. (*Astron. Zhur.*, vol. 38, pp. 898–904; September/October, 1961.) The adoption of Cygnus-A as a standard RF source is considered. Flux density data in the range 12.5–10000 Mc and corrections necessary owing to the proximity of the extended source Cygnus-X are given.

523.164.32 2280
The Origin of the Slowly Varying Component of Solar Radio Emission—V. V. Zheleznyakov. (*Astro. Zhur.*, vol. 39, pp. 5–14; January/February, 1962). Bremsstrahlung mechanisms in different electron layers contributing to RF emission in the range 1–30 cm λ are discussed.

523.164.32 2281
Selected High-Resolution Strip Scans of the 10.7-cm Sun—A. E. Covington, G. A. Harvey, and H. W. Dodson. (*Astrophys. J.*, vol. 135, pp. 531–546; March, 1962.) Strip scans of the solar disk at a frequency of 2800 Mc using a fan-shaped beam 1.2° east-west by 2° north-south are compared with associated optical features.

523.164.32:523.75 2282
On the Association between Noise Storms and Solar Flares—E. v. P. Smith and P. S. McIntosh. (*J. Geophys. Res.*, vol. 67, pp. 1013–1016; March, 1962.) From an examination of I.G.Y. data it is concluded that the association between flares and noise storms is real.

523.163.4 2283
The Discrete Source of Radio Emission $\alpha = 18^h53^m7$, $\delta = 1°16'$—A. D. Kuz'min. (*Astron. Zhur.*, vol. 38, pp. 905–911; September/October, 1961.) Results of observations made at 9.6 cm λ with a 22-m radio telescope are compared with data for other wavelengths. The spectrum of the source is shown to be non-thermal.

523.164.4 2284
Evidence for Polarized 3.15-cm Radiation from the Radio Galaxy Cygnus A.—C. H. Mayer, T. P. McCullough, and R. M. Sloanaker. (*Astrophys. J.*, vol. 135, pp. 656–658; March, 1962.)

523.164.4 2285
Millimetre-Wave Radio Source in Taurus—A. H. Barrett. (*Nature*, vol. 194, pp. 170–171; April, 1962.) Observations at 1.8 cm λ (838 of March) indicate that the mm-λ source in Taurus reported by Kuz'min and Salomonovich (*Astron. Zhur.*, vol. 37, pp. 227–235; March/April, 1960) is of a type hitherto unknown in radio astronomy.

523.164.4 2286
Interpretation of 'Surface Brightness' Measurements of Radio Sources—R. W. Clarke. (*Nature*, vol. 194, pp. 171–172; April, 1962.) Taking account of the change in the apparent surface brightness of a source with distance leads to an ambiguity in the deduced radio luminosity for some cosmological models.

523.165 2287
Detection of an Intense Flux of Low-Energy Protons or Ions Trapped in the Inner Radiation Zone—J. W. Freeman. (*J. Geophys. Res.*, vol. 67, pp. 921–928; March, 1962.) Protons of energy 0.5 kev–1 Mev have been observed in the inner belt by Injun I. An energy flux of about 50 ergs cm² sec^{-1} sterad^{-1} has been measured. For 100 kev particles corresponds to a flux $\sim 3\times 10^8$ cm² sec^{-1} sterad^{-1}, which is much larger than predicted by the neutron albedo theory.

523.165 2288
Rocket Observations of Solar Protons during the November 1960 Events: Part 1—K. W. Ogilvie, D. A. Bryant, and K. R. Davis. (*J. Geophys. Res.*, vol. 67, pp. 929–937; March, 1962.) The results of three Nike-Cajun rocket flights are described.

523.165 2289
A Possible Correction to the Spectrum of Geomagnetically Trapped Protons—G. Haerendel. (*J. Geophys. Res.*, vol. 67, pp. 1173–1174; March, 1962.) The correction takes account of the gradient of the atmosphere over the proton circle of gyration. See also *J. Geophys. Res.*, vol. 67, p. 1697, April, 1962.

523.165 2290
Atmospheric Phenomena, Energetic Electrons and the Geomagnetic Field—J. R. Winckler. (*J. Res. NBS*, vol. 66D, pp. 127–143; March/April, 1962.) X-ray measurements associated with the "dumping" of electrons from the magnetic field are discussed.

523.165 2291
Progressive Rotation of Cosmic-Ray Diurnal Variation Vector—S. P. Duggal and M. A. Pomerantz. (*Phys. Rev. Lett.*, vol. 8, pp. 215–216; March, 1962.) A complete anticlockwise rotation on the harmonic dial was obtained during a disturbed period extending over seven days.

523.5:621.396 2292
The Meteoric Head Echo—B. A. McIntosh. (*J. Atmos. Terr. Phys.*, vol. 24, pp. 311–315; April, 1962.) Several definitive examples of meteoric head echoes are shown and problems involved in explaining them are considered.

523.5:621.396.96 2293
Radio-Echo Determinations of Orbits of Individual Meteors—B. L. Kashcheev, V. N. Lebedinets, and M. F. Lagutin. (*Astron. Zhur.*, vol. 38, pp. 681–691; July–August, 1961.) A diversity-reception technique for measurements of meteor radiants and velocities is described. Observations on 298 meteors of the Geminid stream in December, 1959 are reported in which accuracies within ±2.5° and ±1.8 km were attained.

523.5:621.396.96 2294
Specular Echoes from Dense Meteor Trails—H. Brysk. (*Canad. J. Phys.*, vol. 40, pp. 393–401; April, 1962.) "The scalar wave equation is solved for scattering of a normally incident wave by a cylindrical Gaussian distribution of electrons. The back-scattered intensity is computed for various line densities, as a function of the radius of the Gaussian. The echo intensity for specular backscattering from meteor trails of arbitrary density is thus obtained, including its variation with time."

523.75:551.510.535 2295
The Connection of Type III Absorption with Eruptive Active Regions on the Sun—A. S. Besprozvannaya and V. M. Driatskiĭ. (*Astron. Zhur.*, vol. 38, pp. 611–616; July/August, 1961. The generation and accumulation of charged particles with energies 10–100 Mev, responsible for anomalous absorption in the ionosphere at high latitudes, is discussed. Intense chromospheric flares are considered as a trigger mechanism which allows fast particles accumulated in eruptive regions to escape from the solar atmosphere.

550.38:551.507.362.2 2296
An Evaluation of the Odd Harmonics in the Earth's Gravitational Field—D. E. Smith (*Planet-Space Sci.*, vol. 9, pp. 93–94; March, 1962.) Values for the odd harmonics, J_3 and J_5 are obtained from the eccentricity variations in the orbits of Explorer VIII, Explorer XI and Tiros II satellites.

551.507.362.2 2297
On the Motion of a 24-Hour Satellite—P. Musen and A. E. Bailie. (*J. Geophys. Res.*, vol. 67, pp. 1123–1132; March, 1962.)

551.507.362.2 2298
Lunar and Solar Perturbations in the Orbit of the Third Soviet Cosmic Rocket—V. T. Gontkovskaya and G. A. Chebotarev. (*Astron. Zhur.*, vol. 38, pp. 954–960; September–October, 1961.) Perturbations of the orbit of Lunik III due to the sun and the moon are estimated separately. Results are tabulated.

551.507.362.2 2299
The Influence of Solar Radiation Pressure on the Motion of Artificial Earth Satellites—V. V. Radzievskiĭ and A. V. Artem'ev. (*Astron. Zhur.*, vol. 38, pp. 994–996; September–October 1961.) Description of a method of computation simpler than that of Musen (3492 of 1960) but sufficiently reliable for orbits of small eccentricity. The radiation pressure can give a decelerating effect equivalent to the friction in a medium of density 10^{-16} g cm³.

551.507.362.2:631.391.812.3 2300
The Correlation Analysis of the Fading of Radio Signals Received from Satellites—James. (See 2437.)

551.507.362.2:621.391.812.33 2301
Deduction of Satellite Orientation from Faraday Fading Measurements—J. Mass. (Proc. IRE, vol. 50, pt. 1, p. 466; 1962.) It is shown that satellite orientation can be deduced from the depth of Faraday fading; examples are given from recordings of Explorer VII.

551.507.362.2:621.396.43 2302
Satellite Project Telstar—(See 2444.)

551.510.535 2303
The Electron Density in the Lower Ionosphere—J. E. Titheridge. (*J. Atmos. Terr. Phys.*, vol. 24, pp. 269–282; April, 1962.) Absorption measurements at 720 and 1420 kc show that the electron density in the D region is four times greater at sunspot maximum than at sunspot minimum. Anomalous winter absorption results from increased ionization below 90 km, and fadeouts are caused by extra ionization at heights down to 60 km.

551.510.535 2304
The Stratification of the Lower Ionosphere—J. E. Titheridge. (*J. Atmos. Terr. Phys.*, vol. 24, pp. 283–296; April, 1962.) A series of preferred heights of reflection at intervals of $1\frac{1}{2}$ scale heights is shown to exist throughout the D and E regions. By day reflections occur at 71, 80, 90 and 100 km, and there is negligible seasonal and diurnal variation of these values.

551.510.535 2305
Vertical Movements in the Nighttime Ionosphere—W. Becker. (*Arch. elekt. Übertragung*, vol. 15, pp. 569–577; December, 1961.) Analysis of F-layer electron-density profiles derived from ionograms taken at Lindau from 1957 to 1960. A total vertical shift of 200 km at a velocity of about 30 msec was observed during strong geomagnetic bay disturbances; during geomagnetically calm nights short-term height displacements of up to 60 km were found.

551.510.535 2306
The Distribution of Electrons in the Nighttime Ionosphere—A. R. Long. (*J. Geophys. Res.*, vol. 67, pp. 989–997; March, 1962.) Nighttime $N(h)$ curves are found to be very nearly "α-Chapman" as predicted. The geomagnetic anomaly exists even at midnight at sunspot maximum, and marked nighttime movements occur in equatorial regions such that the ionosphere appears to be rapidly lowered.

551.510.535 2307
Associative Detachment in the D Region—R. C. Whitten and I. G. Poppoff. (*J. Geophys. Res.*, vol. 67, pp. 1183–1185; March, 1962.) Several possible nighttime detachment processes are listed, and are summarized by the equation $O_2^- + O + O \rightarrow O_2 + O_2 + e$. The effect of these processes in producing observed electron concentrations and in explaining an observed polar-cap event is discussed.

551.510.535 2308
On the Nature of Equatorial Slant Sporadic-E—R. Cohen, K. L. Bowles, and W. Calvert. (*J. Geophys. Res.*, vol. 67, pp. 965–972; March, 1962.) Equatorial sporadic-E traces are simulated on a computer, using a thin stratum of magnetic-field-aligned irregularities; it appears that the equatorial electrojet producing these irregularities flows within the E layer.

551.510.535 2309
Photoionization Rates in the E and F Regions—K. Watanabe and H. E. Hinteregger. (*J. Geophys. Res.*, vol. 67, pp. 999–1006; March 1962.) Experimental data on ultraviolet emission from the sun and absorption in atmospheric gases are combined to give ionospheric photoionization rates as functions of height. For overhead sun, the E-region photoionization peak at 105 km is mainly produced by radiation of wavelengths 911–1027 Å; wavelengths 170–796 Å are responsible for the F1 production peak at 140–170 km.

551.510.535 2310
Pulsed Radio Soundings of the Topside of the Ionosphere in the Presence of Spread-F—R. W. Knecht and S. Russell. (*J. Geophys. Res.*, vol. 67, pp. 1178–1182; March, 1962.) Moderate spread F was present on the bottom-side ionogram during the top-side sounding at 4 Mc. In addition to the well-defined "normal" echoes the topside sounding record showed diffuse echoes which, at apogee, were returned from about 7 per cent greater range. Ducting along magnetic-field-aligned irregularities is a possible explanation.

551.510.535 2311
Observation of Large-Scale Travelling Ionospheric Disturbances by Spaced-Path High-Frequency Instantaneous-Frequency Measurements—K. L. Chan and O. G. Villard, Jr. (*J. Geophys. Res.*, vol. 67, pp. 973–988; March, 1962.) Similar frequency fluctuations on the transmission paths from Puerto Rico and Washington, D. C., to Stanford and Seattle have identified nine traveling disturbances during 1600 hours of observation. The velocities range from 1450 to approximately 2750 km/h,

the spatial lengths from 1300 to 2000 km, and the direction of travel is from north to south.

551.510.535 2312

The Form of Disturbances in the Lower Ionosphere and their Interpretation, as shown in the Example of the November Event 1960—E. A. Lauter, G. Entzian, and R. Knuth. (*Z. Met.*, vol. 14, pp. 275–286; November/December, 1960.) The changes in the propagation characteristics of radio waves in the band 128–245 kc are described. During the s.i.d. the reflection height decreased from 80 to 65 km and there was a temporary reduction in signal strength. The influx of cosmic rays at night also caused a large decrease in strength. For about 15 days after the disturbance, low signal strength occurred after sunset and before sunrise; this is attributed to leakage from the outer Van Allen belt of particles which affect the D region even at medium latitudes.

551.510.535:523.75 2313

F-Region Changes associated with the Solar Flare of 23 February 1956—B. N. Bhargava and R. V. Subrahmanyan. (*J. Atmos. Terr. Phys.*, vol. 24, pp. 321–324; April, 1962.) The real height of the F2 layer for various plasma frequencies increased by up to 50 km, and the plasma frequency at various fixed heights decreased, for several hours after the flare. Heights below 325 km were more seriously affected.

551.510.535:550.385.4 2314

The Ionospheric F Region during a Storm—G. A. M. King. (*Planet-Space Sci.*, vol. 9, pp. 95–100; March, 1962.) The recovery phase of a storm is explained by invoking turbulence in and below the lower F region.

551.510.535:551.507.362.1 2315

Rocket Observation of Ion Density in the Ionosphere—Y. Aono, K. Hirao, and S. Miyazaki. (*J. Radio Res. Lab., Japan*, vol. 8, pp. 441–451; November, 1961.) Results of the first Japanese rocket observations of the ionosphere in September, 1960, are given. The rockets reached an altitude of 180 km.

551.510.535:551.507.362.1 2316

Positive Ion Density, Electron Density and Electron Temperature in the Ionosphere by the Kappa-8-5 and -6 Rockets—Y. Aono, K. Hirao, and S. Miyazaki. (*J. Radio Res. Lab., Japan*, vol. 8, pp. 453–465; November, 1961.) A description is given of the resonance probe, Langmuir probe and ionospheric sounding experiments carried out in March and April, 1961.

551.510.535:551.507.362.2 2317

Ionospheric Electron Content Calculated by a Hybrid Faraday-Doppler Technique—F. de Mendoça and O. K. Garriott. (*J. Atmos. Terr. Phys.*, vol. 24, pp. 317–321; April, 1962.) A method of using combined Faraday and differential Doppler-shift observations to deduce true electron content and horizontal grdaients is presented, together with results for 1960 η_1.

551.510.535:621.391.812.63 2318

The Analysis of Ionograms—A. H. de Voogt. (*Nachrtech. Z.*, vol. 15, pp. 1–8; January, 1962.) Models are proposed in which the ionosphere is divided into height zones with alternately increasing and decreasing gradients of electron density. The use of such models for the prediction of propagation conditions on the basis of ionograms is discussed. See also 2148 of 1960.

551.510.535:621.391.812.63 2319

Investigation of Ionospheric Absorption at Delhi—M. K. Rao, S. C. Mazumdar, and S. N. Mitra. (*J. Atmos. Terr. Phys.*, vol. 24, pp. 245–256; April, 1962.) Observations made between June, 1954 and January, 1960 are analyzed. The variations of absorption with frequency, time of day, and season are examined.

551.510.535:621.391.812.8 2320

Ionospheric Storm Forecasts—C. M. Minnis. (*Electronic Tech.*, vol. 39, pp. 172–174; May, 1962.) Comparison of two C.C.I.R. formulas for the assessment of the usefulness of forecasts. The numerical values given by the Japanese formulas [116 of 1959 (Sinno)] are too large and lead in practice to an erroneous assessment. The algebraic sign of the index values obtained by the U.K. formula (2110 of 1953) shows whether action based on the forecasts would have increased or decreased the effectiveness of a communication service.

551.593.5 2321

The Red Line of the Equatorial Night Sky—A. Delsemme and D. Delsemme. (*Ann. Géophys.*, vol. 16, pp. 507–524; October-December, 1960.) The oxygen red line of the airglow at Lwiro (2°S) shows a seasonal annual variation with maximum near March and a minimum near September. Red line intensities at the equator are entirely accounted for by the behavior of the F2 layer.

551.593.5 2322

The Summer Intensity Variations of [OI] 6300 Å in the Tropics—D. Barbier, F. E. Roach, and W. R. Steiger. (*J. Res. NBS*, vol. 66D, pp. 145–152; March/April, 1962.) A relation between airglow and ionospheric F-region parameters is given.

551.594.5:621.396.96 2323

Distribution of Radar Auroras over Alaska—R. S. Leonard. (*J. Geophys. Res.*, vol. 67, pp. 939–952; March, 1962.) Ionospheric disturbances have been observed between 60° and 80° geomagnetic latitude using five auroral radars. The distribution of these disturbances as a function of time and location is presented.

551.594.6 2324

Diurnal Variation of Sweeper Activity—N. C. Gerson and W. H. Gossard. (*J. Geophys. Res.*, vol. 67, pp. 1007–1011; March, 1962.) A description is given of observations made during a 24-h period using a frequency range 23.5–24.0 Mc. The frequency distributions of several different types of sweepers are determined.

551.594.6 2325

The Effect of Positive Ion Collisions on Whistler Propagation—D. W. Swift. (*J. Geophys. Res.*, vol. 67, pp. 1175–1177; March, 1962.) The attenuation caused by positive ion collisions is greater at the lower end of the whistler spectrum, and it peaks in the E and F regions. Below 90 km electron collisions are more effective in producing attenuation.

551.594.6 2326

Investigation of the Geomagnetic Conjugate Point of Poitiers: Nocturnal Variation in the Dispersion of Whistlers—R. Rivault and Y. Corcuff. (*Ann. Géophys.*, vol. 16, pp. 550–554; October-December, 1960.) Distances of lightning flashes which cause atmospherics followed by short whistlers at Poitiers, show good agreement with the distances of the geomagnetic conjugate points. Sunrise and sunset at both points control the noctural variation of dispersion.

551.594.9:523.16 2327

Generation of Radio Noise in the Vicinity of the Earth—P. A. Sturrock. (*J. Res. NBS*, vol. 66D, pp. 153–157; March/April, 1962.) A tentative classification is made of possible sources near the earth by examining separately the available sources of power and known mechanisms for conversion of this power.

LOCATION AND AIDS TO NAVIGATION

621.396.96+621.391.6 2328

Power-Aperture and the Laser—M. D. Rubin. (Proc. IRE, vol. 50, pt. 1, pp. 471–472; April, 1962.) Laser and microwave radar require similar power × aperture products for comparable serveillance. The laser can have advantages at short ranges.

621.396.96 2329

Upwind-Downward Ratio of Radar Return Calculated from Facet Size Statistics of a Wind-Disturbed Water Surface—A. H. Schooley. (Proc. IRE, vol. 50, pt. 1, pp. 456–461; April, 1962.) Results from a wind tunnel experiment with water as a lower surface are used in calculating radar data.

621.396.96 2330

Pulsed Radar Measurement of Back-Scattering from Spheres—S. B. Adler. (*RCA Rev.*, vol. 23, pp. 80–95; March, 1962.)

621.396.96 2331

Coincidence Techniques for Radar Receivers—V. G. Hansen, K. Endresen, and R. Hedemark. (Proc. IRE, vol. 50, pt. 1, p. 480; April, 1962.) Comment on 153 of January and authors' reply.

621.396.96:621.376.33 2332

The Output Spectral Density of a Detector Operating on a F.M. C.W. Radar Signal in the Presence of Band-Limited White Noise—J. Lait and A. J. Hymans. (Proc. IRE, vol. 108, pt. C, pp. 197–207; March, 1961.) The interactions between reference signal, echo and noise are examined in both linear and quadratic detectors. The effect of the pre-detector bandwidth is considered.

621.396.969.1 2333

The Indeterminacies of Measurements using Pulses of Coherent Electromagnetic Energy—R. Madden. (Proc. IRE, vol. 108, pt. C, pp. 247–251; March, 1961.) The accuracy of simultaneous measurements of position and velocity performed by radar is inherently limited, the limitation being a function of the frequency used.

621.396.969.3:621.396.677.832 2334

Radar Corner Reflectors for Linear or Circular Polarization—G. Latmiral and A. Sposito. (*J. Res. NBS*, vol. 66D, pp. 23–29; January/February, 1962.) Polarization conversion effects can be obtained when a grid of parallel wires is put in front of a plane or corner reflector. Trihedral corner reflectors can be made "visible" by radar even with circular polarization.

629.1.05:550.38:551.507.362.2 2335

Use of the Earth's Magnetic Field for Navigation and Attitude Control—N. Avrech. (Proc. IRE, vol. 50, p. 485; April, 1962.) A note of a preliminary study relating to orbiting earth satellites.

MATERIALS AND SUBSIDIARY TECHNIQUES

535.215:061.3 2336

Proceedings of the 1961 International Conference on Photoconductivity—(*J. Phys. Chem. Solids*, vol. 22, pp. 5–407; December, 1961.) The text of 53 papers presented at the conference held in New York, August 21–24, 1961.

535.37:546.47'221 2337

The Growth of ZnS Single Crystals from

the Vapour Phase—H. Hartmann and H. Treptow. (*Mber. dtsch. Akad. Wiss. Berlin*, vol. 2, pp. 670–673; 1960.)

535.37:546.47'48'221 2338
Investigation of the Superlinear Luminescence Yield of ZnCdS Phosphors as a Function of Excitation Intensity and Temperature—H. Eder. (*Z. Phys.*, vol. 166, pp. 328–340; January, 1962.) Part 1 of report on experimental investigations over a range of excitation intensities of eight orders of magnitude and a temperature range from −120° to +23°C.

535.37:546.47'48'221 2339
Determination of the Concentration of Trapping Centres, the Binding Energies and the Recombination Constants from the Luminescence Yield of ZnCdS Phosphors—H. Eder. (*Z. Phys.*, vol. 166, pp. 386–392; February, 1962.) Part 2 of report on experimental investigations. Part 1: 2338 above.

535.37:546.47'86 2340
Investigation of the Luminescence Decay of Tungstate Phosphors after Excitation by Ultraviolet Light and Electrons—V. Schäfer. (*Z. Phys.*, vol. 166, pp. 429–438; February, 1962.) Investigations in the temperature range −180°C to +200°C were carried out on specimens of $CaWO_4$, $CdWO_4$, $MgWO_4$ and $ZnWO_4$, with excitation provided by short pulses of light and by electron beams.

535.376:546.47'221 2341
Electroluminescence in Zinc Sulphide Single Crystals—F. Matossi and G. Schmid. (*Z. Phys.*, vol. 166, pp. 455–459; February, 1962.) Experimental results obtained are interpreted by assuming hole injection to be the cause of the electroluminescence.

537.226/228.1 2342
Piezoelectric and Dielectric Properties of Lead Titanate-Zirconate Ceramics at Low Temperatures—R. Gerson. (*J. Appl. Phys.*, vol. 33, pp. 830–832; March, 1962.)

537.227:546.431'824-31 2343
Thickness Dependence of Polarization Reversal in $BaTiO_3$ Single Crystals—H. Shibata and H. Toyoda. (*J. Phys. Soc. Japan*, vol. 17, pp. 404–405; February, 1962.) The coercive voltage and saturation polarization are measured for different thicknesses.

537.228.1 2344
Electrodeless Excitation of Piezoelectric Crystals—J. J. Gruetzmacher, S. Hess, and P. Eisenberg. (*Hochfrequenz. und Elektroak.*, vol. 71, pp. 28–29; February, 1962.) The excitation is achieved by placing the crystal in the RF field radiated by a transmitter.

537.228.2:547.476.3 2345
The Influence of Mechanical Stresses on the Dielectric Properties of Paraelectric Rochelle Salt—G. Schmidt and K. H. Neumann. (*Z. Phys.*, vol. 166, pp. 207–215; January, 1962.) Report on experimental investigations confirming the dependence of the electrostriction constant on mechanical stress [see 3815 of 1961 (Schmidt)].

537.311.33 2346
Analysis of Semiconductor *p-n* Junctions and Junction Devices by a Flux Method—J. P. McKelvey. (*J. Appl. Phys.*, vol. 33, pp. 985–991; March, 1962.) A method of applying a flux analysis [3819 of 1961 (McKelvey, *et al.*)] to *p-n* junctions is given. A comparison is made of the I/V characteristics derived by this method and those obtained by simple diffusion analysis.

537.311.33 2347
Diffusion and Drift of Minority Carriers in Semiconductors for Comparable Capture and Scattering Mean Free Paths—W. Shockley. (*Phys. Rev.*, vol. 125, pp. 1570–1576; March, 1962.) The basic equations of McKelvey, *et al.* (3819 of 1961) are equivalent to the continuity equation with modified diffusion constants. The treatment is extended to three dimensions with small electric fields.

537.311.33:535.34-1 2348
Optical Spectrum of the Semiconductor Surface States from Frustrated Total Internal Reflections—N. J. Harrick. (*Phys. Rev.*, vol. 125, pp. 1165–1170; February, 1962.) The optical spectrum is obtained by observing directly the absorption of infrared radiation and removing the free-carrier contribution in the space-charge region.

537.311.33:538.569.4 2349
Quadrupolar Nuclear Relaxation in the III–V Compounds—R. L. Mieher. (*Phys. Rev.*, vol. 125, pp. 1537–1551; March, 1962.) Results of measurements on semiconductor compounds and on Ge are compared with theory.

537.311.33:538.632 2350
Electrode Geometries for which the Transverse Magnetoresistance is Equivalent to that of a Corbino Disk—M. Green. (*Solid-State Electronics*, vol. 3, pp. 314–316; November/December, 1962.) Theoretical treatment of electrode configurations for a semiconductor wafer which provide maximum magnetoresistance.

537.311.33:546.23:539.23 2351
Drift Mobilities of Electrons and Holes and Space-Charge-Limited Currents in Amorphous Selenium Films—J. L. Hartke. (*Phys. Rev.*, vol. 125, pp. 1177–1192; February, 1962.) Application of band theory enables the energy levels and densities of electron and hole traps in the gap to be determined. Their origin and energy distribution are discussed. The effects of adding As are investigated.

537.311.33:546.23:539.23 2352
The Faraday Effect in Amorphous Selenium Films—H. Gobrecht, A. Tausend, and I. Bach. (*Z. Phys.*, vol. 166, pp. 76–80; December, 1961.) Faraday rotation was measured in the spectral range 690–930 mμ for values of magnetic induction up to 20 kG.

537.311.33:546.28 2353
Resistivity of Bulk Silicon and of Diffused Layers in Silicon—J. C. Irvin. (*Bell Sys. Tech. J.*, vol. 41, pp. 387–410; March, 1962.) "Measurements of resistivity and impurity concentration in heavily doped silicon are reported. These and previously published data are incorporated in a graph showing the resistivity (at $T=300°$K) of *n*- and *p*-type silicon as a function of donor or acceptor concentration. The relationship between surface concentration and average conductivity of diffused layers in silicon has been calculated for Gaussian and complementary error function distributions. The results are shown graphically. Similar calculations for subsurface layers, such as a transistor base region, are also given."

537.311.33:[546.28+546.289]:548.5 2354
Nomograph Technique for Doping Determination in Germanium and Silicon Crystal Growing—H. Hemmat and A. L. MacDonald. (*Solid-State Electronics*, vol. 3, pp. 309–314; November/December, 1961.)

537.311.33:546.289 2355
Annealing of Quenched-In Defects in Ge Crystal (Dislocation Density 10^4–10^5 Etch-Pits cm^{-2})—A. Hiraki and T. Suits. (*J. Phys. Soc. Japan*, vol. 17, pp. 408–409.) The time dependence and temperature depndence of the annealing process are discussed.

537.311.33:546.289:537.312.9 2356
Effect of Uniaxial Compression on Impurity Conduction in *n*-Type Germanium—H. Fritzsche. (*Phys. Rev.*, vol. 125, pp. 1552–1560; March, 1962.) Results are given of resistivity measurements on Sb-, As-, or P-doped Ge at temperatures between 1.3° K and 300° K under stresses ranging from 2×10^7 to 2×10^9 dynes/cm².

537.311.33:546.289:537.312.9 2357
Effect of Stress on the Donor Wave Functions in Germanium—H. Fritzsche. (*Phys. Rev.*, vol. 125, pp. 1560–1567; March, 1962.) A theoretical discussion leading to a qualitative explanation of the results reported in a previous paper (2356 above).

537.311.33:546.289:539.23 2358
Epitaxy of Germanium Films on Germanium by Vacuum Evaporation—J. E. Davey. (*J. Appl. Phys.*, vol. 33, pp. 1015–1016; March, 1962.) By regeneration of the receiver surface in vacuum prior to the deposition, good crystal propagation was achieved at 300°C.

537.311.33:546.289:548.5 2359
Growing Heavily Compensated Germanium Cyrstals of Known Impurity Concentrations—L. M. Lambert. (*Solid-State Electronics*, vol. 3, pp. 316–317; November/December, 1961.) Note on an application of the modified floating-crucible technique.

537.311.33:546.289:669.046.5 2360
The Selective Melting of Germanium by Thermal Radiation—T. C. Taylor and C. J. Bardsley. (*Solid-State Electronics*, vol. 3, pp. 226–232; November/December, 1962.) To provide the three-dimensional thermal gradients required for selective melting, carbon films locally deposited on the Ge surface are used in conjunction with a radiant-heat source designed to produce a one-dimensional thermal gradient.

537.311.33:546.36'59 2361
Photoemission and Band Structure of the Semiconducting Compound CsAu—W. E. Spicer. (*Phys. Rev.*, vol. 125, pp. 1297–1299; February, 1962.)

537.311.33:546'221:537.323 2362
Thermoelectric Properties of some Cerium Sulphide Semiconductors from 4°K to 1300° K—F. M. Ryan, I. N. Greenberg, F. L. Carter, and R. C. Miller. (*J. Appl. Phys.*, vol. 33, pp. 864–868; March, 1962.)

537.311.33:546.811-17 2363
Reflectivity of Grey Tin Single Crystals in the Fundamental Absorption Region—M. Cardona and D. L. Greenaway. (*Phys. Rev.*, vol. 125, pp. 1291–1296; February, 1962.) The band structure of gray tin determined from reflectivity measurements is discussed in relation to similar data for other semiconductors with diamond and zinc blend structure.

537.311.33:548.5 2364
Growth of Semiconducting Compounds from Nonstoichiometric Melts—D. T. J. Hurle, O. Jones, and J. B. Mullin. (*Solid-State Electronics*, vol. 3, pp. 317–320; November/December, 1962.) Growth characteristics are considered from the viewpoint of constitutional supercooling.

537.312.62 2365
Determination of the Energy Gap of Superconducting Tantalum with the aid of the Tun-

nel Effect—L. Dietrich. (*Z. Naturforsch.*, vol. 17a, pp. 94–96; January, 1962.)

537.312.62:538.24 2366
Magnetization of Hard Superconductors—C. P. Bean (*Phys. Rev. Lett.*, vol. 8, pp. 250–253; March, 1962.)

537.312.62:538.569 2367
Quantum Interaction of Microwave Radiation with Tunnelling between Superconductors—A. H. Dayem and R. J. Martin. (*Phys. Rev. Lett.*, vol. 8, pp. 246–248; March, 1962.) I/V characteristics obtained experimentally with samples of Al–Al_2O_3/Pb, In, or Sn in the presence and absence of a microwave field at frequency ν are discussed. Considerable interaction occurs for $h\nu<2\epsilon_1$. Absorption by a tunneling electron of more than one photon has also been observed.

537.312.62:539.23 2368
Resistance Transitions of Thin Superconducting Films in Magnetic Fields—E. H. Rhoderick. (*Proc. Roy. Soc.* (*London*), *A*, vol. 267, pp. 231–243; May, 1962.) Experiments on evaporated Sn films of thickness 600–10,000 Å reveal characteristics significantly different from those reported for rolled foils.

537.312.62:539.23 2369
Trapped Flux and Critical Currents in Super-conducting Thin-Film Rings—J. E. Mercereau and T. K. Hunt. (*Phys. Rev. Lett.*, vol. 8, pp. 243–246; March, 1962.) Measurements made by a torque method are reported. Current densities $>10^6$A/cm² can readily be achieved in Sn films 700 Å thick within a degree of the transition temperature.

537.323 2370
Thermoelectric Properties of Bismuth-Antimony Alloys—G. E. Smith and R. Wolfe. (*J. Appl. Phys.*, vol. 33, pp. 841–846; March, 1962.)

538:061.3 2371
Proceedings of the Seventh Conference on Magnetism and Magnetic Materials—(*J. Appl. Phys.*, vol. 33, Supplement, pp. 1019–1382; March, 1962.) The full text is given of 145 papers, with abstracts of others, presented at the conference in Phoenix, Arizona, November 13–16, 1961.

538.221 2372
Linear Shift of the Fermi Level in Iron with Applied Magnetic Fields—R. H. Walmsley. (*Phys. Rev. Lett.*, vol. 8, pp. 242–243; March, 1962.)

538.221 2373
Induced Magnetic Anistropy Created by Magnetic and Stress Annealing of Iron-Aluminum Alloys—H. J. Birkenbeil and R. W. Cahn. (*Proc. Phys. Soc.* (*London*), *A*, vol. 79, pp. 831–847; April, 1962.)

538.221 2374
Magnetic Measurements in the System Bismuth-Cobalt—R. Damm, E. Scheil, and E. Wachtel. (*Z. Metallkde*, vol. 53, pp. 196–203; March, 1962.)

538.221:537.312 2375
The *K*-State of some Ferromagnetic Alloys—P. Muth. (*Z. Metallkde*, vol. 53, pp. 203–206; March, 1962.) Report of investigations on mumetal, Mo-permalloy and other alloys, and interpretation of the results with reference to the explanations advanced by Thomas (2751 of 1951).

538.211:538.652 2376
The Volume Magnetostriction of Gadolinium Metal near the Curie Temperature—J. T. Davies. (*Proc. Phys. Soc.* (*London*), *A*, vol. 79, pp. 821–830; April, 1962.)

538.221:539.23 2377
The Variation of the Direction of Magnetization in Domain Walls of Ferromagnetic Films—E. Fuchs. (*Naturwiss.*, vol. 48, p. 450; June, 1961.) Changes in magnetization direction at domain walls can be determined from electron-microscope images, as shown by an example. See 2714 of 1961.

538.221:539.23 2378
The Magnetic Excitation Inside a Cylindrical Thin-Film Ferromagnet—T. H. O'Dell. (*Proc. IEE*, vol. 108, pt. C, pp. 79–82; March, 1961.) An expression for the magnetic excitation inside a cylindrical thin-film ferromagnet is derived, and a table of computed values is given. The results are considered to be relevant to work on thin ferromagnetic films for digital-storage applications.

538.221:621.318.134 2379
Dependence on Heat-Treatment of the Ferromagnetic Resonance Width in Ni Ferrite—H. Sekizawa and K. Sekizawa. (*J. Phys. Soc. Japan*, vol. 17, pp. 359–366; February, 1962.) Various heat treatments, on the same specimen, produce appreciable changes in width, anisotropy constants and g factor.

538.221:621.318.134:538.569.4 2380
Observation of Space Average Harmonic Component of Magnetization due to Spin Waves in Ferrites—P. M. Richards and H. J. Shaw. (*Phys. Rev. Lett.*, vol. 8, pp. 202–204; March, 1962.) It is shown theoretically and experimentally that spin waves can excite fields in microwave circuits, the excitation being at a harmonic of the fundamental resonance frequency.

538.221:621.318.134:621.318.57 2381
The Reversal of Magnetization in Ring Cores of Square-Loop Ferrite—W. Hilberg. (*Frequenz*, vol. 16, pp. 24–31; January, 1962.) Analysis of magnetization reversal processes and their application to switching devices. See also 4023 of 1961.

538.222:538.569.4 2382
Anomalies in Adiabatic Rapid Passage in Ruby—J. S. Thorp. (*J. Electronics and Control*, vol. 11, pp. 439–444; December, 1961.) The presence of impurities in the samples is suggested to be the cause of anomalies in the absorption spectrum of ruby.

538.222:538.569.4 2383
'Forbidden' Transitions in the Paramagnetic Resonance of Mn^{++} in Al_2O_3—V. J. Folen. (*Phys. Rev.*, vol. 125, pp. 1581–1583; March, 1962.)

548.5:671.16 2384
The Synthesis and Uses of Artificial Gemstones—E. A. D. White. (*Endeavour*, vol. 21, pp. 73–84; April, 1962.) Methods of synthesis resulting in improvements of crystalline perfection are reviewed, and applications to low-noise amplifiers, masers and lasers are mentioned.

MATHEMATICS

512+513.83]:621.372.6 2385
The Algebra and Topology of Electrical Networks—Bryant. (*See* 2206.)

512.23:621.372.5 2386
Connection Matrices and Network Algebra—Boisvert. (*See* 2196.)

519:621.372.6 2387
A New Approach to Kron's Method of Analysing Large Systems—Onodera. (See 2207.)

MEASUREMENTS AND TEST GEAR

621.317.337:621.372.412 2388
New Method for Determining the Q-Factor of a Quartz Resonator—E. D. Novgorodov. (*Izmer. Tekh.*, pp. 50–51; November, 1961.) The method is based on measuring the phase shift between the current and voltage when the frequency of the resonator is varied.

621.317.341.089.6 2389
A Method for the Self-Calibration of Attenuation-Measuring Systems—R. L. Peck. (*J. Res. NBS*, vol. 66C, pp. 13–18; January–March, 1962.) The theory and experimental procedures are given for four circuit configurations. Calibrations may be obtained by simple graphical means or by an analytical solution. Measurements on a standard piston attenuator at 30 Mc showed a standard deviation of 0.003 db in.

621.317.342 2390
Technique for the Dynamic Measurement of Differential Phase Shift at Microwave Frequencies—B. P. Israelsen and R. W. Haegele. (Proc. IRE, vol. 50, pt. 1, pp. 474–475; April, 1962.) A null method for ac and dc measurements is described. Two parallel microwave paths are fed from a CW instead of a conventional square-wave source and an AF sweep voltage is applied to one path and to the horizontal input of an oscilloscope.

621.317.342:621.376.33 2391
A Microwave Phase Discriminator—J. R. Chamberlain, H. Daams, and S. N. Kalra. (Proc. IRE, vol. 50, pt. 1, p. 481; April, 1962.) A microwave analog of the Foster-Seely type of ratio detector is described which can be used to measure changes in the relative phase between two fairly low-power signals.

621.317.44:537.312.8 2392
Microsize Magnetic Field Probes with Axial Symmetry—C. A. Shiffman. (*Rev. Sci. Instr.*, vol. 33, pp. 206–207; February, 1962.) Small magnetoresistance probes of Bi for use at extremely low temperatures are described.

621.317.44:538.632 2393
Microprobe for Measuring Magnetic Fields—D. D. Roshon, Jr. (*Rev. Sci. Inst.*, vol. 33, pp. 201–206; Febrary, 1962.) A miniature Hall-effect probe has been produced by vacuum evaporation through a mask. The sensitive area is about 10×10 μ.

621.317.443 2394
Strain-Gauge Balance for Ferromagnetic and Paramagnetic Measurements—N. Lundquist and H. P. Myers. (*J. Sci. Instr.*, vol. 39, pp. 154–155; April, 1962.) Two instruments are described. Designs are based on Sucksmith's ring balance with the ring and optical lever system replaced by a strain-gauge bridge. Relative accuracies for the ferromagnetic and paramagnetic balances are within 0.3 per cent and 0.5 per cent, respectively.

621.317.6:621.317.755 2395
Automatic Measurement of Complex Ratios in the Frequency Range 5–200 Mc/s with Visual Display—H. Eisenmann and K. Lange. (*Nachrtech. Z.*, vol. 15, pp. 17–24; January, 1962.) Description of equipment and its operation, with illustrations of typical locus diagrams obtained.

621.317.72:621.319.4 2396
Using a Vibrating Capacitor as an Electrometer Input—V. J. Caldecourt. (*Electronics*, vol. 35, pp. 48–50; April, 1962.) Design details are given of a vibrating-capacitor unit which converts a dc input signal to ac with power gain;

noncumulative drift rates of ±0.2 mv day can be achieved. See 3510 of 1961 (Riegler).

621.317.727.1.089.6 2397

Voltage Ratio Measurements with a Transformer Capacitance Bridge—T. L. Zapf. (*J. Res. NBS*, vol. 66C, pp. 25–32; March, 1962.) Description of equipment and methods developed at the National Bureau of Standards for calibration of voltage dividers at AF.

621.317.75:537.227 2398

New Type of Loop Tracer for Ferroelectrics—H. Roetschi (*J. Sci. Instr.*, vol. 39, pp. 152–153; April, 1962.) The hysteresis-loop tracer described is simpler in construction than existing types [see *e.g.*, 2249 of 1957 (Diamant, *et al.*)] and is compensated for losses and additional capacitance of the sample holder.

621.317.755 2399

Theory of the Stroboscopic Oscilloscope—C. W. Gerst and H. H. Grimm. (Proc. IRE, vol. 50, pt. 1, pp. 475–476; April, 1962.) Analysis of two methods whereby repetitive waveforms at HF or microwave frequencies may be displayed in LF form.

OTHER APPLICATIONS OF RADIO AND ELECTRONICS

531.787:621.382.23 2400

Tunnel-Diode Hydrostatic Pressure Transducer—M. E. Sikorski and P. Andreatch. (*Rev. Sci. Instr.*, vol. 33, pp. 155–160; February, 1962.) The transducer consists essentially of a Si tunnel diode shunted by a resistor which satisfies the stability conditions for operation in the amplifier mode. Pressure sensitivities as high as 2 mv v per lb in² are observed.

535.376.07 2401

Construction and Performance of an ELF Display System—E. A. Sack, P. N. Wolfe, and J. A. Asars. (Proc. IRE, vol. 50, pt. 1, pp. 432–441; April, 1962.) An experimental system has been constructed using an electroluminescent panel with 256 cells in² [see 225 of 1959 (Sack)]. The pattern is controlled by a ferroelectric microarray.

621.38:57 2402

Bionics: Parts 1, 2, 3 and 4—N. Lindgren. (*Electronics*, vol. 35, pp. 37–42, 40–43, 41–45 & 60–63; March, 1962.) Present developments of equipment based on the principles of living systems are considered. Brain models, neural nets, electronic analog of animal sensors, and learning networks which grow in liquid solution are described. 80 references.

601.384.6 2403

Beam Loading of a Radio-Frequency Cavity—V. K. Neil. (*Rev. Sci. Instr.*, vol. 33, pp. 169–171; February, 1962.) Previous analysis [*Rev. Sci. Instr.*, vol. 32, pp. 256–266; March, 1961 (Neil & Sessler)] is extended to the case in which the characteristic frequency of the cavity does not coincide with a harmonic of the beam circulation frequency. By proper tuning it is possible to minimize the power consumption by bringing the cavity wall currents into phase with the external generator.

621.385.833 2404

Progress in the Production of Microscopic Writing—K. J. Hanszen. (*Naturwiss.*, vol. 49, pp. 56–57; February, 1962.) Description of an electronoptic method for producing fine traces for use in electron-microscope applications.

621.385.833 2405

A New Calculation of Electron Scattering Cross-Sections and a Theoretical Discussion of Image Contrast in the Electron Microscope—R. E. Burge and G. H. Smith. (*Proc. Phys. Soc.* (*London*), *A*, vol. 79, pp. 673–690; April, 1962.)

621.385.833:537.533.73 2406

Fine-Beam Electron Diffraction by means of a Three-Stage Condenser and a Long-Focus Final Condenser Stage—W. D. Riecke. (*Optik, Stuttgart*, vol. 19, pp. 81–116; February, 1962.) A new method is described for producing electron diffraction patterns of small selected areas of transmission specimens in electron microscopes. The minimum area of the diffraction region is about 0.1 μ.

621.385.833:537.533.73 2407

Measurement of the Continuous Phase Shift of Electron Waves in Force-Field-Free Space by means of the Magnetic Vector Potential of an Air-Cored Coil—G. Möllenstedt and W. Bayh. (*Naturwiss.*, vol. 49, pp. 81–82; February, 1962.) Improvements to the electron biprism interferometer noted (*Naturwiss.*, vol. 48, p. 400, May, 1961) are discussed.

621.387.462:537.312.62 2408

Cryotron as Ionizing-Particle Detector—N. K. Sherman. (*Canad. J. Phys.*, vol. 40, pp. 372–376; March, 1962.) A method of using the cryotron as a detector of alpha particles or fission fragments is suggested.

621.9:537.533 2409

Contribution on the Problem of the Production of Electron Beams for Melting, Vaporizing, Welding and Boring by means of Electron Beams—E. B. Bas, G. Cremosnik, and H. Lerch. (*Schweiz. Arch. angew. wiss. Tech.*, vol. 28, pp. 112–121; March, 1962.)

The practical difficulties of achieving high beam current densities are discussed and two types of bombardment-heated cathode are described. Details are given of a 25-kv electron beam system for various applications.

PROPAGATION OF WAVES

621.391.81 2410

On the Diffraction of Spherical Radio Waves by a Finitely Conducting Spherical Earth—L. C. Walters and J. R. Johler. (*J. Res. NBS*, vol. 66D, pp. 101–106; January/February, 1962.) Some computation difficulties are avoided with the aid of modern analysis techniques applied to a large-scale electronic computer.

621.391.812 2411

Radio Propagation over a Sectionally Homogeneous Cylindrical Surface—J. R. Thompson. (*Proc. Roy. Soc.* (*London*), *A*, vol. 267, pp. 183–196; May, 1962.) "The two-dimensional problem is considered of the propagation of H-polarized radio waves over two homogeneous sections, having different electrical characteristics, of a circular cylindrical surface. Though the treatment is in the context of a cylindrical geometry, the results may be cast into a form which is equally applicable to propagation over a sphere."

621.391.812.3 2412

The Short-Term Statistics of a Fading Radio Wave—L. M. Delves and H. A. Whale. (*J. Atmos. Terr. Phys.*, vol. 24, pp. 225–236; April, 1962.) Joint distributions of bearing, elevation, and amplitude are given for the cases of reflection a) from a completely rough ionosphere, b) partly specular, and c) with components grouped about two main directions.

621.391.812.6 2413

Guided Propagation along a Small Atmospheric or (more particularly) Exospheric Layer—J. Voge (*Ann. Télécommun.*, vol. 16, pp. 288–295, November/December, 1961; vol. 17, pp. 34–43; January February, 1962.) Classical theory applied to small stratifications can take account of layer curvature and transverse variations of refractive index. The minimum amplitude of these variations necessary to guide a wave is determined. See also 1006 of 1960 (du Castel, *et al.*). The case of propagation of short waves by the exosphere is also considered assuming that the frequency is very much lower than the gyro-frequency, and a general treatment is given for propagation of very long waves in a layered exosphere.

621.391.812.6.029.45 2414

Propagation of the Low-Frequency Radio Signal—J. R. Johler. (Proc. IRE, vol. 50, pt. 1, pp. 404–427; April, 1962.) A review of theoretical work.

621.391.812.61.029.65 2415

Millimetre-Wavelength Atmospheric Absorption—E. Wolf, R. Kopeck, and A. Mondloch. (Proc. IRE, vol. 50, pt. 1 p. 478; April, 1962.) Atmospheric absorption measurements of 69.9 Gc signals are reported which give a value of 1.35 db/km in fine weather.

621.391.812.62 2416

On the Theory of Wave Propagation through a Concentrically Stratified Troposphere with a Smooth Profile. Part 2—Expansion of the Rigorous Solution—H. Bremmer. (*J. Res. NBS*, vol. 66D, pp. 31–52; January February, 1962.) The height-gain differential equation is analyzed to obtain a series for the complete solution which starts with the extended W.K.B. approximation discussed in part 1 (263 of January).

621.391.812.62.029.6 2417

Radio Meteorology and its Significance in the Propagation of Metre, Decimetre and Centimetre Waves over Long Distances—B. R. Bean, L. Fehlhaber and J. Grosskopf. (*Nachrtech. Z.*, vol. 15, pp. 9–16; January, 1962.) The correlation of the surface value of refractive index with the refractive index gradient, as found, *e.g.*, in measurements made in West Germany, is discussed and its use for the prediction of scatter-link propagation conditions is outlined. See, *e.g.*, 1980 of 1961 (Bean and Cahoon).

621.391.812.624 2418

On the Scattering of Electromagnetic Waves by Nonisotropic Inhomogeneities in the Atmosphere—D. T. Gjessing. (*J. Geophys. Res.*, vol. 67, pp. 1017–1026; March, 1962.) Application of the expression for the scattering cross section explains the very weak dependence of received power on azimuth angle and the observation that maximum average power is received about 0.3° off the great-circle bearing.

621.391.812.624 2419

An Interpretation of U.S.W. Tropospheric Propagation based on Investigations of the Amplitude Fluctuations at 10-cm Wavelength—R. Schünemann and G. Pucher. (*Hochfrequenz. und Elektroak.*, vol. 71, pp. 34–40; February, 1962.) Report of the results obtained from a continuation of earlier field-strength measurements (3642 of 1960). Partial reflections rather than scattering are again shown to be the main contributory factor in propagation over the 76-km path.

621.391.812.63 2420

The Application of Ray Tracing Methods to Calculations of Skip Distances for Radio Communications—I. N. Capon. (*Proc. Phys. Soc.* (*London*), *A*, vol. 79, pp. 808–815; April, 1962.) Parabolic ionospheric profiles are used. The formula of Appleton and Beynon (D.S.I.R. Radio Research Special Report No. 18, 1948) is usually a good approximation to ordinary-ray propagation. Horizontal variations are important.

621.391.812.63 2421

Transmission Curves for the Curved Ionosphere—T. Kobayashi. (*J. Radio Res. Lab., Japan*, vol. 8, pp. 395–411; November, 1961.) The equivalence theorem for a curved ionosphere and curved earth is derived, and two types of transmission curves for M.U.F. calculations are developed.

621.391.812.63 2422

Ionospheric Absorption of H. F. Waves in High Latitudes—N. Wakai and S. Watanabe. (*J. Radio Res. Lab., Japan*, vol. 8, pp. 413–423; November, 1961.) Results of measurements made at Syowa Base, Antarctica, from February, 1959 to January, 1960 are analyzed. Seasonal variations of absorption on quiet days and its correlation with magnetic activity on disturbed days are examined.

621.391.812.63 2423

Reflection and Transmission of Radio Waves at a Continuously Stratified Plasma with Arbitrary Magnetic Induction—J. R. Johler and J. D. Harper, Jr. (*J. Res. NBS*, vol. 66D, pp. 81–99; January/February, 1962.) A theoretical model plasma, together with available data on the ionosphere, is used to evaluate reflections and transmissions during quiescent and disturbed conditions.

621.391.812.63:061.3 2424

Radio Wave Absorption in the Ionosphere—(*J. Atmos. Terr. Phys.*, vol. 23, pp. 1–368; December, 1961.) A collection of papers given at the Fifth Technical Meeting of the Ionospheric Research Committee of AGARD at the University of Athens, June 20–23, 1960.

621.391.812.63.029.4 2425

Fields of Electric Dipoles in Sea Water—the Earth Atmosphere-Ionosphere Problem—W. L. Anderson. (*J. Res. NBS*, vol. 66D, pp. 63–72; January/February, 1962.) The theory of ELF propagation from vertical and horizontal electric dipoles in a half-space separated by in infinite slab from another half-space is discussed, assuming the media to be homogeneous and isotropic. Some calculations have been carried out for fields in sea water at a distance of 1000 km and frequencies of 1, 10, 100 and 1000 cps.

621.391.812.63.029.4 2426

On the Propagation of V.L.F. and E.L.F. Radio Waves when the Ionosphere is not Sharply Bounded—J. R. Wait. (*J. Res. NBS*, vol. 66D, pp. 53–61; January/February, 1962.) An expression is derived for the reflection coefficient of a continuously stratified ionized medium. The result is fitted to previously developed theory for propagation between a spherical earth and a concentric ionosphere.

621.391.812.63.029.45 2427

Results of Measurement of Field Intensity of V.L.P. Radio Waves over Great Distances—A. Sakurazawa, J. Asai, and T. Ishii. (*J. Radio Res. Lab., Japan*, vol. 8, pp. 425–439; November, 1961.) Data for two propagation paths over an 18-month period are given and differences are studied. Attenuation is determined by integrating the attenuation coefficients along the propagation path on the basis of waveguide theory.

621.391.812.63.029.45 2428

An Approximate Full-Wave Solution for Low-Frequency Electromagnetic Waves in an Unbounded Magneto-ionic Medium—W. C. Hoffman. (*J. Res. NBS*, vol. 66D, pp. 107–111; January/February, 1962.) Maxwell's equations for an anisotropic inhomogeneous medium are transformed by means of the Stratton-Chu formula into a vector integral equation.

621.391.812.63.029.62 2429

Reflection of Electromagnetic Waves from Thin Ionized Gaseous Layers—F. H. Northover. (*J. Res. NBS*, vol. 66D, pp. 73–80; January/February, 1962.) The reflection properties of thin ionized layers are examined. Estimates of the rate of attenuation around a curved earth indicate that suitably intense E_s formations may account for freak long-distance transmission of VHF waves.

621.391.812.63.029.62 2430

V.H.F. Radio Propagation Data for the Cedar Rapids-Sterling, Anchoarge-Barrow, and Fargo-Churchill Test Paths, April 1951 through June 1958—G. R. Sugar and K. W. Sullivan. (*J. Res. NBS*, vol. 66D, pp. 113–119; January/February, 1962.) A representative set of data on system loss for D-region scatter and E_s propagation over test paths. See 243 of 1956 (Bailey, *et al.*).

621.391.812.63.029.62:523.5 2431

Evidence that Meteor Trials Produce a Field-Aligned Scatter Signal at V.H.F.—J. L. Heritage, W. J. Fay, and E. D. Bowen. (*J. Geophys. Res.*, vol. 67, pp. 953–964; March, 1962.) Experimental evidence suggests that, to produce scatter, the necessary electrons in excess of ambient are provided near 110 km by a number of sources, *e.g.*, meteors, auroras, and E_s.

621.391.812.63 2432

Radio Waves in the Ionosphere [Book Review]—K. G. Budden. Publisher: Cambridge University Press, 542 pp., 95s; 1961. (*Proc. Phys. Soc.* (*London*), *A*, vol. 79, pp. 872–874; April, 1962.) An authoritative treatise covering the full mathematical theory of the propagation of harmonic waves in a horizontally stratified and stationary ionosphere.

RECEPTION

621.376.23:621.395 2433

A Comparison of Error Rates for Coherent and Phase-Comparison Detection of Two- and Four-Phase Digital Signals in the Presence of Rayleigh Carrier Fading—C. R. Laughlin and R. E. Sullivan. (Proc. IRE, vol. 50, pt. 1, pp. 468–469; April, 1962.) Discussion of expressions for the probability of element error as a function of average signal/noise power ratio when phase detectors are used in the presence of Rayleigh-type fading.

621.376.5:621.372.54 2434

Optimum Combination of Pulse Shape and Filter to Produce a Signal Peak upon a Noise Background—H. S. Heaps. (*Proc. IEE*, vol. 108, pt. C, pp. 153–158; March, 1961.) The optimum system leads to a significantly high signal/noise ratio. It is advantageous to transmit a succession of short pulses of a determined form rather than a single smooth pulse.

621.391.81 2435

The Service Area of the Experimental U.H.F. Transmitter, Vienna—J. Kornfeld. (*Radioschau*, vol. 12, pp. 6–8; January, 1962.) Results are given of field-strength measurements on test transmissions from the band-IV television transmitter Kahlenberg, operating in channel 27.

621.391.812.3 2436

Fading Characteristics Observed on a High-Frequency Auroral Radio Path—J. W. Koch and H. E. Petrie. (*J. Res. NBS*, vol. 66D, pp. 159–166; March/April, 1962.) Observations of fading rate, amplitude fluctuations and fade durations have been made for a 4470 km propagation path through the auroral zone. Fading rates higher than 20 cps were observed. Usually signal amplitudes departed from a Rayleigh distribution.

631.391.812.3:551.507.362.2 2437

The Correlation Analysis of the Fading of Radio Signals Received from Satellites—P. W. James. (*J. Atmos. Terr. Phys.*, vol. 24, pp. 237–244; April, 1962.) It is shown theoretically that the mean height, the height range and the size of ionospheric irregularities can be deduced from the fading records of three spaced receivers.

621.391.812.63.029.62:523.5 2438

The Received-Amplitude Distribution Produced by Radio Sources of Random Occurrence and Phase—W. C. Bain. (Proc. IRE, vol. 108, pt. C, pp. 20–24; March, 1961.) The theoretical amplitude distribution of forward-scatter signals due to meteor ionization is derived and compared with experimental results. A method is outlined for estimating the relative proportions of meteor and turbulent-scattering signal components.

621.391.822 2439

The One-Sided Barrier Problem for Gaussian Noise—D. Slepian. (*Bell Sys. Tech. J.*, vol. 41, pp. 463–501; March, 1962.)

621.396.62.029.62 2440

Some Remarks on the Swiss High-Quality F.M. Broadcast Receiver—R. Netzband. (*Rundfunktech. Mitt.*, vol. 6, pp. 47–48; February, 1962.) The differences between the standard type of German VHF FM receiver and the Swiss receiver conforming to PTT specifications [see 2363 of 1961 (Strohschneider)] are discussed with reference to the results of measurements of selectivity and AM suppression.

STATIONS AND COMMUNICATION SYSTEMS

621.391:621.376.4 2441

Audio Communication with Orthogonal Time Functions—H. F. Harmuth. (Proc. IRE, vol. 108, pt. C, pp. 139–144; March, 1961.) The decomposition of an AF signal by correlation with a set of orthogonal functions enables the phase information to be eliminated. This reduces the bandwidth required for transmission by one-half and the signal power by 3 db.

621.396.216 2442

Single-Sideband Generation—W. Saraga. (*Electronic Tech.*, vol. 39, pp. 168–171; May, 1962.) A new principle of direct frequency translation by quadrature modulation is proposed in which, ideally, the unwanted sideband is never produced. A cheap "symmetric" multiplier, instead of the conventional two, would be required to make the system of practical interest.

621.396.43:551.507.362.2 2443

Geometry of Telecommunication Satellites—C. E. Martinato. (*Ricerca sci.*, vol. 2, pt. 1, pp. 23–33; January/February, 1962.) Optimum orbits and satellite spacings are calculated which would ensure continuity of operation between various telecommunication centers. Systems based on polar and equatorial orbits are compared.

621.396.43:551.507.362.2 2444

Satellite Project Telstar—(*Electronic Tech.*, vol. 39, pp. 198–199; May, 1962.) Brief description of the satellite circuitry including a schematic diagram of the communication circuit. See also *Brit. Commun. Electronics*, vol. 9, pp. 353–355; May, 1962.)

621.396.43:551.507.362.2 2445
G.P.O. Satellite Communications Station—(*Wireless World*, vol. 68, p. 270; June, 1962.) A description of the station at Goonhilly Downs, Cornwall. Equipment includes an 85-ft-diameter steerable paraboloid and transmitters and receivers in the range 1.7–6.4 Gc for projects Telstar and Relay.

621.396.43:551.507.362.2:621.38.004.6 2446
Reliability of Components for Communication Satellites—I. M. Ross. (*Bell Sys. Tech. J.*, vol. 41, pp. 635–662; March, 1962.) Methods for determining reliability and techniques for selection of high-quality components are discussed with reference to life tests on transistors and diodes, traveling-wave tubes, and solar cells.

621.396.65 2447
Future Standby Installation for Radio Links in the German Democratic Republic—H. Hänich. (*Nachrtech.*, vol. 11, pp. 539–541; December, 1961.) Outline of proposed installations and comparison with existing systems.

621.396.65:621.376.3 2448
The Vector Method: a Clear Method for the Treatment of Distortion in Small-Swing F.M. with Application to F.M. Radio Links—M. Müller. (*Arch. elekt. Übertragung*, vol. 16, pp. 25–35 and 93–99; January and February, 1962.) The use of the vector method for the determination of the magnitude and limits of various types of distortion is described.

621.396.712 2449
Automatic Relay Stations—A. L. Hands. (*Wireless World*, vol. 68, pp. 278–280; June, 1962.) A description of the unattended B.B.C. relay station at Llandrindod Wells, Radnorshire. The operational state of the equipment can be checked by telephone.

621.396.97:534.76 2450
Survey of the Different Methods of High-Frequency Stereophony Transmission and a Comparison of their Advantages and Disadvantages—S. Funk. (*Tech. Mitt. BFR, Berlin*, vol. 5, pp. 178–189; December, 1961.)

SUBSIDIARY APPARATUS

621.311.69 2451
New Power Sources and Energy Converters—D. Linden. (*Electronics*, vol. 35, pp. 35–42; April, 1962.) A review of progress since 1959 in the development of nuclear, solar and chemical power sources.

621.311.69:621.383.5 2452
Gettering Effects on the Forward Characteristics of Silicon Solar Cells—W. W. Hooper and H. J. Queisser. (PROC. IRE, vol. 50, pt. 1, p. 486; April, 1962.) A report on the effects of glassy oxide layers on the forward I/V characteristics of p-n junctions.

621.314.63:621.382.233 2453
Characteristics of the Silicon Controlled Cell—A. C. Stumpe. (*Elektrotech. Z., Edn. A*, vol. 83, pp. 81–87; February, 1962. The construction of a p-n-p-n type of Si controlled rectifier is described and the over-all I/V characteristics are derived from the characteristics of the individual junctions. The influence of control current and temperature is investigated.

621.314.63+621.382.2].004.1 2454
Maximum Ratings of Semiconductor Diodes and Rectifiers as a Function of Ambient Temperature—Costamagna and Borri. (See 2479.)

621.362:621.387 2455
Thermionic Generators—D. A. Fraser and G. G. Isaacs. (*Electronic Eng.*, vol. 34, pp. 307–311; May, 1962.) Experimental work shows that generators with outputs of 10 w/cm² of emitter surface and efficiencies of 10 per cent are feasible. Problems to be overcome in developing commercial units are discussed.

TELEVISION AND PHOTOTELEGRAPHY

621.397 2456
Summary of the Most Important Papers on Television published at Home and Abroad during 1960 and 1961—E. Schwartz. (*Rundfunktech. Mitt.*, vol. 6, pp. 26–38; February, 1962.) A review with 180 references arranged under subject headings.

621.397.1:621.395.625.3 2457
Recording and Reproduction of Still Pictures by means of the Foil Storage Device—H. G. Walter. (*Elektron. Rundschau*, vol. 16, pp. 97–100; March, 1962.) A disk-shaped magnetic foil is rotated at 3000 rpm and is supported and stabilized by a current of air at about 1 μ above the magnetic heads. Oscillograms of signal waveforms are reproduced showing the operation of the system which is suitable for the recording of single television pictures.

621.397.13 2458
Some New Developments in B.B.C. Television Technique—D. C. Birkinshaw (*Rundfunktech. Mitt.*, vol. 6, pp. 2–6; February, 1962.)

621.397.13:621.376.56 2459
Video Transmission by Delta Modulation using Tunnel Diodes—J. C. Balder and C. Kramer. (PROC. IRE, vol. 50, pt. 1, pp. 428–431; April 1962.) "A method is described which enables video signals to be transmitted by the pulse code modulation system known as delta-modulation. A tunnel-diode balanced pair (Goto pair) is used for converting the video signal into a binary signal. With a new and very simple circuit, operating at a bit rate of 100 Mc, a ratio of signal-to-quantizing noise of 42 db is obtained. A more conventional circuit, that combines tunnel-diodes with transistors, makes an even lower quantizing noise possible."

621.397.13:621.391.822 2460
The Relative Visibility of Random Noise over the Grey Scale—K. Hacking. (*J. Brit. IRE*, vol. 23, pp. 307–310; April, 1962.) Theoretical relative-visibility curves are deduced for three elementary types of noise source encountered in television systems, by the application of existing data relating to the perception of small differences in luminance.

621.397.132 2461
The Phase Tolerances for a Compatible Colour Television Signal allowing for Colour Retentivity—J. Wobst. (*Tech. Mitt. BRF, Berlin*, vol. 5, pp. 155–165; December, 1961.) The tolerances are determined on the basis of subjective tests carried out by means of color television equipment.

621.397.132 2462
A Constant-Luminance Colour-Television System—I. J. P. James and W. A. Karwowski. (*J. Brit. IRE*, vol. 23, pp. 297–306; April, 1962.) A color television signal employing three basic components $E_Y^{1/\gamma}$, $(E_R^{1/\gamma}-E_Y^{1/\gamma})$ and $(E_B^{1/\gamma}-E_Y^{1/\gamma})$ is proposed. The advantages of this with regard to the quantity and quality of transmitted information are considered.

621.397.132 2463
A Colorimetric Study of a Constant Luminance System—W. N. Sproson. (*J. Brit. IRE*, vol. 23, pp. 311–315; April, 1962.) A set of standard colours typical of modern pigments and printing inks is proposed for the assessment of color and luminance fidelity of a color television system. The method is applied to the system proposed by James and Karwowski (see 2462 above.)

621.397.132 2464
Some Aspects of V.S.B. Transmission of Colour Television with Envelope Detection—G. F. Newell. (*J. Brit. IRE*, vol. 23, pp. 316–320; April, 1962.) The errors liable to result from vestigial-sideband transmission with envelope detection are considered.

621.397.132:621.391.822.3 2465
Fluctuation Noise in Two Forms of the N.T.S.C. Colour Television System—A. V. Lord. (*J. Brit. IRE*, vol. 23, pp. 322–328; April, 1962.) The effects of fluctuation noise in color receivers are analyzed for both the normal N.T.S.C. system and the constant-luminance system suggested by James and Karwowski (2462 above); they are found to be similar.

621.397.331.2 2466
Laminated Picture Tubes—J. A. Shaw and C. H. Laurence. (*Proc. IRE, Aust.*, vol. 23, pp. 61–68; February, 1962.) Molded glass caps bonded by epoxy resin to the tube surface have proved successful in protecting the face of the tube and eliminating internal reflections. Construction techniques are described.

621.397.61:621.42.089 2467
Measurement of Lenses from the Point of View of Television—F. Below. (*Nachrtech.*, vol. 11, pp. 547–549; December, 1961.) Report on experimental investigations of the quality of optical systems for use in television cameras.

621.397.61.029.63 2468
Television Transmitters for Bands IV and V—H. Bosse. (*Radio Mentor*, vol. 28, pp. 35–37; January, 1962.) New design features mentioned include the use of a fixed IF and cavity resonators continuously tunable over the range 470–790 Mc.

621.397.63 2469
Transcription of Television Programme Material to a Different Field Frequency—C. G. Mayo and J. W. Head. (*Electronic Eng.*, vol. 34, pp. 335–336; May, 1962.) Several methods of removing the 10-cps flicker frequency produced during conversion between 50- and 60-fields/sec television material are described.

621.397.63:621.395.625.3 2470
The Influence of the Magnetic Tape on the Quality of Video Tape Recording—O. Schmidbauer and K. Altmann. (*Rundfunktech. Mitt.*, vol. 6, pp. 7–14; February, 1962.) The causes of tape noise are identified, with particular regard to drop outs. Measurements made with the equipment described in 2102 of June (Waechter) are discussed. The economics of the routine testing of tapes and the possibility of "retouching" drop outs in tape are examined.

621.397.63:778.5 2471
Film Recording by the 'Negative' Process—J. Bühler. (*Rundfunktech. Mitt.*, vol. 6, pp. 15–20; February, 1962.) A negative image is displayed on a tube screen and photographed on negative film. Development produces a positive film suitable for use with the suppressed-frame method.

TRANSMISSION

621.396.61:621.372.51 2472

Transmitter Combining Unit—A. B. Shone. (*Electronic Tech.*, vol. 39, pp. 178–186; May, 1962.) A method is described for reducing the size of combining equipment for low-power installations in bands I to III, without increasing insertion loss.

TUBES AND THERMIONICS

621.382 2473

Characteristics of the Space-Charge-Limited Dielectric Diode at Very High Frequencies—J. Shao and G. T. Wright. (*Solid-State Electronics*, vol. 3, pp. 291–303; November/December, 1961.) A theoretical analysis for frequencies comparable with transit times gives a value for incremental admittance essentially confirmed by experimental investigation.

621.382 2474

A Tunnel-Emission Device—R. F. Schwarz and J. P. Spratt. (PROC. IRE, vol. 50, pt. 1, p. 467; April, 1962.) Characteristic curves are shown of an active solid-state triode which achieves gain by a form of controlled internal field emission. It comprises two metallic films in contact with a Ge crystal and separated from each other by a thin insulating spacer such as Al_2O_3. See 2798 of 1961 (Mead).

621.382 2475

Current Gain in Metal Insulator Tunnel Triodes—R. N. Hall (*Solid-State Electronics*, vol. 3, pp. 320–322; November/December, 1961.) Tunneling cannot be responsible for the current gains obtained [see, *e.g.*, 3086 of 1961 (Spratt, *et al.*)] as several associated effects would give too great a loss in electron transfer. An alternative mechanism is suggested.

621.382:537.312.62(083.74) 2476

I.R.E. Standards on Solid-State Devices: Definitions of Superconductive Electronics Terms 1962—(PROC. IRE, vol. 50, pt. 1, pp. 451–452; April, 1962.) Standard 62 IRE 28.S1.

621.382.2/.3 2477

The Calculation of Space-Charge Layer Widths, Maximum Field and Junction Capacitance of *p-n* Junctions with Arbitrary Impurity Profiles—H. W. Loeb. (*J. Electronics and Control*, vol. 12, pp. 31–47; January, 1962.) A semi-graphical method is suitable for junctions of any profile. Examples are given.

621.382.2/.3:537.312.9 2478

Improvement of Semiconducting Devices by Elastic Strain—W. G. Pfann. (*Solid-State Electronics*, vol. 3, pp. 261–267; November/December, 1961.) Elastic strain, when applied in selected crystal directions, can produce positive or negative changes in carrier mobility.

621.382.2+621.314.63].004.1 2479

Maximum Ratings of Semiconductor Diodes and Rectifiers as a Function of Ambient Temperature—G. Costamagna and F. Borri. (*Alta Frequenza*, vol. 31, pp. 39–52; January, 1962.) Detailed description of calculation and measurement procedure carried out to determine the operating limits and characteristics of semiconductor devices.

621.382.23 2480

Tunnel-Diode Power—G. Dermit. (*Solid-State Electronics*, vol. 3, pp. 208–214; November/December, 1961.) An expression for nearly linear tunnel-diode power output (see 3182 of 1961) is derived in a simpler way. Results applicable to all materials and arbitrary values of series resistance are displayed graphically.

621.382.23:539.12.04 2481

Low-Dose Gamma Irradiation of Semiconductor Diodes—D. E. Vaughan. (*J. Electronics and Control*, vol. 12, pp. 233–241; March, 1962.) Report and interpretation of experimental results obtained with Ge junction diodes.

621.382.23:621.372.44 2482

Variable-Capacitance Parametric Diodes—R. E. Aitchison. (*Proc. IRE, Aust.*, vol. 23, pp. 78–85; February, 1962.) The design parameters and V/C characteristics of junction diodes are discussed and a brief review of circuit applications is given.

621.382.23:621.372.44 2483

Maximization of the Fundamental Power in Nonlinear-Capacitance Diodes—J. A. Morrison. (*Bell Sys. Tech. J.*, vol. 41, pp. 677–721; March, 1962.) Particular diodes considered are the abrupt-junction and the graded-junction types, with operation in the foreward-conduction region being permitted.

621.382.23.012.8 2484

Tunnel-Diode Large-Signal Equivalent Circuit Study and the Solutions of its Non inear Differential Equations—S. B. Geller and P. A. Mantek. (*J. Res. NBS*, vol. 66C, pp. 45–50; January–March, 1962.) A model is developed and analog-computer solutions for the nonlinear equations are given for various modes.

621.382.3 2485

The Pinch Effect in Transistors which are Operated in the Breakdown Region—F. Weitzsch. (*Arch. elekt. Übertragung*, vol. 16, pp. 1–8; January, 1962.) The conditions are determined for avoiding the harmful concentration of the emitter-collector diffusion current which occurs during avalanche breakdown.

621.382.333 2486

A Simplified Approach to Transistor Admittances—J. Lindmayer and C. Wrigley. (*Solid-State Electronics*, vol. 3, pp. 278–290; November/December, 1961.) Admittance parameters valid for a limited frequency range are shown to describe high frequency transistors relatively well.

621.382.333 2487

Influence of Wafer Thickness and Carrier Recombination on the Cut-Off Frequency of Alloy-Junction Transistors—S. Amer. (*Solid-State Electronics*, vol. 3, pp. 304–308; November/December, 1961.) Carrier recombination plays a small part in limiting cutoff frequency. It may be increased by reducing the wafer thickness in spite of increased carrier density near the emitter edge.

621.382.333 2488

Indium Antimonide Transistors—H. L. Henneke. (*Solid-State Electronics*, vol. 3, pp. 159–166; November/December, 1961.) Design, fabrication and characteristics at 77°K are discussed. Because of its high electron mobility and consequent very short base transit time, this *n-p-n* InAs transistor compares favorably with any Ge transistor.

621.382.333 2489

Base-Layer Design for High-Frequency Transistors—H. S. Veloric, C. Fuselier, and D. Rauscher. (*RCA Rev.*, vol. 23, pp. 112–125; March, 1962.) Some of the parameters which must be evaluated in the design of a HF double-diffused transistor are discussed.

621.382.333:621.318.57 2490

Dynatron-Like Transistor and its Application—A. Sato, A. Fujie, and K. Kagiyama. (*NEC Res. Developm.*, pp. 6–11; September, 1961.) A new switching device and its mechanism and characteristics are described. It is of similar construction to the double-base diode with *p-n* hook [1820 of 1960 (Tominaga, *et al.*)], except that the bonded region is very close to the collector junction. Applications in the dynatron mode of operation are illustrated.

621.382.333:621.318.57 2491

The Influence of Traps on Transistor Switching Behaviour—J. J. Sparkes and J. R. W. Smith. (*J. Electronics and Control*, vol. 12, pp. 177–194; March, 1962.) The Shockley-Read trap model is extended to high injection levels. A graphical method of solution of the recombination equations is used to account for certain anomalous responses of transistors in a simple switching circuit.

621.382.333.33 2492

Theoretical Current Gain of a Cylindrical Mesa Transistor—D. P. Kennedy and P. C. Murley. (*Solid-State Electronics*, vol. 3, pp. 215–225; November/December, 1961.) The determination of base-region transport efficiency is considered as a boundary-value problem. Resulting equations are applied to the design of practical semiconductor devices.

621.383.292 2493

Random Effects of Transit Times and Secondary-Emission Multiplications in a Multiplier Phototube—H. Dormont. (*Philips Res. Repts.*, vol. 17, pp. 79–94; February, 1962.)

621.383.292 2494

The Properties and Applications of a Grid-Controlled Photomultiplier—A. J. Walton. (*J. Electronics and Control*, vol. 11, pp. 341–359; November, 1961.) A general description of a photomultiplier with a control grid and its static characteristics.

621.385.032.212 2495

Low-Noise Beams from Tunnel Cathodes—G. Wade, R. J. Briggs, and L. Lesensky. (*J. Appl. Phys.*, vol. 33, pp. 836–841; March, 1962.) An analysis is given of the noise associated with the space-charge waves of a beam emitted from a tunnel cathode.

621.385.032.213.23 2496

The Potential Distribution and Thermionic Current between Parallel Plane Emitters—F. H. Reynolds. (PROC. IRE, vol. 108, pp. 159–169; pt. C, March, 1961.) A theoretical analysis is given, the results of which are applied to practical oxide-cathode problems. Numerical values of the generalized Langmuir parameters are tabulated.

621.385.032.213.23 2497

The Conductivity of Oxide Cathodes: Part 9—Thermoelectric Power—G. H. Metson and M. F. Holmes. (PROC. IRE, vol. 108, pt. C, pp. 83–92; March, 1961.) The thermoelectric properties are explained by superposition of two physically separable thermoelectric power functions, each invariant with temperature and temperature gradient. Part 8: 737 of 1961 (Metson and Macartney).

621.385.032.213.23 2498

The Poisoning of Thoriated Tungsten Cathodes—R. O. Jenkins and W. G. Trodden. (*J. Electronics and Control*, vol. 12, pp. 1–12; January, 1962.) The observed resistance to cathode poisoning by oxidizing gases is due to combination of the gases with carbon in the surface. At a critical partial pressure poisoning commences and becomes rapid with further small increases in pressure.

621.385.2 2499

Unstable Electron Flow in a Diode—R. J. Lomax. (PROC. IRE, vol. 108, pt. C, pp. 119

121; March, 1961.) "A perturbation analysis is used to demonstrate the instability of a type of electron flow in a plane diode known as C-overlap flow, which is predicted to be a possible flow in the approximation in which electrons are emitted from the cathode with a uniform velocity."

621.385.2 2500
The Influence of Space Charge on the Characteristics of Diodes under Initial-Current Conditions—H. Pötzl. (*Arch. elekt. Übertragung.*, vol. 15, pp. 578–586; December, 1961.) An approximation method is given for calculating the operational parameters of diodes working under retarding-field conditions.

621.385.23 2501
Estimation of the Total Emission of a Diode—C. H. B. Mee, C. S. Bull, and R. K. Fitch. (*Brit. J. Appl. Phys.*, vol. 13, pp. 182–184; April, 1962.) Critical comment on 1094 of March giving further experimental data and authors' reply.

621.385.6:621.375.9:621.373.44 2502
Subharmonic Parametric Pumping of a Quadrupole Amplifier—J. E. Carroll. (*J. Electronics and Control*, vol. 11, pp. 321–340; November, 1961.) When an Adler-type 350-Mc amplifier was pumped near 250 Mc 10 db gain was obtained. The operation is described in simple physical terms and a more rigorous mathematical theory is also given.

621.385.6.032.26 2503
Derivation of Ideal Electrode Shapes for Electrostatic Beam Focusing—W. W. Siekanowicz. (*RCA Rev.*, vol. 23, pp. 47–59; March, 1962.) A derivation of ideal electrode shapes for es focusing of parallel, laminar, ribbon, hollow and cylindrical electron beams is presented.

621.385.623 .624 2504
The Frequency Stability of Klystron Oscillators—D. Frölich and R. Müller. (*Arch. elekt. Übertragung*, vol. 16, pp. 19–24; January, 1962.) The conversion of supply-voltage fluctuations into frequency variations, *i.e.*, frequency modulation of the beam, is investigated, and methods for the reduction of this effect are proposed.

621.385.623.5.072.6 2505
Frequency Stabilization of a Klystron Oscillator in the 4-Gc/s Range—E. Pietzsch. (*Nachrtech.*, vol. 12, pp. 2–6; January, 1962.) A tunable cavity resonator is used as the control element for frequency stabilization.

621.385.624 2506
Extension of the One-Dimensional (Klystron) Solution to Finite Gaps—L. Solymar. (*J. Electronics and Control*, vol. 11, pp. 361–383; November, 1961.) An analytical solution is derived for the quasi-linear partial-differential-equation system, governing the motion of electrons in the buncher gap and adjoining drift space. See also 4363 of 1961 and 1204 of April.

621.385.624 2507
A High-Efficiency 15-MW, 400-Mc/s Pulsed Klystron—L. D. Clough, J. F. Dix, A. J. Monk, and P. Rowcroft. (*J. Electronics and Control*, vol. 12, pp. 105–118; February, 1962.) A four-cavity pulsed klystron designed for high efficiency is described.

621.385.63:621.375.9:621.372.44 2508
Electron Orbits through a Quadripole Amplifying Structure—H. W. Tuffill and A. D. Williams. (*J. Electronics and Control*, vol. 11, pp. 401–423; December, 1961.) An attempt is made to predict theoretically some characteristics of the four- and two-pole amplifying structures used in Adler tubes; limitations on the maximum obtainable gain due to finite electron-beam width are considered.

621.385.63.032.264 2509
Quantitative Transformation Processes in Low-Noise Electron-Gun Systems—K. B. Niclas. (*Arch. elekt. Übertragung*, vol. 15, pp. 587–599; December, 1961.) The quadripole parameters of the electron gun for a traveling-wave tube are calculated using an approximation method (3584 of 1961). Theoretical and measured minimum noise figures are in good agreement.

621.385.632 2510
A High-Power C.W. Travelling-Wave Tube—M. O. Bryant, A. Thomas and P. W. Wells. (*J. Electronics and Control*, vol. 12, pp. 49–62; January, 1962.) Efficiency is increased by operating the collector at a negative potential. 5 kw output is obtained over a voltage tuning range of about 5 per cent in the 3-cm band.

621.385.633:621.316.729 2511
Frequency Locking of Backward-Wave Oscillators—M. Y. Wong, G. D. Sims, and I. M. Stephenson. (*J. Electronics and Control*, vol. 11, pp. 445–457; December, 1961.) An experimental investigation shows that the minimum signal required to lock a backward-wave oscillator depends upon the point of injection in the slow-wave structure. The actual values are found to be in good agreement with theory.

621.385.832 2512
Cathode-Ray Tubes with Post-Deflection—W. Thommen. (*Arch. elekt. Übertragung*, vol. 15, pp. 565–568; December, 1961.) The sensitivity of cathode-ray tubes cannot effectively be increased by the use of a constant deflection field subsequent to the normal deflection system, because of the resulting deterioration of beam focusing.

621.387:621.362 2513
Thermionic Generators—Fraser and Isaacs. (See 2455.)

MISCELLANEOUS

621.396+621.397]:061.3 2514
The Main Results of the European Broadcasting Conference, Stockholm 1961—W. Klein. (*Tech. Mitt. PTT*, vol. 39, pp. 425–437; December, 1961. In German and French.) Report with particular reference to plans affecting the Swiss broadcast and television systems.

Sylvania helps you put a handle on laser phenomena

Investigating the laser principle and its application in communications, ranging, surveillance? The exciting study of this new area of electronics can be more rewarding if you consider the role these Sylvania products can play.

They provide new facility and handling ease not only in generating stable, reproduceable modes, but in detecting and measuring laser phenomena as well.

Sylvania can be of further help, too, if your program requires modifications of these products or if you'd like to talk over a special problem. Perhaps Sylvania's broad experience, which includes gas discharge, solid state physics, microwaves, luminescence and material synthesis, can bring a quick solution. Write Microwave Device Division, Sylvania Electric Prods. Inc., 1100 Main St., Buffalo 9, N.Y.

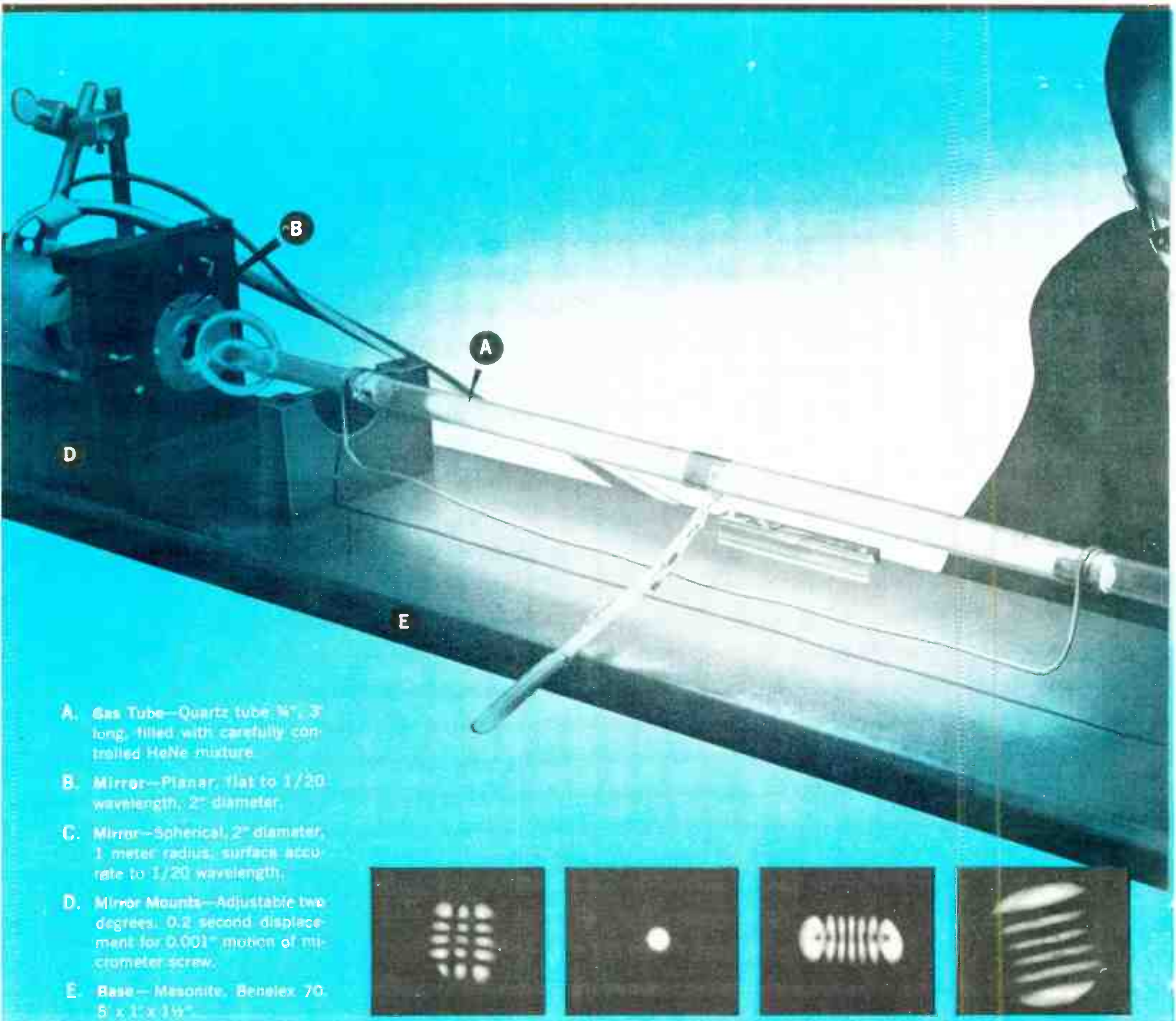

Photographs of simple standing wave modes set up on the GL-6271. Patterns are stable and reproduceable.

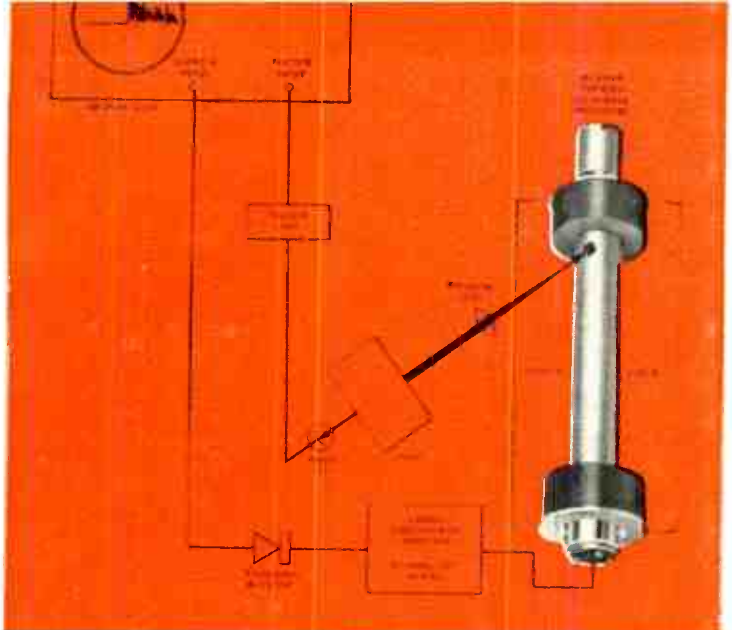

First Practical Device for Laser Detection

The Sylvania SYD-4302 Microwave Phototube fills the important need for receiving light-transmitted microwave modulation in the 1.5Gc to 4.5Gc bandwidth.

Broadband Optical Receiver Use

Capable of response to amplitude modulated light signals, either coherent or incoherent, with a corresponding reproduction of modulation at the output. SYD-4302 makes practicable measurement of natural modulation, multimoding, frequency pulling and spectral width of coherent light.

Optical Superheterodyne Receiver Use

When used with a laser local oscillator, SYD-4302 can serve as the mixer and microwave IF sections of the receiver to detect and demodulate coherent light signals.

This totally new concept in laser reception can deliver sufficient RF power output to drive a low level (10-50mW) TWT such as Sylvania TW-4261. It uses an extremely durable photosensitive-thermionic cathode material and a broadband slow wave helix. Cathode responds to light in the red region of the spectrum and yields up to 0.5mA of photocurrent. It can operate on photocurrent alone or with a low filament voltage for increased output. In addition to this remarkable development for S-band frequencies, Sylvania is currently working on L, C and X-band microwave phototubes.

SYD-4302 Typical Operation

Conditions		Characteristics	
Helix voltage (approx.)	445 Vdc	Cathode current	400 μA*
Grid #1 voltage	0 Vdc		
Grid #2 voltage	445 Vdc		
Heater voltage	3 Vac		

*Measured with approx. 3V on heater and no light energy from laser

New Sylvania Gas Laser

Here is new experimental flexibility for researchers and engineers. A product of Sylvania's accrued knowledge in the field of lasers, the GL-6211 Gas Laser combines outstanding features with unique flexibility.

The GL-6211 provides a continuous output in the milliwatt range at 11,530 Angstroms. Because it employs external optics, the GL-6211 can be adjusted readily to produce simple reproduceable mode operation. Experiments can be made with optical configuration and cavity geometry. Access to the resonant cavity outside the laser tube makes possible easy study of this interesting region of the laser. Optics can be changed without disturbing the laser tube or its fill; confocal, concentric or plane optics can be employed.

This new handling ease can add considerably to research productivity; gaining knowledge and understanding of laser phenomena can be accelerated. At the same time, the GL-6211 offers practical advantages. Its inherent flexibility will not easily be outgrown.

Stability of the GL-6211 is enhanced by its sealed quartz tube, extremely clean gas fill, Brewster angle windows, and good heat dissipation, which virtually eliminates thermal expansion.

See us at WESCON Booths 3301-3306 (Annex-Tent)

SYLVANIA

SUBSIDIARY OF
GENERAL TELEPHONE & ELECTRONICS

GENERAL SYSTEM

Membership

(Continued from page 60A)

Skalbania, F. R., Tonawanda, N. Y.
Smiley, W. J., Kokomo, Ind.
Smith, G. H., Salt Lake City, Utah
Smith, J. R., Webster, N. Y.
Solomon, L. I., Westbury, L. I., N. Y.
Sridhar, R., West Lafayette, Ind.
Staiman, D., Smithtown, L. I., N. Y.
Staite, J. D., Indianapolis, Ind.
Strassberg, G., Bayside, L. I., N. Y.
Swickle, M., Westbury, L. I., N. Y.
Tanghe, R. E., Rock Island, Ill.
Taylor, A. P., Ridgefield, Conn.
Teramoto, M., Shinagawa ku, Tokyo, Japan
Thomas, J. W., Tucson, Ariz.
Thompson, W. S., Raleigh, N. C.
Thoresen, T., Culver City, Calif.
Toth, L. A., Santa Barbara, Calif.
Trick, R. M., Redwood City, Calif.
Tsokris, P. N., Scarsdale, N. Y.
Udell, D. E., New York, N. Y.
Unger, C. T., Canton, Ohio
van Dijck, J. G. R., Antwerp, Belgium
Varley, J. G., Hicksville, L. I., N. Y.
Veneziano, A., New Hyde Park, L. I., N. Y.
Venkateswaran, S., Singleton Park, Swansea, England
Vincent, M. F., Ruislip, Middlesex, England
Vinetz, R. C., Tarzana, Calif.
Ward, P. A., Montreal, Que., Canada
Wassermann, S. A., Jamaica, L. I., N. Y.
Watson, A. M., Chelmsford, Essex, England
Webb, W. C., Greenbelt, Md.
Weckel, W. E., Jr., Ann Arbor, Mich.
Wehrly, P. A., Kokomo, Ind.
Weinberg, H., Merrick, L. I., N. Y.
Weinberg, W. E., Dayton, Ohio

(Continued on page 71A)

The ALL-NEW STODDART NM-22A... is the most advanced RFI Instrumentation in this frequency range. Designed for data recording, the Stoddart NM-22A Radio Interference-Field Intensity Measuring Equipment has built-in capability for performing **spectrum signatures and mil-spec acceptance tests** over the 150 kc to 32 mc range.

The data produced by the NM-22A accurately records the frequencies and amplitudes of signals within this band—clearly defining the portion of the frequencies outside acceptable limits.

Simplified data collection and recording is made possible by such NEW time-saving features as: **Analog Voltage Outputs** for spectrum signature and data recording; **Minimum Gain** change over the frequency range; **Increased Sensitivity**—up to .1 microvolts; **Selectable Bandwidths**—6 db bandwidths of 3 or 10 kc—**constant over the entire frequency range.**

The NM-22A, with its extreme sensitivity and broad Measurement Range of 140 db, permits a wide range of applications for both laboratory and field use.

Other features include: Impulse Generator Calibrator; Remote Rod, Loop Antennas; either Rack Mount or Standard Case. The NM-22A meets the high standard of quality inherent in all Stoddart products.

See the Completely NEW NM-22A at the Wescon Show, Booth 3824. Available from stock September, 1962. Send for detailed literature.

STODDART
AIRCRAFT RADIO CO., INC.
LEADER IN RFI CONTROL
6644 Santa Monica Blvd. • Hollywood 38, California
HOllywood 4-9292

THIS

BRINGS YOU THIS

110

ELECTRONIC NEWS, MONDAY, MARCH 26, 1962

99.997% Reliability Achieved For Minuteman Transistors

KOKOMO, Ind.—The Delco Radio division has succeeded in manufacturing power transistors for the Minuteman missile with 99.997 per cent reliability, based on tests with an assumed acceleration factor of 50. The firm is said to be the first power transistor producer to meet such requirements, according to Delco officials.

This extreme reliability was achieved in a research and development contract with Autonetics, a division of North American Aviation, Inc., associate prime contractor responsible for the inertial guidance and flight control systems for the Minuteman, developed by the Ballistic Systems division of the Air Force Systems Command.

The transistor involved is the Autonetics 251M-1. It is covered by specifications similar to those of the Delco 2N1358. More than 50,000,000 hours were accumulated testing it.

The reliability program at Delco Radio was an effort to accelerate the rate of transistor development to provide power transistors with a failure rate of 0.003 per cent/1000 hours or lower at 60 per cent confidence level.

Part of the program consisted of obtaining histories on specific lots of power transistors. The histories included absolute documentation of all environments, processes, and parts which in any way affect production of the transistors. The lot size was chosen to be the output of transistors from a single germanium crystal.

DOWNEY, Calif.—Autonetics division of North American Aviation, Inc., associate Minuteman contractor responsible for inertial guidance, flight control and aero-space ground equipment, confirmed that Delco Radio power transistors had met Minuteman reliability requirements.

A spokesman said Delco's 251M transistor, for use in Minuteman's guidance and flight control, had achieved the failure requirement of .003 per cent per 1,000 hours.

The Delco Radio 251M-1 Minuteman transistor. Equivalent characteristics are also available for high reliability applications in our 2N1358A version.

251M-1
Germanium Transistor

TYPE	Vcbo @ Icb = 4 ma	Vceo @ Iceo = 1 Amp Sweep	Hfe @ Ic = 5A Min.	Max.	Vce (sat) Ib = 2A Ic = 12A	Thermal Resistance Junction to Case	Junction Temp. (Max.)
251M-1	80V min.	60V min.	25	50	0.7V	0.8° C/w max.	95° C

Write for additional information on the Delco Radio Power Transistor Reliability Story

DELCO RADIO

Sales Offices

Union, New Jersey
324 Chestnut Street
MUrdock 7-3770
AREA CODE 201

Detroit, Michigan
57 Harper Avenue
TRinity 3-6560
AREA CODE 313

Santa Monica, California
726 Santa Monica Blvd.
UPton 0-8807
AREA CODE 213

Syracuse, New York
1054 James Street
GRanite 2-2668
AREA CODE 315

Chicago, Illinois
5151 N. Harlem Ave.
775-5411
AREA CODE 312

General Sales Office: 700 E. Firmin, Kokomo, Ind., Gladstone 2-8211—Ext. 500 • AREA CODE 317 • Division of General Motors, Kokomo, Indiana

Membership

(Continued from page 68A)

Weinstein, J. L., Philadelphia, Pa.
Weisberg, S. A., Great Neck, L. I., N. Y.
Wickert, A. N., Levittown, N. J.
Williamson, R. S., Flushing, L. I., N. Y.
Williams, L. K., North Wilmington, Mass.
Wilser, F. A., Washington, D. C.
Wilson, H. Z., Santa Monica, Calif.
Yngvesson, K. S., Goteborg, Sweden
Zanella, A. J., Montreal, Que., Canada

Admission to Associate

Ahmad, N. U., Oklahoma City, Okla.
Anderberg, S. E., Pyrolavagen, Sweden
Adisusanto, R. A., Magelang, Indonesia
Baker, W. J., San Francisco, Calif.
Balakrishnan, P., Banaglore, India
Barber, C. F., Jr., Littleton, Colo.
Barook, M., Palmdale, Calif.
Batcheller, R. H., Seattle, Wash.
Battat, P., New York, N. Y.
Bennett, M., Calverton, L. I., N. Y.
Bie, T. G., Bandung, Indonesia
Blute, J. F., Jr., Tucson, Ariz.
Buckley, D. C. M., North Surrey, B. C., Canada
Bunevitch, J. G., Scranton, Pa.
Calsyn, L. E., East Moline, Ill.
Clare, S. K., Burnaby, B. C., Canada
Cleve, R. J., Santa Maria, Calif.
Cook, A. B., Lynbrook, L. I., N. Y.
Cork, H. D., Chicago, Ill.
Daroendio, R. M., Bandung, Indonesia
Dasuki, D., Garut, Indonesia
Dayan, D., Brooklyn, N. Y.
Drayer, G. B., Chicago, Ill.
Dunnette, W. H., Rochester, Minn.
Edwards, F. L., Youngstown, Ohio
Eggleston, R. L., Rock Island, Ill.
Ellison, B., Smyrna, Ga.
Entrikin, R. K., East Moline, Ill.
Etzler, H. L., Patrick Air Force Base, Fla.
Fancher, B., Rock Island, Ill.
Fisher, H. T., Drexel Hill, Pa.
Flanagan, T. N., New York, N. Y.
Gadenz, R. N., Pittsburgh, Pa.
Gasparovich, G. M., Alamagordo, N. M.
Gorentlo, F. M., Warren, Pa.
Graham, F. W., Bettendorf, Iowa
Gramenius, H., Jupitervagen, Sweden
Griffin, C., Charleston, S. C.
Gypins, J. J., Midwest City, Okla.
Haworth, J. B., Wallingford, Conn.
Hartnett, J. M., New London, Conn.
Hines, M. E., East Moline, Ill.
Hessler, P. P., Thousands Oaks, Calif.
Howard, T. W., Huntington, L. I., N. Y.
Jacobsohn, W. M., New York, N. Y.
Jann, G., Jr., North Syracuse, N. Y.
Judd, H. W., Westbury, L. I., N. Y.
Kashdan, L., Pomona, Calif.
Kaufman, R. H., El Paso, Tex.
Keradjan, A., Tjimahi, Indonesia
Laney, C. H., Jr., Orlando, Fla.
Larson, J. K., Davenport, Iowa
Lunin, D. R., St. Petersburg, Fla.
Luttrell, E. G., Indianapolis, Ind.
Mangoensoediro, S., Djakarta, Indonesia
Martinez, A. J. R., Buenos Aires, Argentina
McEver, W. L., Levittown, Pa.
Naumann, F. E., Clifton, N. J.
Newman, R. J., Orange, Calif.
Nusser, L. C., Omaha, Neb.
Pace, R. T., Nederland, Tex.
Palmer, J. M., Sierra Madre, Calif.
Pennington, B. E., Charleston, S. C.
Peters, G. T., Juno Riviera, Fla.
Pocock, R. F., Lincolnshire, England
Porcerelli, A. C., Hempstead, L. I., N. Y.
Price, E. D., Chicago, Ill.
Puck, L. F., Davenport, Iowa
Rusinko, J. E., Smolan, Kan.

(Continued on page 72A)

Membership

(Continued from page 71A)

Satenstein, L. S., Outremont, Que., Canada
Schlemmer, A., Rockville, Md.
Schnittman, M., Stamford, Conn.
Sell, E. H., Albuquerque, N. M.
Shackelford, R. D., Davenport, Iowa
Sherman, A., Santa Ana, Calif.
Siebke, M. C., Davenport, Iowa
Soehardjo, Bandung, Indonesia
Soekrisno, Djakarta, Indonesia
Spencer, R. A., Long Beach, Calif.
Steele, J. F., Brookfield, Wis.
Stephan, D. H., Cleveland, Ohio
Stern, L., Jackson Heights, L. I., N. Y.
Sudhono, Tjimahi, Indonesia
Swick, R. H., Warren, Pa.
Tarjudin, T., Paseh Tasikmalaja, Indonesia
Uram, J. D., Clifton, N. J.
Vanderpool, J. H., Cincinnati, Ohio
Waddell, R. E., Abilene, Tex.
Weyls, E. L., Burlington, Iowa
White, H. K., Dayton, Ohio
Williams, D. M., Rock Island, Ill.
Wolf, L. W., Wichita, Kan.
Zimmerman, R. A., Rock Island, Ill.

Positions Wanted

By Armed Forces Veterans

In order to give a reasonably equal opportunity to all applicants and to avoid overcrowding of the corresponding column, the following rules have been adopted:

The IRE publishes free of charge notices of positions wanted by IRE members who are now in the Service or have received an honorable discharge. Such notices should not have more than five lines. They may be inserted only after a lapse of one month or more following a previous insertion and the maximum number of insertions is three per year. The IRE necessarily reserves the right to decline any announcement without assignment of reason.

Address replies to box number indicated, c/o IRE, 1 East 79th St., New York 21, N.Y.

FREQUENCY AND INTERFERENCE SPECIALIST

Retiring officer, 25 years radio & communication experience civil & USAF, desires full or part time position in warm climate. Extensive experience international frequency allocation, and management of operation and maintenance functions. Available Fall of 1962. Write Box 4000 W.

TECHNICAL PUBLICATIONS ENGINEER

Presently Director of Technical Publications and Advertising. Seeks challenging position with increased scope and responsibility. Experience includes ten years of radar and microwave technology and three years in advertising and public relations. Write Box 4001 W.

BIOLOGICAL INSTRUMENTATION

B.S.E.E.—1951. Proficient in micro volt level amplifier design, feedback system analysis, active filter design, and digital circuit design. Desires

(Continued on page 74A)

VIBRATION-PROOF CARD PACKAGING

Pre-test data used to prevent vibration-induced failure of parts leads on printed circuit cards

Probably the most unrelenting adversary of packaging engineers is vibration, the all too persistent specter that hovers malevolently over complex electronic systems. Hours, days, weeks, and even longer, especially during pre-delivery system tests, are repeatedly lost as technicians and engineers patiently stalk malfunctions arising from parts rendered ineffectual by vibration.

Packaging engineers at Litton Systems have devised still another technique of combatting this eternal bugaboo. They have developed a relatively simple pre-test means whereby each of the innumerable parts attached to printed circuit cards in a digital system can be so located and positioned on a card that the probability of its resistance to "the shakes" is virtually 100 percent assured.

The essence of the method, which was perfected for application on an advanced digital tactical data system intended for installation in a carrier-based airborne early-warning and control aircraft, is exemplified in the accompanying diagram. The over 2,000 printed circuit cards in the system were classified into two basic types, the only difference between the two being that type II is equipped along the forward edge with a transistor holder bracket.

Notwithstanding the small size (3″ x 3″) of the card, vibration characteristics were compiled for several zones of each card type. On

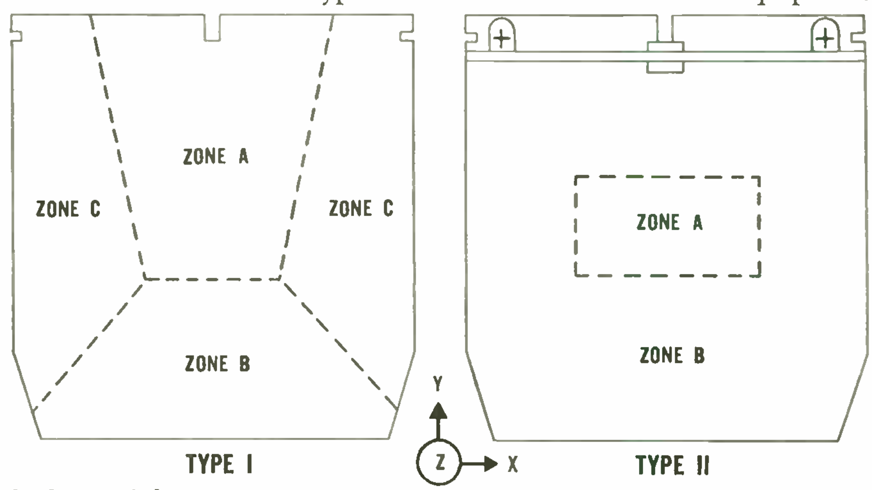

the basis of this data, zones of permissibility and non-permissibility were established for each part to be attached to the card according to the size, weight, and shape of the part.

An A-size capacitor, or equivalent part, for example, could be placed in any zone of either card type with the part axis oriented in any direction. An R-size capacitor or its equivalent, however, could not be placed in zone A of either card type, but could be placed in zone B and oriented along the X-axis on type I, in zone C along the Y-axis of type I, and in zone B along either the X or Y-axis of type II. For another, a .50-inch square by .47-inch high coil could be oriented along the Z-axis in all zones of both card types with the exception of zone A of type I.

The parts placement and orientation data for capacitors, resistors, transistors, diodes, coils, and equivalent parts fit readily on a single oversized sheet. The proof of the technique is in thousands of printed circuit card modules that have consistently met not only the requisite airborne electronic equipment specifications for vibration, but the even more stringent specifications for missile-borne equipment.

Ingenuity of this kind is characteristic of engineering performed at Litton Systems. Those who feel inclined to work in an environment that encourages and inspires thoughtful and fruitful engineering will find satisfaction at Litton Systems. Write to: Harry Laur, Litton Systems, Inc., Data Systems Division, 6700 Eton Avenue, Canoga Park, California; or telephone DIamond 6-4040.

An equal opportunity employer

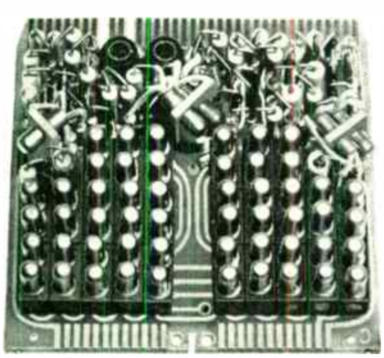

shift-register assembly circuit card with components arranged according to zoning methods.

LITTON SYSTEMS, INC.

A DIVISION OF LITTON INDUSTRIES

DATA HANDLING & DISPLAY SYSTEMS • GUIDANCE & CONTROL SYSTEMS • COMPUTER SYSTEMS • SPACE SCIENCE • BIOELECTRONICS • ADVANCED COMMUNICATIONS TECHNOLOGY

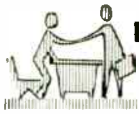

Positions Wanted

By Armed Forces Veterans

(Continued from page 72A)

to work on problems concerned with the life process or on the development of devices for supplementing man's sensory perception. Location on West Coast desirable. Write Box 4002 W.

ELECTRONIC ENGINEER

B.S. (Appl. Phys.), married, age 36. Knowledge of German, Polish, Russian. U.S. Citizen with 12 years of experience in instrumentation research and development. Desires position as Field Engineer for systems installation and customer liaison. Would consider Central European assignment. Write Box 4003 W.

ENGINEER IN FRANCE

American, 36, MSEE, 8 years experience radar systems and 4 years experience professional audio, seeks position or representation full or part time in Paris, France. Fluent French. Write Box 4004 W.

ELECTRONICS TECHNICIAN

B.S. Physics, 1958, 4½ years industrial reserach in Solid State Physics. Veteran USMC, 2 years aviation electronics technician. Married, family. 29 years of age. Seek foreign employment with managerial responsibility. Write Box 4005 W.

COMMUNICATION ENGINEER

B.S. '52. Age 31, married. 10 years in management and engineering of complex communication systems (radio, radar, teletype, telephone

(Continued on page 78A)

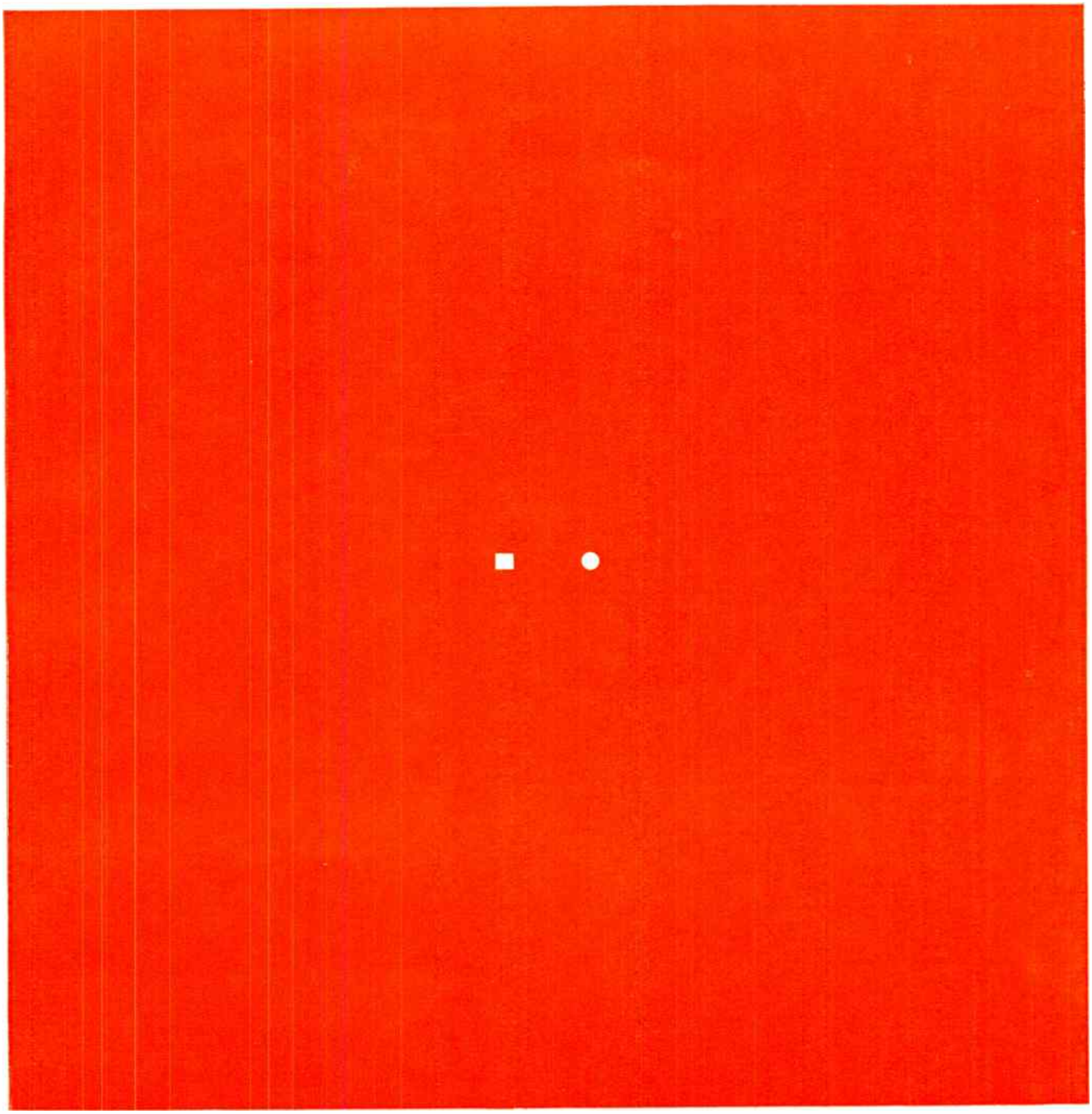

The small white rectangle above represents the approximate size of space required to contain one page of newspaper size document reduced for storage through NCR's PHOTOCHROMIC MICRO-IMAGE process. The small white dot on the right represents the area that would hold thousands of micro-capsules (cell-like structures containing useful materials) produced through NCR's amazing chemical process of MICRO-ENCAPSULATION.

One apparent application of the NCR Photochromic Micro-Image process is that it permits easy and efficient storage, access and reproduction of voluminous data. The process of Micro-encapsulation has applications cutting across many fields of interest including paper coatings (such as on our No Carbon Required paper), food, pharmaceuticals, adhesives, etc.

These are but some of the outstanding achievements of NCR scientists and research and development personnel. Through the years our devotion to the concept of improvement, growth, and service to business and industry has led to many other changes which have benefited the world. Government and military agencies also have an active interest in the advanced work being done by NCR scientists and engineers.

Our Research and Development programs are not limited to the fields of Photochromics and Micro-encapsulation. Rather, the programs extend into many disciplines including physical and chemical research in the areas of semiconductor materials and devices that will have practical application in computer development and add to the total effort of the company. The NCR effort is concentrated on the total systems concept.

To determine whether your career plans fit in with our research and development plans, merely drop us a note with a brief description of your interests and scientific background. Applications at all professional levels will be considered.

Write to:

T. F. Wade, Technical Placement
The National Cash Register Company
Main & K Streets, Dayton 9, Ohio

An Equal Opportunity Employer

NCR

has a light in his eye that money can't

factor. But a man's real warmth for his job—his real measure

check. To find himself in the right emotional

acknowledged masters in their fields—to be an active

—these are the satisfying, the lasting, rewards. And

talent to come to Lockheed Missiles & Space Company.

and civilian space projects as well as other

Here they find inventive and creative freedom. Here

We invite you to join their proud company.

SUNNYVALE, CALIFORNIA • SUNNYVALE, PALO ALTO, VAN NUYS, SANTA CRUZ, SANTA MARIA, CALIFORNIA · CAPE CANAVERAL, FLORIDA · HAWAII

Positions Wanted

By Armed Forces Veterans

(Continued from page 74A)

inside and outside plant). Valid FCC radio-telephone/telegraph licenses with radar and aircraft endorsements. Seeking position in sales or applied engineering western U.S., preferably Pacific coast. Write Box 4006 W.

FREE LANCE TECHNICAL WRITER

Self made electronics engineer reads, writes, and speaks English fluently. Fifteen years experience writing military Tech Orders, Maintenance and Training Manuals Space and Engineering proposals. Commission basis only. Write Box 4007 W.

SALES REPRESENTATIVE—WESTERN CANADA

Professional Electronics Engineer with 12 years experience in a wide range of Communications and Medical-Industrial Electronics equipment and systems design and good sales background, seeks appointment as Manufacturers Representative for a good line of electronics equipment or instruments. Box 3983 W.

LINGUIST-ENGINEERING PHYSICIST

Would enjoy coordinating the research efforts of a laboratory with related research done in other countries to avoid duplication and accelerate results. Training includes: mathematics, management, manufacturing, engineering, graphic arts, Russian, German, French, etc. Interested in automatic language translation (home: Philadelphia; age, 41). Box 3982 W.

(Continued on page 80A)

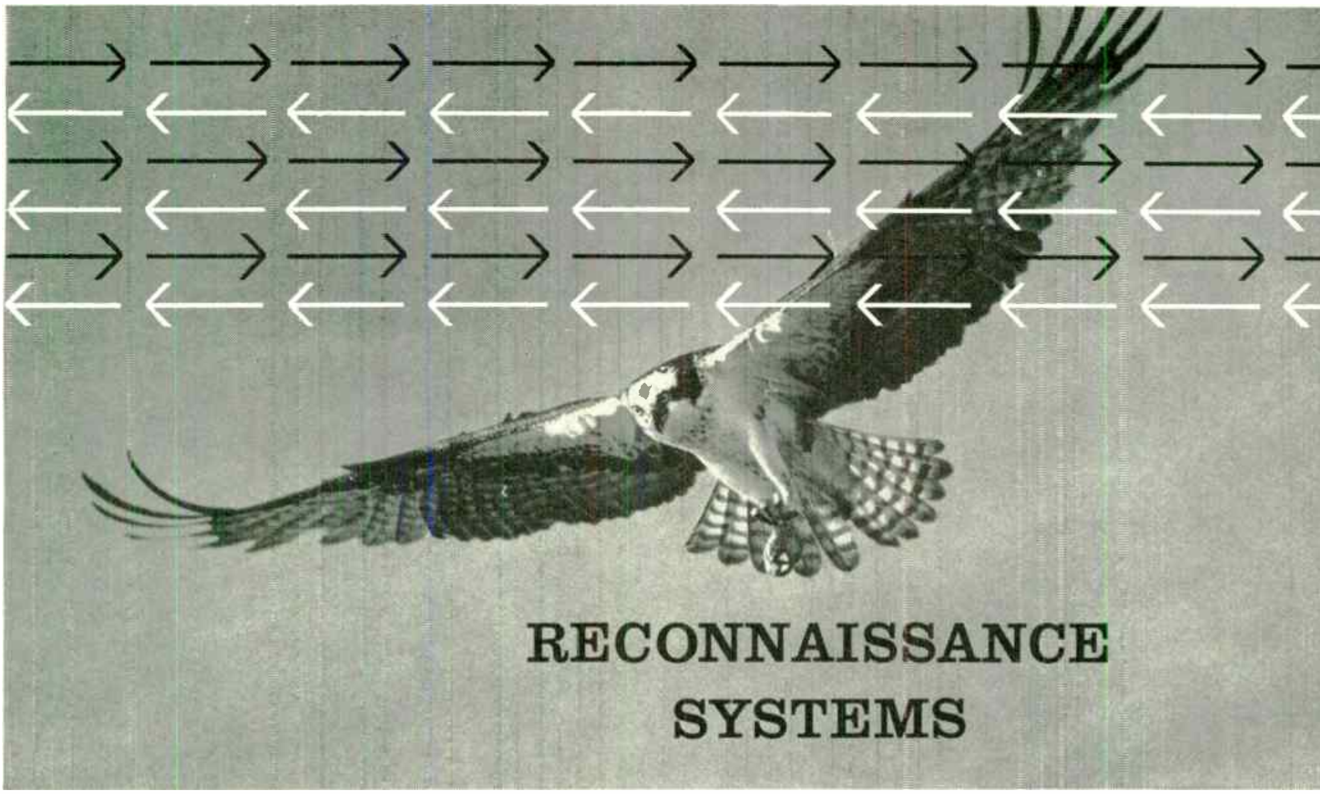

Stimulating career opportunities for Reconnaissance Systems Engineers at Sylvania on the San Francisco Peninsula

SYLVANIA ELECTRONIC SYSTEMS—WEST
offers a broad spectrum of challenging problems involved in Reconnaissance Systems Engineering including: Feasibility Studies, Operational Analysis, System Synthesis and Performance Analysis, Application and Development of Advanced Techniques, Specification of Constituent Subsystems, Human Factors Engineering and Operations Research. Typical areas in which openings currently exist include the following:

DATA ANALYSIS and SIGNAL PROCESSING. Carry out studies, the objectives of which are the design of new, or the refinement of existing data collection systems. Studies range from the analysis required to develop and define operating requirements compatible with economic and state-of-the-art considerations, through systems conceptual design in block diagram form and including specification of hardware design approach.

STATISTICAL ANALYSIS. Perform various statistical analyses at various levels of sophistication, set up mathematical models of stochastic processes. Fields of particular interest include experimental design, theory of queues, theory of mixtures, allocation of resources, search theory, and general operations research.

INTERCEPT AND DETECTION. Direct or perform reconnaissance systems operational and technical requirements studies; electronic signal environment studies; synthesis of electronic intercept systems from conception to hardware specification and system block diagram; analysis of system performance and of data related to telemetry, communications, radar and others. Direct or prepare reports and proposals and maintain technical contact with customer representatives.

ANTENNA AND PROPAGATION. Perform analyses of electromagnetic propagation aspects of reconnaissance and other systems; analyze direction finding problems and develop direction finding techniques; determine antenna requirements and configuration during synthesis of reconnaissance systems. Activities include report writing, and customer contacts.

These openings exist at all experience levels. Advanced degrees in EE, physics, or mathematics desirable.

SYLVANIA ELECTRONIC SYSTEMS
Government Systems Management
for GENERAL TELEPHONE & ELECTRONICS

Complete information may be obtained by writing, in confidence to
Roger Harlan
SYLVANIA ELECTRONIC SYSTEMS • WEST
P. O. Box 188 • Mountain View, California
An Equal Opportunity Employer

7899

Positions Wanted

By Armed Forces Veterans

(Continued from page 78A)

ELECTRONIC ENGINEER

MSEE. 3 years experience in transistorized digital systems for space probe payloads. Desires to do creative work in same or a similar field. Prefers smaller company or autonomous division of larger company. Available in late summer. Write Box 3991 W.

ACADEMIC POSITION

B.S. and M.S. in E.E.; 3 years teaching in a university E.E. department prior to entering USAF for three years. Have begun work on Doctorate. Desires teaching position in Fall of 1962 with opportunity for graduate study. Write Box 3992 W.

ELECTRICAL ENGINEER

USAF Officer, 44 BSEE 1940. MSEE 1957. Reg. P.E. 1947. Experience: radar communications, electronic intelligence and R&D in Special Weapons Fuzing. Prefer Southwest or possibly overseas. Available October 1962. Write Box 3993 W.

FIELD SERVICE ENGINEER

Fifteen years of varied experience in communications and allied fields desires meaningful employment in field service engineering. Would prefer long term, family-type overseas location where command of Russian and German would be an asset. Salary should be interesting, but is secondary to interest in work and satisfaction

(Continued on page 82A)

Of interest to engineers and scientists

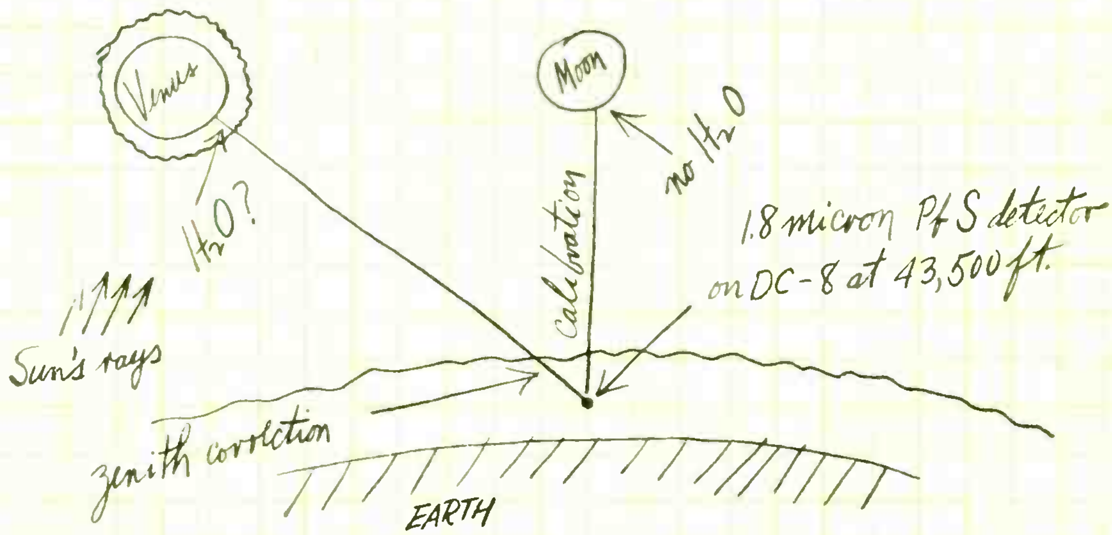

PLANETARY ENVIRONMENTS

...one of more than 500 R&D programs under way at Douglas

The purpose of this Douglas study is to gain a comprehensive insight into the atmospheric characteristics of Venus, Mars and Jupiter. This is to include a detailed knowledge of the following: composition, radiative equilibrium, vertical and horizontal distribution of radiative flux, pressure, temperature, density, and three-dimensional planetary circulation.

Utilizing the most recent observations and advanced theory, working models of these atmospheres are being constructed. New data are being sought through photographic astrometry, spectroscopy and photometry. Feasibility studies of new space instruments are being undertaken as one of many aspects of this investigation.

Of career interest to engineers and scientists

Because leadership in tomorrow's technology is a strong Douglas objective, the company is placing great emphasis on expanding its research and development staff. This has opened outstanding opportunities to scientists and engineers in the multitude of areas related to aerospace, nucleonic and other fields.

An extensive new laboratory complex is being constructed to provide the most modern facilities to aid in R&D operations. If you are seeking a stimulating environment in which to further your career, contact Douglas.

Send us your resume or fill out and mail the coupon. Within 15 days from the receipt of your letter, we will send you specific information on opportunities in your field at Douglas.

Mr. F. V. Edmonds G-3
Missile and Space Systems Division
Douglas Aircraft Company
3000 Ocean Park Boulevard
Santa Monica, California

Please send me full information on professional opportunities in my field at Douglas.

Name __________

Engineering or scientific field __________

Address __________

City __________ State __________

DOUGLAS

Missile and Space Systems Division

An equal opportunity employer

Positions Wanted

By Armed Forces Veterans

(Continued from page 80A)

gained in getting the job done. Age 34. Presently employed in field service division of large electronics firm. Write Box 4011 W.

DATA PROCESSING

B.S. Math, additional grad. Physics. Age 39 with 12 years experience in electronic data processing. Includes management, supervision, systems analysis and programming of such applications as spares provisioning, parts lists, data communications and cost reduction programs. Thoroughly familiar with special and general purpose computer design. Desires responsible position in computer applications area. Write Box 4012 W.

Positions Open

The following positions of interest to IRE members have been reported as open. Apply in writing, addressing reply to company mentioned or to Box No.

The Institute reserves the right to refuse any announcement without giving a reason for the refusal.

Proceedings of the IRE
1 East 79th St., New York 21, N.Y.

ELECTRONIC ENGINEERS

B.S. in EE with experience in electron tube and transistor circuits for work on design, development and application of phase measuring instruments. Any nationality. Permanent position. Pleasant working conditions. Salary commensurate with ability and experience. Detailed resume to Ad-Yu Electronics Lab., Inc., 249 Terhune Avenue, Passaic, New Jersey.

RESEARCH EQUIPMENT SALES

B.S. in Physics, EE or ME. Two or more years experience selling specialized mechanical or electro-mechanical equipment (expensive, semi-custom made items). Must be able to understand customers' special technical requirements and work out engineering solutions, such as modification of standard equipment to meet requirements. Travel half the time and will work with minimum guidance and support. Must be capable of working with clients on all details including financial. Address your resume to: Mr. Donald Sweet, Arthur D. Little, Inc., 35 Acorn Park, Cambridge 45, Mass. An equal opportunity employer.

MANUFACTURING ENGINEER

Redesign of breadboard models of highly engineered electromechanical equipment for cost reduction and semi-mass production. Experienced in mass and semi-mass production operations. Would build manufacturing competence over an R&D base with a thorough knowledge of the problems involved, i.e., when to modify a design to overcome a problem. Address your resume to: Mr. Donald Sweet, Arthur D. Little, Inc., 35 Acorn Park, Cambridge 45, Mass. An equal opportunity employer.

DEVELOPMENT AND DESIGN ENGINEER

Development and design engineer, for advanced work in electronically regulated power supplies. Must have thorough working knowledge

(Continued on page 84A)

NATURE, THE UNBOUNDED VARIABLE

The Electro-Physics Laboratories' research areas are too new to be marked by beaten paths. Our scientists and engineers are engaged in a number of advanced projects, including investigations of ionospheric propagation (in general and as applied to communications), the development of unique long-distance communications techniques, and investigation of upper atmosphere phenomena by means of unusual rocket probe techniques.

Outstanding career opportunities for scientists and engineers are now available in these and other research fields. You will find at Electro-Physics Laboratories a stimulating, creative atmosphere in which ideas can flow freely and in which the rewards are equal to the challenges. Research staff members guide their projects from the concept stage, to applied research, to prototype development. Freed from administrative burdens, they focus their full talents on the scientific aspects of assignments, while the importance of the research effort gives each staff member a very real feeling of contributing to our national purpose.

For additional information, please send your resume to:
Mr. William T. Whelan
Director of Research and Development

ELECTRO-PHYSICS LABORATORIES

ACF ELECTRONICS
DIVISION

ACF INDUSTRIES

3355 52ND AVENUE, HYATTSVILLE, MARYLAND (A RESIDENTIAL SUBURB OF WASHINGTON, D.C.) AN EQUAL OPPORTUNITY EMPLOYER

CAREER OPENINGS AT WESTREX

POSITIONS:

Project Engineers, Development Engineers — senior, intermediate, junior. Engineering Aides • Engineering Writers. Field Engineers, Installation Engineers, Test Engineers, Site Engineers, Training Instructors experienced in carrier, tropo, microwave communications systems for overseas assignments (South Pacific).

AREAS:

SSB Communications Systems
High-Power Radio Transmitters
Oceanographic Navigational Instrumentation Systems
Facsimile Systems
Photo Transmission Equipment
Precise Time Standards
Servo Systems
Navigation Systems
Graphic Recording Papers
Overseas Communication System Support

Send resume to GENE I. ROLLINS, Director of Industrial Relations

An Equal Opportunity Employer

Westrex Company

A DIVISION OF LITTON SYSTEMS, INC.
540 West 58th St., New York 19, New York

Positions Open

(Continued from page 82A)

of solid state circuits and feedback systems. Salary to $16,000 according to qualifications and experience. Position offers a career opportunity in a rapidly expanding organization. Apply to Chief Engineer, Kepco, Inc., Flushing 52, N.Y.

COMMUNICATIONS FOREMAN

U.S. Oil Company, operation Middle East, seeks foreman with FCC or International Radio Telephone and Radio Telegraph First Class to supervise complete communications system with diversified equipment (AM, FM, HF, VHF, Teletype Printer, 100 Line PABX, Multichanneling, etc.). Candidate must have thorough background electronic theory with ten years practical experience (2 to 3 years Supervisory Experience). Approximately $11,600/year which includes $204 month Field Living Allowance; Bachelor Status; 30 day annual vacation with transportation paid; Savings Plan. No U.S. or Foreign Income Tax. Send Resume to Box 2074.

SENIOR PROJECT ENGINEERS

Immediate openings available for Electrical Engineers with Solid State Circuit design experience. Must be capable of assuming project administrative responsibilities. Will handle technical liaison activities with outside contractors. Be capable of directing in-house design effort, component evaluation, and subsystems tests. Masters Degree in Physics or Electrical Engineering desirable, but will accept Bachelors Degree with record of solid project achievement. An Equal Opportunity Employer. Send complete resume to Jet Propulsion Laboratory, 4804 Oak Grove Drive, Pasadena, California.

(Continued on page 86A)

THE *EXCEPTIONAL* MAN

when the position you wish to fill is vital to your organization . . .

when the man you seek requires all the attributes of leadership . . . plus the ability to make significant technical contributions to the work for which he will be responsible . . .

when you need a man who can command the respect of his associates and subordinates because of his intimate knowledge of and first-hand experience in their fields . . .

when you need a man who is well educated and trained in the specialized fields of knowledge you require . . .

you need The Exceptional Man.

Let us locate him for you.

Charles A. Binswanger INCORPORATED ASSOCIATES

EXECUTIVE SEARCH SPECIALISTS
613 PARK AVENUE • BALTIMORE 1, MD. • PLAZA 2-5013

ARA

ELECTRONICS ENGINEERS

Senior and intermediate openings are now available in new programs which require analytic and hardware experience in:

- **Logic**
- **Circuit Design**
- **Instrumentation**
- **Automatic Controls**
- **Servo • Analog**
- **Surveillance Systems**

ARA is a 250-man Research and Development firm active in the fields of space systems, electronics, bionics, physics, geophysics, meteorology, chemistry, aeronautics, and other areas of physical and engineering sciences.

For further information please contact
Mr. Ivan Samuels

ALLIED RESEARCH ASSOCIATES
43 Leon Street, Boston, Massachusetts
"An equal opportunity employer"

AT NASA, YOU'RE IN THE AEROSPACE CENTER OF THE FREE WORLD

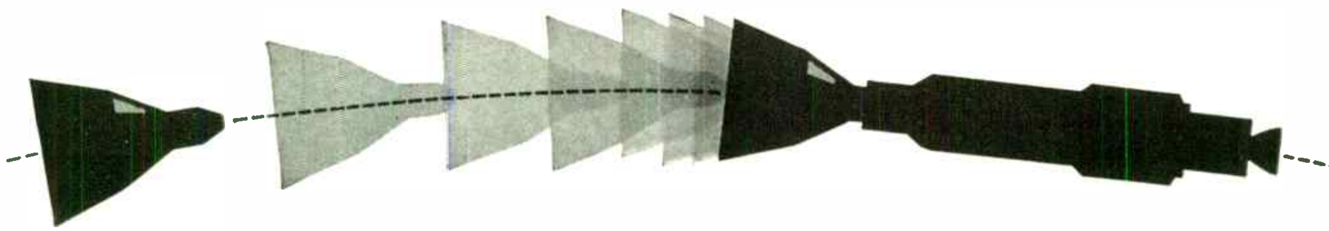

GEMINI

first manned rendezvous in space

How do you dock a two-man spacecraft with another vehicle in earth orbit? What happens when astronauts are weightless for a week or more? Project Gemini is calculated to answer these vital questions. The test of rendezvous techniques alone is a crucial experience in man's drive for the moon—and the results will be invaluable.

Unusual capabilities are needed to solve the intricate and demanding problems of Gemini (and, after Gemini, Apollo).

NASA needs senior aerospace engineers with 6 to 10 years experience in . . . . Systems analysis and studies • Systems engineering • Spacecraft and flight missions • Reliability assessment • Launch vehicles and propulsion • Systems integration and checkout.

NASA offers you unequaled resources and unlimited opportunities for professional growth and recognition. Send just one resume to NASA, Director of Professional Staffing, Dept. 502, NASA Headquarters, Washington 25, D.C. Positions in various locations and in other disciplines—many requiring less experience—are also available.

All qualified applicants will receive consideration for employment without regard to race, creed or color, or national origin. Positions are filled in accordance with Aero-Space Technology Announcement 252-B.

Positions Open

(Continued from page 84A)

TRANSFORMER DESIGN ENGINEER

Transformer design engineer for electronic power supply components and to assist in pioneering development of magnetic type power control devices. Applicants must have a thorough knowledge of magnetic materials and component design. Salary to $16,000 according to qualification and experience. Position offers a career opportunity in an expanding organization. Apply to Chief Engineer, Kepco, Inc., Flushing 52, New York.

ELECTRONIC ENGINEER

A unique position is available for an Electronic Engineer to work in productizing advanced chemical and physical laboratory instrumentation in the field of nuclear magnetic resonance spectroscopy. Successful candidate should have a background including at least 5 years experience in electronic circuit design. Position offers outstanding growth potential and individual should have project engineer capabilities. Outstanding benefit program includes Cash Profit Sharing and Stock Purchase Plans. Submit resume in confidence to: Varian Associates, 611 Hansen Way, Palo Alto, California.

SENIOR ELECTRONIC ENGINEER

Excellent position involves working in the experimental and initial development phases of advanced types of commercial scientific instrumentation. Must be willing to work with unusual circuitry and components which often require extending the state of the art. Some back

(Continued on page 88A)

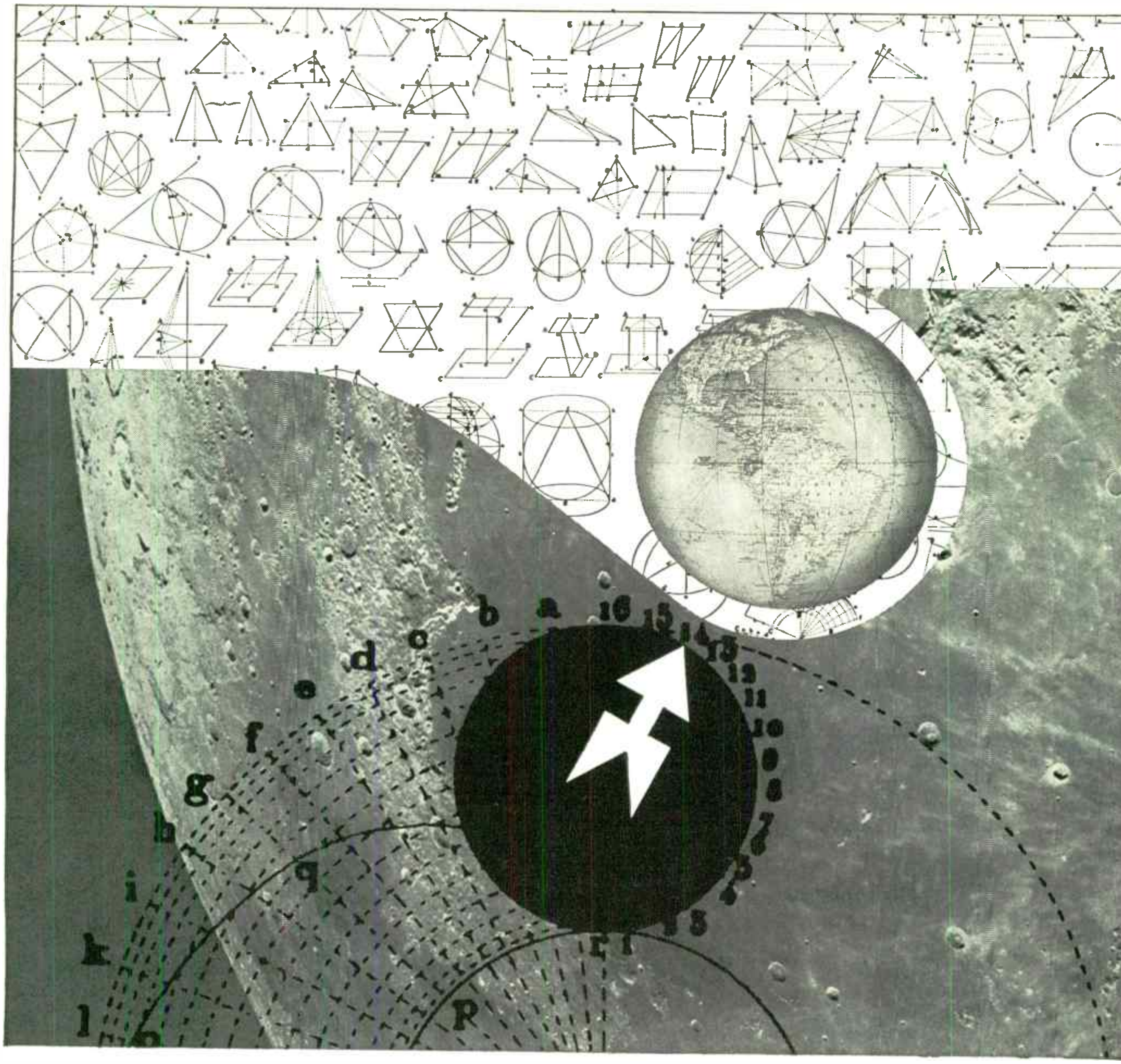

Positions Open

(Continued from page 86A)

ground in tube and transistor circuits, radio frequencies, microwave, stabilized amplifiers and other servo problems is desirable. Work will be in close contact with both physics and chemistry. A BS or MS in EE or Physics plus several years experience. Outstanding Benefit Program includes Cash Profit Sharing and Stock Purchase Plans. Submit resume in confidence to: Varian Associates, 611 Hansen Way, Palo Alto, California.

INSTRUMENTAL SCIENCES FACULTY POSITION

All graduate instruction and research. Young Ph.D. Physicist or Electrical Engineer with strong interest in the multidiscipline field of instrumentation and control. Develop courses and research program for M.S. degree and for expansion into Ph.D. program. Twelve month employment. Reply with resume to: Head, Electronics and Instrumentation, University of Arkansas, Graduate Institute of Technology, P.O. Box 3017, Little Rock, Arkansas.

SENIOR STAFF POSITIONS

Openings exist in the area of nuclear instrumentation system analysis. Personnel with (1) an advanced degree in electrical engineering or physics, (2) several years experience in research and development and (3) a working knowledge in data and control systems analysis, statistical information analysis or instrumentation techniques are being sought. The Instrument Devel

(Continued on page 90A)

Positions Open

(Continued from page 88A)

opment Branch has the responsibility of analyzing and developing data and control systems for nuclear reactors and processes at the AEC National Reactor Testing Station, Idaho. Recent and future expansions have created outstanding opportunities. Write: Philips Petroleum Company, Personnel Administration, P.O. Box 2067 HX, Idaho Falls, Idaho.

SALESMAN

To sell semi-technical instrument in eastern Pennsylvania and Delaware for manufacturers' representative on straight commission (no draw, no expenses; we handle the product on that basis). Degree not needed. Age is immaterial so long as you possess health and integrity. Write Box 2075.

Ph.D. MICROWAVES AND/OR SOLID STATE

Excellent opportunity for Ph.D. with background in microwaves and/or solid state. Some teaching and some research required. Private consulting encouraged. Department has Ph.D. program. Good salary and rank arrangements will be made for exceptional man from either the industrial or academic fields. Address replies to Dr. Fred Schumann, Chairman, Electrical Engineering Departmen., Vanderbilt University, Nashville, Tennessee.

ASSOCIATE PROFESSOR ELECTRICAL ENGINEERING

Ph.D. degree required. Salary $7500 to $8000 per academic year. Opportunity to develop research activity in area of interest. Address replies to: Head, Electrical Engineering Department, South Dakota School of Mines and Technology, Rapid City, South Dakota.

Ph.D. ELECTRICAL ENGINEERING

Unusual opportunity in U.S. Civil Service to recent Ph.D. in Electrical Engineering to continue his research or teaching while administering Army-sponsored basic research projects at U.S. universities, colleges and institutes. Air-conditioned offices located on the Duke University campus immediately adjacent to the Engineering College and Physics-Mathematics Departments. Associates on the Engineering Sciences Staff active in individual research projects at Duke. University campus very attractive in a progressive area of the South. Good family environment. Civil Service levels begin at GS-11 ($7560) to GS-14 ($12,210), depending on background qualifications. Write details of background or submit a Form 57 (obtainable at any post office) to J. J. Murray, Army Research Office (Durham), Box CM, Duke Station, Durham, North Carolina.

ELECTRONIC ENGINEERS

Electronic Engineers for permanent positions with Federal Communications Commission, Washington, D.C., GS-12, $8955 to GS-13 $10,635. Must be graduate engineers with good knowledge of problems involved in the area of space communications. Government will pay expenses for transportation of employee, his family, and household goods to Washington. Attractive fringe benefits include retirement, life and health insurance, automatic pay increases. Good opportunity to enter government career service. Reply to Personnel Officer, Federal Communications Commission, Washington 25, D.C.

(Continued on page 92A)

The Lincoln Laboratory is a center of research and development in advanced electronics, with responsibilities in national defense and space technology. Scientists of many disciplines participate in a program directed toward extending the range and depth of scientific knowledge and solving problems fundamental to the security of the nation.

■ RADIO PHYSICS and ASTRONOMY ■ RE-ENTRY PHYSICS ■ PENETRATION AIDS ■ TARGET IDENTIFICATION ■ SYSTEMS: Space Surveillance, Strategic Communications, Integrated Data Networks ■ NEW RADAR TECHNIQUES ■ SYSTEM ANALYSIS ■ COMMUNICATIONS: Techniques, Psychology, Theory ■ INFORMATION PROCESSING ■ SOLID STATE Physics, Chemistry, and Metallurgy • *A more complete description of the Laboratory's work will be sent to you upon request.* All qualified applicants will receive consideration for employment without regard to race, creed, color or national origin.

Research and Development
LINCOLN LABORATORY
Massachusetts Institute of Technology
Box 16
LEXINGTON 73, MASSACHUSETTS

Yesterday . . . a man named Revere and a dependable steed. Today . . . sophisticated secure weapons command and control systems. The communications media differ but the need is the same... *get the message through.*

For tomorrow's secure communications systems... our scientists and engineers are developing new concepts . . . improving existing communication techniques . . . advancing the state-of-art in survivable communications.

STAFF AND MANAGEMENT OPPORTUNITIES *exist for Electronics Engineers and Physicists with 5-10 years of experience in command and control systems, aerospace communications and familiarity with advanced communications techniques. We are located ten miles northeast of Buffalo in the picturesque suburban community of Williamsville, New York*

SYLVANIA ELECTRONIC SYSTEMS
Government Systems Management
for ***GENERAL TELEPHONE & ELECTRONICS***
GENERAL SYSTEM

Please send resume in confidence to
Robert E. Artman

SYLVANIA ELECTRONIC SYSTEMS—CENTRAL
1181 Wehrle Drive Williamsville, N.Y.

An Equal Opportunity Employer

Positions Open

(Continued from page 90A)

LIFE SCIENCE ENGINEERS

The human factor as a design detail is as old as engineering; as a studied design factor it is relatively new. Engineers with training or experience in the biological or behavioral sciences who are interested in analysis and experimentation in the areas of terrain-following and other radar displays, photointerpretation, advance vehicle handling qualities and heuristic programming techniques are invited to reply to: F. P. Rentschler, Cornell Aeronautical Laboratory, Inc., Buffalo 21, New York.

RESEARCH ASSOCIATE or ASSISTANT PROFESSOR

Immediate opening for professional-level applicant as Research Associate or Assistant Professor to supervise designing, fabricating, and maintaining specialized electronic equipment for research in science and engineering. A properly qualified person will, if he desires, have the opportunity to participate in electronic research or teach. A staff member on full-time appointment may enroll for one course each semester. Salary in range of $7500 to $8500. Annual appointment with one month vacation. Application or further inquiry should be made to: Dean Virgil W. Adkisson, Research Coordinator, University of Arkansas, Fayetteville, Arkansas.

ELECTRONIC ENGINEER

Electronic Engineer, B.S., recent graduate with a few years of practical experience in

(Continued on page 91A)

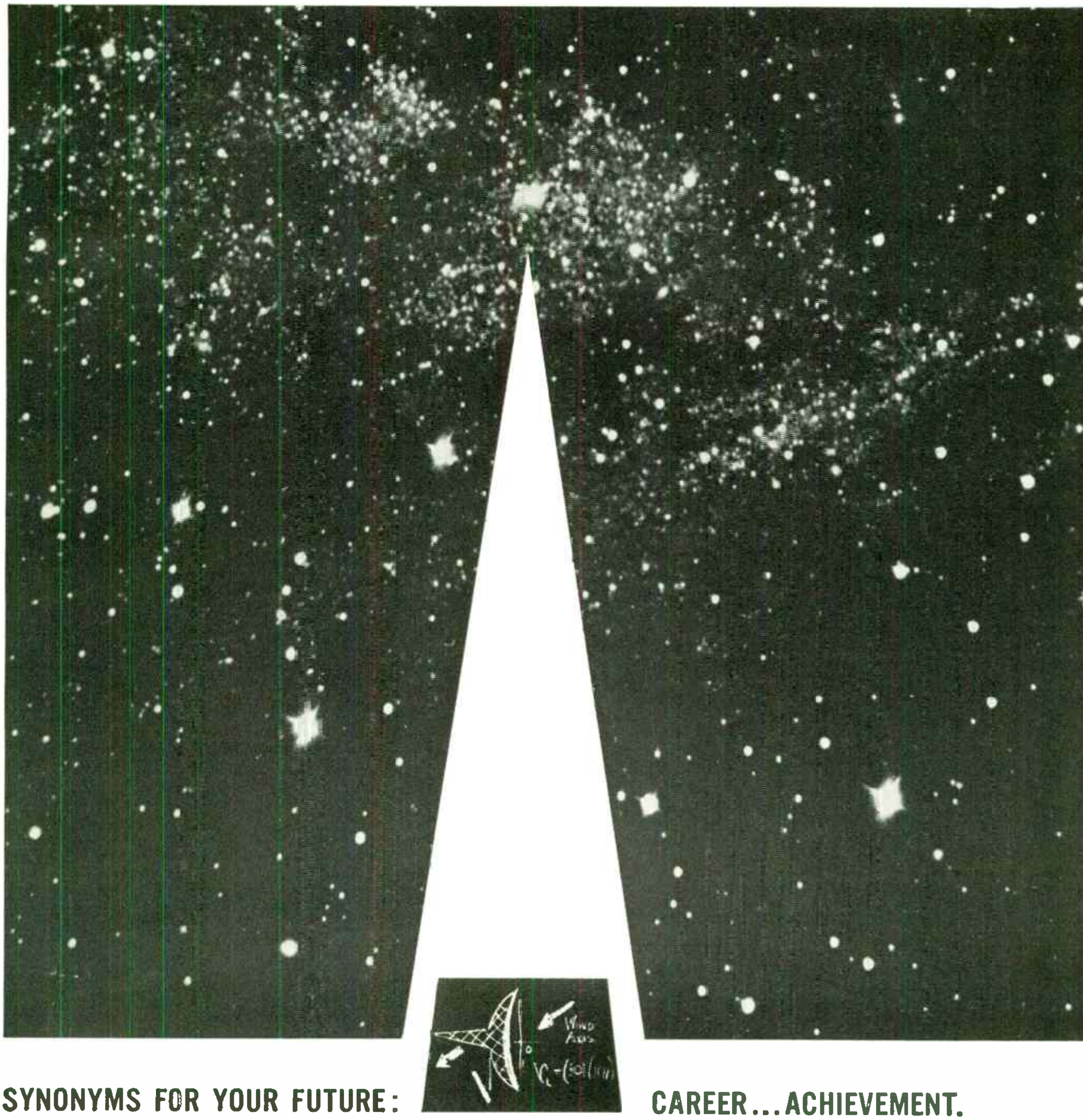

SYNONYMS FOR YOUR FUTURE: CAREER...ACHIEVEMENT.

Working at Philco Western Development Laboratories is synonymous with playing an important role in development of communications and control systems for the nation's frontiers of space. Philco WDL designed and produced the complete satellite package for the Courier Communications Satellite program; other important U. S. satellite programs benefited, too, from advanced technology, research, prototype and fabrication from WDL. This adventure . . . complete program-oriented evolution of tomorrow's answers to tomorrow's space age challenges... is yours, if you want a career that is measured in terms of achievement. Achievement is WDL's history . . . and future.

Write in confidence for information on how you can find your career at Philco WDL, with the additional rewards of ideal living on the San Francisco Peninsula and professional and monetary advancement commensurate with your own ability. Requirements include B.S. or advanced degree (electronics, mathematics, physics), U. S. Citizenship or current transferable D.O.D. clearance. Address Mr. Patrick Manning, Department R-8.

PHILCO *WESTERN DEVELOPMENT LABORATORIES*

A SUBSIDIARY OF *Ford Motor Company*

3875 Fabian Way, Palo Alto, California

an equal opportunity employer

7757

Positions Open

(Continued from page 92A)

electronics or communications, for design and field engineering work. Projects will involve instrumentation for studies of the auroral ionosphere, radio-wave propagation, and geomagnetism. Salary in the $900-$1000 per month range. Write: Geophysical Institute, University of Alaska, College, Alaska.

CRITICAL VACANCIES AT GRIFFISS AIR FORCE BASE, ROME, NEW YORK

Research Psychologist (Engr.)	GS- 7 $5355 pa
Research Psychologist (Engr.)	GS 9 $6435 pa
Electronic Engr. (Electro Magnetics)	GS 11 $8340 pa
Librarian (Adm.) (Physical Sciences & Engr.)	GS 11 $7560 pa
Medical Officer (Occupational Health & Med.	GS 12 $8957 pa

Professional Group Meetings

Aerospace and Navigational Electronics

Boston—May 24

"One Plus One Equals Two," Dr. H. I. Ewen, Ewen-Knight Co. Natick, Mass.

Boston—May 15

"Radar Design for Manned Space Vehicles," G. J. Bonelle, Raytheon, Bedford, Mass.

New York—April 12

"Space GAA Problems and Solutions," R. O. Schroeder, Raytheon, Waltham, Mass.

New York—December 14

"Wide Aperture Direction Finding with Particular Reference to the Doppler System," J. Beukers, Servo Corp. of America, N. Y.

Philadelphia—April 3

"Video Tracker," L. Stinson, FAA-NAFC, Pamona, N. J.

Antennas and Propagation

Washington, D. C.—April 17

"Survey and Analysis of Mapping Antenna Characteristics," C. A. Bolt, Westinghouse, Baltimore, Md.

Antennas and Propagation Microwave Theory and Techniques

Columbus—May 21

"New Techniques for Designing Antenna Arrays," Dr. R. Harrington, Syracuse University, Syracuse, N. Y.

(Continued on page 96A)

Professional Group Meetings

(Continued from page 94A)

Orange Belt—March 21

"Strip Transmission Lines," Dr. S. Cohn, Rantec Corp.

Audio

Boston—May 24

"Room Response Simulation by Digital Computer as an Aid to Subjective Comparison of Audio Systems," Dr. A. G. Bose, MIT.

Milwaukee—May 22

"Future Developments in Magnetic Recording," M. Camras, Armour Res. Foundation, Chicago.

Milwaukee—April 24

"Performance Characteristics of Loudspeaker Arrays," J. F. Novak, Jensen Mfg. Co., Chicago.

Milwaukee—April 3

"Engineering Design Aspects and Problems of Modern Audio Equipment Manufacture," W. Hannah, Heath Co., Benton Harbor, Mich.

San Francisco—May 2

"Acoustic Measurements—What and How?" G. P. Wilson, University of California, Berkeley.

Automatic Control

Akron—February 20

"Adaptive Control Systems," Mr. Dommasch, Dodco, Inc.

Boston—April 10

Symposium "The State of the Art in New England Today."

Papers presented by: R. M. Prased, Foxboro Co.; R. C. McNabb, General Electric Co.; J. O. Faneuf, G. A. Biernson, P. R. Johannessen, Sylvania; Yu-Chi Ho, Harvard University; J. Katzenelson, L. A. Gould, MIT; A. Breecher, St. Regis Paper; A. Pugh, MIT.

New York—January 24

"Are Analog Computers Here to Stay in Process Control?" Dr. P. D. Hansen, Philbrick Researches, Inc., Boston.

New York—December 13

"Digital Techniques in Process Control," Dr. M. Silberberg, IBM Watson Res. Center, N. Y.

Bio-Medical Electronics

New York—April 24

"Instrumentation for the Microscopic Study of Dynamic Events in the Organs of Living Animals," E. H. Bloch, Western Reserve University, Cleveland

(Continued on page 98A)

COLLINS CALL

FOR SCIENTISTS & ENGINEERS

EQUIPMENT DEVELOPMENT

- BSEE — Elec. Eng. — 3 yrs. exp. HF or VHF (CR or D)
- BSEE — Elec. Eng. — 3 yrs. exp. Automatic Test and Checkout (CR or D)
- BSEE — Elec. Eng. — 6 yrs. exp. Power Servo Design (CR)
- BSEE — Elec. Eng. — 3-5 yrs. exp. UHF (CR or D)
- BSEE — Elec. Eng. — 3 yrs. exp. Command Control Systems (CR)
- BSEE — Elec. Eng. — 3 yrs. exp. Radar Beacon Work (CR)
- BSEE — Elec. Eng. — 3 yrs. exp. Television Transmission (CR)
- BSEE — GSE Supervisor — 5 yrs. exp. Equipment Development (CR)
- BSEE — GSE Eng. — 3 yrs. exp. Ground Support (CR)
- BSEE — Digital & Logic Design — 2-5 yrs. exp. (D)
- BSEE — Circuit Design — 1-5 yrs. exp. (D)
- BSEE — ECM — 2-5 yrs. exp. (D)

SYSTEMS

- MSEE — System Analyst — 5 yrs. exp. Modulation Technique (CR)
- MSEE or equiv. — System Analyst — 5 yrs. exp. Tracking and Ranging (CR)
- MSEE — System Analyst — 5 yrs. exp. Communications (CR)
- BSEE minimum — GSE Integration Supervisor — 5 yrs. exp. Ground Support (CR)
- MS or equiv. in Physics or Mechanics — System Analyst — 3 yrs. exp. Classical or Celestial (CR)
- BS — Field Supervisor — 5-10 yrs. exp. Airborne Electronics and Communications (CR)
- BS or equiv. in EE — Field Eng. — 3-5 yrs. exp. Com. (CR)
- BSEE minimum — GSE Layout Eng. — 5 yrs. exp. Layout (CR)
- BSME or equiv. — Mech. Eng. Supervisor — 8-10 yrs. exp. Management and Administration (CR)
- BSME or equiv. — Mech. Eng. — 3-5 yrs. exp. Packaging Designs (CR)
- MSME — Mech. Eng. — 3-5 yrs. exp. Thermal Design and Evaluation (CR)
- BSME or equiv. — Mech. Eng. — 3-5 yrs. exp. Environmental Test and Procedures (CR)
- BSEE — Elec. Eng. — 4 yrs. exp. Circuit Design and Com. (D)
- BSEE — Elec. Eng. — 3-5 yrs. exp. Microwave Systems (D)
- BSEE — Elec. Eng. — 3 yrs. exp. Tropospheric Scatter (D)
- BSEE — Elec. Eng. — 2-7 yrs. exp. UHF, Scatter, Microwave Systems Design (D)

GENERAL

- BSEE or higher — Resident Eng. — 3-5 yrs. exp. Communications (CR)
- BSEE or higher — Senior Staff Asst. — 8-10 yrs. exp. TV Theory (CR)
- BSEE — Test Eng. — 3-5 yrs. exp. Communication Design, Testing (CR)
- BSEE desirable — Logistics Eng. — 2-5 yrs. exp. Space Program Logistics (CR)
- BSEE or higher — R&D Eng. — 1-5 yrs. exp. Antenna Systems (D)
- BSEE — Elec. Eng. — 1-5 yrs. exp. Design Review and Prediction (D)
- BSEE — Project Test Eng. — 1-5 yrs. exp. Quality Assurance (D)
- BSEE — Telephone Eng. — 4-7 yrs. exp. Central Office (D)
- ME or IE — Staff Eng. — 2 yrs. exp. in MTM (CR, D or NB)
- MS or PhD — Solid State Physics — 3 yrs. exp. Thin Film Dev. (D)
- BSIE — Prod. Methods — 1-4 yrs. exp. (CR)
- BSEE or higher — Comp. Designer — Exp. in Network Theory (NB)

DATA

- BSEE or higher — Senior Staff Asst. — 8-10 yrs. exp. Digital (CR or NB)
- MS or PhD — Applied Math — 10 yrs. exp. Business Computing (CR or NB)
- BSEE — Elec. Eng. — 5-8 yrs. exp. Digital Data Design (D or NB)
- MS Applied Math — Business Programming — ext. exp. (D or NB)
- MS Applied Math — Logic Program Designer — 8-10 yrs. exp. (D or NB)
- PhD Applied Math — Logic Program Designer — 8-10 yrs. exp. (D or NB)
- BSEE or higher — Logic Designer — (NB)
- BSEE or higher — Peripheral Equip. Designer — (NB)

PLEASE NOTE

On listings marked (CR), send resume to L. R. NUSS, COLLINS RADIO COMPANY, CEDAR RAPIDS, IOWA

On listings marked (D), send resume to C. P. NELSON, COLLINS RADIO COMPANY, DALLAS, TEXAS

On listings marked (NB), send resume to E. D. MONTANO, COLLINS RADIO COMPANY, NEWPORT BEACH, CALIFORNIA

COLLINS

an equal opportunity employer

Professional Group Meetings

(Continued from page 96A)

New York—October 24

"Disc Electrophoresis," Dr. L. Ornstein, Mt. Sinai Hospital.

North Carolina—May 24

"Indirect Electronic Measurement of Blood Pressure," F. P. Hunter, University of Virginia.

Circuit Theory

Los Angeles—April 17

"Frequency Standards A State of the Art Survey," J. J. Caldwell, Jr., Space Technology Labs., Redondo Beach, Calif.

Los Angeles—January 18

"Solid State Microwave Power Generation," C. J. Carter and H. Miyahira, Space Tech. Labs., Los Angeles.

Philadelphia—May 23

"A Survey of Active RC Network Synthesis," N. Balabanian, Syracuse University.

Communications Systems

Monmouth—May 16

"The Morris Electronic Central Office," R. E. Ketchledge, Bell Telephone Labs., Whippany, N. J.

Monmouth—April 18

"HF Radio Data Transmission," B. Goldberg, U.S.A. Signal Research and Development Lab., Ft. Monmouth.

Monmouth—February 13

"Controlled Communications Concept," Dr. Richard Filipowsky, IBM Communications Center, Rockville, Md.

Monmouth—November 14, 1961

"Broad Aspects of Satellite Communications, Both Passive and Active Types," Dr. Hans K. Ziegler, USA Signal R&D, Ft. Monmouth.

"Advent Synchronous Satellite Communications Systems," Peter Maresca, Advent Agency, Ft. Monmouth.

Northern New Jersey—May 15

"Digital Computer Simulation of Communication Networks," R. L. Dujack, RCA, N. Y.

Rome-Utica—May 8

"Heat Effects in Drosophila Millanogaster," K. Wulff.

"The Effects of Magnetism on Transistors," Lester Gordy.

(Continued on page 100A)

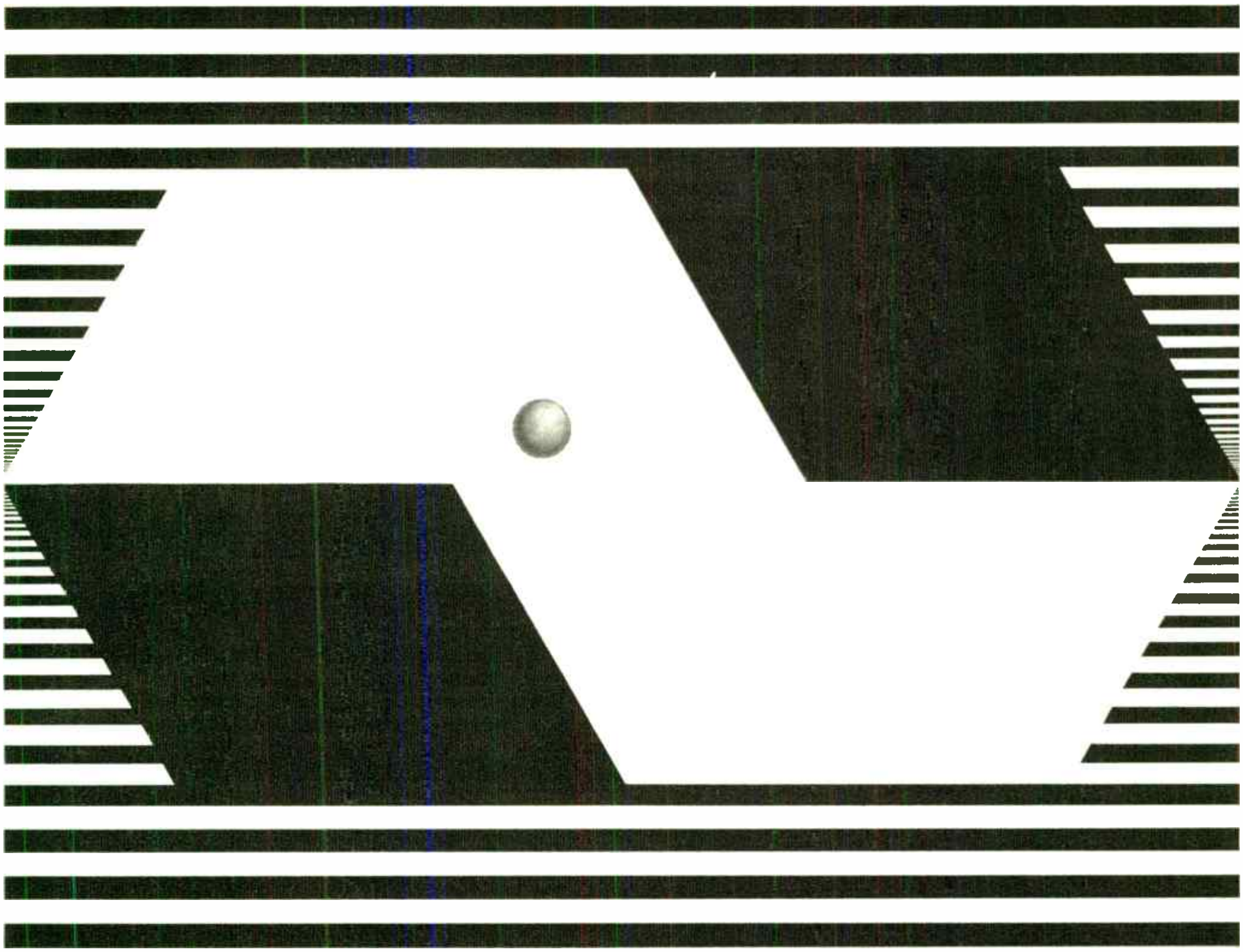

Explorers in the shape of things to come

An idea in the mind of man...that's where every achievement in the world begins. Peer into the minds of Lockheed Scientists and Engineers. There you see ideas in the making—ideas that some day will take on form and substance. Not all, of course. Some are too "far out." But, no matter how visionary, all ideas win serious attention.

As a result, this freedom of imagination has led to many distinguished accomplishments at Lockheed. And the future holds still more. For, among Lockheed's ever-expanding programs are: Spacecraft; Satellites; Man-in-Space Studies; Hypersonic Manned Aircraft; Advanced Helicopter Design; Sophisticated ASW and Ocean Systems.

Scientists and Engineers who thrive in an atmosphere of freedom; whose creative processes flourish through exchange of ideas; who relish exploring the unexplored—to such men we say: Lockheed has a place for you. For example: In Human Factors. Electronics Research; Thermodynamics; Guidance and Control; Stress; Servosystems; Reliability; Dynamics; Manufacturing Engineering; Astrophysics; Astrodynamics; Advanced Systems Planning; RF Equipment Engineering; Bioastronautics and Space Medicine; Weapons Effects; Aerophysics; Digital Communications; Antennas and Propagation Engineering; Tracking, Telemetry and Command Engineering; Communications Analysis. Send résumé to: Mr. E. W. Des Lauriers, Manager Professional Placement Staff, Dept. 1808, 2402 N. Hollywood Way, Burbank, California. An equal opportunity employer.

LOCKHEED
CALIFORNIA COMPANY
A DIVISION OF LOCKHEED AIRCRAFT CORPORATION

Professional Group Meetings

(Continued from page 98A)

"Microwave Plasma Interactions," Leonard Gordy.
Winners of 8th Annual Science Congress sponsored by Science Teachers Assn. of Mohawk Valley.

Rome-Utica—February 21

"Come North With Me," Col. B. Balchen, Dept. of Defense.

Component Parts

Los Angeles—May 14

"Aluminum Electrolytic Capacitors," W. McQueeny, Sprague Electric, North Adams, Mass.
"Power Supply Design," J. Fort, Natl. Cash Register, L. A.

New York—February 28

"Modern Trends in Relay Development," A. C. Keller, Bell Telephone Labs., Murray Hill, N. J.

Philadelphia—April 24

"Crimping as a Means of Termination," C. H. Stuart, Amphenol-Borg, Chicago.
"Systems Approach to Interconnections," E. Leshner, RCA, Camden.

(Continued on page 102A)

Professional Group Meetings

(Continued from page 100A)

COMPONENT PARTS
RELIABILITY AND QUALITY CONTROL

New York—April 9

"Economical Reliability Verification Tests," S. R. Calabro, Internat'l. Electric Corp., Paramus, N. J.

ELECTRON DEVICES

Albuquerque-Los Alamos—May 15

"Purpose of the Professional Group on Electron Devices," A. B. Church, Sandia Corp.

Los Angeles—May 8

"Tunnel Diodes as a General Circuit Element," J. Black, Hoffman Electronics, El Monte, Calif.

New York—May 3

"Introduction and Survey—Sources of High Frequency Electromagnetic Radiation," G. Wade, Raytheon, Burlington, Mass.

New York—April 11

"Recent Advances in Metal Interface Amplifiers," J. P. Spratt, Philco, Blue Bell, Pa.

New York—March 15

"General Theory of the Cesium Plasma Diode Energy Converter," Prof. W. B. Nottingham, MIT.

Philadelphia—May 31

"Electronic Image Converter and Intensifier Tubes," Dr. G. A. Morton, Conversion Devices Labs., RCA, Princeton, N. J.

Washington, D. C.—May 28

"General Techniques and Characteristics of Reading Machines," J. Rabinow, Rabinow Eng. Co., Rockville, Md

ELECTRONIC COMPUTERS

Baltimore—April 17

"BRLESC—The Ballistic Research Laboratories Electronic Scientific Computer," M. Weik, J. Gregory, M. Romanelli, R. Ellis, Computing Laboratory.

Boston—April 25

"Is Artificial Intelligence Just Around the Corner?" E. F. Moore, Bell Telephone Labs.

Detroit—April 5

"Machine Models of Self-Reproduction," Dr. E. F. Moore, Bell Telephone Labs., Murray Hill, N. J.

New York and Northern New Jersey—March 5

"High Density Recording," Dr. A. Gabor, Potter Instrument Co.

(Continued on page 104A)

APL

creator of complete satellite and missile systems

TRANSIT
TYPHON
TALOS
TARTAR
TERRIER

Working in a unique intellectual atmosphere, the professional men of APL play a significant role in advancing the frontiers of science and strengthening the nation's defense. The Laboratory's responsibilities encompass development and design engineering, theoretical and experimental research, and systems synthesis and analysis. Attractive career positions are available in:

Missile guidance and control systems • Digital and analog computing devices • Missile and space communications • Data storage and retrieval systems • Semiconductor micro-electronic devices • Warheads • Missile flight simulation • Flight planning, data acquisition, and analysis • Military operations research • Data processing and reduction • Computer programming and operation • Shipboard missile and fire control systems test • Theoretical and experimental research in fluid mechanics, microwave physics, combustion, and plasma physics.

Direct your inquiry to:
Professional Staff Appointments

The Applied Physics Laboratory
The Johns Hopkins University

8603 Georgia Avenue
Silver Spring, Maryland
(Residential suburb of Washington, D. C.)

AN EQUAL OPPORTUNITY EMPLOYER

ELECTRONICS ENGINEERS & PHYSICISTS

JOIN US IN GIVING A NEW DIRECTION TO AEROSPACE TECHNOLOGY thru RESEARCH & DEVELOPMENT in

aerospace electronics

Republic's Paul Moore Research & Development Center is the most sophisticated and integrated research complex in the East. Advances made here in many critical aerospace problem areas have brought Republic a diversity of new and follow-on R & D contracts leading to next-generation space and re-entry vehicles, satellites, space power and communication systems.

Electronics Engineers and Physicists are invited to consider the challenging opportunities to make important contributions on these programs in the areas of:

SPACE CRAFT COMMUNICATION — B.S., M.S.
Design and develop space vehicle communications systems including telemetry, command and on-board data handling.

DATA HANDLING (AS&SE) — B.S., M.S.
Design and develop ground station and on-board data handling systems for re-entry and space vehicle applications.

COMMUNICATION TECHNIQUES — B.S., M.S.
Develop advanced communications techniques for aerospace and space craft, includes communications theory and network synthesis.

ADVANCED SPACE RADARS — B.S., M.S.
Develop concepts and components for advanced space radar including rendezvous, mapping, acquisition and tracking applications.

RADAR INTEGRATION — B.S.
Develop specifications, install and integrate advanced radar in hypersonic and space vehicles, including antennas, transmitters, receivers, displays, power supplies, controls.

ANTENNA DESIGN — M.S.
Design and development of antennas for re-entry vehicles. Knowledge of wind effects and general re-entry radiation blackout problems.

RADAR TEST (GSE) — B.S.
Test, checkout and maintain ground radar systems. Make required circuit modifications including range gating circuits, modulators. No travel.

RE-ENTRY INSTRUMENTATION — B.S., M.S.
Design instrumentation for specific re-entry and space vehicles including telemetry systems.

MATHEMATICAL ANALYSIS CONTROLS — PhD.
Theoretical analysis of noise effects and non-linear mechanisms on automatic controls. Includes optimal control theory and generalized stability criteria.

ELECTRONIC INSTRUMENTATION — B.S., M.S.
Develop instrumentation for space vehicles. Knowledge of system integration and telemetry desirable.

SPACE GUIDANCE SYSTEMS — M.S., PhD.
Develop and analyze navigation and guidance systems using inertial and Doppler techniques and advanced nuclear gyros.

ECM REQUIREMENTS — B.S., M.S.
Mathematical analysis of ECM requirements for advanced aerospace and space craft, and specification of equipment.

FLIGHT CONTROL DESIGN — M.S.
Automatic flight controls, servo systems, nonlinear dynamic systems for space craft.

PYROTECHNIC CIRCUIT DESIGN — B.S., M.S.
Develop pyrotechnic missile circuits including safe arm, squib ignition and RFI elimination devices.

EXPERIMENTAL PHYSICIST — PhD.
Conduct experimental studies of the application of nuclear or electron resonance to gyroscopics.

ENVIRONMENTAL TESTING — B.S., M.S.
Undertake test programs to estimate component and system reliability using AGREE type methods; monitor offsite testing.

DESIGN REVIEW — B.S., M.S.
Perform mechanical or electronic design reviews, failure analyses, quantitative analyses and reports. Includes circuit analysis, component selection.

STATISTICAL ANALYSIS — B.S., M.S.
Apply statistical theory and method to prediction and analysis of aerospace component performance.

IDEP PRISM PROCEDURES — B.S., M.S.
Participate in "Interservice Data Exchange Programming" and "Program Reliability Information Systems for Management."

Interested applicants are invited to write in confidence to: Mr. George R. Hickman, Technical Employment Manager, Dept. 14H

REPUBLIC
AVIATION CORPORATION

FARMINGDALE, LONG ISLAND, NEW YORK
An Equal Opportunity Employer

Professional Group Meetings

(Continued from page 102A)

New York and Northern New Jersey—February 6

"Data Processing and Communications Requirements," A. Dumey, Data Sciences, Roslyn, N. Y.

New York and Northern New Jersey—November 13

"Marginal Checking in Transistorized Computers," L. W. Snell, IBM, Kingston.

New York and Northern New Jersey—September 28

"Management Games," B. Nanus (for Joel Kibbee), Remington Rand, N. Y.

Santa Ana—May 24

"A Quasi Analog Computer Design Based on the Quantization of Trapped Flux in a Superconductor," Dr. S. Frankel, Computron.

Syracuse—May 22

"Logic Design Trends in Digital Computers," C. W. Adams, Adams Associates.

Engineering Management

Binghamton—April 30

"Engineering—What Do You Want to Do?" W. J. Steen and L. L. Grebe, IBM, Owego, N. Y.

(Continued on page 107A)

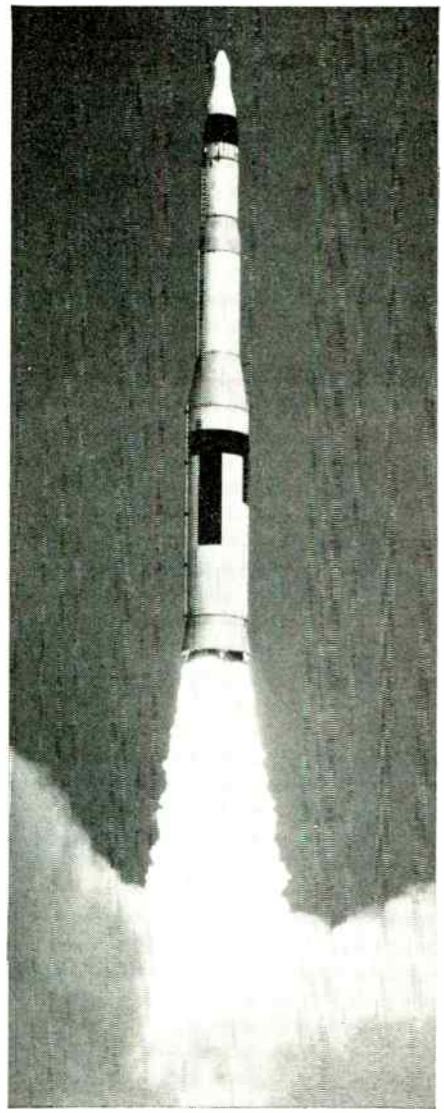

BOEING OPENINGS FOR ELECTRONIC/ELECTRICAL ENGINEERS

Boeing's Aero-Space Division, holder of major contracts on such advanced space programs as SATURN, DYNA-SOAR and MINUTEMAN, has a number of immediate, long-range openings offering professional challenge, and in many instances, unique ground-floor opportunities in newly-formed divisional organizations.

ELECTRONIC/ELECTRICAL engineering assignments are available in many areas, including the design of electronic equipment, the development of improved design techniques, electronic parts, electronic packaging techniques and the design and development of improved electronic systems.

Salaries are commensurate with all levels of education and experience. Minimum requirements are a B.S. degree in any applicable scientific discipline. Most of the assignments are in the uncongested Pacific Northwest, offering outstanding family living and recreational advantages.

Send your resume, today to Mr. Lawrence W. Blakeley, The Boeing Company, P. O. Box 3822 - PRR, Seattle 24, Washington. The Boeing Company is an equal opportunity employer.

P.S. Seattle is the scene, April 21 to October 21, of the science-oriented Century 21 World's Fair. The Fair's Boeing-sponsored Spacearium in the Science Pavilion offers simulated flights through outer space. Fair visitors are invited to stop in at the Boeing Professional Employment Information Center, near the Fair's Science Pavilion entrance.

BOEING

Divisions: Military Aircraft Systems • Transport • Vertol • **AERO-SPACE** • Industrial Products—Boeing Scientific Research Laboratories

Professional Group Meetings

(Continued from page 104A)

Chicago—May 24

"Integrated Management for Integrated Electronics," C. H. Knowles, Motorola.

Chicago—March 16

"Financial Planning for Engineering Managers," M. H. Daskel, M. H. Daskel, Inc., Chicago.

Chicago—January 26

"The Electronic Industry's New Partner—University Research," Dr. T. Jones, Purdue University.

Chicago—October 10

"Future of Chicago Area Electronics," A. Rubenstein

Panel Discussion—E. Terman, W. Everett, D. Noble, J. Kennedy.

Chicago—October 9

"Engineering Management Papers," E. White, Warwick, Skokie, Ill.

Chicago—October 4

"New Products"—Panel Discussion, Chairman—E. White.

San Francisco—March 21

"PERT, a New and Valuable Management Tool," R. M. T. Young, Lockheed Missiles and Space Co.

Engineering Writing and Speech

Philadelphia—May 23

"Suddenly, Upon the Waters"—16 mm color moving picture.

Philadelphia—February 14

"How Better to Tell the Public about Developments in the Several Sciences," Dr. H. C. Wolfe, AIP; P. Fraley, CASW; E. G. Sherburne, Jr., AAAS.

Philadelphia—December 13

"Recent Developments in Graphic Arts and Reproduction," J. P. Banta, Alfred J. Jordan, Inc.; D. Biggs, American Type Founders Co.

Syracuse—May 24

"The Challenging Future of Investigations in Human Communication," J. D. Chapline, Philco Corp., Willow Grove, Pa.

Information Theory

San Francisco—May 10

"Mind, Machine, and Soul," Dr. L. Fein.

(Continued on page 108A)

Professional Group Meetings

(Continued from page 107A)

INSTRUMENTATION

Atlanta—June 1

"Observations of the European Electronics Industry," G. B. Robinson, Scientific Atlanta.

Boston—May 11

"State-of-the-Art in Electrical Measurements," Dr. J. L. Thomas, Natl. Bureau of Standards, Washington, D. C.

Philadelphia—May 14

"Basic Measurements—Present State of the Art," Dr. J. L. Thomas, National Bureau of Standards.

Philadelphia—April 16

"Component and Circuit Analysis Using Swept Frequency Techniques," K. A. Simons, Jerrold Co., Philadelphia.

INSTRUMENTATION RELIABILITY AND QUALITY CONTROL

Chicago—May 11

"Component Noise, Its Measurement and Use in Reliability Prediction," A. P.

(Continued on page 110A)

COMPLETE SOUND and VIBRATION ANALYSIS with THREE PERMANENT VISUAL RECORDS

KAY *Vibralyzer*®

CAT. NO. 651-A

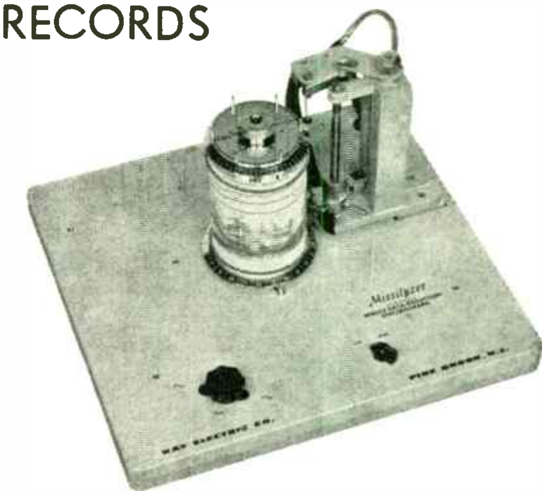

VIBRATION ANALYZER

$2495.00 f.o.b. factory **$2744.50 f.a.s, N. Y.**

An audio and sub-audio spectograph in the 5-4400 cps range, ideal for analysis of transient signals as well as steady state measurements of vibration and noise from aircraft, ships, reciprocating and rotating machinery, and in the fields of acoustics, ordnance, ballistics, seismology, and biophysics. Makes 3 permanent visual records.

SPECIFICATIONS

FREQUENCY RANGES: 5-4400 cps in 3 bands.

Freq. Range	Analyzing Filter-Band Narrow	Wide	Duration of Recorded Sample
5-500 cps	2 cps	20 cps	20 secs.
15-1500 cps	6 cps	60 cps	6.6 secs.
44-4400 cps	20 cps	200 cps	2.4 secs.

Frequency Calibration: Markers at 30 cps or 240 cps intervals may be recorded on analysis paper.

Record-Reproduce Amplifier Characteristics: Frequency response switchable to provide flat (or for transducer usage) 44 or 60 db falling characteristic.

Pickup Devices: Vibration pickups: microphones or other properly matched devices may be used.

Input Impedance: High, 1.8 megohms.

Input Signal Sensitivity: Approx. 3 mv rms for full scale operation.

VISUAL RECORDS

DISPLAY NO. 1

(Vibragram) Frequency vs Amplitude vs Time characteristics. Linear with respect to frequency and time.

DISPLAY NO. 2

(Section) Intensity vs Frequency at any 6 times in recorded 2.4 sec. interval. Makes up to 6 separate sections on one sheet or 300 on 50 sheets of recorded sample using sectioner micrometer plate. Dynamic Ranges: linear scale—10:1; logarithmic scale—35 db.

DISPLAY NO. 3

(with Amplitude Display Unit) Average Amplitude vs Time. Amplitude scale logarithmic over 24 db and 34 db ranges.

AMPLITUDE DISPLAY UNIT (Accessory for recording Display No. 3)........$175.00

PERMANENT RECORDS

DISPLAY NO. 1

Frequency

Time

Frequency & Amplitude vs. Time.—4" x 12" record on facsimile paper.

DISPLAY NO. 2

Frequency

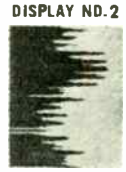

Intensity

Intensity vs. Frequency at Selected Time. Range: 35 db.

DISPLAY NO. 3

Amplitude db

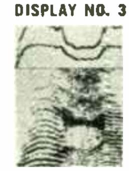

Time

Average Amplitude vs. Time. Logarithmic scale, 24 and 34 db ranges.

KAY *Missilyzer*®

CAT. NO. 675 **5-15,000 cps**

- Two separate channels for simultaneous recording of two signals.
- Remote control of recording and reproducing channel selectors.

The Missilyzer is a wider range spectrum analyzer providing two identical channels for simultaneous recording of two related signals. Built-in, fast-acting relays permit rapid automatic remote control.

SPECIFICATIONS

FREQUENCY RANGE: Standard models, 5-15,000 cps, in bands listed below.

Freq. Range	Analyzing Filter-Band Narrow	Wide	Duration Recorded Sample
5-500 cps	2 cps	20 cps	20 secs.
15-1500 cps	6 cps	60 cps	8.0 secs.
50-5000 cps	20 cps	200 cps	2.4 secs.
150-15,000 cps	60 cps	600 cps	0.8 secs.

Record-Reproduce Amplifier Characteristics: Frequency response switchable to provide FLAT or (for transducer usage) either 44-db or 60-db falling characteristic.

Frequency Calibration: Calibration markers at 30 cps or 240 cps intervals may be recorded on analysis paper.

Input Impedances, Selectable: High, 1.8 Megohms for low level and microphone input. Low, for high level signals, such as from tape recorders.

Price: $2,950.00 f.o.b. factory. **$3,245.00 f.a.s., N. Y.**

For complete details and prices on the entire line of Kay Sound and Vibration Analysis equipment, write:

KAY ELECTRIC COMPANY

DEPT. I-10 MAPLE AVENUE • PINE BROOK, MORRIS COUNTY, N. J. CApital 6-4000

Visit Kay at the Wescon Show • BOOTHS 3411-3412

Professional Group Meetings

(*Continued from page 108A*)

Stansbury, Quan-Tech Labs., Boonton, N. J.

MICROWAVE THEORY AND TECHNIQUES

New York—May 3

"Survey of Microwave Sources of Power," Dr. G. Wade, Raytheon, Burlington, Mass.

Orlando—April 11

"Evaluation and Use of Antenna Ranges for Pattern and Reflectivity Measurements," Dr. E. F. Buckley, Emerson and Cuming, Inc.

Washington, D. C.—May 15

"Cryogenic Metallurgy and Microwaves," Dr. F. E. Werner, Westinghouse Res. Labs.

MICROWAVE THEORY AND TECHNIQUES/ANTENNAS AND PROPAGATION

Albuquerque-Los Alamos—May 10

"Low Level Microwave Power Comparator."

"High Level Microwave Power Comparator," C. A. Denny, C. L. Mavis, and C. J. Still, Sandia Corp.

Baltimore—May 9

"High Efficiency Traveling Wave Tubes for Modern Microwave Systems," G. I. Klein, Westinghouse.

MILITARY ELECTRONICS

Los Angeles—May 23

"Relay Communications Satellite System," M. Brady, Space Technology Labs., Redondo Beach, Calif.

NUCLEAR SCIENCE

Albuquerque-Los Alamos—April 17

"High Voltage Engineering in Sherwood," A. E. Shoefield, Los Alamos Scientific Lab.

Chicago—May 11

"Solid State Particle Detectors," N. J. Hansen, Argonne National Lab.

PRODUCT ENGINEERING AND PRODUCTION

Boston—May 22

"Microelectronics as of May 22, 1962," Dr. H. G. Rudenberg, Arthur D. Little Co.; D. A. McLean, Bell Labs.; S. M. Stuhlbargq, P. R. Mallory, Inc.; G. J. Selvin, Sylvania; E. B. Sussman, Texas Instruments.

(*Continued on page 112A*)

Professional Group Meetings

(Continued from page 110A)

Los Angeles—May 18

"Design Automation at Burroughs," L. L. Bewley, Burroughs Electrodata, Pasadena.

Los Angeles—April 25

"Plastics as a Product Design Medium," G. Clark, W.E.M.S. Inc. Hawthorne, Calif.

Los Angeles—March 19

"Tour and Talks on Burroughs B200 and B500 Computers," Burroughs Personnel, Burroughs Corp., Pasadena.

Los Angeles—February 21

"Thom's Law," C. Weber, Daedalus Co., Woodland Hills, Calif.

New York—February 28

"Modern Trends in Relay Development," A. C. Keller, Bell Telephone Labs., Murray Hill, N. J.

Philadelphia—May 15

"A Night on Site" (A talk and tour of BMEWS at Moorestown), R. Welsh, RCA, Moorestown, N. J.

Washington—May 17

"The Status of Microelectronics," Dr. W. Liben, Johns Hopkins University, Silver Spring, Md.

Radio Frequency Interference

Los Angeles—May 17

"Application of Suppression Components," E. Wheeler, Filtron Co., Los Angeles.

"Power Density vs. Field Intensity RFI Measurements," R. Friedman, Polarad Electronics Corp., N. Y. C.

Reliability and Quality Control

Binghamton—May 14

"Reliability in Space Programs," R. E. Kuehn, IBM, Fort Lauderdale, Fla.

New York—February 12

"Theory of Games Applied to Electronic Reliability Problems," V. Selman, International Electric Corp., Paramus, N. J.

New York—January 15

"The Availability of a System as a Sequential Test Parameter," J. H. Bailey, IBM Corp.

Space Electronics and Telemetry

Philadelphia—May 15

"A Proposed System for the Automatic Determination of the Time and

(Continued on page 114A)

A 300 KC Solid State Counter for $750

Measure frequency and ratio directly; measure speed, rpm, pressure, temperature, acceleration or any phenomena that can be converted with transducers to ac or pulses.

The same design, circuitry and construction features of all new transistorized ⓗⓟ counters are incorporated in this low-priced, general-purpose counter. Time base is derived from the power line, providing 0.1% accuracy—fully adequate for many frequency measurements. The counters have a maximum counting rate of 300 KC. 0.1 v sensitivity permits low-level measurements.

Model 5211A has gate times of 0.1 and 1 second. Model 5211B has an additional gate time of 10 seconds. Otherwise, the instruments are identical. A storage feature, which can be disabled by a rear-panel switch, provides a continuous display, each reading held on the 4-digit neon columnar readout until the count itself changes. The counters provide a 1-2-2-4 BCD code output for systems use or recording devices. Manual gate allows the 5211 counters to be controlled by the front panel, or be operated remotely by contact closure or suitable pulses.

Solid state design and construction provide low power consumption, low heat dissipation, operation over a wide temperature range. The counters are housed in the new ⓗⓟ modular cabinet for bench and rack mount. Plug-in circuit modules and ready accessibility simplify maintenance. Both models weigh but 10 lbs. and can easily be carried in one hand. Conservative design features, such as the use of decade dividers in the gate generating circuits, provide operational stability and eliminate calibration problems.

Specifications

Maximum counting rate:	300 KC
Display:	4 digits, neon column
Input sensitivity:	0.1 v rms sine wave
Temperature range:	—20 to 50°C
Time base:	50 or 60 cps power line
Manual gate:	Controlled by front panel function switch, by external contact closure, or by 3 volt peak positive pulses at least 10 μsec wide at half amplitude point.
Frequency measurement:	2 cps to 300 KC; accuracy ± 1 count, ± time base accuracy
Ratio measurement:	Reads: (f_1/f_2) Range: f_1: 2 cps to 300 KC (0.1 v rms) f_2: 100 cps to 300 KC (1 v rms into 1000 ohms) Accuracy: ± 1 count of f_1, ± trigger error of f_2
Dimensions:	16¾" wide x 3½" high x 11½" deep, 10 lbs.
Price:	ⓗⓟ 5211A, $750.00; ⓗⓟ 5211B, $825.

Data subject to change without notice. Prices f.o.b. factory.

HEWLETT-PACKARD COMPANY

1501 Page Mill Road, Palo Alto, California
Area Code 415, DA 6-7000
Sales and service representatives in all principal areas; Europe, Hewlett-Packard S.A., 54-54bis Route des Acacias, Geneva; Canada, Hewlett-Packard (Canada) Ltd., 8270 Mayrand Street, Montreal.
7903

Professional Group Meetings

(Continued from page 112A)

"Distance of Closest Approach of an Orbiting (Transmitting) Earth Satellite," P. I. Klein, Sophomore, University of Pennsylvania.

Philadelphia—April 17

"Feedback in FM Receiver Systems," L. I. Kozick, ITT Labs., Nutley, N. J.

Vehicular Communications

Detroit—April 25

"Extender Operation—Automatic Electronic Ignition Noise Suppression," J. Germain, Motorola, Chicago.

Detroit—March 29

"Noise Suppression in Mobile Communications Equipment," S. Meyer, Hammarlund Mfg. Co.

Los Angeles—May 17

"Field Trip Through Studios, with Descriptions of Operations," Messrs. Pickett and Pierce, NBC Engineering Dept.

Vehicular Communications Broadcasting

Florida West Coast—May 23

"Review of Up-to-the-Minute Developments in Test Equipment," G. Dashiell, Stiles Associates.

Section Meetings

Albuquerque-Los Alamos

"Experiments to Measure the Gamma Radiation of the Lunar Surface," M. A. Van Dilla, Los Alamos Scientific Laboratory; Election of Officers; 5/18/62.

Joint Dinner Dance with AIEE; 5/29/62.

Atlanta

"Recent Observation of the Electronics Industry in Europe," G. Robinson, Scientific-Atlanta; 6/1/62.

Baltimore

"Responsibilities of Broadcasters to the Public," B. Gunts, WBAL TV; Ladies' Night, Dinner and Dance; 5/12/62.

Binghamton

"Artificial Intelligence and Machine Learning," A. L. Samuel, IBM; 6/7/62.

Boston

"Recent Developments in Lasers," C. Townes, Mass. Inst. of Tech.; Election of Officers; 5/23/62.

Buffalo-Niagara

"Computer Uses II," J. T. Fleck & G. E. Richmond, Cornell Laboratories; 4/18/62.

Installation of New Officers; 5/18/62.

Canaveral

"Development and Flight Test Highlights of Polaris Program," K. Jackson, Lockheed; 5/17/62.

(Continued on page 115A)

New Bourns Subminiature Relay– Its Reliability Is as High as Its Size Is Small

You can see that it's little and you can bet that it's reliable. Only .2" x .4" x .6", but a steady performer even at 40 G, 55-2000 cps, this subminiature SPDT relay is designed to meet all environmental requirements of MIL-R-5757D. Its features include single-coil design, rotary balanced armature, hermetically sealed case and self-cleaning long-life contacts. Efficient coil design and packaging improve sensitivity to just 100 mw maximum.

By subjecting every unit to a 5000-operation run-in, Bourns precludes the possibility of relay "infant mortality." To further ensure consistent quality, Bourns conducts 100% final inspection for all important relay characteristics including mass spectrometer leak testing. The last and most punishing test of quality is the trip taken by monthly samples through the Bourns Reliability Assurance Program. This is one of the most extensive series of electrical and environmental tests in the electronics industry, and has long been the reliability double-check for the famous Trimpot® potentiometer. With Bourns relays, as with Bourns potentiometers, every possible step is taken to see that the quality you specify is the quality you get.

Units are available now from the factory, and will soon be available through Bourns distributors as well. Write for complete technical data.

Size: .2" x .4" x .6"
Maximum operating temperature: 125°C
Contacts: SPDT; Rating: 1.0 amp resistive, 26.5 VDC
Coil resistances: 50Ω to 2000Ω
Pick-up sensitivity: 100 milliwatts
Vibration: 40 G standard, 60 G special
Shock: 150 G

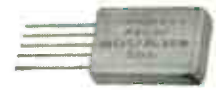

ACTUAL SIZE

Manufacturer: Trimpot® potentiometers; transducers for position, pressure, acceleration. Plants: Riverside, California; Ames, Iowa; and Toronto, Canada

Section Meetings

(Continued from page 114A)

Columbus

"Satellite Communications" Panel Discussion L. Jaffee, NASA; L. Bollinger, Ohio State Univ.; G. Harter, Space Tech. Lab.; J. Glaser, Bell Telephone; 4/26/62.

"L Band Tunnel Diode," J. Phelps, General Electric Co., 5/8/62.

Dallas

"The Effect of the Atmosphere on Radio Transmission," A. N. Straiton, Univ. of Texas; 5/22/62.

Dinner and Dance, Installation of New Officers; 5/26/62.

Detroit

"Parametric Amplifier—Performance and Applications," E. I. Gordon, Bell Telephone Labs.; Discussion of Proposed Merger of IRE with AIEE, T. A. Hunter, Vice President of IRE; 2/23/62.

"Obfuscation by Intent," J. R. Kershaw, Mich. Bell Telephone Co.; "How Electrical Communications Transformed the World," H. Pratt; Secretary of the IRE; Tour of the Electrical Section of the Henry Ford Museum; 4/20/62.

Egypt

"Video Tape Recording," E. M. Fawsy Yassin, UAR Broadcasting & TV; 5/7/62.

Elmira-Corning

"Digital Computer Course Session I," R. Conway, Cornell University; 4/9/62.

"Digital Computer Course Session II," R. Conway, Cornell University; 4/23/62.

(Continued on page 118A)

JFD MAX-C

Sliding Piston Capacitors Specified For Precise Wide ΔC Tuning in Collins RF Phase Stability Analyzer

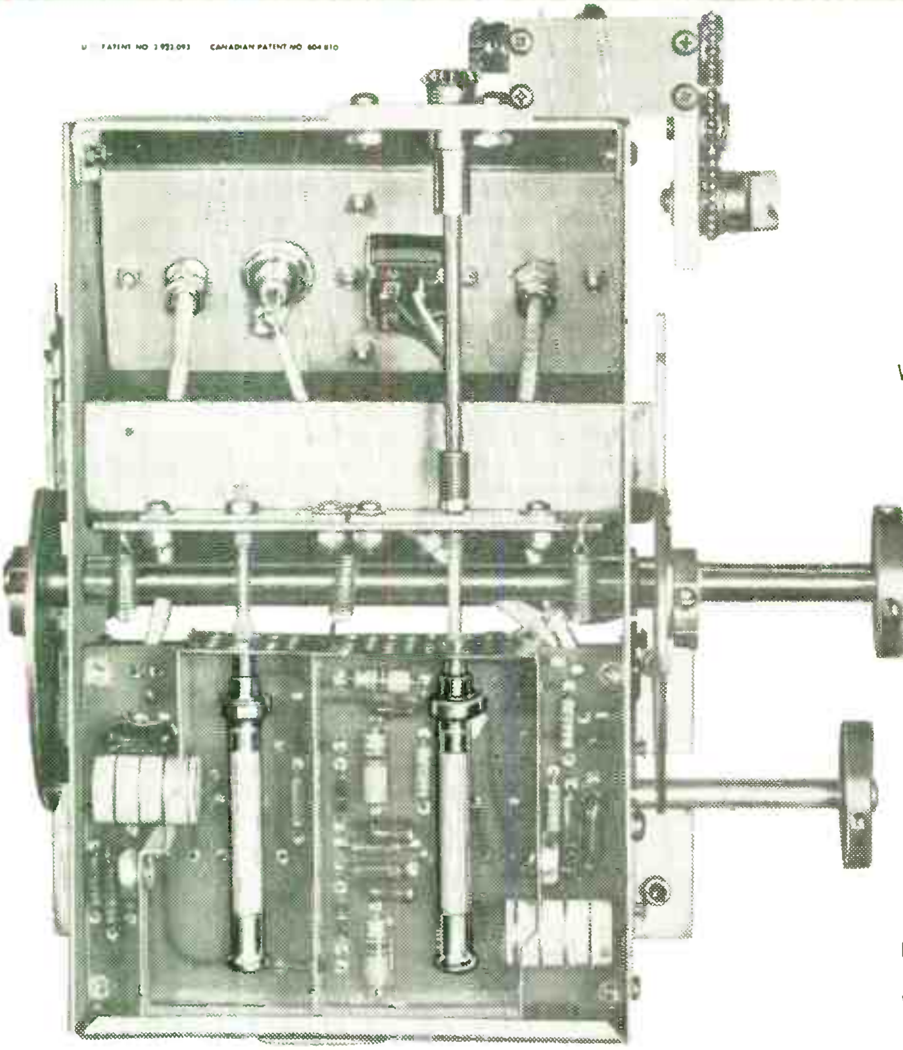

Two ganged cam-driven JFD MAX-C VCJ496 Sliding Piston Capacitors insure precise and stable linear tuning for 1-110 mc. Tunable Phase Detector of Collins RF Analyzer.

When circuit designs of an exclusive new RF Phase Stability Analyzer built for the U.S.A.S.R.D.L.* called for absolutely stable and linear frequency tuning with low noise and minimum microphonics, Collins Radio Company engineers turned to JFD Electronics.

To match the exacting requirements, JFD development engineers came up with the custom-designed VCJ496 and VCJ497 capacitors. One of the outstanding innovations of these capacitors was a sliding piston that was activated by compensated cams for straight line frequency tuning. Another was JFD's MAX-C construction that tripled the tuning range (5-180 pf. per unit) with no increase in size or weight. Use of special glass and invar for zero temperature coefficient provided the absolute stability necessary for exacting measurement.

Today, the Collins Phase Stability Analyzer is performing measurements of instantaneous phase deviation on RF signal sources with a resolution which varies from 0.001 degrees at 1 mc. to 0.11 degrees at 110 mc.

This is one more example of how creative JFD variable capacitor technology added to your engineering team can meet and beat the toughest high frequency specifications.

This is one more reason why you can rely on the skills, the talent, and the resources of JFD for your special or standard trimmer capacitor needs.

Call your local JFD Field Office or your nearest JFD franchised distributor for assistance.

*United States Army Signal Research and Development Laboratory

COLLINS RF PHASE STABILITY ANALYZER

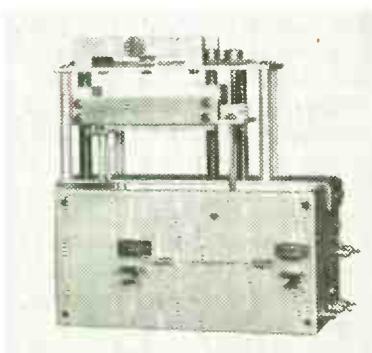

One VCJ497 Sliding Piston Trimmer (not shown) in 1-110 mc. Variable Crystal Reference Oscillator provides necessary frequency stability and accuracy in frequency tuning circuit.

4-Wire Printed Circuit Mounting
JFD VCJ496
MAX-C Sliding Piston Trimmer Capacitor
5 pf. to 180 pf.

actual size

Panel Mount
JFD VCJ497
MAX-C Sliding Piston Trimmer Capacitor
1 pf. to 50 pf.

See JFD Booths 708-709 at WESCON 1962

JFD

AT WORK IN THE NEW FRONTIERS OF ELECTRONICS

JFD ELECTRONICS CORPORATION

Components Division • 6101 16th Avenue, Brooklyn, New York • Phone DEwey 1-1000 • TWX-NY25040

JFD WESTERN	JFD MIDWESTERN	JFD NORTHEASTERN	JFD CANADA
P. O. Box 3416	P. O. Box 588	Ruth Drive, P. O. Box 228	51 McCormack Street
Van Nuys, Calif.	Skokie, Illinois	Marlboro, Mass.	Toronto, Ontario, Canada
Phone: EMpire 4-4131	Phone: 675-1140	Phone: HUntley 5-7311	Phone: ROger 9-1129

VARIABLE TRIMMER PISTON CAPACITORS • FIXED METALIZED INDUCTORS • LC TUNERS • FILTERS • DIPLEXERS
FIXED AND VARIABLE DISTRIBUTED AND LUMPED CONSTANT DELAY LINES • PULSE FORMING NETWORKS

Section Meetings

(Continued from page 116A)

"Digital Computer Course—Session III," R. Conway, Cornell University; 4/30/62.

"Digital Computer Course—Session IV," R. Conway, Cornell University; 5/7/62.

Installation of Officers, 5/31/62.

FLORIDA WEST COAST

"Stanford Two Mile Linear Accelerator Center to be developed at Stanford University, California," G. A. Loew, Stanford University; 5/16/62.

FORT HUACHUCA

Talk about the SHOEBOX, a recognition device at IBM; 2/26/62.

"International Cooperative Space Science," H. Richter, Electro Optical Systems, Inc.; 4/24/62.

"Unintentional Duplication of Effort and Its Organization," R. E. Frese, USAFPG; 5/29/62.

FORT WORTH

"The Air Force Laboratory and its Relationship to Universities and Industry," L. S. Sheingold, United States Air Force; 5/8/62.

INDIANAPOLIS

Student Papers Awards Night; 4/12/62.

"High Fidelity," H. Howard, Graham Electronics; Election of Officers; 5/24/62.

KANSAS CITY

Annual Section Picnic; 6/9/62.

LOS ANGELES

"Space Age Problems," W. Brady, AFSC; Students Nat'l and Local Awards Presentation; Joint with San Fernando Valley; 4/11/62.

"Navy Space Objectives," R. F. Freitag, BuWeps; "Project Transit," R. B. Kershner, Johns Hopkins Univ.; Joint with Buenaventura; 5/11/62.

Annual Installation & Awards Dinner Dance; 6/2/62.

LOUISVILLE

"Developments in Applications of Thermoelectricity," A. Cybriwsky, General Electric Co.; Tour of the Applied Physics Lab. Building 6, Appliance Park; 4/27/62.

MILWAUKEE

"Electronic Data Processing," Personnel of Wisconsin Telephone Co.; 4/18/62.

"The Engineer at the Crossroads," P. Haggerty, President of IRE; 5/3/62.

"Inertial Guidance," R. G. Brown, AC Spark Plug Division; 5/10/62.

MONTREAL

"The Radio Exploration of Space," P. M. Millman, Nat'l Research Council; 5/9/62.

"Bio Medical Electronics," J. Davis, McGill University; 5/25/62.

NEW ORLEANS

"The Two Million Watt Navy VLF Transmitter at Cutler, Maine," M. W. Bullock, Continental Electronics Mfg. Co.; 6/14/62.

NORTH CAROLINA

"Magnetic Memory Devices," J. C. Stuart, Bell Telephone Co.; 5/18/62.

ORLANDO

"Optical Masers," B. M. Oliver, Hewlett Packard Co.; 2/23/62.

"Neural Networks," T. B. Martin, RCA; 3/14/62.

"Telemetry for Large Space Vehicles," W. O. Frost, NASA; Election of Officers; 4/25/62.

PRINCETON

"Hydrogen Fusion and the C-Stellarator," F. K. Bennett, Princeton University; Tour of the C-Stellarator facility; 5/18/62.
Annual Dinner Dance; 5/25/62.

ROME-UTICA

"Come North With Me," B. Balchen, Dept. of Defense; 2/21/62.
"Communications by Orbiting Dipoles," R. M. Lerner, MIT Lincoln Labs.; 4/10/62.
Student Papers Award Night; 5/8/62.

SACRAMENTO

"Light and Gravitation—Some Speculations," C. W. Carnahan, Consultant; 6/14/62.

SALT LAKE CITY

"Propagation of High Frequency Radio Waves by Ionospheric Scattering," C. D. Westlund, Univ. of Utah; 2/16/62.
"The Role of the Tactical Data System in the Free World's Defense Programs," T. M. O'Donnell, Litton Industries; "Prospects for the Salt Lake Plant of Litton Data Systems," V. D. Carver, Litton Industries; 3/16/62.
"Recent Research in Musical Acoustics," H. Fletcher, Brigham Young University; 4/20/62.
Student Papers Competition; 5/11/62.

SAN DIEGO

"The Application of Thin Films to Integrated Circuits," J. R. Black, Motorola; 5/2/62.
"Microwave Tubes and Their Applications," L. W. Clampitt, Raytheon Co.; 6/6/62.

SOUTH BEND—MISHAWAKA

"Computer Control in Petroleum Refining," T. O'Neil, American Oil Co.; 2/23/62.
"Sound Transmission in the Ocean and Its Problems," C. M. Wallis, Univ. of Missouri; 3/29/62.
Annual Banquet; 4/28/62.

SYRACUSE

Description of a trip to the North Pole in a Nuclear Submarine, Commander Steele, USN; Joint Meeting with Ottawa, Canada Section; 5/18/62.

VIRGINIA

"Image Intensifiers (Astracon)," J. A. Hall, Westinghouse Electric Corp.; 4/13/62.
"On-Line Data Transmission," E. B. Lorscheider, IBM; 4/27/62.
Student Papers Competition; 5/11/62.
"Bell System Project 'Telstar'," J. E. Hite, Jr., Chesapeake & Potomac Tel. Co.; 5/18/62.

WASHINGTON

Discussion of the proposed IRE/AIEE Merger, B. Voight, W. Swift, S. Bailey; 5/14/62.

WESTERN MASSACHUSETTS

"You Can Get There From Here," J. Zacharias, Sprague Electric Co.; 5/22/62.

WINNIPEG

Tour of Pelissier's Brewery; 4/27/62.

SUBSECTIONS

CATSKILL

"Electronic Switching System," J. Harr, Bell Telephone Labs.; Election of Officers; 5/24/62.

CRESCENT BAY

"Electronic Design of the Supersonic Transport," W. McCloud, Douglas Aircraft Co.; 4/16/62.
"Automatic Checkout Equipment—Sereb," J. Slocum, Packard Bell; 5/21/62.

LEHIGH VALLEY

"Electrical Engineering Education in the 1960's," Discussion—L. J. Conover, Lafayette College; J. J. Karakash, Lehigh Univ.; R. W. Showers, Univ. of Penna.; W. Smith, Lafayette College; 2/21/62.
"Effects of Specialization on the Development of Leadership," H. A. Schulke, Jr., USA; 3/27/62.
"Biomedical Engineering," D. Geselowitz, Univ. Penna.; 4/19/62.
"A Look Into The Future of Communication Technology," J. D. Tobo, Bell Tel. Labs.; Election of officers; 5/17/62.

MONMOUTH

Field Trip to Industrial Reactor Lab., Inc., Plainsboro, N. J.; R. W. Houston; 3/21/62.
"HF Radio Data Transmission," B. Goldberg, USA, 4/18/62.
"The Morris Electronics Central Office," R. W. Ketchledge, Bell Telephone Labs.; Joint with PGCS; 5/16/62.

PALM BEACH

"Missile Scoring with Nuclear Radiation," R. Wernlund, Franklin Systems Inc.; 1/19/62.
"Data Acquisition at the Atlantic Missile Range," K. Raulins, RCA; "Data Processing at the Atlantic Missile Range," C. Scott, RCA; Installation of New Officers; 2/20/62.
"Nation-wide Data Communications," C. B. McKinney, Southern Bell Tel. & Tel Co.; 3/20/62.

RICHLAND

"Non-Destructive Testing of Hanford Fuel Elements," C. Denton, G.E. Co.; 4/18/62.
"A Biological Study of Alaska," J. R. Davis, G.E. Co.; 5/18/62.

SAN FERNANDO VALLEY

"The X-15 Flight Research Program," J. A. Walker, NASA; 1/17/62.

(Continued on page 120A)

Section Meetings

(Continued from page 119A)

Discussion of the proposed IRE/AIEE Merger, B. Anglin, W. Peterson, J. Guerrera; 2/12/62.

"The Rover Project at the Nevada Proving Grounds," J. H. Germain, Edgerton, Germeshausen & Grier, Inc.; 3/19/62.

"The Long Look Into Space," Gen. Ritland, Aerospace; Joint with Los Angeles Section; 4/11/62.

"New Worlds in Old Oceans," F. P. Higgins, Jr., Lockheed Aircraft Corp.; 5/16/62.

Santa Barbara

"Radio Astronomy (change)," G. Gamow, Univ. of California; 5/15/62.

Southern

"System Engineering Aspects of the Air Force Space Programs," E. J. Barlow, Aerospace Corp; 5/16/62.

Westchester

"A System Designer Surveys the Radio Spectrum," D. J. Blattner, RCA; 2/28/62.

"VHF Ionospheric Scatter Communications," R. C. Kirby; Natl. Bureau of Standards; 3/7/62.

"Data Processing (Receive) Functions that can be Obtained by Combining Certain Electro-Optical Techniques," M. Arm, Columbia University; 4/4/62.

"Interplanetary and Interstellar Communication Potential of the Laser," D. S. Fayley, General Precision, Inc.; 4/11/62.

"Tropospheric Scatter Communications," L. P. Yeh, Page Communications Engrs., Inc.; 4/25/62.

"Performance Predictions for Tropospheric Communications Circuits," A. P. Barsis, Natl. Bureau of Standards; 5/9/62.

IRE People

(Continued from page 46A)

Joseph J. Martus (M'62) has joined the Essex Electronics Division of Nytronics, Inc., Berkeley Heights, N. J., as Engineering Manager. He was formerly assistant chief engineer at the Hanovia Lamp Division of Engelhard Hanovia, Inc., Newark, N. J. He attended Stevens Institute of Technology where he received a degree in Mechanical Engineering. Mr. Martus is a member of the Illuminating Engineering Society.

❖

Wardwell Montgomery (A'54–M'57) has been named Marketing Manager of Hospital Communications Products by Motorola, Inc. He will have the responsibility for product planning, market research, merchandising and distribution of Motorola/Dahlberg hospital communications systems with headquarters in Minneapolis.

He joined Motorola in 1951, after working as a radio communications sales representative and sales manager in Ohio. Since 1960, he has served as the staff marketing assistant in Motorola's national sales offices in Chicago. An electrical engineering graduate of Northwestern University, Montgomery is a registered professional engineer.

❖

Thomas J. King (M'56–SM'60) has joined the Reconnaissance Systems Laboratories (RSL) of Sylvania Electric Products Inc., as supervisor, equipment analysis section, in RSL's reliability engineering department.

He has extensive experience in the design and installation of equipments, instruments, and electronic and electrical systems in aircraft, as well as broad experience in design and reliability work in ground and space electronic systems and equipments. Prior to joining Sylvania, he was reliability manager for the Midas program at Philco Corporation's western development laboratories in Palo Alto, Calif., and earlier held managerial positions with the Martin Co. in Baltimore, Md.

Mr. King received the B.S. degree in electrical engineering from Johns Hopkins University. He is now working toward the M.S. degree at the University of Santa Clara.

❖

(Continued on page 122A)

IRE People

(Continued from page 121A)

Louis B. Horwitz (S'48–A'50–SM'56) has been named technical director for Beckman Instruments, Inc., Fullerton, Calif., manufacturer of electronic instrumentation, it was announced recently. In the newly-created position, he will coordinate technical programs of the company's domestic divisions and foreign operations. He will be responsible for reviewing individual projects and total programs and recommending plans for the most effective utilization of funds, personnel and facilities as they relate to technical programs.

A member of the Beckman organization since 1957, he served most recently as operations manager for the company's Systems Division. Previously, he held engineering positions with the Continental Oil Co., Ponca City, Okla., for eight years. He was graduated from the University of Texas with a B.S. degree in Electrical Engineering, and received his M.S. degree in Electrical Engineering from Stanford University.

(Continued on page 124A)

DELTASTRIP DIODES®

CUT CIRCUIT ASSEMBLY TIME UP TO 50%!

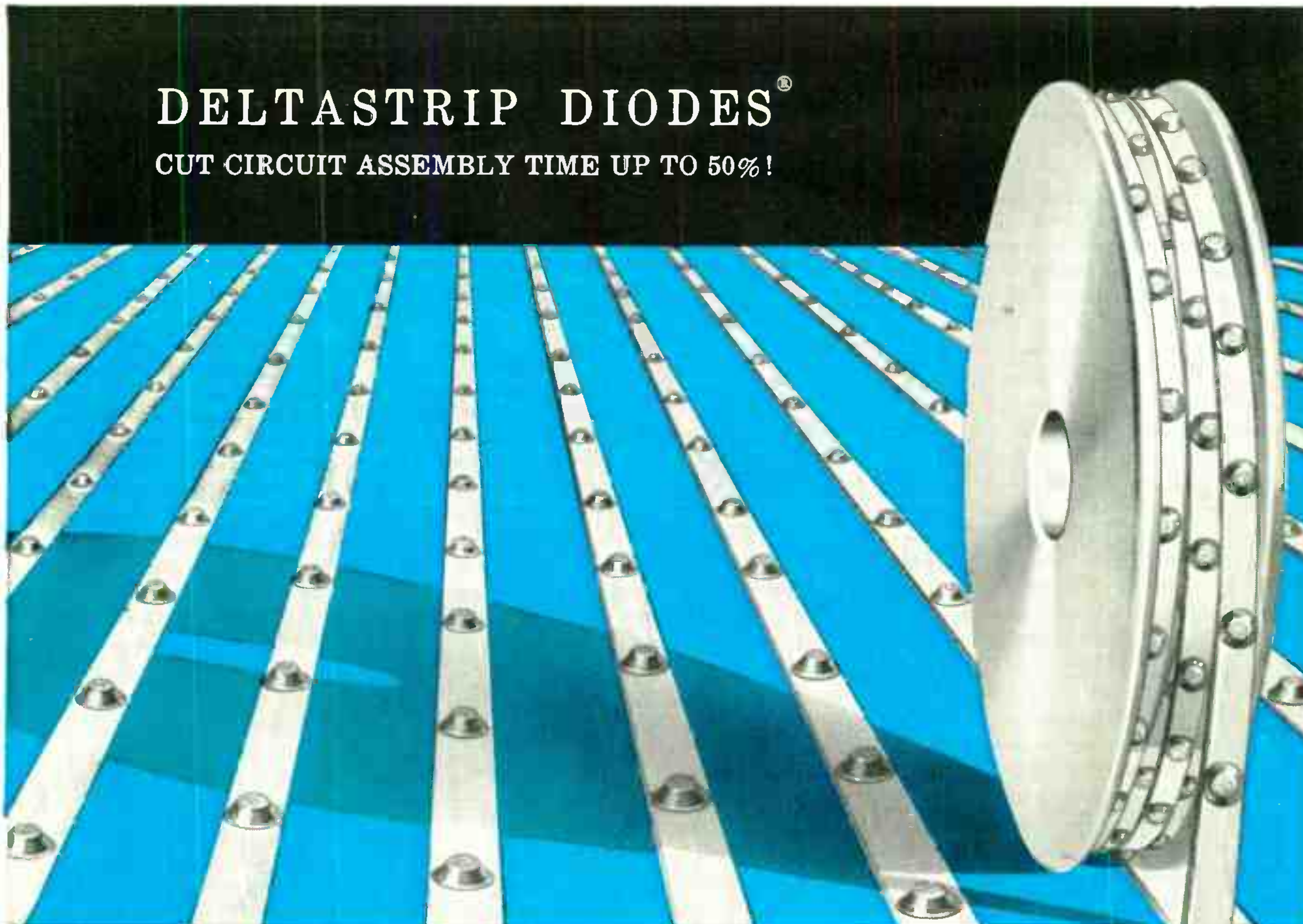

approx. 10 times actual size

THE GREATEST ADVANCE IN DIODES SINCE THE GLASS PACKAGE!

The remarkable new Deltastrip Diodes® provide the fastest circuit assembly time ever achieved . . . at low competitive prices. The first fully automated diode manufacturing technique, allows silicon junction diodes to be fused directly onto continuous gold-plated ribbon . . . literally "diodes-by-the-foot". The result is lower cost diodes *and* the most practical approach yet, toward truly automated circuit assembly.

Greater reliability is achieved through the use of a hyper-pure glass seal fused to the junction, providing a complete hermetic seal and elimination of floating impurities. Deltastrip Diodes® can be supplied with or without leads, in any number of junction combinations required. They provide a basic building block for any common anode or cathode connected circuit and can be sweat-soldered directly onto etched circuit connections or utilized in practically any circuit packaging technique. Let Delta engineers assist you in solving your design problems with Deltastrip Diodes.®

Delta Semiconductors manufacture a complete line of standard diodes, micro-diodes, high-speed switching diodes, subminiature rectifiers, gate circuit Poly-Diodes® and temperature-compensated zener diodes.

Write today for complete information and technical data.

Deltastrip Diodes® shown actual size

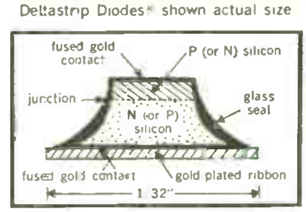

Cross-section of the Deltastrip Diode®

VISIT DELTA AT WESCON-BOOTH 3201

DELTA SEMICONDUCTORS, INC.

835 PRODUCTION PLACE · NEWPORT BEACH, CALIFORNIA

"New Dimensions in Diodes"

PROFESSIONAL CONSULTING SERVICES

IRE People

(*Continued from page 122A*)

G. L. Musser

Dr. Glenn L. Musser (SM'57) has been named President of HRB-Singer, Inc., to succeed **Dr. John L. McLucas** (S'50–A'51–SM'52–F'62) who has accepted the position of Deputy Director of Defense Research and Engineering, Tactical Warfare Program, The Pentagon.

Dr. Musser has held the post of Vice President for Systems and Operations since 1958. In this capacity, he was responsible for more than 45 per cent of the company's active personnel. During his eleven years with the company, he has also held such positions as Head, Intelligence Department, and Vice President and Head, Operations Department. Before joining HRB-Singer, he was Research Physicist and Assistant Chief of Antenna Branch, Aircraft Radiation Laboratory, Wright-Patterson Air Force Base, for two years; and acting Head of the Physics Department, Susquehanna University, for one year.

He received the B.A. degree in physics and mathematics from Susquehanna University in 1941; the M.S. degree in physics from Case Institute of Technology in 1943; and the Ph.D. degree in physics from Pennsylvania State University in 1951. He attended an Executive Management Program at Pennsylvania State University in 1958. He belongs to numerous professional fraternities, and is a member of the Armed Forces Communications and Electronics Association.

Dr. McLucas became associated with the company in 1949 as Project Engineer, and quickly advanced to the position of Vice President and Technical Director. He became President of the company, then known as Haller, Raymond and Brown, in 1957, and retained the post when it became a subsidiary of Singer in 1959. He holds patents on numerous inventions, including a radar-relay system, oscillograph and oscilloscope recorders, and band-compression devices. He has published articles in various journals, and holds positions in many professional and community organizations.

❖

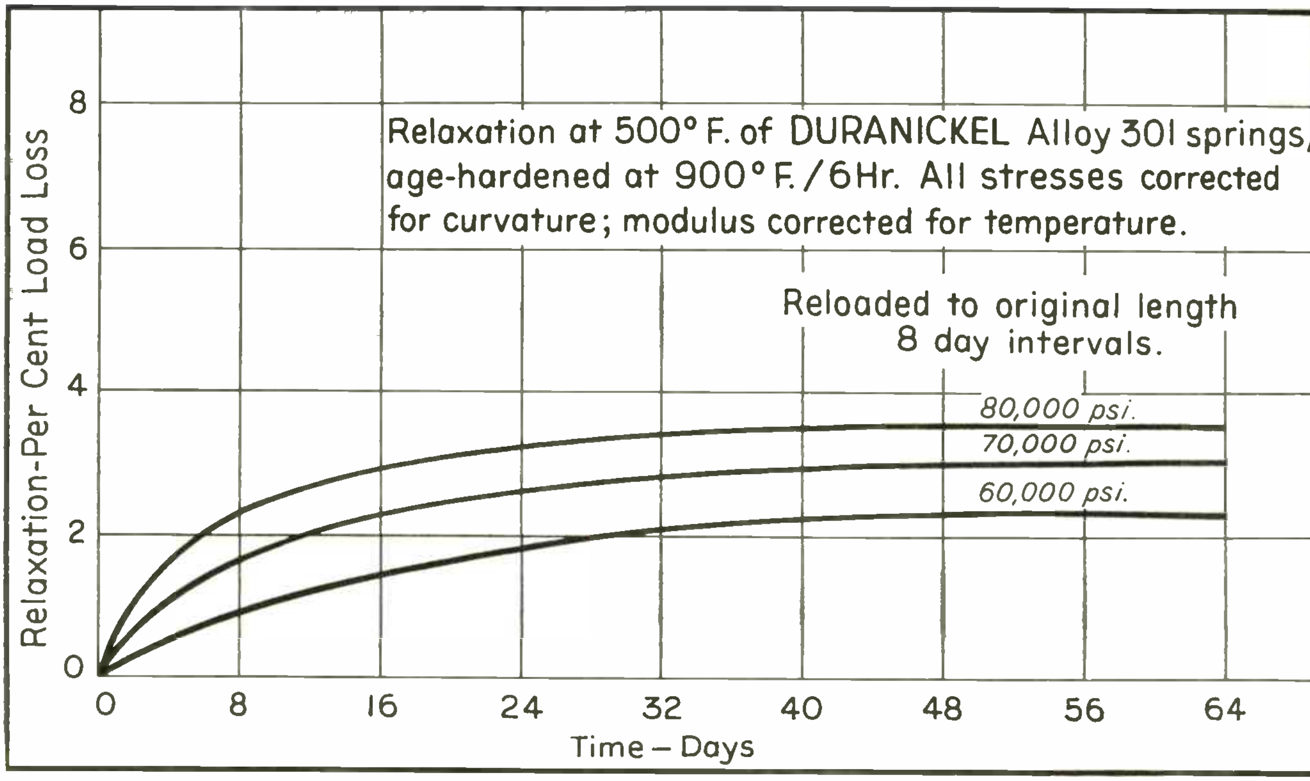

Nickel Alloy Springs last longer in Corrosive Environments and at High Temperatures

Kick out switches, relays, circuit breakers, solenoid valves, diaphragms and other spring type assemblies play a vital part in the efficiency of electrical equipment. If corrosion or high temperatures are important factors in the reliability and service life of your spring assembly, make sure they are made from a high nickel alloy for: (1) high strength stability; (2) resistance to relaxation at elevated temperatures; (3) oxidation resistance; (4) resistance to corrosive environments with good electrical properties.

INCONEL* Alloy X-750 is the outstanding choice for springs operating up to 1200° F because of its high strength stability, good oxidation and corrosion resistance, and resistance to relaxation.

DURANICKEL* Alloy 301 gives excellent service at temperatures up to 600° F. It is used for infrared bulb spring contacts, springs in sun lamps and spark plugs, electric toaster coils and numerous other applications requiring relaxation resistance at elevated temperatures.

The physical constants of DURANICKEL Alloy 301 and PERMANICKEL Alloy 300

PHYSICAL CONSTANT	DURANICKEL Alloy 301	PERMANICKEL Alloy 300
SPECIFIC GRAVITY, GM/CM	8.26	8.75
DENSITY, LB./CU. IN.	0.298	0.316
THERMAL CONDUCTIVITY AT (32°-212°F.) BTU./SQ. FT./HR. °F./IN.	128/137**	400
ELECTRICAL RESISTIVITY OHMS/CIR. MIL. FT. (68°F.)	260 **	94.5**
MICROHMS/CM. (20°C.)	43**	15.7**
TEMP. COEF. OF RESISTIVITY PER°F. (68°-212°F.)	0.0006	0.002
PER°C. (20°-100°C.)	0.001	0.0036
MEAN COEF. OF THERMAL EXPAN. AT (77°-212°F.), IN./IN./°F.	0.0000072	0.0000072
AT (25-100°C.) CM./CM./°C.	0.000013	0.000013
MAGNETIC TRANSFORMATION TEMP. F. (APPROX.)	200 **	563**

**Age-Hardened

Design Stress for age-hardened DURANICKEL Alloy 301 and PERMANICKEL Alloy 300 springs at elevated temperatures.

Coiling Method	Maximum Shearing Stress for temperatures (°F.) indicated	
	Up to 400°F.	550 to 600°F.
Cold	70,000 psi	60,000 psi
Hot	70,000 psi	60,000 psi

Other nickel alloys recommended for electrical spring assemblies include — PERMANICKEL* Alloy 300 high electrical and thermal conductivity requirements, MONEL* Alloy 400 for general applications requiring corrosion resistance in addition to toughness and strength up to temperatures of 450° F and INCONEL Alloy 600 for good strength, ductility, resistance to oxidation and good spring properties up to 750° F.

You can get the complete story on nickel alloy springs. Write for our technical bulletin T-35. "High Nickel Alloy Helican Springs." Our corrosion and high temperature engineers will be glad to help with any specific problem you have.

*Registered trademark

HUNTINGTON ALLOYS INCO

HUNTINGTON ALLOY PRODUCTS DIVISION
The International Nickel Company, Inc.
Huntington 17, West Virginia

Advertising Index

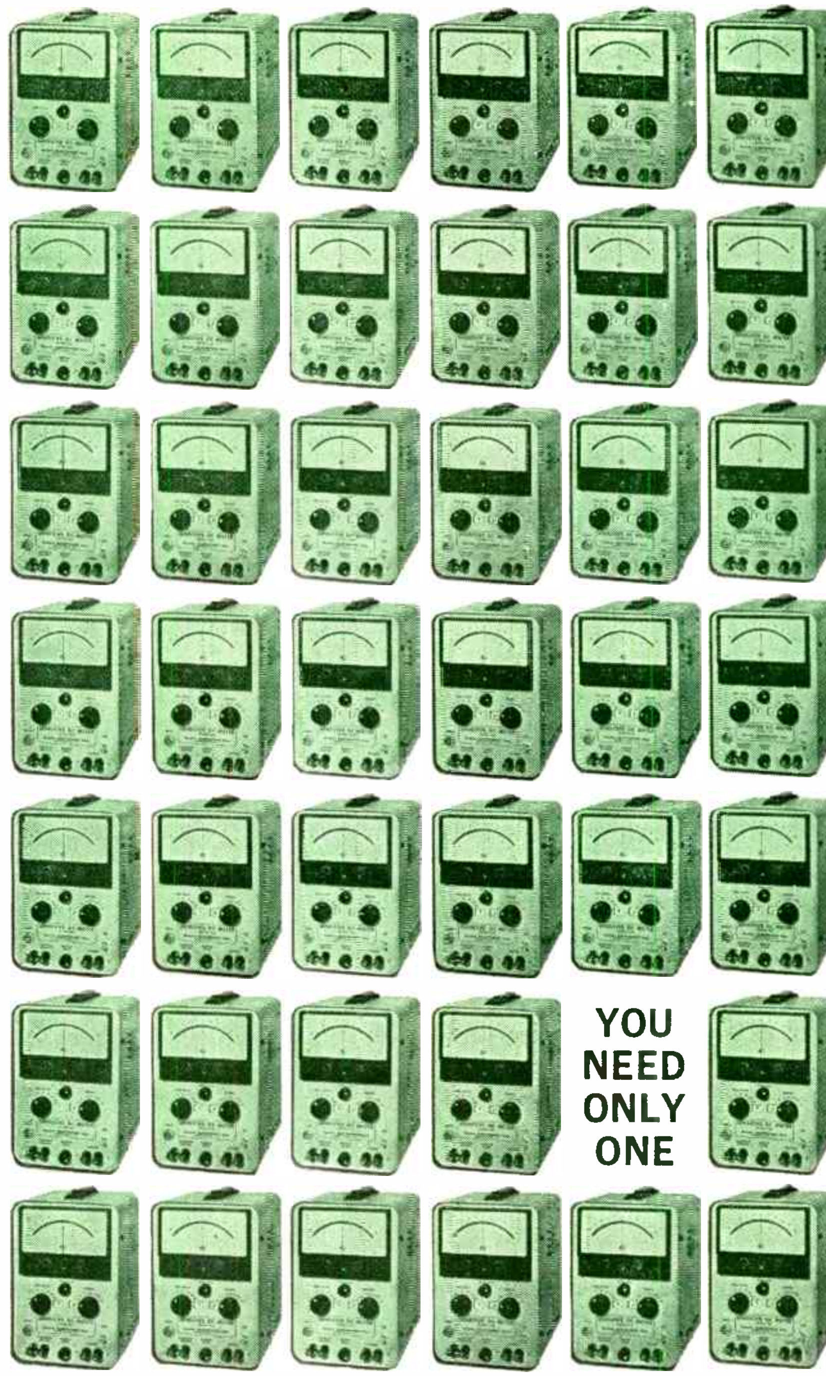

Advertising Index

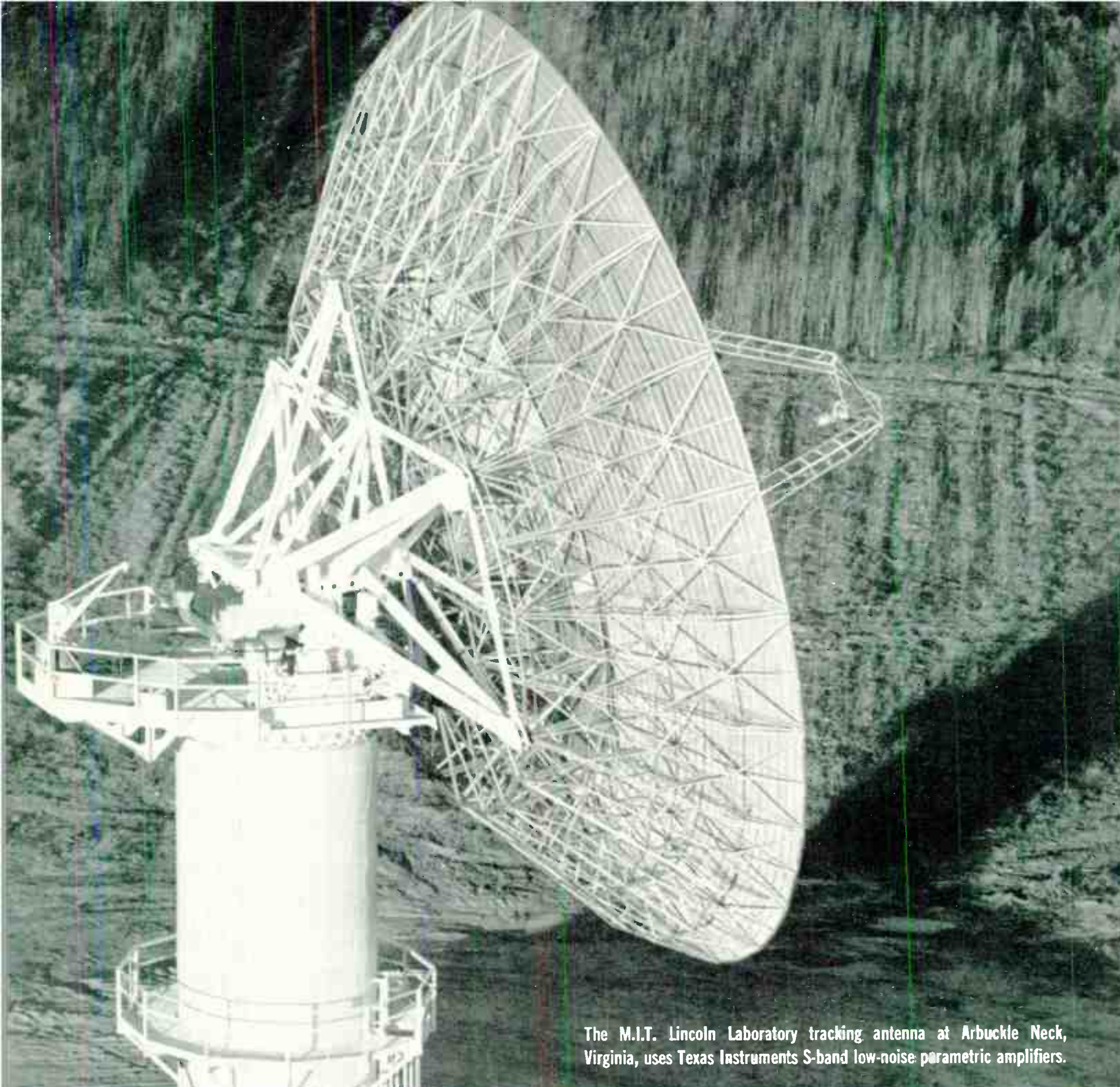

The M.I.T. Lincoln Laboratory tracking antenna at Arbuckle Neck, Virginia, uses Texas Instruments S-band low-noise parametric amplifiers.

Hearing better with TI paramps!

Many microwave communication and radar systems now incorporate parametric amplifiers and low-noise receiver assemblies from Texas Instruments. From L band through K_u band, standard and custom equipments operate efficiently and dependably in monopulse radar, polarization diversity tracking, troposcatter communication, and other airborne and ground applications. ■ Texas Instruments staff of experienced applications specialists will help you analyze your systems requirement. Call today. ■

APPARATUS DIVISION
PLANTS IN DALLAS
AND HOUSTON, TEXAS

TEXAS INSTRUMENTS
INCORPORATED
6000 LEMMON AVENUE
P. O. BOX 6015 • DALLAS 22, TEXAS